Third International Meeting
on
Wind Turbine Noise
Aalborg, Denmark 17 – 19 June 2009

Monitoring, Analyzing, and Adjusting Wind Turbine Systems

Daryoush Allaei and Dave Tarnowski

QRDC, Inc., 125 Columbia Court North, Chaska, Minnesota, 55318, USA.
dallaei@qrdc.com

Abstract

The QRDC team have proposed the development Monitoring, Analyzing, and Adjusting Wind Turbine Systems (MAATS). MAATS will have intelligent capabilities including self-monitoring, self-diagnostics, and self-corrections or self-adjustment online while a wind turbine is in operation. Smart sensors, actuators, and control system will be optimally incorporated in MAATS that will make online corrections for a wide range of maintenance issues critical to the efficient and failure-free operation of wind turbines. Ultimately, MAATS will be integrated in current and future wind turbines offering the capability to monitor their operating conditions and making the proper adjustments. MAATS will significantly boost performance, maintainability, and reliability while reducing downtime and catastrophic failures of wind turbines which are crucial to meeting our national renewable energy goals.

MAATS significantly enhances long-term reliability of wind turbines as they increase their penetration into the national and international electrical power base. MAATS offers new tools and methods to perform real time and predictive condition monitoring on major wind turbine subsystems and structure, including blades, gearboxes, generators, bearings, and towers. MAATS utilizes advanced acoustic and vibration sensor array systems and instrumentation to effectively monitor the health of a wind turbine. Blade mistuning, misalignment, gearboxes, and bearing models are used to predict real-time performance and component failure. In addition to having system capability for determining structural condition, MAATS reduces unscheduled outages, and predicts needed maintenance to avoid failures in order to achieve near zero downtime. The first part of this effort will lead to a tested laboratory prototype and preparation for full demonstration in the second stage.

Commercial application of this technology is in the wind turbine industry. The wind turbine technologies have found a wide range of applications in recent years. In 2008, the United States provides enough wind electrical power to power 5 million homes in 2008. The average annual power consumption of each household is estimated at 10,000 kWh. The U.S. must provide 20% of the nation's electricity by the year 2030. While no breakthrough in wind power technology is needed to achieve this goal, power transmission lines, reliability of wind turbines, reduction of operation and maintenance costs, and reduced outage need to be enhanced. The proposed MAATS will improve the reliability while reducing operation and maintenance costs and outage of wind turbines.

Introduction

Figure 1 Example of delaminated blades

Figures 1 and 2 show two examples of failures in wind turbines [7]. Long before these types of failures occur, the damages make the wind turbine power generation inefficient. Using proper sensors, some or all these failures may be detected before they become failure statistics. MAATS will respond to this need by significantly enhancing long-term reliability of wind turbines as they increase their penetration into the national electrical power base.

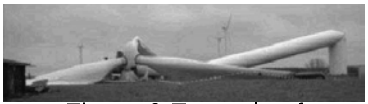

Figure 2 Example of collapsed wind turbine tower due to fatigue cracks and wind loading

One of the goals of the U.S. Department of Energy is that wind energy must provide 20% of the nation's electricity by the year 2030. This level of wind power will support 500,000 jobs while saving the consumers $128 billion by lowering the price of natural gas. In addition, it will cut greenhouse gas emission as much as taking 140,000,000 cars off the road. While no breakthrough in wind power technology is needed to achieve this goal, power transmission lines, reliability, reduction of operation and maintenance costs, and reduction of downtime and failure of wind turbines is crucial. The proposed MAATS will offer significant improvements in these areas.

The operational and maintenance costs of wind turbines should be reduced to make conversion of wind energy to electrical power economically more viable. The wind turbines must also become more reliable with reduced downtime and failures. For example, for offshore wind turbines, the costs for operation and maintenance are estimated [5-6] in the order of 30 to 35 % of the costs of electricity. Roughly 25% to 35% is related to preventive maintenance while 65% to 75% is due to corrective maintenance. The revenue losses for offshore wind turbines are estimated in the same order as the direct costs for repair. One of the approaches to reduce the cost of corrective maintenance is the application of condition monitoring for early failure detection and reduction of unpredicted or catastrophic failures. If wear and damages can be detected at their early stages, the propagating wear and damage can be contained, the cost of repairs will be lessened, and failures may be prevented. Offshore wind turbines however, will benefit the most from the fact that with early wear and failure detection, repairs can be better planned. This will lead to shorter downtimes and less revenue losses.

Wind turbines are complex machines with several sub-machines that convert the kinetic energy of moving air to electrical power. Extraction of a significant amount of energy requires high wind speeds and large turbine diameters. In general, turbine speeds are slow (about 20 rpm) and the speed must be increased to a useful generator speed. A typical wind machine has a 3-blade turbine with more than 60 meters in diameter. This turbine drives a generator through a speed-increasing gearbox that generally has a planetary first stage and one or two additional parallel shaft stages. The generator runs at about 1500 rpm and produces about 1.5 MW. Many wind turbines are variable speed machines; the speed depends on the wind conditions and can vary over a wide range. For these machines, high power output requires high levels of torque and accompanying high gear-mesh forces. Because of the low speed of the turbine, the various gearbox components are usually supported by rolling element bearings. These bearings are subject to significant radial loads and need to be carefully monitored to detect any degradation.

The application of condition monitoring has grown considerably in the last decade in several branches of industry. The interest in condition monitoring is also increasing in the wind turbine manufacturers and operators. Because of small financial margins in the wind turbines, the relatively small production losses, and the minor effects on the electricity network (a wind turbine is operating stand-alone), the application of continuous condition monitoring has remained limited. Additionally, most components have been designed for the lifetime of the turbine, which implies that degradation leading to replacement is not expected to occur.

At present, with the increasing installed power of the wind turbines, the application of off shore wind turbines and major problems with turbine blades and gearboxes, the necessity of condition monitoring can no longer be neglected. Some components, although designed for the turbine lifetime, may require repair or fail earlier than expected. This is emphasized by the approach of warranty and insurance companies that simply require application of monitoring provisions. Otherwise, expensive preventive replacements or inspections should be carried out periodically. Also the development of special purpose instrumentation for wind turbines results in the use of off-the-shelf systems for a reasonable price.

Table 1 Reported causes of machinery failures

Cause No.	Causes of Vibrations	Rate of Occurrenc
1	**Blade Mistuning**	**N/A**
2	**Misalignment**	**30%**
3	**Mass Imbalance**	**30%**
4	**Resonance**	**15%**
5	Looseness/Tightness	10%
6	Bearings	10%
7	Others	5%

The main root causes of wind turbine wear, damage, failure is excessive vibration. Noise and vibration is used as wear and damage detecting signals that can reveal the health of the wind turbine and needed maintenance. MAATS will monitor and make certain online adjustments (while a wind turbine is operating) in order to eliminate excessive noise and vibrations in wind turbine systems. Reduced noise and vibration in turn will result in reduction of component wear and failure. Eventually, the proposed Monitoring, Analyzing, and Adjusting Wind Turbine Systems (MAATS) will eliminate the top six of the most important causes of wind turbine machinery failures (see Table 1) that occur due to excess vibration or noise/vibration could be the symptom of such causes of wear or damage. Such root causes are <u>blade mistuning</u>, <u>misalignment</u>, <u>imbalance</u>, <u>resonance</u>, fastener <u>looseness</u>, and <u>bearing damages</u> and defects. In this project, our focus is on online correction of blade mistuning, misalignment, imbalance, and resonance that have shown to be responsible for over 75% of machinery wear, failure, and downtime. Table 1 shows the potential causes (or sources) of machinery noise and vibration, and thus, wear and failures. Note that 30% of the machinery failures are due to misalignment between coupled driven and driver units, 30% due to imbalance, and 15% due to machinery resonance. It should be noted that even though blade mistuning has been reported to be a major fatigue problem for high speed turbines (i.e., high speed jet engines), it has not been previously investigated for low speed machines, such as wind turbines. The QRDC team believes that blade mistuning could result in very high stress concentrations in wind turbines because of their unusually long blades (more than 105 ft in length for a 1.5MW wind turbine) even though the rotational speed is relatively low. The causes of blade mistuning are known [1-3] to be manufacturing processes, variation in material properties, and environmental and operational conditions. In this project, we monitor blade mistuning because it can cause high stress concentration and thus catastrophic failure. Furthermore, blade mistuning will be used to assess the mechanical health of wind turbine systems. The use of the proposed MAATS in wind turbines will result in significant savings in operation and maintenance cost of the U.S. wind power generation farms. MAATS not only monitors and predicts the required repairs, but also makes adjustments to correct some of the problems so the uptime is optimized. These savings will directly benefit wind turbine systems due to decreased operational cost and thereby, reduced cost per unit power generation.

Blade to blade variations in wind turbine rotors may lead to the well-documented [1-4] phenomenon of mistuning. Mistuning can cause an amplification of resonant response by up to 400%. Mistuning has been identified as a primary factor in high cycle fatigue failures in high speed turbines. To improve robustness in turbine designs, the blade-hub assemblies need to be inspected for their mistuning characteristics. High-response rotors will be identified for refurbishment. This leads to a need for a rapid mistuning evaluation. Further, when components are in the field, usage may change the blade to blade characteristics of the rotor, requiring additional mistuning evaluation. MAATS is focused on the monitoring, correcting mistuning, or reducing its adverse effects in wind turbines whose degree of mistuning may increase due to operational and environmental conditions such as bird collisions and collection of dust. None of the current condition monitoring systems has the capability to inspect blade mistuning in wind turbines.

Integral components of wind turbine power generation systems are blade-hub assemblies that also function in compressors, turbines, and turbo-pumps, for example. Bladed-disk assemblies are rotating fan-like structures designed to transfer energy to or from a moving fluid or gas. In a wind turbine blade assembly, a set of identical blades is assumed to be positioned symmetrically around a central hub. Such a cyclic or symmetric set-up allows the blade-hub assembly to rotate about an axis directed along the fluid flow. Disturbances in the flowing fluid (or wind) induce fluctuating loads on the blades which in-turn are subjected to severe vibrations. In the case of wind turbines, due to the large length of blades (over 105 ft for 1.5 MW wind turbine), the resulting dynamics generate very large and damaging vibrator loads. The latter poses limits to the functionality, performance, and useful life of the turbine blade-hub assemblies. In the case of high speed bladed systems, the performance of the system is reduced due to the occurrence of flutter that is a dynamic instability caused by interactions between aerodynamic loads and vibrations of the blades. On the other hand, the useful life of the system is usually lowered due to high cycle fatigue that is a degradation of the structural integrity of the blades resulting from time dependent, vibrating loads. Due to the catastrophic nature of flutter-type failures, much research and development have been previously conducted [1-4] to assess the flutter boundaries and thereby reduce the chance of the occurrence of flutter by improving the design of bladed-disk assemblies. However, even though there has been much research work on reducing high cycle fatigue, there still exists a lack of conclusive, effective, and universal techniques to minimize high cycle fatigue. In particular, in the case of wind turbines, even though the speed is much lower, due to the long length of the blades, the adverse effects of the mistuning could be as much as or higher than a high cycle fatigue system. Due to long length of the blades, small mistuning of the blades will result in high vibration loads that propagate throughout the gearbox, bearings, shafts, and even in the turbine tower. The proposed Monitoring, Analyzing, and Adjusting Wind Turbine Systems (MAATS) will monitor the degree of mistuning and the resulted high vibratory loads during operation of the wind turbines. MAATS has a strong promise to yield substantial economic, energy, and environmental benefits leading to enhanced competitiveness by reducing the cost of the renewable electrical power generation.

Current vibration-based condition monitoring system providers have one thing in common; they mostly monitor gear and bearing vibrations and make an attempt to predict the required maintenance. These conventional vibrating monitoring systems do not monitor blade mistuning, and they do not have any capability for online corrections and adjustments. MAATS addresses these shortcomings.

The ultimate goal of this project is to develop MAATS that will be integrated in the wind turbines replacing the manual vibration-based monitoring systems. MAATS will have MEMS vibration sensors and miniaturized microphones to monitor both structural vibrations and air-borne noise. It will incorporate the award winning [8-14] energy managing techniques to effectively monitor blade mistuning. This innovative technology has won several R&D awards from Army, Navy, Air Force, DOE and commercial organizations. This is the first time that our technology is proposed for reducing operation and maintenance cost while improving power generation efficiency of wind turbines.

Overall Approach

MAATS offers new tools and methods for performing real time and predictive condition monitoring on major wind turbine subsystems and structure, including blades, gearboxes, generators, bearings, and towers. MAATS will utilize advanced acoustic and vibration sensor array systems and instrumentation to effectively monitor the health of a wind turbine. Blade mistuning, misalignment, gearboxes, and bearing models will be used to predict real-time performance and component failure. In addition to having system capabilities for determining structural condition, MAATS will reduce unscheduled outages, and will predict needed repairs to avoid failures for achieve near zero downtime. This effort will lead to a tested laboratory prototype and preparation for full demonstration in the next stage of the project.

MAATS will have intelligent capabilities including self-monitoring, self-diagnostics, and self-corrections or self-adjustment online while a wind turbine is operating. Smart sensors, actuators, and control system will be optimally incorporated in MAATS that will make online corrections for a wide range of maintenance issues critical to the efficient and failure-free operation of wind turbines. Ultimately, MAATS will be integrated in current and future wind turbines offering the capability to monitor their operating conditions and making the proper adjustments while wind turbines are in operation (i.e., online adjustment). MAATS will significantly boost performance, maintainability, and reliability while reducing downtime and catastrophic failures of wind turbines which are crucial to meeting our national renewable energy goals. MAATS must meet certain requirements.

(1) MAATS will be capable of withstanding extreme environments, including high temperatures, high humidity, extreme cold, corrosive offshore environments, and wind-blown sand and dust

(2) MAATS will be flexible in nature, capable of providing a variety of crosscutting condition monitoring applications;

(3) MAATS will be easily integrated into the total wind control platform. This includes integration into wind turbine fleets or into remote, stands alone, unattended turbines;

(4) MAATS (both its sensors and data acquisition systems) must be capable of lifetimes on the order of 20 years or be of such a cost as to make more regular replacement economically viable; and

(5) This effort will lead to a demonstration of the MAATS system in either simulated or actual operating environment.

The targeted markets are vibration-based analysis, machinery condition monitoring, and predictive maintenance. Even though these niche markets have been fast growing with several major advancements, wind turbine farms still face significant downtime and excess operational costs. At its best, the current maintenance technology applied to wind turbines relies on the procedure outline below.

1. Wind turbines are monitored on a periodic basis (intervals vary from a week to several months).
2. The operator (or an automated system) reports excess vibrations.
3. A vibration technician identifies the source of vibrations. The process may take 1 to 10 days.
4. The vibration technician (analyst) issues a work order to the mechanics.
5. The mechanics replace (or repair) the damaged parts while shutting down the system. This has resulted in downtime and often loss of production.
6. The quality of the repair is checked and another work order issued if the repair is unsatisfactory.
7. The mechanics conduct the final fine-tuning of the wind turbine before starting it up.

The above procedure and technologies have four disadvantages. (1) The time interval between inspections could result in damage becoming a catastrophic failure. (2) By the time excess vibrations are sensed, the damage could have propagated throughout other sections of the machinery, thus damaging other components. (3) The time spent on data analysis is often long and costly. In complex systems, the analysis of data and correct diagnostics may take weeks. This deficiency may result in costly downtime and/or catastrophic failures and loss of lives. (4) Wind turbine downtime is a major source of excess operational cost and lack of power generation. In summary, even though it has been successfully demonstrated that condition monitoring and predictive maintenance have had a significant role in reducing operational costs, the advancements in the technologies have not found their way in the wind turbines.

To minimize machinery maintenance cost and downtime, new technologies have been introduced. These new technologies (or procedures) are continuous monitoring, multi-domain analysis, automated reporting and worksheets, and total reliability maintenance. Even with these new ideas, the downtime is still significant since none of the methods eliminates the time spent on analysis of data by an operator and the time a machine is shut down for repair (i.e., downtime).

The MAATS approach has three innovative features that make MAATS unique and effective. (1) It will explore and address the occurrence of blade mistuning that can result in damages and eventually failure in wind turbine gearbox, bearing, and tower. (2) In addition to the conventional gear and bearing frequencies and signals, we will measure and analyze blade mistuning frequencies and wave forms in order to asses the condition of a wind turbine. (3) For certain causes of excess noise/vibration and wear, it will induce corrections and adjustments online while a wind turbine is operating. These three features are not addressed in any of the condition monitoring systems currently applied to wind turbines.

This team proposes to optimally combine mistuning and vibration-based condition monitoring technological advances and the state-of-the-art energy management (patented by the author), and control algorithm. These concepts have been investigated by QRDC for deployment to critical systems in the U.S. Department of Defence. DARPA, NSF, Army, Navy, Air Force, MDA, and DOE have contributed to the development of parts of this technology for use in military systems and processing industry. In particular, with the support from DOE [13], the QRDC team has successfully applied part of the technology to particle separation using vibrating screens applicable to taconite processing, food processing, dry powder processing, and dewatering machines.

Anticipated Public Benefits

Wind turbines have become more established as an economically viable alternative to fossil-fuel power generation in the last decade. Wind farms consisting of hundreds of units have been adding a significant amount of electrical generating capacity around the world and in America. As the size of wind farms continues to increase business economics dictate careful asset management to minimize downtime and maximize availability and profits. To help end users and operators more proactively detect mechanical problems in wind turbines, MAATS can have both permanently mounted and portable offerings for wind turbine vibration- and noise-based condition monitoring. Integral to the MAATS offerings is a signal processing technology based on blade mistuning waveforms, and gears and bearing vibration and noise signals, which can be particularly beneficial when applied to wind turbines.

Wind turbines can be separated into two general types based on the axis about which the turbine rotates. Turbines that rotate around a horizontal axis are most common. Vertical axis turbines are less frequently used. Wind turbines can also be classified by the location in which they are to be used. There are onshore and offshore wind turbines.

Because financial margins are very small for wind turbines, economic aspects play a very important role. The installed power per wind turbine is relatively small. Wind turbines are available in the order of 1 MW, while other power generation units are in the range of 10 up to several hundreds of MW's. At the present time, the production losses due to failures are very small for onshore wind turbines, as compared with other branches of renewal energy industry. Moreover, due to the low installed power per wind turbine, the investment level for condition monitoring system is relatively high for the current onshore wind turbines. Due to the energy crisis in USA and around the world, the number of wind power generation farms are rapidly increasing, and thus from economical point of view, the investment for condition monitoring and online corrections will be justified.

For offshore application, the situation is quite different. Due to the restricted accessibility of wind turbines for maintenance, the waiting and repair periods, following a failure will be considerably longer, which implies increasing production losses and repair costs. Together with decreasing prices of condition monitoring systems, the economical break even will decrease significantly. A condition monitoring systems, based on vibration analysis is in the range of $15,000 to $20,000. Although the robustness with respect to failure detection/forecasting is yet to be demonstrated, the level of investment makes application feasible. Wind turbine power generation farms will benefit from the proposed MAATS product. Specifically, the key benefits are listed below.

1) Significant economic improvement to offshore wind turbine operations where repairs and maintenance are much more difficult and costly than onshore wind turbines.
2) Significant energy and cost savings by optimizing power generation efficiency of wind turbines.
3) Significant performance and uptime improvement that results in greater savings.
4) Significant reduction in maintenance cost (75% or more reduction in maintenance cost).
5) Significant improvement in environment around wind turbines. Noise and vibration levels will be significantly reduced. Up to 15 dBA reduction in noise level is expected.
6) Significant reduction in waste such as lubrication, bearings, and other spare parts.

Economic Benefit –

1) The outage (downtime) of wind turbines will be reduced by 75%. For a small wind turbine (1.5 MW), the current annual cost of downtime due to reactive maintenance is about $11,340 in loss of power. This is based on the following assumption: 10 days downtime for maintenance, 1500 kW turbine, capacity factor of 0.3, and an average cost of power at 12¢ per kWh. We anticipate a saving of about 75% of downtime resulting in annual economic benefit of about $8,505 per small turbine. If a farm has 100 small turbines, the annual saving could be as high as **$850,500**.

2) The maintenance cost will be reduced by at least 50% per year. For a small wind turbine (1.5 MW), the current annual cost of repairs (including labor, material, equipment) due to reactive maintenance is about $15,264. Our projected saving will result in an annual economic benefit of $7,632. Assuming the wind power generation farm has 100 small turbines, the total annual saving will be about **$763,200**.

3) Excess noise and vibration level will be reduced by 10 dBA.

Proper installation and maintenance of wind turbine is critical to their optimum operation, higher efficiency, lower excess noise and vibration, and reduced downtime. In particular, alignment, balanceed system, and tuned blade assembly of the turbine parts is necessary to secure highest possible efficiency and a low noise level. Maintenance of wind turbines is carried out at regular intervals. Quality minded turbine producers chose a maintenance program for the propellers, gearboxes, bearings, and generators in order to optimize efficiency and reduce noise and unexpected maintenance and failure. The following could be economic benefits of the MAATS technology.

1) Condition monitoring does not prevent failures from happening but if failures can be recognized at an early stage, appropriate measures can be taken to limit the consequence damage and unexpected failure.
2) Maintenance actions can be better planned which leads to less unexpected failures, thus less downtime.
3) The largest benefits from condition monitoring can be expected for offshore wind energy to change from corrective maintenance to condition based maintenance. The economic benefits will significantly increase when going from condition based maintenance to online correction that is offered by the proposed MAATS.

Environmental Benefits –

MAATS systems will have a significant positive environmental impact due to improving power generation by wind turbines, reduced energy consumption, and far fewer throw-away parts such as bearing, lubrication, bolts, etc.

Anticipated Improvements to Worker Health and Safety –

MAATS will reduce (or eliminate) excess noise and vibrations and thus, present minimum or no hazard exposure to environment and operators. Furthermore, safety will be improved by reducing noise.

Conclusions

Reducing the current unscheduled maintenance and failures, decreasing maintenance cost, improving wind power generation, and reducing downtime or power outage in wind turbine operations are not trivial tasks. Care must be taken to ensure that economic and engineering data generated in this work is truly scalable to the industry needs. Because of the extensive industry interactions that are an important part of this proposal, and considerable experience in the research needs for the project that reside at QRDC and its partners, we believe that the transfer of lessons learned into successful industrial-scale practice will be rapid and successful. Technical barriers that must be overcome are listed below.

- Determine the number of sensors and their locations required to generate sufficient monitoring data.
- Determine the most effective frequency range that can be used to detect problems.
- Determine if structural fatigue is an issue when mistuning occurs.
- Investigate the path of vibration propagation from the rotation of the blades to gearbox, shaft, bearings, and tower. This can be used to identify the best location for the sensors.
- Determine if an effective packaging of the miniaturized sensors is possible for survival in harsh environmental conditions.
- Determine if MASST is scalable to a variety of wind turbine farms.

References

1. Sang-Ho Lim, Christophe Pierre, Matthew P. Castanier, *"Mistuning Identification and Reduced-Order Model Updating for Bladed Disks Based on a Component Mode Mistuning Technique",* Thesis, Department of Mechanical Engineering, The University of Michigan, Ann Arbour, MI.
2. D.M. Feiner and J.H. Griffin, *"Mistuning Identification of Bladed Disks Using a Fundamental Mistuning Model – Part II: Application",* Journal of Turbomachinery, Vol. 126, January 2004
3. D.M. Feiner and J.H. Griffin, *"Mistuning Identification of Bladed Disks Using a Fundamental Mistuning Model – Part I: Theory",* Transactions of the ASME, Vol. 126, January 2004.
4. M.P. Mignolet and A.J. Rivas-Guerra, *"Identification of Mistuning Characteristics of Bladed Disks From Free Response Data – Part I",* Journal of Engineering for Gas Turbines and Power, Vol. 123, April 2001.
5. Hatch, C., "Improved Condition Monitoring Using Acceleration Enveloping," 2Q04 ORBIT, pp. 58-61, 2004.
6. Verbruggen, T. W., "Wind Turbine Operation & Maintenance Based on Condition Monitoring: WT-OMEGA," ECN (Energy research Center of the Netherlands) Final Report, January 2003.
7. M. A. Drewry and G. A. Georgiou, "A review of NDT techniques for wind turbines", document at www.ndt.net/search/docs.php3?id=4550, 2007.
8. "Moving DARPA Technologies into the Marketplace," DARPA, 1998.
9. "Technology 2000: Innovation on Display," NASA Tech Briefs, January 2001
10. "Minnesota Member Leads Way by 'Smart Skin' Technology", S. of Manufacturing Eng., SME News, 1/01
11. "Smart Control Systems Reduces Vibrations," MDA Update, # 37, Mar 2001.
12. "25 Hot New Companies", Fortune Small Business, May/June 2000.
13. "Smart Screen systems", R&D100, 2003.
14. "Energy-based Smart Skins," Technology Award of the Year, Smart Structure Conference, 2002.

Third International Meeting
on
Wind Turbine Noise
Aalborg Denmark 17 – 19 June 2009

Sound Emission and Sound Propagation for Wind Turbines in Forest Terrains

Martin Almgren, Stephan Schönfeld and Josefin Grönlund
P.O. Box 1551, SE-40151 Göteborg, Sweden
Martin.almgren@afconsult.com

Abstract

Measurements of sound emission according to IEC 61400-11 and sound immission up to 520 m distance has been made for a wind turbine at Ryningsnäs in Hultsfreds municipality in Sweden. The wind turbine is a 2,5 MW turbine with 100 m hub height and 90 m rotor diameter. The measurements show that the determined apparent sound power level is some decibels lower than the level guaranteed and also below the level measured by the manufacturer. The hypothesis was that the wind turbine shall be noisier in a forest terrain. The measurements on sound propagation indicate a rise of sound pressure level inside the forest with 1 – 2 dB. This may be due to reverberation and a temperature lapse inside the forest among the trees. Simulation of a distributed source in Nord2000 compared to a point source at hub height shows that the model with an apparent point source at the hub position is working good. The standard for sound emission measurement should be improved by stating the sound power level as a function of wind speed at the hub height and not at 10 m height. Further, for large wind turbines, the atmospheric sound absorption shall be accounted for.

Introduction

For wind turbines in a forest terrain, it is, in Sweden, not clear how the sound power level shall be determined. In the Swedish model, published by the Swedish Environmental Protection Agency, Naturvårdsverket (2001), the sound power is corrected due to the difference in wind speed profile depending on the ground roughness deviating from the conditions under which the sound power is stated according to IEC 61400-11. This has led to increased calculated sound pressure levels at dwellings, sometimes with more than 1 dB and the wind parks have been planned to produce less renewable energy. This may be valid for the old type of stall controlled wind turbines, where the radiated sound power often increased linearly with shaft speed. The newer type of turbine, that is controlled with blade pitch and shaft speed, does not show this behaviour. The radiated sound power increases with increasing wind speed up to approximately 8 m/s. For higher wind speeds, the sound power is often constant or may even decrease somewhat.

There is also a hypothesis that turbulent winds and higher wind shear will lead to an increased sound radiation from the rotor.

Measurements of sound emission according to IEC 61400-11 have been made of a wind turbine placed in a forest terrain. Further, measurements of sound pressure level downwind at distances up to 520 m and upwind at 125 m has been made with the purpose to compare with sound propagation models.

Sound emission measurement

Determination of apparent sound power level according to IEC 61400-11 (2006) has been applied on a wind turbine in Ryningsnäs in Hultsfreds municipality in Sweden. The wind turbine is of the type Nordex N90-2500-LS. It has a three-bladed rotor with diameter 90 m and hub height 100 m. The rotor is pitch and rotor speed controlled and the turbine has a nominal power of 2,5 MW. In the park, that is owned by Vattenfall Vindkraft AB, there are at present two turbines. Vattenfall conducts several types of investigations in the park.

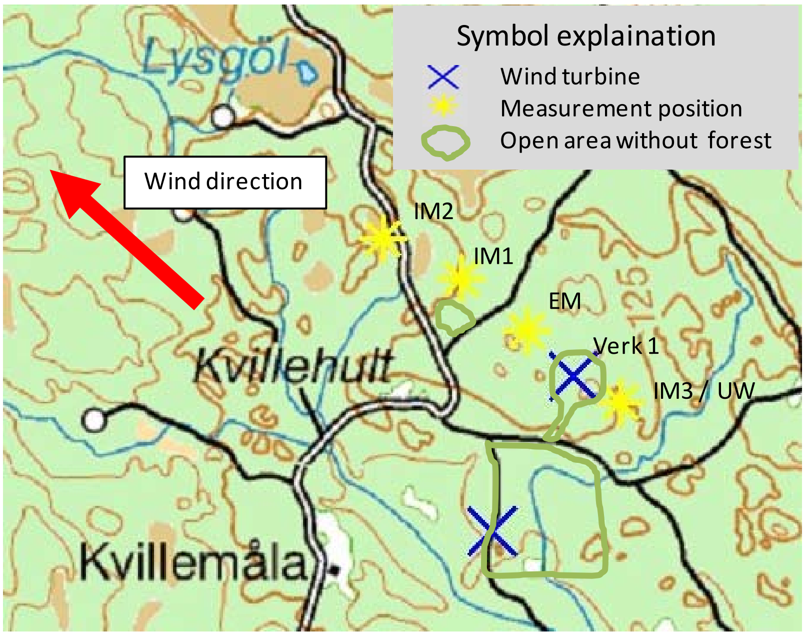

Figure 1 Map showing the position of the measure turbine, "Verk 1", the emission measurement point EM.

Figure 2 The microphone is placed under a secondary large windshield on a hard board on the ground in the forest at the sound emission measurement.

Figure 3 The wind turbine as seen from a position close to the emission measurement location

The sound emission measurement report is in appendix 1 to Almgren (2009). The determination of the so called apparent sound power level has been made for the wind speed 5,7 m/s at hub height, corresponding to 4 m/s at 10 m height recalculated from hub height according to the rules in IEC 61400-11 (2006)

The recalculation of the wind speed to 10 m height has been made under the assumption of a logarithmic wind speed profile and the reference ground roughness 0,05 m, as prescribed by the standard. This wind speed is a fictive wind speed, which would appear at 10 m height if there was no trees and if the ground would have a roughness equal to a flat farmland instead of an uneven forest ground surface. Inside the forest among the trees, the wind speed was negligible. In the analysis of the results it was tricky to know what was correct when relating the sound power level to wind speeds transformed from 100 m to 10 m and later transformed back to 100 m under the assumption of another ground roughness, when using the sound power in the sound immission calculations.

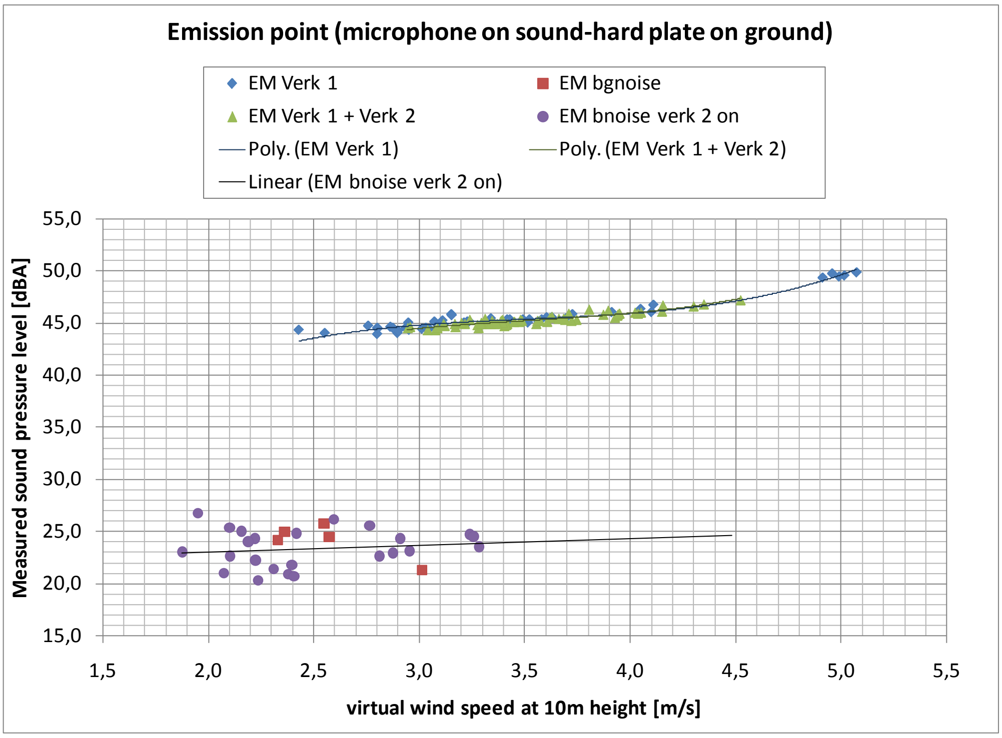

Figure 4 The measured sound pressure level on the hard board at 150 m horizontal distance from the turbine tower related to the wind speed at 10 m height. The wind speed was determined from the wind speed at hub height under the assumption of 0,05 m ground roughness. The wind speed at hub height was determined from the produced electric power in one minute intervals. The second turbine, "Verk 2" was also operating during some of the measurements. "bg" stands for background

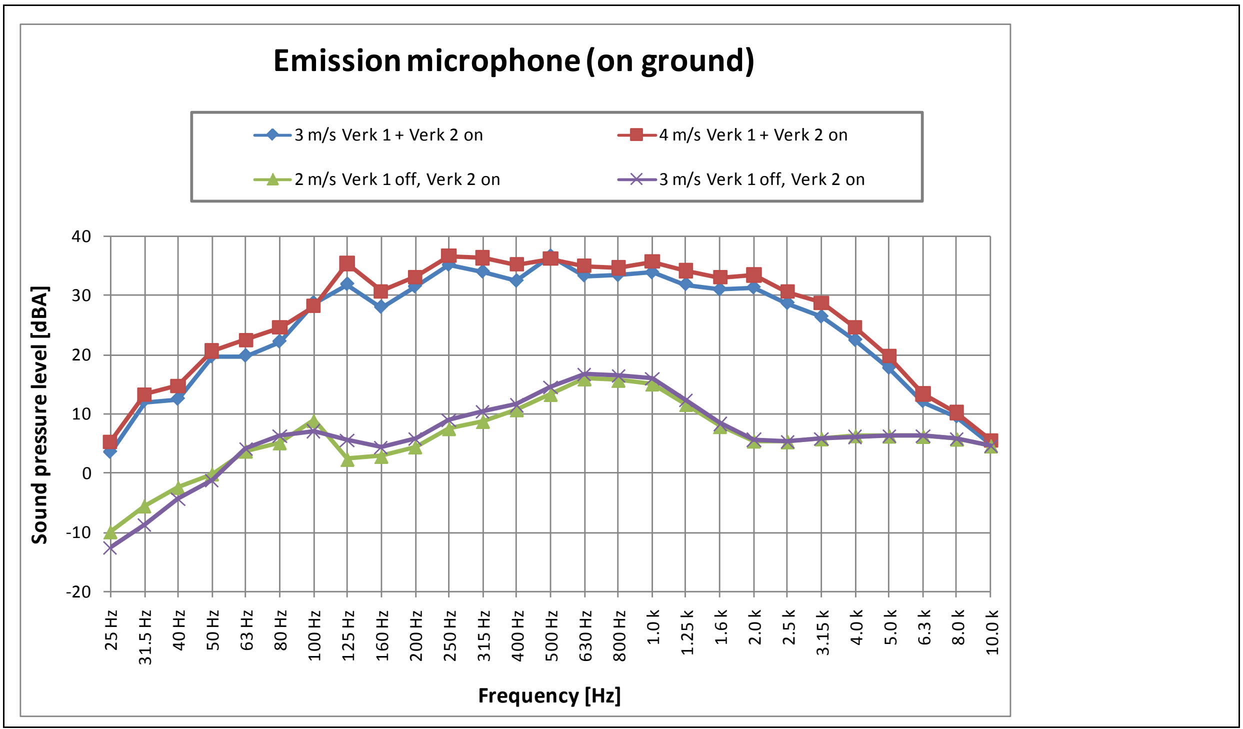

Figure 5 The measured third-octave spectra of the sound pressure level at the sound emission measurement. 2, 3 and 4 m/s refers to the wind speed at 10 m height determined as described in Figure 4.

The resulting apparent A-weighted sound power level is shown in Table 1 together with the warranted sound power level from the supplier. The data from the supplier has been collected from the web, Nordex (2009) and Windtest (2005).

Table 1 Measured and warranted sound power level of the turbine

Measured sound power level at 4 m/s at 10 m height at the reference ground roughness 0,05 m $L_{WA,4}$, dB re 1 pW	Warranted sound power level at 4 m/s at 10 m height $L_{WA,4}$, dB re 1 pW
96,2	99,0

The warranted sound power level is probably determined by the supplier from the measured sound power level of one or several turbines with a hub height of 80 m on flat farmland. An extract from one such measurement is shown in Windtest (2005). In that extract, the sound power level is shown at 6, 7, 8 and 8,6 m/s at 10 m height recalculated from the wind speed at the rotor under the assumption of ground roughness 0,05 m and a frequency spectrum is given for 8,6 m/s wind speed at 10 m height.

The difference between the warranted sound power level and the sound power level that has been measured by the supplier for a turbine with 80 m hub height is shown in table 2.

Table 2 Sound power level warranted and measured by the supplier for a Nordex N90-2500LS turbine with 80 m hub height on flat farmland with an estimated ground roughness length 0,05 m,

Wind speed at 10 m height m/s	Warranted sound power level $L_{WA,k}$, dB re 1 pW	Measured sound power level $L_{WA,k}$, dB re 1 pW	Difference dB
6	103,0	100,9	2,1
7	104,0	101,7	2,3
8	104,0	102,8	1,2
8,6	-	103,3	-
9	104,8	-	-

The warranted sound power level should normally be higher than what has been measured for a specific turbine, since there may be individual variations. The sound power level shall be declared according to IEC TS 61400-14 (2005). In the actual case, the supplier obviously. according to Table 2, has a difference of 1 – 2 dB. The warranted sound power level 99,0 dBA re 1 pW of a turbine with 100 m hub height on flat farmland, thus corresponds to a measured value of 97 – 98 dBA re 1 pW.

The formula that is used in the IEC standard to calculate the sound power level $L_{WA,k}$ from the sound pressure level, $L_{Aeq,c,k}$, only takes the the slant distance, R_1, from the hub to the measurement point into account

$$L_{WA,k} = L_{Aeq,c,k} - 6 + 10 \cdot \log\left(\frac{4 \cdot \pi \cdot R_1^2}{S_0}\right)$$

S_0 is 1 m2. For such a tall turbine as in this case, the atmospheric sound absorption has an influence. In this case with a temperature 2,4 °C and a relative humidity RH slightly below 100%, the effect of the atmospheric absorption is around 1 dB that should be added to the evaluated sound power level. A lower relative humidity may lead to higher attenuation than 1 dB.

Sound immission measurement

Figure 6 The microphone on a stand at the immission measurement point IM2 at 520 m distance downstream from the turbine

During the emission and immission measurements, the wind speed inside the forest at a height of 7 m was very low. It was less than 0,5 m/s.

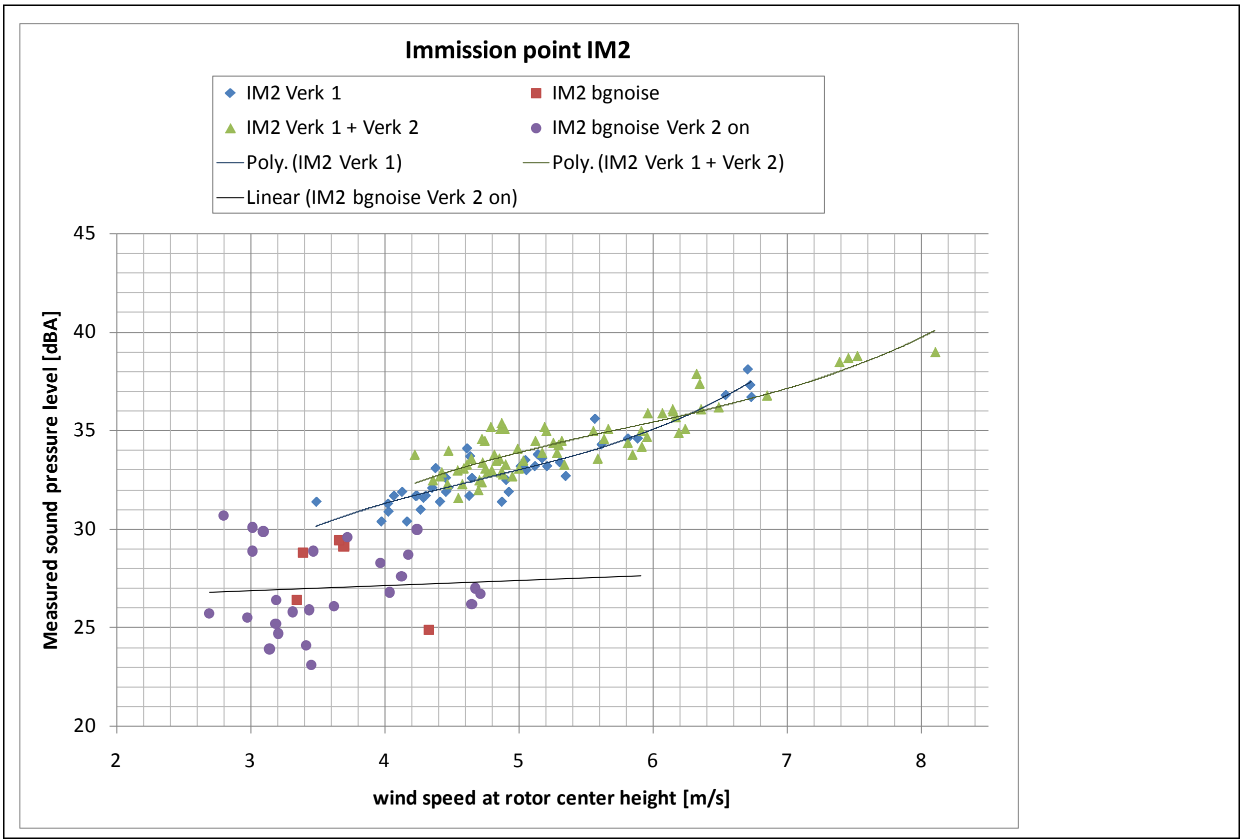

Figure 7 Measured sound pressure levels in one minute intervals in the immission point IM2 520 m downstream of the turbine related to the actual wind speed at hub height. The wind speed was evaluated using the produced electric power in the corresponding one minute interval

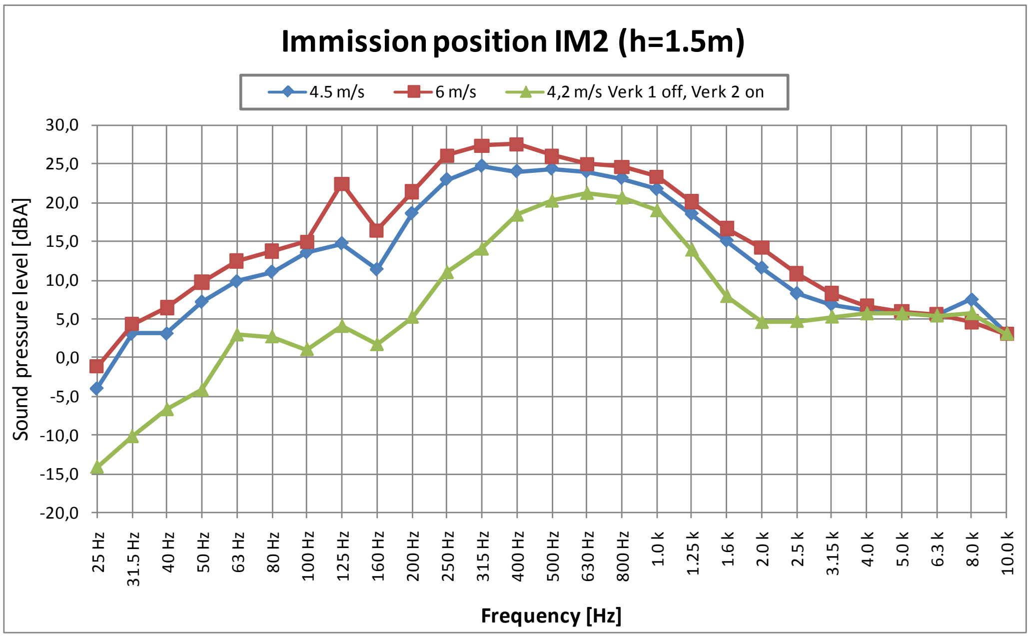

Figure 8 The third-octave band frequency spectrum in the measurement point IM2 averaged between ten one minute intervals for wind speeds around 4,5 and 6 m/s at hub height. The background noise levels including the second wind turbine are evaluated around 4,2 m/s.

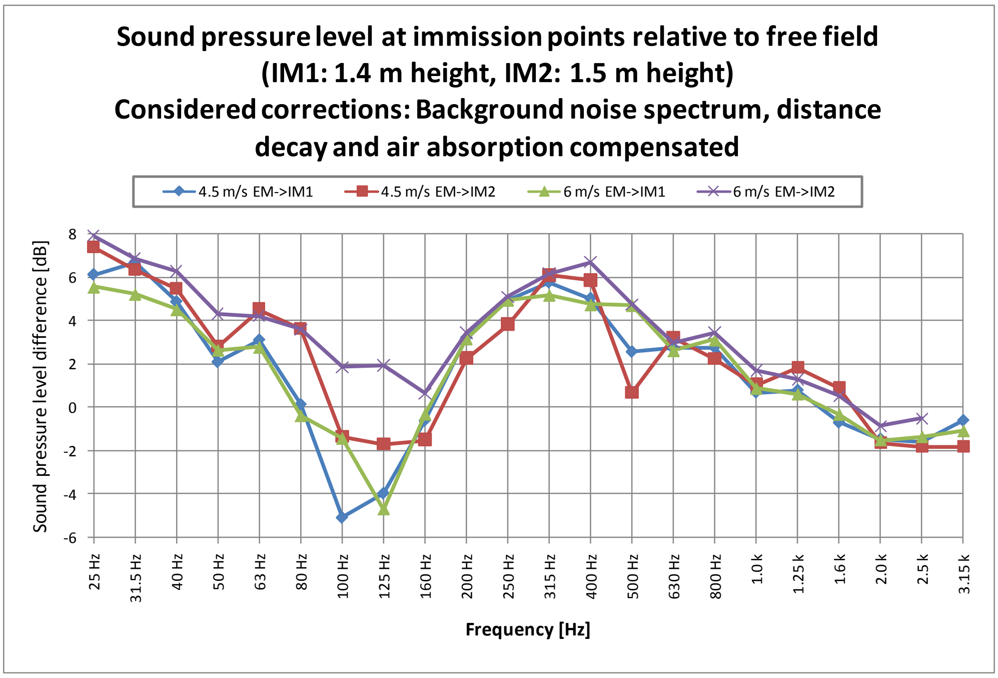

Figure 9 The sound pressure level in the immission points at 330 and 520 m distance relative to spherical sound propagation in free field. The calculated atmospheric sound absorption has also been subtracted

The ground effect is clearly identified in Figure 9. At low frequencies, the ground leads to amplification with around 6 dB. A dip in the curve due to the ground interference effect appears in the frequency range 80 to 200 Hz in this case.

Sound immission prediction and sound propagation in the forest

The sound pressure levels in the four immission points were calculated using Nord2000. Three points are placed downstream the turbine at 150, 330 and 520 m and one point was placed upstream at 125 m, see the following figure.

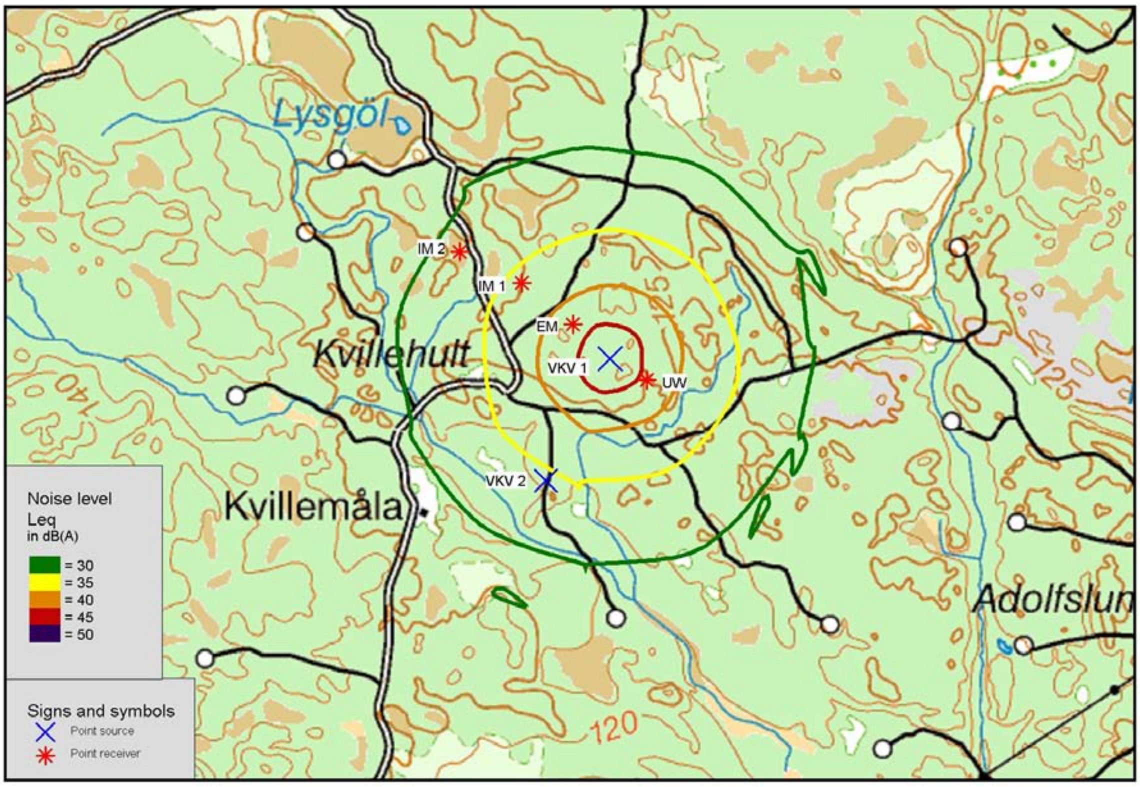

Figure 10 Sound pressure level contours calculated with Nord2000.

In the table below the measured and the calculated sound pressure levels are compared.

Table 3 Measured and calculated sound pressure level at 6 m/s wind speed at hub height. The predictions have been made with Nord2000 in the commercial software SoundPlan. The sound power level determined according to IEC 61400-11 has been used for hub height wind and has been corrected for atmospheric sound absorption to be 97,8 dBA re 1 pW.

Measurement point	Measured dBA re 20 μPa	Calculated at 1,5 m above porous ground dBA re 20 μPa	Calculated at 1,5 m above hard ground dBA re 20 μPa
EM, 150 m, measured on a hard board on the ground	46,5	-	-
EM, 150 m. The measure level transformed to 1,5 m above porous ground	42,2	42,7	43,5
IM1, 330 m 1,4 m above the ground	37,3	35,9	36,9
IM2, 520 m 1,5 m above the ground	34,3	31,8	32,9
IM3/UW, -125 m 1,3 m above the ground	45,8	43,7	44,4

The measured sound pressure level at point EM has been transformed to 1,5 m height above porous ground with a calculation in Nord2000 in the software ExSOUND2000 developed by Delta in Denmark. The spectrum in third octave bands has been adjusted for ground attenuation.

The sound pressure level calculated with Nord2000 is in average lower than the measured sound pressure level. The difference is the largest at the two largest distances. The difference is 2,1 to 2,5 dB under the assumption of soft ground and 1,4 dB under the assumption of hard ground.

The reason for the level difference has to be examined further. Two likely explanations are that reverberation inside the forest raises the sound pressure level as in a room and that the temperature may have been increasing with height inside the forest. The reverberation is caused by scattering of the sound waves between the tree stems.

The Nord2000 in SoundPlans version does not include the attenuation due to scattering from trees. If the ISO-model for scattering is used, the calculated sound pressure level still lower see variant 4 in the table below.

Table 4 Calculated sound pressure level in the four immission points. Variant 1 is calculated with the sound power level warranted by the supplier. Variant 2 is calculated with 97,8 dBA sound power and soft ground. Variant 3 is calculated assuming a distributed sound source and variant 4 is the same as variant 3 but with sound attenuation due to ISOs scattering model in the forest.

Description	Variant 1	Variant 2	Variant 3	Variant 4
IM 1	37,8	36,0	35,9	32,1
IM 2	33,6	31,7	31,8	28,1
EM	44,4	42,6	42,7	39,2
UW	45,3	43,8	43,7	41,1

In variant 3, the sound power was equally distributed between ten point sources place along the circumference of the rotor with a diameter of 90 m. The difference compared to a single apparent point source placed in the hub is negligible. The levels are within ±0,1 dB.

Conclusions

The apparent sound power level that has been determined according to IEC 61400-11, for the wind turbine at Ryningsnäs is one or a few dB lower then what has been warranted by the supplier for a corresponding turbine placed on flat farmland. The hypothesis that the sound emission should be larger for the turbine placed in the forest terrain due to increased turbulence and wind shear could thus not be strengthened.

The method to state the apparent sound power level at the wind speed recalculated to 10 m height instead of at hub height increases the risk of errors.

IEC 61400-11 should be revised so that the sound power is stated at the actual wind speed at hub height and electric power production in order to avoid misunderstanding. It should further be revised to take the atmospheric sound absorption into account. For a 100 m tall wind turbine, the effect may lead to that more than 1 dB shall be added to the A-weighted apparent sound power level. The effect on the evaluated frequency spectrum is larger.

It seems that reverberation inside the forest results in an increased sound pressure level compared to an open field. To start with, it was assumed that the scattering of sound waves from the tree stems would lead to a reduced sound pressure level. The effect of reverberation may be larger than the attenuating effect of the trees.

The method to assume that the sound power from the entire wind turbine appears to radiate from the hub functions well in this case. The assumption of ten point sources placed on the circumference of the 90 m diameter rotor gives a calculated sound pressure level that deviates only insignificantly, less than 0,1 dB.

References

Naturvårdsverket (2001) Ljud från vindkraftverk (In Swedish; Sound from wind turbines), report 6241

Almgren M (2009) Ljudemission och ljudutbredning för vindkraftverk i skogsterräng (in Swedish), Elforsk rapport 09:22

IEC 61400-11 (2006) Wind turbine generator systems – Part 11: Acoustic noise measurement techniques. Edition 2.1

Nordex (2009) Noise emission Nordex N90/2500 LS, Warranty levels according to IEC 61400-11:2002. Hub height 90 m – 105 m. From http://www.nordex-online.com/

Windtest (2005) Windtest Kaiser-Wilhelm-Koog GmbH. Auszug WT 4226/05 aus dem Prüfbericht WT 4212/05 zur Schallemisson der Windenergieanlage vom Typ Nordex N90/2500 LS, Messdatum 2005-04-18/19. From http://www.nordex-online.com/

IEC TS 61400-14 (2005) Wind turbines – Part 14: Declaration of apparent sound power level and tonality values

Nord2000 (2002) Nordic environmental noise prediciton methods, Nord2000. Summary report. General Nordic sound propagation model and applications in source-related prediction methods. Report AV 1719/01 Delta, Lyngby, Denmark

Third International Meeting
on
Wind Turbine Noise
Aalborg Denmark 17 – 19 June 2009

Long distance sound propagation over a sea surface

B.L. Andersson[1], K. Bolin[2], A. Cederholm[1] & I. Karasalo[1,2]
Addresses:
[1)]FOI - Swedish Defence Research Agency, Stockholm, Sweden
[2)]KTH - Royal Institute of Technology, Stockholm, Sweden
e-mails:

brodd.leif.andersson@foi.se, kbolin@kth.se, alex.cederholm@foi.se, ilkka.karasalo@foi.se

Abstract

Results from measurements of sound propagation over a sea surface to a 10 km distant receiver are compared to modelling with the Green's Function Parabolic Equation (GFPE) method by Gilbert and Di. The purpose is to assess the accuracy of prediction of atmospheric sound propagation by methods that use detailed knowledge of the local geographical and meteorological conditions.

Experimental data were collected during a one-week period in June 2005, and consist of data on the transmission loss (TL) of narrow band signals with frequencies 80, 200 and 400 Hz. Meteorological data were provided from radio sounding and balloon tracking up to 2-4 km in height at the receiver location and from meteorological sensors mounted on a 90 m high mast at the emission point. An atmospheric model including a laminar and a superimposed turbulent wind field was fitted to the meteorological data.

Comparisons between the experimentally observed TL and predictions by the GFPE-model are presented. A satisfactory agreement is observed of the model-predicted transmission loss as a function of time to the experimental data.

Introduction

In the light of global warming the transition to renewable power sources is a crucial challenge to today's society. A power source that will probably play a major role in the future is wind turbine power. Until now most of the wind turbines are land based, however large off-shore farms are under construction or planned all over the world. These will exploit the vast wind resources available in at sea and by 2020 50 GW of installed capacity is planned in Europe [1]. Off-shore wind turbines are often located near a coast due to cost increases with increasing water depth. Such installations have given rise to concerns for noise pollution on shore, often in recreational regions unaffected by community noise. Since atmospheric sound propagation is highly dependent upon the changing meteorological conditions, the level of such noise varies strongly with time.

Measurements of long distance sound propagation over water surfaces concurrently with meteorological observations have been performed by Konishi and Tanioku [3,4]. However, the meteorological data were registered up to a few hundred meters height only, while knowledge of the meteorological conditions (wind velocity, humidity and temperature) further up in the atmosphere is in general needed for accurate predictions of the soundfield.

The aim of this paper is to present measurements of sound propagation at 10 km distance [5] and evaluate the reliability of a sound propagation model with detailed knowledge of the meteorological and geographical conditions at the measurement times. This has been conducted by comparing transmission loss (TL) of the predictions to the measurements.

Measurements

The measurements were performed between the 15th and the 21st of June 2005 in the Kalmar strait and the island Öland in the Baltic Sea. A motivation for this choice of experimental period was that most annoyance from wind turbine noise could be expected in the summer due to increased recreational outdoor activity.

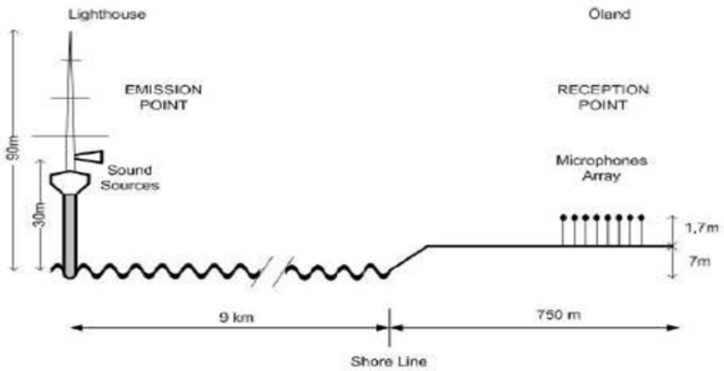

FIG. 1: Measurement setup.

Acoustical measurements

Source site

Two sound sources were placed on Utgrunden lighthouse located 9 km from shore. The sources were mounted at height 30 m on the lighthouse roof, with reference microphones placed 1 m front of respective source for recording the emitted signals.

The first source was a compressed-air-driven siren (Kockum Sonics Supertyfon AT150/200 with Valve Unit TV 784). It produced a 10-second signal with an average level of 130 dB and average frequency 200 Hz. Both this fundamental frequency and the first harmonic at 400 Hz were used in the analysis. The signal presented variations of the order of 1% in frequency and about 20 dB in sound level within each sound pulse, caused by the decreasing pressure of the compressed air driving the siren.

The second source consisted of a sound generator coupled to a loudspeaker and a 1.2 m-long resonator tube. It produced a 1 minute long 80 Hz tone with constant sound pressure level of 113 dB at 1 m distance. Both sound sources were employed simultaneously.

Receiver site

The receiver site was on the island Öland 750 m from shore with ground height 7 m above sea level (see Fig. 1 for the experimental setup). The site was adjacent to the houses closest to the shoreline, in a quiet residential area.

The receiver was a horizontal linear array of eight ½-inch microphones oriented parallel to the direction to the source. The array was placed at 1.7 m height accordingly to ISO 1996. The distance between the microphones was set to 40 cm, equal to half the wavelength at 400 Hz, to ensure a beam pattern free from grating lobes at all three frequencies. The signals were transmitted through a preamplifier to an UA100 analyzer and then processed in Matlab as explained in Ref. [5].

Meteorological measurements

Source site

The wind speed was measured at 38, 50, 65, 80 and 90 m above sea level on a meteorological mast at the emission point. The wind direction was determined with wind vanes at 38 m and 80 m heights. The temperatures were measured at five heights: 6, 38, 50, 65 and 80 m. The relative humidity was measured at 38 m height. Data from these sensors were registered at 10 minutes intervals, and the average and standard deviations were recorded.

Receiver site

During the measurements performed in June 2005, wind profiles at the receiver site were measured during the day using radio probes and theodolite tracking of free flying balloons [6]. These measurements were performed by staff from the Department of Earth Sciences, Uppsala University. Wind velocity (horizontal components), humidity and temperature were measured up to 3500 m height.

GFPE Model

The GFPE method was developed by Gilbert an Di [7,8] and later slightly improved by Salomons [9]. The method is particularly designed for atmospheric sound propagation and can use considerably longer range-steps than conventional PE methods. Because of its computational efficiency, the GFPE model was used in this study.

Model description

The method computes a 2D field in the *rz*-plane where r is the radial distance from the source and *z* is the vertical axis. From the 3D Helmholtz equation for the sound pressure, *p*, in cylindrical coordinates combined with a variable substitution $\varphi = exp(-i\, k_0\, r)\, pr^{0.5}$ two expressions (1) and (2) can be derived [7,9]

$$\phi(r+\Delta r, z) = \exp(i\frac{\Delta r \delta k^2(z)}{2k_r}) \times$$
$$\times \left[\begin{array}{l} \frac{1}{2\pi}\int_{-\infty}^{\infty}(\Phi(r,k') + R(k')\Phi(r,-k')) \times \exp(i\Delta r(\sqrt{k_r^2 - k'^2} - k_r))e^{ik'z}dk' + \\ + 2i\beta\Phi(r,\beta) \times \exp(i\Delta r(\sqrt{k_r^2 - \beta^2} - k_r))e^{-i\beta z} \end{array} \right] \quad (1)$$

where *Δr* is the horizontal step size, $k(z)=\omega/c(z)$ is the wave number, k_r is a reference wave number ($k_r=k_0=k(0)$ in this paper [9]), $R(k')=(k'\, Z_g-k_r)/(k'\, Z_g+k_r)$ is the plane-wave reflection coefficient, Z_g is the normalized ground impedance, $\beta=k_r/Z_g$ is the surface-wave pole in the reflection coefficient and Φ is given in Eq.(2)

$$\Phi(r,k) = \int_0^{\infty} \exp(-ikz')\phi(r,z')dz' \quad (2)$$

which combined constitute the fundamental step in the GFPE-algorithm.

Parameter selection

The parameters were selected by suggestions from Ref. [7,9,10]. The horizontal step was set to 10λ and the vertical step size was 0.1λ in accordance to recommendations in Ref. [9]. An absorption layer that suppress spurious reflections from the upper limit of the numerical integration has an absorption parameter, A, calculated according to Ref. [9] with a depth of 75λ. The attenuation coefficients were calculated according to ISO/DIS 9613-1 [11]. To calculate the surface impedance the model by Embleton et. al. [12] was used. The ground impedance is determined by the sound frequency and a flow resistivity parameter, which was selected to a value representative of grass in a rough pasture [12]. The water surface was treated as perfectly reflecting.

Turbulence

Effects of wind and temperature fields were included in the GFPE model following the approach in Appendix I and J of Ref. [10]. Thus, the turbulent components of these fields are modelled as homogeneous random fields with von Karman type horizontal wavenumber spectra. The effect of such turbulence on the GFPE solution is represented by including a random z-dependent phase factor in the GFPE propagator, without requiring explicit computation of realizations of the fields. According to this turbulence model the transmission loss to the receiver is a stochastic variable, and statistics of the transmission loss were determined by carrying out 50 Monte Carlo runs for each frequency at every hour of the experimental week.

Meteorological assumptions

Meteorological inputs to the GFPE model were balloon measurements (horizontal wind velocity), radio balloon (relative humidity and temperature) and the anemometers on the mast (standard deviation of wind speed and temperature). The wind and radio balloon data were used as meteorological parameters (***U**(z), rh, T*) of the laminar atmosphere. Linear interpolation was used between measurement points in the vertical direction as well as in time. The mast data (horizontal wind speed and the variances of wind velocity and temperature) were used to estimate the turbulence intensities.

Results

As previously stated our objective is to investigate the accuracy of the model predictions compared to measurements, in particular to investigate the effect of turbulence on the model-predicted transmission loss.

Turbulence excluded

The black curves in Fig. 2 show the simulated TL, the average of the simulated TL during measurement periods are shown as horizontal yellow lines. Red dots show measured TL values, with their daily averages shown by horizontal green lines.

It can be clearly seen that the predictions show larger variations of TL with time than the experimental data. Periods with low TL show good agreement between the measured and the modelled TL, whereas the modelled TL is severely overestimated in periods periods where TL is high. High TL values occur when the sound speed decreases as function of height, causing the emitted sound to be refracted upwards and shadow zones to occur at the receiver. An example is shown in Fig. 3. Low TL values occur when the sound speed has a local maximum at relatively low height (e.g. induced by a low level jet [6]), causing the sound to be refracted downwards and trapped within a channel below the local wind maximum. Such meteorological conditions occurred e.g. around noon of June 17 as can be seen in Fig. 4.

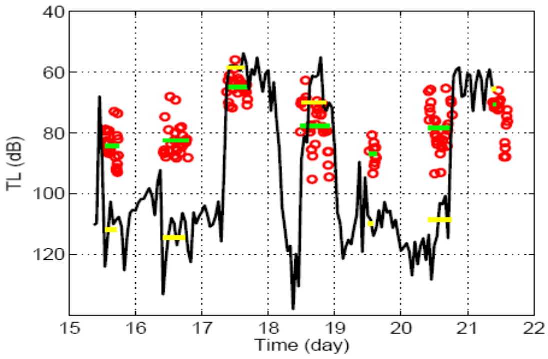

a) TL at 80 Hz as function of time. Black curve: Predicted with a laminar atmosphere model. Red dots: Measured data.

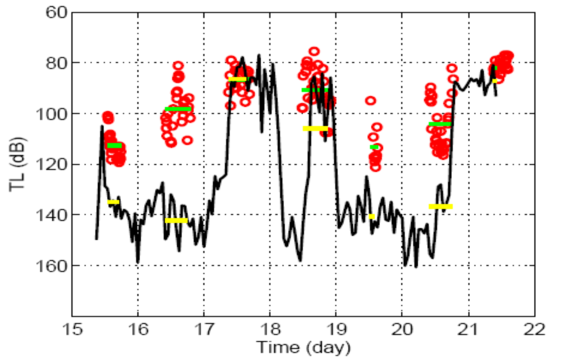

b) TL at 200 Hz as a function of time Black curve: Predicted with a laminar atmosphere model Red dots: Measured data.

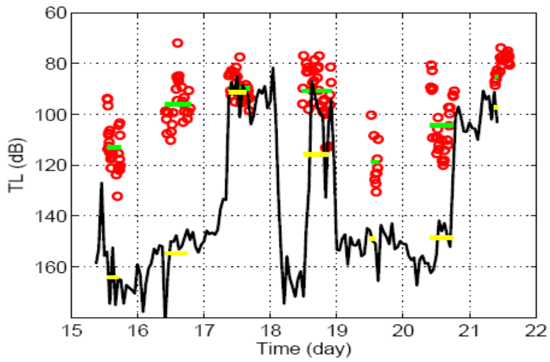

.

c) Transmission loss at 400 Hz as a function of time.
Black curve: Predicted with laminar atmosphere in the model.
Red dots: measured data.

FIG 2: TL as function of time. (o): Measured (-): Predicted with a laminar atmosphere in the model. Daily averages for measured and predicted TL are shown as green respectively yellow lines.

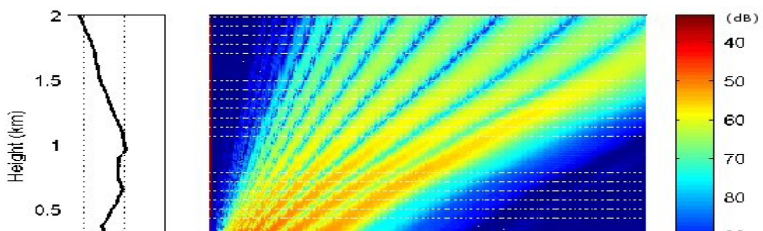

FIG 3: Sound speed profile (left figure) and simulated 80 Hz sound field (right) at noon on June 16. The sound speed decreases with height and the receiver is in sound shadow. Atmosphere modelled as laminar.

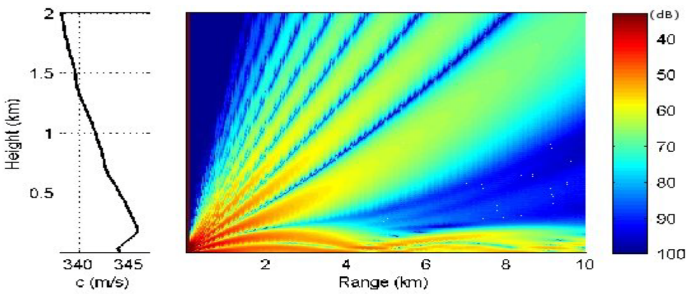

FIG 4: Sound speed profile (left figure) and simulated 80 Hz sound field (right) at noon on June 17. The sound speed has a maximum at height 200 m and a sound channel below this height can be observed. Atmosphere modelled as laminar.

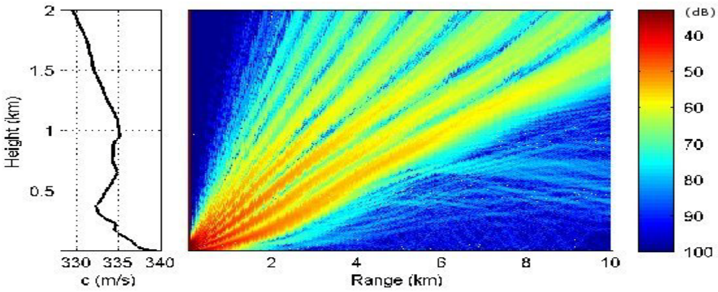

FIG. 5: Simulated soundfield in the 80 Hz case of Fig 3, with effects of a turbulent atmosphere included.

Turbulence included

As discussed in Chapter 5 of Ref [10], the effect of turbulence is a random scattering of sound, leading to increased sound levels in refractive shadow zones. This effect is illustrated in Fig. 5, showing the model-predicted 80 Hz soundfield of Fig 3, but with the atmosphere modelled as turbulent. Clearly, the shadow zone of the laminar case (Fig 3) becomes less pronounced when turbulence effects are included (Fig 5).

In Fig. 6 the simulations of Fig 2 are repeated, now including effects of turbulence. The thick black curve shows the average value of the TL from the Monte Carlo simulation and the thinner black curves surrounding the average show the interval of the standard deviations. Comparing Fig. 2 and Fig. 6 it can be seen that the most prominent change in the predictions caused by turbulence is a significant decrease of the high TL values, leading to a significantly improved agreement between the predicted and measured TL levels.

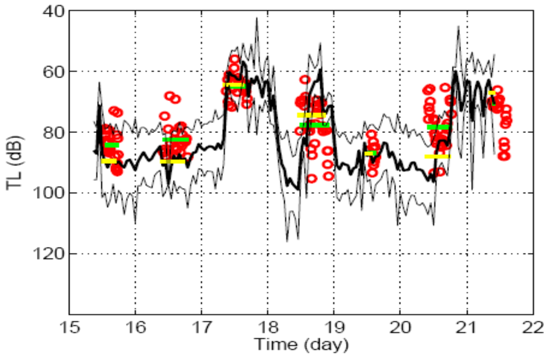

a) TL at 80 Hz as function of time. Black curve: Predicted with a turbulent atmosphere model. Red dots: Measured data.

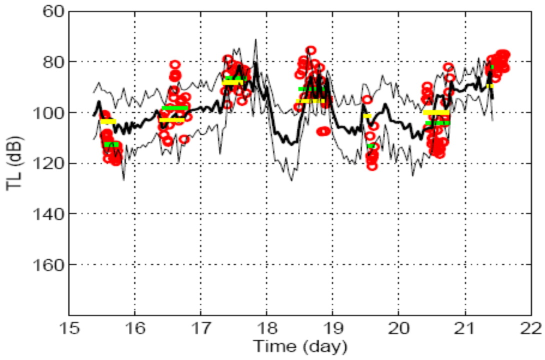

b) TL at 200 Hz as a function of time Black curve: Predicted with a turbulent atmosphere model Red dots: Measured data.

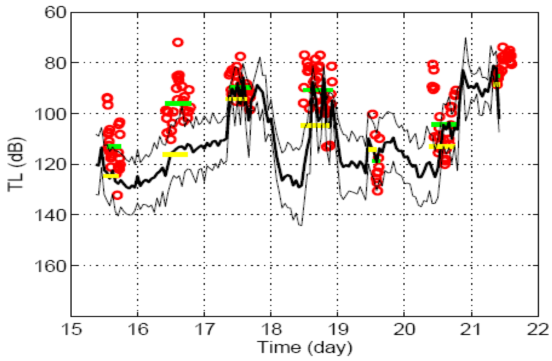

c) Transmission loss at 400 Hz as a function of time.
Black curve: Predicted with turbulent atmosphere in the model.
Red dots: measured data.

FIG. 6. TL as function of time. (o): Measured. (**-**): Predicted with a turbulent atmosphere in the model. Daily averages for measured and predicted TL are shown as green respectively yellow lines.

Conclusions

The results indicate that sound propagation modeling including effects of detailed meteorological data can be used for reliable prediction of transmission loss. In particular, the predicted TL remains reasonably accurate under varying meteorological conditions, and follows the variations observed in the TL measurements in a realistic way. The results further indicate that the sound propagation model must include effects of turbulence in the atmosphere for accurate predictions of the TL into shadow zones.

Acknowledgements

The authors wish to thank Prof. Sten Ljunggren, Prof. Hans Bergström, and Civ.Ing. Hans Olsson for helpful comments and discussions. Vindforsk II is acknowledged for their financial support.

References

[1] E. W. E. Association, “Ewea’s response to the European commission’s green paper”, Technical Report, (COM (2006) 275 Final) (2007).

[2] L. Johansson, “Sound propagation around off-shore wind turbines -long-range parabolic equation calculations for Baltic sea conditions”, Technical Report, Licentiate thesis, KTH/ Building sciences (2003).

[3] Z. M. K. Konishi, Y. Tanioku, “Long time measurementof a long range sound propagation over an ocean surface”, Applied Acoustics 61 (2000).

[4] Z. M. K. Konishi, “Interpretation of long term data measured continuously on long range propagation over sea surfaces”, Applied Acoustics 62 (2001).

[5] M. Boué, “Long-range outdoor sound propagation over sea, applications to wind turbine noise”, Technical Report TRITA-AVE 2007:22, KTH (2007).

[6] K. T¨ornblom, “Thermally driven wind modification in coastal areas and its influence on sound propagation with application to wind power”, Technical Report, Department of Earth Sciences, Uppsala University (2006).

[7] K. E. Gilbert and X. Di, “A fast green’s function method for one-way sound propagation in the atmosphere”, Journal of the Acoustical Society of America 94, 2343–2352 (1993).

[8] X. Di and K. E. Gilbert, in Proceedings of the Fifth International Symposium on Long Range Sound Propagation, 128–146 (Milton Keynes, England) (24-26 May 1992).

[9] E. M. Salomons, “Improved greens function parabolic equation method for atmospheric sound propagation”, Journal of the Acoustical Society of America 104, 100–111 (1998).

[10] E. M. Salomons, Computational Atmospheric Acoustics (Kluwer Academic Publishers) (2002).

[11] International Organization for Standardization, Geneva, Switzerland, ISO/DIS 9613-1: Attenuation of sound during propagation outdoors- Part 1: Atmospheric absorption (1995).

[12] T. F. W. Embleton, J.E. Piercy and G. A. Daigle. Effective flow resistivity of ground surfaces determined by acoustical measurements, *Journal of the Acoustical Society of America,* **1983***, 74*, 1239-1244

Third International Meeting
on
Wind Turbine Noise
Aalborg Denmark 17 – 19 June 2009

Design of low noise airfoil with high aerodynamic performance

Christian Bak,
Franck Bertagnolio,
Helge Aa. Madsen

Risø DTU National Laboratory for Sustainable Energy, Wind Energy Division, P.O.Box 49, DK-4000 Roskilde, Denmark
chba@risoe.dtu.dk, frba@risoe.dtu.dk, hama@risoe.dtu.dk

Abstract

This paper presents the design of a high performance airfoil for incompressible flow and for Reynolds numbers at $6x10^6$ with a lift performance, which is resistant to surface contamination and turbulence intensity. The new airfoil is dedicated for MW-size wind turbines, which are exposed to varying inflow conditions and surface contamination from bugs and dust. The objectives in the design process were to have high maximum lift coefficient, while maintaining high aerodynamic efficiency and reduced noise emission. The results from the design process showed that the design tool was capable of designing airfoils with reduced noise using Risø-C2-18 as a basis. Thus, airfoils showing 1.5dB to 3dB reduction of maximum SPL were designed, with increasing relaxation of the constraints on the geometry around the trailing edge. However, evaluating the designs using A-weightening on maximum SPL showed another picture. It appears that the Risø-C2-18 has around 1dB higher SPL(A) as the Risø-B1-18 and that the new design obtained a similar maximum SPL(A) as the Risø-B1-18. Thus, the conclusions when analyzing the maximum SPL with A-weight is that it is possible to reduce the A-weighted noise compared to the initial airfoil and that the new airfoil showed a thinner trailing edge, the same low noise emission as the Risø-B1-18, and higher aerodynamic performance.

Introduction

Design of tailored airfoils for wind turbine rotors is essential for the continuing development of wind turbines. It has been known for decades that wind turbine airfoils should differ from traditional aviation airfoils in choice of design point, off-design characteristics and structural properties. The development of wind turbine airfoils has been ongoing since the mid 1980's. Significant efforts have been made by Tangler and Somers[1], Timmer and Van Rooij[2], Björk[3], and Fuglsang and Bak[4]. For wind turbine airfoils operating in the atmospheric boundary layer there is influence from the turbulence intensity and contamination of bugs and dust and the airfoils should under these conditions show both high performance in terms of high lift-drag ratio, constant maximum lift and low noise.

A new airfoil was designed for MW-size wind turbines. The blade lengths for such rotors are at the moment, year 2009, between 35m and 63m corresponding to 1MW and 5MW, respectively. Modern blades are commonly designed with thicknesses between 15% and 100% with thin airfoils (*t/c*<24%) on as much of the blade as possible. The airfoil was designed for rotors controlled with variable rotor speed and pitch control to maintain the optimum ratio between tip speed and wind speed (tip-speed-ratio). Many characteristics from the Risø-C2-18 airfoil[5] were inherited because this airfoil has shown to be both efficient and to have a high degree of insensitivity to leading edge roughness. However, there is a need for reducing the noise emission for airfoils to be mounted on the outer part of rotor blades. Finally, the new airfoil was as well designed to be aerodynamically very efficient both with and without a contaminated surface.

The design was carried out with a Risø DTU in-house multi disciplinary optimization tool, AIRFOILOPT, that has been developed since 1996[6]. The numerical optimization algorithm works directly on the airfoil shape providing a direct and interdisciplinary design procedure, where multiple design objectives for aerodynamics and structure may be handled simultaneously. This paper describes the extension of the airfoil design tool and the development of a new noise reduced airfoil.

III. Method for airfoil design

The airfoil design tool can be divided into a 2D design tool and a 3D design tool. The 2D design tool has been used to design the former Risø airfoil families except of the Risø-C2 family[4,5]. It uses a direct method where numerical optimization is coupled with either the flow solver XFOIL[7], which is a panel code with inviscid/viscous interaction, or the flow solver EllipSys2D, which is a code based on the solution of the Navier Stokes equations in 2D[8,9,10]. The latter solver is not used in the present work. A number of design variables form the airfoil shape, which is optimized subject to design objectives and constraints. Direct methods, such as the method used, are basically interdisciplinary and multi-point and they allow direct use of integrated response parameters such as airfoil c_l, c_d and trailing edge noise directly as design objectives. Also, boundary layer response parameters, e.g., skin friction and transition point location can be constrained or used as objectives. Structural characteristics can be controlled by constraining the shape in terms of coordinates, gradients, curvatures or moment of resistance.

The 3D tool models a complete blade with all its airfoil sections to form the blade surface and compute the aerodynamic rotor performance. Gradients and curvatures in the direction from the root to the tip were included to quantify the compatibility. Also, the 3D tool opens up the possibility of maximizing the rotor power performance in terms of, e.g. the power coefficient C_P. With the 3D tool follows a graphical user interface so that information about the geometry can either be extracted for use in the optimization process or existing blades can be inspected visually and quantitatively.

A. Design algorithm

The design variables are changed in an optimization problem to minimize the objective function. This is done subject to constraints. In this case the design variables are the control points that describe the airfoil shape. The constraints are side values for the design variables and bounds on response parameters from flow and structural calculations. A traditional Simplex optimizer was used with a finite difference sensitivity analysis. This is a simple and robust solution method, which however, is computationally expensive because of the large number of necessary flow calculations. The optimization process is iterative involving numerous calculations of flow and structural response parameters where the design gradually changes to improve the objective. The calculated flow and structural response parameters are used to estimate the value of the objective function and the constraints. Multiple angles of attack are calculated to allow off-design optimizations. The combination of flow and structural responses allows multidisciplinary optimization (MDO).

B. Geometry description

A smooth shape is important for the optimization results. The 2D airfoil shape was represented by a single B-spline defined from the trailing edge around the airfoil contour by a set of control points. The blade shape, which however was not modeled in this work, is represented by cubic B-splines fixed at the top and bottom of the 2D sections and at the leading and trailing edge. In between these four fixed points at the sections the splines were distributed evenly along the surface length. The splines creating the 2D sections and the connection between the 2D sections form a mesh from where coordinates, gradients and curvatures can be extracted and used either for inspection or for use in the optimization process.

C. Flow analysis

The XFOIL code by Drela[7] was used for the flow calculations during the optimization. For a given *AOA* and *Re*, XFOIL provides the c_p-distribution and c_l, and c_d. In addition, numerous boundary layer parameters are calculated. Transition was modeled by the e^n method with n = 9. Prescribing transition to x/c = 0.001 after the leading edge on the suction side and at x/c = 0.10 after the leading edge on the pressure side simulated leading edge roughness. XFOIL is well suited for optimization because of the fast and robust viscid/in-viscid interaction scheme. However, the integral boundary layer formulation is not well suited for separated flows. XFOIL should therefore be used with caution at and above $c_{l,max}$. Others find that it may be necessary to modify or even tune XFOIL to better match measured results[2], but the computations seem to compare relatively well with EllipSys2D computations especially in the attached flow region.

D. Noise analysis

The noise emission is in earlier investigations, e.g. by Brooks, Pope and Marcolini[11], divided into five different sources: 1) Tip noise, 2) Blunt trailing edge noise, 3) Laminar vortex shedding noise, 4) Turbulent inflow noise and 5) Turbulent trailing edge noise. Experience shows that especially the last source is important because the trailing edge noise is broadband and a distributed source. This is the reason for focusing on this source and two models for predicting this source in detail are developed: The TNO model[12] and the Glegg *et al* model[13]. These two models are implemented into AIRFOILOPT[14]. A single or few entities for evaluating the noise emission is important to simplify the design process. The simplification of the noise emission could either be integration of the spectrum or simply the maximum noise. The simplification of the noise emission was investigated in this work.

IV. Strategy for airfoil design

The desirable airfoil characteristics form a complex matrix of properties of which some are in conflict with others. This has been a topic of discussion in the literature[15,16,17]. There seems to be consensus on most of the general desirable characteristics. However, the means of achieving them are strongly related to the design method and the philosophy of the designer. The new airfoil was designed for operation on a wind turbine rotor. The force that contributes to the rotor power is the tangential force, T, whereas the force that contributes to the rotor thrust, is the normal force, N. As it was the case with the Risø-B1 airfoil family T can be used as the objective function, but also the lift-drag ratio (c_l/c_d) can be used. The latter is a common measure of the airfoil efficiency because c_l can be considered as the production and c_d can be considered as the loss. The new airfoil was designed with maximum c_l/c_d ratio as was the case for the Risø-C2 series. Some of the characteristics that are taken into account in the design process will be described in the following.

A. Structure

A wind turbine blade may be divided into the root, mid and tip parts. The mid and tip parts are determined mainly from aerodynamic requirements whereas structural objectives are relevant mainly for the inboard part of the blade, e.g., for t/c > 24%. Another issue is the geometric compatibility between airfoils of the same family to ensure smooth transition from neighboring airfoil sections. However, in this work the structure was not part of the design process, but was used to evaluate the influence of the noise requirements on the structural stiffness.

B. Insensitivity of cl_{max} to leading edge roughness

Roughness on the airfoil leading edge region formed by accumulation of dust, dirt and bugs is well recognized as a main design driver for wind turbine airfoils[15]. The new airfoil was designed for minimum sensitivity of $c_{l,max}$ to leading edge roughness by two separate design objectives: (1) The suction side natural transition point was constrained to move to the very leading edge for AOA around 3° below $c_{l,max}$ predicted with forced transition. This determined the local shape of the leading edge region so that a small pressure rise at the leading edge caused natural transition to turbulent flow at the leading edge a few degrees before $c_{l,max}$. Premature transition caused by roughness will therefore be eliminated close to $c_{l,max}$ by a very forward position of the natural transition point. (2) The level of $c_{l,max}$ resulting from a flow analysis with simulation of leading edge roughness, i.e. forced transition from the very leading edge, was constrained to a sufficiently high value compared to results from analysis assuming free transition. This shapes the airfoil suction side so that the pressure recovery region does not separate prematurely because of an increase of the boundary layer thickness caused by roughness, which would reduce $c_{l,max}$. Even with this constraint massive roughness will inevitably reduce $c_{l,max}$. Also, the existence of even minor leading edge roughness will result in an unavoidable reduction in the c_l/c_d ratio.

C. Design $c_{l,max}$

The airfoil sections were designed for high $c_{l,max}$. This was chosen because the airfoil sections can be used for design of slender blades and in general ensuring minimum fatigue loads and extreme loads. Also, this choice was made to compare to the Risø-B1 and Risø-C2 airfoils. However, a disadvantage from this choice is the loss of stiffness for the blade if the relative airfoil thicknesses are maintained even though the chord distribution is reduced. Thus, the choice of high maximum lift is closely related to the choice of concept in the blade design. No matter which concept is used in the blade design, the inner part of the rotor needs airfoil sections with both high relative thickness and high maximum lift.

D. Design objective

A compound objective function was defined as a weighted sum of c_l/c_d ratio values resulting from multiple angles of attack in the design *AOA* range and trailing edge noise values at one angle of attack close to maximum c_l/c_d. Some were for a clean airfoil surface whereas others were for flow with simulated leading edge roughness to ensure good performance at both conditions. The airfoil design *AOA*-region is also determined from the requirements to the wind turbine off-design operation. Because of the stochastic nature of the wind, turbulence gusts and wind direction changes will always lead to some off-design operation due to non uniform inflow. However, the degree of off-design is mainly given by the power control principle. In most cases it is desirable that the design *AOA*-region is close to $c_{l,max}$ since this enables low rotor solidity and/or low rotor speed. For all the new airfoils the design point region was AOA_r = [5°;14°], where c_l/c_d are computed both assuming transition from laminar to turbulent forced at the leading edge (fully turbulent) and free transition. High aerodynamic performance is important because the power output from wind turbines is very dependent on this. For instance, an increase from c_l/c_d=140 to 150 for a rotor results in an increase of around 0.4% in power output. The chosen angles of attack for maximizing c_l/c_d will lead to an expected high $c_{l,max}$ at around AOA_r =16° corresponding to $c_{l,max}$ = 1.8 assuming a lift curve slope of 2π */rad*. The airfoil family was designed for $Re = 6x10^6$, because this corresponds to modern blade designs of the 3MW size. Furthermore, it will be investigated whether to include the noise prediction as constraints or in the objective function.

V. Airfoil designs with noise reduction

The results from the design process of the new airfoil with *t/c*=18% can be divided into three parts:

- The entity to measure noise: Should maximum values or integrated values of the spectra be used in the design process? Should A-weighted values be used? And should noise from fully turbulent airfoil flow or free transitional airfoil flow be used as the noise entity?
- Setup of the design problem: Because the aerodynamic characteristics of airfoils for wind turbine are very important, should the noise reduction be handled as constraints to the design problem or should it be a part of the objective function?
- The final airfoil design

In the design process the Risø-C2-18 airfoil was the starting point and most of the characteristics for this airfoil were inherited. However, because this type of airfoil typically is used on the outer part of a rotor, the bending stiffness is of secondary importance and therefore it was allowed in the design process to reduce this stiffness somewhat.

The entity to measure noise

Because noise is experienced at a wide range of frequencies and the human ear dampens some frequencies in this range, it is not straight forward to state an unambiguous measure for noise. Basically, there are four ways to evaluate the noise 1) Maximum sound power level (SPL) without A-weight, 2) Maximum SPL(A) with A-weight, 3) Integrated SPL spectrum without A-weight and 4) Integrated SPL spectrum with A-weight. Because aerodynamic noise from wind turbines are integrated from all airfoil sections along the rotor blades, the main contribution to the total wind turbine SPL at the different frequencies stems from airfoil sections at different radii. This can be seen in Figure 1, where SPL spectra are seen for the Nordtank 500/41 (500kW turbine with 41m diameter rotor) using an implementation of the semi-empirical noise model described by Fuglsang and Madsen[18] and based on Brooks, Pope and Marcolini[11] and Lowson and Fiddes[19], which in short is called the BPM model. The spectra show the SPL for the entire rotor (red curve) and for annular elements as stated in the plot. Maximum SPL appears at 630Hz at the outer part of the rotor continuously decreasing to 200Hz at the mid part of the blade span. For the entire rotor maximum SPL appears at 315Hz. Thus, SPL is greater at some frequencies in the spectra even though the maximum value is decreasing with decreasing radius of the rotor. Also, the plot shows that the noise from the outer part of the rotor contributes more than from the mid or inner part of the rotor. This plot also makes it clear that when reducing the aerodynamic noise, focus should mainly be put on the airfoils on the outer part of the rotor.

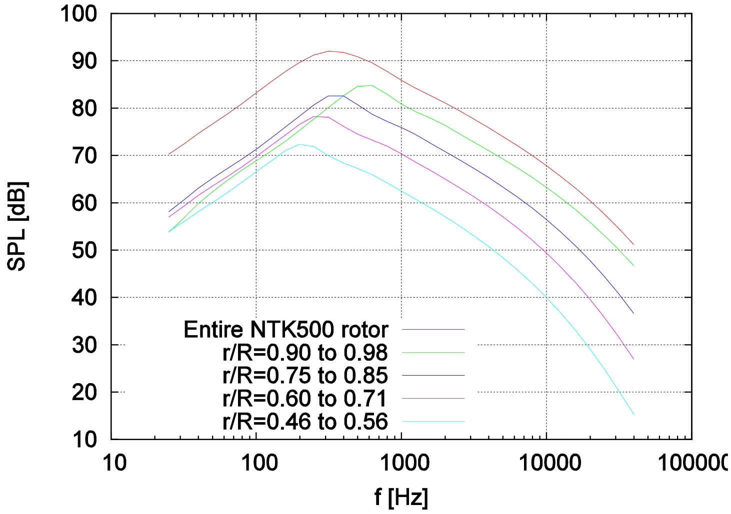

Figure 1 SPL spectrum for the NTK 500/41 for the entire rotor and for sections of the rotor at different radii using the BPM model.

Figure 2 shows the computed maximum and integrated SPL and SPL(A) for the Risø-C2-18 airfoil assuming both free transition and fully turbulent flow in the XFOIL computations. An increase in both maximum and integrated SPL as a function of

AOA is seen in contrast to maximum SPL(A) that shows only a very weak increase with AOA. Also, integrated SPL(A) shows no unambiguous increase with AOA. Even though maximum and integrated SPL for fully turbulent flow is significantly higher compared to flow with free transition, this is not the case for the A-weighted values. Therefore, designing airfoils using maximum or integrated SPL(A) will potentially cause some difficulties. From this investigation either maximum or integrated SPL can be used as a measure for the noise. In this work it was decided to measure the noise using maximum SPL. Finally, as stated before it is seen from Figure 2 that maximum SPL from fully turbulent flow is higher than for flow assuming free transition. That is the reason for choosing maximum SPL (or alternatively SPL(A)) for fully turbulent flow as the entity to reduce.

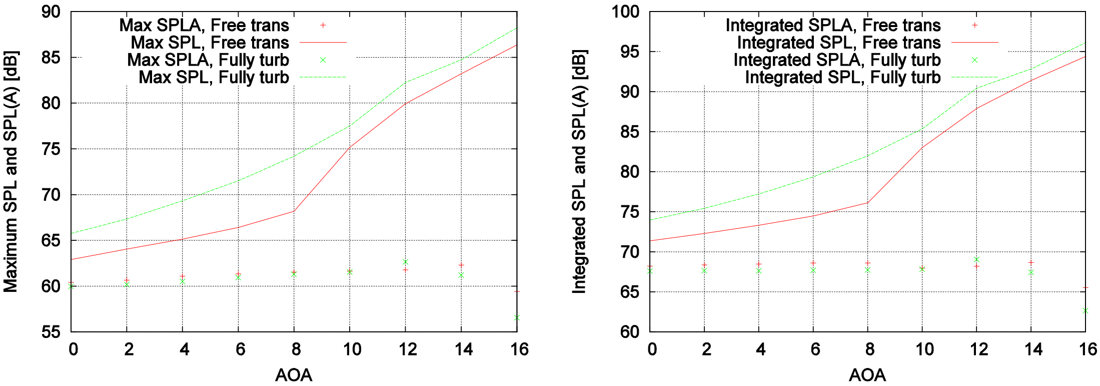

Figure 2 Left: Maximum SPL and SPL(A) as function of angle of attack, Right: Integrated SPL and SPL(A) as a function of angle of attack.

Setup of design problem

There are two ways of including the noise modeling in the design process. Either it is included as constraints or in the objective function. This is investigated in the following. One design, where the noise was put as a constraint, was carried out so that the noise emission was reduced as much as possible without reducing or changing the aerodynamic performance. Another design, where the noise was a part of the objective function, was carried out. However, the question to be answered for this type of setup was how the weight between aerodynamic and noise characteristics should be. In Figure 3 is shown the changes in the surface contour, when including noise in the objective function, compared to the surface contour, when including the noise in constraints. The pressure/lower side of the airfoil is plotted as negative values of x/c and the suction/upper side is plotted as positive values. It is seen that a weight of 10 for the noise in the objective function ensures the contour that best matches the contour designed using noise as constraints because the maximum changes in the contour is below 0.002. The noise for the four airfoils were maximum SPL=74.5dB for the airfoil designed with constraints and maximum SPL=75.4dB, 74.6dB and 74.5dB for the three airfoils designed using noise in the objective function with weight 1, 10 and 100, respectively, compared to the aerodynamic performance. Figure 4 shows the corresponding airfoil characteristics evaluated using XFOIL, which reflects that no significant changes in the airfoil performance were introduced when the trailing edge noise was reduced except for the case with a weight of the noise in the objective function of 100. From the Figures it is indicated that using an objective function with the weight of the noise 10 times higher than the c_l/c_d ratio resulted in a fairly good weight between noise and aerodynamics, because the noise was reduced sufficiently without sacrificing the aerodynamic performance and the surface contour agreed well with an airfoil designed with noise as constraints. The weight relation between noise and aerodynamic performance of 10 to 1 was kept in the objective function in the rest of the investigation.

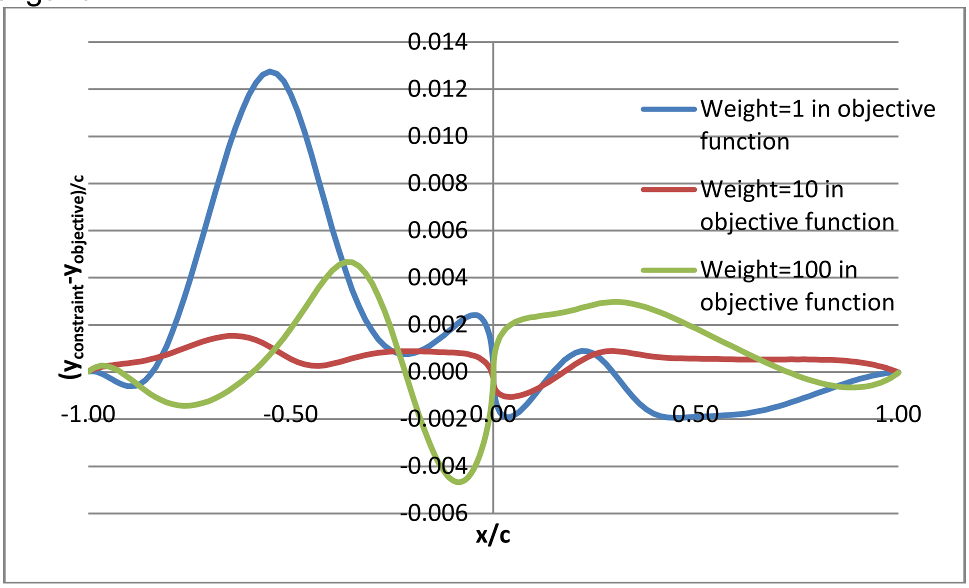

Figure 3 Difference in surface contour for the airfoils designed with noise in the objective function compared to the airfoil designed with noise as constraints denoted by the y-coordinates $(y_{constraint}\text{-}y_{objective})/c$.

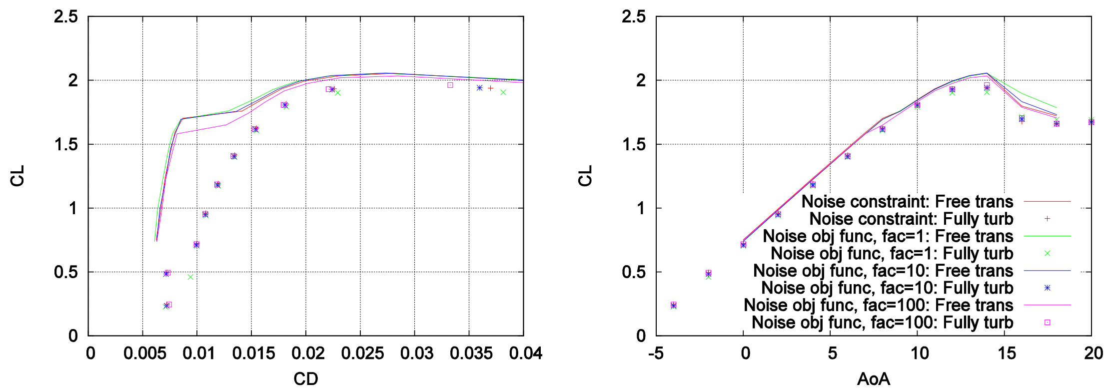

Figure 4 Airfoil characteristics of different designs to determine the weights in the compound objective function.

Final airfoil design

With the Risø-C2-18 airfoil as the starting point in the design process several airfoils were designed:

Airfoil name	Description
#1	Similar constraints as for Risø-C2-18
#2	Up to 20% reduction in airfoil thickness close to trailing edge
#3	Up to 40% reduction in airfoil thickness close to trailing edge
#4	Up to 60% reduction in airfoil thickness close to trailing edge
#5	Up to 80% reduction in airfoil thickness close to trailing edge

More airfoils were designed in the investigation, where constraints especially on the airfoil contour were relaxed. However, it turned out that the listed constraints where the most important concerning the reduction of trailing edge noise.

Figure 5 shows how the design maximum SPL at an angle of attack of 14° from zero-lift angle-of-attack reduces for decreasing trailing edge thickness. Thus, reducing the trailing edge thickness has a significant effect on maximum SPL. However, when reducing the trailing edge thickness, the total bending stiffness of the airfoil reduces as showed in Figure 6. However, loosing stiffness at the outer part of wind turbine blades is acceptable compared to, e.g. the inner part of blades.

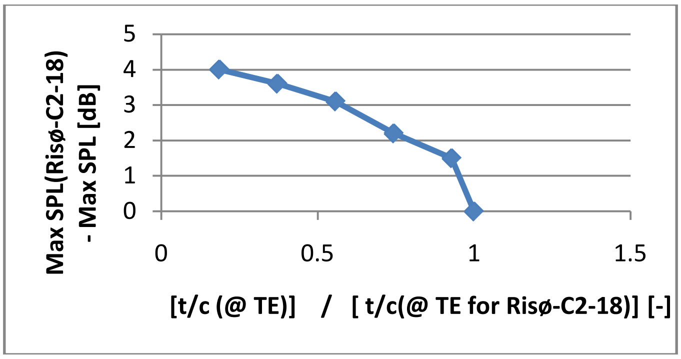

Figure 5 Reduction of maximum SPL as a function of the airfoil thickness ratio at the trailing edge

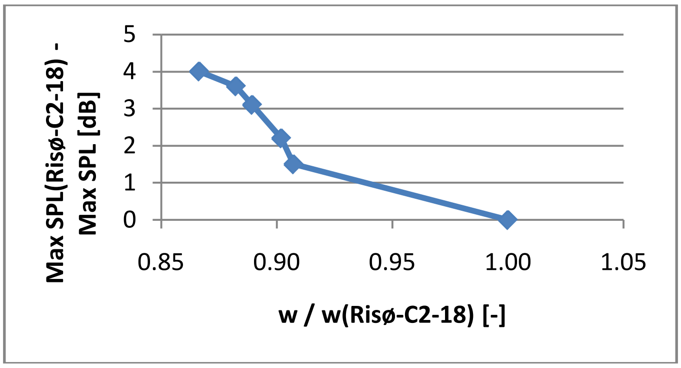

Figure 6 Reduction of maximum SPL as a function of the airfoil bending stiffness for the Risø-C2-18.

Figure 7 shows the aerodynamic performance of some of the new airfoil designs, the Risø-C2-18 airfoil and the Risø-B1-18, which is a well established airfoil design[4]. No significant changes from Risø-C2-18 airfoil are seen. However, even though the performance of c_l is similar for the Risø-B1-18 compared to Risø-C2-18, c_l/c_d is significantly higher for the Risø-C2-18 airfoil at c_l values between 1.2 and 1.7 making this airfoil aerodynamically much more efficient. Figure 8 shows to the left maximum SPL as a function of c_l and to the right SPL spectra for c_l around 1,2. Apart from the Risø-C2-18 airfoil and two of the new airfoil designs also Risø-B1-18 and NACA 63-418[20] are shown. Reductions of maximum SPL are seen for the two new designs of 1.5dB and 3dB respectively, confirming the ability of the design tool to design airfoils with reduced noise emission. Furthermore, Risø-B1-18 shows similar noise emission as the Risø-C2-18, but the NACA 63-418 has significantly higher maximum SPL for a given c_l value. Investigating the trends using A-weight shows, however, another picture. Figure 9 shows to the left maximum SPL(A) as a function of c_l. and to the right SPL(A) spectra for c_l around 1.2. It appears that the Risø-C2-18 has somewhat higher SPL(A) (1dB) as the Risø-B1-18 and that the design #5 obtains a similar maximum SPL as the Risø-B1-18. Thus, the conclusions when analyzing the maximum SPL with A-weight is that it is possible to reduce the A-weighted noise compared to the initial airfoil and that the new airfoil showed the same low noise emission as the Risø-B1-18, but with higher aerodynamic performance.

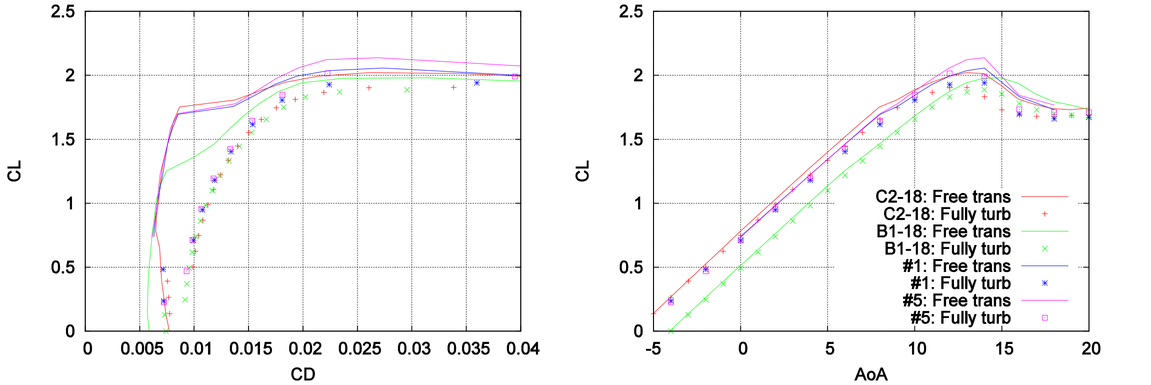

Figure 7 Aerodynamic characteristics of two of the new design, #1 and #5 compared to Risø-C2-18 and Risø-B1-18. To the left: c_l as function of c_d and to the right c_l as a function of *AOA*.

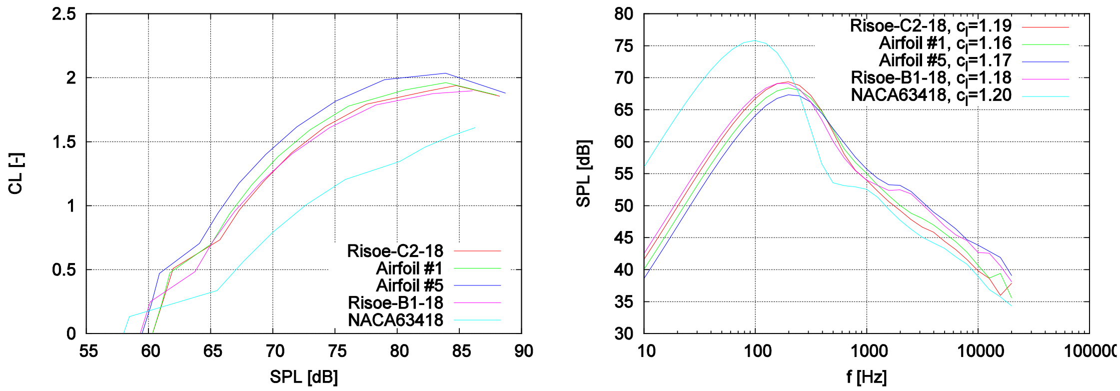

Figure 8 Left: Maximum SPL as a function of c_l for different airfoils. Right: Spectra of SPL at c_l around 1.2 for different airfoils.

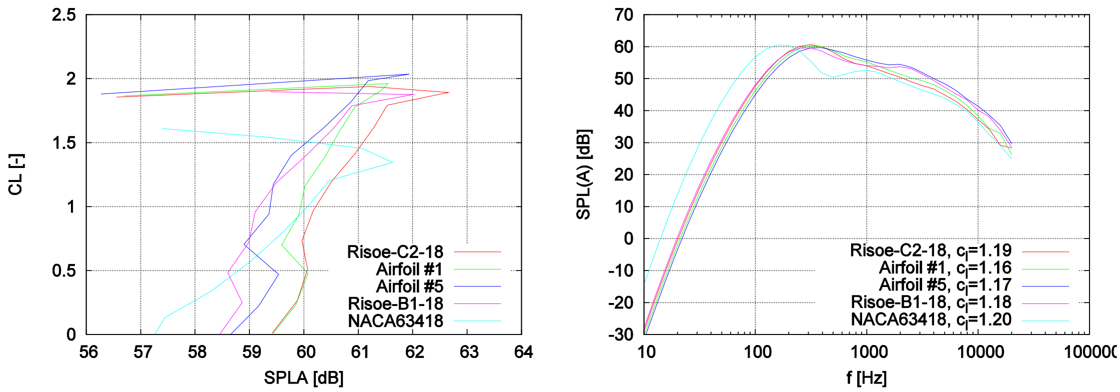

Figure 9 Left: Maximum SPL(A) as a function of c_l for different airfoils. Right: Spectra of SPL(A) at c_l around 1.2 for different airfoils.

The conclusions above were based on designs with maximum SPL in the objective function. However, using maximum SPL(A) in the objective function did not reduce the maximum SPL(A) further.

VI. Conclusions

This paper presented the design of a new low noise airfoil with 18% thickness. The airfoil dedicated for wind turbines was developed considering excellent aerodynamics and low noise. For this purpose the airfoil design tool AIRFOILOPT was used. The airfoil was developed for variable speed operation and pitch control of large megawatt sized rotors. Design objectives were used with simultaneous use of airfoil flow simulations assuming both free and forced transition. A compound objective function was used, where the c_l-c_d ratio over a range of design angles took care of the design for aerodynamic efficiency, and where the trailing edge noise predicted by the TNO model took care of the reduced noise. Also, numerous constraints on flow and structural response parameters to ensure a high maximum lift coefficient and insensitivity of this to leading edge roughness were put on desired characteristics.

The results from the design process showed that AIRFOILOPT was capable of designing airfoils with reduced noise using Risø-C2-18 as a basis. Thus, airfoils showing 1.5dB to 3dB reduction of maximum SPL were designed, with increasing relaxation of the constraints on the geometry around the trailing edge for increased reduction in SPL. However, evaluating the designs using A-weight on maximum SPL showed another picture. It appears that the Risø-C2-18 has around 1dB higher SPL(A) as the Risø-B1-18 and that the design #5 obtained a similar maximum SPL(A) as the Risø-B1-18. Thus, the conclusions when analyzing the maximum SPL with A-weight is that it is possible to reduce the A-weighted noise compared to the initial airfoil and that the new airfoil showed a thinner trailing edge, the same low noise emission as the Risø-B1-18, and higher aerodynamic performance.

Nomenclature

AOA	Angle of attack [°]
AOAr	Angle of attack relative to zero lift AOA [°]
c	Chord length [m]
c_l	Lift coefficient [-]
c_d	Drag coefficient [-]
c_p	Normalized coefficient for the pressure on the airfoil surface [-]
C_P	Normalized coefficient for the wind turbine rotor power [-]
f	Frequency [Hz]
N	Force on airfoil normal to the rotor plane [N]
Re	Reynolds number [-]
SPL	Sound Power Level [dB]

SPL(A)	A-weighted Sound Power Level [dB]
t	Airfoil maximum thickness [m]
T	Force on airfoil parallel to the rotor plane [N]
U	Flow speed [m/s]
x	Coordinate in chordwise direction [m]

Acknowledgments

The Danish Energy Authorities, EFP2007 II are acknowledged for funding the airfoil design investigation.

References

[1] Tangler J.L. and Somers D.M. Nrel airfoil families for hawt's. *Proc. WINDPOWER'95, Washington D.C.*, pages 117-123, 1995.

[2] Timmer W.A. and van Rooij R.P.J.O.M. Summary of the delft university wind turbine dedicated airfoils. *Proc. AIAA-2003-0352*, 2003.

[3] Björk A. Coordinates and calculations for the FFA-w1-xxx, FFA-w2-xxx and FFA-w3-xxx series of airfoils for horizontal axis wind turbines. Ffa tn 1990-15, FFA, Stockholm, Sweden, 1990.

[4] Fuglsang P. and Bak C. Development of the Risø wind turbine airfoils. *Wind Energy*, 7:145-162, 2004.

[5] Bak C, Andersen *P B*, Madsen *H A*, Gaunaa M, Design and Verification of Airfoils Resistant to Surface Contamination and Turbulence Intensity. AIAA 2008-7050, 26th AIAA Applied Aerodynamics Conference 18 - 21 August 2008, Honolulu, Hawaii

[6] Fuglsang P. and Dahl K.S. Multipoint optimization of thick high lift airfoil wind turbines. *Proc. EWEC97, Dublin, Ireland*, pages 468-471, 1997.

[7] Drela M. *XFOIL, An Analysis and Design system for Low Reynolds Number Airfoils. Low Reynolds Number Aerodynamics*, volume 54. In Springer- Verlag Lec. Notes in Eng., 1989.

[8] Michelsen J.A. Basis3d - a platform for development of multiblock pde solvers. Technical report afm 92-05, Technical University of Denmark, 1992.

[9] Michelsen J.A. Block structured multigrid solution of 2d and 3d elliptic pde's. Technical report afm 94-06, Technical University of Denmark, 1994.

[10] Sørensen N.N. General purpose flow solver applied to flow over hills. Risø-r-827(en), Risø National Laboratory, Denmark, June 1995.

[11] Brooks, T.F., Pope, d.s., Marcolini, M.A., 1989, ''Airfoil Self-Noise and Prediction,'' NASA Reference Publication 1218, USA

[12] Parchen, R., "Progress report DRAW: A Prediction Scheme for Trailing-Edge Noise Based on Detailed Boundary-Layer Characteristics", TNO Rept. HAG-RPT-980023, TNO Institute of Applied Physics, The Netherlands, 1998.

[13] Glegg, S., Morin, B., Atassi, O., and Reba, R., “Using RANS Calculations of Turbulent Kinetic Energy to Provide Predictions of Trailing Edge Noise”, 14th AIAA/CEAS Aeroacoustics Conference (Proc.), AIAA Paper 2008-2993, Vancouver, Canada, 2008.

[14] Bertagnolio F., Madsen H A, Bak C, ‘Experimental validation of TNO trailing edge noise model and application to airfoil optimization’, Presented at: 2009 European Wind Energy Conference and Exhibition. Marseille (FR), 16-19 Mar, 2009, In: EWEC 2009 Proceedings online, p. 10 pages EWEC, 2009

[15] Tangler J.L. and Somers D.M. Status of the special purpose airfoil families. *Proc. WINDPOWER'87, San Fransisco*, 1987.

[16] Björk A. Airfoil design for variable rpm horizontal axis wind turbines. *Proc. EWEC'89, Glasgow, Scotland*, 1989.

[17] Fuglsang P. Aerodynamic design guidelines for wind turbine rotors. *Proc. 4th GRACM Congress on Computational Mechanics GRACM 2002, Patra, Greece*, 2002.

[18] Fuglsang P. and Madsen H. A., 1996, Implementation and Verification of an Aeroacoustic Noise Prediction Model for Wind Turbines., Risø-R-867(EN), Risø National Laboratory, Denmark, March 1996

[19] Lowson, M.V., Fiddes, S.P., 1994, ‘’Design Prediction Model for Wind turbine Noise, ETSU W/13/00317/REP

[20] Abbott, I.H.; von Doenhoff, A.E., ‘Theory of Wing Sections’, Dover Publications Inc. New York, 1959

Third International Meeting

on

Wind Turbine Noise

Aalborg Denmark 17 – 19 June 2009

Seismic Effect on Residents from 3 MW Wind Turbines

Bakker, H.H.C.,

School of Engineering and Advanced Technology, Massey University,

H.H.Bakker@Massey.ac.nz

Bennett, D.J., Kea Petroleum Limited, Wellington NZ 6012

davebennett@xtra.co.nz

Rapley, B., Atkinson & Rapley Consulting, Palmerston North,

arg@paradise.net.nz

Thorne, R., Noise Measurement Services, Brisbane,

bob@noisemeasurement.com.au

Abstract

Residents on a river plain at the foot of the Tararua Ranges, New Zealand, experience ongoing noise problems, including sleep deprivation, thought to emanate from a nearby wind farm in the ranges to the east (closest V90 turbine is 3 km away). The problem is worst when wind is from the eastern quadrant. Installation of 'Hush Glass' only partly alleviated the problem indoors.

Continuous time series recording of seismic noise using a buried L4 geophone and acoustic surface microphone attached to a wall inside the house, was conducted during March 2009. Use of night hours records minimised extraneous noise, and seismic noise from vegetation was also guarded against by analysis of site wind records.

Early analysis of 196s seismic samples identifies noise bursts lasting 10 seconds or more, every minute or so, associated with easterly wind conditions; with broad spectral power peaks centred on approximately 10 and 28 Hz. Audio playback of the seismic records was identified by the residents as similar to the noise they experienced.

We conclude that seismic energy from the turbines, most likely as Rayleigh waves, is coupled through its concrete foundations into the house, where various vibrational modes are stimulated, thus producing the effects experienced. We note that residents experience these strongest when lying down, i.e. when best aurally coupled to the foundations.

These results provide an initial indication that seismic effects should be assessed in consideration of offset distances from turbines to residences.

Ongoing work will consider such factors as directionality of seismic noise, proximity to the range front fault as possibly accentuating seismic response, either through standing wave or dispersion, and constructive/destructive interference between turbines associated with wind variability as a cause of the intermittent nature of the phenomenon.

Introduction

The Tararua Ranges in New Zealand provides some of the best wind farm sites in the world with generation factors of over 40%. Several windfarms have recently been constructed and several more are in the planning stages. One of these will be located within ten kilometres of the centre of the city of Palmerston North (pop 75,000).

While much has been published on the acoustic emanations from wind farms (Hayes McKenzie Partnership Ltd (2006), Pedersen & Persson-Waye (2004), van den Berg (2006)) little work has been carried out on vibration. This paper studies the case of residents on the river plain at the foot of the Tararua Ranges who have experienced noise problems from a wind farm with the closest V90 turbine 2.8 km to the south-east. One of the observations made by the residents was that the noise could be heard "through the pillow," suggesting involvement of seismic, as well as acoustic, effects.

This study was undertaken to investigate two issues:

1. whether the noise reported by the residents could be detected and analysed, and

2. whether it was related to the nearby windfarm.

Background

The residence in question lies at the edge of a river plain at the base of the Tararua Ranges on a spur. Two wind farms lie to the east through to the southeast at the top of the ranges. The older wind farm consists of 48 Vestas V47's, commissioned in 1999, and 55 Vestas V47's which were commissioned in May 2004. The newer windfarm comprises 31 Vestas V90's with commissioning beginning in 2007 and is still on-going. The closest Vestas V90's are approximately 2.8 km south-east of the residence. The onset of noise problems coincides with the installation of the newer V90 turbines with noise being experienced by a number of neighbouring properties around the residence which is being monitored.

After initial complaints from the residents the power company installed 'Hush Glass' in the master bedroom (surface microphone location - see Figure 1). This reduced the acoustic noise, however, there are still noise issues.

The residence is of timber and brick facade construction with a concrete slab foundation. It is 52.5 metres long and between 9 to 13.5 metres wide with the long axis pointing towards the wind farms. It is divided into three distinct sections with the house separated from a large workshop and office by a carport. The workshop lies closest to the windfarms.

The residents have observed the following pattern to the noise occurrences:

• The noise is audible only when the wind is coming from the south-east.

• It is most noticeable at night, particularly in the early hours of the morning.

• The noise is 'audible' when lying down, "through the pillow," but is also audible in the main bedroom and in the hallway when more severe.

• It consists of a low rumbling noise reminiscent of a jet landing.

• The residents find some alleviation of the problem by transferring to another bedroom of the house, suggesting that the geometry of the main bedroom and its outlook may be a contributing factor.

•

Figure 1: Site layout and position of sensors. (© Copyright 2009 Google Map Data)

Some of the neighbouring residents also observe similar noise issues but report disturbances on different nights, suggesting that the effect is localised.

Figure 2: View of the V90 windfarm to the east south-east of the residence.

The Vestas V90 turbine is a 3MW unit with a variable-speed gearbox that allows it to adjust the blade speed to be optimal for the existing wind speed while adjusting blade pitch and the gearbox ratio to smooth the incoming power. The operational speeds range from 0.14Hz to 0.31Hz. Vestas (2008)

Seismic Effects

Ground acceleration associated with earthquakes is a well known phenomenon. In NZ some local authorities produce maps of ground response to illustrate areas of high earthquake hazard. For example, the Wellington Regional Council has such maps on its website, one of which shows that the area immediately west of the Tararua Ranges, just to south of the study area, is predicted to have high ground shaking response to a driving signal from an earthquake. Basically, this is because the geologically ‘young’ and relatively unconsolidated rocks and fill west of the range front, will wobble like jelly when seismically excited; whereas the geologically older and better consolidated rocks of the ranges will have a much smaller response.

In the field of seismic surveying the phenomenon is also well known as ‘ground roll’; an unwanted ‘jelly wobble’ most obvious when working over unconsolidated surface fill such as river gravels or sediments in confined valleys. Seismic companies make routine use of DIN 4150 and similar standards to ensure that ground accelerations at nearby houses, due to the operation of their equipment, fall within acceptable standards since the phenomenon of unwanted vibration and noise within a residence is a common cause of complaint. Rayleigh Waves, or ‘ground roll’, propagate energy along the air-earth boundary, with particle motion confined to the vertical plane in the direction of travel. The energy propagates outwards with a geometrical spreading attenuation factor of 1/(range). This contrasts with propagation of compressional (acoustic) energy through the air which attenuates as 1/(range**2).

Styles (2005) reported on the measurement of seismic vibrations from a wind farm in Scotland. He noted that such seismic signals can travel for tens of kilometres and still be measurable. The seismic vibrations observed were predominantly at the rotational and blade-passing frequencies and their harmonics. In the case of the Vestas V90 turbines this would be 0.14-0.31Hz and 0.43-0.92Hz respectively. However. Styles is careful to comment that these seismic signals are below human perception threshold.

The question, therefore, is not whether turbines actually generate seismic energy, but whether this signal can be significant for nearby residents. In the present instance, the turbines are well coupled into the mechanically competent ‘old’ rocks of the ranges by their concrete bases, which will ensure good coupling of whatever seismic energy they generate into the ground. Rayleigh Wave energy will then propagate outwards, including towards the range front to the west, where they will meet the unconsolidated sedimentary rocks and sediments of the river terraces to west, on which the residents' house is situated. The range front fault system will be a driving point for energy propagation into the sedimentary rocks to the west, rather analogous to shaking a carpet from the edge and sending waves through it. Given the Rayleigh velocity in such rocks, at frequencies of 1-10 Hz typical wavelengths will be hundreds of metres to ~1 km, with standing waves setting up nodal and antinodal points. It is possible that the residents' house, some 2 km west of the range front, is at an antinodal point in certain conditions. The effect may also be exacerbated by the trace of the range front, which effectively runs due north to the north, and southwest to the south of the residents' house. This may serve to focus Rayleigh energy propagating west from the range front into the vicinity of the residents' house, rather like the focal point of a parabolic reflector; and may explain why the unwanted effects are localised to a few neighbouring houses.

Experimental

Initial measurements used two sensors to measure the vibrations in the main bedroom and seismic vibrations in the ground adjoining the house. An acoustic Soho surface microphone was placed on the wall of the main bedroom equidistant from the underlying studs and cross-members. A Mark Products L4 1Hz geophone was buried in the ground at the workshop end of the residence.

Figure 3: Photo of L4 geophones in situ; bonded to the carport floor and buried in the ground.

Two separate data acquisition units were used to record data. A LabJack U3-HV was used to record two channels at a 100Hz-sampling rate and 10 bits of resolution. Another PC-based instrument, SAM - a spectroaudiometer, (Rapley and Atkinson Consulting, Palmerston North, New Zealand) was used to capture data.

SAM is based on National Instruments' Virtual Instrumentation core and provides the ability to record and analyse sound data, providing real time power spectra as well as statistical data on environmental noise every second, such as the equivalent sound level. It is more commonly used to monitor nuisance noise and is capable of creating a number of different on-the-spot reports including a noise abatement notice (complete with trace of noise level over time and GPS-based location.) It was used for this work for its ability to continuously record data at 100Hz as well as 44.1kHz data captures when set power levels were exceeded.

The standard microphones that come with the equipment were replaced by the surface microphone and L4 geophones. Data was measured at 44.1kHz and 16 bits of resolution and decimated to 100Hz for continuous recording. The full signal was also recorded for 60s after power levels exceeded a set threshold with a hold-off period of 10 or 20 minutes thereafter.

A USB sound card was used to digitise the incoming signals after they had been passed through an Australian Monitor AMIS-PRE1 preamplifier and a low-pass antialiasing filter. The acoustic microphone had an additional preamplifier at the main bedroom to boost the signal before being sent the 30m to the data acquisition systems.

An Acer laptop computer was initially used to run SAM but was later changed to a desktop computer when issues were found with interference from the internal circuitry of the Acer and with its ability to handle the data load.

A WS1083 Black Weather Station PC USB was installed at the residence providing half-hourly summaries of wind direction, wind speed, rainfall as well as other sundry data.

Figure 4: Weather station mounted close to the south-eastern end of the residence.

Data was periodically retrieved and analysed using Matlab (The Mathworks, Natick, USA). The data was first presented for rapid visual inspection by plotting three minute periods of time series, power spectrum, wind speed/direction and rainfall data and converting the resulting plots into a movie. (see Figure 5) This provided an effective method of scanning the data rapidly, with frame-by-frame control both backwards and forwards, as well as providing a low data storage method to summarise the data.

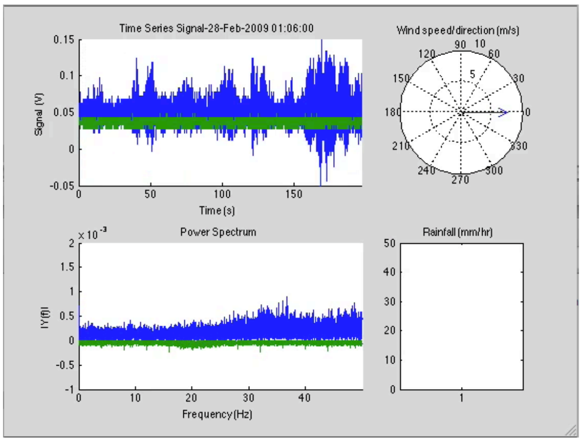

Figure 5: One frame of a movie to store a day's worth of data in a readily viewable form. (For wind direction, 0° is east.)

From these plots events were identified and analysed. Only events that occurred between about 10:30pm and 5am were considered as possible seismic events as the residents were not active during these times. Where possible the 44.1kHz sampled data was used, i.e. when a one-minute sampled interval aligned with the event in question.

Events were then compared with the residents' recollections from the same times, backed up by a diary that they kept of instances of noise. Some events were played back to the residents using either earphones or a stereo system (to provide reasonable playback of the low frequencies in the signals) to help identify the event.

Cross-correlations and auto-correlations were taken of the two signals.

Results

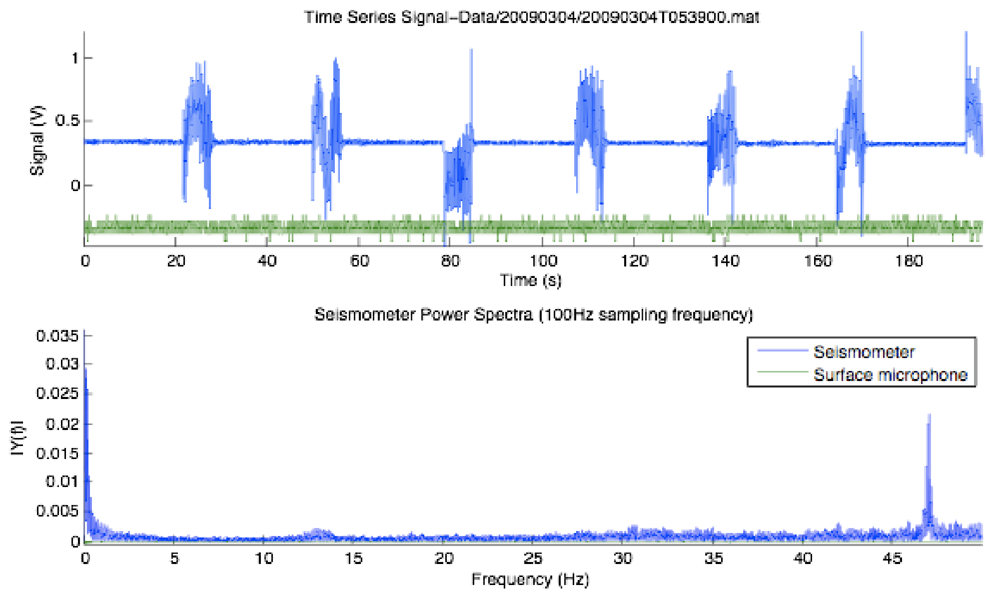

Figure 6: Time series signals and power spectra of domestic water pump.

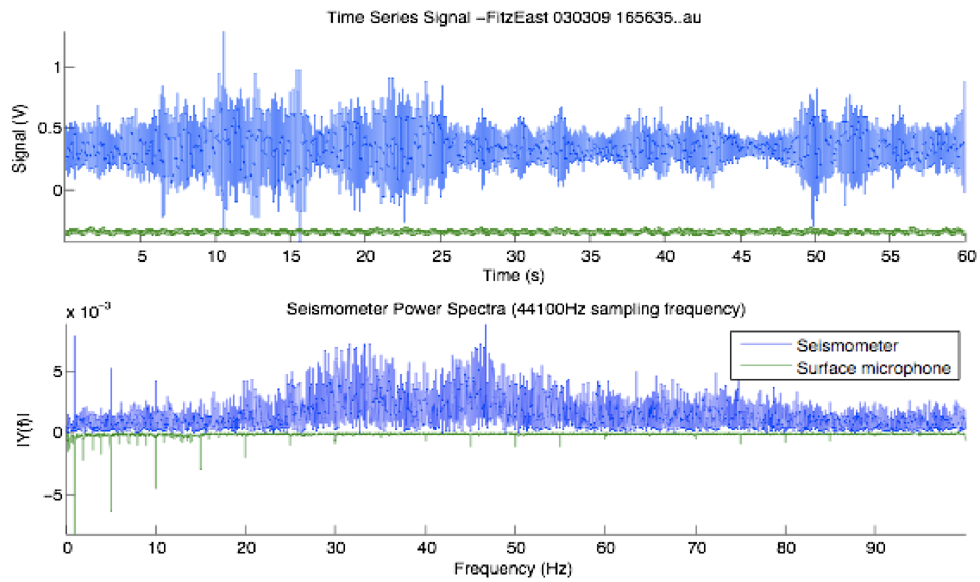

Figure 7: Time series signals and power spectra during strong winds with an average speed of 8.8m/s and a peak gust of 12.9m/s.

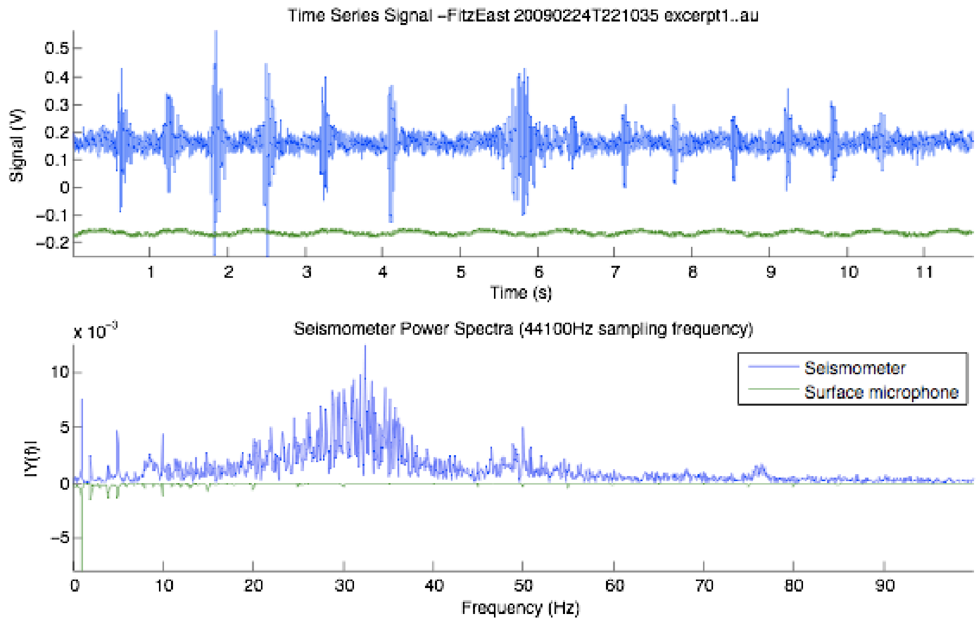

Figure 8: Time series signals and power spectra of human footsteps in the workshop and closing of the workshop door (centre).

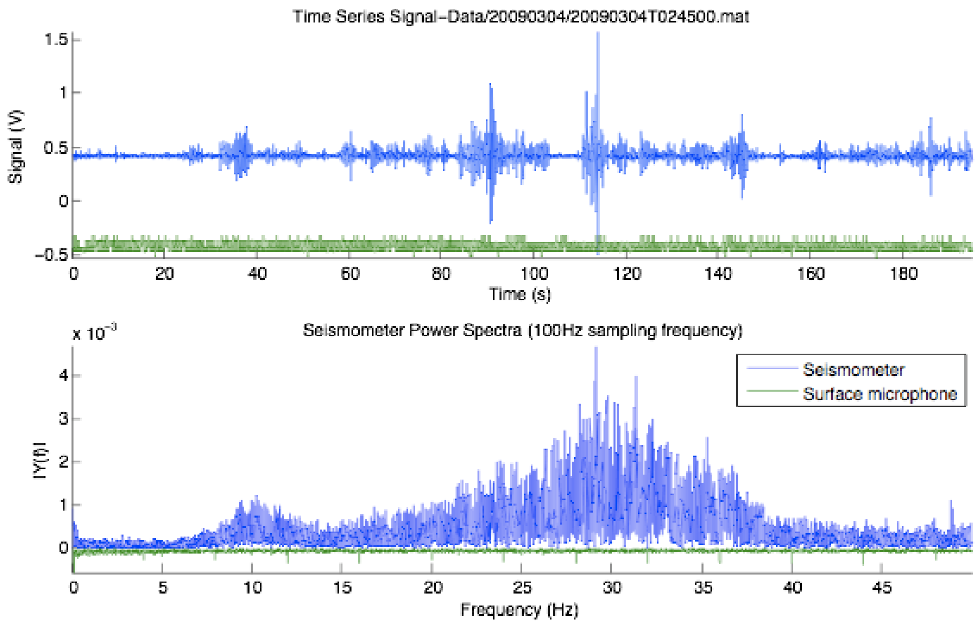

Figure 9: Time series signals and power spectra of a typical seismic event (recorded at 2:45am at an average wind speed of 1.4m/s and a peak of 2m/s).

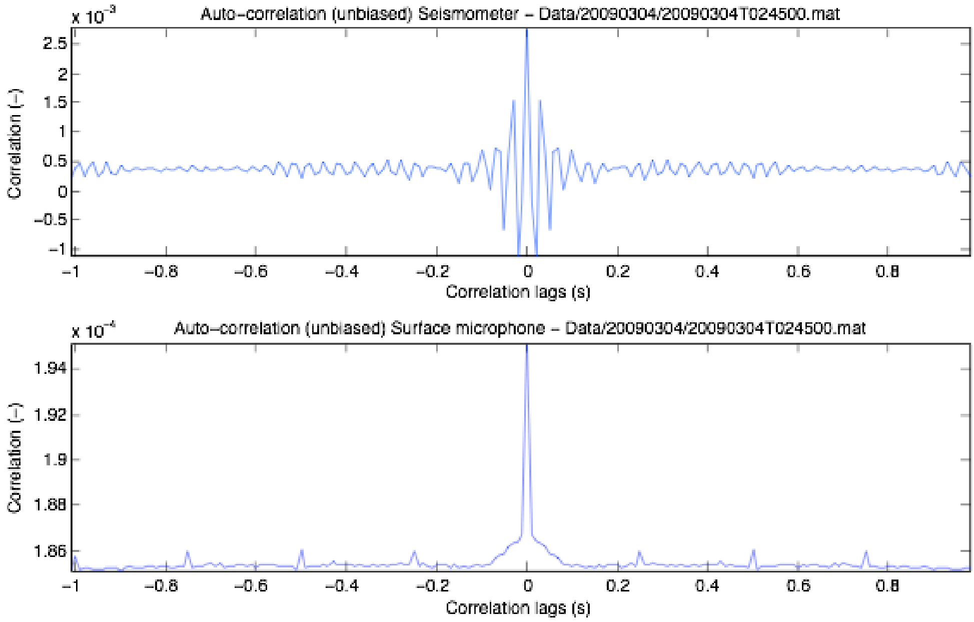

Figure 10: Auto-correlation plots of the time series signals in Figure 9.

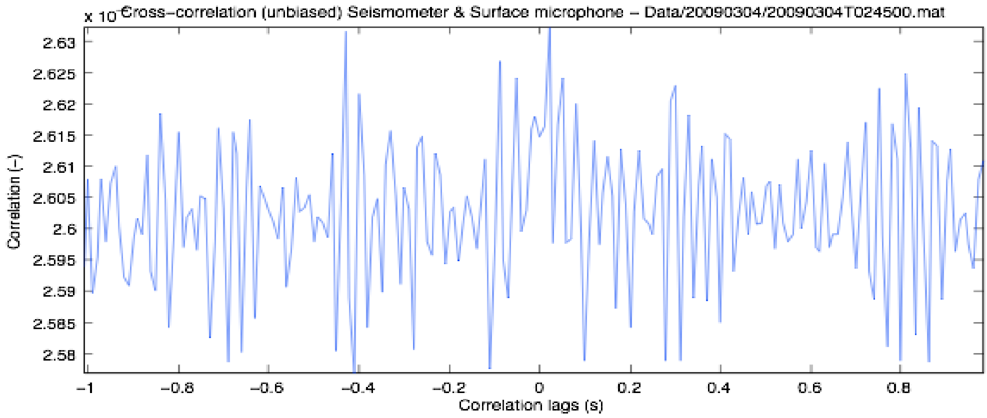

Figure 11: Cross-correlation plot of the time series signals in Figure 9.

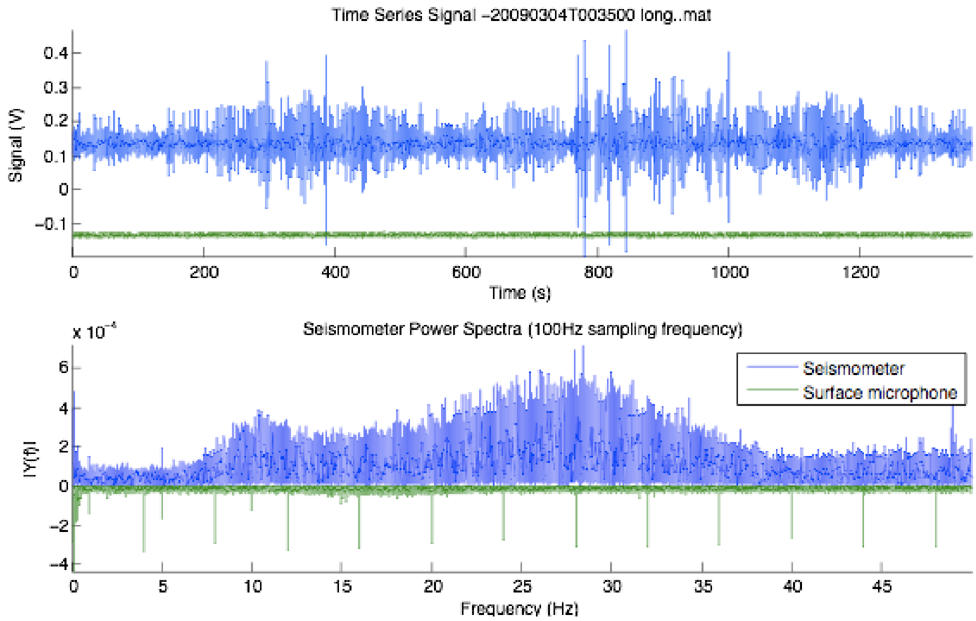

Figure 12: Time series signals and power spectra of a typical seismic event over a long baseline taken at an average wind speed of 5m/s with gusts to about 7m/s.

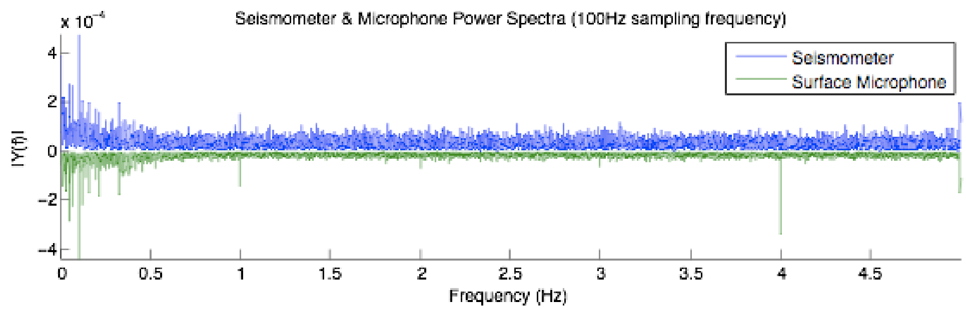

Figure 13: Detail of Figure 12 from 0Hz to 5Hz.

Discussion

Initial results indicated that artefacts were generated at 1Hz and 5Hz for many signals and at 4Hz for the surface microphone signals. These appeared to be due to electrical noise injection from the laptop computer in to the USB sound card, which was replaced for later experiments.

A number of extraneous events were identified and removed from subsequent analysis:

- The water pump supplying domestic water. As shown in Figure 6 this produced tight bursts of high intensity noise in the time domain with a large near-DC content in the power spectrum and a peak at 47Hz. This latter is a strong indicator of an AC motor running, with slip, at slightly less than the 50Hz mains power.

- High wind. As shown in Figure 7, this presumably coupled to the ground through the house itself. This was characterised by many spread impulses of varying amplitudes in the time domain and fairly constant energy from DC to beyond 100 Hz in the frequency domain. Broad peaks at 32Hz, 46Hz are present. Note the artefacts at 1Hz, 5Hz and their harmonics.
- Footsteps in and around the workshop. These provided a rough calibration of the seismometer gain, which was otherwise uncalibrated. Figure 8 shows a typical event with regularly spaced impulses in the time series signal both increasing and decreasing in intensity and associated with a broad peak at 32Hz and smaller peaks at 8Hz and 50Hz in the power spectrum.

After eliminating these events there were a number remaining with similar characteristics that appeared only when the wind was from a south-easterly direction, and reached maximum intensity on those nights when the residents reported the loudest nuisance noise. One of the clearest and strongest events is shown in Figure 9 with sharp and complex bursts in the time series signal generally lasting in the order of 10 seconds and with broad peaks at 28Hz and 10Hz. The intensity of these events was seen to increase with wind speed above about 1m/s and appeared to disappear for wind speeds much above about 6m/s.

The frequencies of 28Hz peak are near the lower threshold of human hearing—normally quoted as 20Hz—but there is significant energy as high as 35-40Hz. This would be perceived as a very low rumble similar to that described by the residents and would be amplified by mechanical coupling. As noted by Moller (2004), at these frequencies the dynamic range of human hearing is markedly decreased and with a spread of individual thresholds. This can lead to large differences in perceived loudness; a sound that is inaudible to one person can be loud to another.

When recordings of these were played back to the residents through either earbuds or a stereo system (good bass response was required to make the low frequencies audible) they reported that the recordings were similar to the noise that they experienced. This represents good evidence that the noise reported by the residents has been detected by the seismometer. In conjunction with the relative success of the 'Hush Glass,' it is possible to conclude that there are two parts to the nuisance noise; an acoustic wave modulated in amplitude, and possibly frequency, and a seismic wave that is 'perceivable' within the residence creating sleep disturbance.

Auto-correlations of the signals were carried out (Figure 10) showing that both signals had a strong non-periodic component although the seismometer signal showed a periodic component at close to 30Hz. The cross-correlation of the two signals (Figure 11) suggests a similar component at close to 30Hz.

One interpretation of these data would be that the broad peaks in the spectrum of Figure 9 were caused by vibrational modes in the windfarm structures. One could postulate either a vibrational resonance mode or multi-turbine constructive interference as sources of these vibrations. If the vibrations were coupled to the ground as Rayleigh waves, they could propagate principally in the upwind and downwind directions from the towers, and therefore only be noticed when the wind was blowing from the south-east or north-west. They would dissipate with distance rather than its square and be measurable at larger distances.

In this case the concave shape of the fault front at the base of the range could act as a lens, focussing these vibrations to a small area in which the residence in question, and one or two others, was situated.

From previous experiments, Styles (2005), seismic recording of wind turbines have shown peaks at the rotational and blade-passing frequencies as well as their harmonics. The relevant frequencies for this windfarm are 0.14-0.31Hz and 0.43-0.92Hz respectively. A long baseline sample was analysed to provide higher definition at these lower frequencies (Figure 12). Apart from several small peaks close to 0.1Hz, there are no significant peaks suggesting either the rotational frequency, blade-passing frequency or any of their harmonics (Figure 13) that might be emitted from the windfarm. As noted in Styles (2005a) these frequencies were at very small levels of vibration and would not normally be detectable with conventional instruments.

An alternative explanation for the seismic events are that the house is not seismically coupled to the windfarm but acoustically. In this case it would be the acoustic noise making the house and concrete pad vibrate thereby causing the seismic vibrations measured by the geophone. This would explain the similarity in the power spectra of the footsteps and the seismic events.

Further work needs to be undertaken to differentiate between the competing hypotheses and should consider such factors as directionality of seismic noise, proximity to the range front fault as possibly accentuating seismic response—either through standing wave or dispersion—and constructive/destructive interference between turbines associated with wind variability as a cause of the intermittent nature of the phenomenon.

Conclusions

Seismic and acoustic measurements were undertaken at a residential site at the base of the Tararua Ranges close to a windfarm to determine whether nuisance noise reported by the residents could be detected and whether it could be traced to the windfarm.

Extraneous events were eliminated from the measurements by using only night time records, by removing known events and by eliminating events that did not correlate with the timing of the residents' perception.

The remaining events were characterised by bursts of around 10 seconds duration and with broad peaks in the power spectra at 28Hz and 10Hz.

When the residents were played these events, through earbuds or a stereo system, they decided that they were closely similar to the noise they had been reporting. We therefore conclude that the noise 'perceived' by the residents is measurable, consists of separate acoustic and seismic parts and can cause annoyance by disturbing sleep.

Seismic emanations recorded at other windfarms, Styles (2005), were not observed in the records. Several hypotheses have been suggested for the source of the seismic spectral peaks involving the windfarm but the data available cannot confirm or disprove any of them. Ongoing work will continue to analyse the events and seek to do so.

References

Hayes McKenzie Partnership Ltd (2006) "The measurement of low frequency noise at three UK wind farms", report to DTI, URN number 06/1412

Moller H, Pedersen CS. (2004) "Hearing at low and infrasonic frequencies", Noise Health [serial online] [cited 2009 May 3];6:37-57. Available from: http://www.noiseandhealth.org/text.asp?2004/6/23/37/31664

Pedersen, E & Persson-Waye, K (2004) "Perception and annoyance due to wind turbine noise - a dose - response relationship", Journal of the Acoustical Society of America, 116(6), pp. 3460-3470

Styles, P, Stimpson, I, Toon, S, England, R & Wright, M, (2005) “Microseismic and Infrasound Monitoring of Low Frequency noise and Vibration from Windfarms: Recommendations on the Siting of Windfarms in the Vicinity of Eskdalemuir, Scotland", Report, Keele University, Keele, UK.

Styles, P, Toon, S (2005a) "Wind Farm Noise", Article, British Wind Energy Association, http://www.bwea.com/ref/lfn_keele.html.

van den Berg, GP, (2006) "The sounds of high winds - the effect of atmospheric stability on wind turbine sound and microphone noise", Science Shop for Physics, Netherlands, Electronic version available from:

www.ventdecolere.org/archives/nuisances/VAN%20DEN%20BERG%202006.pdf

Vestas (2008) 'V90 - 3.0MW An efficient way to more power', Product Brochure, Vestas Wind Systems A/S, Randers, Denmark

Third International Meeting
on
Wind Turbine Noise
Aalborg Denmark 17 – 19 June 2009

Optimization of energy production of a large windfarm with noise constraints: a numerical toolkit

Andrea Bartolazzi
Via Lagrange 1, 00197 Roma
a.bartolazzi@studiorinnovabili.it

Michelangelo Mariani
Via Lagrange 1, 00197 Roma
m.mariani@studiorinnovabili.it

Abstract

When building a large windfarm developers can encounter the problem of noise constraints for sensible receivers. More and more these windfarms are built in inhabited zones, therefore the number of sensible receivers increases. To solve eventual problems with the receivers there is the need to control turbine noise. Noise control would diminish the energy production. There is the need to forecast what would be the impact of noise control of the turbines after the building of the windfarm. In particular the investors that are financing the park want to know what is the best noise control strategy to control the noise and what is its economical effect in order to include it in the risk assessment of the financing. To complicate the model, turbines and background are varying with wind velocity. This problem has a manageable solution when the number of turbines and receivers is low, but if the number increases the problem becomes complex and a numerical toolkit helps to discover what is the best strategy, which receivers are hit and when, what turbines have to be reduced in noise and what amount of energy is at risk. The authors, consultants at Studio Rinnovabili, present a numerical toolkit developed in Matlab that solved the problem for a 80 turbines wind farm with more than 200 receivers.

Introduction

This is the story of a study done by our company Studio Rinnovabili for the technical due diligence of a large windfarm of over 80 turbines, with more than 200 noise receivers. At the beginning the developer wanted to evaluate if there where noise problems due to local laws. Afterwards, discovering that there could have been problems, they wanted to evaluate what could have been the result of the need to reduce the noise.

Role of Studio Rinnovabili in the measurement, analysis and finalization of the toolkit

Our company decided at the beginning of this project to use a commercial software to solve the problem. We performed a complete noise measurement campaign. We analysed the background and modelled both background and turbine noise. Later we discovered that the problem given by our customer was not solvable with that software. The main problem was that the software was not able to manage the complications given by the laws. Moreover the model given by the software did not allow the calculation of the final noise control level of every turbine.

Description of the problem solved – time constraints, background noise model and its need, legal constraints, clients norm constraints

Noise reduction after a project has been authorized and the position of turbines is fixed means that the developer needs to reduce or even switch off some turbines, hence reducing the power output. Therefore they asked to evaluate what would have been the power reduction needed to stay within laws. Not to overestimate this power reduction there was a problem to find the optimal solution of reduction/switching the turbines. The problem had a very high level of complexity if you consider: the large numbers of sources, the large number of receivers, the multiple conditions required by laws, the change of background noise with wind velocity, the cross effect of reducing one noise level for one receiver on the other receivers, the necessity to consider wind transportation effect. This high complexity made impossible to use one of the existing software, mainly because of difficulties in inserting all laws constraints, and also impossible to do the calculation with spreadsheet mainly because of complexity of calculation and necessity to complete it in short times.

Law limitation in Italy can be described as a three level constraint. A first level of constraint indicates what is the max noise level depending from the receiver classification. On our site we had two classes: residential sites with a max noise level of 60 dBA during night and 70 dBA during day, then we have Industrial receivers with a max noise level of 70 dBA during night and day.

In residential receivers there is second level of control, a differential level of 3 dBA during night and 5 dBA during day to be respected. Differential level indicates the difference of noise between noise produced by the plant in exercise and pre-existing background noise.

A third level of constraint is that differential constraint applies only if total noise is over 40 dBA.

To let the reader understand what the root of the problem is we will describe the principal workflow to analyse the noise and to verify if this noise is out of law limits.

As first we will need to evaluate the background noise of all sites that we consider sensible (these are residential). This must be done measuring noise over a few days and measuring wind velocity at the same time. This is needed to construct a model of noise in function of wind. As a matter of facts background noise is modelled as if it is composed by two noises, a first noise which is not depending from wind (e.g. Cars, human activity, animals and so on), and a second noise depending on wind that creates a growing noise hitting vegetation (Fegeant 99), houses and other objects. For wind depending noise we considered a logarithmic noise.

Therefore the formula describing the noise will be

$$L = 10\log_{10}\left[10^{\frac{K_w \log_{10} v_w}{10}} + 10^{\frac{K_b}{10}}\right]$$

Where:

K_w = wind noise coefficient (equal to average wind noise with wind of 10m/s)

K_b = base noise coefficient (equal to average background noise without wind)

v_w = wind velocity

L = noise level at the receiver

This model is necessary because we need to check legal constraints at all possible wind speeds.

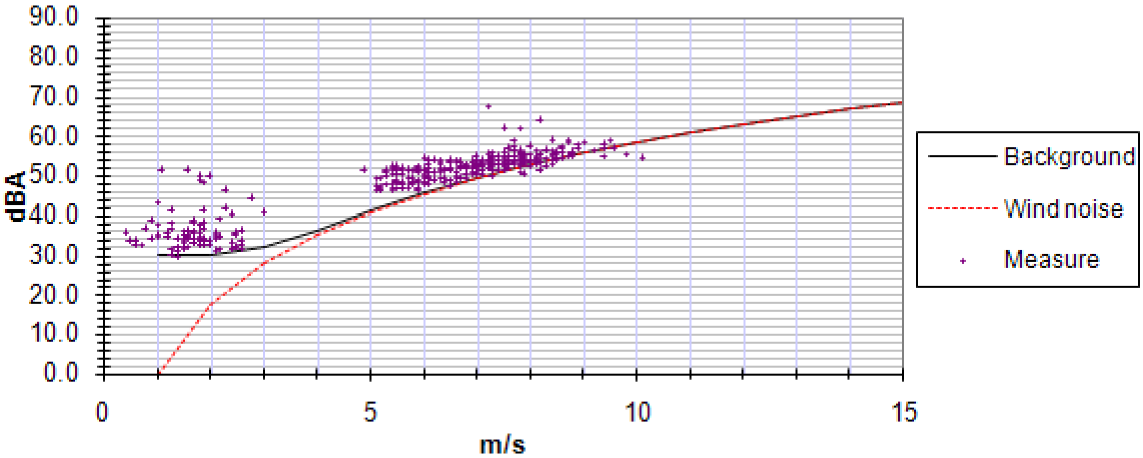

Figure 2 - Background noise (dBA) modelling for one sensible receiver in function of wind (m/s) derived on the site from wind at the meteo station. Small crosses are 10 minute measurements of noise and the corresponding wind. Black line is the model (L90) of noises coming from wind and non-wind related noise. Red dotted line is the wind related noise.

When we have background noise we can add noise created at the receiver by the turbines. This is calculated with another commercial software (CADNA-A), which applies the ISO 9613 for noise calculation.

This describes the respect of limits on a single receiver noise limits be them differential or total. Of course the noise created by turbines at different wind speed is changing because turbines tend to produce lower noise at lower wind speeds.

So for the example receiver we can say that legal limits are not respected for wind velocities of 4 m/s.

This means that we will have to reduce noise at the turbines for those turbines and wind speeds in which we have noise problems.

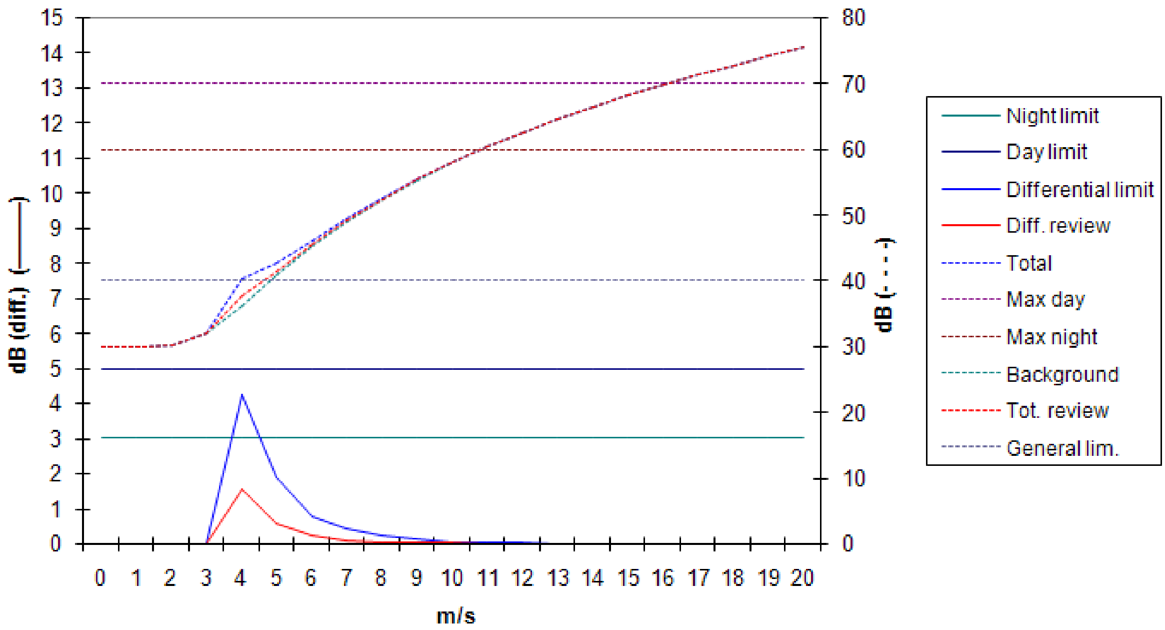

Figure 1 - On this figure there is represented noise and differential noise in function of wind. Dotted lines are total noise, and in particular background, total (which is background and noise noise from turbines), and total review (of total which is the description of noise after turbine noise reduction). Horizontal dotted lines represent limits (40, 60 and 70 dBA). Continuous lines represent differential noise: differential (difference between total noise before review and background) and differential review (difference between total noise after review and background). Horizontal continuous lines represent differential limits (3 and 5 dBA).

To implement this calculation on Matlab we needed as first a method to evaluate effect on receivers of change of output noise. This is done by CADNA-A that can give as an output a matrix where the element describes the noise produced on a single receiver by a single source (turbine).

So if we transform this matrix we may write that the vector of noises at every single receiver if given by

Noise = FdT * Source

Where:

FdT = matrix where every element $FdT_{i,j}$ represents that number that multiplied by the i-element of vector Source gives the contribution of the i-turbine to noise at j-receiver

Source = vector of noise coming form i-turbine

Noise = Vector representing noise coming from turbines at receiver

This matrix FdT anyway is valid for a situation in which the effect of source noise on single receiver is constant. The problem has a further degree of complexity due to the fact that depending on wind direction the noise on receivers changes. Receivers downwind receive generally a higher noise impact than received that are placed upwind respect to turbines. To represent this change we used a CADNA-A routine that is based on CONCAWE procedure built in the software CADNA-A. For this reason it is necessary to repeat the calculation for every interesting noise direction. This implies a certain number of FdT matrixes one for every wind direction and condition.

To reduce noise at turbine means to reduce output power, because noise control strategies imply a non-optimal use of wind energy. So when noise constraints are not respected at more receivers there is the need to understand what is the most economical turbine to reduce in power, and to calculate what is the power reduction or energy reduction that is generated.

Further to this result it can be interesting to produce a scenario in which, for every single receiver, we can forecast what the possible energy loss is.

Complexity – why a numerical toolkit is needed, limits of commercial software for solving this issues,

All this procedure is rather complex if done for one receiver because it implies the calculation of noise reduction for all wind classes, for all directions, for different sets of turbine noise reduction. The choice of the turbine to reduce in noise isn't immediate because it depends on energy losses.

To do it for two receivers becomes almost impossible due to mutual effects of turbine noise reduction on the receivers. For this reason to calculate the reduction strategies of a large windfarm with a large number of receivers is necessarily a task for a software algorithm.

There are already software that approach this problem. For example Windpro calculates the noise on all the wind curve, and gives an energy reduction due to stop or noise control strategies. The limits of Windpro are that it does not calculate the set of noise control level for every wind class forevery turbine. Further the software is not so flexible in deciding legal constraints. As a matter of facts the constraints that we have described are only for the present situation. If the municipality decides to put in place a background noise law, the coefficients could be strongly reduced and/or differentiated per receiver. In this case while in our case night max limit is supposed to be 60dBA, if there is a background noise niveau this could easily be 10 or 15 dB lower.

Description of algorithm, linearity of ISO 9316 relationship between source levels and effects on the receivers,

The source code is basically built in such a way to load the input data and to process them. The aim is to define the optimized power level according to which each single turbine has to be set to satisfy the noise constraints imposed by law.

The main input data consist in double arrays which contains several kind of information concerning:

- A measure of the noise magnitude with which each single turbine can affect each single receiver (FTrasf Matrix)
- All possible Turbine noise levels related to the imposed power regime and the wind classes chosen for the analysis (Livelli Matrix)
- Background noise measured for each receiver (Fondo Matrix)
- The power loss rate related to the imposed power regime (Perdita Matrix)

A brief picture of those input data can be found in Table 1.

Type	***Array Name***	***rows***	***columns***
Double array	*FTrasf*	*Turbine number*	*Receiver number*
Double array	*Livelli*	*Power level*	*Wind class*
Double array	*Fondo*	*Receiver number*	*Wind class*
Double array	*Perdita*	*Power level*	*Power loss rate*

Table 1 – Arrays used for the software

The initial power level configuration is stored in another double array (TurbinedB Matrix). That variable is periodically updated during the run of the code until the final configuration, which can ensure the respect of the legal noise limits.

By the application of a noise calculation model from TurbinedB Matrix and FTrasf Matrix is possible to estimate the intensity of the noise caused by the turbines at each receiver (L_{eq}, Turbines). Then by a noise addition (sum of the noise power and 10* logarithm to obtain the noise in dB) the code sums the Turbine noise with the background noise, in order to obtain the total noise at the receivers (L_{eq}, Total).

At this point the total noise can be compared with the noise constraints imposed by law both for the nightime and daytime case, considering three different wind regimes (General, Northern Wind, Southern Wind).

If the first test reveals that there’s no problem for every receiver the routine ends giving the final solution. This means that every turbine can be set at the maximum power level. However if noise levels of one or more receivers exceed the noise constraints, the program starts a loop in order to turn down the working power level of some turbines.

The bulk of this problem stays in choosing a suitable strategy which can represent the best power configuration of the wind farm to minimize production loss and of course to respect noise limits.

The problem has been solved by programming an external function (MR function), which can implement a trivial rank sort algorithm.

The function MR works in such a way to forecast different noise scenarios after each single turbine has been weakened, and afterwards it indexes the whole turbine list with a parameter (pp index) based on the expected production loss and the noise drop for one fixed receiver. So the best turbine to be weakened is chosen according to the index values suggested by the MR function. Therefore it passes to a lower noise level emission for the analyzed receiver and, of course, to a lower power regime.

Then the process continues until the final test on the noise constraints isn't satisfied for all the receivers.

Thus, once the code has found one solution it stores the results in the output files.

As explained before we have considered six different cases which refer to three wind regime both for nightime and daytime condition, so the output arrays (Initial and final noise at the receivers and the chosen final power configuration of the windfarm) are written on three files for the six considered cases.

Thus the final output consists in eighteen ASCII files.

A more clear view insight the code can be provided by the following Flow-Chart (Figure 1):

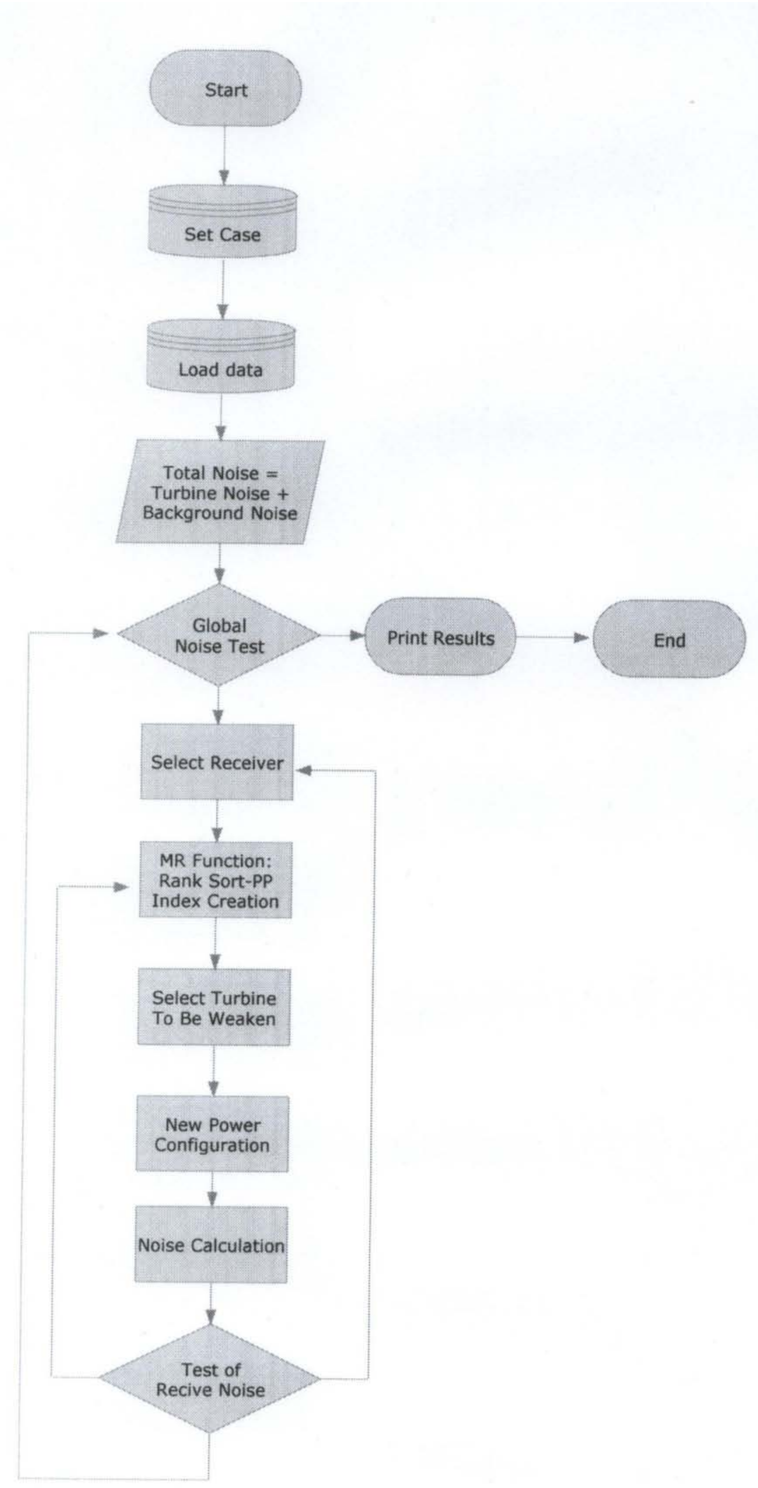

Figure 1 - Flow Chart of The Code

Description of results and remarks

This code represents an easy and quick tool to solve the problem of noise impact, above all, in cases of big wind farms built in wide areas with hundreds of sensible receivers.

Moreover it is quite user friendly because it gives the possibility to change and manage the main input data in form of ASCII files which can be created by simple text editing programs.

On the contrary it has been implemented on PC using a not very sophisticated programming language (MATLAB C) whose interface with the user is only based on text editing.

It offers few occasion to see on the screen the updating of the arrays during the run and unfortunately in complex cases takes long time to give the final solution.

The results show that the more impacted receiver decides Turbines power turning down strategy. That is unavoidable because, even if it's possible to find a solution for the less impacted receivers which minimize production losses, the most impacted receiver would still remain unsolved.

The code can be refined by applying a more sophisticated noise calculation model and a more efficient rank sort and test algorithms which can improve calculation time.

A limit of the software is also the relationship between the wind level at the receiver, and the wind level measured by the wind park meteo station. These are not always well correlated.

Moreover it's also important to test this software on some other different and complex situations in order to better manage cases in which the code can't identify quickly the best turbine to be weakened among several turbines with the same index pp at the end of the rank sort routine.

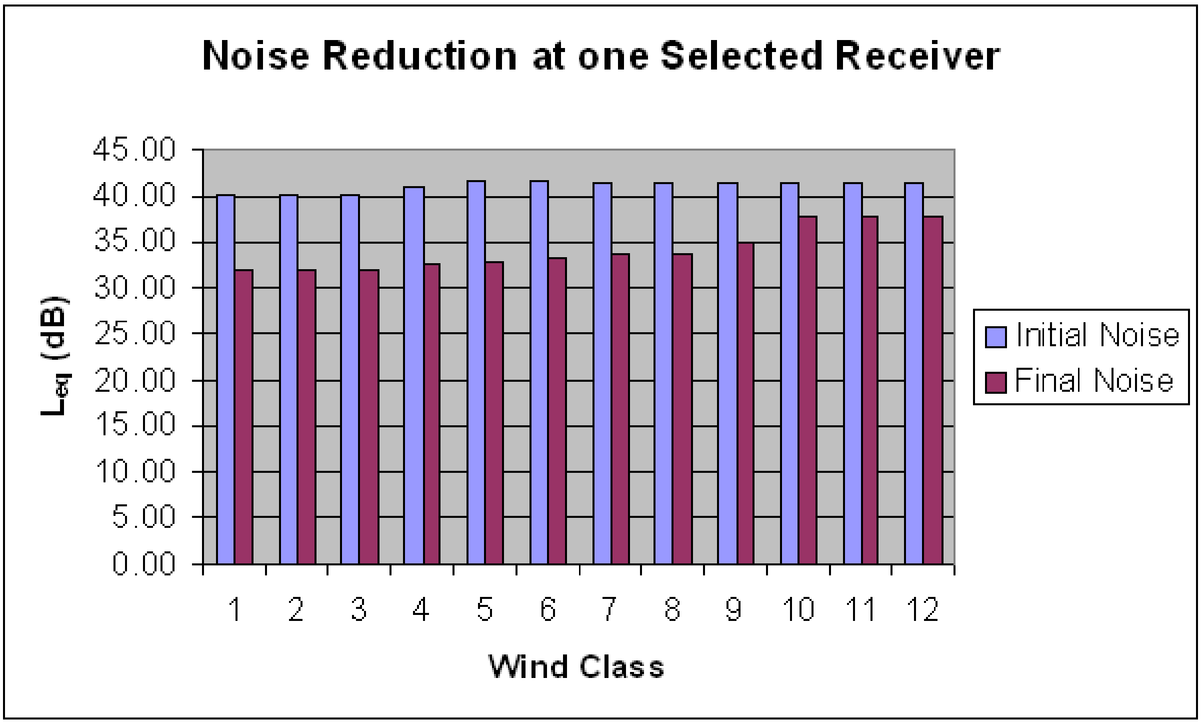

Figure 1 – Noise emission of all turbines at one receiver in function of wind. Final noise represents noise coming from control strategy

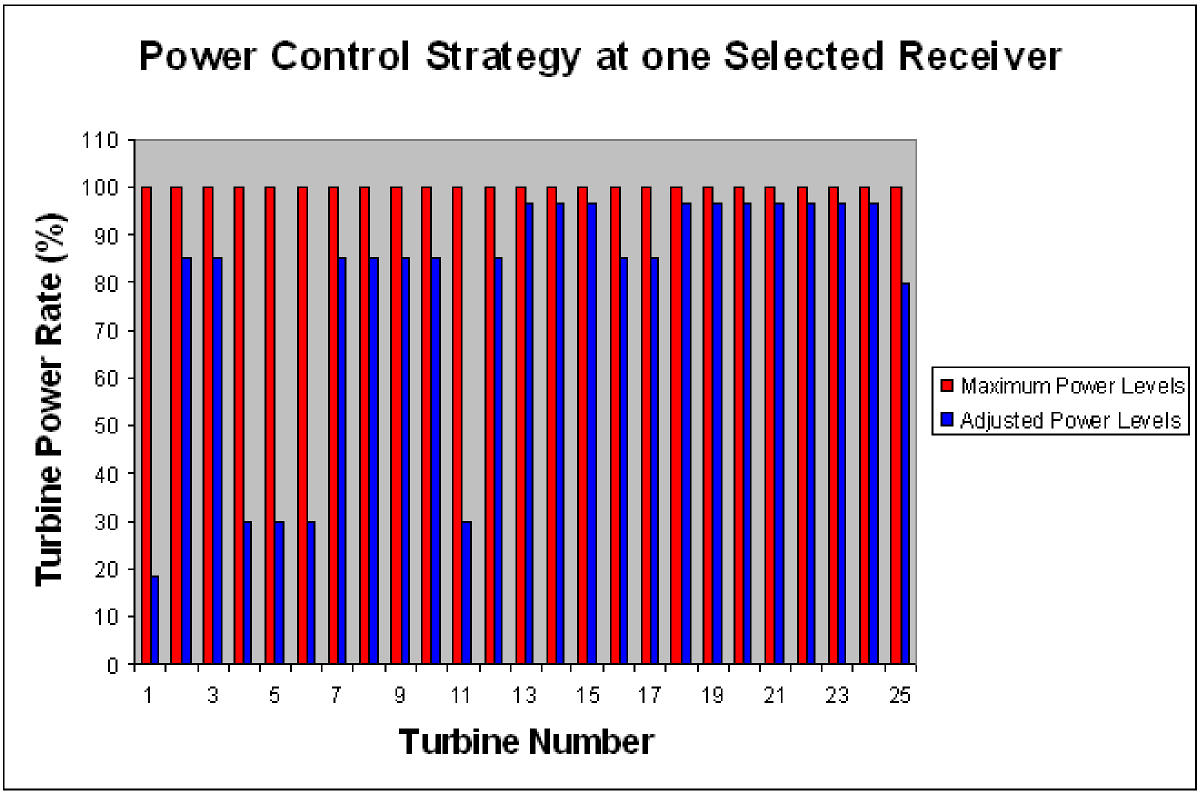

Figure 1 – Example of power level reduction of turbines calculated to comply with legal constraints at one receiver.

References

(Fegeant 99) O. Fegeant: Wind-induced vegetation noise. Part I: A prediction model. Acustica–Acta acustica 85 (1999) 228–240. Part II: Field measurements. Acustica–Acta acustica 85 (1999) 241–249

Third International Meeting
on
Wind Turbine Noise
Aalborg Denmark 17 – 19 June 2009

Oregons Wind Turbine Noise Regulations

Mark Bastasch
CH2M HILL
2020 SW 4th Avenue
Portland, OR 97201
Mark.Bastasch@ch2m.com

Abstract

The State of Oregon's noise regulations were revised to specifically address wind projects in 2004. The States noise regulations require new industrial projects to comply with two requirements, the ambient degradation test and the Table 8 test. The ambient test requires a wind project to demonstrate that the noise level increase resulting from the project will not exceed the existing ambient L50 or L10 by more than 10 dBA or 36 dBA at non-participating landowners. The Table 8 test requires the project to demonstrate that the maximum project noise level will not exceed an L50 of 50 dBA at any residence – participating or not. This paper provides a summary of the rules and developments since their implementation.

Introduction

The permitting of commercial-scale wind turbines had been restricted by noise standards adopted 30 years ago—a time when wind energy development did not exist on Oregon's rural lands. The Oregon noise regulations (Oregon Administrative Rule [OAR] Chapter 340 Division 35) contain two standards that are generally referred to as the "Table 8 test" and the "ambient degradation test" (other portions of the rules address octave and third-octave band limits). The "Table 8 test" refers to Table 8 of the rule (reproduced here as Table 1), which limits the maximum permissible statistical noise levels generated by a project. The "ambient degradation test" limits the increase in the existing L_{10} or L_{50} to a maximum of 10 dBA. The "ambient degradation test" had proved to be the greatest impediment in permitting wind energy facilities. The "ambient degradation test" required extensive monitoring to determine existing (that is, pre-project) noise levels and results in large setbacks from landowners who may be indifferent to the increase in noise and who may directly benefit from project royalties.

The rule contained some potentially helpful procedures to establish variances; however, the Oregon Department of Environmental Quality (DEQ) no longer has the authority or funding to work on noise-related issues. Thus there was no mechanism to establish a variance. The process was further complicated by the fact that energy facilities that exceed a nominal electrical production threshold must obtain a Site Certificate from the Oregon Energy Facility Siting Council (EFSC), a division of the Oregon Department of Energy (ODOE). In issuing a Site Certificate, EFSC must ensure that the facility will comply with the regulations of other agencies, including

DEQ's noise rule. It was determined that EFSC cannot grant a variance or waiver of another agency's rules even when that agency is no longer actively administering their rules. Therefore, on larger projects, the noise rule remained in effect and was enforced through the EFSC site certification process. Projects that do not exceed the nominal electrical production thresholds are not considered "energy facilities" and are subject to a less rigorous permitting process governed primarily by local land use regulations. These smaller projects are likely still at risk if they do not comply with the noise rule; however, DEQ is unlikely to take enforcement action.

In at least one instance the ambient degradation rule as it had been administered by EFSEC prevented a landowner from re-occupying a dwelling on her land notwithstanding the fact that she has stated she does not find the noise bothersome. In another case a home was vacated because the landowner was concerned that occupation would adversely impact or complicate the landowner's chances of being included in a large wind development.

With the support of the Governor's Office of Sustainability, the ODOE established a joint rule making with DEQ to amend the existing noise rule to explicitly address noise standards for wind turbines.

Establishing Minimum Existing Ambient Levels

The relatively calm conditions that are ideal for establishing existing noise levels for other industrial noise sources are not necessarily representative of the existing noise levels when a wind turbine would be expected to generate power and noise. Thus a correlation between background noise level (at the receiver location) and wind speed (preferably at hub height at the proposed turbine location) is necessary to establish the existing noise levels. This creates several challenges. Addressing these issues required extensive monitoring, which proved to be challenging and costly in terms of both equipment and time. Successful implementation would also require a statistical method to analyze the collected data to be legislated to ensure that project proponents and/or opponents do not unfairly skew the results.

To avoid these difficulties, the modified rule establishes a minimum background L_{50} of 26 dBA. This was based in part on field measurements conducted for a Site Certificate application and in part because the resulting limit of 36 dBA was generally consistent with available British and Australian guidance[1,2].

Similar to both the British and Australian guidelines at the time, the changes to the Oregon rule will allow the project developer to submit evidence that the actual existing level is more than 26 dBA. Given the level of effort required to conclusively demonstrate the existing noise levels, many projects in Oregon have not pursued this option.

Establishing Landowner Consent

One of the more significant changes was to allow affected landowners to consent to waive the ambient rule on their properties. The "Table 8" limits—namely an L_{50} of 50 dBA—would apply at the properties of consenting landowners. Landowners who choose not to consent would still be governed by the ambient degradation limit of 10 dBA.

It is very often the case that nearby residents are involved in the project and may not be concerned with noise increases near their homes as a result of the wind facility. Many landowners, including one audiologist, provided testimony to substantiate this. Annoyance from changes in ambient noise levels is subjective, and some rural landowners can be fairly accepting of noise from agriculture, forestry and other natural resource development. “Different individuals have different sensitivities to different types of noise and this probably reflects differences in expectations and attitude … depending almost entirely on personal preferences, lifestyles and attitudes of the listeners and on the context in which the sound is heard[3]”. In many situations the resident potentially affected by noise also would benefit financially from leasing land to the wind development project. Texas Rancher and wind project landowner Louis Woodward is quoted in a Public Citizen brochure: “Yep, they make some noise, but it’s the soothing sound of money being made”.

The ODOE’s December 2003 draft rule language addressing landowner consent was limited. It allowed an increase in the ambient degradation threshold from 10 to 15 dBA provided that the landowner consented and one or more turbines were located on the same parcel of land as the home. Other landowners could not consent to a higher noise limit unless they were granted an “exception” by EFSC or DEQ. The requirement that a turbine be located on the same parcel of land as the home is problematic in rural Oregon where a single landowner may own several parcels of land. Under this proposal, even though turbines were located on parcels under the same ownership as the home, the owner would not be able to consent to the increase in the ambient degradation limit unless a turbine was on the same parcel as the home. It was also unclear as to how DEQ could grant an exception when it no longer has the authority or funding to work on noise-related issues. EFSC would be able to grant an exception only on the larger projects that it has jurisdiction over; thus, it wasn’t clear how an exception could be obtained for smaller projects that fall outside of EFSC jurisdiction.

The ODOE Hearings Officer report revised the rule language to allow all affected landowners the option of entering into a consent agreement. This avoids a potentially complicated exception process and provides certainty needed for financing both large and small wind projects. The report also found that the resulting Table 8 level of 50 dBA for consenting landowners was sufficient to avoid health impacts: “If landowners want to agree to this level of noise for compensation, I see no reason to deny them this ability to do so … this is a reasonable compromise since it provides some flexibility for wind for willing landowners, while maintaining the noise degradation standards for those unwilling to waive this standard[4]”. This provides certainty needed for financing both large and small wind projects.

Incorporating IEC61400-11

Historically ODOE required that wind projects demonstrate that the Table 8 limits were complied with under the maximum operating conditions, typically around 25 m/s. The ODOE’s December 2003 draft rules reduced the wind speed requirement to 16 m/s at hub height. ODOE staff believed that above this wind speed the wind itself would create substantial noise, making it difficult to accurately measure the wind turbine noise. Although somewhat better than 25 m/s, the 16-m/s proposal resulted in several complications.

Most if not all turbine manufacturers provide sound power level data determined in accordance with International Electrotechnical Commission's (IEC) International Standard IEC 61400-11, *Wind Turbine Generator Systems – Part 11: Acoustic Noise Measurement Techniques.* At the time of the rule making, the IEC method established the acoustic reference wind speed of 8 m/s at 10-meter height. Although often misunderstood, this did not require that a measurement be made with 8 m/s winds at a height of 10-meters. Rather, the 10-meter height was part of IEC's calculations to standardize the results for comparison of different turbines and different hub heights.

The modified rule requires the maximum sound power level, determined in accordance with IEC 61400-11, be used to demonstrate compliance with both Table 8 and the ambient degradation limits. This ensures that the maximum sound power level is used for prediction purposes and that measurements (if required) would be conducted when the hub height wind speeds correspond to the maximum noise emissions. While the IEC 61400-11 data may not have disclosed the maximum sound power level of some stall related wind turbines, this data was ultimately obtained.

By referencing the maximum sound power level and IEC 61400-11, the modified rule has ensured that a projects noise level at non-consenting landowners will remain 36 dBA, regardless of turbine type. Most importantly, it has also avoided potential complications resulting from a reference to 10-meter height wind speeds as well as wind shear.

Remarks on the Modified Rule

Comments regarding the implementation of the rule over the past 5 years will be discussed during the presentation of this paper.

Conclusions

The revised Oregon noise rules provide needed flexibility to effectively develop wind farms while providing those individuals that desire it, the same level of protection as was previously afforded. In summary, the proposed rules result in the following changes for wind energy facilities 1) establish a baseline preproject noise level of 26 dBA, 2) provide any willing landowner the ability to waive the 10 dBA ambient degradation standard while maintaining the Table 8 limits (50 dBA), 3) ensure that the maximum sound power level determined in accordance with IEC 61400-11 is used to evaluate project noise during permitting and compliance phases.

Tables

TABLE 1
Oregon's "Table 8 Limits": Maximum Permissible Levels for New Industrial and Commercial Noise Sources

Statistical Descriptor	Daytime (7 a.m. – 10 p.m.) (dBA)	Nighttime (10 p.m. – 7 a.m.) (dBA)
L_{50}	55	50
L_{10}	60	55
L_1	75	60

Source: OAR 340-35-035

TABLE 2
Oregon's Median Octave Band Standards for Industrial and Commercial Noise Sources

Octave Band Center Frequency (Hz)	Daytime (7 a.m.-10 p.m.)	Nighttime (10 p.m.–7 a.m.)
31.5	68	65
63	65	62
125	61	56
250	55	50
500	52	46
1000	49	43
2000	46	40
4000	43	37
8000	40	34

Source: OAR 340-35-035

References

1. Noise Working Group. *The Assessment & Rating of Noise from Wind Farms*. ETSU-R-7. (September 1996).

2. *Environmental Noise Guidelines: Wind Farms*. Environmental Protection Authority of South Australia. (February 2003).

3. L. Finegold. "Recommendations for an Expanded Environmental Noise Impact Assessment and Mitigation Process." *Proceedings of InterNoise 02*. Dearborn, MI. (2002).

4. Michael W. Grainey. "Draft Hearings Officer Report to the Oregon Environmental Quality Commission On Noise Rulemaking Standards for Wind Energy Facilities." Prepared by Michael W. Grainey, Director of the Oregon Department of Energy. March 22, 2004. Viewed online April 15, 2004, at http://www.energy.state.or.us/renew/Wind/Noise/Hearing_Officer_Report.pdf.

Third International Meeting
on
Wind Turbine Noise
Aalborg Denmark 17 – 19 June 2009

Comparison and Validation of Trailing Edge Noise Models

Franck Bertagnolio, Helge Aa. Madsen, Christian Bak
Wind Energy Division, Risø-DTU National Laboratory for Sustainable Energy
P.O. Box 33, DK-4000 Roskilde, Denmark
franck.bertagnolio@risoe.dtu.dk; Helge.Aagard.Madsen@risoe.dtu.dk; Christian.bak@risoe.dtu.dk

Abstract

The aim of this work is the comparison and validation of two trailing edge noise models from the literature. The models assumptions and formulations are shortly reminded and their differences emphasized. Measurements of surface turbulent pressure, which constitutes an intermediate component in the formulation of both models, are used for comparisons. Far field noise levels measured in various experiments are then considered as a second validation test for the models. Conclusions are drawn concerning the respective quality of the models.

1 Introduction

In order to increase public acceptance of wind turbines, there is a strong need to reduce their noise emission. There is a general agreement that one of the main sources of high-frequency noise originates from the scattering of aerodynamic noise at the trailing edge of the blades.

There exist various models that can be used to predict the acoustic noise radiated from an airfoil trailing edge[1,2,3]. In this paper, two models are compared and validated against various experimental results. The theoretical foundations behind each model are analogous, however the mathematical approach used to numerically solve the problem differs.

The first so-called TNO model was originally proposed by Parchen[4]. It is based on an approximate solution of the Poisson equation for the turbulent boundary layer pressure field giving access to the airfoil surface pressure (see Blake[5] for details). Various hypotheses are used to facilitate the solution procedure and express the contribution of the Lighthill tensor which appears as a source term in the previous equation.

The second considered model was recently proposed by Glegg *et al* [6]. It is also based on a solution of the turbulent boundary layer problem. However, in this case, the whole turbulent velocity field is determined first. Then, the pressure field can be solved using the same Poisson equation for pressure turbulent fluctuations as for the previous model, but this time no approximation is needed for defining the source term (apart from its linearization) since the flow velocity is known. Instead, approximations are made when establishing a solution to the Navier-Stokes equations to determine the velocity field.

From the knowledge of the surface pressure near the trailing edge obtained with the above two models, it is possible to express the acoustic noise scattered by the trailing edge in the far field using a theory originating from the work of Ffwocs-Williams and Hall[7]. It was subsequently improved by various authors[8,9] as summarized and unified by Howe[10]. The simplified formula by Brooks and Hodgson[14] is used.

The goal of this paper is to compare the two approaches by a detailed analysis of the numerical results obtained with the two models. At the same time, these data are validated against available measurements from the literature, involving both pressure measurements on airfoil surfaces (with microphones mounted beneath their surface) and far field noise measurements.

The paper is organized as follows. The second section describes both models formulations. The procedures to obtain these formulae are not reported here since these are quite lengthy and involve rather complicated developments. The reader is referred to the original papers for details. The second section is dedicated to surface pressure measurements performed in the LM wind tunnel. The third section is concerned with the NACA0012 airfoil and far field noise measurements in two anechoic wind tunnels, as well as surface pressure measurements in one case. In the fourth section, the model results are compared to those of a Computational Aero-Acoustic code.

2 Models Formulations

2.1 TNO Model[4,11]

This model originally proposed by Parchen[4] is gathering several results from previous studies. These are used to formulate a far field noise Sound Pressure Level (SPL) expression as a function of turbulent boundary layer characteristic quantities.

In more detail, the first part of the model is based on a formula expressing the contribution of the mean-shear/turbulence interaction in the boundary layer, which relates the turbulent boundary layer characteristic quantities to the fluctuating surface pressure (see Blake[5]). Manipulating the previous formula, Parchen[4] arrived to the following result for the wavenumber-frequency surface pressure spectrum:

$$\Phi_P(k_1,k_3,\omega) = 4\rho_0^2 \frac{k_1^2}{k_1^2+k_3^2} \int_0^{+\infty} L_2\, \overline{u_2^2} \left(\frac{\partial U_1}{\partial y_2}\right)^2 \Phi_2\, (k_1,k_3,L_2)\, \Phi_m\left(\omega - U_C\, k_1\right) e^{-2|\boldsymbol{k}|y_2} \mathrm{d}y_2$$

where the subscripts 1, 2, 3 denote directions parallel to the airfoil surface in the main flow direction, perpendicular to the surface, and along the trailing edge, respectively, $|\boldsymbol{k}|$ is the norm of the 'surface' wavenumber $\boldsymbol{k} = \{k_1, 0, k_3\}$, ω is the circular frequency, ρ_0 is the density, $L_2(y_2)$ is the vertical integral length that characterizes the vertical extent of the turbulent eddies, $\overline{u_2^2}(y_2)$ is the vertical velocity Reynolds stress component assumed proportional to the turbulent kinetic energy $k_t(y_2)$, $U_1(y_2)$ is the streamwise mean velocity (its derivative, the mean shear, actually appears in the integral), Φ_{22} is the spectrum of the vertical velocity fluctuations (modeled using the classical Von Karman theory, and depending as well on y_2 through L_2), Φ_m is the so-called moving-axis spectrum that describes how Φ_{22} is distorted by the generation and destruction of eddies during their convection past the trailing edge, and $U_C(y_2)$ is the convection velocity of these eddies. The various quantities involved in the previous formula can be deduced from a fluid flow solver (such as for the velocity profile) or from theoretical results (usually assuming isotropy as for Φ_{22}), or a combination of both. Turbulent kinetic energy is directly available from a Computational Fluid Dynamics (CFD) code or can be related to the mean shear[11] if using a coupled inviscid-integral boundary layer code such as XFOIL[12]. As for the integral length scale, the approach followed by Lutz *et al* [13] is implemented when using CFD, otherwise it is determined using Prandtl theory [11]. The remaining quantities are defined as specified in the model implementation by Moriarty *et al* [11].

2.2 Model by Glegg *et al* [6]

The approach proposed by Glegg *et al* [6] considers as a starting point the turbulent boundary layer Navier-Stokes equations. The model is based on an analytical solution of these equations for the turbulent fluctuations in the Fourier space. Such a solution can be obtained by assuming incompressibility, linearizing the set of equations, neglecting viscous effects, assuming homogeneity in planes parallel to the surface and that these planes can be individually considered as uncorrelated vortex sheets. In addition, the spectral content of each sheet is also assumed using isotropic turbulence results. To close the model, the resulting turbulent kinetic energy across the boundary layer is calibrated so that it matches computational or experimental results from an exterior source (such as a CFD code). Once the flow turbulent velocity field is known, a solution for the pressure field is obtained by solving the Poisson equation (with linearized source term, i.e. by only considering mean-shear/turbulence interaction and neglecting the turbulence/turbulence one) using Green's functions.

The first main result of this formulation is the expression of the turbulent kinetic energy k_t across the boundary layer:

$$k_t(x_2) = \int_0^{\delta_{\mathrm{BL}}} A(y_0)\left[Q_s(y_0, x_2) + Q_w(y_0)\delta(x_2 - y_0)\right]\mathrm{d}y_0$$

where δ_{BL} is the boundary layer thickness, y_0 is an integration variable across the boundary layer, $A(x_2)$ is a calibration function across the trailing edge that will be specified later, and $\delta(x_2)$ is the Dirac function. The two functions used in the integral reads:

$$Q_s(y_0, x_2) = \frac{\pi}{2}\int_0^{+\infty} E\left(\lambda L_2(y_0)\right) 2q_s(y_0, x_2, \lambda)\,\lambda\,\mathrm{d}\lambda$$

$$Q_w(y_0) = \frac{\pi\, U_1'(y_0)}{2\,\delta_{\mathrm{BL}} U_1''(y_0)}\int_0^{+\infty} E(\lambda L_2)\,\lambda\,\mathrm{d}\lambda$$

where $\lambda = \sqrt{k_1^2 + k_3^2}$ is a wavenumber, $E(\lambda L_2)$ is a function characterizing the turbulent kinetic energy spectrum, L_2 is the vertical integral length defined earlier, and the prime $'$ denotes a derivative with respect to x_2. The function q_s is defined as:

$$q_s(y_0, x_2, \lambda) = e^{-2\lambda|x_2 - y_0|} + e^{+2\lambda|x_2 - y_0|} + 2H(x_2 - y_0)e^{-2\lambda x_2}$$

where $H(x_2)$ is the Heaviside function. The previous equations can be discretized, yielding a matrix product in the form:

$$\sum_{n=1}^{N} Q_{mn} A_n = k_m \qquad \text{for } m \in \{1, \ldots, N\}$$

where N is the number of discretization points across the boundary layer, k_m and the coefficients A_n corresponds to the turbulent kinetic energy k_t (assumed to be known) and calibration factor $A(x_2)$ (to be calculated), respectively, at these points. Inverting this matrix yields the calibration coefficients. These calibration factors being given, it is possible to express the turbulent velocity flow field across the boundary layer.

A Poisson equation for the turbulent pressure fluctuations can be obtained by taking the divergence of the Navier-Stokes equations. After linearization, it reads:

$$\nabla^2 p = -2U_1'(x_2)\frac{\partial u_2}{\partial x_1}$$

where p is the fluctuating pressure. Transforming this equation in the k_1-k_3 Fourier space and using the Green's functions methodology, an analytical solution can be obtained. The resulting pressure spectrum at the wall surface reads:

$$\Phi_p(k_1, k_3, \omega) = \int_0^{\delta_{\mathrm{BL}}} A(y_0) E\left(\lambda L_2(y_0)\right) P_E\left(y_0, \lambda\right) \left(\frac{k_1}{\lambda}\right)^4 \delta\left(\omega + kU_1(y_0)\right) \mathrm{d}y_0$$

where the function P_E is defined as:

$$P_E\left(y_0, \lambda\right) = \int_0^{\delta_{\mathrm{BL}}} U_1'(y)\left(e^{-\lambda|y-y_0|} + e^{-2\lambda|y+y_0|}\right) \mathrm{d}y$$

The spectrum $E(\lambda L)$ characterizing the turbulent kinetic energy spectrum is defined as an extension of the Von Karman spectrum as:

$$E\left(\lambda L\right)\lambda L = \left(1 + \frac{c}{\lambda L}\right)\frac{(\lambda L)^4}{\left(1 + (\lambda L)^2\right)^{17/6}}$$

where the constant c is set to 0.5 (The Von Karman spectrum is recovered by setting $c = 0$). Note that in the original paper by Glegg *et al* [6], this constant was set to 0.05, but this proved to be far too small in our case to produce consistent results. The effect of this modification of the original Von Karman spectrum is to increase the relative contribution of larger vortices, i.e. that the low-wavenumber part of the spectrum is amplified.

2.3 From Surface Pressure to Far Field Noise

Both models use the same approach for calculating the far field noise as a function of the previously calculated wavenumber-frequency spectrum of the surface pressure fluctuations. According to the formula by Brooks and Hodgson[14], the far field acoustic pressure spectrum can be expressed as an integral of the wall pressure spectrum over the wavenumber component in the flow direction:

$$S(\omega) = \frac{L}{4\pi R^2} \int_{-\infty}^{+\infty} \frac{\omega}{C_0 k_1} \left(\Phi_P(k_1, k_3, \omega) \right)_{k_3=0} \, \mathrm{d}k_1$$

where R denotes the distance from the trailing edge to the observer (located 90° with respect to the main flow direction above the trailing edge), L the span extent of the trailing edge, and C_0 is the speed of sound. The Sound Pressure Level (SPL) in decibels can then be calculated using the formula:

$$SPL(f) = 10 \, \log_{10} \left[2\pi \, \Delta f \; S(\omega) / (2 \times 10^5)^2 \right]$$

where Δf is the chosen frequency band-width distribution used to express the SPL.

In addition, note that the frequency spectrum of the surface pressure can be easily deduced from the wavenumber-frequency spectrum by integrating over the whole wavenumber space:

$$\Phi_p(\omega) = \int_{-\infty}^{+\infty} \int_{-\infty}^{+\infty} \Phi_P(k_1, k_3, \omega) \, \mathrm{d}k_3 \mathrm{d}k_1$$

which can be performed numerically.

Note that for all numerical results presented in this work (unless specified as in Section 5), fluid flow calculations used to define the different flow parameters in the above described models are performed with the in-house two-dimensional incompressible Reynolds-Averaged Navier-Stokes CFD code EllipSys2D. The k-ω SST model by Menter[15] is used as a turbulence model. The e^N transition model by Drela and Giles[16] is used when transition is set free in the experiment with which the models are compared. The reader is referred to previous publications for details about this code[17,18,19].

3 LM Wind Tunnel Surface Pressure Measurements

LM Glasfiber's wind tunnel is designed for the testing of wind turbine airfoils[20]. The actual test section dimensions are 1.35m in width, 2.70m in height, and 7m in length. Two airfoil sections are considered in this work: the NACA0015 and the wind turbine designed airfoil RISØ-B1-18[21]. These were instrumented with an array of high-frequency microphones mounted beneath their surface. Two inflow velocities, V_∞=50 and 100m/s resulting in Reynolds numbers based on the airfoil chord equal to *Re*=3×10^6 and 6×10^6, and various angles of attack before stall are considered in this section.

In the absence of turbulence grid, a previous study showed that the inflow turbulence intensity is quite small[20]. Hot-wire measurements analysis revealed that it is roughly of the order of 0.1% at all wind tunnel inflow velocities. All measurements data presented here were obtained for the configuration where no turbulence grid was present in the wind tunnel.

Figure 1 and Figure 2 display surface pressure for *Re*= 3×10^6 and 6×10^6, respectively, at the chordwise position *x/C*=0.567 and for 4 different angles of attacks α=0,4,8,12^o for the NACA0015 airfoil section. As it can be seen, the models (in particular Glegg *et al*'s model) largely overestimate the measured spectrum at zero angle of attack for higher frequencies. But as the angle of attack increases, both models predict quite well the measured spectra for frequencies larger than 100 to 1000Hz depending on the cases. The quite good prediction of the spectra slopes compared to the measured ones at higher frequencies and for larger angles of attack indicates that the isotropy assumption might be reasonable in these cases. A generally observed tendency concerning the spectra is the increase of spectral intensity and a decrease of the spectrum peak frequency as the angle of attack increases, which is correctly reproduced by the models. Measured pressures at lower frequencies from which the models depart significantly might be largely influenced by ambient sound waves and other acoustic disturbances present in the wind tunnel (which is not anechoic). It could as well originate from measurements noise present in the microphones electrical or recording system.

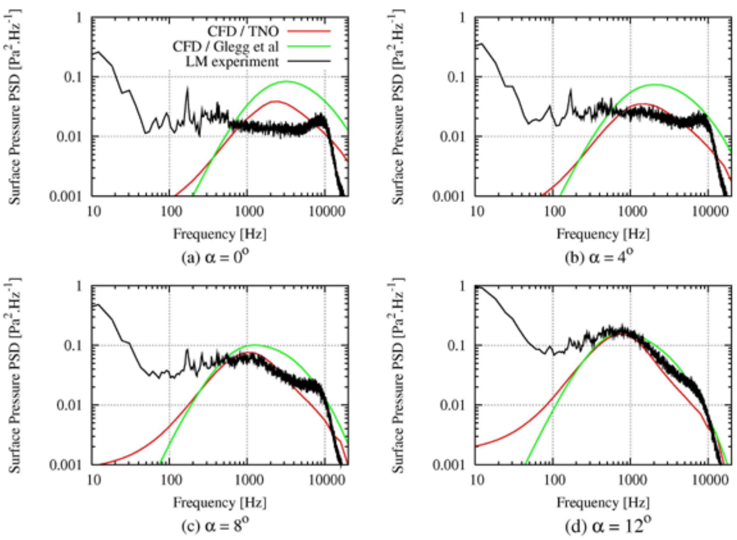

Figure 1 – NACA0015 – LM Experiment – *Re* = 3×10^6 - *x/C* = 0.567

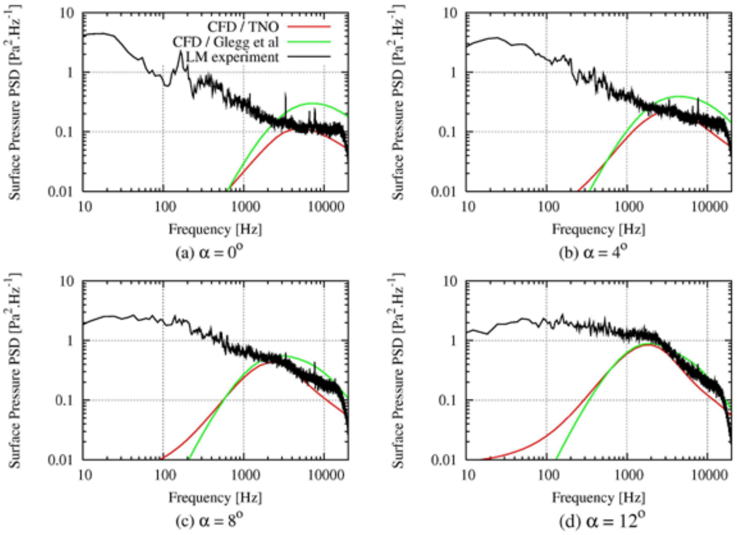

Figure 2 – NACA0015 – LM Experiment – *Re* = 6×10^{6} **- *x/C* = 0.567**

The same spectra as above are now displayed for the RISØ-B1-18 airfoil in Figure 3 and Figure 4 at the chordwise location *x/C*=0.833. The largest considered angle of attack is now α=10°, instead of 12°, as this airfoil stalls at lower angle of attack than the NACA0015. Stall is characterized by large shed vortices which generate powerful (incompressible) pressure waves that are captured by the microphones, but which the models are not designed to predict. In such case (not displayed here), the measured surface pressures largely exceed the model results. Nevertheless, the same conclusions drawn for the NACA0015 airfoil can be applied to the RISØ-B1-18 case.

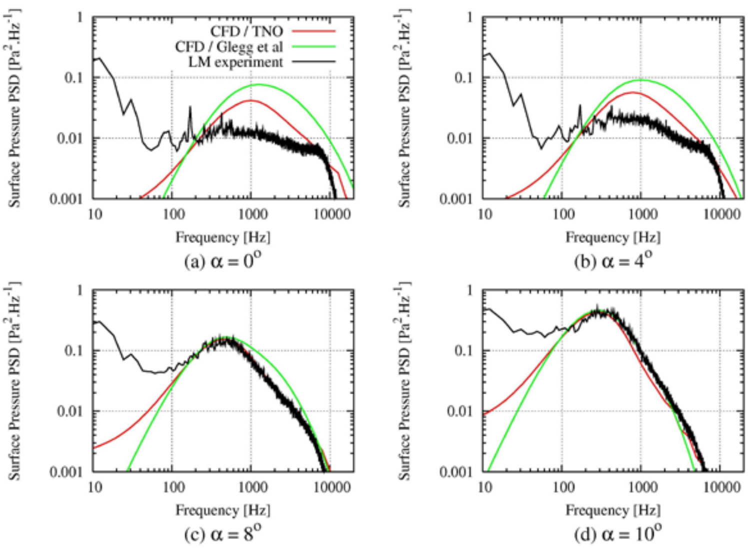

Figure 3 – RISØ-B1-18 – LM Experiment – *Re* = 3×10^{6} **- *x/C* = 0.833**

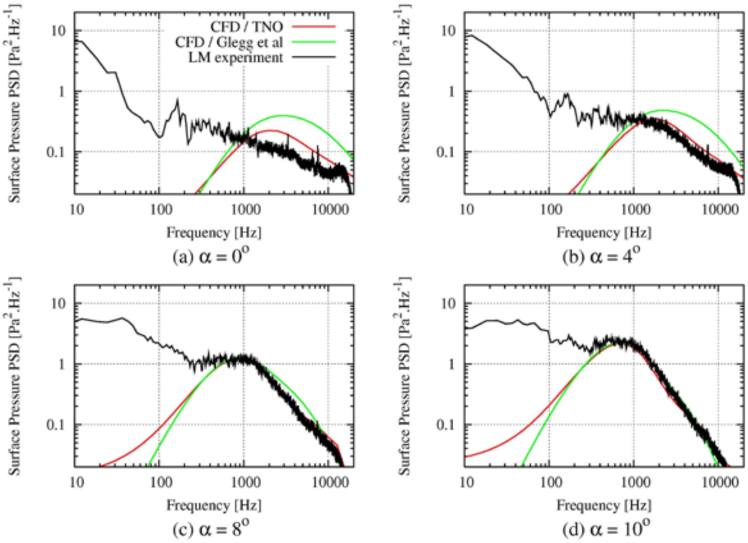

Figure 4 – RISØ-B1-18 – LM Experiment – *Re* = 6×10^6 - *x/C* = 0.833

The evolution of the surface pressure along the airfoil chord is investigated for the RISØ-B1-18 airfoil. Figure 5 and Figure 6 display the surface pressure spectrum for angles of attack α=4 and 8°, respectively, for *Re*=3×10^6. The following chord locations are considered: *x/C*=0.543, 0.688, 0.736 and 0.833. It can be seen for the lowest angle of attack that the overestimation of the spectra observed earlier is independent of the chord location, whereas for the higher angle of attack the spectra are well predicted at all considered chord positions.

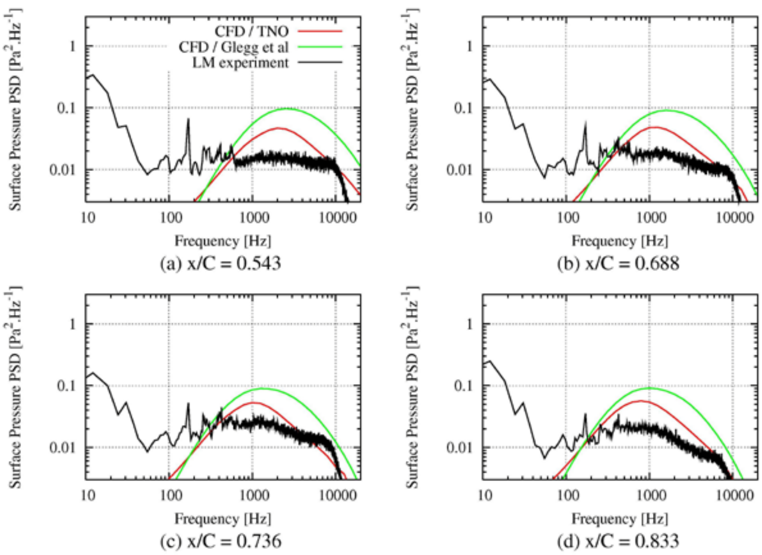

Figure 5 - RISØ-B1-18 – LM Experiment – *Re* = 3×10^6 - α = 4°

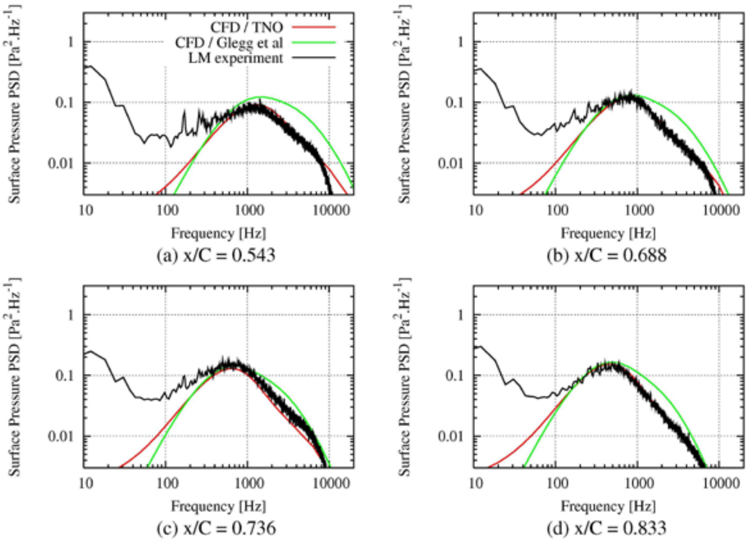

Figure 6 - RISØ-B1-18 – LM Experiment – *Re* = 3×10^6 - α = 8°

In view of the previous results and focusing on comparing the two models, it seems that the TNO model performs generally better. However, in a few cases the Glegg *et al*'s model performed slightly better (see Figure 1(d) and Figure 2(d)).

The overestimation of the surface pressure spectra at lower angles of attack may be caused by different mechanisms. A first possibility is the influence of transition. Indeed, at low angles of attack, the transition location may be located far downstream along the airfoil chord (in particular at low Reynolds numbers), and it can be difficult for the transition model implemented in the CFD code to accurately predict the transition location. Missing the correct transition location influences the development of the turbulent boundary layer further downstream and thereby the turbulence characteristics near the trailing edge required for the above models. At higher angles of attack, the rapid acceleration of the flow around the leading edge from the stagnation point to the suction side usually results in transition to turbulence relatively close to the leading edge, in any case far from the trailing edge, and therefore the turbulence characteristics at the trailing edge might be better estimated in this case. Experimental conditions for which the transition was tripped were investigated, but no significant improvement was observed in the results, possibly ruling out the above explanation.

A second possibility could be the spectral characteristics of turbulence. As the angle of attack increases, the turbulent boundary layer will rapidly thicken near the trailing edge and it could be that the assumptions made when deriving the models, in particular the isotropic turbulence assumption, might be more valid when the boundary layer is thicker.

At last, both model derivations only consider mean-shear/turbulence interaction as a source of surface pressure fluctuations. It might be that the neglected turbulence/turbulence interaction plays a significant role, as it was proven to be the case for certain flow configurations[22], at lower angles of attack. Note that the introduction of this second mechanism would decrease the surface spectral intensities at low angle of attack (as desired if one wants to improve the models results) only if the two interaction mechanisms (mean-shear/turbulence and turbulence/turbulence) are coherent in some way. Otherwise, this would only increase the spectral intensities and worsen the results.

4 NACA0012 Measurements in Anechoic Wind Tunnels

In this section, two different experiments in anechoic wind tunnel involving the NACA0012 airfoil section are considered.

4.1 NASA Langley Measurements

The first one was conducted in the anechoic quiet-flow facility at NASA Langley Research Center. The results presented in this report were reported in the paper by Brooks and Hodgson[14]. The tunnel consists of a free jet originating from a nozzle with rectangular exit dimensions of 0.3x0.46m. The test airfoil placed in this jet has a chord of 0.62238m and a span of 0.46m. Note that the previous chord is measured with an additional sharp trailing edge extension. The original profile with blunt trailing edge is slightly shorter. Measurements presented in this report are always performed with the sharp trailing edge.

A series of pressure sensors were mounted under the airfoil surface near the trailing edge. The chord locations of the sensors for which data are displayed in this work are: x/C=0.648, 0.773, 0.876 and 0.97. The radiated noise was measured with a series of microphones located in the plane perpendicular to the airfoil mid-span. The far field trailing edge noise is extracted using a cross-spectral analysis technique. Two inflow velocities V_∞=38.6 and 69.5m/s (resulting in Reynolds numbers equal to *Re*=1.6×10^6 and 2.9×10^6) and two angles of attack are considered: α=0 and 5^o.

Figure 7 displays the surface pressure spectra at zero angle of attack and for the highest inflow velocity. It can be seen that none of the models accurately predicts the measurements. Since the present experimental conditions (apart from the wind tunnel itself) are not very different than in Section 3, as far as Reynolds and Mach numbers are concerned, the possibility of the use of different conventions for displaying the spectra could be suspected. Nevertheless both models seem to correctly predict the increase of spectral intensity and the decrease of the spectrum peak frequency as one gets closer to the trailing edge.

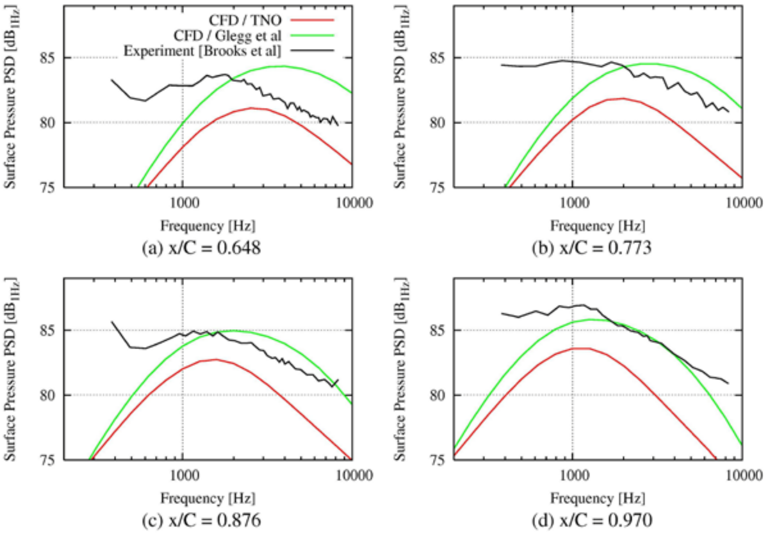

Figure 7 - NACA0012 - Brooks *et al* Experiment – α = 0^{o} – *Re* = 2.9×10^{6}

Figure 8(a) and (b) display the far field noise spectra (in term of SPL) at angles of attack respectively equal to 0 and 5^{o}. In this case, it is quite clear that the Glegg *et al*'s model provides much better prediction of the measured spectra than the TNO model, which significantly underestimates the measurements. It must be noted that it is in accordance with the fact that the former model predicted higher surface pressure spectral intensities than the later one (see Figure 7).

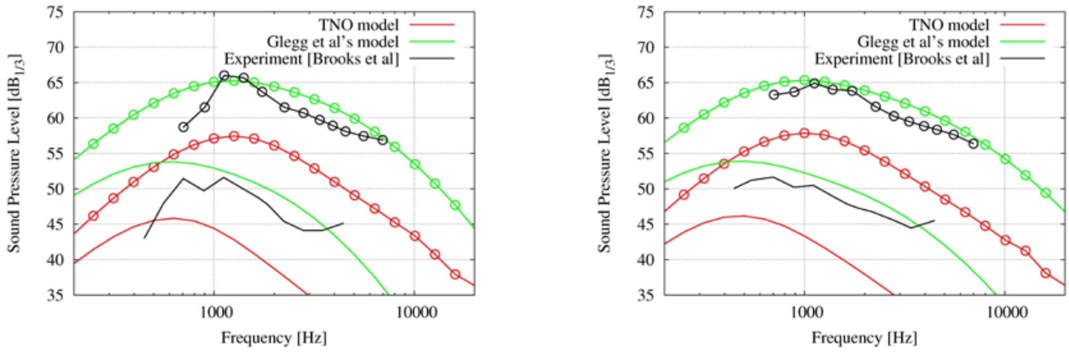

(a) α = 0^{o} **(b) α = 5^{o}**

Figure 8 – NACA0012 - Brooks *et al* Exp. (No point: *Re*=1.6×10^{6}; With points: *Re*=2.9×10^{6})

4.2 AWB Measurements

The second experiment was performed in the Aeoroacoustic Windtunnel Braunschweig (AWB) facility at the Institute für Aerodynamik und Strömungstechnik (DLR) and reported by Herr [23]. The acoustic measurement device consists of an elliptic mirror system. The considered measurements involve the 0.4m chord

NACA0012 airfoil at zero angle of attack and for wind speeds equal to 40 and 60m/s corresponding to *Re*=1.1×10^6 and 1.6×10^6, respectively.

Far field SPL at α=0^o are displayed in Figure 9(a) and (b). As in the previous section, a similar offset of the SPLs is observed between the TNO and the Glegg *et al*'s model. Again, the latter model is in quite better agreement with the measurements. Nevertheless, both models reproduce the tendencies of the measurements (increase of SPL and of the spectrum peak frequency) with respect to increasing velocity.

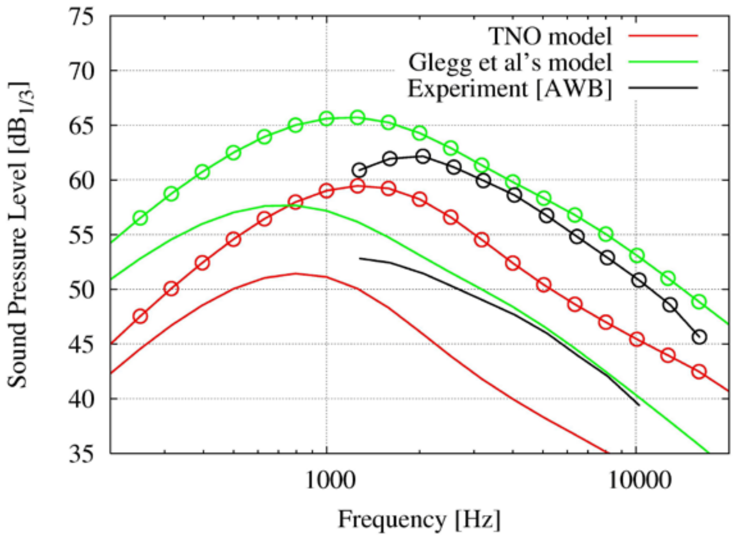

Figure 9 – NACA0012 - AWB Exp. – α = 0^o (No point: *Re* =1.1×10^6; With points: *Re* =1.6×10^6)

5 Computational Aero-Acoustic Calculations of NACA0015

In this section, the trailing edge noise models are compared with results from a Computational Aero-Acoustic (CAA) code. This code combines in a decoupled manner a Large Eddy Simulation code for the incompressible flow and a Direct Numerical Simulation of the compressible Navier-Stokes equations that resolves the acoustic waves propagation (see Shen and Sørensen[24] for details on the algorithm). The case of a NACA0015 airfoil at an angle of attack α=4^o and for a Reynolds number equal to *Re*=0.1×10^6 performed by Zhu[25] is considered. This corresponds to an airfoil with a chord of 0.022m at an inflow velocity of 68.6m/s. The acoustic field was calculated for a Mach number equal to 0.2.

In this section, the TNO and Glegg *et al*'s models are fitted with input data originating from the LES calculation in order to check to which extent the results from the CFD calculations (which use a Reynolds-Averaged Navier-Stokes approach) that have been used so far may corrupt the predicted far field noise. From the LES unsteady calculation, the following time-averaged data are extracted near the trailing edge: boundary layer thickness δ_{BL}, the velocity profile across the boundary layer U_1 (from which the mean shear is deduced), and the turbulent kinetic energy k_t across the boundary layer. To complete the model input data, the integral length scale is still needed. It is deduced from Schlichting approximation for the mixing length scale[26] divided by the Karman constant κ=0.41.

Figure 10 displays the SPL obtained with the CAA code as well as model results obtained either with the classical CFD calculation or with input data from the LES calculation. As it can be seen the latter approach (with LES input data) noticeably improves the results, in particular for the TNO model, compared to the CAA results which may be considered as a reference. It was shown in a previous work[27] that the improvement mainly originates from the turbulent kinetic energy and the integral length scales which are underestimated by the CFD calculation in this case. Note that these poor results might be attributed to the quite low Reynolds number of this test case.

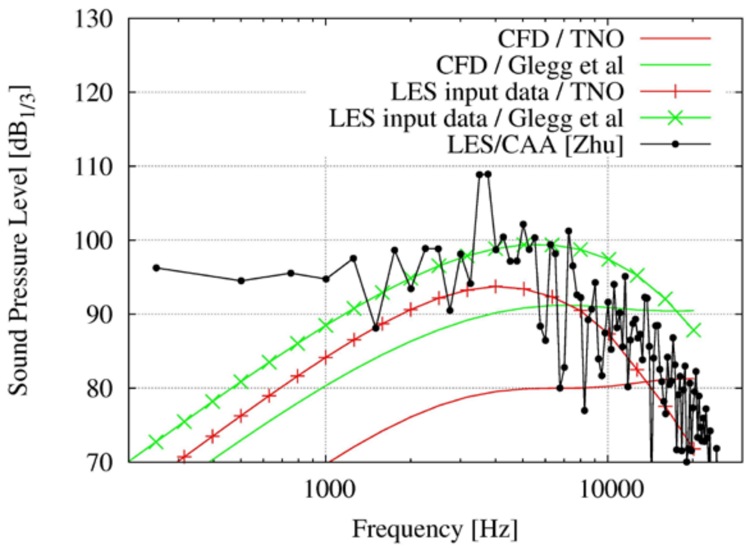

Figure 10 – NACA0015 – *Re*= 0.1×10^6 **-** α **= 4°**

6 Conclusions

Two trailing edge noise models from the literature, namely the TNO model[4] and Glegg *et al*'s model[6], were implemented and compared with various experimental and numerical results.

Surface pressure spectra predicted by the models showed quite good agreement compared to measured ones in one case (Section 3). Small discrepancies were observed at lower angles of attack and various possible explanations for these discrepancies were given. They relate to the assumptions made for deriving the models. In a second case (Section 4.1), surface pressure measurements didn't really allow for clear conclusions.

Relative comparison of the two models suggests that the TNO model performs better for surface pressure prediction, whereas the Glegg *et al*'s model proved to be superior in predicting the far field noise. This could indicate that the theory on which is based the expression of the far field noise as a function of the surface pressure (see Section 2.3) is deficient in some way.

Further investigations of the assumption made in the models, as well as evaluations of the turbulent quantities used in the model formulae, are under way in order to estimate the models respective validity and improve their prediction capabilities.

References

[1] Brooks, T.F., Pope, S.D., and Marcolini, M.A. (1989) “Airfoil Self-Noise and Prediction”, Tech. Rep., NASA Reference Publication 1218, Langley Research Center.

[2] Amiet, R.K. (1976) “Noise due to Turbulent Flow Past a Trailing Edge”, J. Sound Vib., Vol.47, No.3, pp.387-393.

[3] Fukano, T., Kodama, Y., and Senoo, Y. (1977) “Noise Generated by Low Pressure Axial Flow Fans, I: Modeling of the Turbulent Noise”, J. Sound Vib., Vol.50, No.1, pp.63-74.

[4] Parchen, R. (1998) “Progress report DRAW: A Prediction Scheme for Trailing-Edge Noise Based on Detailed Boundary-Layer Characteristics”, TNO Rept. HAG-RPT-980023, TNO Institute of Applied Physics, The Netherlands.

[5] Blake, W.K. (1986) Mechanics of Flow-Induced Sound and Vibration, Vol.II, in Applied Mathematics and Mechanics, Frenkiel, F.N. and Temple, G. (eds.), Academic Press.

[6] Glegg, S., Morin, B., Atassi, O., and Reba, R. (2008) “Using RANS Calculations of Turbulent Kinetic Energy to Provide Predictions of Trailing Edge Noise”, 14th AIAA/CEAS Aeroacoustics Conference (Proc.), AIAA-2008-2993, Vancouver.

[7] Ffowcs Williams, J.E., and Hall, L.H. (1970) “Aerodynamic Sound Generation by Turbulent Flow in the Vicinity of a Scattering Half Plane”, J. Fluid Mech., Vol.40, No.4, pp.657-670.

[8] Chandiramani, K.L. (1974) “Diffraction of Evanescent Waves with Applications to Aerodynamically Scattered Sound and Radiation from Unbaffled Plates”, J. Acoust. Soc. Am., Vol.55, No.1, pp.19-29.

[9] Chase, D.M. (1972) “Sound Radiated by Turbulent Flow off a Rigid Half-Plane as Obtained from a Wavevector Spectrum of Hydrodynamic Pressure”, J. Acoust. Soc. Am., Vol.52, pp.1011-1023.

[10] Howe, M.S. (1978) “A Review of the Theory of Trailing Edge Noise”, J. Sound Vib., Vol.61, No.3, pp.437-465.

[11] Moriarty, P., Guidati, G., and Migliore, P. (2005) “Prediction of Turbulent Inflow and Trailing-Edge Noise for Wind Turbines”, AIAA Paper 2005-2881, Proc. of the 11th AIAA/CEAS Aeroacoustics Conf., Monterey.

[12] Drela, M. (1989) “XFOIL: An Analysis and Design System for Low Reynolds Number Airfoils”, in Low Reynolds Number Aerodynamics, Mueller, T.J. (ed.), Lecture Notes in Engineering, Springer-Verlag, Berlin, Vol.54, pp.1-12.

[13] Lutz, T., Herrig, A., Würz, W., Kamruzzaman, and Krämer, E. (2007) "Design and Wind-Tunnel Verification of Low-Noise Airfoils for Wind Turbines", AIAA Journal, Vol.45, No.4, pp.779-785.

[14] Brooks, T.F., and Hodgson, T.H. (1981) "Trailing Edge Noise Prediction from Measured Surface Pressures", J. Sound Vib., Vol.78, No.1, pp.69-117.

[15] Menter, F.R. (1993) "Zonal Two-Equations k-w Turbulence Models for Aerodynamic Flows", AIAA Paper 93-2906.

[16] Drela, M. and Giles, M. B., ``Viscous-Inviscid Analysis of Transonic and Low Reynolds Number Airfoils'', AIAA Journal, Vol.25, No.10, pp.1347-1355, 1987.

[17] Michelsen, J.A. (1992) "Basis3D - A Platform for Development of Multiblock PDE Solvers", Technical Report AFM 92-05, Technical University of Denmark.

[18] Michelsen, J.A. (1994) "Block Structured Multigrid Solution of 2D and 3D Elliptic PDE's'', Technical Report AFM 94-06, Technical University of Denmark.

[19] Sørensen, N.N. (1995) "General Purpose Flow Solver Applied to Flow over Hills", PhD Thesis, Risø-R-827-(EN), Risø National Laboratory, Roskilde, Denmark.

[20] Papenfuss, H.D. (2006) Aerodynamic Commissioning of the New Wind Tunnel at LM Glasfiber A/S (Lunderskov), Private Communication, Institut für Thermo- und Fluiddynamik, Ruhr-Universität Bochum, Bochum.

[21] Fuglsang, P., Bak, C., Gaunaa, M., and Antoniou, A. (2004) "Design and Verification of the RISØ-B1 Airfoil Family for Wind Turbines", J. Sol. Energy Eng., Vol.126, No.4, pp.1002-1010.

[22] Kim, J. (1989) "On the Structure of Pressure Fluctuations in Simulated Turbulent Channel Flow", J. Fluid Mech., Vol.205, pp.421-451.

[23] Herr, M. (2007) "Design Criteria for Low-Noise Trailing-Edges", AIAA Paper 2007-3470, Proc. of the 13th AIAA/CEAS Aeroacoustics Conf., Rome.

[24] Shen, W.Z., and Sørensen, J.N. (2001) "Aeroacoustic Modeling of Turbulent Airfoil Flows", AIAA J., Vol.39, No.6, pp.1057-1064.

[25] Zhu, W.J. (2008) "Aero-Acoustic Computations of Wind Turbines", PhD Thesis, Technical Report MEK-PHD 2007-09, Institute for Mechanics, Energy and Construction, Danish Technical University.

[26] Schlichting, H. (1968) Boundary Layer Theory, McGraw Hill.

[27] Bertagnolio, F. (2008) "Trailing Edge Noise Model Applied to Wind Turbine Airfoils", Tech Rep. Risø-R-1633-(EN), Risø National Laboratory, Roskilde, Denmark.

Third International Meeting
on
Wind Turbine Noise
Aalborg Denmark 17 – 19 June 2009

The influence of natural ambient sounds on wind turbine noise

Karl Bolin[1] and Mats E. Nilsson[2]

[1)] The Marcus Wallenberg Laboratory, Kungliga Tekniska Högskolan, Stockholm, Sweden
[2)] The Gösta Ekman Laboratory, Stochholm University, Stockholm, Sweden

e-mails: kbolin@kth.se, mnn@psychology.su.se

Abstract

A psycho-acoustic test was performed to study the influence of ambient sounds on perceived loudness of wind turbine noise. The masking potential of ambient sounds is important because natural ambient sounds may be facilitated in order to create a positive soundscape that conceals wind turbine noise. A magnitude estimation method was used to measure perceived loudness and annoyance of wind turbine noise heard together with natural ambient sounds. The investigation was restricted to natural sounds. This because it is questionable to introduce additional noise sources in an already noise polluted environment. The test showed that ambient sounds influenced the perception of wind turbine noise. The main message of the present study was that masking of wind turbine noise by using positive natural sounds may be a useful soundscape design tool.

Introduction

Noise from wind turbines is the main source of annoyance reported by nearby residents [1]. The adverse effects from noise can be compensated for by introducing “positive” sounds [2]. For example, sound from vegetation or the sea could mask wind turbine noise [3]. The noise emission guidelines in Britain take masking into account by determining the allowed noise emission limit with respect to the ambient sound level [4]. The need to investigate total masking but also how the perception of wind turbine annoyance is influenced by other sounds can therefore be considered important.

Method

Recordings

Sound samples from coniferous and deciduous trees were chosen because these two types of sounds are distinctively different; compare the upper and middle diagram of Figure 1. Both vegetation sounds were recorded on a digital analyzer SONY PC216Ax using an omni-directional 1/2" microphone. The microphone was placed on 1.2 m above the ground level [5]. In order to decrease the pseudo-noise generated by the wind into the microphone, a foam windscreen 10 cm in diameter enclosed the microphone. The recordings were conducted at times with high wind speeds, around 8 m/s, contributing to relatively high S/N ratios when vegetation noise levels are compared to the levels of other ambient noises. The sea wave sound shown in the lower diagram of Figure 1 was recorded close to the shoreline at the island Öland in the Baltic Sea. The significant wave height $H_{1/3}$ [6] was 1 m.

The WT noise spectrogram, shown in Figure 2, was recorded at a distance of 400 m from the Rhede WT park at night time [7]. The microphone was mounted on a pole 4.5 m above the ground level. The park consists of seventeen 1.8 MW WTs with a height of 98 m and 35 m blade radius.

Listeners

Ten listeners participated in the study, mainly staff and students from the Kungliga Tekniska Högskolan (KTH), Stockholm, Sweden. Their ages varied between 16 and 45 years. Seven were men and three were women. The subjects had no reported hearing losses.

Procedure

The participants took part in one listening test, conducted in a semi-anechoic room. All sounds were monaurally recorded signals and presented through headphones AKG k-501. Both tests were programmed in MATLAB® 7.3.0 (R2006b). The listener was positioned approximately 2 m from the computer and shielded from computer noise by a 5 cm thick sound insulator to ensure that they were not influenced by noise from the computer. A training session with twenty sounds was conducted prior to the first session. Perceived loudness or annoyance was assessed with the method of free number magnitude estimation [8]. The participants entered their magnitude estimates in tables on paper.

The test consisted of five sessions presented in random order. In each session 40 noise signals were presented. Backgrounds of natural sounds were presented in three sessions with A-weighed sound levels, $L_{A,BG}$, of 40 dB, 44 dB or 48 dB respectively. Two of the sessions were performed in silent background. The sessions with background sound contained wind turbine noise mixed with ambient sound. The signal-to-noise ratio varied in 2 dB steps between -10 dB to +6 dB for the wind turbine noise, also presented was one blank signal containing no wind turbine noise. These ten different stimuli were presented four times in random order within each session. The sessions without background sound contained wind turbine noise in 2 dB steps with A-weighed sound levels ($L_{A,WT}$) from 30 dB to 54 dB. These sessions also contained samples of pink noise. The pink noise was presented in 4 dB steps with A-weighed sound levels from 30 to 54 dB. The duration of the signals was 2.5 s and the pause between each stimulus was equally long. A 30 s pause was inserted between each session. The complete test time was 20 minutes.

Half of the subjects rated the perceived loudness from the signals while the remaining half rated the *additional* annoyance from the signal. If the subjects experienced no increased annoyance because of the signal they were instructed to give the grade zero.

Results

Pink noise equivalent sound level (PNE_{loud})

The perceived loudness of each traffic sound was expressed as the pink-noise equivalent sound level (PNE_{loud}). The PNE_{loud} of a traffic sound is the sound level of an equally loud pink noise. The main advantage of expressing loudness as PNE_{loud} is (a) that it gives loudness a meaningful unit (pink-noise sound level in dB), and (b) that it does not presuppose that listeners are able to produce magnitude estimates with ratioscale properties. The only assumption is that, on average, equal numbers (magnitude estimates) means equal loudness (cf. Refs. [9,10]). PNE_{loud} -values were determined by first calculating the geometric mean magnitude estimate (R_{pn}) for each listener and pink-noise sound level (L_{pn}). These geometric means were used to derive individual psychophysical functions,

$$\left[\ln(R_{PN}) = a\right] + bL_{PN} \qquad (1)$$

where a and b are constants unique to each listener.

Second, for each listener and wind turbine noise, the geometric mean magnitude estimate (R_{WT}) was calculated. These geometric means were then transformed into pink-noise equivalent sound levels, using each listener's unique set of constants (*a* and *b*). The logic behind the transformation was as follows: Equal loudness of a wind turbine noise and a pink-noise sound level would imply that a listener, on average, would give the two sounds the same magnitude estimate. Thus, PNE_{loud} can be calculated from Eq. (1),

$$\mathrm{PNE}_{\mathrm{loud}} = \left[\ln(R_{WT}) - a\right]/b \qquad (2)$$

PNE_{annoy}-values of annoyance were calculated in the same way as described in connection with Eqs. (1)–(2), but with R_{PN} and R_{WT} now referring to annoyance rather than to loudness.

Loudness

The results from the loudness estimation test are shown in Fig. 1. Intra-individual averages are shown for PNE_{loud} with background sounds (blue dots) and without (red dots). As can be seen, the loudness estimate is depending on both wind turbine sound level but also on the background sound level. For example, the equivalent loudness (PNE_{loud}) of $L_{A,WT}$= 40 dB varies from 26.5 dB in the loudest background to

39.8 dB without background sound. The masking effect (difference between the blue and red dots $PNE_{loud,WT}$- $PNE_{loud,WT+BG}$) seems to be higher at 44 and 48 dB background sound levels than in 40 dB background.

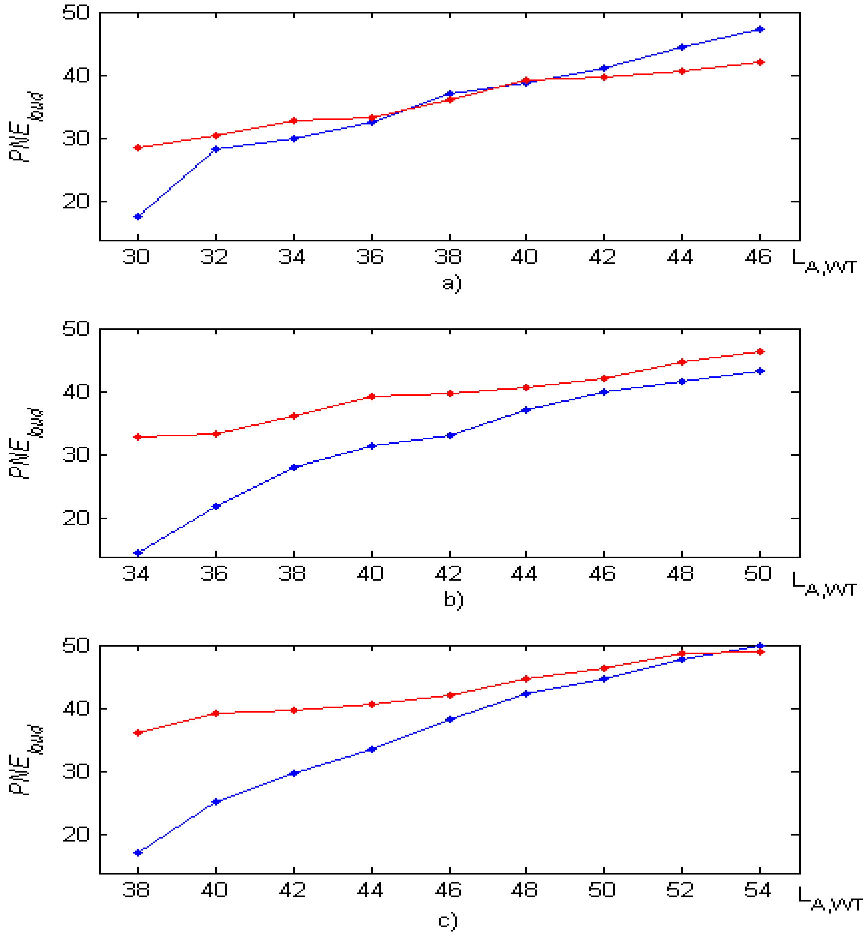

FIG 1: The equivalent pink loudness PNE_{loud} as a function of wind turbine sound level $L_{A,WT}$. The red lines show wind turbine noise alone while the blue line show the WTV loudness when mixed with background sound. Figures a, b, and c show PNE_{loud} with background sound levels of 40, 44 and 48 dB.

Annoyance

Fig 2 shows the perceived annoyance. Intra-individual averages are shown for PNE_{annoy} with background sounds (blue dots) and without (red dots). As revealed by the graphs, the annoyance seems to be higher when heard alone compared to the same level when mixed with background sounds. The PNE_{annoy} for 40 dB wind turbine noise varies from 24.1 dB at 48 dB background level to 42.7 dB in silent environment. All three background levels show lower annoyance ratings compared to when heard alone. When compared to Fig 1 the backgrounds effect on annoyance seems to be more pronounced than on loudness.

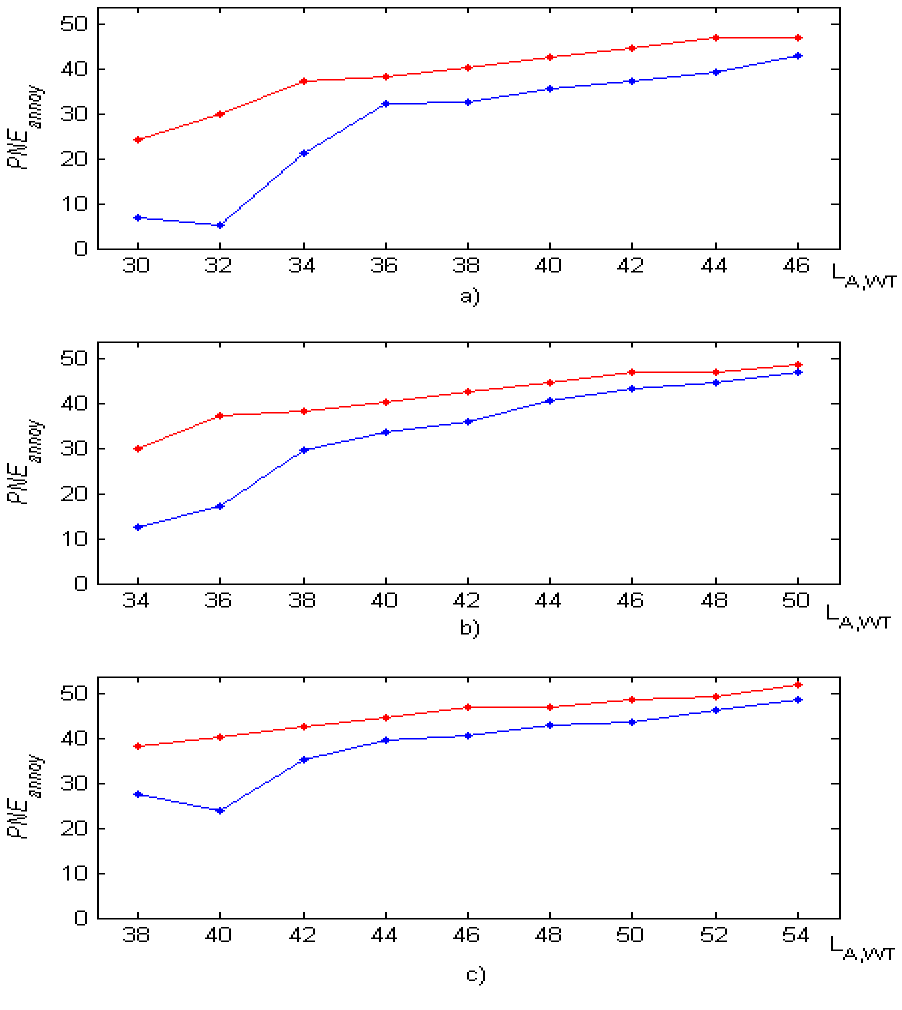

FIG 2: The equivalent pink annoyance PNE_{annoy} as a function of wind turbine sound level $L_{A,WT}$. The red lines show wind turbine noise alone while the blue line show the WTV loudness when mixed with background sound. Figures a, b, and c show PNE_{annoy} with background sound levels of 40, 44 and 48 dB.

Conclusions

The results from the test show that both the loudness and annoyance seems to be strongly influenced by introducing natural sounds. The ambient sounds effect on annoyance is larger than on loudness. One reason for this might be that the background sound was considered more annoying than the wind turbine noise. Thereby, the *added* annoyance was less compared to the partial loudness.

The experiment only included one sample of wind turbine noise and three samples of background sounds. Therefore, the general applicability of the result needs to be evaluated in further studies including other natural sounds and wind turbine noises. An important message of the present study is that masking of wind turbine noise by adding "positive" natural sounds may be a useful soundscape design tool. This would be especially relevant for quiet areas where wind turbine noise typically is perceived as highly unwanted, even at low levels. Examples of such environments would be national parks or areas used for recreational purposes where the absence of artificial noise, including wind turbine noise, is considered a significant value. Furthermore, the present results suggest that guideline values for wind turbine noise may benefit from being defined in terms of relative levels. This approach would be better than guideline values in terms absolute wind turbine noise levels, since the perceived loudness of a given wind turbine level may vary considerably due to complete or partial masking by natural sound sources.

References

[1] van den Berg, E. Pedersen, J. Bouma F and R. Bakker. Wind Farm Perception, visual and acoustic impact of wind turbine farms on residents. Technical report, EU project: FP6-2005-Science-and-Society-20, 2008.

[2] Brown, A. L., & Muhar, A. (2004). An approach to the acoustic design of outdoor space. *Journal of Environmental Planning and Management, 47*(6), 827-842.

[3] Bolin K., Wind Turbine Noise and Natural Sounds- Masking, Propagation and Modelling, PhD-thesis, Report no. Trita/AVE 2009:19 ISSN1651-7660, KTH, Sweden

[4] R. Meir & et al.: The assessment and rating of noise from wind farms. Technical report ETSU-R-97, Department of Trade and Industry (1996).

[5] ISO1996: Acoustics – Description and measurement of environmental noise, International Organization for Standardization, Geneva, Switzerland (1986).

[6] R. G. Dean and R. A. Dalrymple, Coastal processes with engineering applications (Cambridge University Press) (2001).

[7] G. P. van den Berg: Effects of the wind profile at night on wind turbine sound, Journal of Sound and Vibration 277, 955-970 (2004).

[8] S.S. Stevens, Psychophysics. Introduction to its Perceptual, Neural and Social Prospects, New York, Wiley-Interscience, 1975.

[9] B. Berglund, Quality assurance in environmental psychophysics, in: S.J. Bolanowski, G.A. Gescheider (Eds.), Ratio Scaling of Psychological Magnitudes—In Honor of the Memory of S.S. Stevens, Erlbaum, Hillsdale, NJ, 1991, pp. 140–162.

[10] L.E. Marks, Sensory Processes. The New Psychophysics, New York, Academic Press, 1974.

Third International Meeting
on
Wind Turbine Noise
Aalborg Denmark 17 – 19 June 2009

ASSESSMENT OF ACOUSTIC EMISSIONS OF A WIND TURBINE IN INDIA

K. Boopathi, Scientist, Deepa Kurup, Scientist, R. Katyal, Senior Scientist, R&D, Dr. S. Gomathinayagam, Executive Director

Centre for Wind Energy Technology, (Under the Ministry of New and Renewable Energy Sources- GOI), Chennai, India

boopathi@cwet.res.in,deepa@cwet.res.in,katyal@cwet.res.in, ed@cwet.res.in

Abstract

Horizontal axis wind turbines under the influence of atmospheric wind turbulence are a prolific source of noise. Genesis of noise emissions are predominantly from the mechanical components and aerodynamic profile interactions and controls. Noise problems are always looked at the perspective of possible environmental impact and extensive studies have gone into identifying the effects. The scope of this paper is to do an assessment of the noise generated from a wind turbine coupled with an induction generator having constant speed drive train mechanism & power regulation by active pitch control at an Indian wind farm site. IEC standard 61400-11:2002 guidelines for acoustic noise measurement techniques is used for the assessment. The experimental study is carried out at a distance of 100 m away from the central vertical axis of the turbine tower. During the measurements, all the wind turbines in the vicinity were turned off to avoid interference. Meteorological parameters like temperature, pressure and humidity were measured during the course of the test and equivalent wind speed was calculated for the reference height. Based on the measurements, the apparent acoustic power level, audibility and tonal level are determined, to assess whether the test turbine in the wind farm has been generating noise within the limit of the stipulated levels. Diagnosis of the source turbine component causing the noise is also done from the noise measurements. The various issues/methods involved in identification of sub-components which may trigger noise are based on the case study. The results obtained are compared with the values stipulated by the environmental standards presently in vogue and an inference is evolved on whether they are within the permissible noise levels.

Keywords: Environmental impacts, acoustic noise, apparent acoustic power level, audibility, tonal level

Introduction

Among other non renewable energy sources wind energy is one of the most acceptable, significant and cleanest natural resource which neither pollutes the environment, nor emits harmful gases during the energy conversion process. Even though it has the said advantageous the wind turbine poses some environmental problems. These problems are noise, vibration, & visual impacts etc. These factors may have negative effect on people, pose a danger to flying birds and harm local soil conditions. Besides ecological problems caused by the wind turbines the landscape view can be disrupted. Among these one of the serious problem from wind turbine is the noise which can cause inconvenience to the residents in the nearby locations.

Wind energy Development in India.

The development of wind power has taken place in India since 1990s, and has been drastically increasing for the last few years. Although a relative newcomer to the wind industry compared with Denmark or the US, a combination of domestic policy support for wind power prevalent in the country has made this possible. India is the country with the fifth largest installed wind power capacity in the world, and the installed capacity of wind power in India till Nov.2008 was 9587.14 MW. It is estimated that another 6,000 MW of additional wind power capacity will be installed in India by 2012. Wind power accounts for 6% of India's total installed power capacity, and it generates 1.6% of the country's power.

Sources of Noise from wind turbines

There are two potential noise sources from the wind power plant; one is mechanical and other from aerodynamic noise.

Mechanical noise

The Mechanical noise is emitted from the wind turbine due to relative rotation of drive train components like gearbox, generator, yaw motors, cooling fans, hydraulic pumps and other accessories. The noise from these components frequently contains more or less prominent tones, whose amplitude and also frequency fluctuates slightly in rhythm with the blade passing frequency of the rotor. Occasionally low levels of mechanical noise also arise from pitch control motors. All mechanical noise sources are contained within the wind turbine nacelle. Several techniques are used to mitigate this noise source. These include special gears, belt drives, mounting of vibrating components on vibration isolating mounts and the use of acoustic isolation to dampen noise.

Aerodynamic rotor noise

When wind turbine rotor blade moves in a flow field or interact with air stream a pressure distribution is established around the blade. While the blades are interacting with the air stream the aerodynamic noise generated along with a number of complex phenomenon occurs around the blade, each contributing the noise emission from the wind turbine generator system.

The rotor noise from a well designed wind turbine would have broad band type with some amount of low frequency or even tonal component, a characteristic amplitude modulated pattern in rhythm with the blade passing frequency, providing a typical “swishing” sound. At larger distances from the turbine the amplitude modulation decreases and the sound gains a more stationary character. Some observations indicate that the modulation can be strong, even at rather large distances, in a stable atmosphere which can occur at night time when the wind is not too strong. Aerodynamic noise is generally affected by some of the factors viz. shape of the blade tip, tip speed ratio, pitch setting, trailing edge thickness, blades’ surface finish and twist distribution.

Noise measurement from wind turbine:

The noise emission from a wind turbine is generally expressed in terms of its sound power level. The typical sound power level from a single wind turbine is usually in the range of 95 dB (A) -105 dB (A). This creates a sound pressure level of 50 dB (A) – 60 dB (A) at a distance of 40 m from the turbine.

Investigation:

Noise measurements were carried out on a 600 kW pitch regulated wind turbine with constant speed drive train mechanism and using a precision analyser 2260, of Bruel & Kjaer (Danish make), and the wind turbine’s technical descriptions are presented in Table 1.

Table 1. Technical description of the wind turbine

Rotor	Power regulation	Active Pitch regulated
	Number of blades	3
	Rotor diameter	52 m
	Hub height	75 meter
	Rotor speed	24 rpm (Revolutions per minute)
	Rotation direction	Clockwise
	Cut in wind	3.5m/s
Blade	Length	25 meter
Gear Box	Type	3 stage (1 planetary and 2 helical)
Generator	Type	Single speed induction generator
	Rated/peak power	600 kW
	RPM	1500 rpm
	Frequency	50 Hz
Yaw System	Type	Polyamide slide Bearing
	Cut out wind	25 m/s
	Type	Lattice

Measurement Methodology:

Sound pressure level was measured on the ground in and around a test turbine at a distance of Ro = H + (D/2), Ro is the reference distance, H is the hub height, D is the diameter of the rotor in the downwind direction as shown in Fig 1. Simultaneous wind measurements were carried out at a height of 10 m on a met mast. The sound level meter was placed on a 12 mm thick plywood of circular shape having 1 m diameter. Additionally, a primary windscreen of about 95 mm diameter was used. The acoustic measurements were carried out at 4 positions laid out in a pattern around the vertical centreline of the WTGS tower as shown in Fig 2.The sound pressure level at a wind speed 8 m/s has to be determined from the data pairs by means of linear regression. A linear regression analysis was done with 10 pairs of equivalent continuous sound pressure level from the microphone at the reference positions. The reference position sound pressure level, L_{Aeq} is the value of the regression line at the acoustic reference wind speed. A similar analysis yields the background noise level at the acoustic reference wind speed.

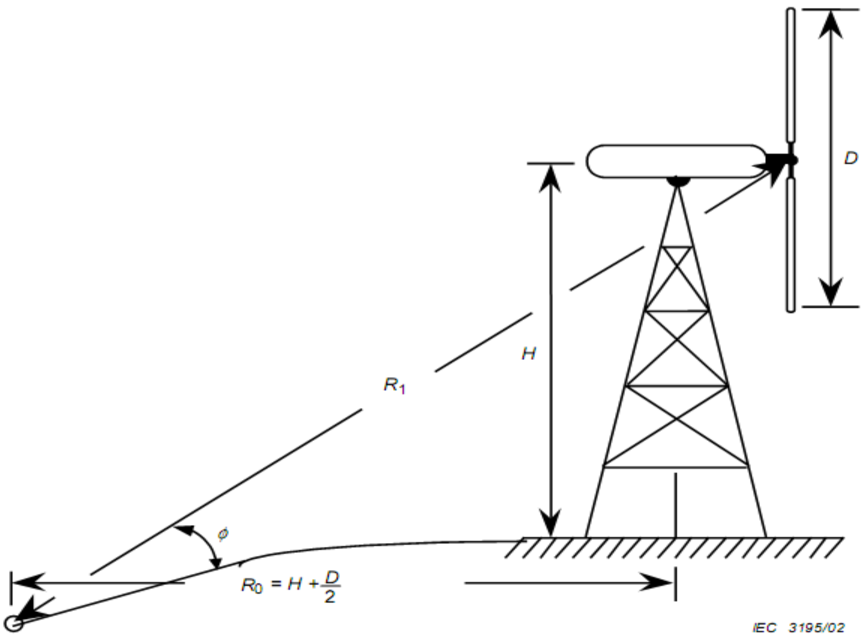

Fig 1. Instrument location(source IEC 61400-11)

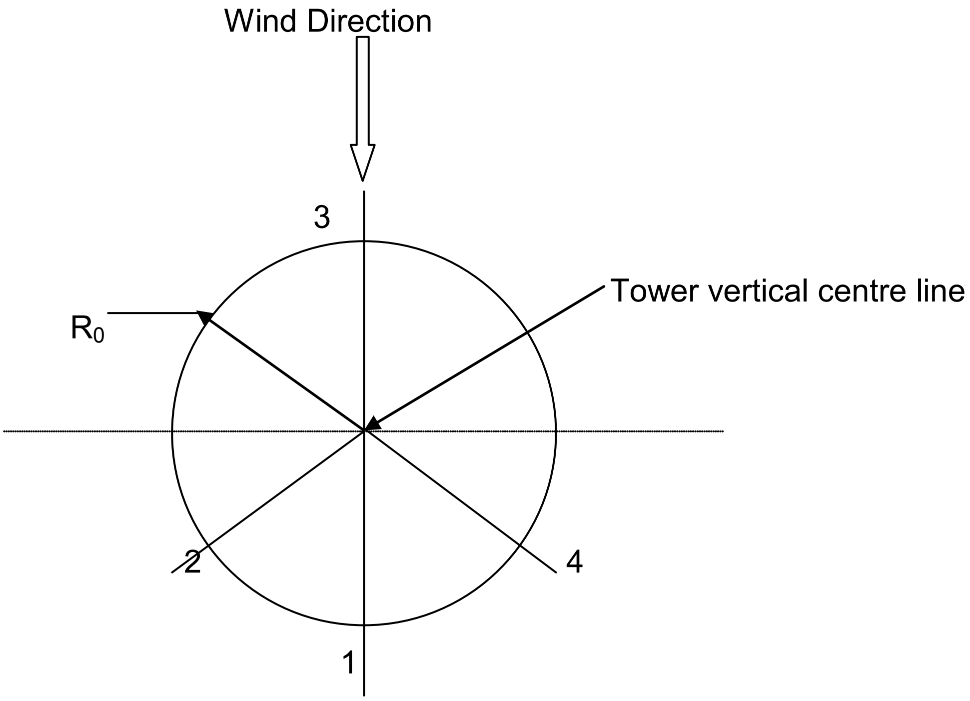

Figure 2 – Pattern of Microphone measurement positions

Results and discussions:

A case study was carried out on a 600 kW wind turbine at wind turbine test station, at Kayathar wind farm. The wind speeds during the measurements were ranging between 4 to12 m/s. The turbine was allowed to operate in its normal mode during the test period, except when it was shut down to measure the background noises. The sound level meter was set up to record successive measurements of L_{Aeq} as 1 minute averages as per the stipulations prescribed in the standard. During the test period, potentially interfering background noise like vehicle noise were noted, so that these could be filtered out & muted during the data analysis. Measurements with the turbine on shut down mode allows an assessment of the steady background noise at the site where measurements were conducted, so that the measured noise level from the turbine could be corrected. A 10 m met mast was installed in front of the turbine at a distance of 150 mtrs with a bearing of 257^0 w.r.t true north. Anemometer, wind vane, temperature sensor, humidity and pressure sensor were mounted on the mast. Synchronized wind speed and wind direction measurements were made using NRG #40 anemometer and NRG #200P wind vane, mounted at the same 10m height connected to a Nomad data logger placed at the base.

A-Weighted Sound Power Level

Fig 3, 5 & 7 show the scatter plots of the wind turbine and the background noise data for the reference microphone position 1 which was placed in the down wind direction, microphone position 3 is the upwind, and microphone positions 2 & 4 placed on either side of the turbine. At Microphone position 1, 60 measurement data were taken at different time periods and used for the analysis. The apparent sound power level for all the microphone positions were determined from the turbine & its background data, in the wind speeds ranges of 6 to 10 m/s. Table 2 portrays the calculated apparent sound power level for the four microphone positions from around the turbine.

The Fig 4 depicts the binned average wind speed against the average sound power level of the integer wind speed between 6 m/s to 10 m/s, both for the turbine under operation mode and in parking mode. The average sound pressure level of turbine at 8 m/s was recorded as 55 dB. The Fig 4 clearly indicates the background sound pressure level for different integer wind speeds as between 44 dB (A) to 50.5 dB(A). The turbine background (Turbine in operational mode) sound pressure level were between 51 dB (A) to 55 dB (A), which indicates that the difference is 4 dB and is less than the 6 dB specified in the standard. For each integer wind speed, the background level was subtracted from the turbine level, to give a corrected level, as per standard. The results are summarized in Table 2, together with the calculated sound power level:

Table 2. Apparent Sound Power Levels for the Acoustic Reference Wind Speed

Description/Microphone position	Unit	Ref.1	Ref.2	Ref.3	Ref.4
Apparent sound power level at 8 m/s	dB (A)	101.78	*	103.1	102.5
Turbine sound pressure level at 8 m/s	dB(A)	55.53	53	56.52	56.2
Background sound pressure at 8 m/s	dB(A)	47.5	47.3	46.1	47.52
Difference between background and turbine	dB(A)	8.03	5.7	10.42	8.68
Number of turbine points		60	20	10	10
Number of background points		60	20	20	20

* - The difference between the turbine and background noise was between 3 and 6 dBA, so the apparent sound power level cannot be determined.

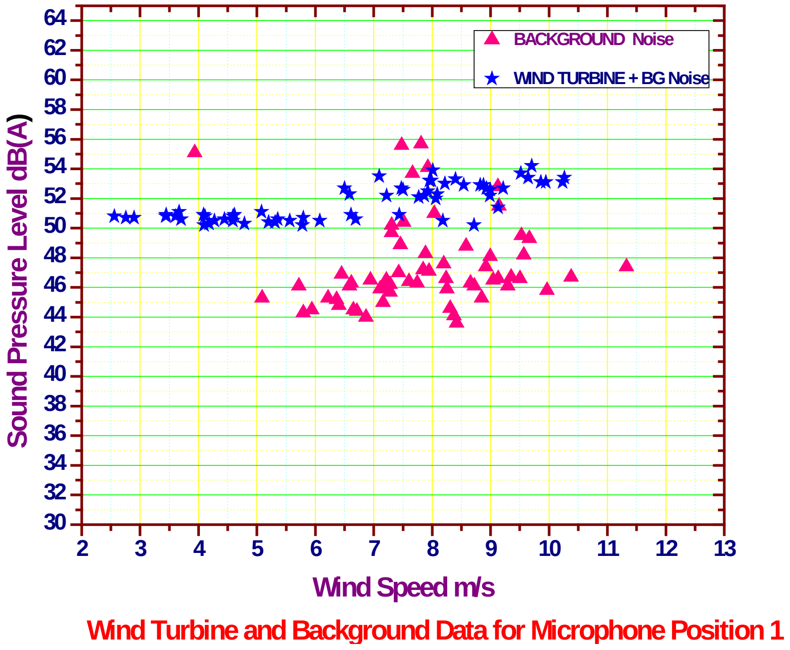

Fig 3. Wind turbine and background data for microphone position 1

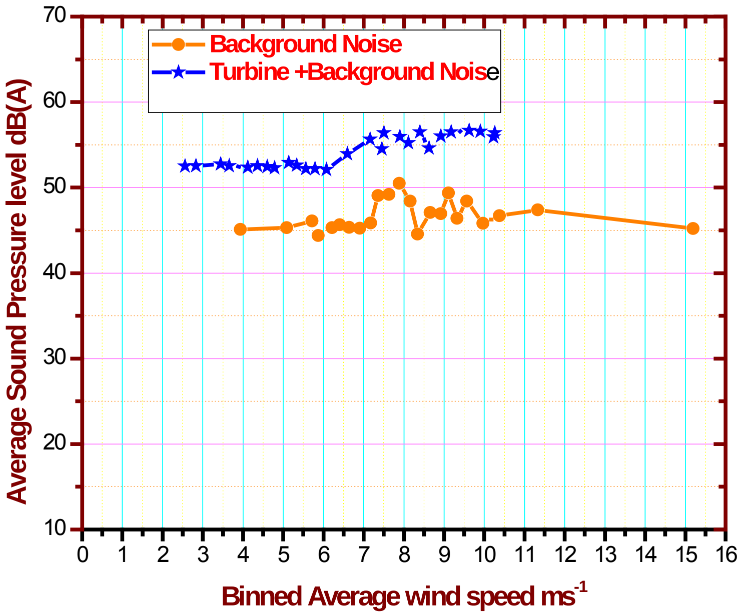

Fig 4.Wind turbine and background data for microphone position 1

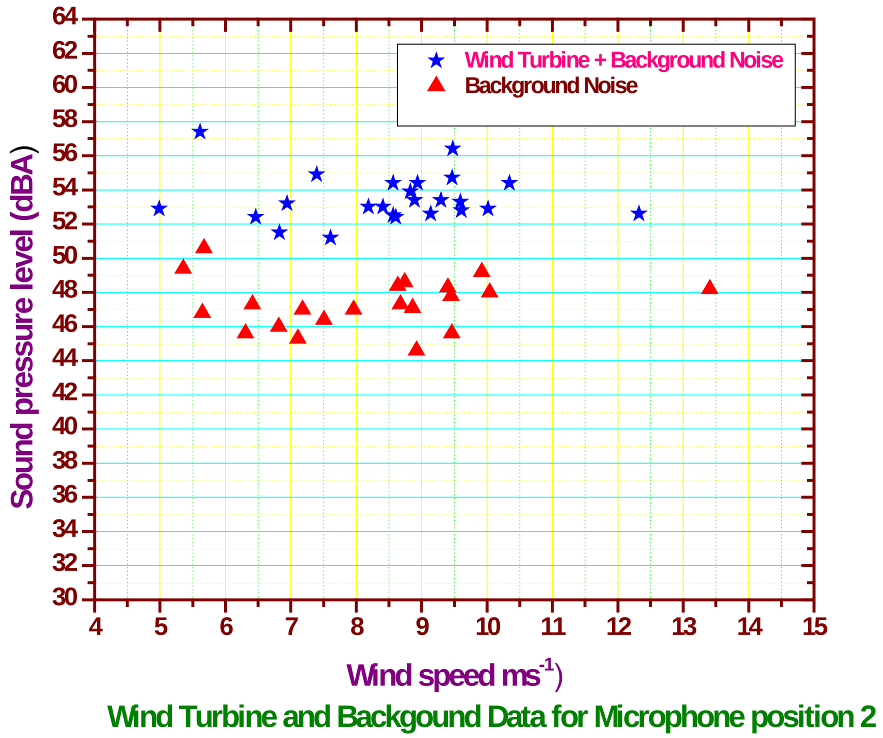

Fig 5 Wind turbine and background data for microphone position 2

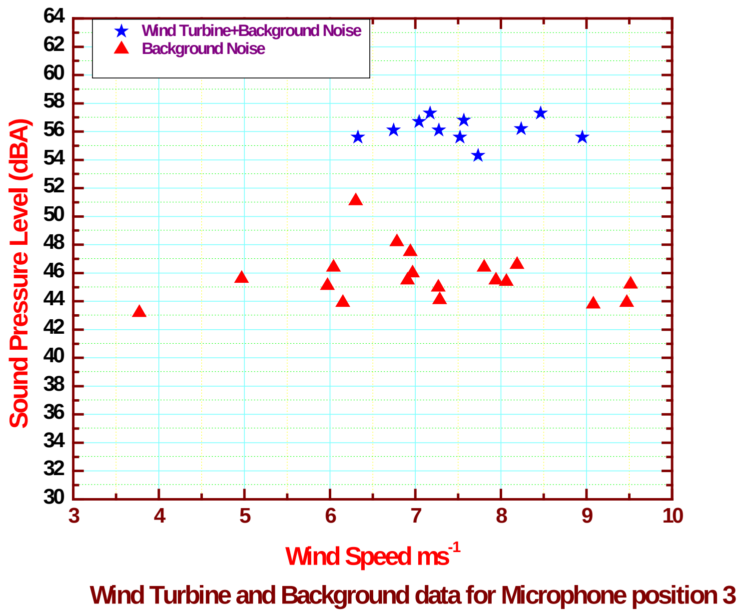

Fig 6. Wind turbine and background data for microphone position 3

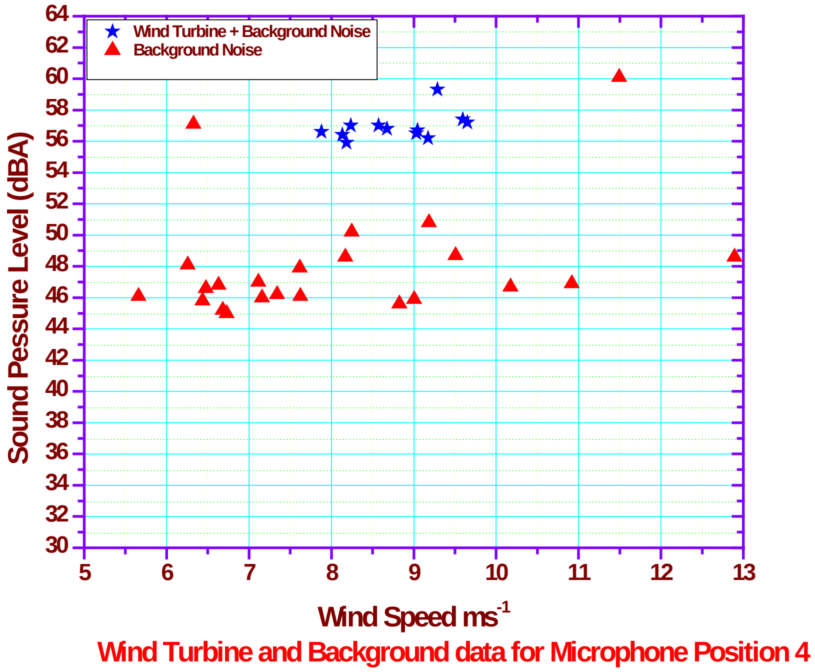

Fig 7. Wind turbine and background data for microphone position 4

Source Sound Power Level

The sound power level of a noise source is normally expressed in dB re: 1pW. Table 3 and Fig 8, show the Turbine Sound Power Level of a 600 kW Turbine.

Table 3. Sound power level of standardized wind speed

Wind Speed at 10m Height (m/s)	Sound Power Level (dB LW_{Aeq})
6	101.95
7	102.17
8	102.25
9	102.44

The recommended sound power level for modern turbines which have already been designed are as follows ***(Source-Wind Turbine Technology –Erick Hau)***

- Small wind turbines up to 20 m rotor diameter / 100 kW ~ 95 dB (A)
- Medium-sized wind turbines up to 40 m rotor diameter / 500 kW ~ 98 dB (A)
- Large wind turbines with 70–80 m rotor diameter / 2000 kW 103–105 dB (A)
- Multi Megawatt wind turbines, 100–120 m rotor diameter 105–107 dB (A)

The test turbine sound power level at integer wind speeds 6-10 m/s are between 101.95 – 102.44 dB, these values lie within the recommended values.

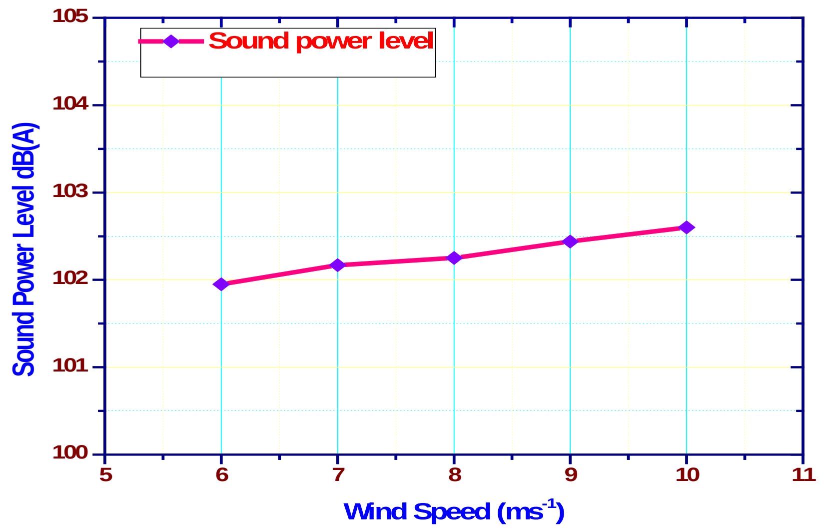

Fig 8. Sound power level vs. Standardized wind speed

Tonal Analysis

Quantification of the tonal characteristics is the most important feature of analysis. The tonality assessment at the acoustic reference wind speed (8 m/s) was made according to JNM2 standard. Data sets where the wind speeds were close to 8 m/s, for a minimum of 2 minutes were used for the analysis. The signal analyser was set to perform Fast Fourier Transforms (FFTs) using a Hanning window in the time domain.

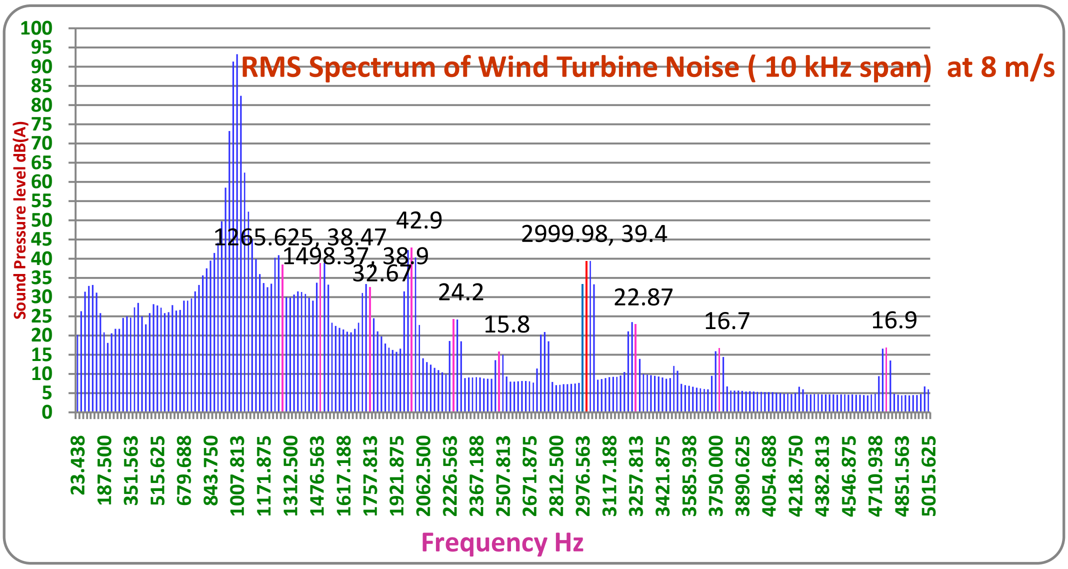

Fig 9. RMS spectrum of Wind turbine noise at 10 kHz

Table 4 –Tonal component details at 8 m/s, (span10 kHz) ,NBW 35.2

width	Critical Band	Penalty k	Audibility Δlta	Tonality Lpt	Corrected frequency	Corrected dB	masking noise	Most prominent tone level	ΔLtn max=Lpt-Masking Noise
609.40	2695.3-3304.7	6	22.4	39.4	2999.98	39.4	21.1	39.6	18.3
375.00	1687.5-2062.5	6	18.8	42.9	2000	42.9	28	43.4	14.9
375.00	1687.5-2062.5	6	18.8	33.4	1749.28	33.4	28	43.4	5.4
632.80	2812.5-3445.3	6	22.4	23.5	3249.76	23.5	21.1	39.5	2.4
586.00	2578.1-3164	6	22.6	20.9	2750.28	20.9	20.7	39.5	0.2
703.10	3164.1-3867.2	6	7.5	16.7	3758.67	16.7	21	24.4	-4.3
960.90	4289.1-5250	6	2.2	16.9	4763.2	16.9	19.1	16.9	-2.2
562.50	2484.4-3046	6	22.8	16.3	2498.96	15.8	20.5	39.5	-4.2
421.00	1898.4-2320.3	6	22.4	24.3	2249.2	24.2	24.1	43	0.2
281.20	1242.2-1523.4	6	7	39.1	1498.37	38.9	39.3	43.1	-0.2
257.00	1125-1382.8	6	3	40.9	1250.32	40.9	41	40.9	-0.1

Table 5. Tone identification and classification

Adjacent line Frequency	Level above average	Classification
2929.688	17.34	Masking
2953.125	17.17	Masking
2976.563	8.52	Tone
2999.98	14.54	Tone
3000.000	14.53	Tone
3023.438	8.51	Tone
3046.875	16.37	Masking
3070.313	16.18	Masking
3093.750	15.93	Masking

In Fig 9 the RMS spectrum of the wind turbine noise at 10 kHz, at reference wind speed is shown. In this analysis it was found that the noise had pronounced tones at different frequencies namely 1250.32 Hz,1498.37 Hz,1749.28 Hz,2000 Hz,2249.2

Hz,2498.96 Hz,2750.28 Hz,2999.98 Hz,3249.76 Hz,3758.67 Hz,4763.2 Hz. Out of these the most prominent tone level was found at 2999.9 Hz, where the tonality observed was 39.4 dB. The difference between the tone level & the masking noise level is 18.3 dB as shown in Table 4.

The Table 5 gives the details about the adjacent frequency line tone and masking noise level. It was found from that the adjacent frequencies of 2976.5 Hz, 3000.0Hz, and 3023.43Hz also have tone level.

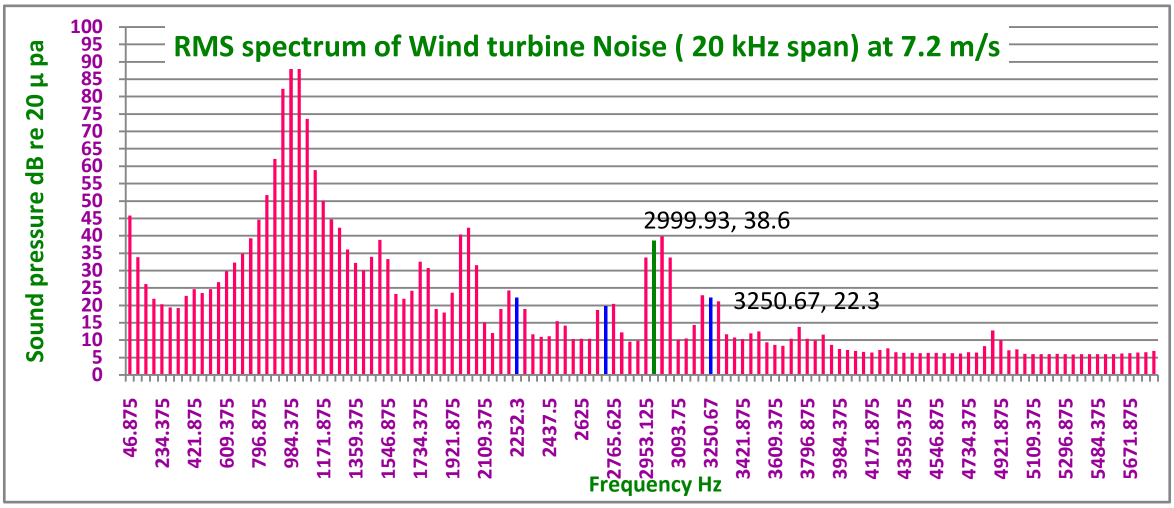

Fig 11. RMS spectrum of Wind turbine noise 20 kHz span

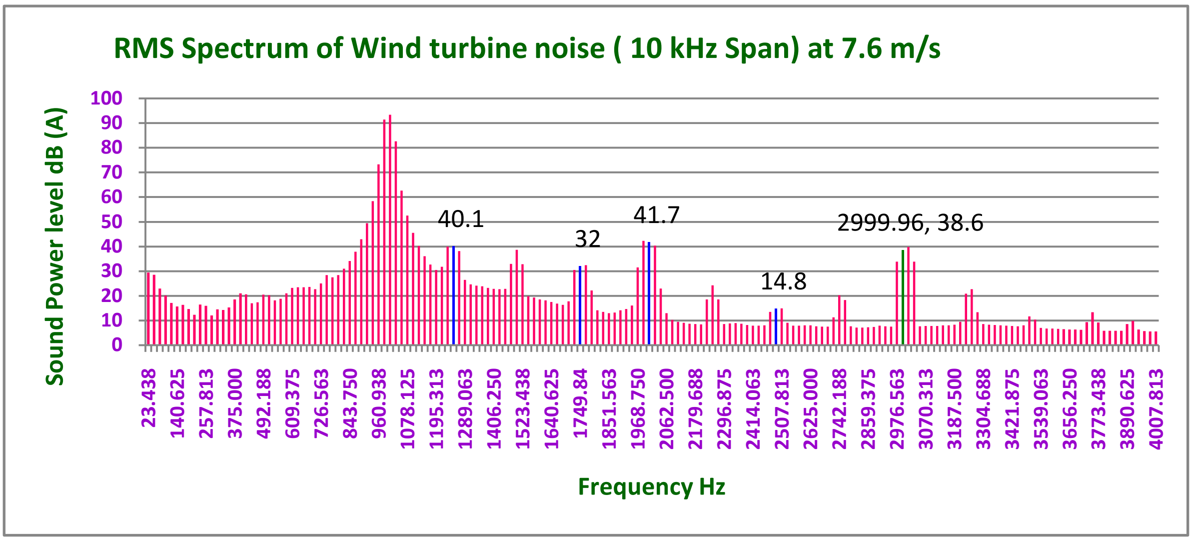

Fig 12. RMS spectrum of Wind turbine noise span 10 kHz

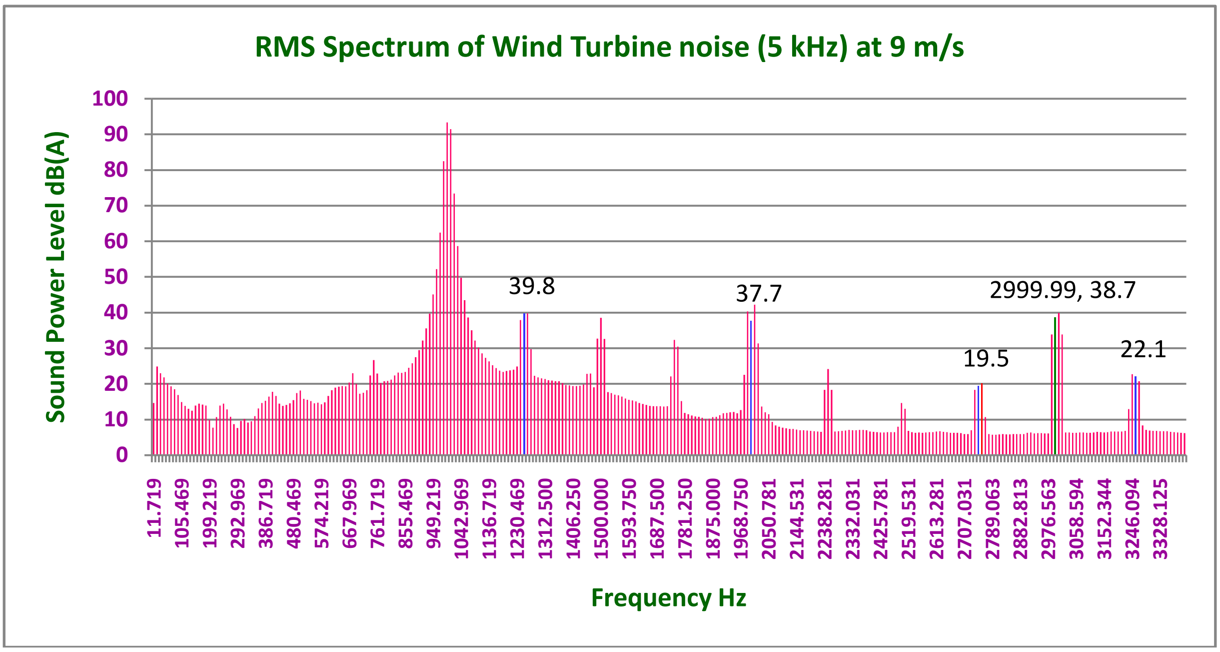

Fig 13. RMS spectrum of Wind turbine noise span 5 kHz

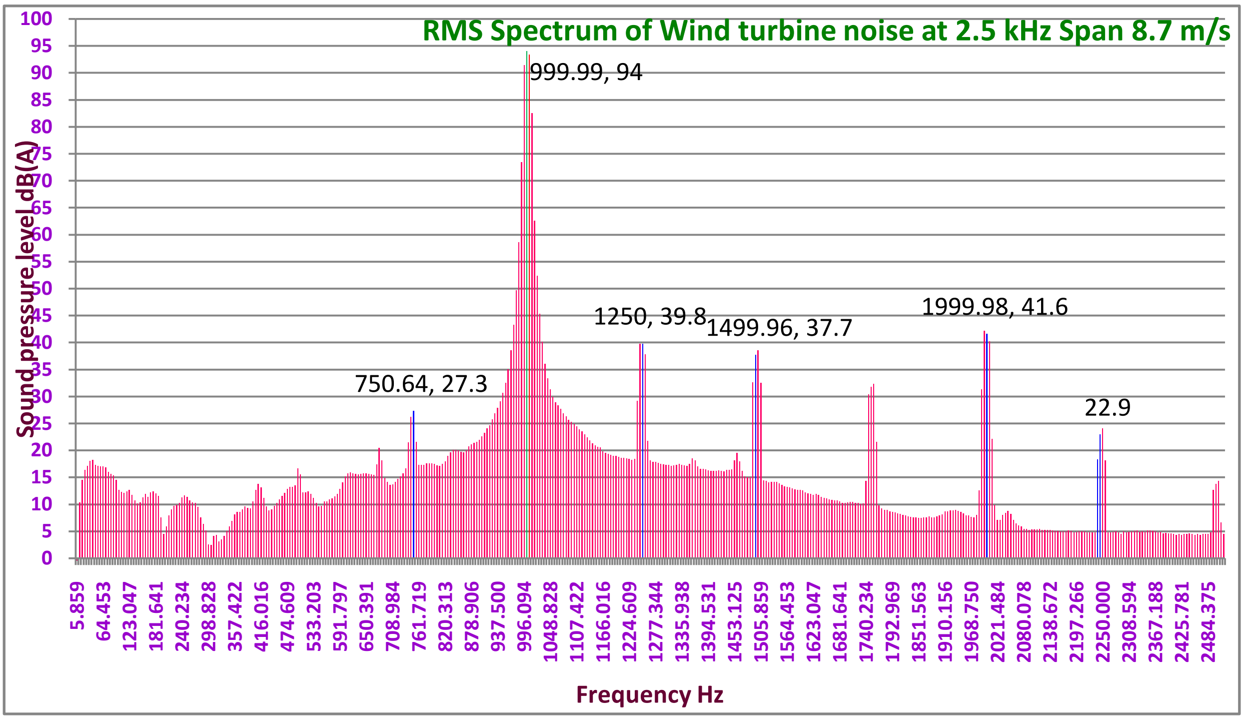

Fig 14. RMS spectrum of Wind turbine noise at 2.5 kHz

Figs 11-14 show the RMS spectrum of wind turbine noise at different wind speeds ranging from 7.2 to 9 m/s. It was found that the prominent tone at frequency of 2999.9 Hz.

Conclusion

The broad band and narrow band analysis (20 kHz) were carried out for the case study. The analysis of broadband noise indicates that the sound power level of the turbine is within the stipulated level of 101.95 dB (A) – 102.44 dB (A) specified for a wind turbine of comparative size. The “A” weighted sound pressure level measured for the wind turbine was observed to be in the range of 51 dB (A) - 55 dB (A) which is within the values stipulated by the Indian Noise pollution (Regulation and control) rules-2000 for residential areas. The stipulated values are 55 dB (A) during the day time and 45 dB (A) during night time. Hence from the observation it is found that the sound pressure levels have exceeded the stipulated levels during night time. The existence of prominent tone at 2999.99 Hz in the narrow band analysis indicates that the noise is not of aerodynamic nature, but generated from a mechanical component, probably the gear box. The actual cause of this tonal identified frequency needs further investigation.

References:

a) IEC 61400-11 ,2002 Acoustic Noise measurement techniques

b) Whisper H-40 Acoustic noise test report- National Wind Technology Center National Renewable Energy Laboratory ,A. Huskey, M. Meadors ,June 01, 2001

c) The assessment of the noise level generated a wind turbine based on the results of the acoustic pressure measurement ,T. Boczar, S. Borucki, A. Cicho , M. Lorenc

d) Acoustic Tests of Small Wind Turbines ,P. Migliore, J. van Dam, and A. Huskey ,To be presented at the 2004 Wind Energy Symposium ,Reno, Nevada ,January 5–8, 2004

e) Acoustic Noise Test Report for the AOC 15/50 Wind Turbine at the National Wind Technology Center

f) Golden, Colorado by National Wind Technology Center ,National Renewable Energy Laboratory

g) 1617 Cole Boulevard ,Golden, Colorado 80401 ,July 1, 1999

h) North Dover Wind Park Environmental Statement, Chapter 11: Noise

i) Wind turbines and sound: review and best practice guidelines submitted to: CanWEA ,Canadian Wind Energy Association ,Canada K1P 5Z9

j) Ministry of environment and forests notification, New Delhi, the 30th, December, 2002

k) The Noise Pollution (Regulation and Control) Rules, 2000, Standardising noise Dr. G. Madhusoodanan Pillai,

l) Wind Turbine Acoustic Noise ,A white paper ,Prepared by the Renewable Energy Research Laboratory ,Department of Mechanical and Industrial Engineering ,University of Massachusetts at Amherst ,Anthony L. Rogers, Ph.D. James F. Manwell, Ph.D. June 2002 ,Amended January 2006.

Third International Meeting
on
Wind Turbine Noise
Aalborg Denmark 17 – 19 June 2009

An Alternative Approach to Explaining Wind Farm Noise to Community Groups

Paul Botha

Meridian Energy, PO Box 10840, Wellington 6143, New Zealand
Paul.botha@meridianenergy.co.nz

Fraser Clark

New Zealand Wind Energy Association (NZWEA), PO Box 553, Wellington 6140, New Zealand
Fraser@nzwea.org.nz

Abstract

The public's perception and understanding of the acoustic effects of wind farms remains one of the major issues to be addressed during the consenting of wind farms in New Zealand. The traditional method of trying to explain what is a very complex subject to the general public has been to use summarised information such as "fact sheets". These summary documents have their limitations and an alternative method has been investigated. The result has been the production of a 19 minute DVD which explores some basic acoustic concepts and goes on to investigate the noise levels around an operational wind farm in New Zealand. The production has been titled "Sound Advice – Measuring wind farm noise" and is envisaged to be used as a tool by developers when undertaking consultation with the public living in close proximity to proposed wind farms.

Introduction

Summarised information on wind farm acoustic effects or "fact sheets" are regularly used during the public consultation phase of wind farm consenting in New Zealand. These fact sheets, together with the complete noise impact assessment report which forms part of the AEE (Assessment of Environmental Effects) are used to assist the public in trying to better understand any acoustic effects of a proposed wind farm on neighbouring properties.

Meridian Energy, with support from the New Zealand Wind Energy Association (NZWEA) have undertaken a project to try and present information on wind farm acoustics in an alternative, and easy to understand, way. The concept was to put together a short informative DVD which serves to answer questions on key issues about wind farm acoustics.

The 19 minute DVD will be played to the delegates at the 3rd International Conference on Wind Turbine Noise, and three very short clips are included in the conference proceedings.

Objectives of the Sound DVD

The primary objective of the project was to produce a short documentary on wind farm acoustics that could be understood by a lay audience and was sufficiently interesting that it would hold the audience's attention for the duration of the movie. Whilst being engaging it also had to hit the correct note of authority, that is, it had to be believable and the presenter had to gain the audience's trust.

The story being told had to attempt to put wind farm noise issues in context with some 'every-day' noises and had to try and answer some of the wind farm specific acoustic issues. Many of these are regularly raised by the public, especially when a new wind farm is proposed in an area that is currently unfamiliar with wind turbines and their only experience with them is from what they can find on the internet or other 'third-party' sources. The DVD attempts to bridge the gap between a written description of the nature of wind turbine noise and what they might experience by visiting a wind farm itself.

Theme of the DVD

It was finally decided to present the subject in an investigative manner. Peter Elliot, a relatively well known New Zealand actor was engaged to investigate wind farm noise and present the measurements and findings he makes. He has a number of discussions including those with an industry acoustics expert, a family living adjacent to an operational wind farm (who had initially objected to it being installed) and some local residents. Measurements of an operational wind farm were made at a wind farm site known as Project White Hill, in Southland, New Zealand, which comprises twenty nine 2MW wind turbines.

DVD Content

The DVD commences by investigating the sound levels of every day noise sources inside and outside a house. Peter goes on to measure noise at a party (a common source of noise complaints in New Zealand) before having a detailed interview with Malcolm Hayes of Hayes McKenzie Partnership. While this interview covered a number of interesting issues on wind farm noise, it was limited in the final cut as it had the potential to lose the audience due to the highly technical nature of the subject matter. However, the full technical interview is included as an extra menu option on the DVD so those people who want to explore and understand the subject to a greater degree can do so.

After the meeting with Malcolm, Peter heads off to White Hill wind farm where he takes some noise measurements from the operational wind farm and discusses noise matters with the local residents and wind farm neighbours.

Conclusions

Initial screenings of the "Sound Advice" DVD have been positive with the majority of comments being that the DVD does a much better job at addressing the subject of wind farm noise than that of the traditionally used printed noise fact sheet. The most significant hurdle was to cover sufficient acoustic facts and terminology without completely losing or boring the audience. NZWEA will be licensing the DVD to interested parties – both in New Zealand and internationally.

Three short video clips from presentation are embedded here.
These can also be played directly from the CD

Third International Meeting
on
Wind Turbine Noise
Aalborg Denmark 17 – 19 June 2009

Wind Shear and its Effect on Noise Assessment

Dick Bowdler

The Haven, Low Causeway, Culross, Fife, Scotland KY12 8HN

dick@dickbowdler.co.uk

Abstract

In 2003 and the following years van den Berg pointed out that the impact of wind shear on turbine noise at night had two effects – that of increasing turbine noise levels for a constant 10m wind speed and that of increasing amplitude modulation due to greater variation in wind speed. But it is still not widely agreed when and where excess wind shear is most prevalent.

This paper looks at the difference and similarity of wind shear conditions at different locations and at different times of day and times of year using actual data collected at wind farm sites. It examines the effect of this on the relative noise level of turbines and the background.

The paper looks at both vertical shear and horizontal shear ("twist") and at differences in wind speeds and wind directions round the blade tip trajectory that might cause excessive amplitude modulation.

Introduction

The first question we need to ask is why are we interested in wind shear in relation to turbine noise.. There are three answers to that question. The first is that it has an influence on the way sound is propagated from the wind turbine to the neighbouring housing. On the whole we tend to deal with this by calculating the "worst case", that is to say the most efficient propagation method. Downwind with hard ground and a low air absorption coefficient. I do not intend to deal with this further in the paper.

The second reason is that we reference turbine sound power levels to the 10m wind speed using a fixed wind shear. This is because IEC 61400-11 measures sound power level related to hub height wind speeds but reports them related to 10m high wind speeds using a standard wind shear equal to a roughness length of 0.05m. As van den Berg pointed out in 2003[1] increasing wind shear results in increasing sound power level output of the turbine for the same 10m wind speed – and so the sound level may be higher than expected. The third reason is that there is some evidence (again from van den Berg[2] and others) that increased wind shear across the face of the turbine results in increased amplitude modulation which may be perceived as exacerbating the noise. It is these last two that I intend to address.

Sites 1 and 4 are flat sites in Eastern England. Sites 2, 3 and 6 are about 200 to 250m above sea level with gently rolling hills as is common in areas of South West England, parts of Northern England and the lower lands of Scotland. Site 5 is a very exposed site in Scotland but rolling moorland, not mountainous.

How Wind Varies with Height

Wind speed increases with height above the ground. This is first due to the fact that winds at higher level are slowed down near the ground because of the friction of the surface. This resulted in an algorithm for the variation of wind speed with height using a “roughness length”. It was thought that the length of the “roughness” of the ground would be the determining factor in how much friction there was. For example a roughness length of 50mm might represent short grass. The actual dimension used however bore little relation to the real life dimension. For example the European Wind Atlas states that “Very large cities with tall buildings and skyscrapers” should have a roughness length of 1.6m. Nevertheless the algorithm provided a useful tool as long as the actual values were not taken too seriously.

The alternative method was to use the wind shear exponent. This is a formula with an arbitrary exponent designed to fit the wind shear described in practice. These two methods are described in many publications so I do not intend to detail them here.

An examination of the two methods shows that there is nothing to choose between them as far as providing a fit to a given situation. Fig 1 shows the graphs of Roughness length 0.05 (in red) and exponent 0.16 (in blue).

Fig 1 – Roughness and Exponent (1)

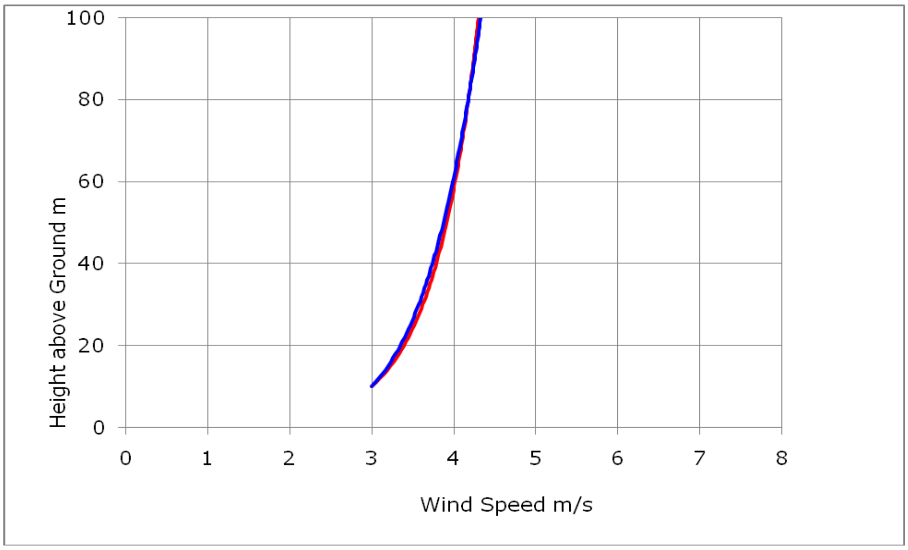

The graphs are so close together as to be indistinguishable. Fig 2 shows the curves for a Roughness length of 0.3 and an exponent of 0.22. Again the curves are very close.

Fig 2 – Roughness and Exponent (2)

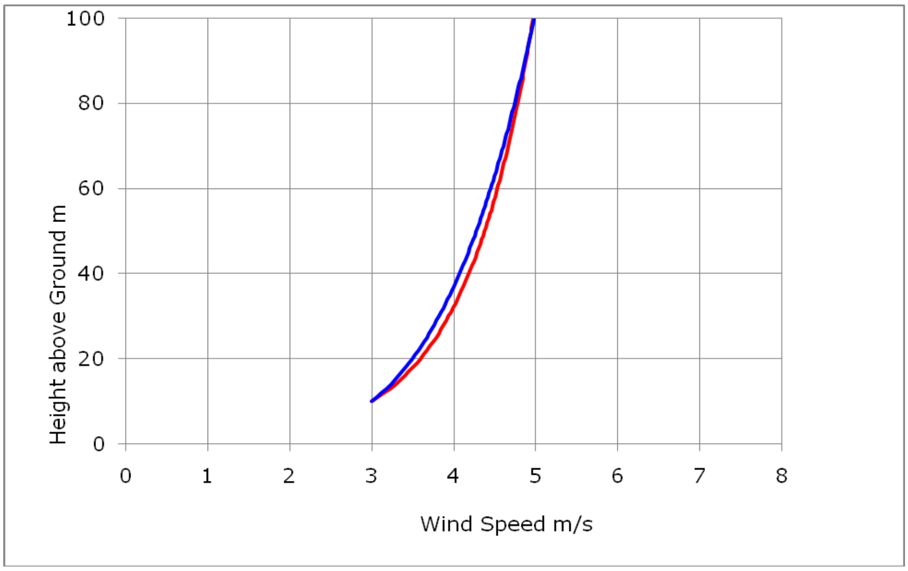

In this paper I use the exponent method for all the calculations and presentations.

Wind Shear

Fig 3 shows the result of measurements of wind speed on Site 2. The measurements are 10-minute periods over about nine months making over 30,000 data points in all. The horizontal axis shows the 10m wind speed as measured by a 10m anemometer. The vertical axis is the value of the shear exponent "m" calculated from wind speeds at 60m and 40m. It can be seen that, with the exception of a few outliers, there is a well defined maximum value of m for each wind speed. The blue line is an approximation to the maximum shear value and is the line defined by the formula $m=2/V_{10}+0.2$ where V_{10} is the 10m wind speed and m is the shear exponent.

Fig 3 – Typical Wind Shear

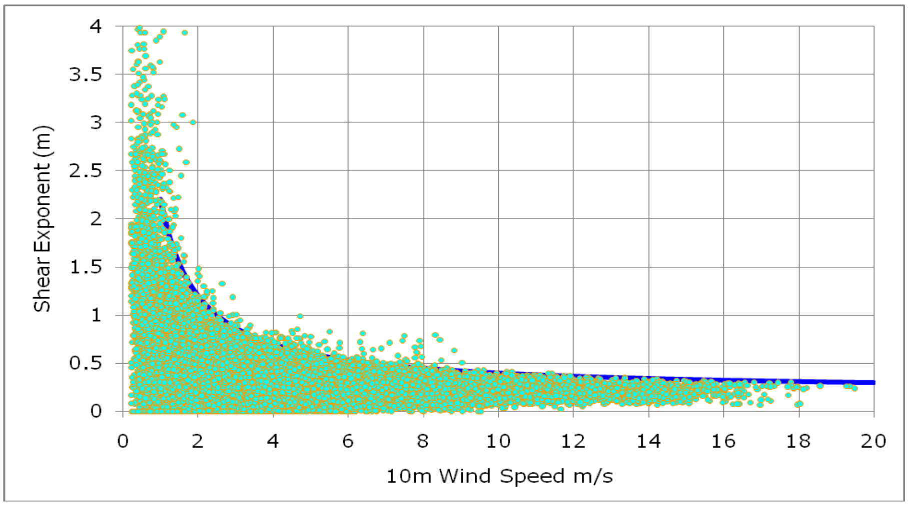

This is a typical pattern shown by all analysis of shear data, though I have not looked at any data for mountainous regions. On flat land and hill land, in principle, the pattern is always the same irrespective of location, time of day or time of year. There are differences in detail which I will come to later.

At low wind speeds the wind shear can be very high but the degree of shear reduces with wind speed. In this case at a 10m wind speed of 8m/s the shear exponent can more or less be said never to exceed m=0.5. (Put into context the handful of points on the graph above the blue line compare with the total number of over 30,000 points on the graph). The other feature is that above 6 to 8m/s there is always some shear.

If we take the data in fig 3 and use them to plot the 80m wind speed against the 10m wind speed we get the result shown in Fig 4. 80m is chosen to represent a typical hub height so that wind at hub height can be compared with the standard 10m wind.

Fig 4 – Typical relation between 80m and 10m Wind Speeds

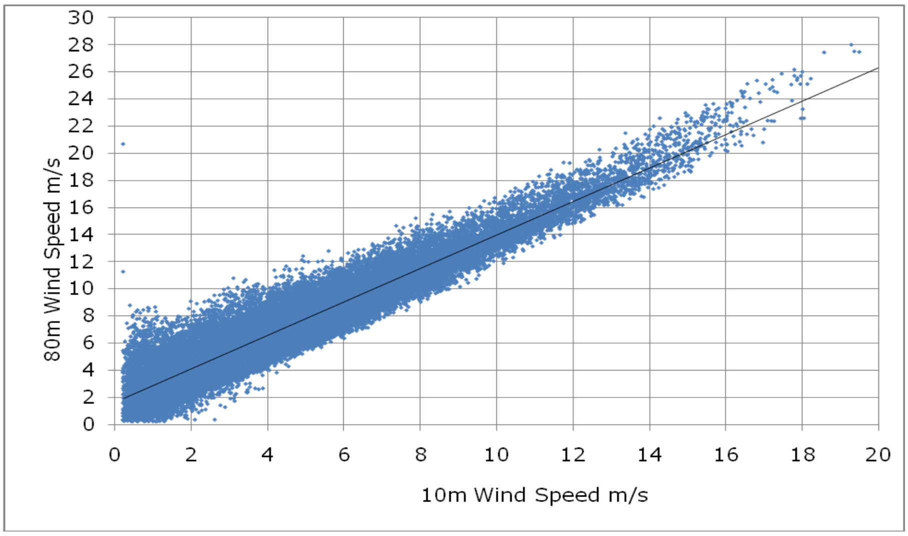

The graph shows that there is a greater proportional spread of 80m wind speeds at low wind speeds. At a 10m wind speed of 4m/s the 80m wind speed can vary between 4 and 10m/s, a range of 150% of the 10m speed but at a 10m wind sped of 10m/s the range is only 40%.. The absolute spread also decreases from 6 to 4m/s in the two cases described.

Generally the most sensitive 10m wind speeds for residents are between 4m/s and 8m/s. This is when background noise levels may not have started rising significantly but turbine noise is often near its maximum. It is the wind shear in this area that is important for assessing the impact of noise on residents.

Diurnal patterns

The first variation of wind shear that I want to look at is diurnal variation. Van den Berg[3] and others have shown that wind shear is greater at night during the day. Fig 5 below shows 10 minute data for Site 4 between 1000 and 1600hrs over a year. These times are chosen because they are in daylight for the whole year. Fig 6 shows data from the same site recorded between 2200 and 0400hrs, the time that is in darkness throughout the year.

Fig 5 Day – Flat Site

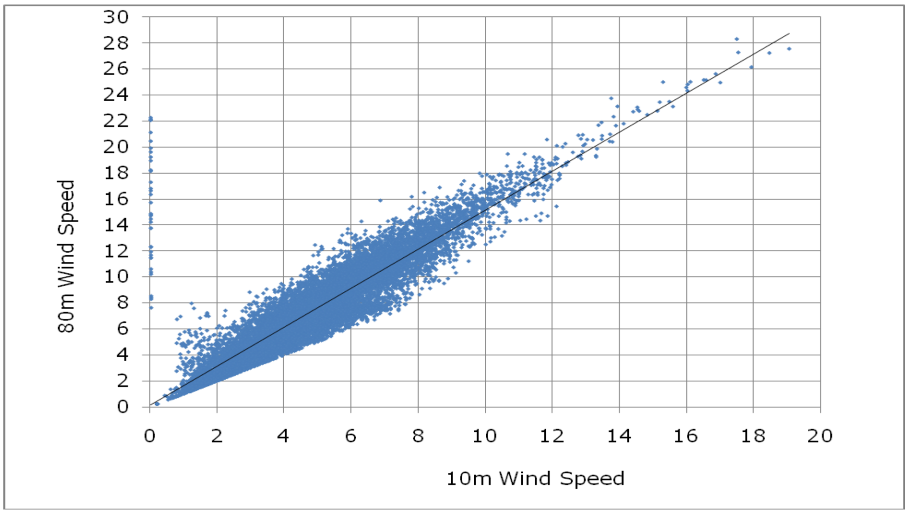

Fig 6 – Night – Flat Site

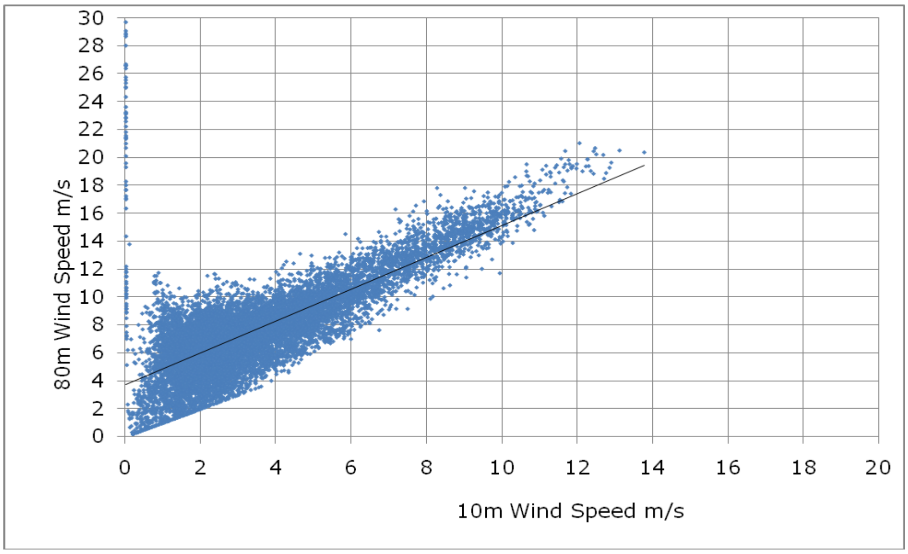

The difference between the two can be clearly seen. Perhaps the most striking result is the much greater spread of 80m wind speeds at night. This means that, at a 10m wind speed of 2m/s, when background noise is likely to be very low the turbines could be running at full sound power in a wind of 8m/s for a small but significant amount of time whilst during the day the hub height wind speed would never exceed 6m/s. The large spread of data indicating high wind shear that can be seen at lower wind speeds in Fig 4 is entirely due to the large spread that occurs at night time. If we look at the most sensitive 10m wind speeds of 4, 6 and 8 m/s the position is shown in Tables 1 and 2. Table 1 shows the average 80m wind speed at each 10m wind speed. Table 2 shows the 10-percentile speed – the 80m speed that is exceeded 10% of the time.

Table 1 – 80m Wind Speeds

Flat Site	10m Wind Speed		
Average	4m/s	6m/s	8m/s
Day	6.2	9.4	12.4
Night	8.3	10.7	12.8

Table 2 – 80m Wind Speed

Flat Site	10m Wind Speed		
10 Percentile	4m/s	6m/s	8m/s
Day	8.1	11.3	13.9
Night	9.8	11.7	14.1

An inspection shows that the average shear at night is similar to the 10-percentile shear during the day. The averages for this site over all wind speeds are a day shear exponent of 0.20 and a night shear exponent of 0.43.

Annual Patterns

Fig 7 shows the plot of 80m wind speed against 10m wind speed again, this time for all times of day and night in the months April to September – the Summer period – for site 4. Similarly fig 8 shows the same thing for the winter months of October to March.

Fig 7 – Summer – Flat Site

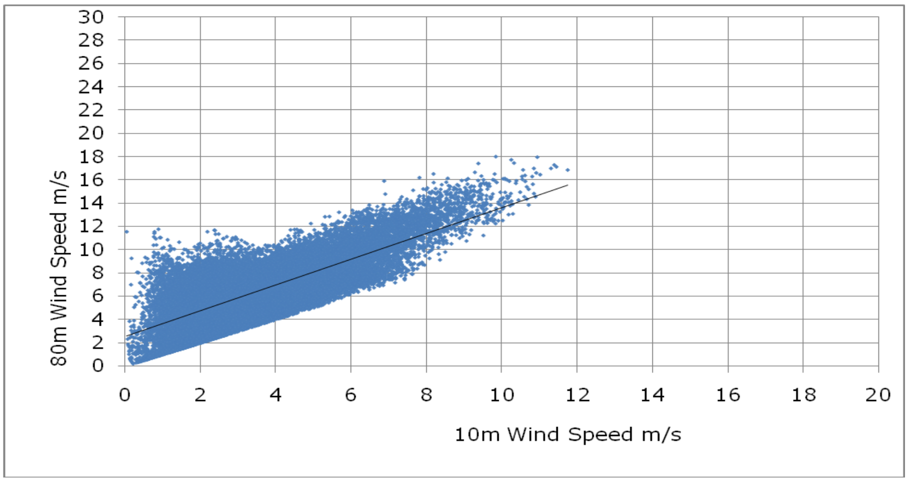

Fig 8 – Winter – Flat Site

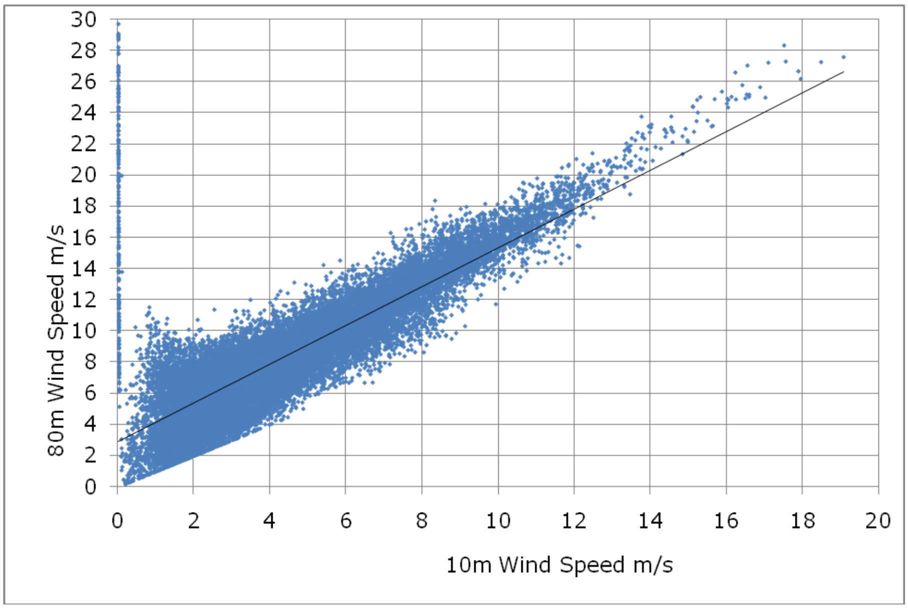

The main difference between summer and winter is that the there are more higher wind speeds in winter. The average wind shear exponent in winter is 0.35 and in summer is 0.30 for this site. At a 10m wind speed of 6m/s the 80m wind speed averages about 9m/s in summer and 10m/s in winter. These figures suggest a slightly greater wind shear in winter but perhaps not sufficient to be significant. In any case it might be expected that there would be higher wind shear in winter because of the longer nights. More investigation is required.

Topography and Local Conditions

It is often thought that wind shear is higher on flat sites. Figs 9 and 10 show the day and night on Site 6 during the day and night (as defined earlier).

Fig 9 – Day – Hilly Site

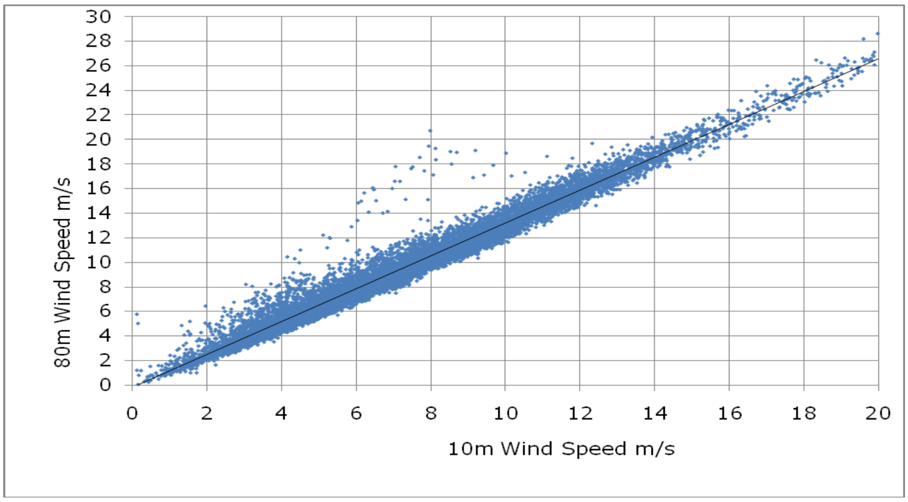

Fig 8 – Night – Hilly Site

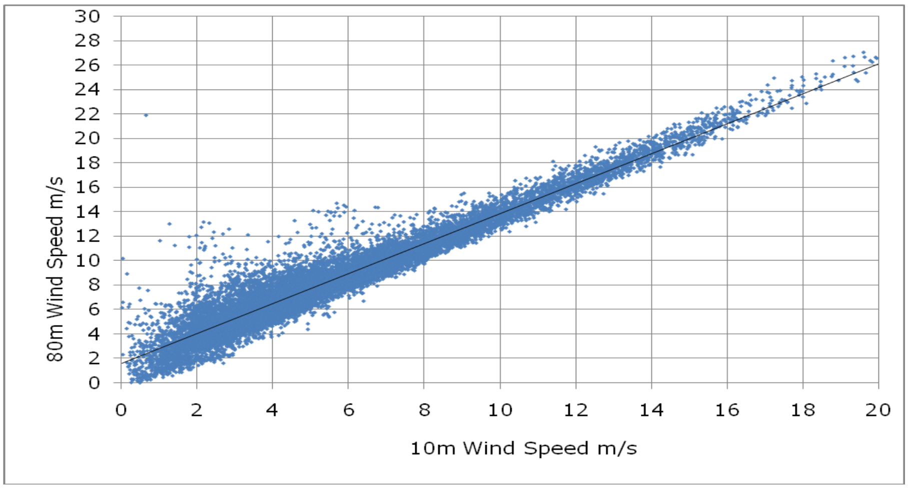

Comparing the above with Figs 5 and 6 it is clear that, overall, there is much less spread on the hilly site than the flat site. There is still the same pattern of more spread at night and higher shear generally at night. Tables 3 and 4 below give the average and 10-percentile figures as before.

Table 3 – 80m Wind Speeds

Hilly Site	10m Wind Speed		
Average	4m/s	6m/s	8m/s
Day	5.1	8.0	10.5
Night	6.5	8.8	11.3

Table 4 – 80m Wind Speeds

Hilly Site	10m Wind Speed		
10 Percentile	4m/s	6m/s	8m/s
Day	6.1	8.7	11.5
Night	7.9	10.0	12.0

Hub height wind speeds are significantly higher on the flat site than on the hilly site for the same 10m wind speed. The averages for this site are a day shear exponent of 0.13 and a night shear exponent of 0.22. This compares with the flat site with a day shear exponent of 0.20 and a night shear exponent of 0.43.

I have also examined wind shear at site 5 where the topography is similar to site 3 but is in a much more exposed part of the country. I do not have a full set of comparative figures for all three types of sites but I can compare the summer data.

The average summer shear exponent is 0.3 at the flat site 4, 0.24 at the hillier site 3 and 0.16 at the very exposed site 5. However, caution needs to be exercised in relying too much on averages. Some part of the reason that shear varies in the way it does is that the more exposed the site the higher the average wind speed and it has been well established that shear is lower at higher wind speeds. The table below shows this data.

Table 5 – Average Wind and Shear

Site	Av 10m Wind	Shear (m)
Site 5 - Exposed	6.4m/s	0.16
Site 3 - Hilly	4.7m/s	0.24
Site 4 - Flat	3.8m/s	0.30

It is more instructive to examine the degree of shear at wind speeds around 6m/s where the impact of noise on residents is likely to be most significant. At a 10m wind speed of 6m/s the 80m wind speed at sites 5 and 3 are about 8m/s whilst, at site 4 it is about 9m/s.

Twist

It is not only wind speed that changes with height but wind direction. Meteorologists appear to call the variation of wind direction with height “shear” in the same way as the variation of speed with height. I have called it “twist” to distinguish the two. It seems unlikely that twist will make a significant difference to sound power output, though it may make a difference to the sound characteristics of the turbine in that increased amplitude modulation may take place where the wind direction at the top of the trajectory is significantly different from that at the bottom.

The convention I have used for describing twist is that it is positive when the wind direction at the upper level is clockwise of the wind direction at the lower level. Twist is normally positive in the northern hemisphere and negative in the southern hemisphere.

Fig 9 Wind Shear and Twist

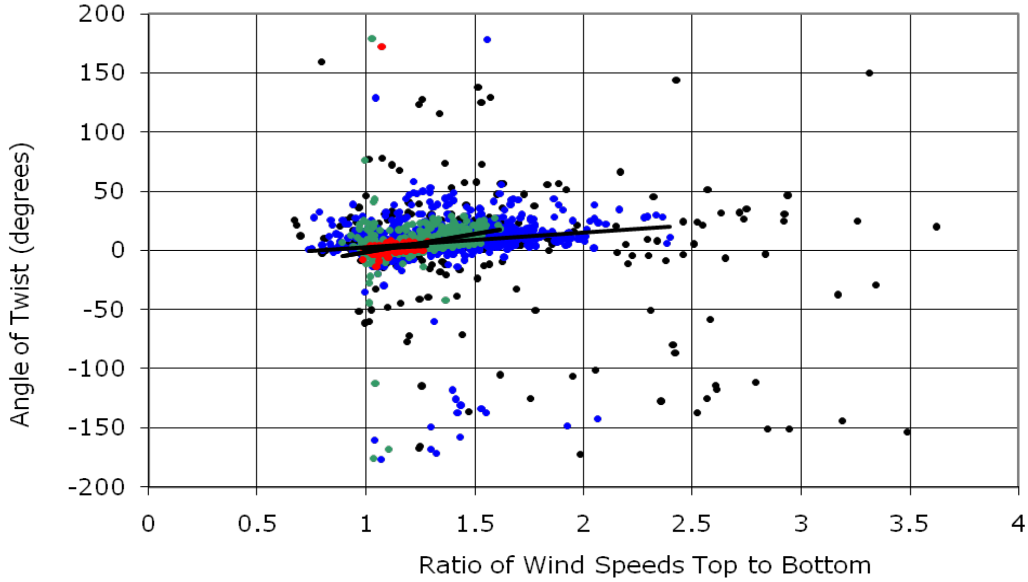

The diagram shows a typical pattern of wind variation with height.

The X-axis shows the ratio of wind speed at 125m to the wind speed at 45m. The further to the right we move the greater the vertical shear. The Y-axis shows the angle of twist. These heights are chosen to represent the top and bottom of the trajectories of a typical turbine blade.

Black shows wind speeds up to 2.5m/s at 10m. These would be wind speeds where it is unlikely that the turbine would be operating. As it can be seen the vertical shear and the twist are widely scattered around the graph.

The blue series shows wind speeds at 10m of 2.5 to 4.5m/s. At these speeds the turbines would normally be operating but, if 2-speed or variable speed, not at full speed and so at a reduced noise level. As can be seen the points are much tighter together. On average there is a wind speed ratio around 1.5 and a twist of about +10 degrees. However, there are many data points where the twist is as high as 30 to 40 degrees.

The green series is 4.5 to 7.5m/s 10m wind speed which is the speed where turbines are most likely to have noise levels in excess of background by the greatest margin. Here the twist is generally less than 10 degrees and the speed ration less than 1.5. Finally the red series shows wind speeds greater than 7.5m/s at 10m high where both shear and twist are much smaller..

If a high wind speed ratio and high twist are contributory factors in excessive amplitude modulation then it is more likely to occur at lower wind speeds than at higher ones

Conclusions

Wind shear is highest and exhibits the greatest spread at low wind speeds . It reduces with increasing wind speed to the point where it is, on average, of a similar value as that used in IEC 61400-11 to define wind turbine sound power levels.

The spread at low wind speeds is more predominant at night on all sites. Night time wind shear is, on average, higher than day time.

There does not appear to be a large difference between average wind shear in summer and winter. The evidence suggests that shear in winter may be slightly higher but this may be due to the fact that there are longer nights when shear is higher.

Wind shear on a flat site is significantly higher than that on a hilly site, even a hilly site with low rolling hills. The spread of wind shear is also higher on a flat site. This is true at all times of day and all times of the year.

High twist tends to occur together with high vertical shear. Twist is more significant, like shear, at lower wind speeds.

References

---

[1] G.P.van den Berg. Wind turbines at night: acoustical practice and sound research. Euronoise 2003.

[2] G.P.van den Berg "Do wind turbines produce significant low frequency sound levels?" 11th International Meeting on Low Frequency Noise and Vibration. 2004.

[3] G.P.van den Berg. As note 1.

Third International Meeting
on
Wind Turbine Noise
Aalborg Denmark 17 – 19 June 2009

Comparison of Wind Turbine Manufacturers' Noise Data for Use in Wind Farm Assessments

Sylvia Broneske

Hayes McKenzie Partnership Ltd., 16a The Courtyard, Dean Hill Park, West Dean, Salisbury, SP5 3TF, United Kingdom

sylvia@hayesmckenzie.co.uk

Abstract

Input data for wind farm noise assessments are provided by the turbine manufacturers in the form of sound power level values for 'standardised' 10 m height wind speeds. The format, in which sound power levels are provided, together with possible uncertainties, differs from manufacturer to manufacturer. Some specifications recommend the use of an additional safety margin to allow for measurement uncertainties. Others state measurement uncertainties from test reports, standard deviation from averaging several test reports, K-values depending on the extent of the confidence level (according to IEC/TS 61400-14:2005) or no information about uncertainties at all. An overview of different methods of publishing wind turbine sound power levels and the result of comparing different wind turbine types for the same development site is given.

Introduction

Wind farm noise assessments are carried out according to country-specific requirements; for example ETSU-R-97 in the United Kingdom, Planning Guidelines from the Department of the Environment, Heritage and Local Government in the Republic of Ireland and TA Lärm plus further specifications in Germany. In general, the international standard ISO 9613 *Acoustics - Attenuation of sound during propagation outdoors* is used to calculate sound pressure levels which result from wind farm developments at noise sensitive properties. Sound power level data is the fundamental input parameter for such calculations. The values, that manufacturers specify, can be based on a variety of sources; theoretical calculations, noise measurements of a single turbine representing a certain make and model, or mean values over a certain number of noise measurements, with or without adding a measurement uncertainty. Depending on the input data, the result can vary widely.

Documents from several of the larger wind turbine manufacturers have been reviewed and the difference in the way the noise data is provided is discussed.

Manufacturers' Methods of Presenting Noise Data

The way in which wind turbine sound power level data is presented by the manufacturers varies significantly. There is no standardised approach.

Some manufacturers issue warranted noise levels for use in noise assessments; others state noise levels for information only but attach a noise warranty to their contract with the buyer, others in turn warrant sound power levels at hub height and give calculated sound power levels referenced to 10 m height for information only. It can also happen that no official document from a manufacturer is available and that noise assessments are based only on a single turbine sound power level test report. If the sound levels from the measurement report are used without adding a measurement uncertainty, there will be no safety margin to allow for measurement uncertainties, uncertainties of the calculation model or slight variation within a batch of turbines.

Every manufacturer has their own method of providing published noise data. In the absence of measurement reports on which noise warranties/statements could be based, calculations are often used to derive noise levels. Calculations can be based on wind turbines of a similar size from the same manufacturer, up- or down-scaled to the new turbine size, or on the same blade model, with amendments to account for a different rotational speed. Only follow-up noise measurements can show how accurate such methods are. In this case, the manufacturer should provide an appropriate safety margin to allow for uncertainties with such a methodology.

A more common method is to conduct a turbine test according to IEC 61400-11 *Wind turbines – Part 11: Acoustic noise measurement techniques* on the prototype or the first erected turbines and, based on that measurement, issue a warranty/statement. The margin between measured and warranted/stated value may vary between only a few tenths of a dB up to 3 or 4 dB depending on the manufacturer.

Noise data is normally given for standardised wind conditions i.e. wind speed at 10 m height based on a ground roughness of 0.05 as specified in IEC 61400-11, but guaranteed noise levels may also be supplied with reference to hub height wind speeds, or specified for 10 m height with alternative roughness factors or values of shear exponent.

Declaration of Tonality Values

In most countries a "penalty" is added for prominent tones in broadband noise when carrying out noise assessments. Information about tones, or warranties for the absence of tones, in the turbine noise, however, is not always given in the manufacturers' documentations.

Some manufacturers claim that their wind turbines don't emit any noise with tonal components and therefore don't make any official statement at all.

Other manufacturers give warranties applicable to the near vicinity of a turbine. A minor tonality of 0-2 dB at the turbine should not be relevant at the receptor and therefore should not lead to a penalty.

Others give a warranty that the tonal audibility ΔL_a is smaller than or equal to 4 dB, measured at the turbine in a test according to IEC 61400-11. But how does this tonal component appear at a receptor? Will it be masked by broadband noise at the receptor location or will it still be audible? In the UK, ETSU-R-97, which refers to measurements at receptors, specifies that a measured tone level of 4 dB above the audibility threshold results in the application of a penalty of 3 dB.

Another method is to warrant the absence of tones at receptors. In this case, tonal noise would not have to be considered in the noise assessment but it would be the responsibility of the manufacturer, to ensure that no tonal noise is present at the neighbouring properties.

Uncertainty of Noise Data

Very often, no information about the accuracy of the provided noise data is given and local authorities have to trust that an adequate safety margin has been added to allow for uncertainties of the measurements and propagation model.

In some turbine warranty documents it is stated that warranties are only valid for sound power levels measured according to IEC 61400-11. In these documents it is often not stated whether a measurement uncertainty has been taken into account in the derivation of the stated sound power levels. It is not always clear whether the warranty level is deemed to be met if the apparent sound power level, plus or minus the measurement uncertainty, is equal to or below the warranted noise levels.

There are manufacturers that recommend a certain safety margin added to the warranted sound power level. One manufacturer, for example, recommends adding 1 dB to allow for such uncertainties. In this case, the warranty is valid for noise levels as described in a table, plus/minus 1 dB. For a worst case calculation, this 1 dB would have to be added to the given sound power levels.

In another document, it is stated that the noise levels in the document are the 'average expected values L_W'. To gain the declared apparent sound power level L_{Wd}, according to IEC TS 61400-14, it is stated that L_W should be increased by 2 dB. This is one of the few manufacturers' documents in which the technical specification IEC TS 61400 *Part 14: Declaration of apparent sound power level and tonality values* is mentioned at all.

One very comprehensive document has been found so far, which includes all the required information such as standard deviation for test reproducibility, mean values of measurement test reports including uncertainty, standard deviation for product unit-to-unit variability and the K-value for 95% confidence level according to IEC 61400-14.

Conditions for Sound Power Level Measurements/Validity

Not all the considered documents mention particular conditions for which the sound power levels are valid. Others are more specific in that respect. Examples of such conditions are:

- measurement standard for the verification of the turbine noise sound power level: IEC 61400-11:2002
- roughness length z_0 = 0.05 for calculating the standardised wind speed at 10 m height
- clean blades, no dirt, no ice, no rain on the blades, no damage to the leading edge
- a certain turbulence intensity
- a certain (vertical) wind shear
- a certain (vertical) inflow angle

The question that arises here is, what happens to the noise levels when those stated conditions are not present at a site? What allowance has to be given for "non-ideal" conditions, which one would expect in practice for most of the time? How do wind turbines within a wind farm interact?

1/3 Octave/Octave Band Data

In general, octave or 1/3 octave band data is not warranted at all. If included in official manufacturers' data, it is given 'for information only'. Some manufacturers publish a sample measurement report together with the noise document from which the relevant octave data can be taken.

Some measurement reports contain octave or third octave band data, or both, for the whole measurement range. Others only state the ones at either the highest wind speed or the wind speed at 10 m height, where 95% of the rated power is reached.

When calculation of receptor noise levels for each wind speed is required, for example according to ETSU-R-97 in the UK, and if the relevant information is available, octave band data for each wind speed could be used. The method commonly used in practice is to take the octave band data for the highest noise level, at reference or other wind speed, and adjust it to the other noise levels at the relevant wind speeds.

If the manufacturers don't supply a specific set of octave band levels for use in the noise assessment, or if there are several measurements reports for one turbine type, consultancies have to take the decision which octave band data to use for noise predictions. This may lead to variation in the assessment.

If, on the other hand, several measurement reports are available, one approach could be to calculate the mean value for each frequency band across the various reports.

In one manufacturer's document, the octave data of all the noise measurements have been plotted in a graph and three different sets of octave data have been derived: an optimistic model with higher noise levels at higher frequencies, a pessimistic model with higher levels at lower frequencies and the average with 50%

of each of the previous models. It is up to the consultant who carries out the noise assessment, which model is preferred.

Other Issues

There are other issues currently not addressed by wind turbine manufacturers' warranted/stated noise data, such as

- the minimum separation distance needed between wind turbines so that turbulence intensity does not increase to such an extent that the sound power levels increase significantly
- amplitude modulation
- a clear declaration of two speed machines and the relevant noise data for each generator stage
- noise data when the turbine is braking for changing generator stages (two speed).

This information is important when examining the effects of wind turbine noise on surrounding properties.

Technical Specification IEC TS 61400-14

As there are individual variations between different turbines of the same batch, turbine noise specification based on measurement results from a single turbine of a particular make and model can hardly be seen as representative of these turbines as a whole. The technical specification IEC TS 61400-14 *Wind Turbines - Part 14: Declaration of apparent sound power level and tonality values* provides a method to determine declared noise emission values from a sample of turbines of the same type. Its aim is~~,~~ to facilitate the comparison of apparent sound power levels and tonality values of different wind turbine types and to increase the reliability of wind farm noise assessments.

IEC TS 61400-14 allows the calculation of the mean apparent sound power level $\overline{L}_W$ and the standard deviation 'σ' from a minimum of three noise measurements at individual turbines of the same type.

The declared apparent sound power level L_{Wd} is then calculated from

$$L_{Wd} = \overline{L}_W + K$$

where L_{Wd} is the declared apparent sound power level of wind turbines of the same make and model

$\overline{L}_W$ is the mean apparent sound power level of at least three measurements

K represents a certain confidence level.

K is equal to 1.645·σ for a probability of 95 %~~,~~ that the apparent sound power level, derived from a turbine test in accordance with IEC 61400-11 at wind turbine of a certain batch, does not exceed the declared value for this batch. For a lower confidence level, a smaller multiplier than 1.645 may be used.

The standard deviation used for the declaration is calculated from three standard deviations: the standard deviation ‘s’, which is determined when averaging the apparent sound power levels, the standard deviation of reproducibility ‘σ_R’ and the standard deviation of production ‘σ_P’.

The more measurement results are available for the determination of $\overline{L}_W$, the more reliable L_{Wd} will be. Increasing the number of measurements will usually result in decreasing ‘s’ and ‘K’, unless the individual measurement results differ significantly.

The declaration of tonality according to IEC 61400-14 should not be performed in the same way as for the apparent sound power level. The results of all measurements should be stated individually.

Comparison of Noise Data

In the following figures, apparent sound power levels with examples of differently derived uncertainty margins are displayed for comparison.

Figure 1 shows the apparent sound power level L_W from one measurement in black, the same L_W with the measurement uncertainty of this measurement report added in a dashed black line, the mean apparent sound power level $L_{W,mean}$ (=$\overline{L}_W$ in the previous chapter) derived from three measurement results in green, and the declared apparent sound power level according to IEC TS 61400-14 with an added confidence level K in orange.

It can be seen, that in this case, the average apparent sound power level of three measurements is higher than the apparent sound power level of the first test result for wind speeds below 9 m/s.

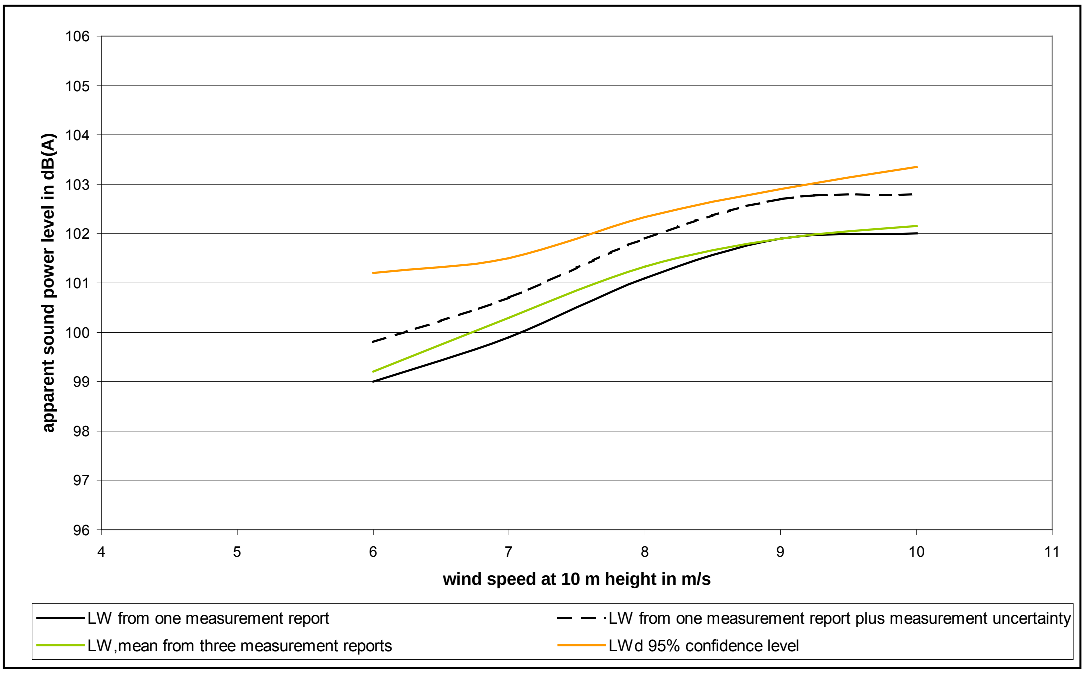

Figure 1: Comparison of measurement results from one measurement L_W, L_W plus measurement uncertainty, mean apparent sound power level derived from three measurement results $L_{W,mean}$ and declared apparent sound power level L_{Wd} with 95% confidence level.

Figure 2 shows the same mean apparent sound power level as in Figure 1 in green, warranted noise data in red and the sound power level which could be recommended for the use in a noise assessment, assuming the safety margin in this recommendation would be + 1 dB.

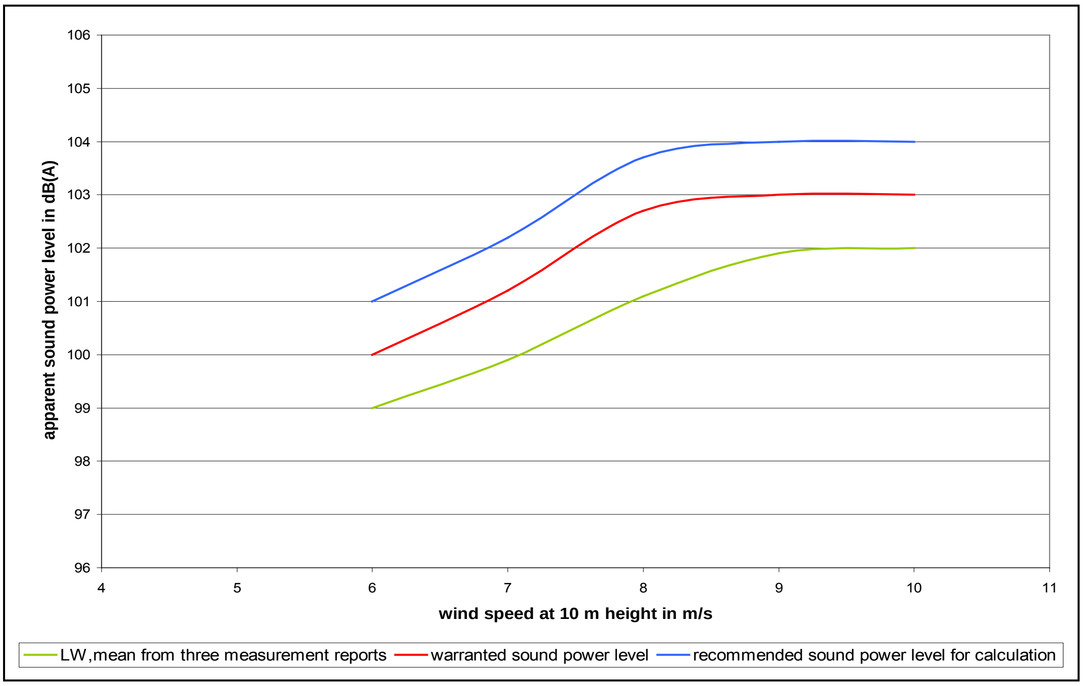

Figure 2: Comparison of mean apparent sound power level derived from three measurement results with warranted apparent sound power level and with recommended sound power level for noise assessments.

In Figure 3 all of the above mentioned noise data are combined.

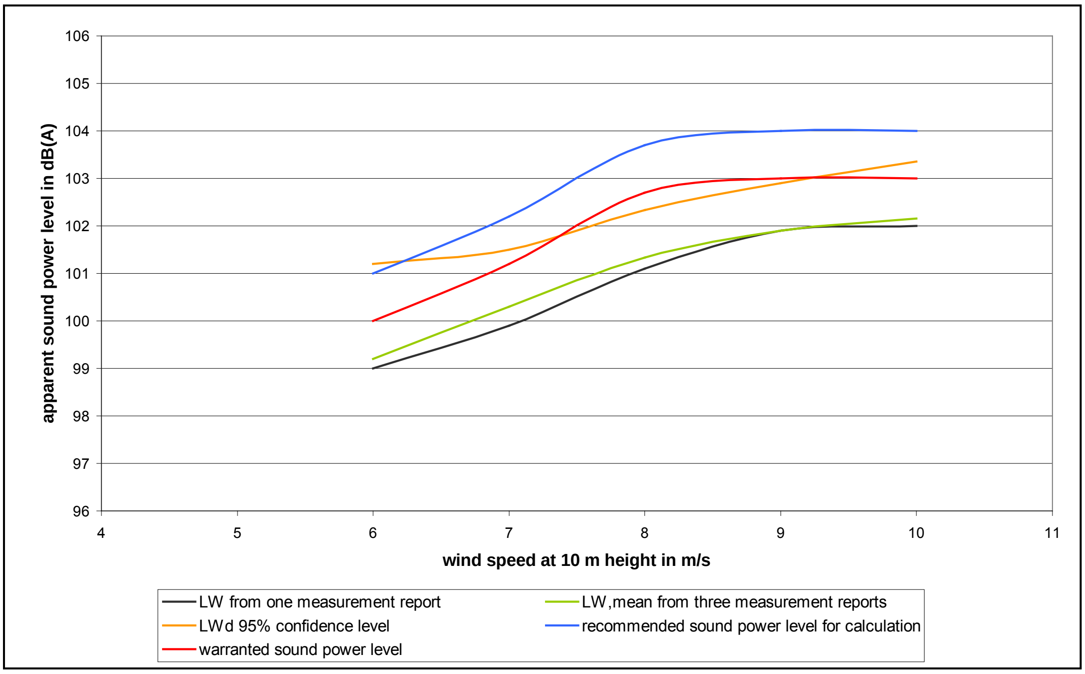

Figure 3: Combination of Figure 1 and 2.

Figure 3 reveals how different the results of a noise assessment may be depending on which set of noise data is used for the prediction.

The orange line symbolises the declared apparent sound power level. When using these noise levels it can be assumed that with a probability of 95% the actual apparent sound power level of a turbine of the same batch, is below this stated declared apparent sound power level. In the presented case, the warranted noise levels are lower than the declared apparent sound power level for wind speeds below 7.5 m/s and above 9 m/s. For these wind speeds the probability that the actual sound power level is above the warranted sound power level increases compared to wind speeds between 7.5 and 9 m/s.

In this case, using the manufacturer's recommended sound power level gives sufficient planning reliability. But it may also be overcautious and result in a layout with fewer wind turbines than might actually be possible.

Figure 3 also indicates graphically the implications of manufacturers using different methods for deriving warranted/stated noise data. It is difficult to interpret the results of an assessment for several candidate wind turbine types unless the input data from all manufacturers is presented in a standardised format.

The quality of the declared sound power level, however, depends on the available measurement reports. The more measurement reports available for a batch, the more representative the mean apparent sound power level will be.

Conclusions

At the moment it is difficult to compare turbine noise data as specified in manufacturers' documents on a like for like basis because the methods for deriving the input data are not comparable.

To gain confidence in manufacturers' noise data, it is important to know how they are derived. Full measurement reports, including measurement uncertainty to verify the stated noise data, are desirable if not essential. If no measurement reports of a turbine model are available, the noise data should be handled with care.

Consultants can calculate the declared apparent sound power level for a turbine model themselves when at least three measurement reports of the same turbine make are provided. In doing this for all the candidate wind turbines at one site, a useful comparison could be achieved regardless of the different methods used by turbine manufacturers for providing a warranty or statement of wind turbine sound power levels.

It would be preferable for all manufacturers to state their noise levels in accordance with IEC TS 61400-14 with the relevant uncertainties, standard deviation and so on, so that it is clear, how noise levels are derived and thus allow noise assessments to be compared on a like for like basis. The noise documents should also include the full measurement reports used to calculate the declared apparent sound power level.

In terms of tonality, octave data and other factors referred to, more information in official noise documents from the manufacturers would be beneficial for noise assessments.

References

The turbine manufacturers' wind turbine noise data documents are examples of the vast amount of documentations, which are available for all sorts of different wind turbine types. This list is not exhaustive.

ENERCON GmbH: 'Sound Power Level E-70 E4', Document SA-04-SPL Guarantee E-70-Rev5_1-ger-eng, 2006

Department of Trade and Industry: 'ETSU-R-97, The Assessment and Rating of Noise from Wind Farms', 1996

GAMESA Corporación Tecnológica, S.A.: 'Design Calculation & Compliance Report – Power Curve and Noise Emission G87 2MW 50/60 Hz', Document GD022914-en, 2008

GAMESA Corporación Tecnológica, S.A.: 'Analysis of the Noise Emission for G8X Wind Turbines', Document GD027805-en, 2008

GE Energy: 'Commercial Documentation Wind Turbine Generator Systems GE 2.5xl – 50 Hz & 60 Hz: Product Acoustic Specifications – Normal Operation according to IEC 61400-11', 2009

International Electrotechnical Commission: ‘IEC 61400-11 Wind turbines – Part 11: Acoustic noise measurement techniques’, 2002

International Electrotechnical Commission: ‘IEC 61400-14 Wind turbines – Part 14: Declaration of apparent sound power level and tonality values’, 2005

NORDEX AG: ‘Noise Levels N90/2500 HS’, Document F008_149_A03_EN, 2007

REpower Systems AG: ‘Power Curve & Sound Power Level Repower MM92’, Document SD-2.9-WT.PC03-A-A-EN, 2008

Vestas Wind Systems A/S: ‘General Specification V90 – 3.0 MW VCS 50 Hz’, Document 0000-5450 V02, 2008

Third International Meeting
on
Wind Turbine Noise
Aalborg Denmark 17 – 19 June 2009

Wind Farm Noise Predictions and Comparison with Measurements

Andrew Bullmore, Justin Adcock, Mark Jiggins, Matthew Cand

Hoare Lea Consulting Engineers
140 Aztec West Business Park
Bristol, UK
BS32 4TX

andrewbullmore@hoarelea.com
justinadcock@hoarelea.com
markjiggins@hoarelea.com
matthewcand@hoarelea.com

Abstract

Conservative approaches to the prediction of noise immissions from wind farms reduce the risk of compliance failure. However, overly conservative approaches introduce the risk of not capturing the true energy generating capacity of a given wind farm site. Unlike other forms of development, conservative planning of wind farms cannot be offset by increased mitigation without incurring such lost energy generating potential. The large scale of modern wind farms means that seemingly small conservatisms in the prediction of noise immission levels can translate to substantial lost development opportunities.

A worst case assessment methodology assumes that a receiver is located downwind of every turbine, all turbines experience the same wind conditions as the first upwind turbine, the ground acts as a hard reflective surface, and all turbines are emitting sound power greater than test levels. Minimal reductions, if any, are factored for the excess attenuation provided by the atmosphere and barrier effects. In practice, all these factors are unlikely to transpire simultaneously. To gauge the pessimism of this approach, several campaigns of long term measurements were carried out near operational wind farms and compared to noise levels predicted using several techniques. Initial results were presented previously; this paper presents further results and analysis and discusses the opportunities for more realistic prediction techniques. The paper then continues to discuss the potential impact that the use of more realistic prediction techniques may have on increasing the potential generating capacity of wind farm sites.

Introduction

It is common practice in many countries to control the noise impact of proposed wind farm developments by setting limits for the maximum level of noise that may occur at surrounding noise sensitive receptor locations. An important distinction in this practice is that the test of compliance in some countries may be based on predicted noise levels alone, whilst in others the test is based on the actual noise levels that occur in practice, as demonstrated by measurements. The latter method offers benefits for regulators in that there is a definitive limit for the noise that may occur in practice. However, measurement based compliance places the onus on developers and their advisors to plan and design wind farms in a way that adequately addresses the risk of a failed compliance test and the subsequent power generation losses that could be incurred to address the failure. The prediction of wind farm noise immission levels (i.e. the noise occurring at the receiver location, in contrast to the emission level that defines the sound power output of the sources) is therefore an integral element of the planning process for measurement based noise compliance regimes. However, prediction of environmental noise immissions from wind farms is influenced by a range of variables. This means that choices have to be made in the calculation parameters adopted for these variables in any assessment, and these choices can have a significant bearing on the outcome results.

The propagation of environmental noise immissions, and therefore its prediction, is influenced by a number of variables. This is evident in the measured noise levels observed around wind farms. Such noise levels tend to show a relatively wide range of temporal variation, even under relatively stable downwind propagation conditions. The key focus of a prediction exercise is usually the upper noise level that will occur under such downwind conditions, for which the following factors must be addressed:

- the turbine sound power and any associated uncertainties;
- the source height;
- the receiver height;
- the wind speed experienced by the turbine rotors, how this may vary across the rotor diameter, how it may vary between individual turbines across a multi-turbine site, and how these variations relate to reference wind speeds derived at other heights or locations;
- the wind direction, and the range of angles to the direct line between the source and receiver for which downwind conditions are considered to occur, along with the portion of an expansive site that can simultaneously lie within these angles;
- temperature and humidity;
- the terrain profile with respect to intervening ground height and noise screening features;
- the ground characteristics of the surrounding area and any regional or seasonally varying changes to its composition;
- the selection of noise index adopted to quantify the calculated noise immission levels (L_{Aeq}, L_{A90}, L_{A50}, etc.).

These variables, and the manner in which they are accounted for, will impact on the likelihood of the predicted noise immission levels being higher or lower than the actual immissions that occur in practice. Understanding the nature of these factors to enable informed selection of prediction input parameters is therefore vitally important for designers and developers alike if they are to make truly informed selections of their noise prediction methodologies and likewise the relevant input parameters for their selected methodology. Ultimately, there will be a trade-off of considerations, which will need to strike the appropriate balance between the potential generating capacity losses of conservative approaches and the compliance risks of more optimistic approaches.

In most instances, environmental noise predictions are made on the basis of established engineering methods such as ISO 9613[1]. The use of these methods has been supported by various studies such as the EU Joule report[2] which found that such methods offered a robust means of estimating downwind noise levels that would not generally be exceeded in practice, and generally offered a margin of conservatism depending on the choices made regarding input parameters. However, despite the relative simplicity of such prediction methods (when compared to advanced numerical or analytic methods), informed choices still need to be made on a site by site basis. Experience suggests, however, that these choices can have a significant effect on the outcome findings of individual noise assessments and thus can often become the focus of considerable dispute between developers/designers and other interested parties.

Previous papers[3] produced by Hoare Lea Acoustics highlighted the effect that seemingly minor assessment choices can have: differences of less than 3 dB(A) can translate in effect into large differences in the potential generating capacity of individual wind farm sites, which has implications for national-scale wind energy potential. To provide an improved basis for making noise prediction choices, Hoare Lea Acoustics have carried out noise monitoring exercises around a number of UK wind farm sites for the purpose of comparing predicted and actual noise immission levels. A key element of this investigation was to compare predicted noise levels that are derived from techniques that are normally used during the design phase of a wind farm with the actual immission levels that occur in practice. This investigation has considered predicted and measured turbine noise levels that occur for the wind speed experienced at the turbine rotors, thus focussing the analysis on sound power and propagation effects by limiting the influence of uncertainties related to reference wind speeds and wind shear.

This paper presents the findings of the measurements and analysis completed to date and sets out the requirements of any further studies.

Site Descriptions

For commercial reasons, it is not possible to disclose the full details of the wind farms chosen for this study, and thus the following general descriptions are provided. All three sites (A, B and C) were located in rural areas and comprise wind farms with more than 20 turbines. The turbines in all three cases were two speed active stall regulated machines rated at over 2 MW generating capacity per machine, with hub heights of 60 to 70 meters.

Site A

The wind farm is located on a relatively high plateau characterised by moderately undulating terrain and minimal vegetation. Ground conditions were a mix of partly grassland and mainly peat bog, but given the undulation, the land was not prone to complete saturation. In addition, ground conditions were effectively frozen for the most part of the measurements because of low ambient temperatures.

Site B

The wind farm is located in reasonably flat terrain with minimal vegetation. The ground surrounding the wind farm was almost entirely composed of peat bog. These ground characteristics, coupled with the very high rainfall in the area, meant that the ground is believed to have been totally water logged for the entire duration of the survey, thus providing effectively hard ground propagation conditions.

Site C

The terrain was lightly undulating but effectively flat in acoustic terms, and ground conditions were a mix of grassland and flooded areas. Minimal vegetation was present in the immediate surroundings of the turbines, but large areas of forestry were located further away.

Survey Description

At each site, automated Type 1 sound logging meters (SLMs) were positioned at varying distances from the nearest turbine, with an installed microphone height of approximately 1.5 m above ground.

For all sites, the SLMs were set to log continuous periods of 10 minute noise levels, recording statistical and equivalent noise level parameters. The internal clocks on the SLMs were synchronised with the wind farm control system. All systems were calibrated on deployment, during interim data collection and following collection from site, no significant drifts in sensitivity were found (typically below 0.5 dB(A)).

Supplementary non-acoustic data was obtained from the Supervisory Control & Data Acquisition (SCADA) System of each wind farm for the operation of the turbines and met mast during the period of noise monitoring. The SCADA data provided the following information:

- date/time at the end of each 10 minute period;
- primary wind speed from the turbine nacelle (mean);
- turbine power output (kW) (mean);
- turbine rotor speed (min/mean/max);
- turbine nacelle orientation (mean);
- met mast wind speeds at hub height (mean);
- met mast wind direction at hub height (mean);
- rainfall indication;

- temperature and humidity (not used in the present assessment but effects to be studied).

Site A

3 sound level meters were positioned to the northwest of the wind farm at distances ranging from 415 m to 920 m. The equipment comprised Svantek SVAN949 logging SLMs housed in environmental enclosures with battery power. The enclosures have an integral pole to provide a mounting for the microphone and windshield system. A two layer windshield system was used to reduce wind induced noise on the microphone. The primary windshield and rain protection were provided by a 01dB BAP21 outdoor microphone adaptor which enclosed the standard microphone and pre-amplifier. The secondary windshield was custom made from open cell foam approximately 25 mm thickness formed as a domed cylinder 170 mm diameter and 300 mm high. A lower disc of 40 mm thick open cell foam formed total enclosure of primary windshield. The outer windshields were custom designed following the guidance given in the report Noise Measurements in Windy Conditions[4]. The report indicates that the insertion loss of this type of windshield assembly is likely to be less than ±1 dB between 50 Hz and 5 kHz. The positioning of the meters was largely driven by practical access constraints. A total measurement period of approximately 47 days was obtained at this site.

Site B

5 sound level meters were positioned along a single line directed just to the west of north. The alignment of this array of meters was chosen for the availability of stable ground conditions and to avoid local streams to the north east of the site which would have been sufficient to contaminate the measurements with water flow noise. The measurement distances were 101 m, 270 m, 466 m and 754 m. The equipment was the same as that used at Site A. A total measurement period of approximately 34 days was obtained at the 100 m location and more than 57 days at the other locations.

Whilst the northwest positioning of the meters for both sites A and B was out of the direct down-wind line according to the prevailing UK south westerly wind direction, it offered a broader mix of wind directions to be acquired enabling both downwind and crosswind noise propagation conditions to be investigated.

Site C

At site C, five sound level meters were positioned along two lines directed to the North and North-East, at distances of 100 m to 820 m from the closest turbine, in recognition of prevailing wind directions and site constraints such as streams and forestry. Individual positions surrounding the site, at distances of 700 m to 1000 m were also installed. In addition to the Svantek SLMs, systems based on RION NL-31 SLMs in similar enclosures were used, and the microphones equipped with large diameter windshields.

To reduce uncertainties due to ground absorption effects and help characterise the effective noise emissions of the sources, the closest position consisted of a microphone installation on a circular hard board with a double hemispherical windshield arrangement, following the guidance of IEC 61400-11[5] for turbine sound power certification. In addition, several other individual positions were located at varying distances around the wind farm. A total of approximately 2 months measurement data was obtained.

Analysis

The first element of the data analysis was to correlate the measured noise level information with the prevailing wind conditions. At the design stage of a wind farm, predictions would normally be based on a single reference 'free condition' wind speed value which is taken to be experienced simultaneously by all wind turbines (with the exception of very large sites where more than one reference may be used). Thus, for this study, it was initially chosen to relate the measured noise levels to a single wind speed and direction representation for the site. Generally, this information was acquired from the site meteorological masts. However, at Site B, it was known that under certain directions, the reference meteorological masts would be downwind of the wind farm and the wind speed measurement would therefore be influenced by the wind farm's presence. For these directions, the wind speed was taken from turbine locations that were upwind of the remainder of the site. The wind speed data at the turbines were deduced from the nacelle anemometer readings, subsequently corrected to free-flow conditions (using site-specific nacelle corrections supplied by the site operators). In all instances, the wind speed reference for the correlation related to hub height wind speeds. Due to differing client requirements for sites, the wind speed data was either corrected to 10m wind speed heights assuming reference roughness conditions (z=0.05) (Sites A and C), or raw hub height wind speed data was referenced (Site B).

The correlated noise and wind speed data were then filtered to eliminate any periods in which rainfall was indicated to have occurred, or during the times when service personnel were known to have been near the sound level meters.

At site A, additional data filtering comprised reduction of the data set to wind directions from 90 to 200 degrees to provide a 110 degree wide arc of downwind propagation conditions (required to encompass the distributed measurement locations).

At Site B and C, data filtering resulted in the production of two datasets for downwind angle ranges +/-15 degrees from directly downwind and +/-45 degrees from directly downwind. The former angle range is specified in the relevant turbine sound power output standard (BS EN 61400 Part 11:2003[5]) whilst the latter represents an extended range often regarded as still representing downwind conditions (although downwind propagation can ultimately occur for wider angles due to the range of wind speeds considered for wind farm sound propagation). An additional dataset was also formed for wind directions within +/-45 degrees of directly upwind conditions for the nearest turbine and the measurement line. In addition, the study focussed on the periods in which all turbines were generating in high speed mode.

For each of these correlated 10 minute records, predicted noise levels were generated using the ISO 9613 prediction methodology according to the following parameters:

- source height equal to hub height;
- receiver height equal to 4 m and free-field conditions;
- 10 degrees Celsius and 70% relative humidity;
- flat and level ground cover for two separate conditions: G = 0 and G = 0.5 (for source, middle, and receiver ground) to consider hard and mixed ground cover conditions, according to site-specific considerations;
- turbine sound power data provided by the manufacturers and measured according to BS EN IEC 61400 Part 11:2003[5], excluding any margin for test uncertainty or manufacturers warranties (i.e. raw measurement turbine noise levels). The turbine sound power data was converted to hub height wind speeds (assuming reference ground roughness of 0.05 m) and plotted to obtain a 3rd order polynomial best fit curve. This curve was then used to obtain the sound power value for non-integer wind speeds when required;
- the subtraction of 2 dB(A) to correct for the use of the L_{A90} rather than L_{Aeq} index, according to ETSU-R-97[6]. This assumption was found to be consistent with the analysis of the measured data.

The predictions are first made without inclusion of any margin for test uncertainty or manufactures warranties. It is common practice for manufacturers to add approximately 2 dB, although actual values may be considerably different to this according to commercial factors. The IEC 61400-11 standard requires an estimate of the test uncertainty to be presented along with the determined turbine sound power, and reported values tend to be less than 2 dB.

Results & Discussion

Site A

The analysis of Site A was subject to a greater degree of complexity due to factors such as ground terrain profile and the varied orientations of the measurement locations relative to the wind farm. Thus, whilst the analysis of Site A was supportive and consistent with that of the other sites, for brevity only partial results are presented within this paper.

Figure 1 presents the results of measurements at the most distant measurement locations: position 3, approximately 900 m from the nearest turbine. Predictions were made using hard ground cover (ISO 9613 G=0 for the source, middle and receiver ground) because of site observations of a frozen ground surface for which G=0 would be expected to be the appropriate ground characterisation. The predictions for each 10 minute period only included for the turbines which are known to have been operating, as the number of operational turbines varied during the survey; this results in lower predicted levels, particularly apparent in lighter wind conditions.

The predicted immission levels, excluding any margin for uncertainty, generally exceed measured levels; the margin above typical, average immission levels is approximately 3 dB(A). The addition of a further 2 dB(A) sound power uncertainty margin would then correspond to a significant over-estimate of typical immission levels. Furthermore, background ambient levels have likely influenced the measurement to some extent; this aspect is discussed in more detail for site B below.

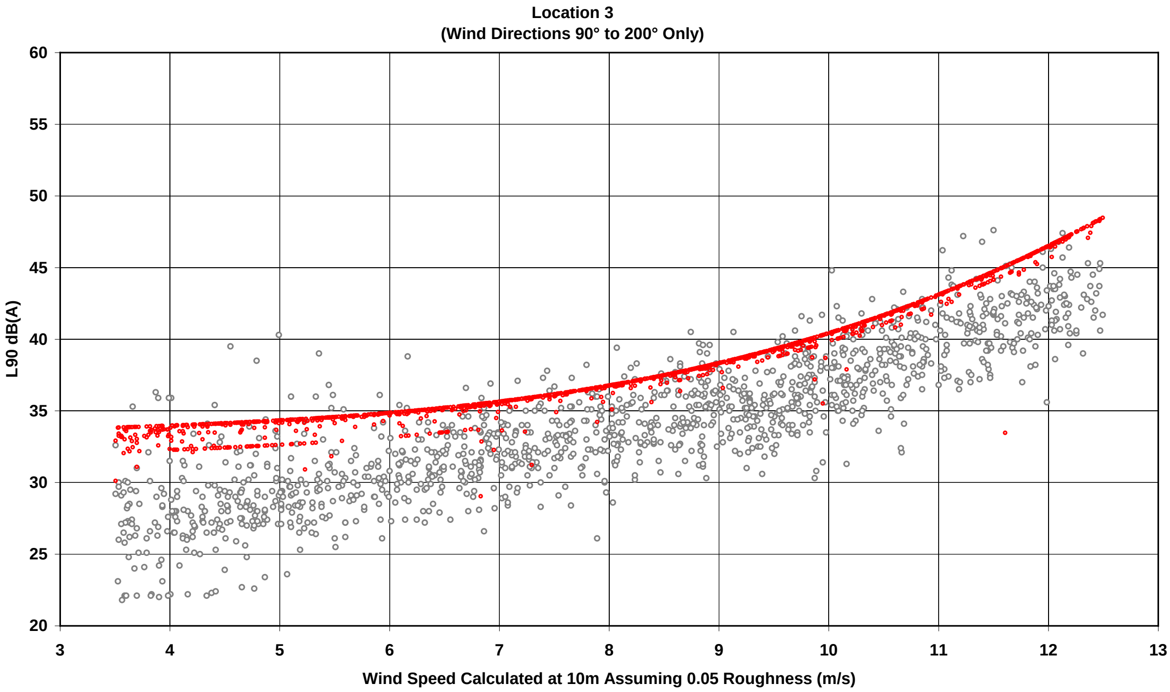

Figure 1 - Comparison of Site A measured (grey) and predicted (red) noise levels at measurement location 3 only.

Site B

It was more straightforward for this site to directly compare the 4 different measurement locations, situated at increasing distance from the wind farm.

The group of charts presented in Figures 2a to 2d relate purely to the Site B measurements, with associated noise immission predictions presented for a single prediction methodology, which is based on hard ground cover (ISO 9613 G=0 for the source, middle and receiver ground). This is because site observations indicated the soil to be almost totally submerged by ground and surface water for which G=0 would be expected to be the appropriate ground characterisation. A single reference free-field wind speed for each ten minute period is assumed to occur at all of the turbines

The indicated upwind measurements for all four sites are the +/-45 degree upwind measurements taken from the furthest position (where upwind noise levels are more likely to relate to background noise levels). The indicated downwind measurements are for the +/-15 degrees angle only. Comparison of the results for the four separate measurement locations indicates the following:

- The upwind and downwind measurements show a very clear noise level difference which supports the view that downwind measurements have been strongly influenced, if not controlled by, the wind farm's emissions. At the furthest location, the difference between the downwind measurement trend line and the general trend of the upwind values is around 6 to 7 dB(A). Previous studies such as the EU Joule project[2] have indicated differences between upwind and downwind turbine noise levels of the order of 10 dB(A) to 15 dB(A) at distant locations. The observation of a lower difference at the furthest position may indicate that either the 10 dB(A) to 15 dB(A) reduction has not been realised at this site, or more likely, that the background noise is dominating the upwind measurements, thus limiting the observed difference.
- At all locations, the predicted immissions trend line generally exceeds (by up to approximately 1 dB(A) at the nearest measurement location) or just equals the downwind measured data trend line. The exact background noise level influence at each measurement location for each 10 minute period cannot be known. It is however likely that the background noise level may have contributed 1 dB(A) or more to the total measured noise levels at the furthest location. The margin between actual turbine contribution and the predicted immission levels will therefore be greater than indicated by the total measurement comparison represented in the charts.
- At hub height wind speeds up to approximately 12 m/s, the margin between the prediction trend line and measurement trend line is relatively constant for increasing wind speed at each site. At higher wind speeds, the prediction and measurement trend lines diverge at each site, with the predictions showing an increasing margin above the measured noise levels. Subsequent results discussed later tend to suggest this is due to the increased significance of wind speed variations across the wind farm at higher wind speeds.
- The margin between the prediction trend line and measurement trend line tends to progressively decrease with increasing distance from the turbines. The most obvious potential cause of this effect is the increasing influence of background noise at increasing distance. However, another important consideration is the changing angle between the turbines and the measurement locations relative to the wind direction with increasing distance from the turbines. As the receiver location approaches the turbine locations it becomes increasing unlikely that the receiver location could lie downwind of every turbine simultaneously. This means that some turbines at peripheral positions may contribute less than the directly downwind propagation assumed in the prediction. At increasing distance, this effect is reduced, and the turbines located at the periphery of the site will then increasingly contribute to the total wind farm noise level (i.e. a greater portion of the turbines at the wind farm site will be propagating sound under conditions closer to direct downwind propagation).

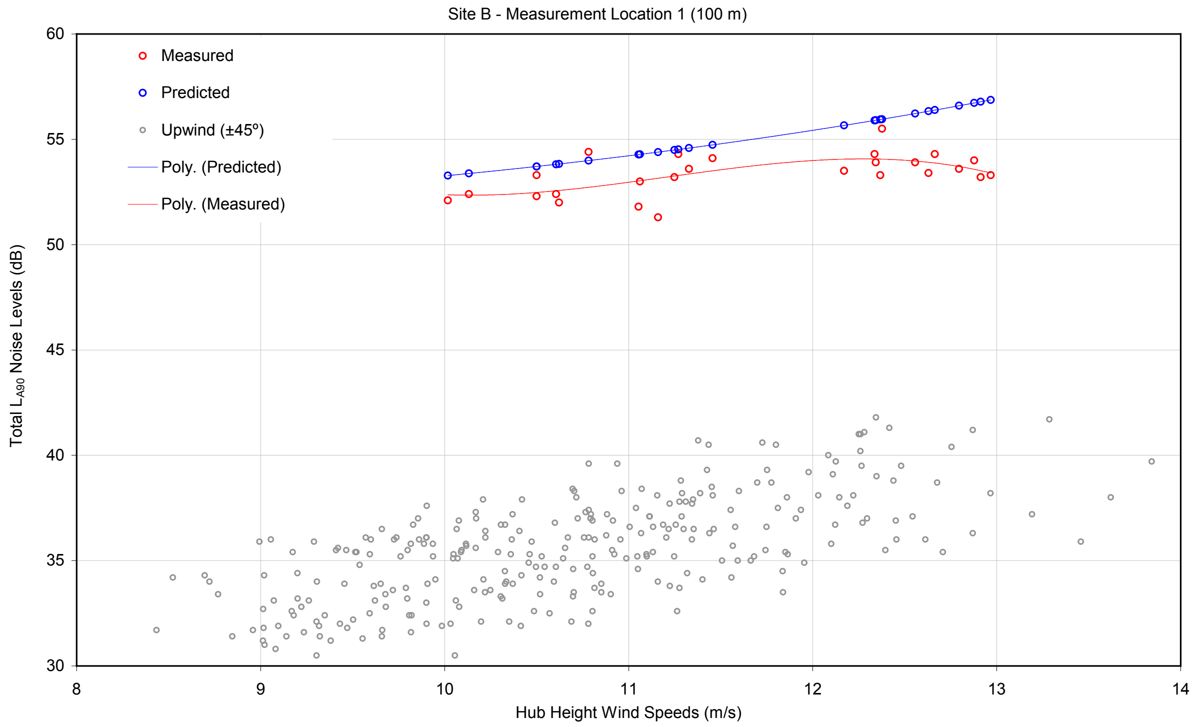

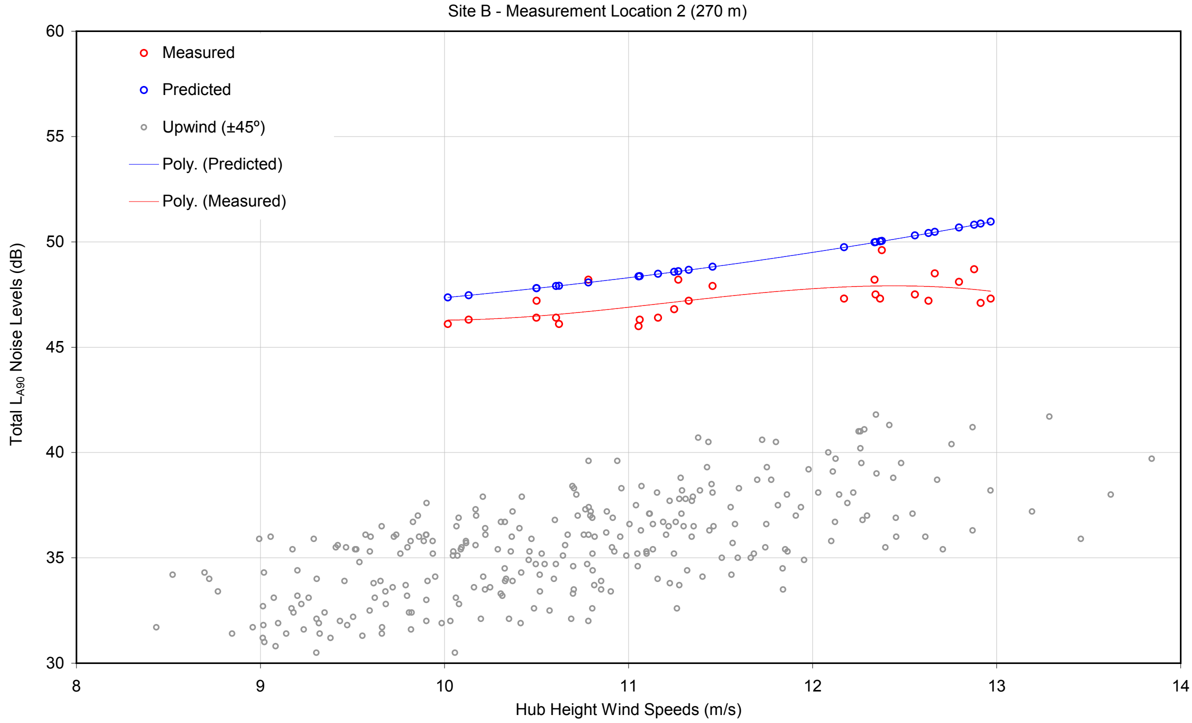

Figure 2(a & b): Sample analysis group set to compare Site B measured and predicted noise levels at the 4 measurement distances. All downwind angles restricted to +/-15 degrees. Predicted noise levels based on a single site wind speed reference and G = 0.

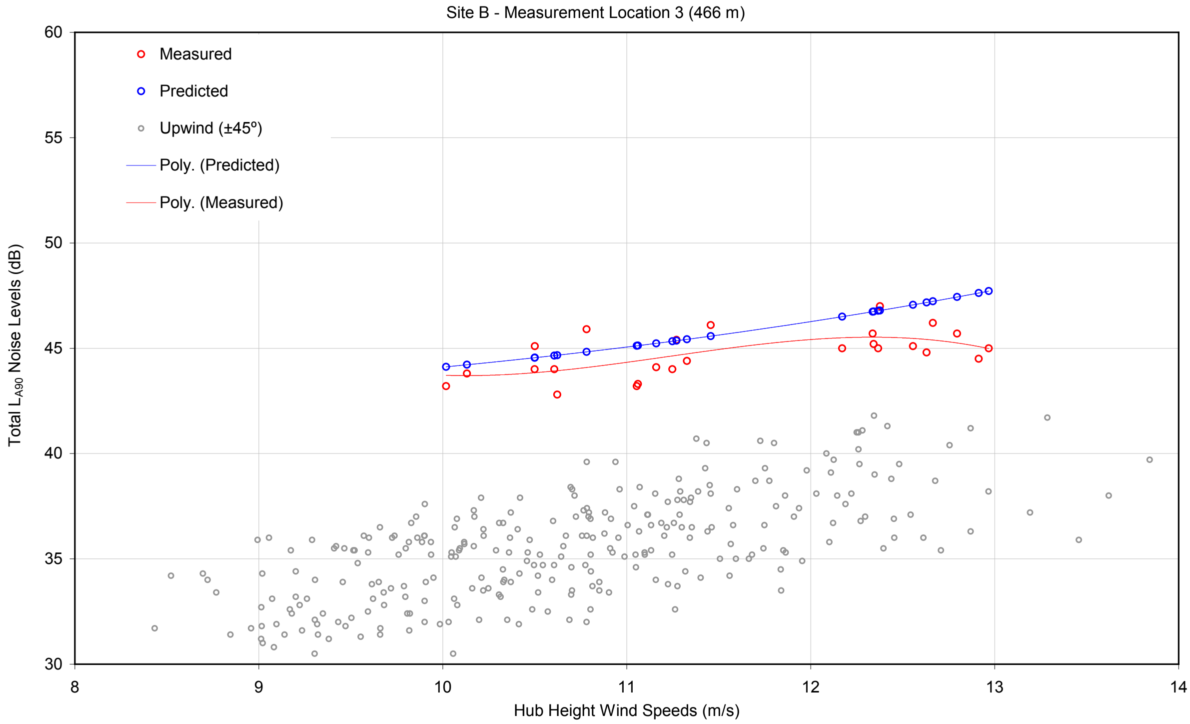

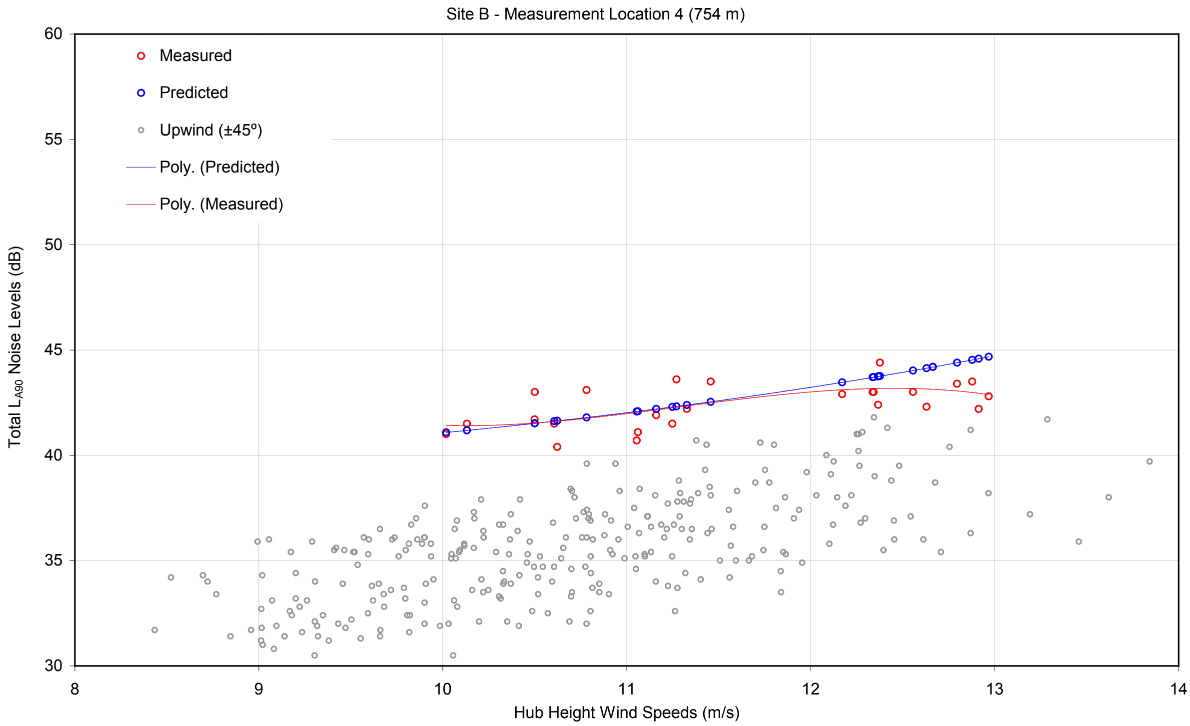

Figure 2 (c & d): Sample analysis group set to compare Site B measured and predicted noise levels at the 4 measurement distances. All downwind angles restricted to +/-15 degrees. Predicted noise levels based on a single site wind speed reference and G = 0.

The group of charts presented in Figures 3a and 3b relate only to measurement location 4 (754 m) of Site B. The 2 charts for this location present +/-45 degrees downwind conditions, and differ in terms of the wind speed reference used for the predictions: initially a single wind speed reference as presented in figure 2, but then modifying the predictions to account for the actual wind speed seen by each individual turbine in each 10 minute period. Comparison of the results indicates that:

- Expansion of the range of downwind angles from +/-15 degrees to +/-45 degrees indicates the predictions exceed the total measured noise levels by a slightly greater margin for the widened downwind angle. This may be due to the increased number of data samples offering a better representation of the true relationship between measurements and predictions. Alternatively, this may indicate that the contribution of the dominant/nearest turbines to the measured levels is progressively reduced as the wind direction moves away from directly downwind conditions and this effect is not represented in the predictions.

- The predictions made on the basis of the individual wind speed experienced by each turbine rather than a single site wind speed reference indicate immission levels which no longer diverge from the measurement trend line at higher wind speeds. This tends to suggest that the margin of conservatism demonstrated at higher wind speeds is strongly related to the reduced level of wind seen by the nearest turbines to the measurement location which may be due to sheltering and/or wake effects of upwind turbines. To investigate this further, a statistical analysis of the difference between the single wind speed reference and the wind speed of each of the turbines indicated the following key figures:

  - *Mean difference = -0.5 m/s*
  - *Standard deviation of differences = 1.2 m/s*
  - *Maximum decrease = -5.1 m/s*
  - *Maximum increase = 4.3 m/s*

  [Values shown are derived from the individual turbine specific wind speeds minus the single site reference wind speed. A negative number indicates the reference wind speed is overestimating the wind speed at each individual turbines.]

  A wind speed changes of the order of 0.5 m/s would correspond to a 0.4dB difference in the sound emissions of the turbines. The values above are averages, but immission levels are dominated by the closest turbines which are also the most shielded in down-wind conditions. The scatter of the predicted data also appears closer to that of the measurement data when using the variable wind speed reference, which suggests this effect could be a significant source of the variability observed in practice.

- Although the predictions appear to match with measurements at the most distant location, the latter were likely influenced by background noise to a certain degree. If the typical upwind measured noise levels are taken as an estimate of the background levels, this influence would then equate to an increase of 1 dB to 2 dB. The true margin between predictions and measurements would then be similar to the margin observed at closer locations. The further addition of a 2 dB(A) uncertainty margin would then correspond to a significant over-estimate of typical immission levels.

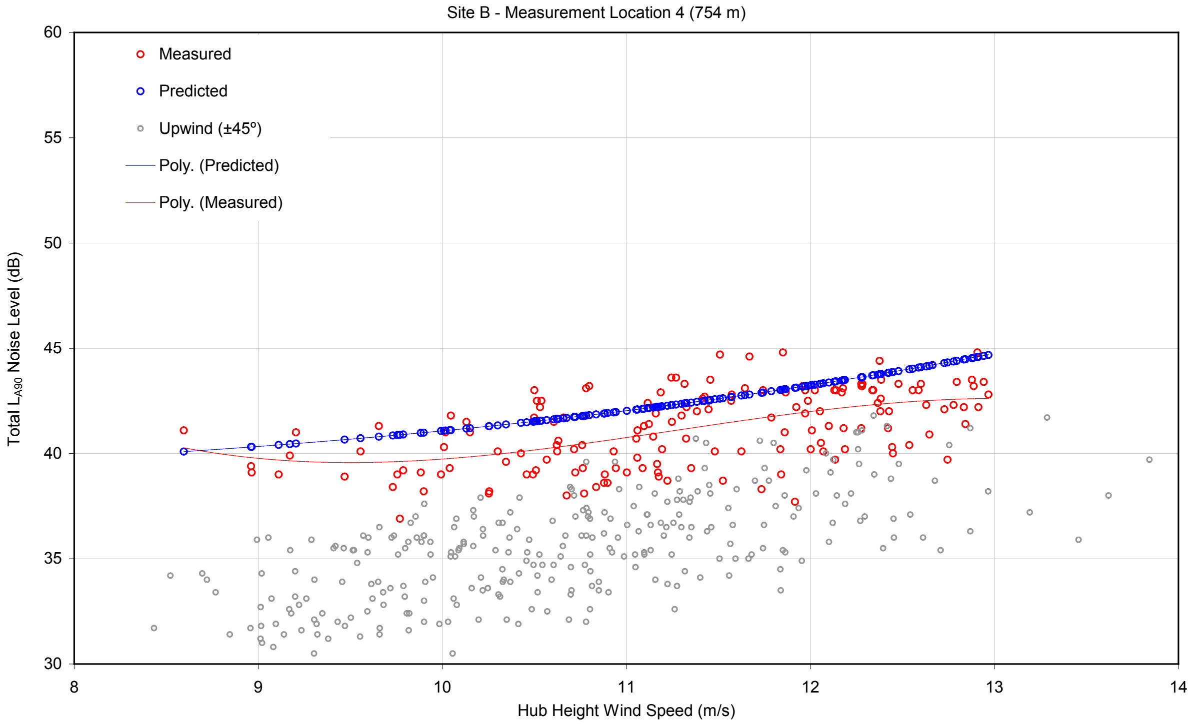

Figure 3a: Comparison of Site B measured and predicted noise levels at measurement location 4 only. All downwind angles restricted to +/-45 degrees. Predicted noise levels based on a single site wind speed reference and G = 0.

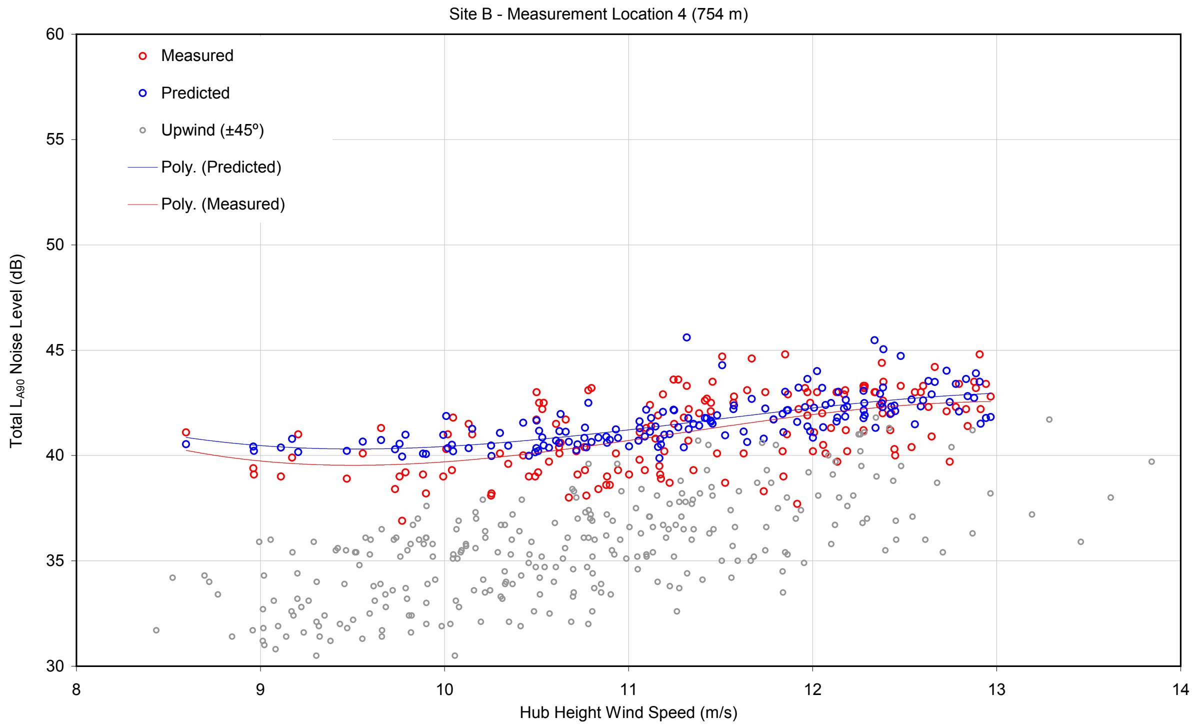

Figure 3b: Comparison of Site B measured and predicted noise levels at measurement location 4 only. All downwind angles restricted to +/-45 degrees. Predicted noise levels based on turbine specific wind speeds and G = 0.

Site C

The prediction methodology for this site was based on a mixed ground cover (ISO 9613 G=0.5 for the source, middle and receiver ground) based on site observations described above.

The results obtained for site A and B suggest that adding a 2 dB “uncertainty” margin, typical of the commercial warranty margin used for some turbine models, to the raw tested sound power values, is likely to lead to an over-estimate of actual turbine noise immission levels. The stated test uncertainty, as required by the relevant IEC 61400-11 standard, has therefore been referenced instead. For the turbines installed at site C, the predictions were made by using the measured sound power data and adding the corresponding stated uncertainty value of 1 dB.

Figure 4 shows the noise levels measured at position 1, situated 100 m from to the closest turbine on a reflective board. At this position, the influence of background noise levels is minimal. However, comparisons with predictions at this location were complicated by the proximity of the measurement location to the turbines which makes it unlikely it could lie downwind of every turbine simultaneously. The effect of the wind speed variations across the site (described below) was also identified as significant.

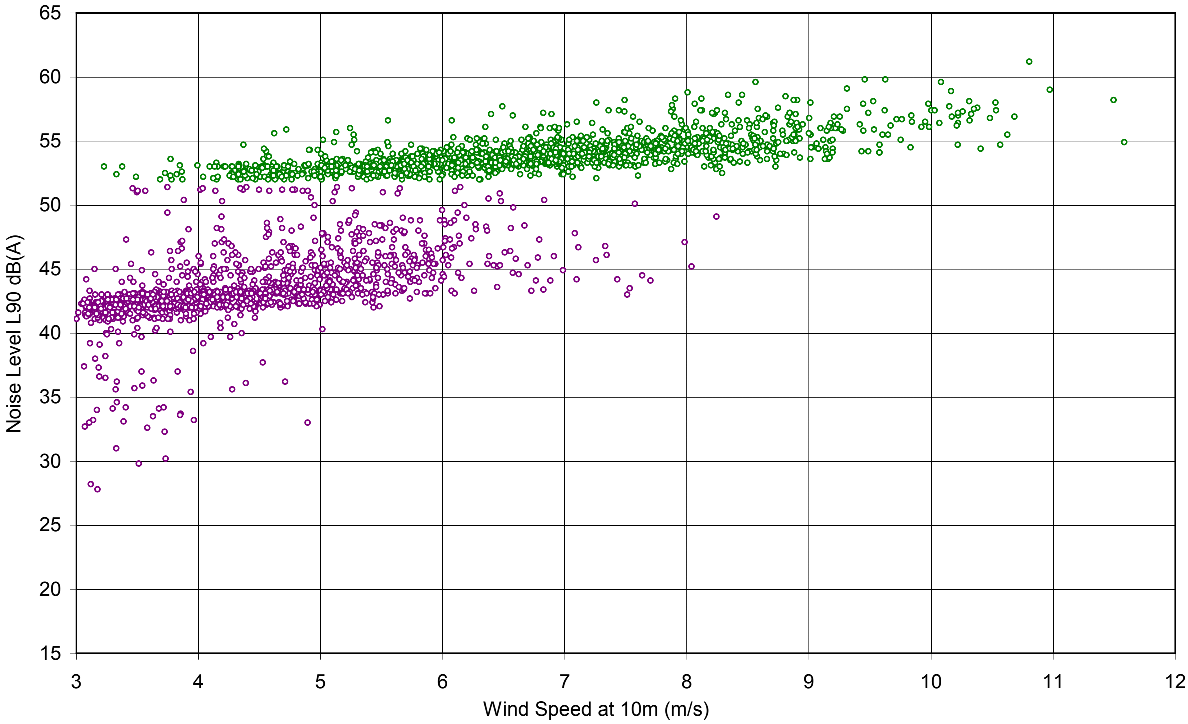

Figure 4: Levels measured at site C, position 1. Green points correspond to high-speed operation of the site, and purple points to some turbines operating at low-speed or not at all.

The 2-speed pattern of operation of the turbine installed at site C is clearly apparent in Figure 4, with the turbines operating in a lower speed in lighter wind, and a higher fixed speed (with corresponding louder noise emissions) in stronger winds. Intermediate levels correspond to times where only part of the site was operating in a high-speed mode. In the remainder of the analysis, this region of high-speed operation was the focus of the study, in order to obtain the highest signal-to-noise ratio. In particular, it is expected that the region where turbines have switched to high-speed operation while wind speeds remain moderate will correspond to the least background-affected measurements.

Figures 5a and 5b display the levels measured at the two locations situated respectively 450 and 750 m from the closest turbine, along the North-East line. Similar general observations can be made as were made for site B, above. Compared to the latter site, the more distant measurement locations of site C were situated close to forestry and vegetation which created higher wind-related background noise levels, affecting the measurements; it was not possible to operate site shutdowns to characterise more precisely the background noise levels, but figure 5b indicates that the margin between noise levels measured in upwind and downwind conditions is low. Comparing figures 5a and 5b, it is apparent that the margin between raw measured values and predictions is constant over the wind-speed range in the first case, but increases in the second: this suggests that this increased margin is not related to changes in the noise source but in background-related effects. Therefore, in both cases the turbine immission noise levels are thought to be close or lower than the predictions.

The exact background noise level influence at each measurement location for each 10 minute period cannot be known. It is however likely that the background noise level may have contributed approximately 1 dB(A) to the total noise levels measured at location 3 (750 m distance). In addition, historical background data measured in nearby locations suggests that the background levels measured in downwind conditions were marginally higher, because of site-specific effects, suggesting that the background levels described above are underestimated to some extent.

Figures 6a and 6b display a similar comparison for the measurements made at positions 4 and 5, which were situated respectively 700 and 820 m from the closest turbine. Similar observations can be made as for locations 2 and 3 above.

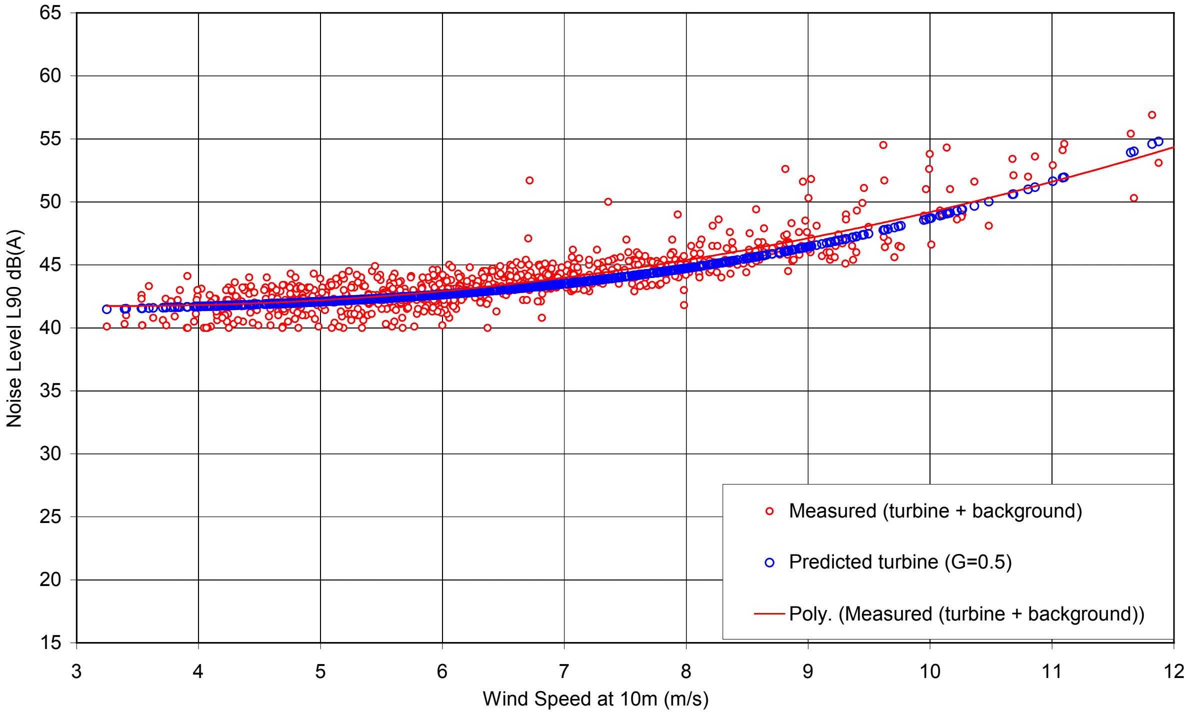

Figure 5a: Levels Comparison of Site C measured and predicted noise levels at measurement location 2 (450 m distance). All downwind angles restricted to +/-45 degrees. Predicted noise levels based on a single site wind speed reference and G = 0.5.

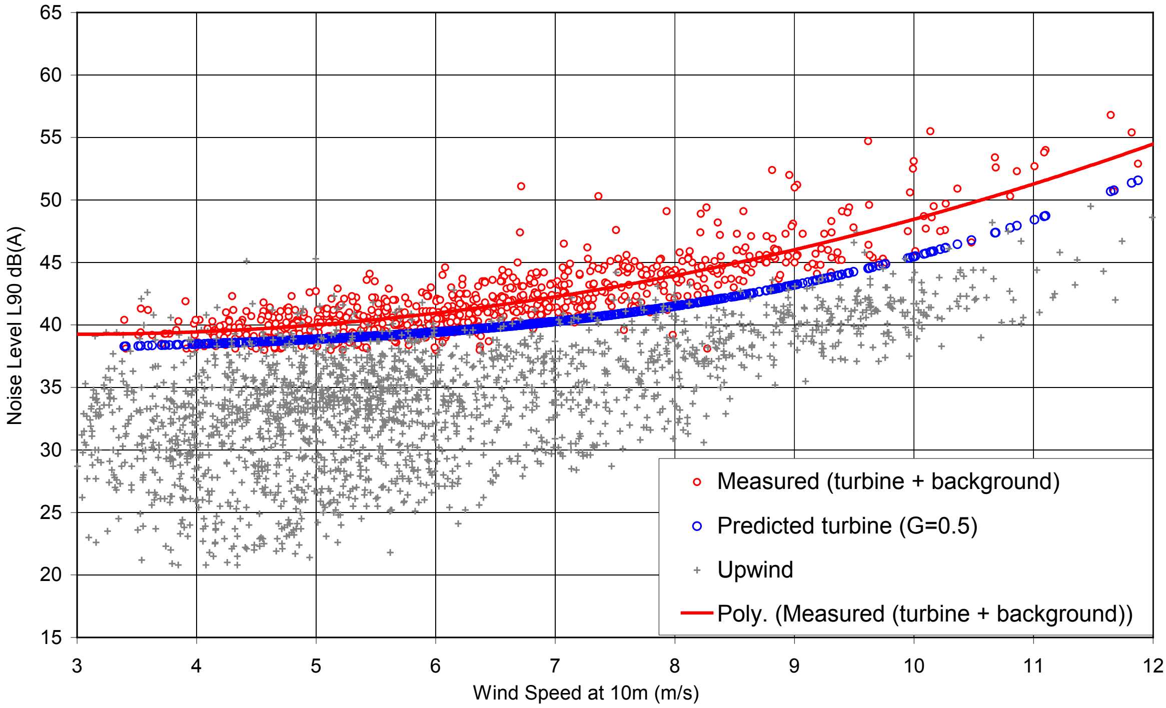

Figure 5b: Levels Comparison of Site C measured and predicted noise levels at measurement location 3 (750 m distance). Downwind and upwind angles restricted to +/-45 degrees. Predicted noise levels based on a single site wind speed reference and G = 0.5. The low margin above background levels suggests that actual turbine noise levels will be closer to the predictions.

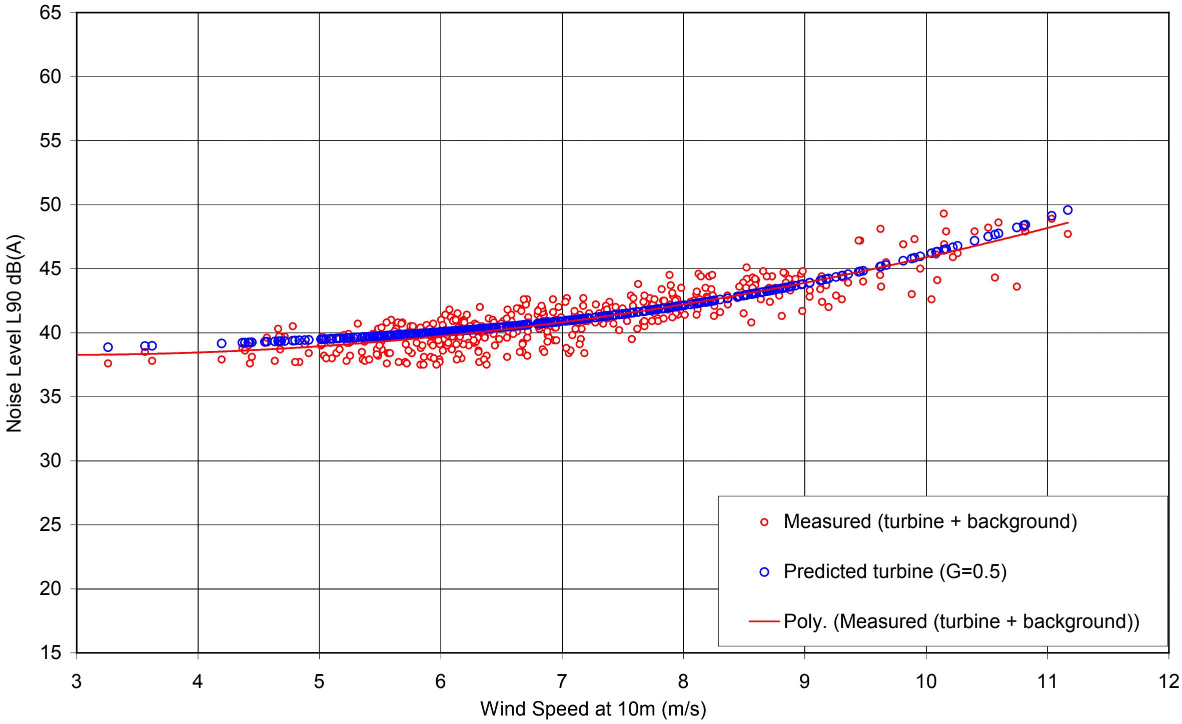

Figure 6a: Levels Comparison of Site C measured and predicted noise levels at measurement location 4 (700 m distance). All downwind angles restricted to +/-45 degrees. Predicted noise levels based on a single site wind speed reference and G = 0.5.

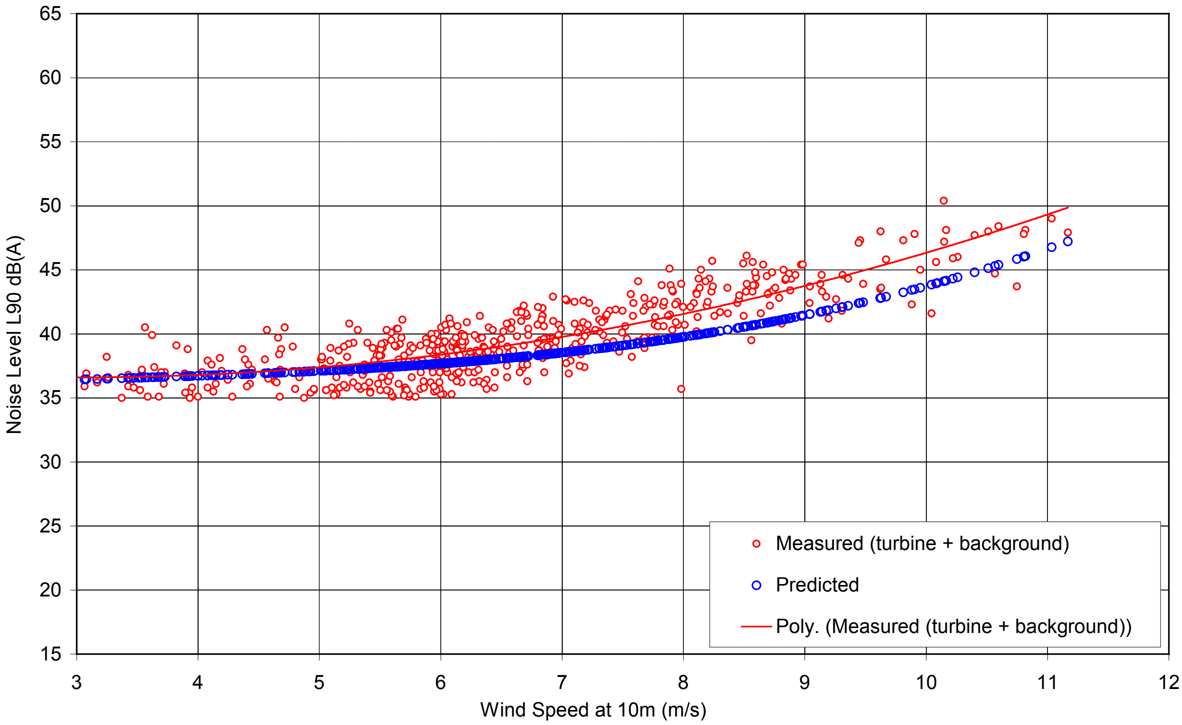

Figure 6b: Levels Comparison of Site C measured and predicted noise levels at measurement location 5 (820 m distance). All downwind angles restricted to +/-45 degrees. Predicted noise levels based on a single site wind speed reference and G = 0.5.

Noise levels were also measured at several positions surrounding the site, at distances of 700 to 1000 m: for these locations, complexities due to the influence of background noise levels hindered the interpretation of the results, but observations were generally consistent with the comments made above.

Finally, observations could be made for site C in terms of the difference between the single wind speed reference and the wind speed of each of the turbines, with the following results:

- *Mean difference = -0.4 m/s*
- *Standard deviation of differences = 1.4 m/s*
- *Maximum decrease = -8.9 m/s*
- *Maximum increase = 7.8 m/s*

Figure 7 demonstrates the trend that the reduction in effective wind speeds between the upwind and downwind extremities of the wind farm site tends to be higher with increasing wind speeds. These observations are similar to those made for site B.

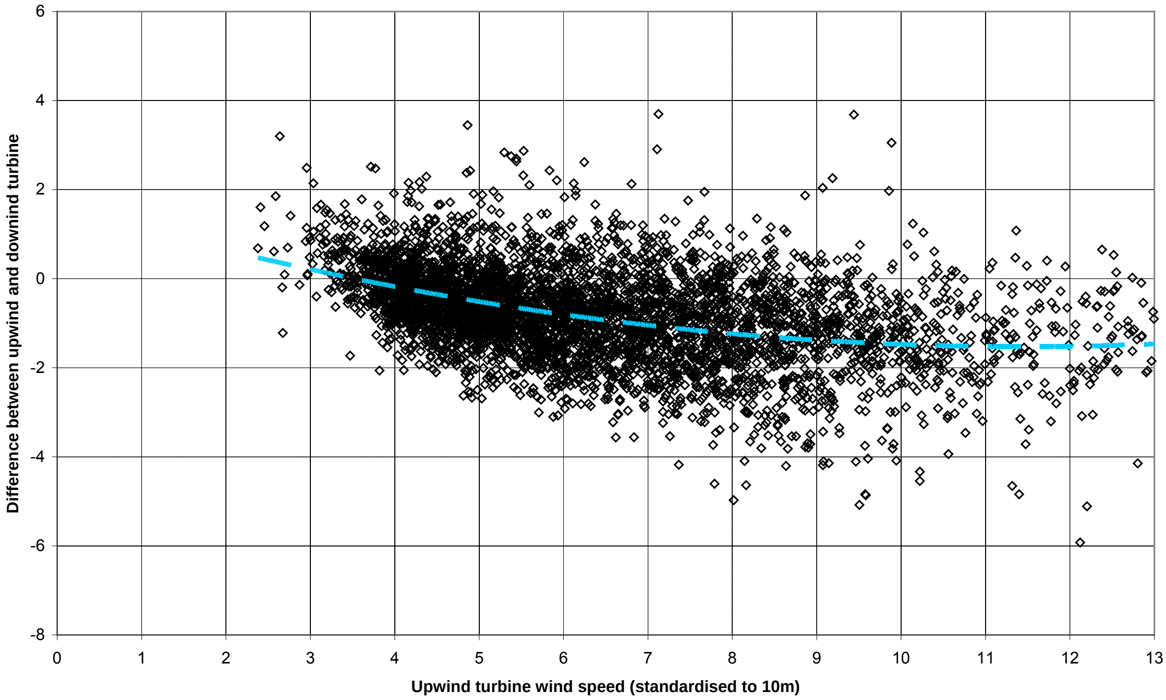

Figure 7: Difference between the wind speed measured at hub height (standardised to 10 m) between the most upwind and the most downwind turbine at site C, over a period of approximately 3 months. A negative number indicates that the downwind wind speed is lower.

Conclusions

The results of the study of noise emissions from large operating wind-farm sites have supported the view that engineering methods such as ISO 9613 offer a robust means of determining the upper turbine immission levels that may occur in practice under favourable, downwind propagation conditions.

Detailed analyses made to date of completed large-scale measurement studies illustrate the extent of conservatism that may be inherent to certain prediction methods and choices. Our studies also illustrate the difficulties encountered in noise immission measurements, and in particular evaluating the measurement contribution directly attributable to turbine immissions alone and defining a relevant wind speed reference. Measurements made closer to the source can help in evaluating the different contributions within the measurements.

Predictions using relatively conservative methods tend to equal or exceed total measured noise levels in practice. In particular, the addition of relatively high uncertainty margins corresponding to the use of commercial warranted sound power, as well as the choice of pessimistic propagation parameters, both have the propensity to result in significant design conservatism. Whilst these conservatisms may seem numerically small, and will be of limited significance subjectively, the consequences in power generating losses can be substantial.

The results are in line with recommendations for best practice in wind farm noise predictions as recently set out by several practitioners in the field in the UK[7]. Whilst certain choices of parameters have been found to be effective in practice, further detailed studies would be required to determine exact propagation effects occurring.

The findings have also shown that the assumption of a single wind speed reference for all turbines that form a large wind farm site may overestimate the actual wind speed seen by each individual turbine. This is particularly the case for the turbines nearest to a location of interest which may be partly shielded by the furthest upwind turbines which experience uninterrupted (by the wind farm) and higher wind speed conditions. This means that a single wind speed reference will likely overestimate the sound emissions of the turbines nearest to a location of interest. This effect appears to be most significant at higher wind speeds for the sites studied.

In summary, better knowledge of the relationship between predicted and actual noise immission levels has the potential to reduce un-necessary conservatism and enable substantially enhanced generating capacity during the design phase of a wind farm. This requires that careful account is taken of the specifics of each site under consideration and that compatible design choices are made to avoid cumulative pessimism which may be unlikely to simultaneously occur in practice.

Further study works would be beneficial to identify in more detail and in isolation the influence of different ground conditions, of more complex terrains profiles, and other types of turbines such as variable speed machines. Further study of directional propagation effects would be beneficial given their relevance to large wind farm site and cumulative impacts.

References

[1] ISO 9613-2 '*Acoustics – Attenuation of sound during propagation outdoors – Part 2: General method of calculation*', International Standards Organisation, ISO 9613-2, 1996.

[2] JOR3-CT95-0091 '*Development of a Wind farm Noise Propagation Prediction Model'*, Bass J H, Bullmore A J, Sloth E, Final Report for EU Contract JOR3-CT95-0051, 1998.

[3] *Wind Farm Noise Predictions - The Risks of Conservatism*, J. Adcock, A. Bullmore, M. Jiggins and M. Cand, Second International Meeting on Wind Turbine Noise, Lyon, France, September 2007

[4] ETSU W/13/00386/REP '*Noise Measurements in Windy Conditions*', Davis R A, Lower MC, 1996

[5] BS EN IEC 61400 Part 11:2003. *Wind turbine generator systems - Part 11: Acoustic noise measurement techniques*. British Standards Institute.

[6] *The Assessment and Rating of Noise from Wind Farms - ETSU-R-97*. The Working Group on Noise from Wind Turbines. September 1996.

[7] *Prediction and Assessment of Wind Turbine Noise - agreement about relevant factors for noise assessment from wind energy projects*, Proceedings of the Institute of Acoustics (Acoustics Bulletin), Vol34, No 2, March/April 2009, pp35-37; Bowdler, Bullmore, Davis, Hayes, Jiggins, Leventhall, McKenzie.

Third International Meeting
on
Wind Turbine Noise
Aalborg Denmark 17 – 19 June 2009

Wind Turbine Noise in the United States: The Environmental Speed Limit vs. Worst Case Noise Analyses

Tim Casey
Acoustics Program Manager
HDR Engineering, Inc.
701 Xenia Avenue South
Minneapolis, Minnesota 55416, USA
(763-591-5450)
tim.casey@hdrinc.com

Abstract

Wind turbine noise is often a topic of debate in the United States. Most state and local environmental noise regulatory programs have not evolved to specifically address wind turbine noise (including noise from ancillary equipment). The National Environmental Policy Act (NEPA), which doesn't address wind turbine noise, does not require worst-case impact analyses. Rather, NEPA requires that the assessment of a project's environmental effects consider only representative operating conditions. This concept of evaluating representative or typical operational conditions is generally practiced by consultants who perform analyses of wind turbine noise in the United States. The author considers this approach "doing the environmental speed limit". Other consultants, often employed by opponents of wind farm developments who are engaged in wind turbine-related litigation, endorse use of "worst-case noise analyses". There is merit to both approaches. This paper discusses these conflicting perspectives, some of the components of a worst case noise analysis, and the uncertainties in data and predictive methods. The paper highlights recent developments in the body of knowledge of wind turbine noise. The paper concludes that, until environmental noise regulations evolve in the United States, developers and their consultants can strike a balance between "the environmental speed limit" and use of worst-case noise analyses for siting and approvals purposes.

Introduction

According to the American Wind Energy Association, wind turbines generate approximately 28,000 megawatts (MW) of electricity in the United States (as of April

2009). Wind farms exist in numerous states throughout the USA. Three tables at the end of this paper show some of the largest wind farms in operation in the USA, some of the proposed large wind farms, and the top ten wind energy-producing states. Clearly wind-derived energy has established itself as a meaningful source of electricity in the United States. Wind farms are often located in rural areas, where the wind resource is well documented and reliable and background noise levels are perceived to be quiet (but actual wind noise levels are high). Problematic-levels of wind turbine noise have been identified at noise-sensitive land uses near wind farms throughout the world. These problems are well publicized.

Publicizing Controversy Surrounding Wind Turbine Noise

The internet is undeniably the most effective communication resource for critics of wind farms. An inherent flaw of the internet is that the power of print is stronger than ever, regardless of the relative merit of what is put in print. Wind farm critics can now compile, publish, and distribute information so efficiently that it is truly revolutionary (this is the age of information). The internet contains an abundance of information regarding wind turbines and wind turbine noise. One of my favourite websites is YouTube.Com, and I highly recommend you spend some time there. A search of “wind turbine” on YouTube turned up 7,950 videos such as:

- People base-jumping off of wind turbines;
- Construction of wind turbines and the crowd it draws;
- Turbines malfunctioning and breaking apart, and;
- Explosions, accidents, crashes, etc.

Search YouTube for ”wind turbine noise” and you’ll find at least 187 video clips. Many are critical of wind turbines, and some point out how quiet they are. Titles or topics you’ll see at You Tube include:

- Wind turbines at Montreathmont (Scotland), with captions that claim:”the ground around the turbines vibrates with a deep dull thud…”
- Footage of wind turbines entitled, “Do Wind Turbines Make Noise?
- Eagle, New York No Wind Turbine Noise. A Bigger Lie!
- Wind Turbine Noise Levels 106 db-Yes they do make noise
- Wind Turbine Shadow Flicker and Noise, Byron Wisconsin
- Does an industrial scale wind turbine sound like a refrigerator to you?
- Wind Turbine Noise – Suncor Wind Farm Ripley Ontario
- Milwaukee Channel Six News Report on Wind Turbine Trouble in Fond du Lac County, Wisconsin

- Wind turbine noise in Canada
- Wind Turbine Noise samples from New York State, Fenner and Tug Hill turbines.
- Wind turbine noise – NOT! (wind turbines in Swaffham, England are not loud!)
- Wind turbines are not noisy
- Lawsuit over wind turbine noise

The list goes on and on. Critics of wind turbines effectively use the internet to distribute their materials. The internet levels the playing field, it gives people access to enough information to allow them to ask challenging questions – and to make developers and their consultants work harder to achieve siting approvals.

Differences in the Way States Regulate Wind Turbine Noise

Wind turbine noise is regulated in different ways throughout the United States. Some states apply their general environmental noise rule (if they have one) to wind turbine projects. In some states that do not regulate environmental noise, counties sometimes have wind turbine noise limits. In other cases where the county does not regulate wind turbine noise, they sometimes enact minimum setback distances between turbines and residences. These setback distances have an approximate range of 500-1200 feet. It is also not uncommon for a Public Utility Commission (a state-level quasi-regulatory agency that regulates certain public services like energy, telecommunications, etc.) to enact either noise limits or setback distances for wind turbines.

From state to state, environmental noise limits vary. Some states regulate using broadband noise limits, others employ spectral limits. Some states regulate noise using hourly equivalent levels (Leq), and others use statistical metrics like L_{10} and L_{50}. Additionally, some states employ A-weighted noise limits, others regulate using unweighted noise limits. There is not universal agreement on the relative merit of any of these regulatory methods in the context of wind turbine noise; a subject that merits review.

National Environmental Policy Act (NEPA)

The United States Congress passed the National Environmental Policy Act (NEPA) in 1969, establishing a national policy for protecting the environment. NEPA requires federal agencies to, among other things, prepare an Environmental Impact Statement when those agencies propose activities that may harm the environment. In general, NEPA requires agencies to consider:

- The environmental impact of the project
- Any adverse environmental effects which cannot be avoided if the project is implemented
- Alternatives to the proposed project

- The relationship between local short-term uses of the environment and the maintenance and enhancement of long-term productivity
- Any irreversible and irretrievable commitments of resources associated with the project.

A consideration of NEPA is relevant to a discussion of wind turbine noise because NEPA establishes a context for environmental assessment, and in particular – the level of rigor that an environmental assessment should exhibit. NEPA does not impose a substantive duty on agencies to mitigate adverse effects or to provide a fully developed mitigation plan. It requires agencies to take a “hard look” at the consequences of a proposed project, and to provide the general public with relevant information about the project and potential consequences. NEPA does not require agencies to produce particular results. NEPA requires that mitigation measures be discussed in sufficient detail to ensure that environmental consequences have been adequately evaluated. It does not require that a complete mitigation plan be formulated and implemented. Additionally, in 1985 CEQ amended NEPA, and eliminated the requirement for agencies to perform “worst case analyses”.

These concepts and context are important when assessing the divergence between how wind turbine noise is evaluated and regulated in the United States, and – at the other end of the spectrum – claims that those regulations and evaluations are inadequate. In the United States there exists a great variety of environmental regulations, statutes, media- and resource-specific limits on emissions and activities. In my view, if a company is complying with environmental rules, they are doing the environmental speed limit. This concept is important to me. Citizens are allowed to drive at speeds that equal the speed limit on whatever roadway they are driving at. Citizens are allowed certain freedoms as defined by our laws.

As a consultant, it has always been my opinion that my job is to help my clients “do the environmental speed limit”. That means I should help my clients define and achieve levels of operational activity that comply with applicable environmental limits, and then help them demonstrate and maintain their compliance. This is the environmental speed limit.

As a consultant in environmental acoustics, I apply this perspective while performing analyses of noise from highways, transit systems, industrial and infrastructure-related projects, and wind turbine developments. Our environmental laws are based on science and health-related research, and they are amended when the preponderance of research demonstrates the need to amend them. There is a growing body of evidence relating to wind turbine noise. However, this body of evidence has not yet reached a point where the preponderance of evidence requires a paradigm shift in noise regulations.

Worst-case Noise Analyses

Existing wind farms are well documented in the literature and on the internet. We know a lot about their productivity, cost to construct and operate, financing and subsidy-related issues, and environmental issues. The body of knowledge includes contributions from advocates and critics of wind-derived energy. The Not-In-My-Backyard (NIMBY) camps maintain websites that highlight problems with wind farms around the world. Noise is often one issue they highlight.

Like any new noise source, wind turbines have potential to annoy people who have no prior exposure to them. Often it appears that the people who are most annoyed, or who express the most annoyance are people who did not support the proposed wind farm or who have uncommon sensitivities to noise. Common complaints include changes in viewshed and audioscape. Some claim that noise from wind turbines is too high for the quiet nature of rural communities, and that wind turbine noise is clearly audible to rural residents occasionally during night time and daytime. Rarely do they note how loud the wind itself is.

There is growing evidence that wind turbine noise has potential to disrupt sleep in the most sensitive subset of the population. There is also evidence of additional health effects associated with the introduction of wind turbine noise in areas with no prior exposure to wind turbine noise and populated by members of the most sensitive subset of the general population.

Some of the body of knowledge associated with supposed human health effects of wind turbines is self-reported. This raises questions of validity, statistical significance, and general questions of merit. I am not a medical researcher, and will not deny reports of such health effects. However, it is clear that some of this evidence does not have the same merit as other, traditional clinical health studies whose results form the bases of established environmental laws, statutes, emission limits, etc. This creates conflict between advocates of “the environmental speed limit” and advocates of “worst case analyses”.

Advocates of worst-case wind turbine noise analyses raise interesting notions. For example, they highlight the uncertainty and error in wind turbine noise analysis methodologies. These include, but are not limited to:

- +/- 3 dB in the IEC 61400-11
- +/- 3 dB in the commercially available noise models that are based on ISO 9613 due to the limitations of that standard in assessing noise from elevated sources.
- +/- 3-5 (or more) dB due to commercially available noise models inability to assess noise propagation during temperature inversions and during different meteorological stability conditions.

Advocates of worst-case noise analyses suggest that a measure of conservatism be added to noise analyses to account for these uncertainties. There is merit to this notion; however there is also merit to the notion that these claims are somewhat academic arguments.

Consider other environmental noise assessment methods. The Federal Highway Administration's (FHWA) traffic noise assessment guidelines require use of peak hour traffic volumes in the calculation of traffic noise levels associated with a proposed roadway project. The peak hour traffic volumes are based on annualized average daily traffic volumes and projections of future traffic. FHWA does not require a demonstration that the traffic volume used in a traffic noise analysis is actually a worst-case traffic volume. In fact, one significant noise source that is omitted is engine compression brake noise, which is unfortunately growing in the frequency of its occurrence throughout the United States. Also, FHWA's traffic noise model does not account for temperature inversions, which have been documented to have dramatic long-range effects on traffic noise propagation.

Similarly, the Federal Transit Administration and Federal Railroad Administration (which have virtually identical noise assessment methods) advocate spreadsheet-based calculations of noise from trains, buses, and other modes of mass transportation. Clearly these methods do not account for all the factors that could constitute a worst-case noise analysis.

The commonality in these methods is that they require the project sponsor to take a "hard look" at typical operating conditions. This level of rigor is commensurate with NEPA's general intentions (regardless of whether or not NEPA applies), and creates a context in which wind turbine noise analyses should be performed in the United States.

Developments in the body of knowledge

The body of knowledge associated with wind turbine noise is broad and deep. It spans topics including:

- Meteorological dynamics associated with wind turbine noise generation and propagation;
- Mechanical dynamics of wind turbine noise generation;
- Studies of noise from wind turbines operating in different terrain regimes, under different meteorological regimes;
- Reports of health effects associated with wind turbines, including sleep disruption and hypertension;
- The effects of wind turbine noise on wildlife;
- The interaction of wind turbine noise with residential structures, and more.

Here again, the internet serves an important communication function to allow wind turbine noise researchers to interact with each other and expand our knowledge base. This is important work, and there is merit in advocating that more funding be directed towards it. Ultimately this will better inform regulators and allow them to amend or promulgate turbine noise limits so they better protect human health and welfare.

Conclusions

The body of knowledge relating to wind turbine noise is growing in important directions. This includes mechanisms of noise generation and propagation, noise assessment methods and algorithms, health effects of exposure to wind turbine noise, and more. The body of knowledge has not reached a critical mass that overwhelmingly supports rigorous reform in wind turbine noise regulation. The paper concludes that, until environmental noise regulations evolve in the United States, developers and their consultants can strike a balance between “the environmental speed limit” and use of worst-case noise analyses for siting and approvals purposes.

Like any new noise source, wind turbine noise is going to bother some people. The same is true of highway noise, industrial noise, noise from dogs and other animals. It is important to bear in mind that land owners do not own the audioscape or the viewshed. Property rights end at the property line. While you may object to wind turbine noise, your neighbour may object to noise from your dogs. If there is not a law limiting either one, you are left to rely on patience and tolerance or to relocate.

Additional research should also be performed to assess people’s acclimation to wind turbine noise. We know that the introduction of new noise sources can interfere with sleep. There is general agreement that people can acclimate to noise sources. This commonly occurs when people move into a new neighbourhood and are exposed to train noise for the first time. I experienced this personally, and wonder if the same acclimatization occurs with people exposed to wind turbine noise from new wind farms.

There is also merit in studying the relationship between people who complain about wind turbine noise and whether or not they supported the wind farm before it was constructed and began operating. The potential for psychoacoustic issues merits study. I also advocate refining commercial acoustical analysis models to better process hourly meteorological data and profiles. The United States Environmental Protection Agency (EPA) distributes software for evaluating air emissions from industrial sources (ISC2). In a typical air quality analysis, the ISC2 models process five years worth of hourly meteorological data, including temperate inversions and a variety of stability conditions. Surely these algorithms can be added to modern noise models and will improve our predictive tools.

Tables

Large wind farms in the United States[1][2]		
Farm	**Installed Capacity (MW)**	**State**
Adair Wind Farm	174	Iowa
Altamont Pass Wind Farm	606	California
Ashtabula Wind Farm	196	North Dakota
Barton Wind Farm	160	Iowa
Barton Chapel Wind Farm	120	Texas
Benton County Wind Farm[3]	130.5	Indiana
Big Horn Wind Farm	200	Washington
Biglow Canyon Wind Farm	125	Oregon
Blue Canyon Wind Farm	225	Oklahoma
Blue Sky Green Field Wind Farm	145	Wisconsin
Brazos Wind Ranch	160	Texas
Buffalo Gap Wind Farm	523	Texas
Buffalo Ridge Wind Farm	225	Minnesota
Bull Creek Wind Farm	180	Texas
Camp Grove Wind Farm	150	Illinois
Camp Springs Wind Energy Center	130	Texas
Capricorn Ridge Wind Farm	662	Texas
Carroll Wind Farm	150	Iowa
Cedar Creek Wind Farm	300	Colorado
Centennial Wind Farm	120	Oklahoma

Century Wind Farm	150	Iowa
Champion Wind Farm	126	Texas
Colorado Green Wind Farm	162	Colorado
Crystal Lake Wind Farm	350	Iowa
Desert Sky Wind Farm	160	Texas
Dutch Hill/Cohocton Wind Farm	125	New York
Elbow Creek Wind Project	122	Texas
Elk River Wind Farm	150	Kansas
Fenton Wind Farm	206	Minnesota
Forest Creek Wind Farm	124	Texas
Forward Wind Energy Center	129	Wisconsin
Fowler Ridge Wind Farm	750	Indiana
Goodland I	130	Indiana
Green Mt. Energy Wind Farm	160	Texas
Gulf Wind Farm	283	Texas
Hackberry Wind Project	165	Texas
High Winds Wind Farm	162	California
Horse Hollow Wind Energy Center	736	Texas
Inadale Wind Farm	197	Texas
Intrepid Wind Farm	160	Iowa
Judith Gap Wind Farm	135	Montana
Kibby Wind Power Project	132	Maine
King Mountain Wind Farm	281	Texas
Klondike Wind Farm	400	Oregon
Langdon Wind Energy Center	159	North Dakota

Lone Star Wind Farm	400	Texas
Maple Ridge Wind Farm	322	New York
Marengo Wind Farm	140	Washington
McAdoo Wind Farm	150	Texas
Milford Wind Corridor Project	203	Utah
Mount Storm Wind Farm	264	West Virginia
NedPower Mount Storm I	164	West Virginia
New Mexico Wind Energy Center	204	New Mexico
Panther Creek Wind Farm	257	Texas
Peetz Wind Farm	400	Colorado
Peñascal Wind Farm	202	Texas
Pine Tree Wind Farm	120	California
Pioneer Prairie Wind Farm	293	Iowa
Pomeroy Wind Farm	196	Iowa
Pyron Wind Farm	249	Texas
Roscoe Wind Farm	781[4]	Texas
San Gorgonio Pass Wind Farm	619	California
Sherbino Wind Farm	750	Texas
Shiloh Wind Farm	300	California
Smoky Hills Wind Farm	249	Kansas
Stanton Energy Center	120	Texas
Stateline Wind Project	300	Oregon
Story County Wind Farm	150	Iowa
Sweetwater Wind Farm	585	Texas
Tatanka Wind Farm	180	No. & So. Dakota

Tehachapi Pass Wind Farm	690	California
Trent Wind Farm	150	Texas
Turkey Track Wind Farm	169	Texas
Twin Groves Wind Farm	396	Illinois
Walnut Wind Farm	153	Iowa
Wethersfield Wind Park	124	New York
White Creek Wind Power Project	204	Washington
Wild Horse Wind Farm	229	Washington
Wildorado Wind Ranch	160	Texas
Woodward Wind Farm	159	Oklahoma
Wyoming Wind Energy Center	144	Wyoming

Proposed Large Wind Farms		
Wind Farm	**Capacity (MW)**	**State**
Banner County Wind Farm	2,000	Nebraska
Beech Ridge Wind Farm	186	West Virginia
Buzzards Bay Wind Farm (offshore) [5]	300	Massachusetts
Cape Wind (offshore)	420	Massachusetts
Delaware Offshore Wind Project	600	Delaware
Franklin County Wind Farm[6]	200-300	Iowa
Garden State Offshore Energy Wind Park[7]	350	New Jersey
Golden Hills Wind Farm[8]	400	Oregon
Hartland Wind Farm	500-1,000	North Dakota
Long Island Offshore Wind Park[9]	144	New York

McAdoo Wind farm [10]	150	Texas
Glacier Wind Farm[11]	210	Montana
Pampa Wind Project	4,000	Texas
Pine Canyon Wind Farm[12]	150	California
Pine Tree Wind Project[12]	120	California
Shepherds Flat Wind Farm	909	Oregon
Tehachapi Renewal Project	4,500	California
Titan Wind Project	5,050	South Dakota
Valley City/Lake Ashtabula Wind Farm[13]	200	North Dakota

Top Ten States with the Largest Wind Energy Generation Capacity			
State	**Existing MW**	**MW Under Construction**	**Rank in USA**
Texas	7,907	1,102	1
Iowa	2,883	210	2
California	2,653	125	3
Minnesota	1,803	0	4
Washington	1,479	0	5
Oregon	1,363	126	6
New York	1,261	21	7
Colorado	1,068	0	8
Kansas	1,014	0	9
Illinois	915	312	10

NOTES

1. ^ AWEA 3rd Quarter 2008 Market Report

2. ^ Drilling Down: What Projects Made 2008 Such a Banner Year for Wind Power?

3. ^ Benton County Wind Farm

4. ^ E.ON Delivers 335-MW of Wind in Texas

5. ^ Buzzards Bay wind farm proposed

6. ^ 40,000-Acre Wind Farm Proposed for Iowa

7. ^ Garden State Offshore Energy

8. ^ Golden Hills Wind

9. ^ Long Island Offshore Wind Park

10. ^ Wind farm whips up activity around McAdoo | AVALANCHE-JOURNAL

11. ^ Glacier Wind Farm goes live

12. ^ ***a b*** Winds of Change A-Blowin': Pine Tree Wind Project

13. ^ Barnes County wind project would be state's largest

References

American Wind Energy Association (2009)

Environmental Impact Analysis Handbook, Edited by John Rau and David Wooten (1980)

YouTube.Com (2009)

Wikipedia.Com (2009)

Third International Meeting
on
Wind Turbine Noise
Aalborg Denmark 17 – 19 June 2009

A risk management strategy related to wind farm noise emissions

Francois COSTES

EDF Energies Nouvelles
Technical Support
Paris, France

Email: francois.costes@edf-en.com

Abstract

Wind farm noise predictions and measurements of background noise level are dependent on so many variables that designing an optimal layout on development stage and managing noise of turbines in operation may be quite challenging. Facilities must as well comply with local regulations as ensure non disturbance of local inhabitants. These issues are often addressed by a mere study aiming at getting project financing and approval, and a measurement during operation (if required). Generally, no risk management methodology is applied.

This paper describes a risk management approach at each stage of the project (development, construction and operation) with specific tools and methods enabling to analyze and to mitigate the risks related to the wind farm noise emissions. Examples and feedback are given at each project milestone in order to illustrate the risk management methodology (layout design, environmental impact assessment, project financing and approval, commissioning).

1. Introduction

Wind farm noise predictions and background noise level measurements are dependent on so many variables that they may prove quite challenging. When evaluating the potential impact of wind farm noise, the objective is therefore to assess risk rather than to obtain an accurate instant picture. The physical phenomenon is not knowable in a deterministic way. Data are processed into one or several indicators, which are essential for making objective decisions and for analysing a project's impact.

A risk is an event that may occur (with some degree of uncertainty) and that may prevent the project objectives from being achieved. Identifying objectives is thus the first step to consider when addressing risk management.

Preventing the impact on local residents is one of the main objectives of a wind farm project. As far as noise is concerned, this objective carries two major risks, one being the disturbance of local residents, the other being non-compliance with local regulations. The variety of wind farm project locations, as well as discrepancies in local residents' perceptions, makes it hard to predict and measure noise impact.

The night-time limits set by the French and UK regulations illustrate the differences from one country to another. In France, the regulations concerning wind farm noise are more restrictive at night than during the day. Conversely, the UK has assumed that higher noise levels during the night are unlikely to disturb residents. UK noise limits were proposed based on a 35 dBA sleep disturbance criterion, and an allowance of 10 dBA has been made for attenuation through an open window. In general, inhabitants rarely complain of wind farm noise at night-time. However, the risk of disturbance at night is, for example, higher in the south of France than in the north of England. Due to higher temperatures, inhabitants are more likely to spend evenings outside and sleep with open windows in the south of France.

This paper describes a risk management approach covering each stage of a project (development, construction and operation) using specific tools and methods to analyse and to mitigate the risks related to wind farm noise emissions.

2. Wind farm noise risk assessment and mitigation

In general, risk assessment is outsourced and addressed merely through a study aimed at securing project financing and approval. Although this study forms the cornerstone of wind farm noise impact analysis, a risk management strategy is essential in order to mitigate noise risks from the early development stage.

A noise survey is generally performed after the wind farm layout has been finalised, and its goal is to verify that noise levels are below the limits set in the regulations. By that stage, the project is too far advanced to modify the positioning of wind turbines easily. Risk detected at this point usually entails designing an acceptable noise management plan that will not be too detrimental to production. To predict risk at an early stage, we have developed tools and methods designed to assist project developers in designing the wind farm layout. Equally crucial for this advance planning is monitoring the risks affecting operation of the turbines.

Risk has to be assessed and mitigated at various project milestones. Early detection of risk makes developing a solution less expensive. Conversely, a comprehensive assessment of the impact of wind farm noise is costly and not economically viable if undertaken at every stage of a project, especially early in the development of the wind farm when confidence in the project is low. Risk has to be assessed in order to balance cost and complexity based on how likely the project is to succeed.

A wind farm project is constantly evolving and so risk assessment and mitigation is a continuous process throughout the project's life.

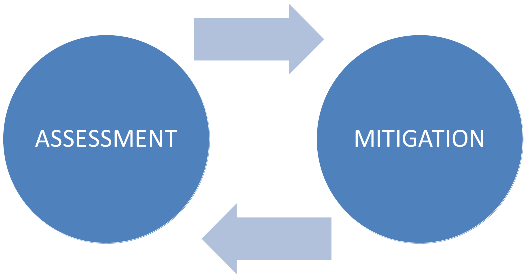

To prevent the occurrence of risks related to wind farm noise, a choice between two alternatives has to be made. One way of mitigating risk is to alter the layout or type of turbines used, while another is to adapt power generation through noise reduction modes. The first solution is highly effective but due to the intricacies and many constraints of a wind farm project, the second solution may be used in some cases.

Risk is commonly assessed using two parameters

- Probability, i.e. the likelihood of occurrence of the Risk
- Severity, i.e. a comparative measure of the impact on the project if the Risk occurs

How to measure each parameter, i.e. Probability and Severity, varies from country to country.

What follows is a proposal as to how to measure the Probability and Severity parameters with regard to wind turbine noise:

- Probability

  Noise levels are assessed at residential locations. Depending on the country, wind farm noise, emergence or difference is then computed. Thresholds are specified based on experience.

- Severity

  For given conditions (wind speed and direction, night and day, etc.), turbines that entail a risk are identified. Severity is measured as the number of turbines that need to be removed or halted in order to decrease the Probability below a given level.

The distinction between Probability and Severity is crucial for efficient risk management. Even though the two indicators are not entirely independent, the insight they provide is of a different nature. Probability may be high while Severity is low, such as a large wind farm at which only one turbine is close to a residential location. Probability may as well be low and Severity high, such as where there are a large number of turbines a long way but at the same distance from a residential location.

Case 1: high Probability - low Severity

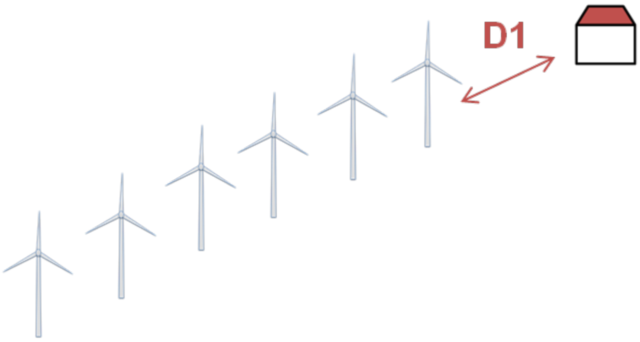

A residential location is close to one turbine. The wind farm noise level is likely to be high, especially in certain specific meteorological conditions. However, mitigation efforts on this single turbine are sufficient to eliminate the risk.

Case 2: low Probability - high Severity

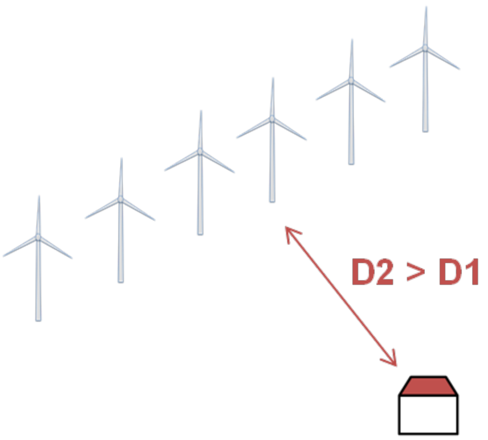

A residential location is almost equidistant from a number of turbines. Even if we assume the wind farm noise level, and therefore the Probability is lower than in case 1, mitigation could require action on several turbines to eliminate the risk. The Severity is therefore higher than in case 1.

3. AcousEole - Tools for wind farm noise assessment

AcousEole is a set of tools we have developed to simulate wind farm noise at various stages of the project. The objective is to assess Risk from early development right through to operation. As discussed in the previous section, cost and efficiency are balanced depending on the status of the project.

Three tools have been developed: AcousEole0, AcousEole1, and AcousEole2.

3.1. AcousEole0

AcousEole0 computes wind farm noise. The propagation model is simplistic and does not include topography. It is based on the ISO 9613 standard. Only two damping values are calculated: geometrical divergence and atmospheric absorption. Due to the hub-height location of the noise source, these are the major damping factors as far as wind turbine farm is concerned, and accuracy is sufficient at an early stage of wind farm development. Current practice when designing the preliminary layout is usually to maintain a given distance between each residential location and the closest turbine (500 or 700 meters, for example). Given changes in wind farm layouts and wind turbine design, the distance does not ensure a low-risk probability.

AcousEole0 maps the wind farm noise. Noise is assessed at every point on a 2D grid. The grid step is 20 meters. The grid size is specified by user and depends on the size of the wind farm. The default value is a 2km radius area around the turbines. It takes less than 5 minutes to perform the calculations for a 50 wind turbine farm.

Calculation requires only the position of turbines and the maximum sound power level. Results are written out to a text file with two columns containing the location point coordinates and one column containing the noise level. The file can then easily be imported into a mapping information system to display noise levels on a map.

A sample noise map is provided below.

3.2. AcousEole1

AcousEole1 is similar to AcousEole0 as far as the propagation model is concerned. However, it was developed for real-time assessments at given residential locations.

Calculation requires the positions of turbines and residential locations, the background noise levels at each location, as well as the sound power level. Wind farm noise is computed at three wind speeds.

Below is an illustration of the table of results.

DAYTIME													
Direction : SE	Wind Speed (Hub)	5. m/s				8. m/s				10. m/s			
	Wind Speed (10m)	3.6 m/s				5.7 m/s				7.2 m/s			
		WT	Back.	Amb.	E.	WT	Back.	Amb.	E.	WT	Back.	Amb.	E.
LP1	Location Point 1	25.5	30	31.3	1.3	34.9	34	37.5	3.5	37.2	38	40.6	2.6
LP2	Location Point 2	26.7	32	33.1	1.1	36.0	36	39.0	3.0	38.3	42	43.5	1.5
LP3	Location Point 3	21.3	37	37.1	0.1	28.3	38	38.4	0.4	28.5	38	38.5	0.5

Figure 1: AcousEole1 interface – results
(WT: wind farm noise; Back.: background noise; Amb: ambient noise; E: emergence)

Although the calculations are similar to AcousEole0, AcousEole1 makes it possible to modify the sound power level in real time, as well as switching on and off each turbine separately. The results are instantly updated so that the impact of individual choices can be displayed.

Below is an illustration of the interface.

Sound Power						
AutoFill						
Wind Speed (Hub)	5. m/s		8. m/s		10. m/s	
Wind Speed (10m)	3.6 m/s		5.7 m/s		7.2 m/s	
WTG1	97	1	106	1	108	1
WTG2	94	1	103	1	104.5	1
WTG3	94	1	103	1	104.5	1
WTG4	94	1	103	1	104.5	1
WTG5	94	1	103	1	104.5	1
WTG6	94	1	103	1	104.5	1
WTG7	94	1	103	1	104.5	1
WTG8	94	1	103	1	104.5	1
WTG9	94	1	103	1	104.5	1
WTG10	97	1	106	1	108	1
WTG11	97	1	106	1	108	1
WTG12	97	1	106	1	108	1
WTG13	97	1	106	1	108	1
WTG14	97	1	106	1	108	1

Figure 2: AcousEole1 interface - sound power

3.3. AcousEole2

The AcousEole2 graphical user interface is identical to that of AcousEole1. The only difference lies in the propagation model. In AcousEole2, wind farm noise is not computed directly, but assessed using imported simulation results. Sophisticated simulations are usually performed during the noise survey, which includes the effect of topography and wind on propagation. The results are then imported into AcousEole2 and the sound power level of each individual turbine can be modified.

Below is an example of imported data. The first column shows the sound power level (LwA) used in the simulation and the following columns show wind turbine noise levels at each residential location.

DATA

Wind speed (Hub) 8. m/s — Wind Speed (10m) 5.7 m/s — Direction NO

Parc	LWA	LP1	LP2	LP3	LP4	LP5	LP6	LP7	LP8	LP9	LP10	LP11	LP12	LP13	LP14	LP15	LP16
WTG01	105.0	0.0	6.2	16.5	7.9	0.0	0.0	0.0	7.2	0.0	0.0	23.9	17.2	20.7	19.2	18.1	0.0
WTG02	105.0	0.0	0.0	29.9	14.0	1.8	0.0	0.0	16.0	3.2	0.0	11.6	31.3	22.7	27.9	20.5	0.0
WTG03	105.0	0.0	0.0	33.1	20.5	7.0	0.0	0.0	23.6	8.5	0.0	7.0	25.9	16.7	21.9	13.3	0.0
WTG04	105.0	0.0	0.0	34.2	18.5	5.4	0.0	0.0	21.1	6.8	0.0	8.4	27.5	18.4	23.4	17.8	0.0
WTG05	105.0	0.0	0.0	27.2	14.7	3.9	0.0	0.0	18.1	5.2	0.0	11.9	27.1	21.1	24.1	17.5	0.0
WTG06	105.0	0.0	0.0	26.7	13.1	2.4	0.0	0.0	16.1	3.7	0.0	13.5	27.8	22.4	24.9	18.5	0.0
WTG07	105.0	0.0	0.0	24.2	11.4	0.8	0.0	0.0	14.1	2.1	0.0	15.1	28.3	23.9	25.6	19.6	0.0
WTG08	105.0	0.0	0.0	32.6	16.6	4.0	0.0	0.0	19.0	5.4	0.0	9.8	29.9	20.0	24.5	18.8	0.0
WTG09	105.0	0.0	0.0	27.6	11.9	0.2	0.0	0.0	13.9	1.6	0.0	13.2	31.7	24.9	28.9	21.8	0.0
WTG10	105.0	0.0	0.0	15.9	4.9	0.0	0.0	0.0	8.0	0.0	0.0	23.7	20.2	23.5	21.6	20.3	0.0
WTG11	105.0	0.0	0.0	17.4	6.6	0.0	0.0	0.0	9.8	0.0	0.0	21.1	23.5	23.6	22.0	20.3	0.0
WTG12	105.0	0.0	0.0	24.6	15.2	3.9	0.0	0.0	16.5	5.1	0.0	13.2	23.6	18.7	21.4	15.3	0.0
WTG13	105.0	0.0	0.0	22.2	10.9	2.3	0.0	0.0	14.7	3.5	0.0	15.1	24.0	19.7	21.9	19.4	0.0
WTG14	105.0	0.0	0.0	21.5	9.3	0.7	0.0	0.0	12.8	1.9	0.0	17.2	24.0	22.9	22.1	19.8	0.0

Figure 3: AcousEole2 interface for input data

Like AcousEole1, AcouEole2 makes it possible to alter sound power levels in real time, as well as switching on and off each turbine separately.

AcousEole2 assumes that noise propagation is linear as far as sound power emissions are concerned. Since the propagation models available on the market are linear, the results in AcousEole2 are as accurate as if they had been computed by the simulation from which data are imported. However, turbine or residential location coordinates cannot be modified. New input data are then required.

4. A four-phase noise risk management approach

A consistent approach to risk management is fully embedded in the project management process. Key project milestones were identified to control risks related to wind farm noise.

- Preliminary Layout
- Final Layout
- Building Permit
- Project Approval
- Commissioning

Risk is reviewed at every milestone. A risk review includes a risk assessment and a list of points to be checked.

We have developed a four-phase approach. Each phase is associated with a risk assessment methodology adjusted to balance cost and efficiency.

- **Phase 0** - Preliminary Layout

  A noise map is established using AcousEole0 to **assist project developers in designing a preliminary layout**.

- **Phase 1** - Final Layout

  Confidence in the project is higher and expenditure may be committed for background noise measurements. At each given location point, wind farm noise is assessed using AcousEole1. **The wind farm layout is optimised**.

- **Phase 2** - Project Approval

  A complete noise survey is performed, including sophisticated wind farm noise simulations. The results are imported into AcousEole2 to **define and optimise noise management planning**.

- **Phase 3** – Wind Farm Noise Measurement

  Wind farm noise is measured to refine phase 2 simulations. Based on the results, **a noise management plan can be implemented**.

The illustration below summarises the key points of noise risk management related to a wind farm project.

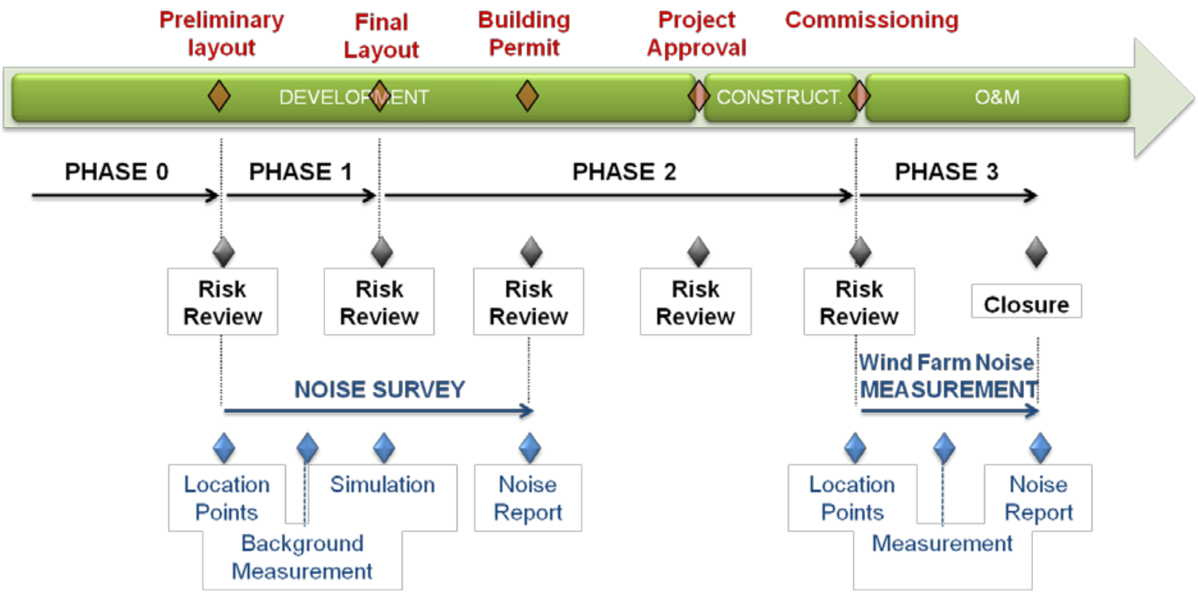

Figure 4: Milestones related to Wind Farm Noise risk management

Details on how risk is controlled at each phase, as well as examples on wind farm projects, are presented below.

4.1 Phase 0 - Preliminary Layout

AcousEole0 is used to establish a noise map. The map is an effective tool for detecting noise risks at specific residential locations and identifying which turbines carry the risk.

A value of 2 dB/km is usually chosen for atmospheric absorption. Results are generally representative of a worst-case scenario (a residential location downwind of the wind farm).

A sample noise map for a fictitious project is shown below.

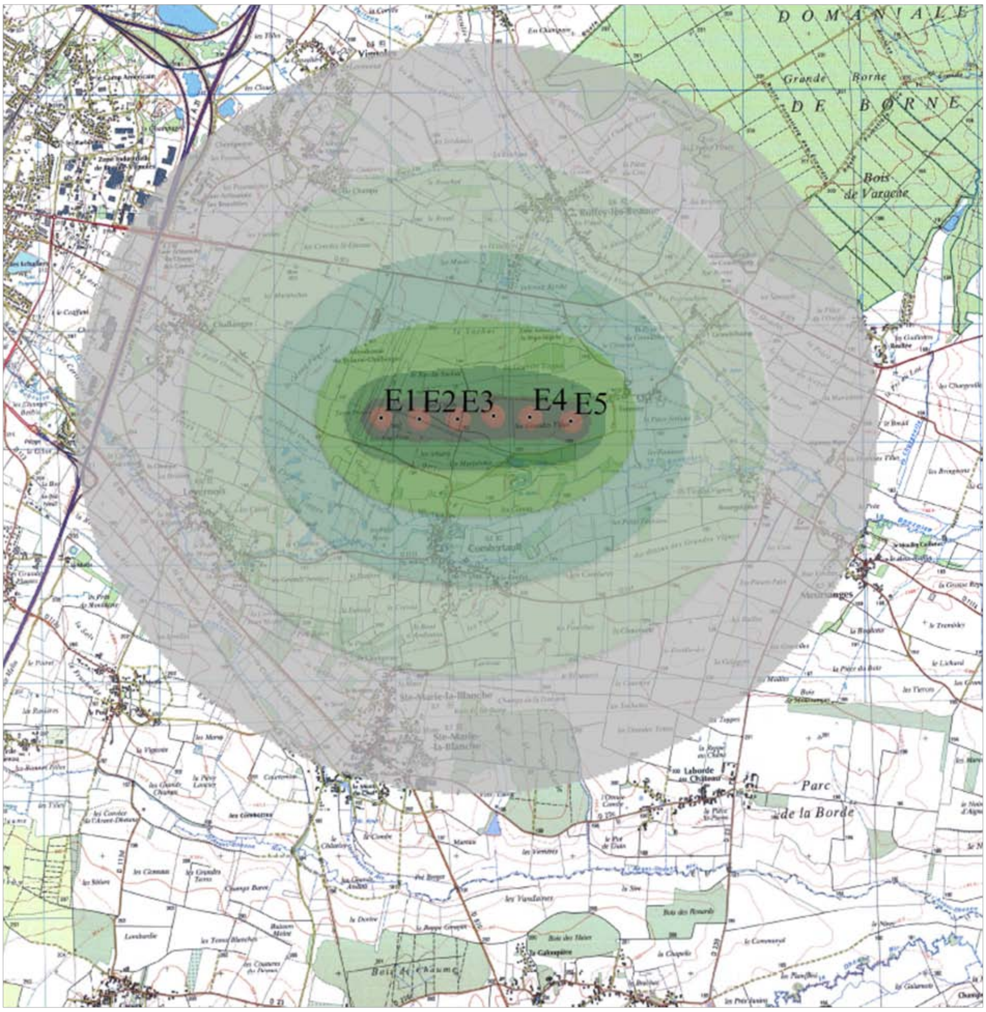

Figure 5: AcousEole0 noise map on a fictitious wind farm project

A risk is likely to occur when wind farm noise exceeds a given threshold. The threshold depends on the position of wind farm and residential locations, background noise (quiet or loud) and the direction of the prevailing wind.

Phase 0 is completed when a preliminary layout is produced. Risk is reviewed as follows:

- Control AcousEole assumptions,
- Check layout version,
- Check for any residential locations where level is above threshold.

4.2 Phase 1 - Final Layout

After a preliminary layout is produced, only minor modifications of turbine positions are subsequently expected. Moreover, confidence in the project is higher. Therefore, sensitive residential locations are identified and background noise measurements are performed (if needed).

Wind farm noise is assessed at each location using AcousEole1. Results are compared to the limits specified in the local regulations.

Risk is assessed as follows:

- Probability

  Probability is measured as the difference between calculated levels (wind farm noise, difference or emergence) and the regulatory limits. Four categories are specified: "low", "moderate", "high", and “critical". Thresholds depend on various parameters and are set based on feedback.

- Severity

  Turbines that entail a Probability higher than "low" are identified.

The following tables illustrate a Probability and Severity assessment for a fictitious project.

	Wind Speed 10m ref	5. m/s		6. m/s		8. m/s	
		Jour	Nuit	Jour	Nuit	Jour	Nuit
LP1	location point 1	1	2	1	1	1	1
LP2	location point 2	1	1	1	1	1	1
LP3	location point 3	1	2	1	2	1	1
LP4	location point 4	1	3	1	4	1	1
LP5	location point 5	1	1	1	1	1	1

(1 : low - 2 : moderate - 3 : high - 4 : critical)

Figure 6: Phase 1 Probability assessment for a fictitious wind farm project

	WTGs
LP1	WT3, WT4
LP2	
LP3	WT5
LP4	WT7
LP5	

Figure 7: Phase 1 Severity assessment for a fictitious wind farm project

In this example, LP1 Probability is "moderate" but a decrease from "moderate" to "low" would require the removal of two turbines (WT3 and WT4). In contrast, LP4 Probability is high, i.e. higher than LP1 whereas only one turbine (F4) carries the risk. In other words, risk occurrence is less likely for LP1 than LP4. However, should the risk occur on LP1 and LP4, mitigation on LP1 will be more costly and/or difficult than mitigation on LP4. This illustrates the dual nature of Risk (Probability and Severity).

Phase 1 is completed when a final layout is produced. Risk is reviewed as follows:

- Check layout version,
- Check relevance of chosen location points,
- Check period and whether background noise measurements are representative,
- Control the quality of background noise measurement,
- Check the AcousEole1 assumptions,
- Assess Probability and Severity.

4.3. Phase 2 - Project Approval

Phase 2 starts when the layout is definitive. Sophisticated noise simulations are performed. Generally, an engineering company is commissioned for the overall noise survey, including both background measurements and wind farm noise predictions.

The company commissioned for the noise survey delivers a report and simulation results in dBA (noise of each turbine at every residential location). Simulation data are then used as input for AcousEole2.

Risk is assessed as follows:

- Probability

  Wind farm noise, emergence or difference serve as a measure of Probability.

- Severity

  Severity is measured as the expected percentage of production losses due to a potential noise management plan designed to reduce Probability. It is assessed either for each location point or for each wind turbine.

Unlike during phase 1, no thresholds are specified for Probability. To illustrate this, let us assume emergence of 4.1 dB and 4.9 dB. In phase 2, the Probability is higher in the second case. In phase 1, due to uncertainties the gap between 4.1 and 4.9 dB is not significant and the Probability is identical.

The following table illustrates a phase 2 Probability assessment for a fictitious project.

	Wind Speed 10m ref	5. m/s		6. m/s		8. m/s	
		Day	Night	Day	Night	Day	Night
LP1	location point 1	0.2	1.2	0.7	2.1	0.6	0.5
LP2	location point 2	0.3	**3.8**	1.2	**5.6**	0.9	**3.8**
LP3	location point 3	0.1	1.9	0.6	3.0	0.5	1.2

Figure 8: Phase 2 Probability assessment for a fictitious wind farm project

	LOSSES
WTG01	0%
WTG02	1.5 %
WTG03	0%
WTG04	0%
WTG05	2 %
WTG06	0%

Figure 9: Phase 2 Severity assessment for a fictitious wind farm project

At the Building Permit stage, Risk is reviewed as follows:

- Check layout version,
- Check turbine sound power level,
- Check the AcousEole2 assumptions,
- Compare AcousEole1 and AcousEole2 results to detect potential errors,
- Review noise survey,
- Assess Probability and Severity at every residential location.

The Risk review is subsequently updated at the Project Approval and Commissioning stages. Phase 2 is completed when the wind farm is commissioned.

4.4. Phase 3 - Wind Farm Noise Measurement

Once turbines are in operation, wind farm noise can be measured and the noise survey can be updated.

Owing to the complexity of operating wind farm measurements, it is difficult in many cases to gather data reflecting every possible combination of wind speeds and directions. At this point, the wind farm noise simulations are usually calibrated using the measured data.

The potential noise management plan may be optimized using AcousEole2.

Phase 3 is completed when noise management plan is drawn up.

5. Discussion and conclusions

The AcousEole calculation results have been compared with a variety of propagation models and on-site measurements.

The following is a case in point. Noise levels were measured at an operational wind farm at three different locations with a north-westerly wind. Measurements were used to calibrate a sophisticated ray tracing model, and noise levels were assessed for a south-easterly wind. AcousEole1 simulation was run in parallel.

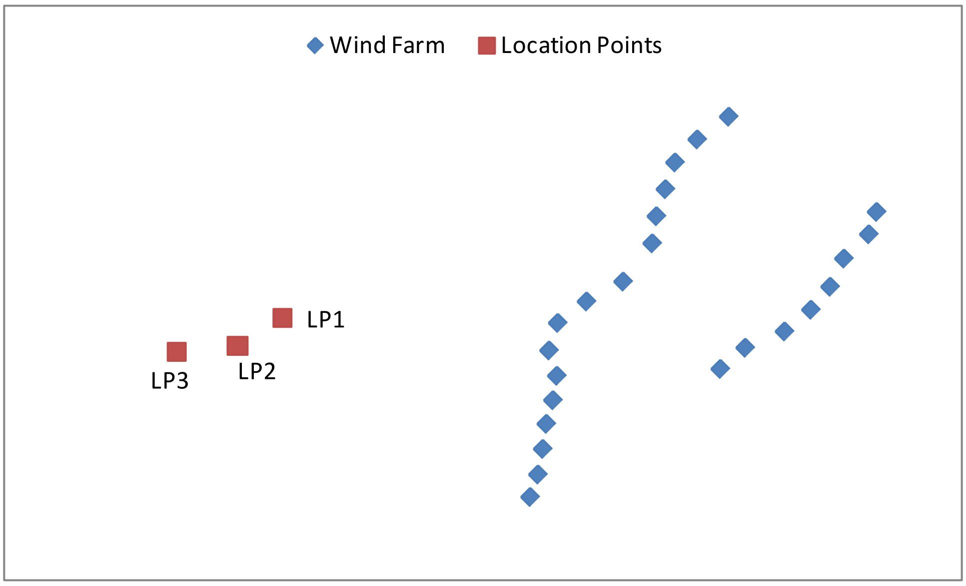

Figure 10: AcousEole1 vs. Measurements - Location points and wind turbine positions

	LP1	LP2	LP3
Wind Speed (10m)	8 m/s	8 m/s	8 m/s
Survey NO	31.5	30.4	29.0
Survey SE	40.0	39.1	37.7
AcousEole1 2dB/km	40.3	39.3	37.8

Figure 11: AcousEole1 vs. Measurements - Wind Farm Noise

In favourable propagation conditions (SE), AcousEole1 results are close to the noise survey results. This confirms that AcousEole1 results are conservative. Similar studies have been carried out at other wind farm sites.

The risk management method was tested on a few selected projects. Initial results were conclusive. The risk management approach is now being implemented at all our projects in France. Procedures are being drafted to control Risk at every project milestone. The process will be developed continuously through feedback from our wind farms in order to adapt to future changes.

6. Glossary

Background Noise

The ambient noise level already present in the environment without an operational wind farm.

Difference

The arithmetical difference between Wind Farm Noise and Background Noise.

Emergence

The arithmetical difference between ambient noise with an operational wind farm and Background Noise.

Probability

The likelihood of occurrence of a specific Risk.

Risk

An event or a situation that may occur (with some degree of uncertainty) during the Project and may prevent from the Project objectives from being achieved.

Risk Assessment

The overall process of assessing the Risk impact.

Risk Control

The overall process of controlling and monitoring Risk exposure.

Risk Severity

The comparative measure of the impact on Project results, if Risk occurs.

Sound Power

The total sound energy radiated by a source per unit time.

Wind Farm Noise

The rated noise due to the combined effect of all the Wind Turbines.

7. References

[1] ISO 9613-2 Ed. 1: Acoustics - Attenuation of sound during propagation outdoors - Part 2: General method of calculation. 15 December 1996.

[2] IEC 61400-11-am1 - Ed. 2.0: Amendment 1 - Wind turbine generator systems - Part 11: Acoustic noise measurement techniques. 29 May 2006.

[3] Décret n° 2006-1099 du 31 août 2006 relatif à la lutte contre les bruits de voisinage. JO Rep. Française. 01 September 2006

[4] ETSU-R-97: The Assessment & Rating of Noise from Wind Farms. Final Report. September 1996.

[5] Impact sanitaires du bruit généré par les éoliennes. Avis de l'AFFSET. March 2008.

Third International Meeting
on
Wind Turbine Noise
Aalborg Denmark 17 – 19 June 2009

Investigation into onshore noise emanating from piling operations during the construction phase of GunfleetSands offshore wind farm.

Martin Patrick Court, Senior Environmental Health Officer and Andrew Rutson-Edwards BSc. (Hons), Environmental Science Manager

Pollution and Environment team, Environmental Services, Tendring District Council, Weeley, Essex CO16 9AJ.

mcourt@tendringdc.gov.uk
arutson-edwards@tendringdc.gov.uk

Abstract

The construction of an array of 48 wind turbines and one substation is being undertaken in the locale of Gunfleet Sands, off of the Essex coast in England. With the commencement of piling operations, complaints were received by Tendring District Council from the General public. Investigation into the noise alleged was undertaken in October 2008. With the potential for further complaints, Tendring District Council's Environmental Services in conjunction with DONG Energy carried out a more detailed longer term study and investigation into the impact of piling operations on residential areas in November and December 2008.

Continuous monitoring at 3 sites adjacent to properties on the seafront was undertaken to establish the levels. The measurement locations were chosen to be representative of the existing noise climate to which the closest noise sensitive residences are exposed.

Background monitoring between the piling operations showed that the noise levels followed a diurnal pattern due to the influence of wave action on the foreshore adjacent to the monitoring sites. The existing noise climate at Sites 1 and 3 is largely dominated by tidal noise with occasional local traffic at this time of year. Site 2 is more dominated by road traffic noise during the day, on a busy suburban approach road into Clacton on Sea. In the early hours, again, tidal noise dominates this noise climate.

During piling operations the weather conditions and wind direction had a significant impact on the sound propagation over the water between the piling and the onshore SLM's . Weather conditions play a large part in onshore noise perception. Psycho-acoustics may also play a part in people's perception of noise disturbance from these

piling works. It is a new noise source and has considerable AM properties which are generally considered more noticeable.
This shows a peak SPL of 53dBA, but more pertinently a maximum Amplitude Modulation (AM) of approx 17dB. That is, the difference between the highest and lowest readings giving a significant contrast in the noise climate.

Atmospheric absorption, humidity, wind and temperature gradients, ground and water effects reflecting sound greater distances inland than would be expected, as confirmed by complaints received from some miles inland.

In the U.K. BS 5228, in conjunction with the Control of Pollution Act 1974, gives advice on noise and vibration control on construction sites. Part 4 refers to a code of practice for noise and vibration control applicable to piling operations. In essence it gives source data for different types of noise source and methods for calculating noise produced by these sources, using sound power levels or LAeq levels and standard attenuation over distance calculations. Given the large distances involved, and the high levels of impact noise at the Gunfleet Sands site it is open to discussion whether this is appropriate for these piling operations.

Introduction

In 2007 United Kingdom Government Energy Minister, John Hutton announced plans for the installation of 7000 offshore wind turbines around Britain's 7,760 miles of coast. Planning permission was granted by Tendring District Council for two arrays (Gunfleet Sands 1 and 2) consisting of 48 turbines and an offshore substation to be built at the location of Gunfleet Sands off of the North East Essex coast see Figure 1. The planned arrays Gunfleet Sands 1 (108MW) and Gunfleet Sands 2 (65MW) are designed to power 120,000 average (4 person households) (Pers Comm Sills, 2008). In line with the UKs carbon reduction commitment under the Kyoto protocol, a reduction in CO_2 emissions is required. By utilising wind turbine technology to generate electricity the Gunfleet Sands array will provide a total CO_2 saving of 480,000 tonnes per annum compared to coal fired station producing the same output.

Figure1 Location of Gunfleet Sands wind park

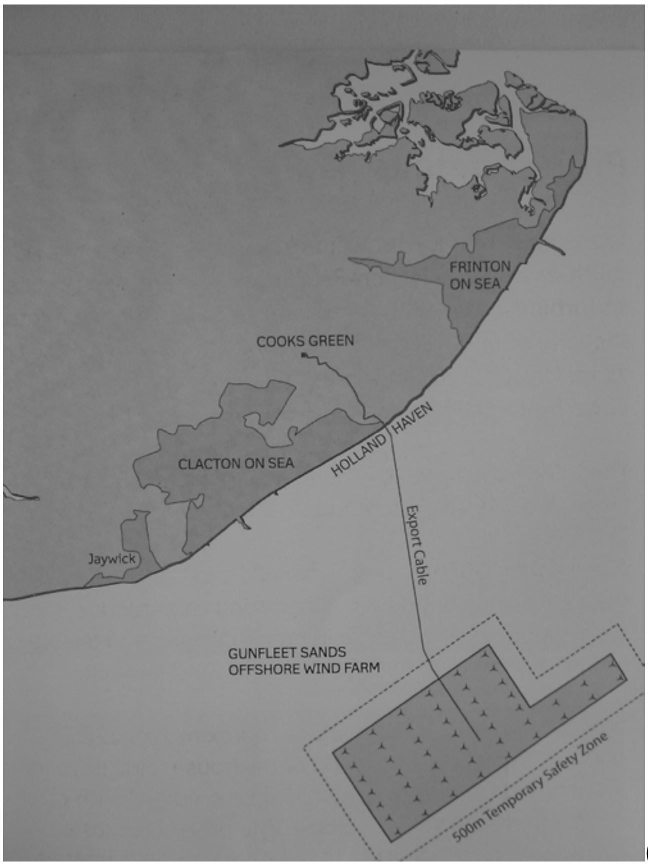

(Image courtesy of Dong,2008)

Planning was also granted by Tendring District Council for the associated onshore cabling works. Meetings were held between Tendring District Council's Planning Services, Environmental Services and the company carrying out the installation on behalf of the energy supplier, Dong energy. It was established that the piling works would need to be carried out at times consistent with suitable tidal states and weather windows; the piling rig would only be able to gain access at certain times due to the shallow depths on and around the sand banks.

The piling equipment used was a Menck hydraulic hammer, this equipment was used aboard one of two vessels throughout the project it would be either based on board Excalibur or Svanen (Fig 2) which was floated to site at the relevant times prior to the piling operation.

Figure 2 Svanen

(Image courtesy of Dong,2008)

With the start of the piling phase of the construction process in October 2008, (delayed by one month due to inclement weather conditions) Tendring District Council's Environmental Services received complaints regarding noise from the operation. Unfortunately due to tidal restrictions, the first piling was undertaken at night. The piling rig and associated barges were visible off shore for some hours prior to the piling operation actually commencing. The fact that the piling rig was so visible may have compounded the perceived "annoyance levels" to some of the complainants. Pedersen & Larsen, (2008) discuss "the interactions and influence of vision on the response to the auditory stimuli". Describing that, "seeing the noise source has been found to increase noise annoyance".

Initially manual noise monitoring was carried out during night time piling.

There were indications from the initial measurements that that there may be potential for further complaints due to the time to drive in each pile, (potentially up to four hours) and the extended nature of the piling phase of the works (in the region 5 months).

Cobo et al (2007) concur stating that"The two noisier phases of a wind farm lifecycle are construction and operation. The most significant activity during wind farm construction is foundation installation, specially piling".

From BS5228 source noise levels (*Lsource dB)* of 121dB(A) are given for a Hydraulic drop hammer.

"British Standard, BS5228 as amended provides guidance on acceptable noise levels during construction. In urban areas, Lequivalent should not exceed 75 dB at the outside of a noise sensitive building (i.e. a residential or office building), with a lower limit of 70 dB applying in rural areas. "White et al(2008)

Concern was raised as to the validity of using BS5228 as there appeared to be little relevance to offshore piling.

During a subsequent meeting between Dong energy and Tendring District Council it was proposed that a longer term monitoring programme should be carried out. Tendring District Council in conjunction with DONG Energy monitored noise levels in November – December 2008 from the piling operation of the construction of Gunfleet Sands wind turbine farm. This assessment is based on the highest sound pressure levels (SPL) associated with the construction of Gunfleet Sands 1 and 2, namely the piling aspect of the construction works. Due to the locations of the piles the areas most likely to be affected by the piling operations were identified as being along the seafronts of Clacton on Sea and Holland on Sea. Consequently, three locations were selected for monitoring purposes, which were: 1. The Esplanade, Holland on Sea . 2. Marine Parade East ,Clacton on Sea, and 3. The Coastguards Offices, West Clacton, Martello Bay.

This paper provides an overview of the impact of piling operations on residential areas. This will focus on results obtained for the period 2/12/08 through to 4/12/08 at Sites 1 and 2. This period included a piling operation on 3/12/08, between approximately 2000 – 2215 hours. A large amount of data is available for the total period of one month continuous monitoring at the three locations, however, for the purposes of this report, the period referred to above is considered representative

Assessment methodology and criteria

Initial investigations and literary review looking for research into airborne noise nuisance from offshore piling offered very little information and advice. Most of the previous papers found, related mainly to under water noise disturbance effects to cetaceans or noise nuisance issues raised once the wind turbines are operational.

In the absence of any specific assessment criteria or standards for long range piling noise over sea, it was deemed appropriate to adapt and have regard to all of the standards below when making any assessment of nuisance or interference with an individual’s use and enjoyment of their property.

The effect produced by the introduction of a noise source into an environment may be determined by:

- reference to guideline noise levels. The World Health Organisation (WHO) *Guidelines for Community Noise* and British Standard (BS) 8233:1999 “Sound insulation and noise reduction for buildings” contain such guidance values. This method is well suited to the assessment of noise from an activity that is fixed within a defined boundary to a relatively small number of receptors. But the noise from the piling during the wind array project potentially has a large number of receptors although it does emanate from within a defined boundary.

- reference to the existing background noise level (L_{A90}). This is the method employed by BS 4142:1997 “Method for rating industrial noise affecting mixed residential and industrial areas” to determine the likelihood of complaints about noise "… of an industrial nature in commercial premises..." amongst others.

Guideline values

There are a number of guidance documents that contain recommended guideline noise values. These are discussed below.

- BS 8233 is principally intended to assist in the design of new dwellings; however, the Standard does state that it may be used in the assessment of noise from new sources being brought to existing dwellings.
- BS 8233:1999 this document is based on "Guidelines for community noise". A draft of a document issued by the World Health Organisation in 2000.
- The WHO guideline values are appropriate to what are termed "critical health effects". This means that the limits are at the lowest noise level that would result in any psychological, physiological or sociological effect. Shown below in Tables 1 and 2:

TABLE 1: BS 8233 Noise Reduction

Guidance Document	Level	Level of annoyance
World Health Organisation "Community Noise 2000"	L_{AeqT} = 55 dB	Serious annoyance, daytime and evening. (Continuous noise, outdoor living areas)
	L_{AeqT} = 50 dB	Moderate annoyance, daytime and evening. (Continuous noise, outdoor living areas).
	L_{AeqT} = 35 dB	Moderate annoyance, daytime and evening. (Continuous noise, dwellings, indoors)
	L_{AeqT} = 30 dB	Sleep disturbance, night-time (indoors)
	L_{AMAX} = 60 dB	Sleep disturbance, windows open at night. (Noise peaks outside bedrooms, external level).
	L_{AMAX} = 45 dB	Sleep disturbance at night (Noise peaks inside bedrooms, internal level)

Table 2: WHO Guidelines for Community Noise

Guidance Document	Level	Recommended levels
BS 8233:1999 "Sound Insulation and noise reduction for buildings"	L_{AeqT} = 55 dB	Upper limit for external steady noise. (Gardens and balconies).
	L_{AeqT} = 50 dB	Desirable limit for external steady noise. (Gardens and balconies).
	L_{AeqT} = 40 dB	Reasonable resting/sleeping conditions for living rooms during the day. (Internal – steady noise)
	L_{AeqT} = 35 dB	Reasonable resting/sleeping conditions for bedrooms, night time. (Internal – steady noise)
	L_{AeqT} = 30 dB	Good resting/sleeping conditions for bedrooms, night time (Internal – steady noise)
	L_{AMAX} = 45 dB	Limit for individual noise events for a reasonable standard in bedrooms at night

- BS 4142:1990 considers that the difference between the rating level of noise from industrial development and the background noise level of the area is indicative of the likelihood of complaint. U.K. Planning Policy Guidance PPG 24 (due to be replaced by Planning Policy Statement PPS24) incorporates and refers to BS4142:1990 as follows:

  "The likelihood of complaints about noise from industrial development can be assessed, where the Standard is appropriate, using guidance in BS 4142:1990. Tonal or impulsive characteristics of the noise are likely to increase the scope of complaints and this is taken into account by the "rating level" defined in BS 4142. This "rating level" should be used when stipulating the level of noise that can be permitted. "A difference of around 10 dB or higher indicates that complaints are likely. A difference of around 5 dB is of marginal significance".

BS 4142 also considers night noise measurements. Within the guidance given in PPG 24 the times for night noise are 2300 to 0700. The reference period of measurement and assessment, "T", used when following BS 4142 procedures is five minutes for night time (23:00-07:00) and one hour for day time (07:00-23:00).

- BS 5228: 1997 as amended when used in conjunction with the Control of Pollution Act 1974, (COPA1974) gives advice on noise and vibration control on construction sites. Part 4 refers to a code of practice for noise and vibration control applicable to piling operations. In essence it gives source data for different types of noise source and methods for calculating noise produced by these sources, using sound power levels or LAeq levels and standard attenuation over distance calculations. Given the large distances involved, and the high levels of impact noise at the Gunfleet Sands site it is open to discussion whether this is appropriate for these piling operations.

- The Environmental Protection Act 1990 (EPA1990) provides powers for Local Authorities to serve a Noise Abatement Notice in order to demand that an individual or company who the Local Authority believes is generating unnecessary and objectionable noise refrains from causing a nuisance in the future.

At first due to the fact that the piling operation was beyond three miles from the U.K. shoreline it wasn't established whether Tendring District Council were able to take any action under the EPA 1990 but: Tendring District Council instructed Counsel to investigate this. Counsel did establish that if a Statutory Nuisance was identified then authorised officers from Environmental Services shall serve abatement notices under The EPA1990 on the operator of the equipment causing that nuisance.

As previously mentioned in BS5228 source noise levels (*Lsource dB)* of 121dB(A) are given for a Hydraulic drop hammer. In contrast, the sound pressure levels from the piling equipment used during the operation off shore, ranged between 130-150dB(A) as measured 1m from the source. This figure was variable due to the different power levels used within the piling hammer equipment to carry out the piling dependent on the strata the piles are driven into.

Predicted levels at the facades of noise sensitive residential properties were calculated using the distance attenuation equation for a point source:

$SPL = L_1 - 20\log(r_2/r_1)$

where $_{r1}$ is the measurement distance,

$_{r2}$ is the receiver distance and

L1 is the sound level as measured at $_{r1}$

The predicted levels at the noise sensitive properties, as calculated for the piling taking place at 7Km from the noise sensitive properties ranges from:

$=130 - 20\log(7000/1)$

$= 130 - 20\ (3.85)$

$=130 - 77$

SPL = 53dB(A)

to

$=150 - 20\log(7000/1)$

$= 150 - 20\ (3.85)$

=150 – 77

SPL = 73dB(A)

Equipment and Noise Survey details

A noise survey was undertaken between Friday 7th November and Friday 5th December 2008. The survey consisted of long term unmanned readings taken at the three different locations.

1: (Cllr B) The Esplanade, Holland on Sea. Lat 51°48.3'N, Long 1°12.4'E
2: (SLooker) Marine Parade East, Clacton on Sea Lat 51°47.7'N, Long 1°10.4'E and
3: (CG) The Coastguards Station, Hastings Avenue, West Clacton. Lat 51°46.8'N, Long 1°8.4'E
(Google earth plan shows relative locations)

Figure 3 Location of SLM as indicated by yellow markers

(Image Google 2009)

The measurement locations were chosen to be representative of the existing noise climate to which the closest noise sensitive residences are exposed. This, together with the need for access to service the equipment, download information and for the security of the unmanned equipment.

Noise measurements were taken using a Norsonic 140 type 1 and two Norsonic 131 Type 1 sound level meters. (The Norsonic 131's, were hired from Campbell Associates courtesy of DONG Energy). The Norsonic sound level meters meet the following standards: IEC 61672-1:2002 class 1, IEC 60651 class 1, IEC 60804 class 1, IEC 61260 class 1, ANSI S1.4-1983 (R2001) with amendment S1.4A-1985 class 1, ANSI S1.43-1997 (R2002) class 1, ANSI S1.11-2004 class 1.

All sound level meters were factory calibrated by Campbell Associates. Prior to the installation of each meter the microphone was connected using a 5metre extension and environmental kit fitted with a wind muff. The meters were field calibrated at the start, during and at end of the survey using a Norsonic 1251 precision sound calibrator compliant with IEC 942, class 1 with an output of 114dB SPL. No variation in levels was noted. Weather conditions varied considerably throughout the survey, and any readings in high winds and storm conditions will be ignored. The noise measurements were undertaken 1m from the façades of the respective locations.

The existing noise climate at Sites 1 and 3 is largely dominated by tidal noise with occasional local traffic at this time of year. Site 2 is more dominated by road traffic noise on a busy suburban approach road into Clacton on Sea. In the early hours, again, tidal noise dominates this noise climate.

Results

There was a large amount of monitoring information available over the continual monitoring period. The measured noise levels from the part of the survey for this paper are summarised below. i.e 2nd December 2008 – 4th December 2008. These dates were chosen as being representative of the piling operations as a whole.

The weather conditions during the piling operation on the 3rd December between 2000 and 2215 hours were: Clear, very light SW breeze, 0% cloud cover, good visibility, air temperature 1 degree C, sea temperature 10 degrees C.

Figure 4. Survey results for Site 1 for this period show a maximum SPL of 51dBA with LAeqt of 43dB.

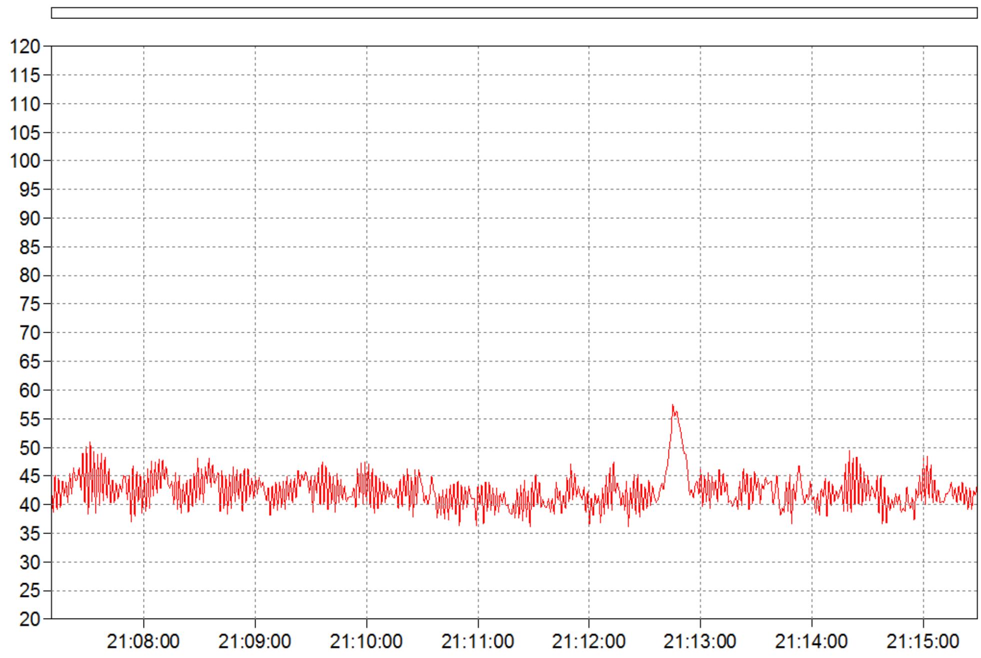

Figure 5 shows the same time period the previous day 2/12/08 as a reference for when there was no piling operation. This shows a maximum SPL of 60dBA which is probably attributable to a passing vehicle given the shape of the noise spike. LAeqt is 38dB for this period.

Figure 5

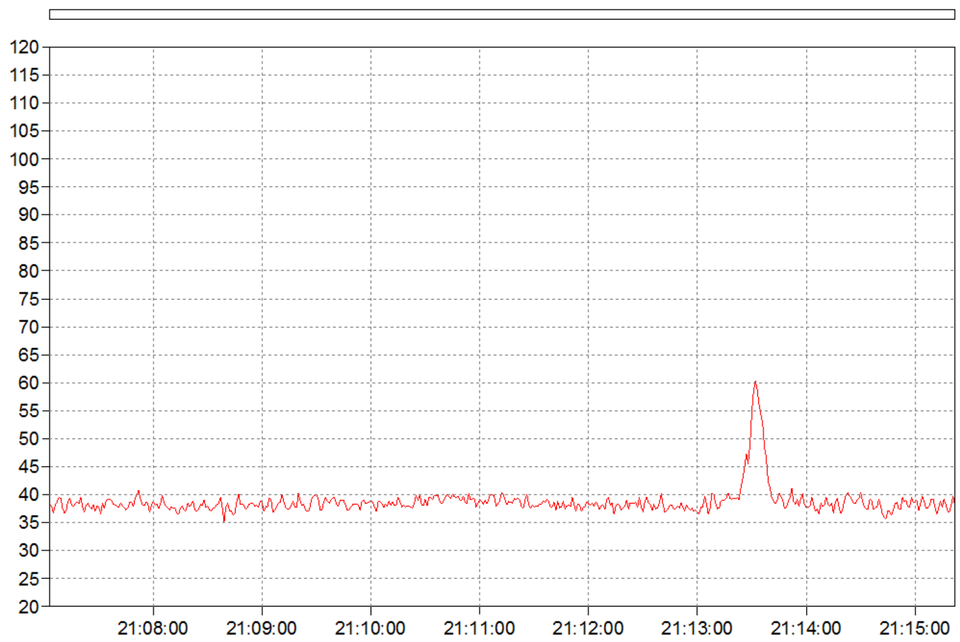

Interestingly Figure 6 shows relatively high noise levels with LAeqt of 60dB, which is purely as a result of high wind and tidal action. This level would be similar to that of a fairly busy road.

Figure 6

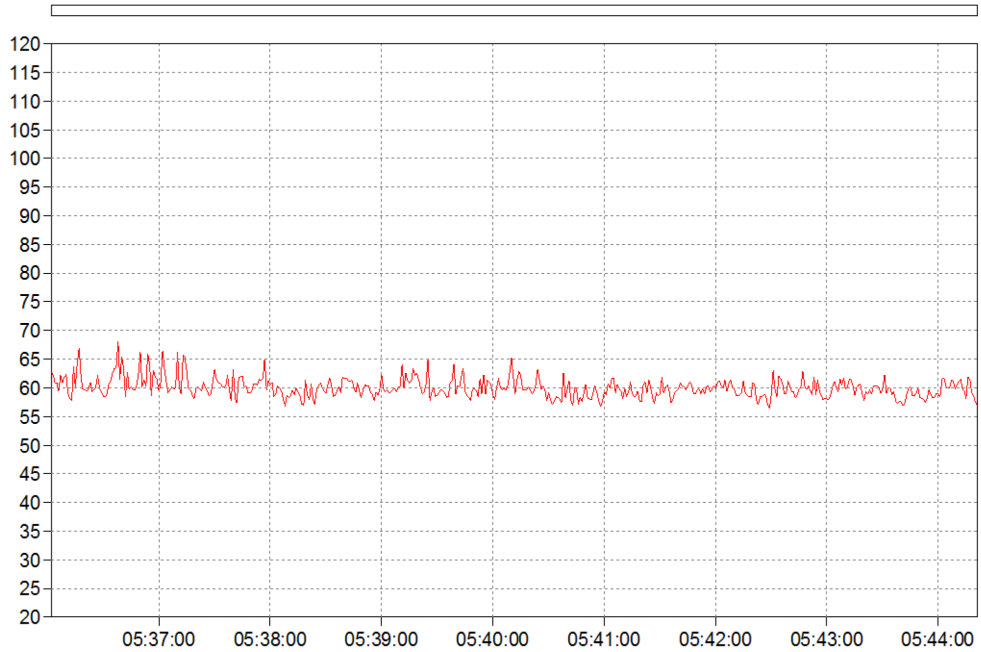

Figure 7 shows an expansion of 2 minutes of piling noise to give greater clarity. This shows a peak SPL of 53dBA, but more pertinently a maximum Amplitude Modulation (AM) of 17.1dB. That is, the difference between the highest and lowest readings giving a significant contrast in the noise climate

Figure 7

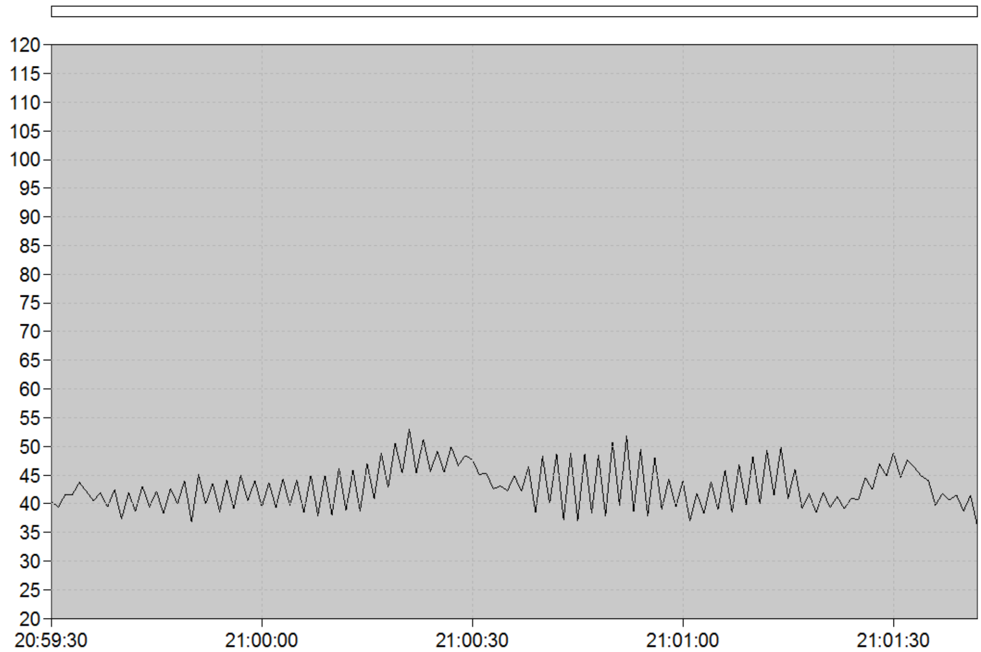

The results for Site 2 for the same time period show the influence of road traffic noise on the noise climate for this area. Figure 8 clearly shows the percussive piling compared to peaks of traffic noise which peak at approx 72dBA.

Figure8 Site 2 3/12/08. Busy road showing piling between passing cars. Illustrates high La90

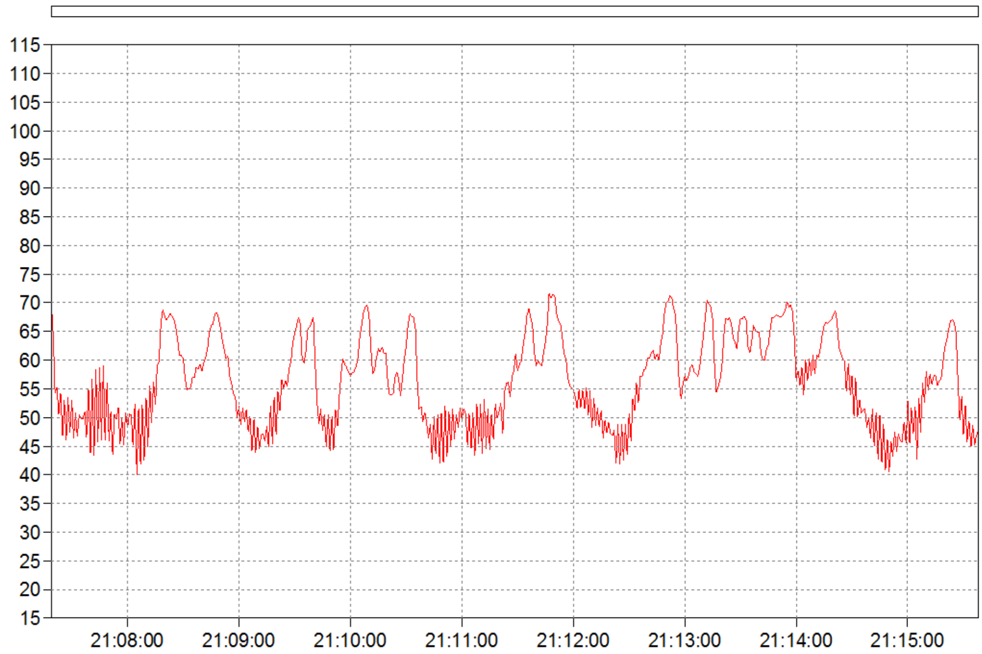

Figure 9 shows similar peaks and profiles for the previous day at the same time when there were no piling operations. This profile is due to RTN.

Figure 9 .Site 2. 2/12/08. No piling, showing high Road Traffic Noise.

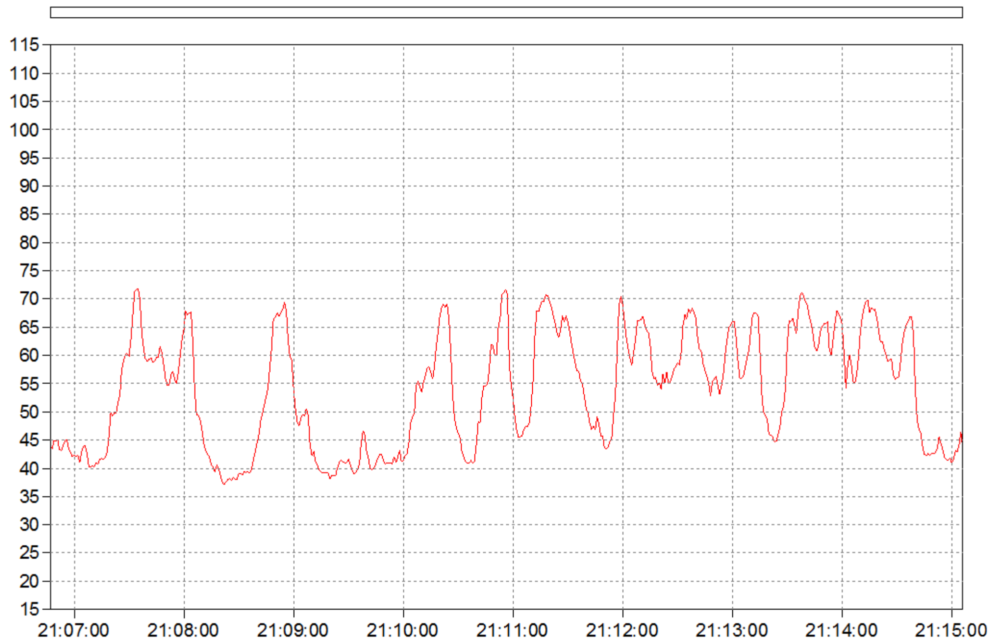

Figures 10-13 show background noise an hour before high tide and summaries of levels versus time over the whole sample period.

Figure 10

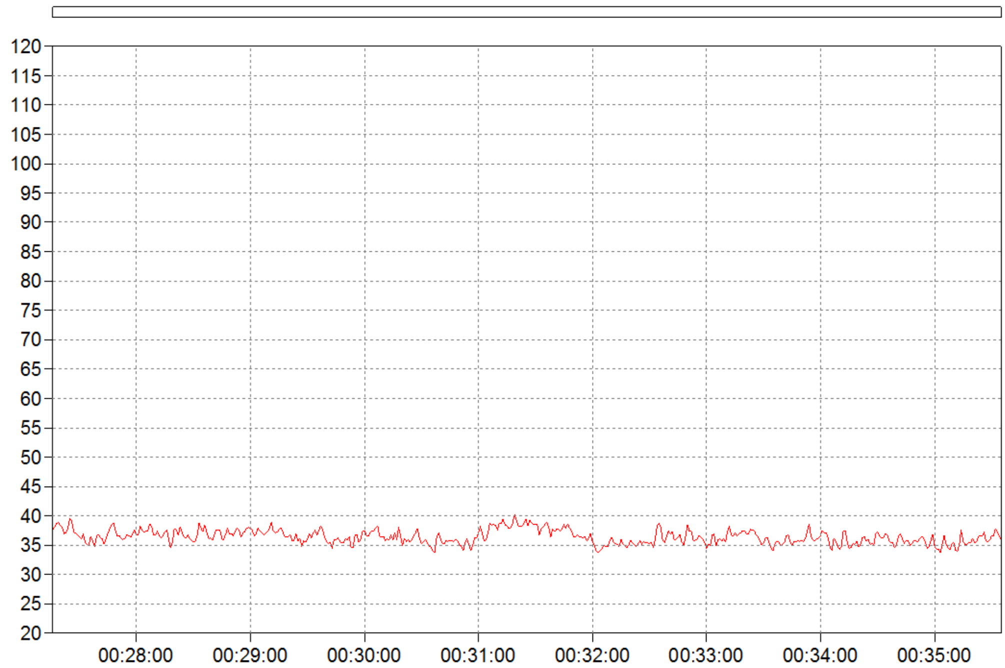

Figure 11. Site 2 2/12/08, 1 hour before high tide Peaks are passing cars.

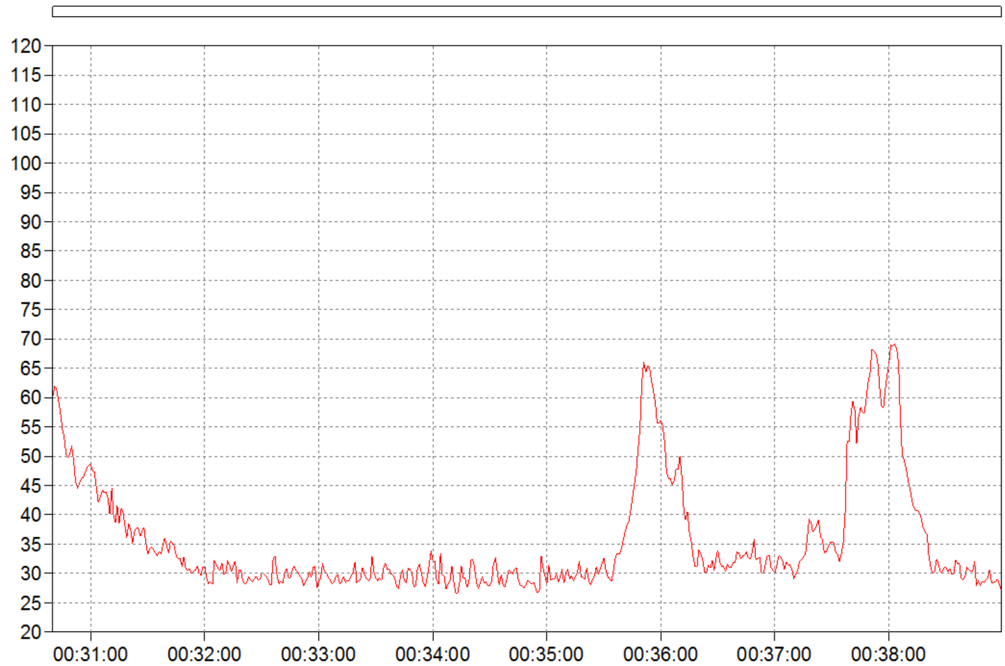

Figure 12. Summary for site 2, 2/12-5/12/2008.

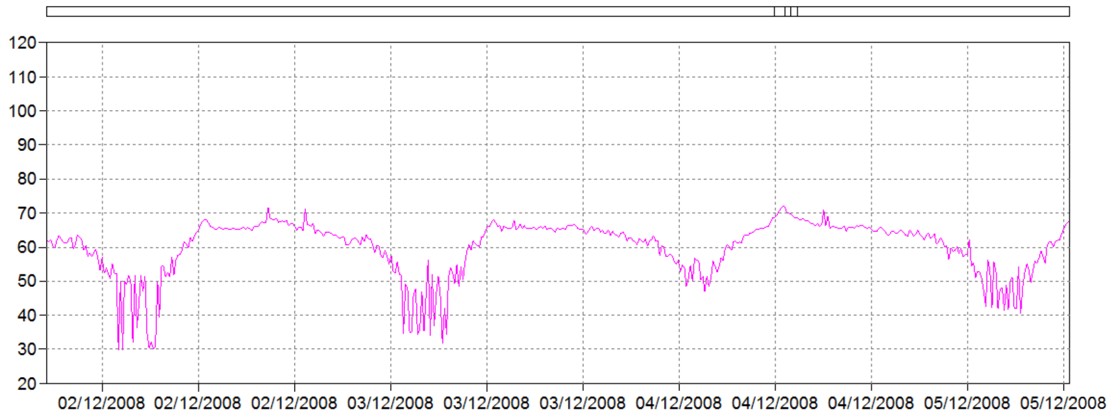

Figure 13 Site 1 summary 2/12/08-4/12/08

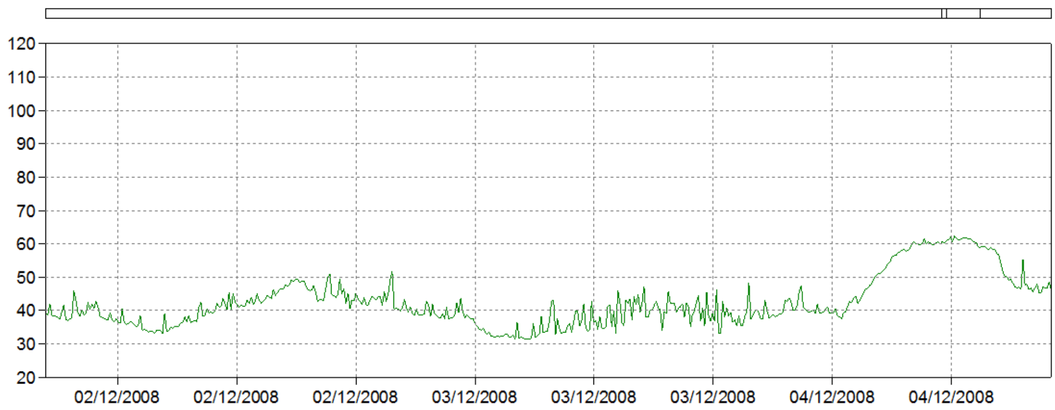

Discussions and Conclusions

The large amount of data collected in the entire monitoring programme does not support any claims of a Statutory nuisance arising from the piling works. For $L_{Aeq\ T}$ criteria the time base (T) given in the documents is 16 hours for daytime limits and 8 hours for night time limits. However, given the nature of the impact noise from piling operations La(max) would appear to be the most appropriate parameter. Amplitude Modulation (i.e the difference between highest and lowest sound levels) may also be a factor in its comparison with La90.

There is scope for debate on the long range outdoor sound propagation over sea, and the likely effect of tidal noise and the influence of wind speed on the results. Low level jets and the reflective properties of water are variable dependant on how 'rough' the water is compared to the usual modelling that is carried out on flat water giving sound reflective tendencies. There is also the phenomenon of the shoreline effect on the sound propagation. Boue (2007), discusses that there is a supplementary change of attenuation due to the change of direction of travel of the sound waves and that the temperature and wind gradients are also changed modifying the characteristics of attenuation at this boundary.

Weather conditions play a large part in onshore noise perception. Atmospheric absorption, humidity, wind and temperature gradients, ground and water effects reflecting sound greater distances inland than would be expected, as confirmed by complaints received from some miles inland although the nearest sensitive properties and those with the sound monitoring equipment installed reported that there were no disturbances heard on the nights in question.

Psycho-acoustics may also play a part in people's perception of noise disturbance from these piling works. Within the Glossary of Planning Policy Guidance (PPG) 24 – Planning and Noise it states that:

"A change of 3 dB(A) is the minimum perceptible under normal circumstances, and a change of 10 dB(A) corresponds roughly to halving or doubling the loudness of the sound."

The piling operation noise is a new noise source and has considerable AM properties which are generally considered more noticeable the results showed a 17.1dB (A) AM. "The analysis of the psycho-acoustic parameters of loudness, sharpness, roughness, fluctuation strength and modulation were carried out at by Professor Weber and colleagues at the working group of acoustics/psychoacoustics at the University of Oldenburg". The psycho-acoustic profiles obtained gave some information on characteristics in the noise that were important for perception and annoyance" They went on to describe "two major groups of psycho-acoustic descriptors could be distinguished, where "lapping", "swishing" and "whistling" can be hypothesised to be related to easily noticed and potentially annoying sounds, while "grinding" could be less annoying and therefore tolerated" (Person Wayne and OGHrstrog , 2002). It can be seen that piling falls within the first category as an impulsive sound.

Existing background levels will contribute to the noise climate. Previous surveys undertaken by Tendring DC have shown LA90 of up to 45dB for night time noise in

Central Clacton on Sea, these figures again depend on wind and weather conditions. Generally, any further noise would need to be 10dB above background level in order to be appreciably noticeable.

There may need to be further noise monitoring activities once both arrays are completed and the wind farm is commissioned and operating.

References

Boué M. (2007). *Final report for the Swedish Energy Agency project 21597-3*

(TRANS)LONG-RANGE SOUND PROPAGATION OVER THE SEA WITH APPLICATION TO WIND TURBINE NOISE
TRITA-AVE 2007:22 ISSN 1651-7660

Cobo P, Kormannl J., Ranzl C. (2007) *UNDERWATER NOISE IMPACT OF OFFSHORE WIND FARMS DURING CONSTRUCTION AND OPERATION PHASES* Technical Report for 1Instituto de Acústica. CSIC. Serrano 144, 28006 Madrid, Spain

Dong Energy (2008) photograps

Google (2009) Map imagery

Pedersen E, Larsman P. (2008) *The Impact of visual factors on noise annoyance among people living in the vicinity of wind turbines.* Journal of Environmental Psychology 28:379-389

PERSSON WAYE K., OG HRSTROG E. (2002) *PSYCHO-ACOUSTIC CHARACTERS OF RELEVANCE FOR ANNOYANCE OF WIND TURBINE NOISE* Journal of Sound and Vibration 250(1), 65:73

Sills P.(2008) Pers comm.

White D., Finlay T., Bolton M., Bearss G.(2008) *Press-in piling: Ground vibration and noise during pile installation.* Proceedings of the International Deep Foundations Congress. Orlando, USA. ASCE Special Publication 116: 363-371

Acknowledgements

Tendring District Council

DONG Energy for hiring the sound level meters

Campbell associates for supplying the sound level meters at short notice.

Appendix

Acoustic Terminology

1. Noise, defined as unwanted sound, is measured in units of decibels, dB. The range of audible sound is from 0 dB to 140 dB. Two equal sources of sound, if added together will result in an increase in level of 3 dB, i.e. 50 dB + 50 dB = 53 dB. A 10 dB increase in sound is perceived as a doubling of loudness.

2. Frequency (or pitch) of sound is measured in units of Hertz. 1 Hertz = 1 cycle/second. The range of frequencies audible to the human ear is around 20 Hz to 18000 Hz (or 18 kHz). The capability of a person to hear higher frequencies will reduce with age. The ear is more sensitive to medium frequency than high or low frequencies.

3. To take account of the varying sensitivity of people to different frequencies a weighting scale has been universally adopted called “A-weighting”. The measuring equipment has the ability to automatically weight (or filter) a sound to this A scale so that the sound level it measures best correlates to the subjective response of a person. The unit of measurement thus becomes dBA (decibel, A-weighted).

4. The second important characteristic of sound is amplitude or level. Two units are used to express level a) sound power level - Lw, and b) sound pressure level - Lp. Sound power level is an inherent property of a source whilst sound pressure level is dependent on surroundings/distance/directivity etc. The sound level that is measured on a meter is the sound pressure level, Lp.

5. External sound levels are rarely steady but rise or fall in response to the activity in the area - cars, voices, planes, birdsong, etc. A person’s subjective response to different noises has been found to vary dependent on its temporal distribution (i.e. its variation with time). For this reason a set of statistical indices have been developed.

6. There are four main statistical indices in use in the UK:

L_{A90} The sound level (in dBA) exceeded for 90% of the time. This unit gives an indication of the sound level during the quieter periods of time in any given sample. It is used to describe the “background noise level” of an area.

L_{AeqT} The equivalent continuous sound level over a period of time, T. this unit may be described as “the notional steady noise level that would provide, over a period, the same energy as the varying noise in question”. In other words, the energy average level. This unit is now used to measure a wide variety of different types of noise of an industrial or commercial nature, as well as road traffic, aircraft and trains.

L_{A10} The sound level (in dBA) exceeded for 10% of the time. This level gives an indication of the sound level during the noisier periods of time in any given sample. It has been used over many years to measure and assess road traffic noise.

L_{AMAX}	The maximum level of sound, i.e. the peak level of sound measured in any given period. This unit is used to measure and assess transient noises, i.e. gun shots, individual vehicles, etc.

Third International Meeting on Wind Turbine Noise
Aalborg, Denmark 17 – 19 June 2009

A Comparison of Background Noise Levels Collected at the Portland Wind Energy Project in Victoria, Australia

Christophe Delaire (Marshall Day Acoustics)
Daniel Walsh (Pacific Hydro)

ABSTRACT

The New Zealand Standard 6808:1998 *Acoustics - The assessment and measurement of sound from wind turbine generators* (the "New Zealand Standard") is currently used in the State of Victoria, Australia to assess noise emissions from wind farms.

The New Zealand Standard requires that background noise monitoring be undertaken at the nearest affected residential properties before the wind farm is operational. The measured background noise levels are then correlated with wind speed data collected on site to determine noise limits.

Once the wind farm is operational, ambient noise levels must be measured at the same location as was used for background noise monitoring. The background noise levels are then subtracted from the measured ambient noise levels to determine the derived "wind farm only" noise levels.

In practice, background and ambient noise levels are usually measured a few years apart.

For their approved Portland Wind Energy Project (PWEP), developers Pacific Hydro carried out the required background noise monitoring at nearby residential properties for a minimum 10 day period during 2004/2005 before submitting their planning application. In addition, they have carried out further background noise monitoring campaigns at the same residential properties during 2005 to 2008, in order to collect a more comprehensive dataset and determine whether seasonal variations significantly affect the noise impact assessment.

This paper presents a comparison of background noise levels measured at the PWEP together with the respective wind roses. It discusses changes in background noise levels and the impact of those changes on the noise impact assessment.

1. INTRODUCTION

As part of their planning permit application for the development of the Portland Wind Energy Project (PWEP) in Victoria, Australia, developers Pacific Hydro have undertaken background noise monitoring at selected properties in the vicinity of the proposed site between 2004 and 2005. In addition to this monitoring, they have repeated background noise monitoring at the same properties between 2005 and 2008 in order to collect a more comprehensive dataset and determine whether seasonal variations significantly affect the noise impact assessment.

The results of this extensive background noise monitoring campaign have been analysed and are presented in this paper.

2. SITE DESCRIPTION

The PWEP is located in south western Victoria and comprises the following four projects:

- Yambuk (PWEP I)
- Cape Bridgewater (PWEP II)
- Cape Nelson South (PWEP III)
- Cape Nelson North and Cape Sir William Grant (PWEP IV)

Yambuk (PWEP I) has not been included in this study as background noise monitoring was only undertaken once at properties in the vicinity of this site, for the noise impact assessment.

The Cape Bridgewater wind farm can be considered to comprise two sites. With the two sites also considered for PWEP IV, a total of five sites, across 3 wind farms, are considered in this paper. These sites are presented in Figure 1.

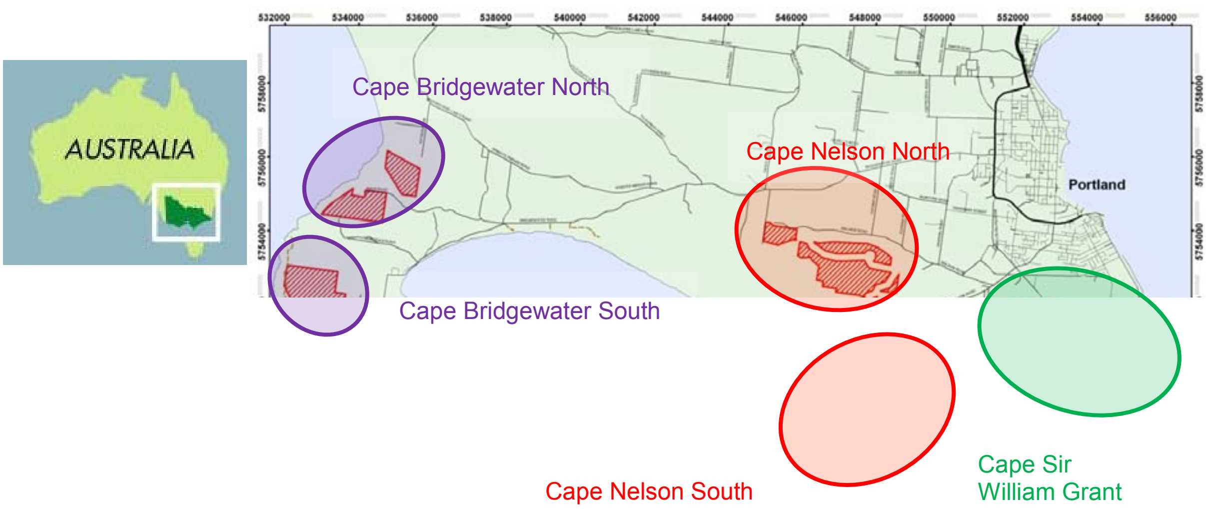

Figure 1 – Study sites location

The Cape Bridgewater wind farm covers a significant proportion of Cape Bridgewater along its western side. It comprises **Cape Bridgewater North (CBN)** and **Cape Bridgewater South (CBS)**. The coastal escarpment on the west is 30 to 40m above sea level, and away from it the area features a gently undulating landscape. The north area offers a slightly more complex topography than the south area. Most native vegetation has been cleared from this site and there is predominantly introduced vegetation, mainly in the form of grazing pasture.

The **Cape Nelson South (CNS)** wind farm is located in a coastal headland surrounded by coastal cliffs and escarpments which rise between 40 to 70m above sea level. The cape itself undulates slightly, generally rising up to Picnic Hill in the centre at 110m, and from this point the landform slopes downwards undulating gradually inland to the north east at an average height of 70-80m before dropping down to around 30m closer to Portland. In general, the area has a reasonably undulating pastoral landscape character. Although predominantly open, the pastoral setting supports scattered, stands of low remnant vegetation. The western coastal edge and southern section of the Cape have a dense cover of low remnant vegetation.

The **Cape Nelson North (CNN)** site is situated 2 km to the east of Portland northwards of Cape Nelson and approximately 3 km inland. Generally the site shows strong undulating character and is dominated by low sand dunes which forming irregular ridges. The average elevation above sea level is 65m. The site is divided along the south-western direction from the beach zone by a massive dune system with elevation up to 110m above sea level.

The **Cape Sir William Grant (CSWG)** site is located approximately 3 km to the south of Portland and shows generally coastal landscape character. The area consists of the cape itself and some narrow sections along the coastline which are delimited to the seaside by partially steep escarpments. The top of the cape is predominantly flat and features large cleared areas. From the edge of the cape the landform rises very gradually inland towards the north, containing of undulating and swampy areas before descending back down to the township of Portland. The easterly part of the site is dominated by the infrastructure of the Portland Aluminium Smelter which is situated between Portland and Cape Sir William Grant. Significant re-vegetation has occurred around the smelter in the past and has since given way to a dense cover of low coastal vegetation.

Dwellings located in the vicinity of the study sites along with the noise monitored locations are shown in the site plans of Appendix A.

3. THE NEW ZEALAND STANDARD

The New Zealand Standard 6808:1998 *Acoustics - The assessment and measurement of sound from wind turbine generators* (referred herein as “The New Zealand Standard”) is currently used in the State of Victoria to assess noise emissions from wind farms.

Section 4.5 of the New Zealand Standard details recommended methodology for measurement of background noise levels at selected properties in the vicinity of a proposed wind farm site.

The New Zealand Standard recommends collecting 10 minute L_{A95} noise levels for a period of at least 10-14 days in order to give a suitable range of data (typically 1,400 data points). Furthermore, the data should be obtained for the wind speed range of 5-8m/s.

Concurrently, 10 minute averaged wind speeds should be measured on the wind farm site.

In Section 4.5.5, the New Zealand Standard requires that background noise measurements be correlated with wind speeds and that a regression curve is to be used to describe the average background noise level versus the wind speed.

Noise emissions from the proposed wind farm must comply with the background noise level plus 5dBA or 40dBA, whichever is the greater.

Background noise levels are therefore extremely important for the pre-construction noise assessment as different background noise levels will lead to different noise limits.

Furthermore, background noise levels are also subtracted for the post-construction noise levels to obtain a derived “wind farm only” noise level.

4. WIND DATA

Wind speed data used for this analysis has been measured using the wind monitoring masts (met masts) presented in Table 1.

Table 1

Met masts

Site	Met mast	10m AGL wind dataset	Period

CBN	CBN45	10m extrapolated from 30m	2005 - Feb 2007
	CBS70	10m extrapolated from 50m	Feb 2007 - 2008
CBS	CBS70	10m extrapolated from 50m	2005 - 2008
CNN	CNN50	*Climatronics* 10m measured	2004
	CNN70	10m extrapolated from 20m	2008
CNS	CNS50	*NRG* 10m measured	2004 - Apr 2007
	CNS50	10m extrapolated from 50m	Apr 2007 – Jun 2007
	CNS50	10m measured	Jun 2007 - 2008
CSWG	CSWG50	10m measured	2004 – 2008

All wind speed data has been measured with calibrated **Risø** anemometers unless otherwise indicated and has been referenced to 10m above ground level (AGL). When measured 10m AGL data was not available, wind speeds were extrapolated using the average roughness factor for the site.

For each of the monitoring periods, wind roses based on frequency and mean wind speed sector distributions are presented in Appendix B, while average and maximum wind speeds for each period are reported in Appendix C.

5. BACKGROUND NOISE LEVELS

Background noise monitoring was undertaken in accordance with the New Zealand Standard at selected properties in the vicinity of the PWEP between October 2004 and June 2008. The monitored properties together with the monitoring periods are presented in Appendix C.

Background noise levels and wind speeds have been correlated and a regression curve of 2^{nd} or 3^{rd} order has been fitted for each monitoring period. Furthermore, a regression curve has been fitted for the set of *all* data points for each house, which we shall refer to as the *all data regression curve*. Equations for the regression curves are presented in Appendix C together with the coefficients of determination (R^2) and the correlation coefficients.

The correlated data together with the regression curves are provided in Appendix B.

6. DATA ANALYSIS

Background noise levels in rural areas are dependent on many variables, such as:

- Wind generated noise through surrounding vegetation
- Wind generated noise around surrounding buildings
- Traffic noise
- Animal noise (dogs, cows, birds, insects, frogs, etc.)
- Farming activities
- Ocean noise

The influence of wind generated noise on background noise levels may depend on the following:

- Wind speed
- Wind direction
- Meteorological conditions
- Changes in surrounding buildings
- Changes in surrounding vegetation

Whilst the New Zealand Standard assumes the same background levels would be found whenever logging occurs, this may not always be the case.

Indeed, these factors can vary between monitoring periods, seasons and years, potentially affecting the resulting background noise levels. For this paper, we have limited our assessment to the influence of seasonal changes

6.1. Seasonal changes

At each property, the background noise level regression curves for each monitoring period have been compared to the all data regression curve. By considering seasonal variation in this way, it is implied that the all data regression curve is representative of the long term average background noise level. The results of the comparisons are presented in Appendix B.

Wind turbine sound power levels are commonly given for wind speeds between 6 and 10m/s, therefore it is for this range that noise limits and hence background noise levels are the most critical during pre-construction noise assessments.

In order to provide a summary of seasonal variations across all monitored properties, the difference between each seasonal noise level and the average noise level has been averaged over the wind speed range of 6 to 10m/s. The results are presented in Figure 2 below.

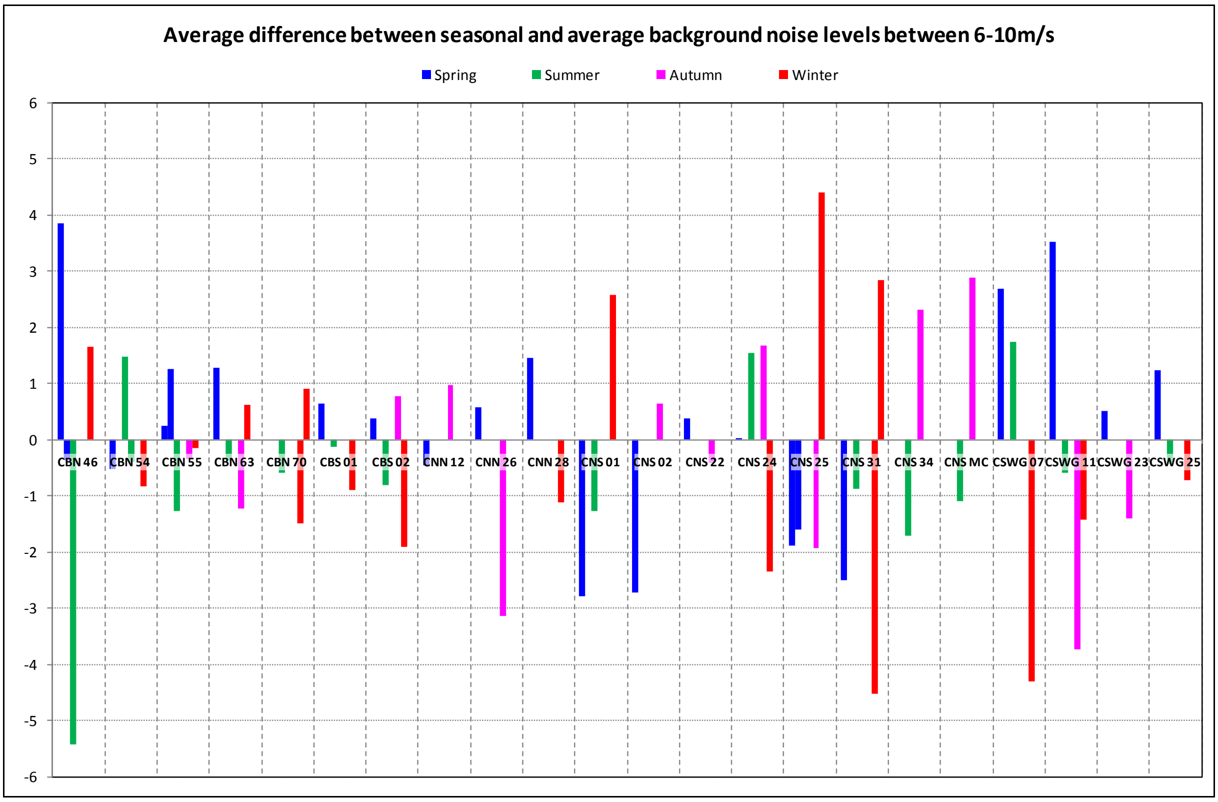

Figure 2 – Seasonal background noise levels comparison

It can be seen from Figure 2 that there no obvious trends in seasonal variations. For a given season, background noise levels are at times higher than the average background noise levels and at other times lower.

It can even be seen that the levels of the same season may be higher than the average background noise level during one year and lower during another. This is shown for the winter seasons at Houses CBN 70 and CNS 31.

In Figure 3, the average differences shown in Figure 2 are plotted as a time history.

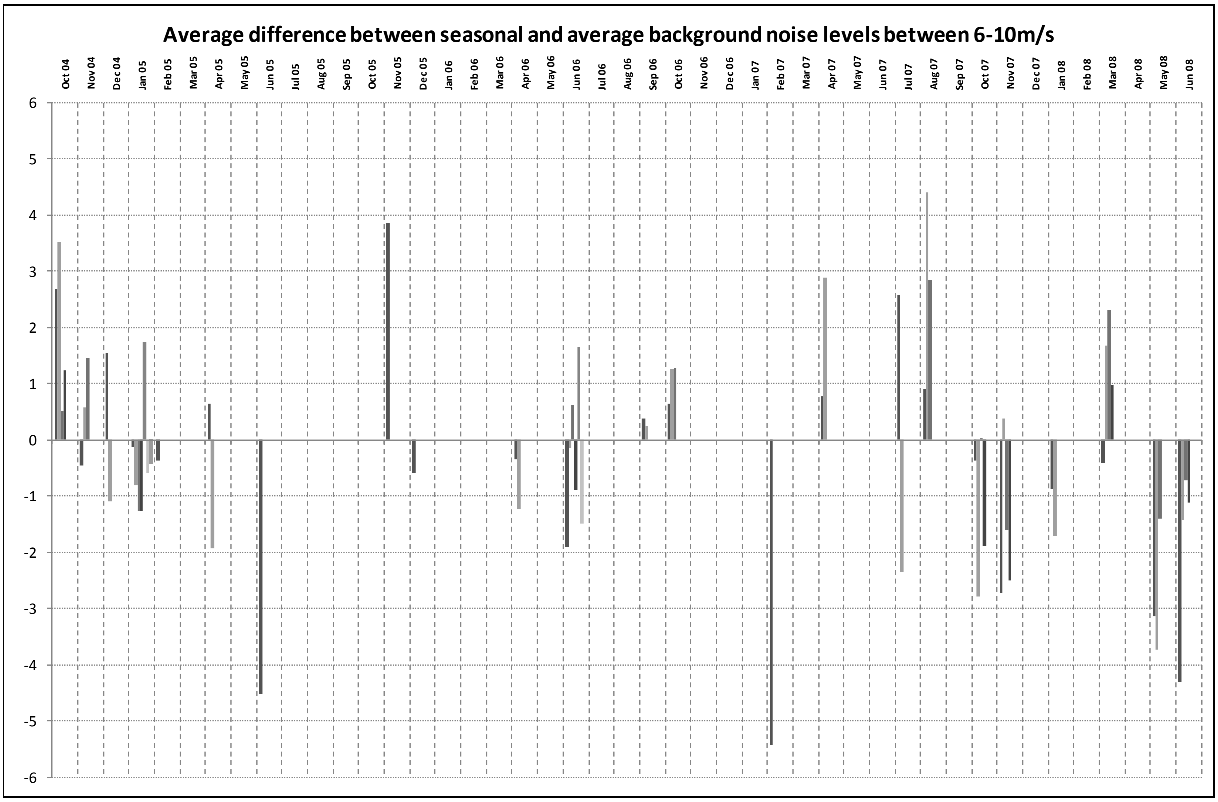

Figure 3 – Seasonal background noise levels comparison – time history

It can be seen from Figure 3 that certain survey periods consistently provide lower or higher seasonal background noise levels (ie: Oct 04, Oct 07, Nov 07, May 08 and June 08). However background noise levels measured during the same month can be higher than the average background noise levels one year (Oct 04) and lower during another (Oct 07).

Attempts have also been made to analyse the effect of wind direction, including consideration of vegetation near the noise monitor as the likely dominant noise source for each direction quadrant to explain the variations in background noise levels. This did not lead to any obvious trends for the houses analysed and therefore an extensive wind direction analysis of the data has not been carried out.

Panorama and aerial photos are only available for some periods and therefore such a detailed study across the sites is beyond scope of this study.

6.2. Wind speed distribution

During the seasonal changes analysis, background noise levels scatters at some houses presented interesting trends, when the wind speed range varied across the monitoring periods. Selected examples are presented in Figure 4 and 5.

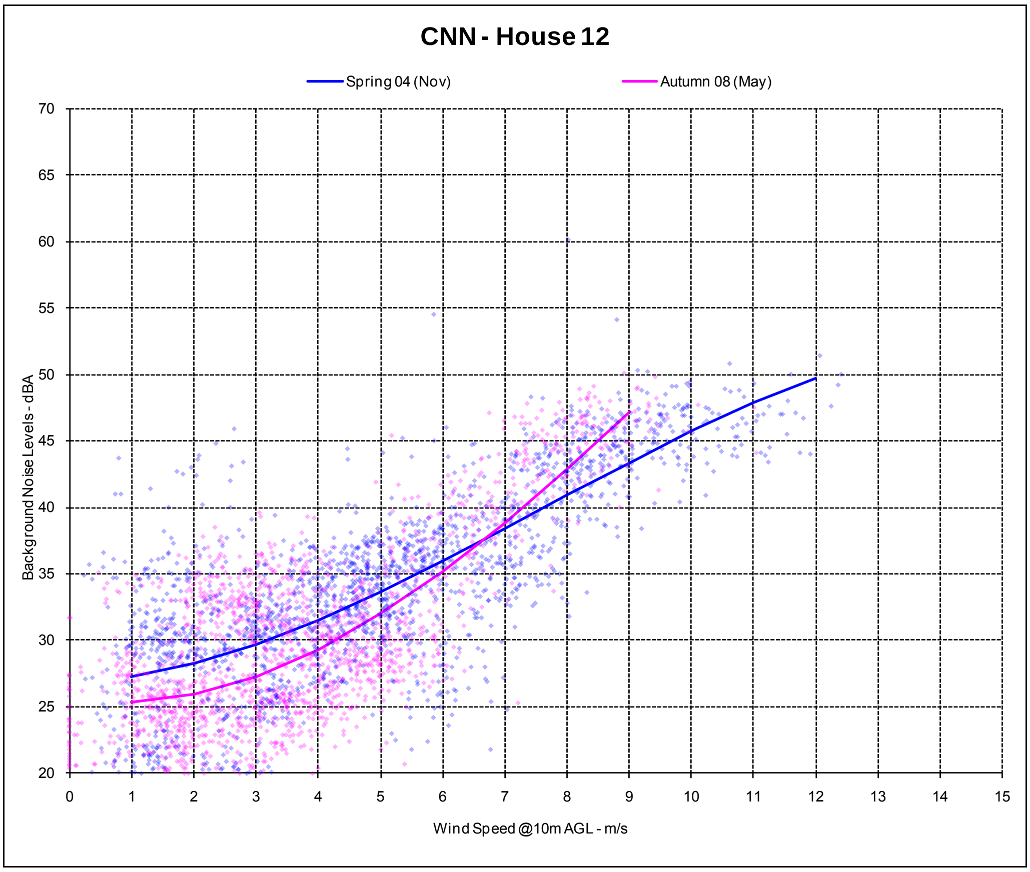

Figure 4 – Background noise levels at CNN 12

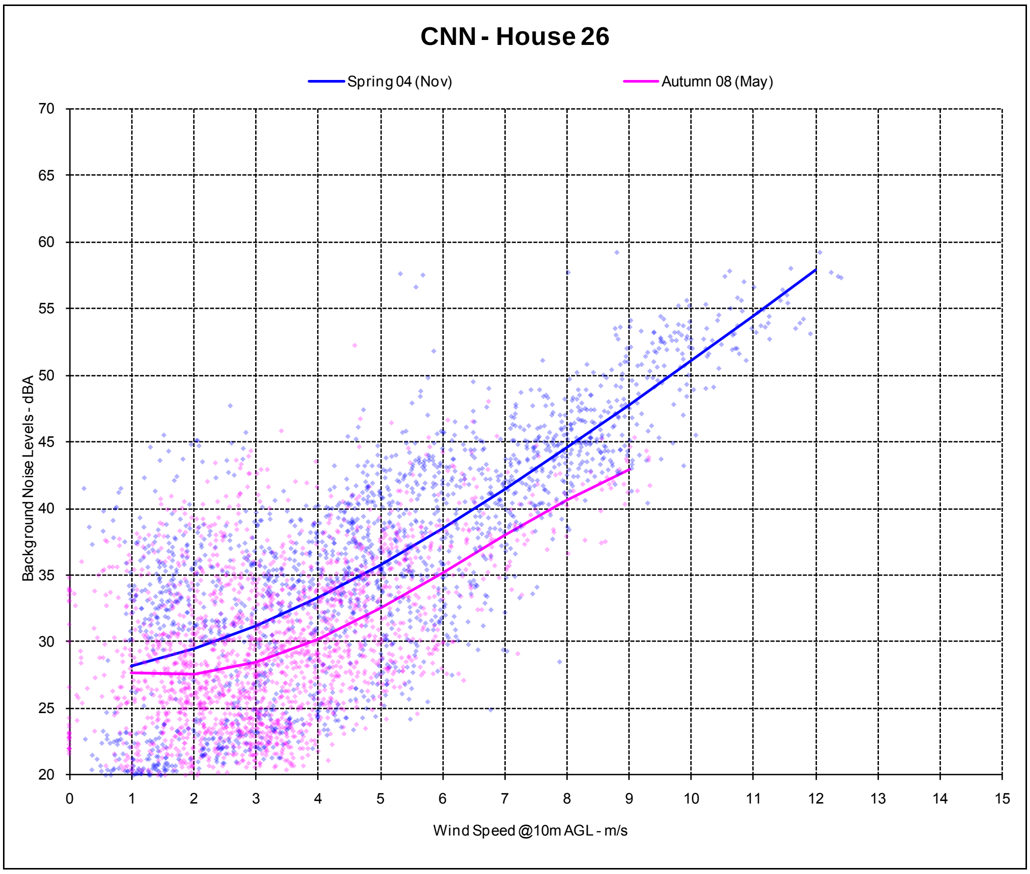

Figure 5 – Background noise levels at CNN 26

It can be seen from Figures 4 and 5 that wind speeds during the Spring 04 period exceeded 12m/s at both CNN 12 and CNN 26 whereas wind speeds during the Autumn 08 period rarely exceeded 9m/s. Both measurements complied with the wind speed range requirement of the New Zealand Standard (5-8m/s).

It can be seen that background noise level scatters below 9m/s are fairly similar during each period for both houses. However, in each case, a lack of data points above 9m/s during the Autumn 08 period leads to a very different regression curve of best fit compared to the Spring 04 regression curve.

Considering that wind farm noise emissions are usually predicted between 6 and 10m/s, the shape of the regression curve of best fit within this range is most critical as it can change the noise limit significantly. For example, in the case of CNN 12, monitoring during Autumn 08 would have lead to a noise limit at 9m/s 5dBA higher than the actual noise limit, which was derived from the Spring 04 data.

Based on these observed trends, to obtain a representative background noise level regression curve for the critical wind speed range of 6-10m/s, we recommend that a significant amount of data be collected both above and below this wind speed range. For example, to obtain a representative background noise level curve at the higher wind speeds of 9-10m/s, it may be necessary to obtain monitoring data up to at least 12m/s, with a suitable number of data points (say 30) at each of the 11 and 12m/s wind speed bins.

7. UNCERTAINTIES

Whilst remaining mainly within the requirements of the New Zealand Standard, the analysis employs a number of uncertainties. These are presented below.

7.1. Wind data

Uncertainties linked to the wind data are as follows:

- measured 10m wind speed data is highly affected by terrain and roughness, in some sites this has a more significant impact than others
- data extrapolated to 10m height, using an average site roughness factor (and not time series)
- for some dwellings the met mast used and anemometer level was not consistent throughout seasons
- met masts may not be in the most appropriate location for all dwellings
- instrument mounting arrangements have not been consistent for all monitoring masts

7.2. Noise data

Uncertainties linked to the noise data are as follows:

- some minor changes to logger locations (from A to B locations) throughout seasons (as shown in the Site Plans and Summary Parameters) , namely at;
  - CBS – House2
  - CNS – House 31
  - CNS – MC
  - CNN – House 28
  - CSWG – House 11
  - CSWG – House 23
  - CSWG – House 25

- data points potentially affected by rain were removed using rainfall data provided by the nearest Bureau of Meteorology weather stations located at Portland and Cape Nelson
- whilst rain affected measurements were removed, measured background noise levels were also influenced by non wind related sources, mostly at lower wind speeds

7.3. Correlations

Uncertainties linked to correlation between background noise levels and wind speeds are as follows:

- datasets with correlation coefficients inferior to 0.4 were not included in this study
- a visual assessment of the shape of the data scatter was performed to choose between using 3rd or 2nd order regressions
- use of the all data regression curve as representative of the long-term average background noise level
- outlier data points have not been removed from the analysis

8. FURTHER WORK

This paper mainly focuses on seasonal variations in background noise levels. However we recognise that this extensive amount of data could be further analysed.

For example:

- Further assessment on effect of wind speed distribution
- Determination of background data collection guidelines

- is there a “real” background noise dataset?
- should we aim to collect as much data as possible, or to capture representative conditions (long term wind speed and direction distributions of site) or ‘worst case’ conditions?

- Statistical regression guidelines
  - what distribution of wind speeds should be included in the regression curve analysis
  - what order regression should be used?
- Suitability of using representative data from proximate dwellings
- Detailed study of the effect of vegetation and wind direction

Acknowledgments

We would like to thank Pacific Hydro for releasing the background noise and wind speed data and Daniel Griffin for his very valuable contribution.

APPENDIX A

SITE PLANS

532000
533000
534000
535000
536000
5757000
5756000
5755000
5754000
5753000
5752000
KITTSON RD
AMOS RD
PEACOCKS RD
BLOWHOLES RD
CBN45
CBN70
63
70
55
56
54
46
B
A
2
1
DRAFT
N
Dwellings
Noise Logger Locations
Monitoring Mast
Site Boundary
10m Contours
Cadastral Boundaries
Roads
PROJECT
PWEP II: Cape Bridgewater, Australia
TITLE
Noise Logger & Dwelling Locations
CREATED BY
M.Barnett
DATUM
MGA 94
DATE
04/05/09
CLEARANCE BY
D.Walsh
SCALE
1:25,000
DRAWING NO
PH-0236
REV
A
APPROVED BY
PacificHydro

- Dwellings
- Noise Loggers
- Monitoring Mast
- Site Boundary
- 10m Contours
- Cadastral Boundaries
- Roads

PROJECT PWEP III, Australia			
TITLE Noise Logger & Dwelling Locations			
CREATED BY M.Barnett	DATUM MGA 94	DATE 04/05/09	
CLEARANCE BY D.Walsh	SCALE 1:25,000	DRAWING NO PH-0238	REV A
APPROVED BY	PacificHydro	Level 11, 474 Flinders Street, Melbourne Victoria 3000 Australia Telephone +61 3 8621 6000 Facsimile +61 3 8621 6111 www.pacifichydro.com.au	

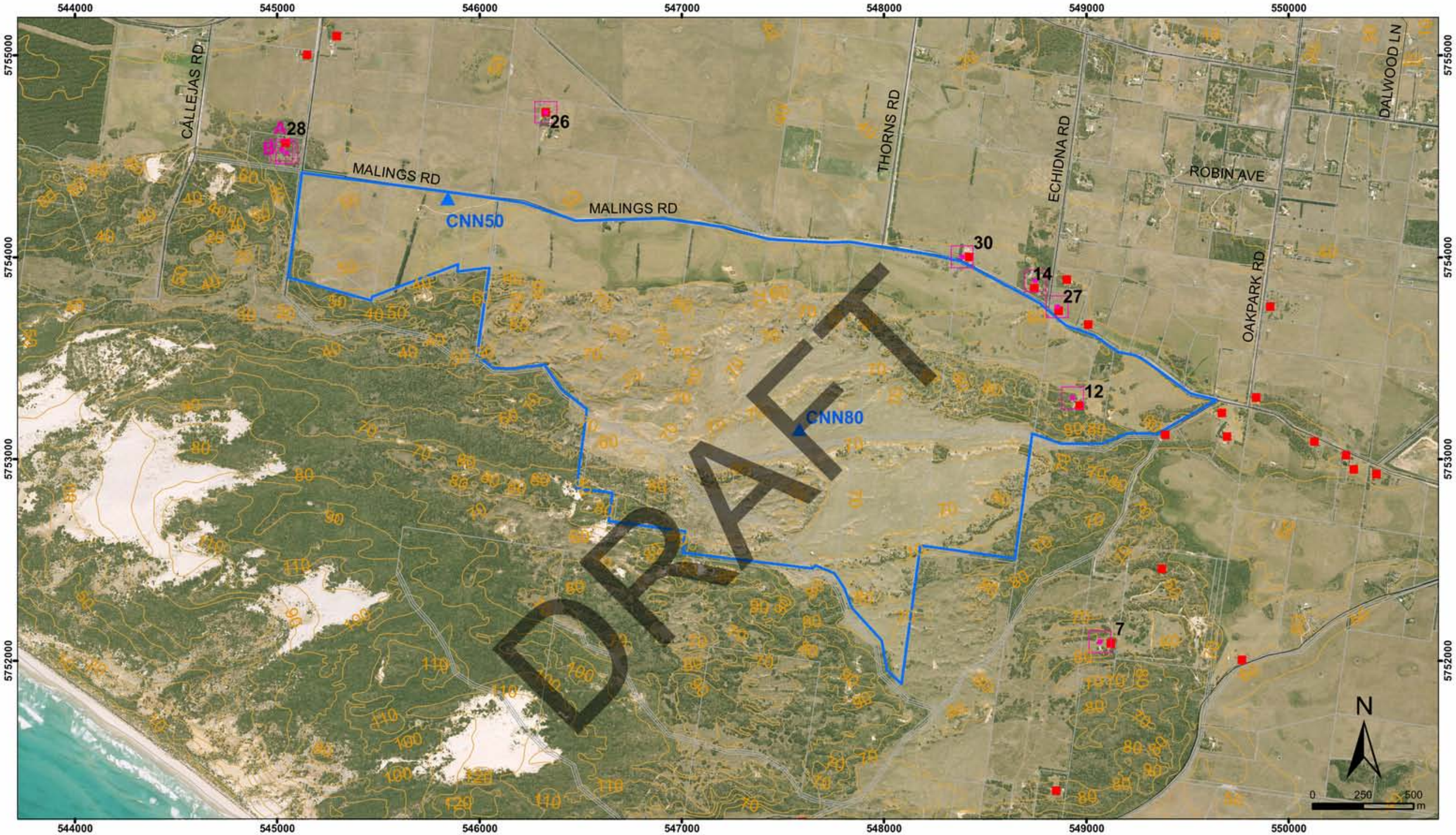

■	Dwellings
▣	Noise Logger
▲	Monitoring Mast
▭	Site Boundary
—	10m Contours
—	Cadastral boundaries
—	Roads

PROJECT			
PWEP IV, Cape Nelson North			
TITLE: Noise Logger & Dwelling Locations			
CREATED BY: M.Barnett	DATUM: MGA 94	DATE: 04/05/09	
CLEARANCE BY: D.Walsh	SCALE: 1:25,000	DRAWING NO: PH-0237	REV: A
APPROVED BY	PacificHydro	Level 11, 474 Flinders Street, Melbourne Victoria 3000 Australia Telephone +61 3 8621 6000 Facsimile +61 3 8621 6111 www.pacifichydro.com.au	


DRAFT
PROJECT
PWEP IV, Cape Sir William Grant
TITLE
Noise Logger & Dwelling Locations
CREATED BY
M.Barnett
DATUM
MGA 94
DATE
04/05/09
CLEARANCE BY
D.Walsh
SCALE
1: 25,000
DRAWING NO
PH-0239
REV
A
APPROVED BY
PacificHydro
Dwellings
Noise Logger
Monitoring Mast
Site Boundary
10m Contours
Cadastral Boundaries
Roads
N
0 250 500 m
CSWG50
CSWG70
GREAT SOUTH WEST WALK
AMITY RD
BARKLY ST
REBECCA RD
DERRIL RD
WELLINGTON RD
MADEIRA PACKET RD
QUARRY RD
THISTLE RD
TECOMA RD
OLERIA RD
MALINGS RD
CAPE NELSON RD
SHEOKE RD
11
23
25
7
5753000
5752000
5751000
5750000
550000
551000
552000
553000
554000
555000
556000

APPENDIX B

SEASONAL BACKGROUND NOISE LEVELS

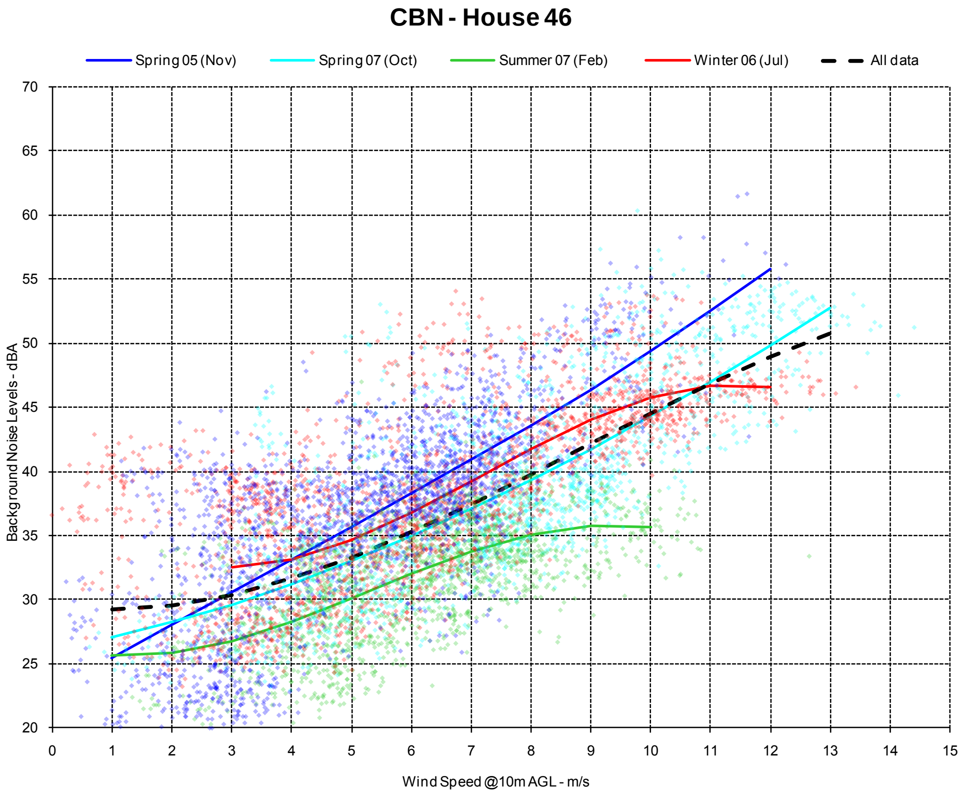

CBN - House 46
Spring 05 (Nov)
Spring 07 (Oct)
Summer 07 (Feb)
Winter 06 (Jul)
All data
Background Noise Levels - dBA
Wind Speed @10m AGL - m/s

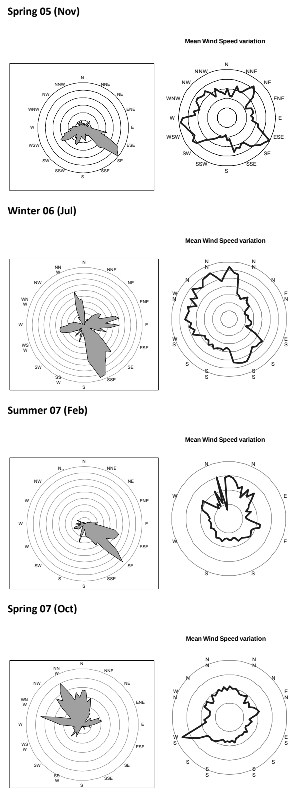

Spring 05 (Nov)
Mean Wind Speed variation
Winter 06 (Jul)
Mean Wind Speed variation
Summer 07 (Feb)
Mean Wind Speed variation
Spring 07 (Oct)
Mean Wind Speed variation

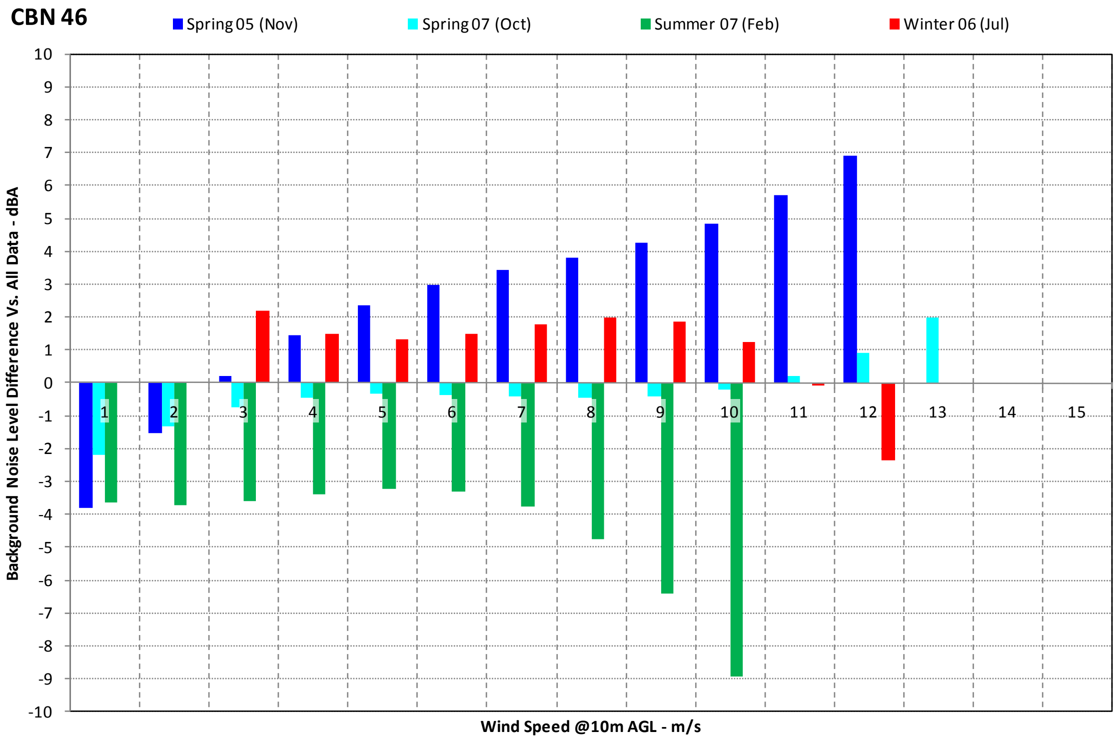

CBN 46
Spring 05 (Nov)
Spring 07 (Oct)
Summer 07 (Feb)
Winter 06 (Jul)
Background Noise Level Difference Vs. All Data - dBA
Wind Speed @10m AGL - m/s

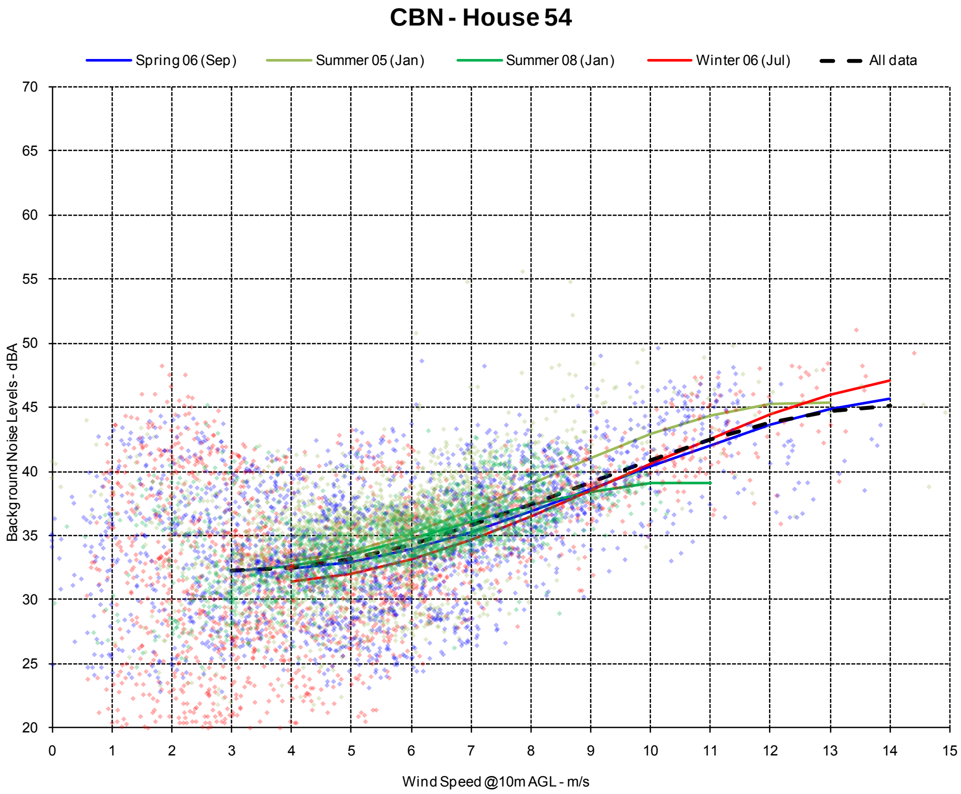
CBN - House 54
Spring 06 (Sep)
Summer 05 (Jan)
Summer 08 (Jan)
Winter 06 (Jul)
All data
Background Noise Levels - dBA
Wind Speed @10m AGL - m/s
70
65
60
55
50
45
40
35
30
25
20
0 1 2 3 4 5 6 7 8 9 10 11 12 13 14 15

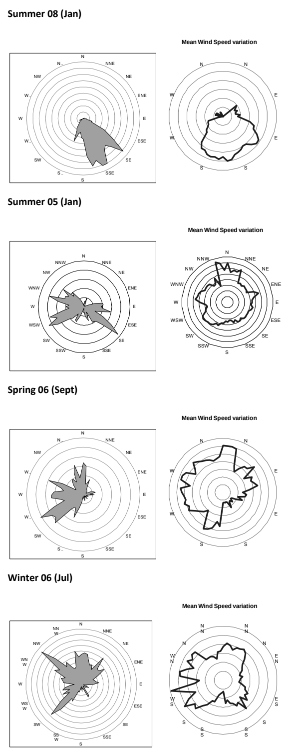
Summer 08 (Jan)
Mean Wind Speed variation
Summer 05 (Jan)
Mean Wind Speed variation
Spring 06 (Sept)
Mean Wind Speed variation
Winter 06 (Jul)
Mean Wind Speed variation

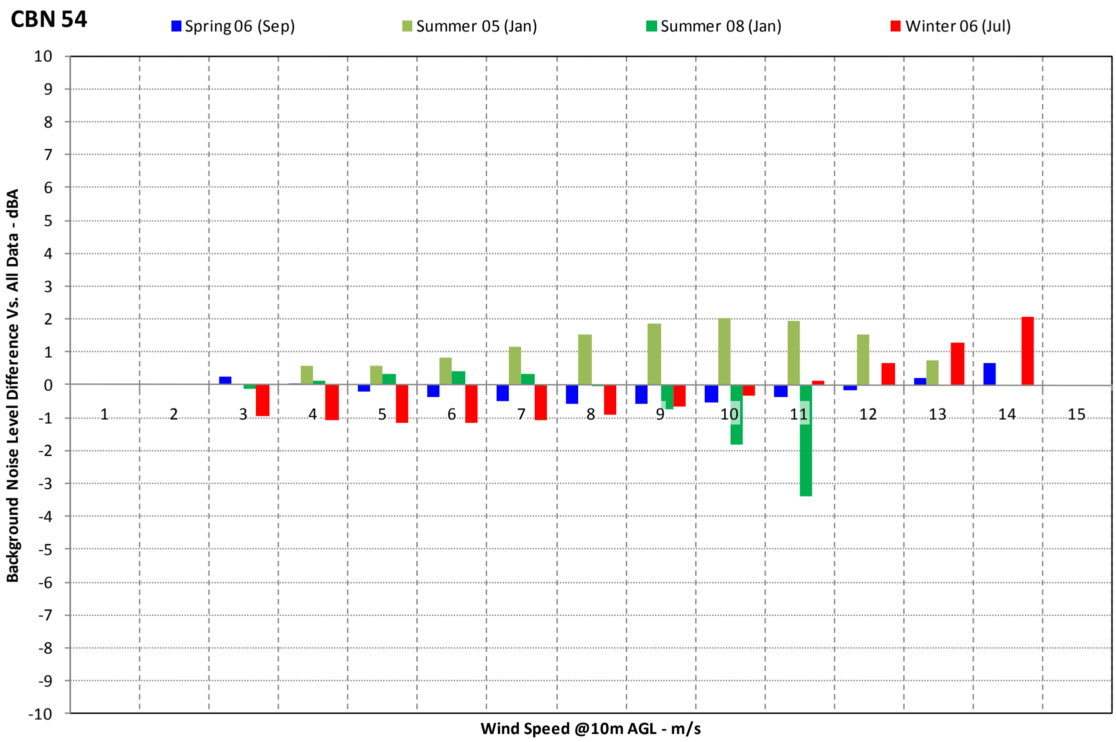
CBN 54
Spring 06 (Sep)
Summer 05 (Jan)
Summer 08 (Jan)
Winter 06 (Jul)
Background Noise Level Difference Vs. All Data - dBA
Wind Speed @10m AGL - m/s
10
9
8
7
6
5
4
3
2
1
0
-1
-2
-3
-4
-5
-6
-7
-8
-9
-10
1 2 3 4 5 6 7 8 9 10 11 12 13 14 15

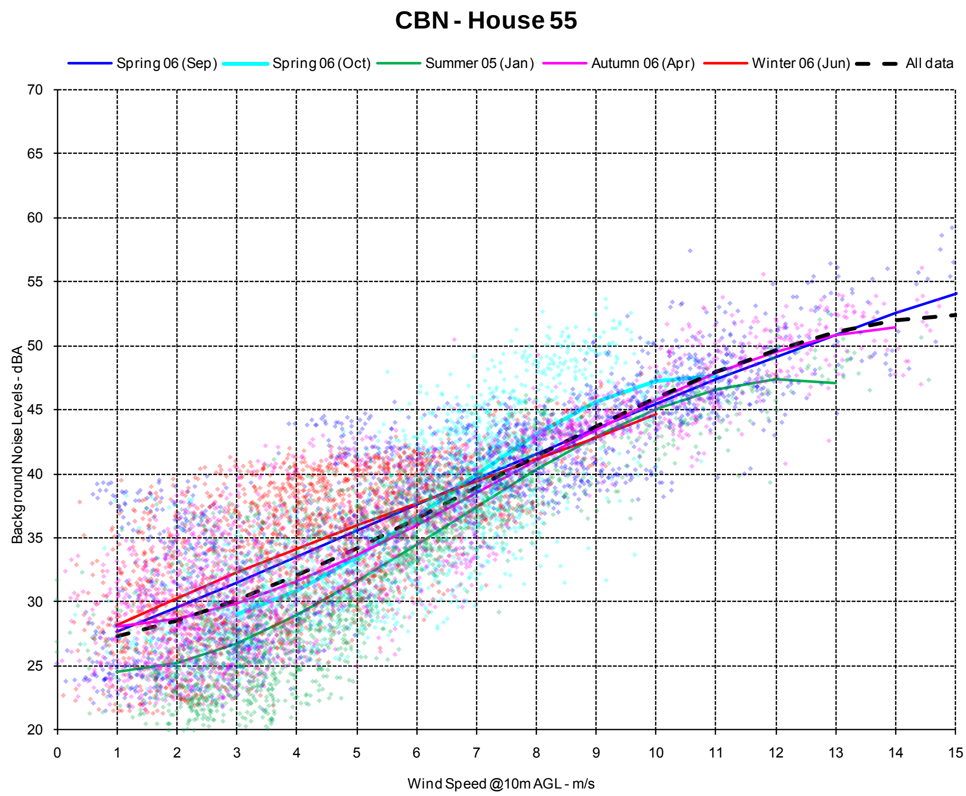

Spring 06 (Sept)

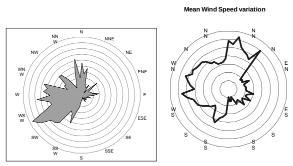

Spring 06 (Oct)

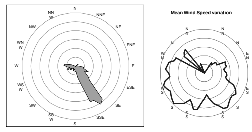

Autumn 06 (Apr)

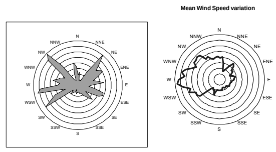

Summer 05 (Jan)

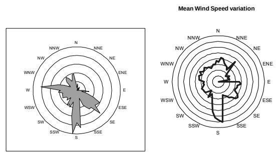

Winter 06 (Jun)

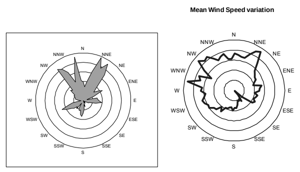

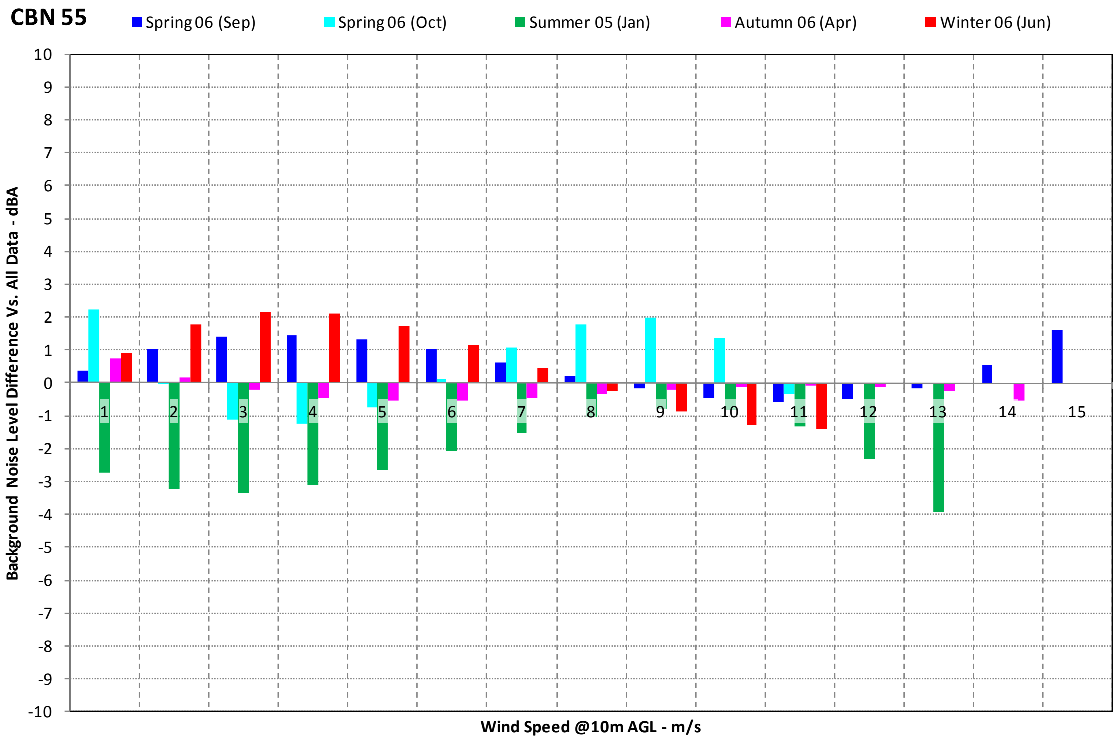

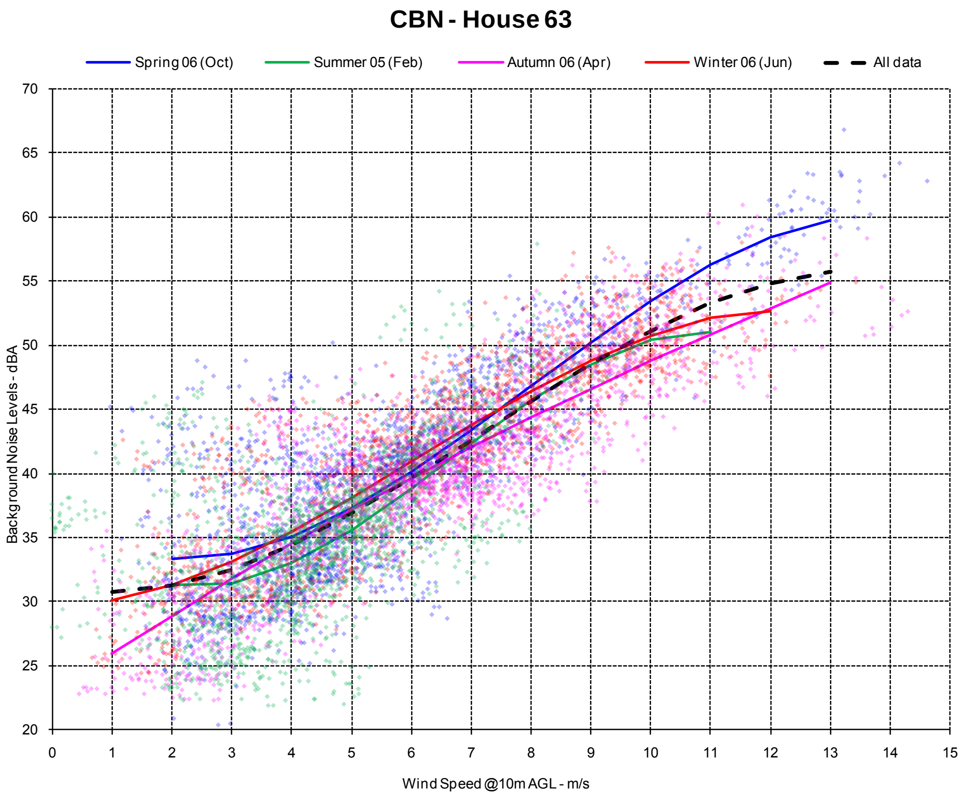
CBN - House 63
Spring 06 (Oct)
Summer 05 (Feb)
Autumn 06 (Apr)
Winter 06 (Jun)
All data
Background Noise Levels - dBA
Wind Speed @10m AGL - m/s

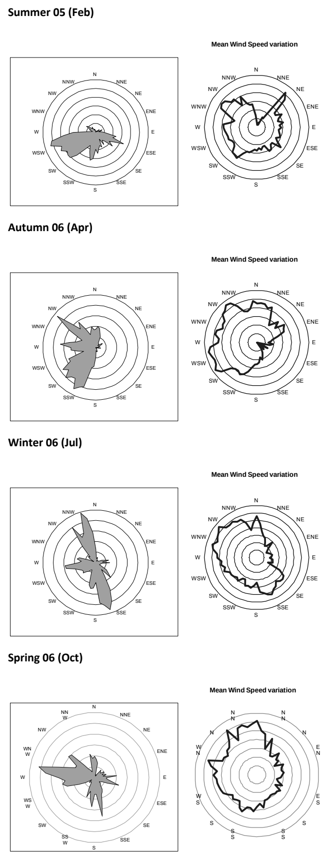
Summer 05 (Feb)
Mean Wind Speed variation
Autumn 06 (Apr)
Mean Wind Speed variation
Winter 06 (Jul)
Mean Wind Speed variation
Spring 06 (Oct)
Mean Wind Speed variation

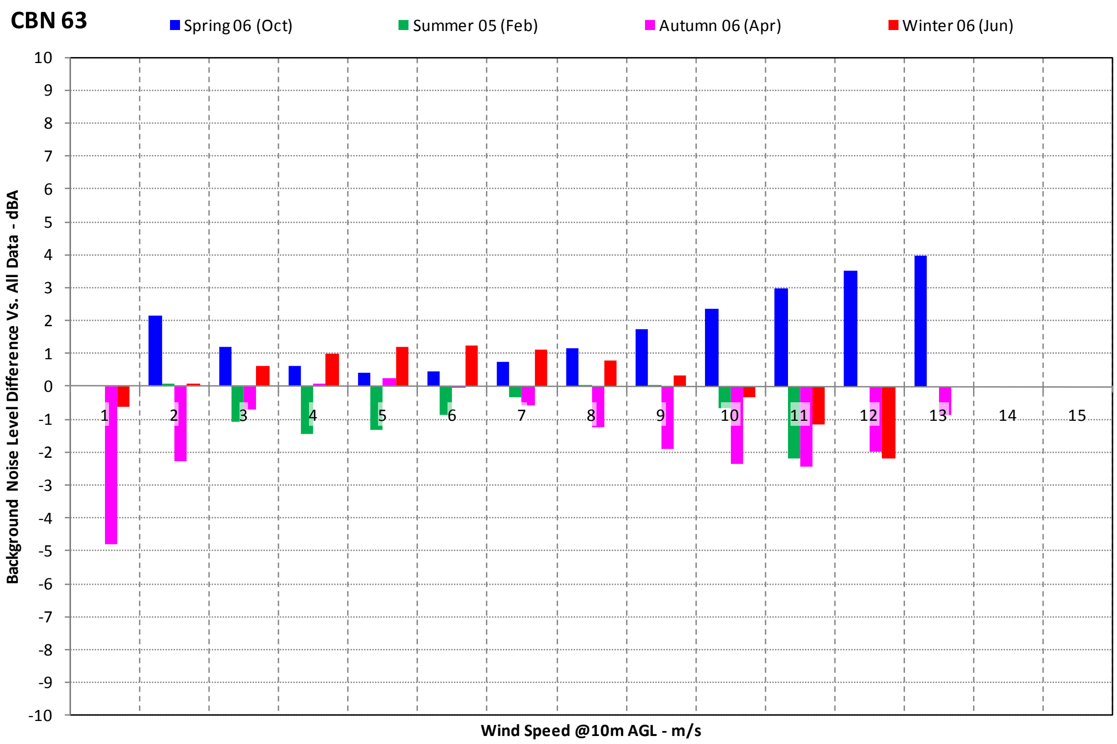
CBN 63
Spring 06 (Oct)
Summer 05 (Feb)
Autumn 06 (Apr)
Winter 06 (Jun)
Background Noise Level Difference Vs. All Data - dBA
Wind Speed @10m AGL - m/s

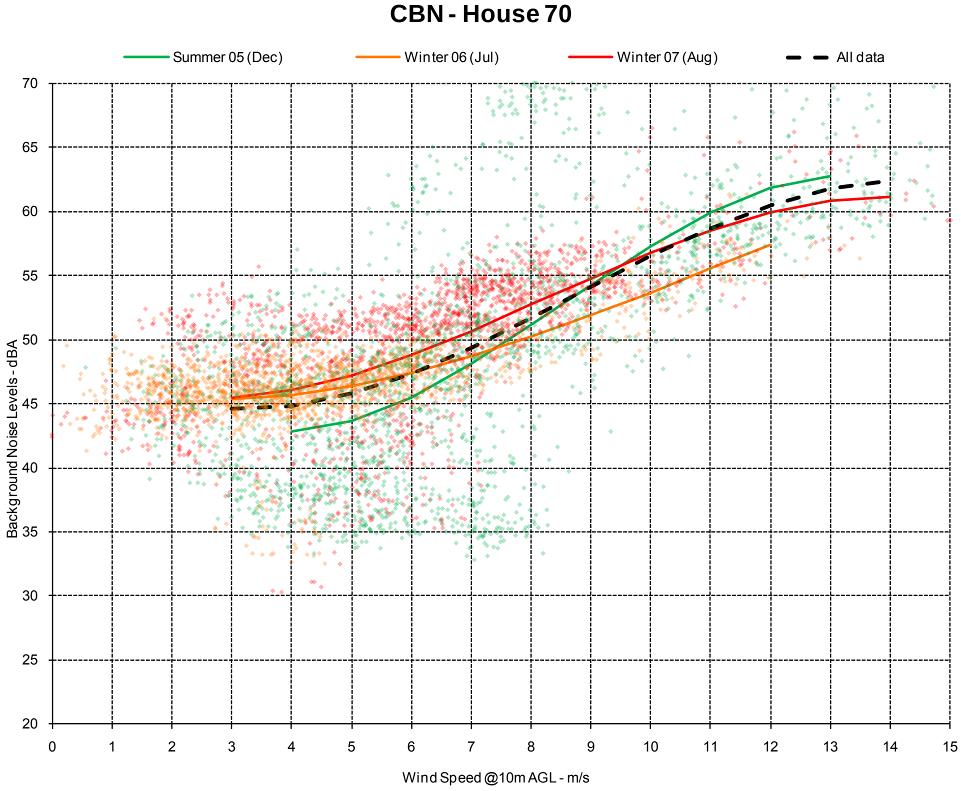

Summer 05 (Dec)

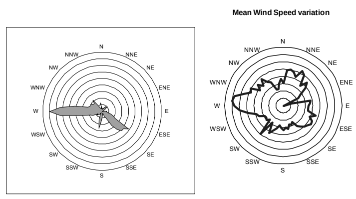

Winter 06 (Jul)

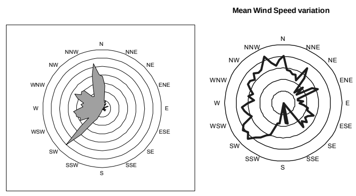

Winter 07 (Aug)

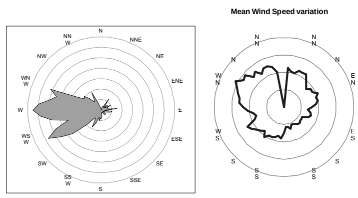

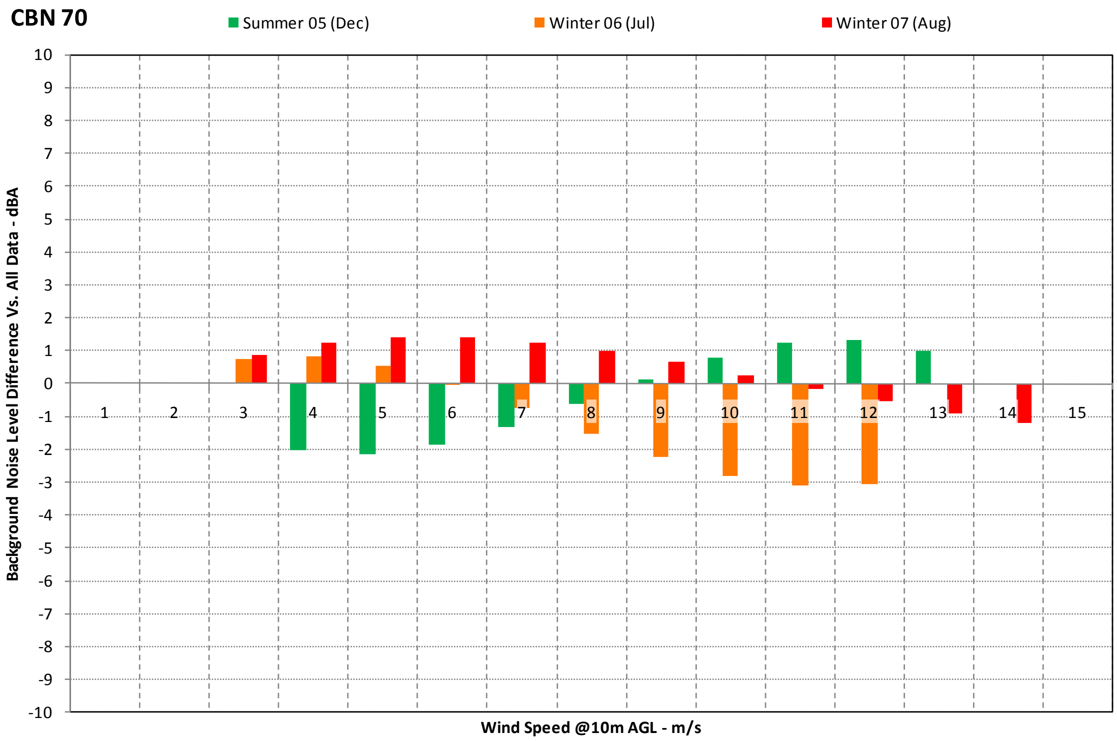

CBS - House 1

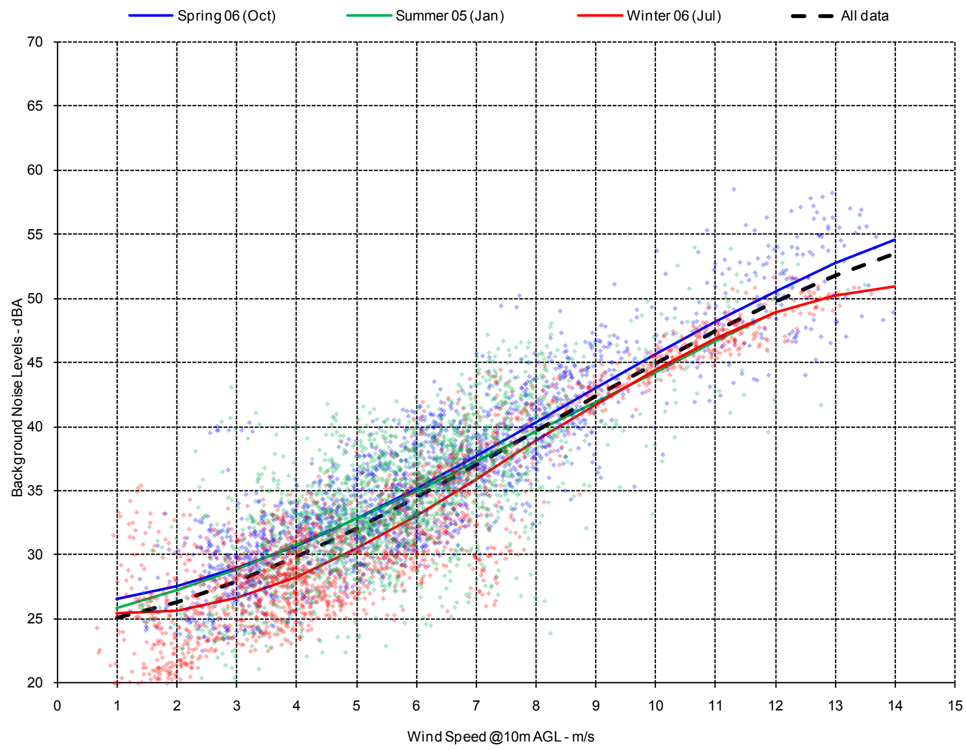

Spring 06 (Oct)

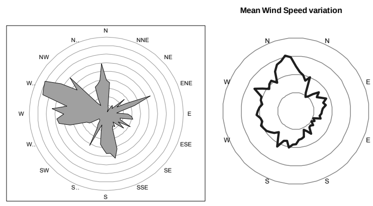

Summer 05 (Jan)

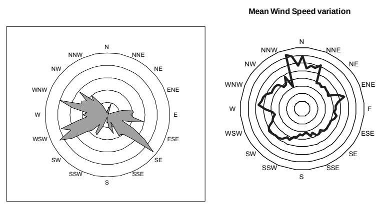

Winter 06 (Jul)

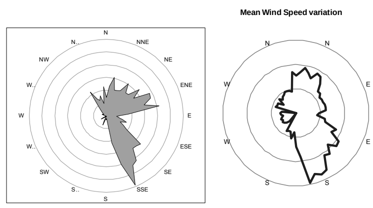

CBS 01

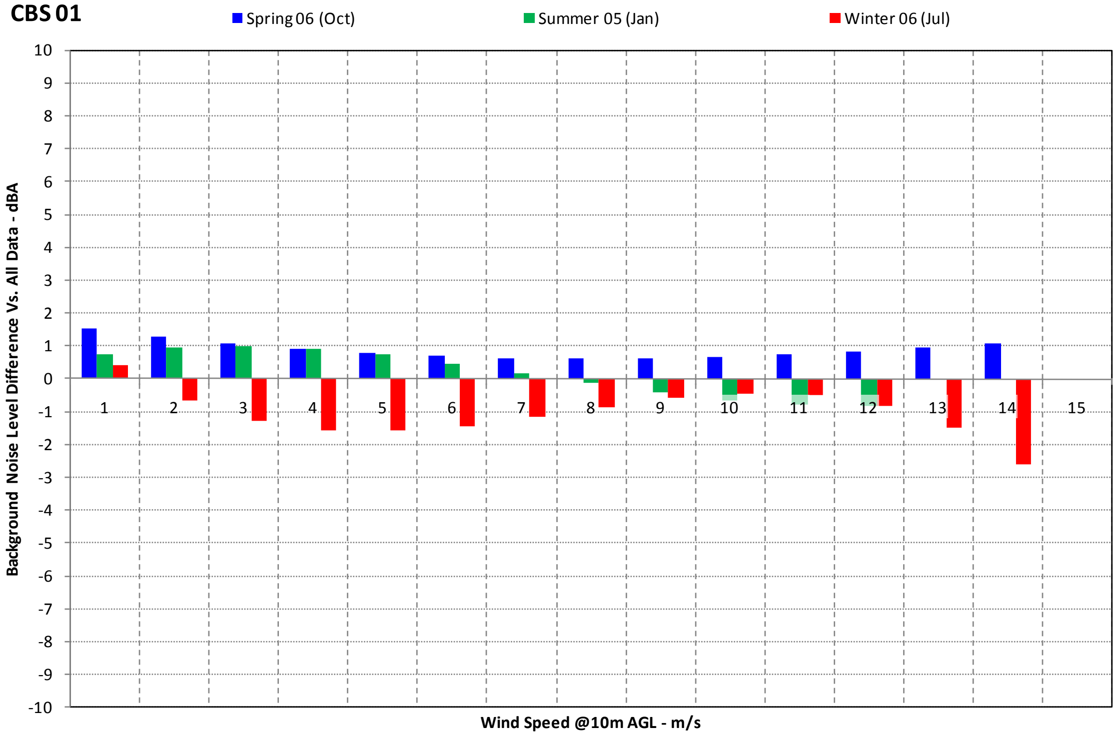

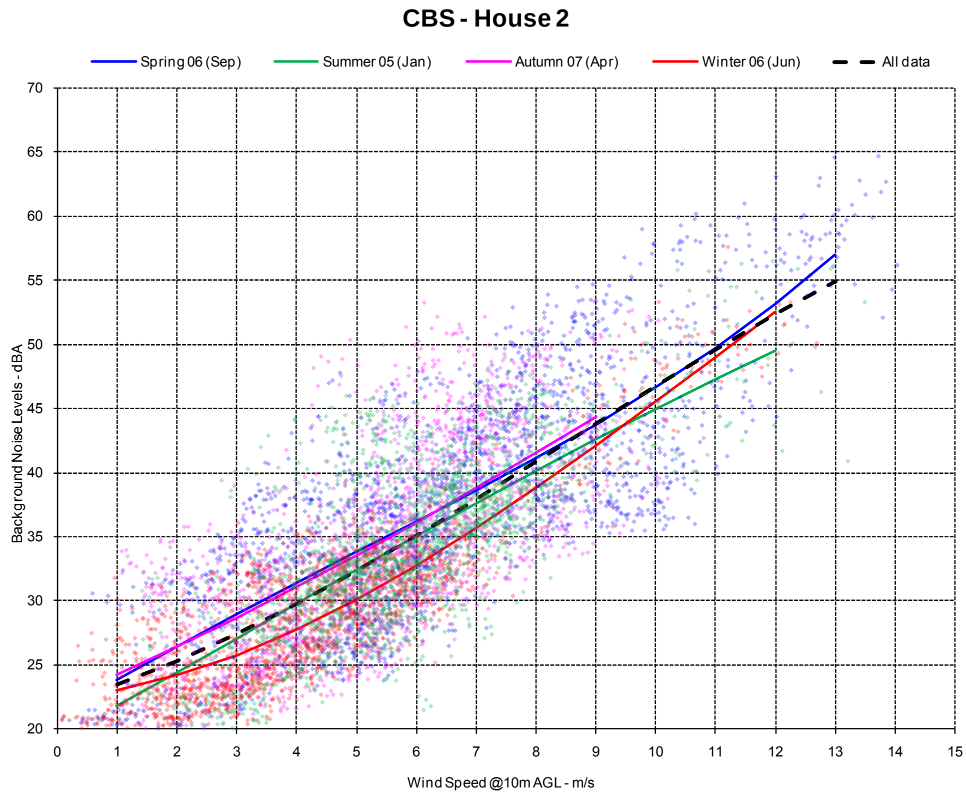

Spring 06 (Sep)

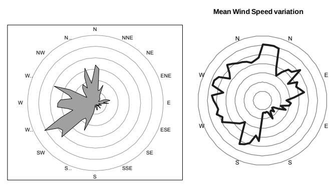

Summer 05 (Jan)

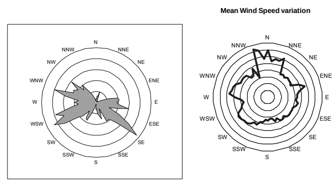

Autumn 07 (Apr)

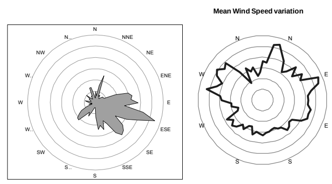

Winter 06 (Jun)

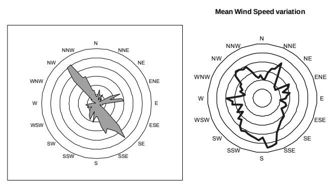

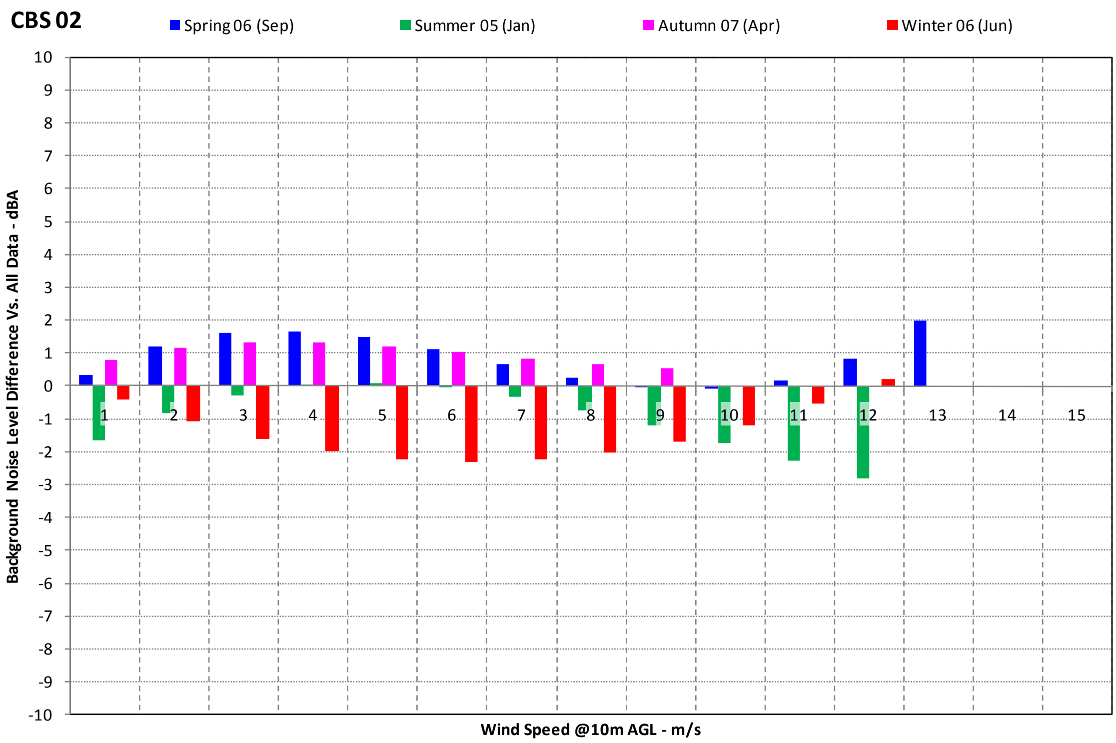

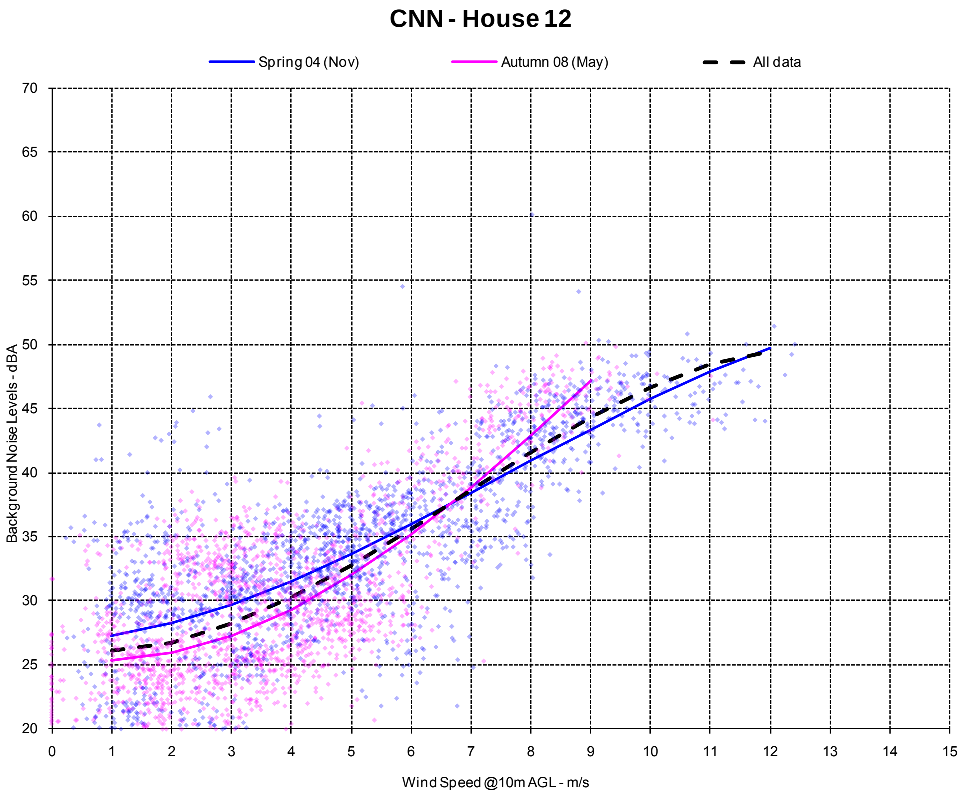
CNN - House 12
Spring 04 (Nov)
Autumn 08 (May)
All data
Background Noise Levels - dBA
Wind Speed @10m AGL - m/s
70
65
60
55
50
45
40
35
30
25
20
0 1 2 3 4 5 6 7 8 9 10 11 12 13 14 15

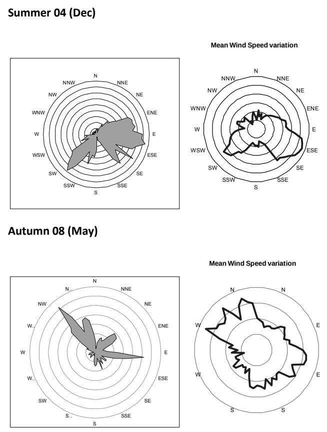
Summer 04 (Dec)
Mean Wind Speed variation
Autumn 08 (May)
Mean Wind Speed variation

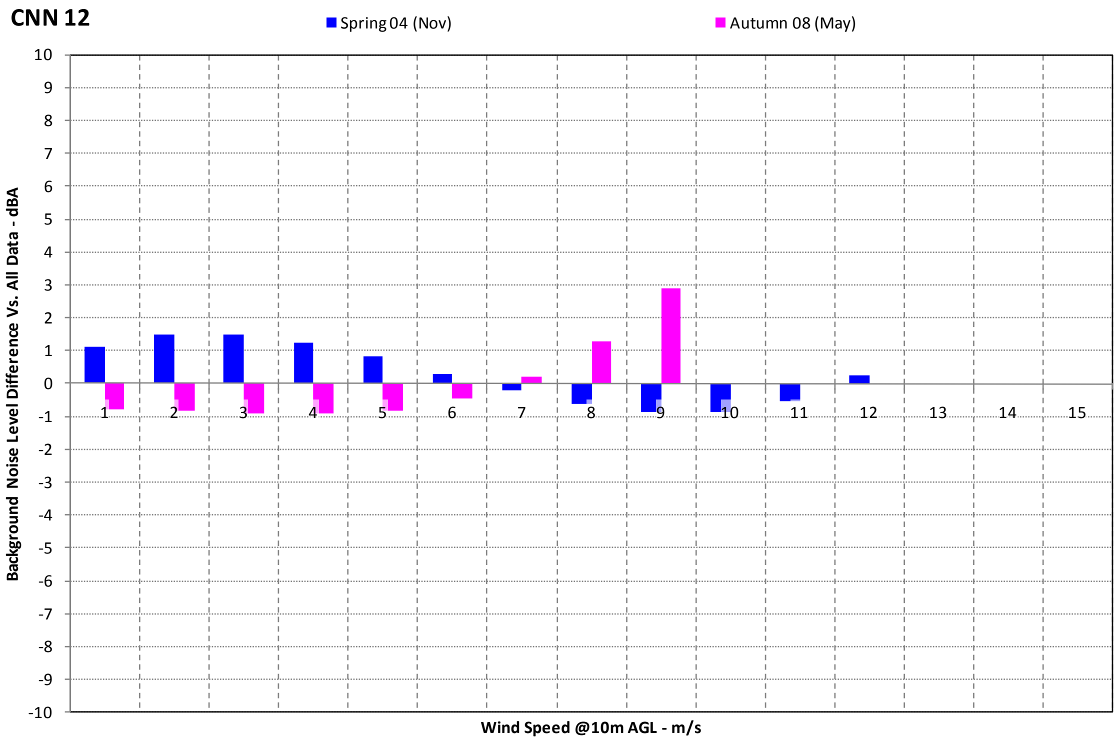
CNN 12
Spring 04 (Nov)
Autumn 08 (May)
Background Noise Level Difference Vs. All Data - dBA
Wind Speed @10m AGL - m/s
10
9
8
7
6
5
4
3
2
1
0
-1
-2
-3
-4
-5
-6
-7
-8
-9
-10
1 2 3 4 5 6 7 8 9 10 11 12 13 14 15

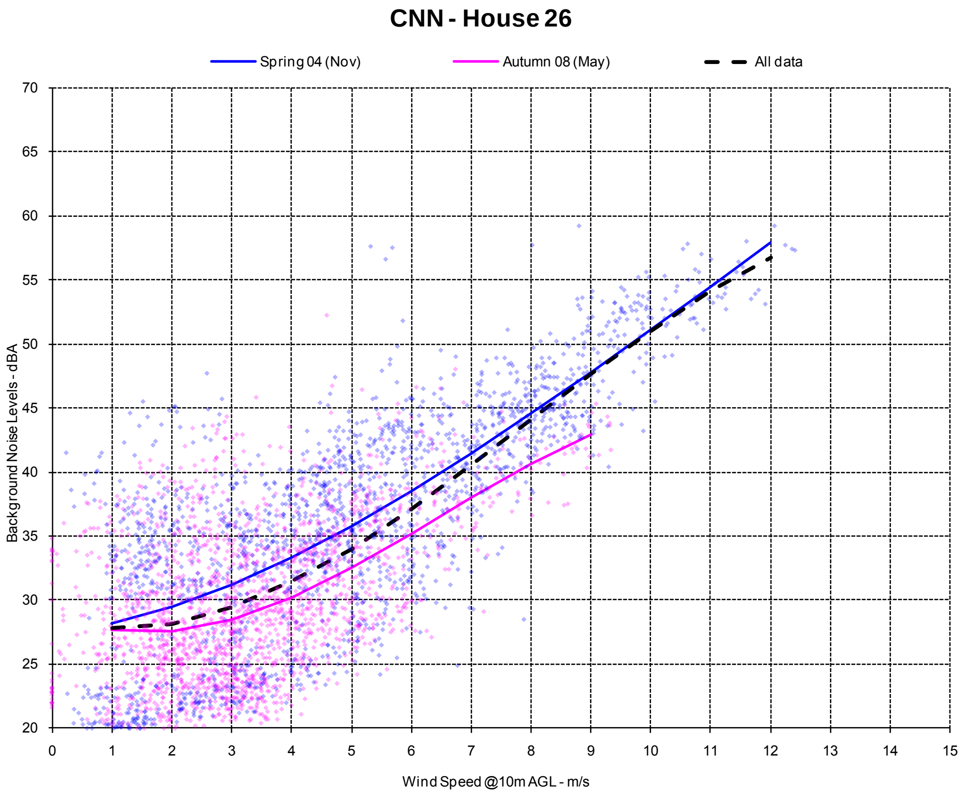
CNN - House 26
Spring 04 (Nov)
Autumn 08 (May)
All data
Background Noise Levels - dBA
Wind Speed @10m AGL - m/s

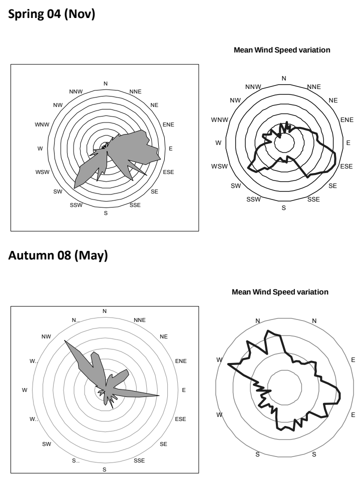
Spring 04 (Nov)
Mean Wind Speed variation
Autumn 08 (May)
Mean Wind Speed variation

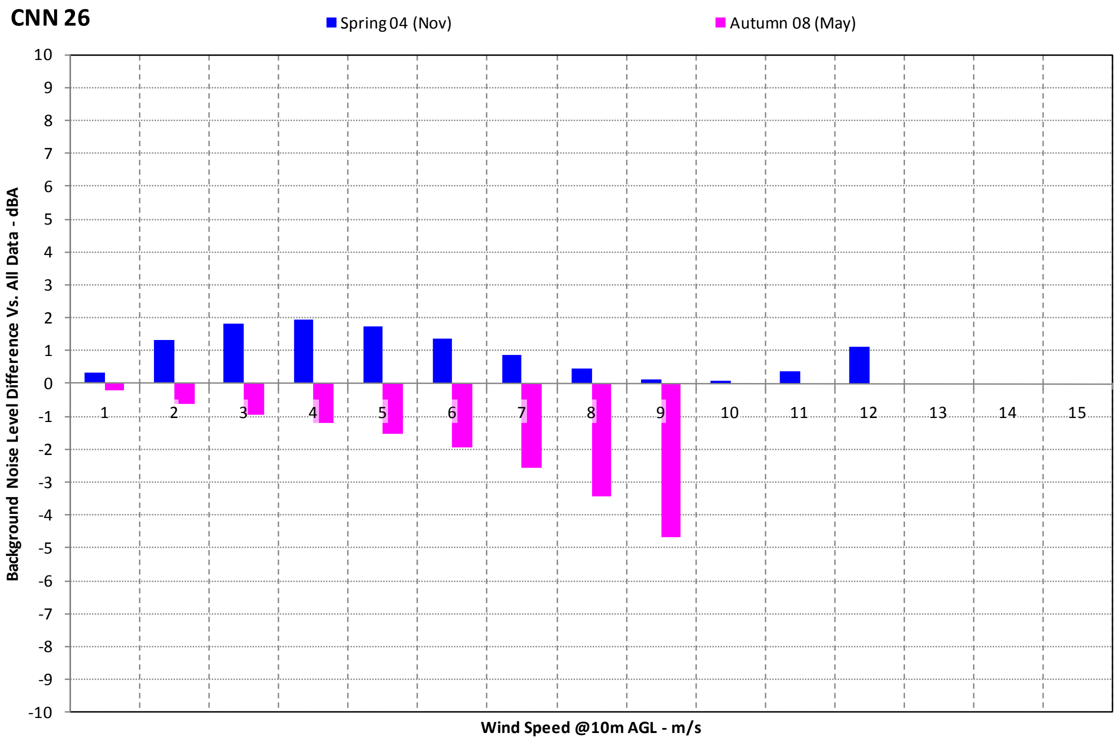
CNN 26
Spring 04 (Nov)
Autumn 08 (May)
Background Noise Level Difference Vs. All Data - dBA
Wind Speed @10m AGL - m/s

CNN - House 28

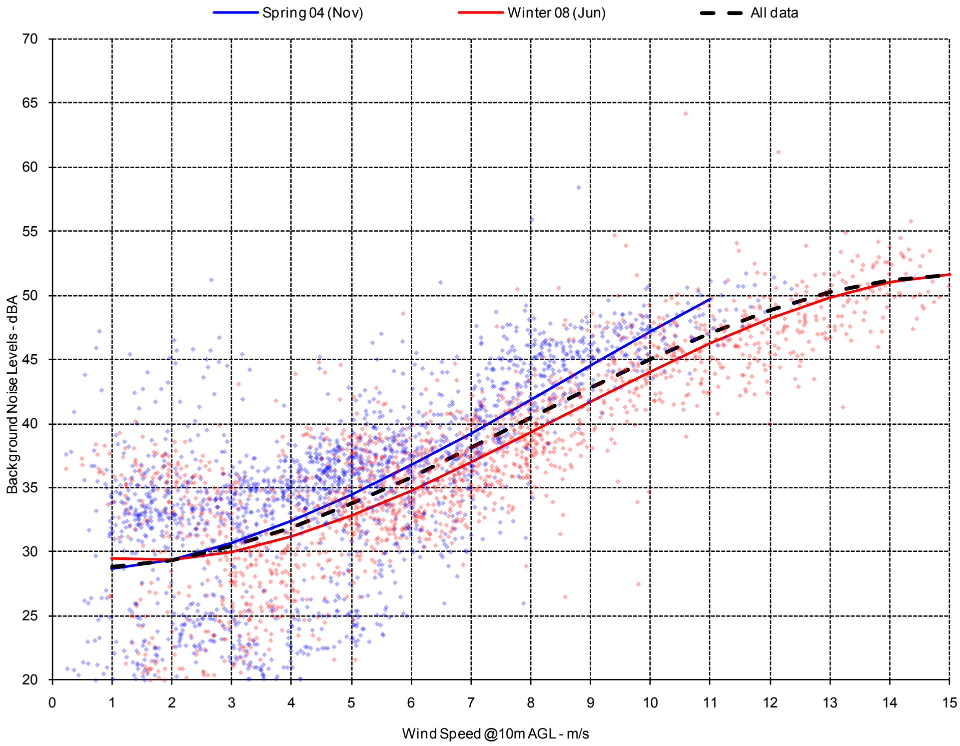

Spring 04 (Nov)

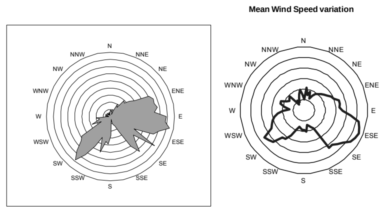

Winter 08 (Jun)

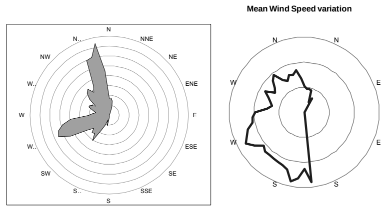

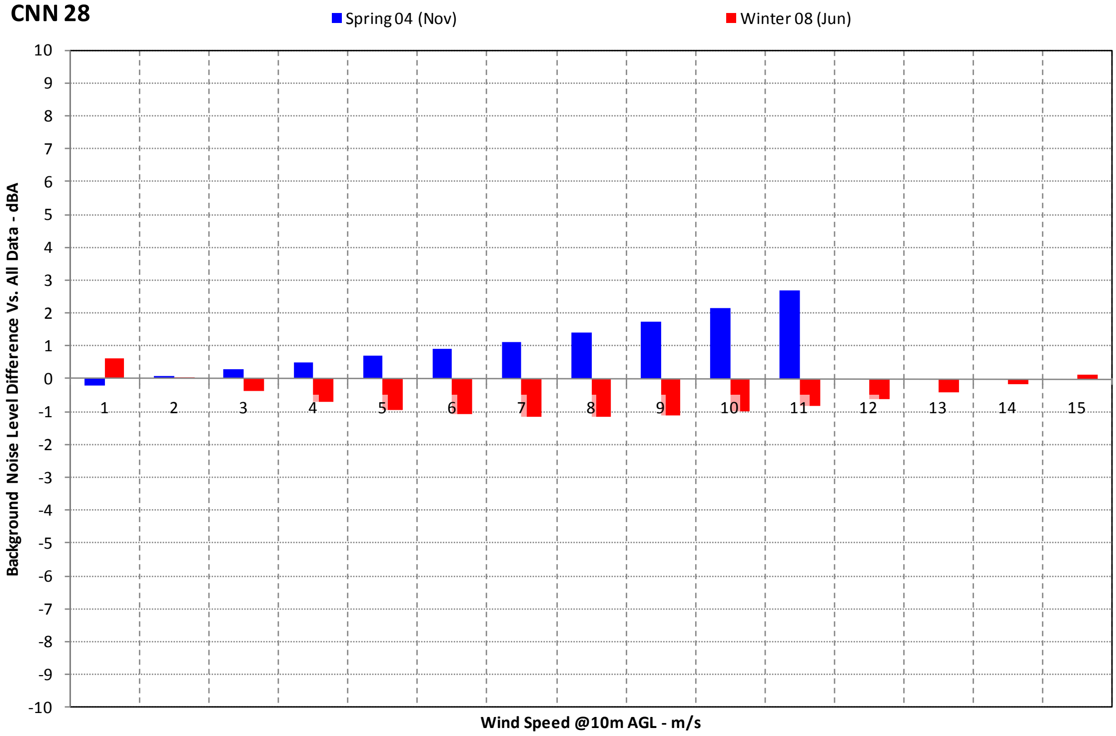

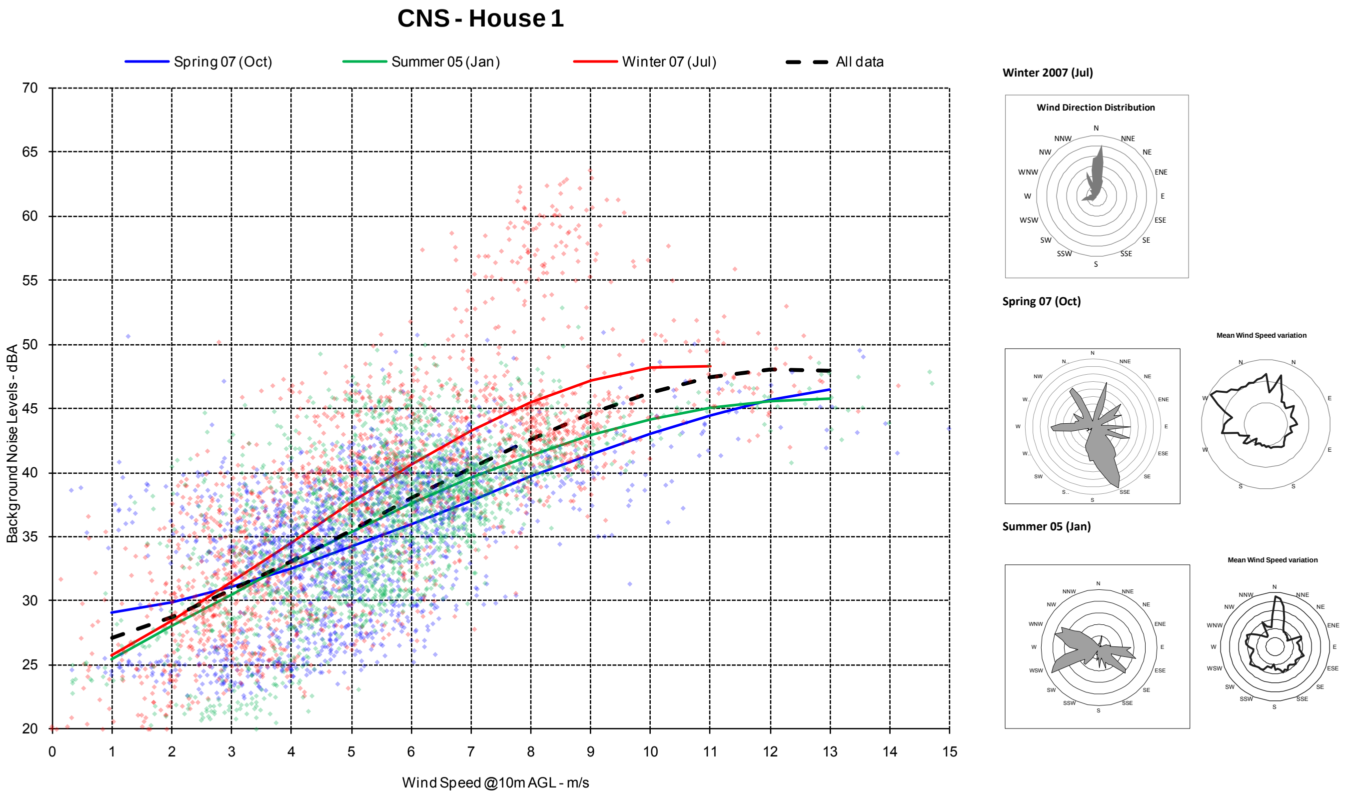
CNS - House 1
Spring 07 (Oct)
Summer 05 (Jan)
Winter 07 (Jul)
All data
Background Noise Levels - dBA
Wind Speed @10m AGL - m/s
Winter 2007 (Jul)
Wind Direction Distribution
Spring 07 (Oct)
Mean Wind Speed variation
Summer 05 (Jan)
Mean Wind Speed variation

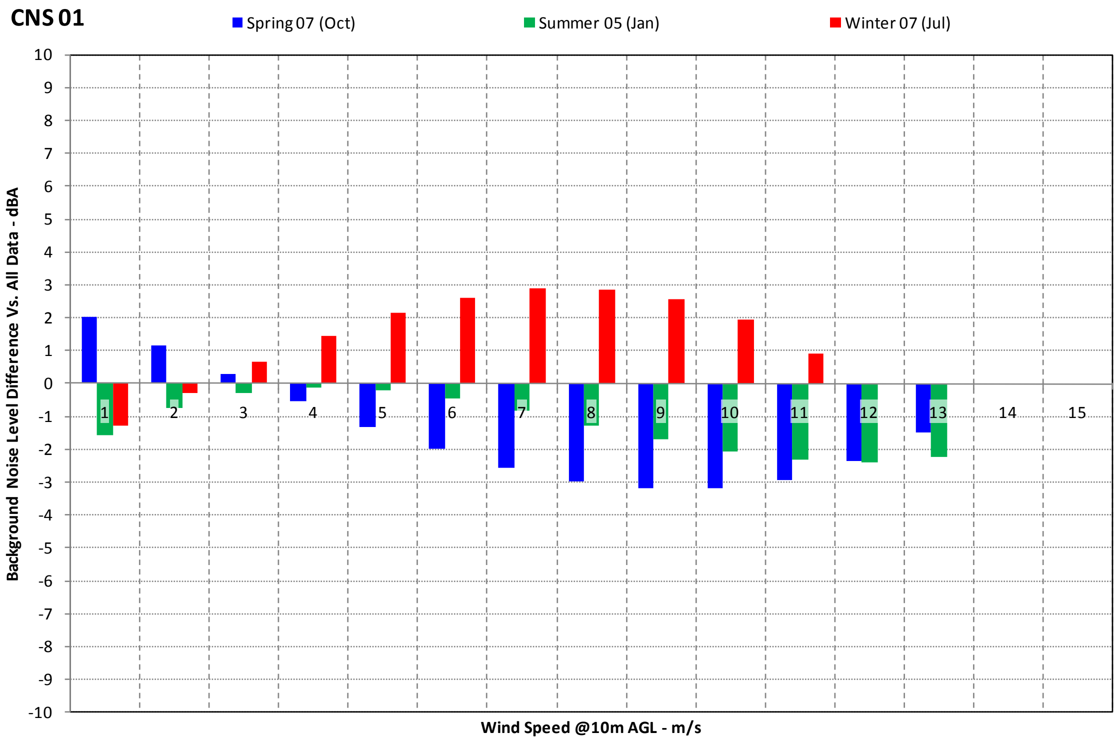
CNS 01
Spring 07 (Oct)
Summer 05 (Jan)
Winter 07 (Jul)
Background Noise Level Difference Vs. All Data - dBA
Wind Speed @10m AGL - m/s

CNS - House 2

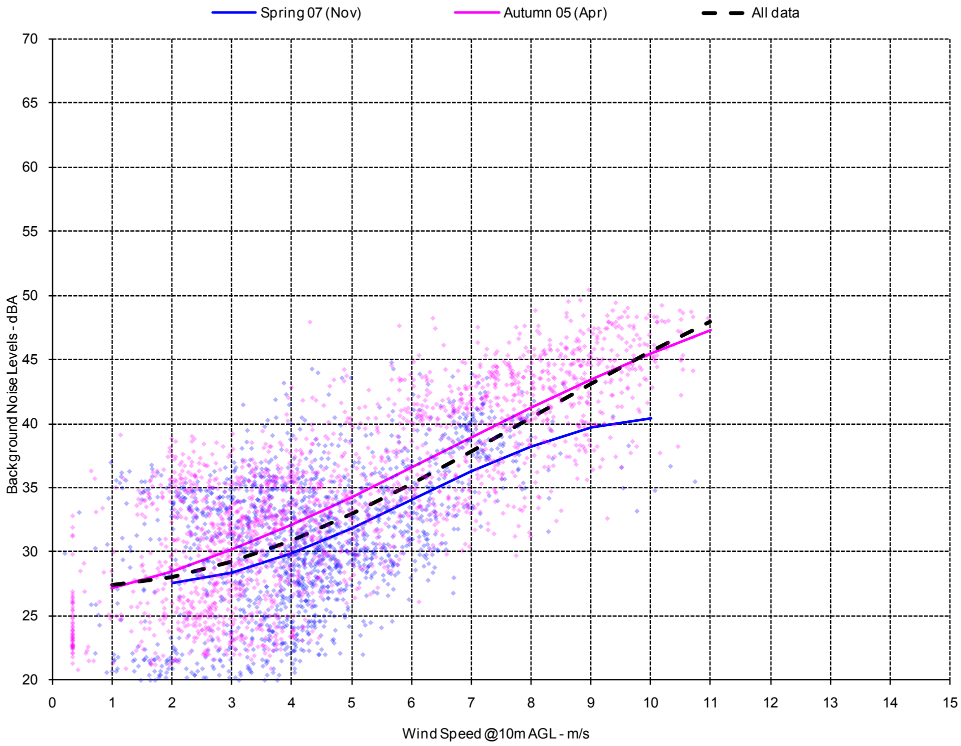

Spring 07 (Nov)

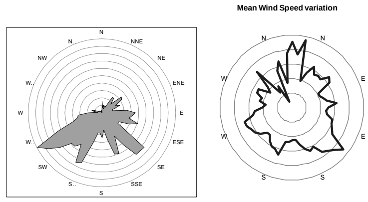

Autumn 05 (Apr)

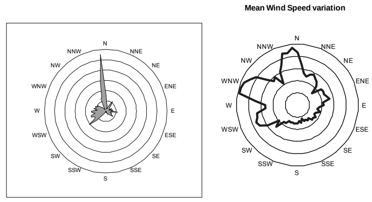

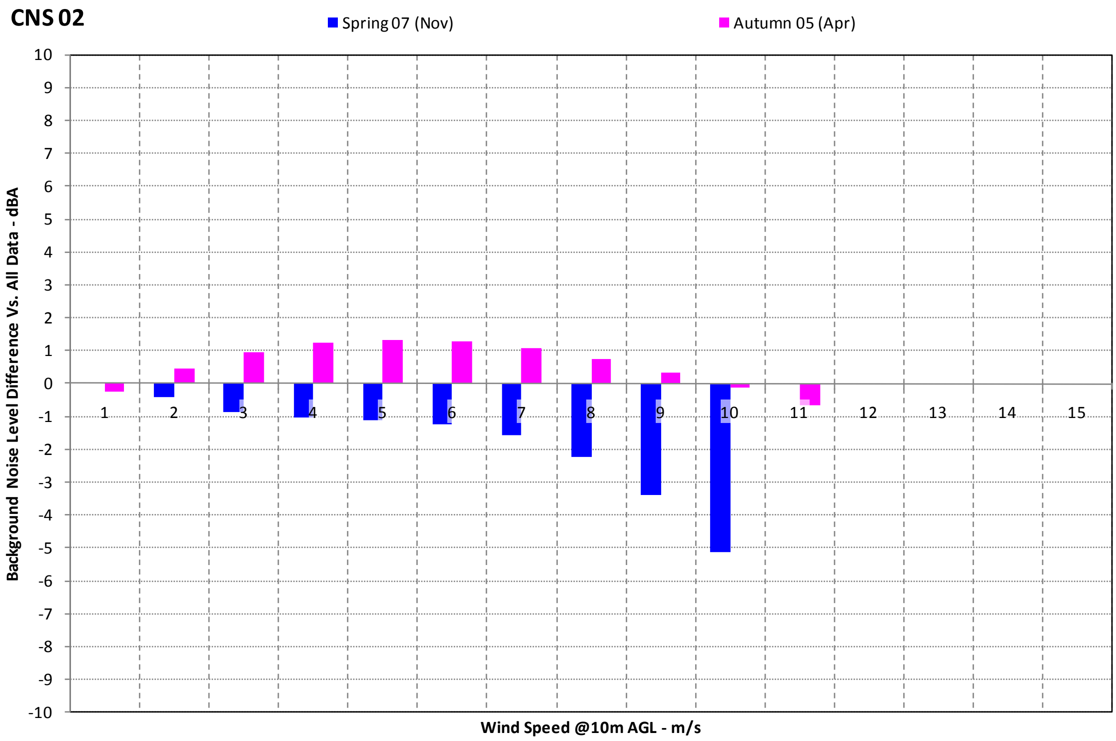

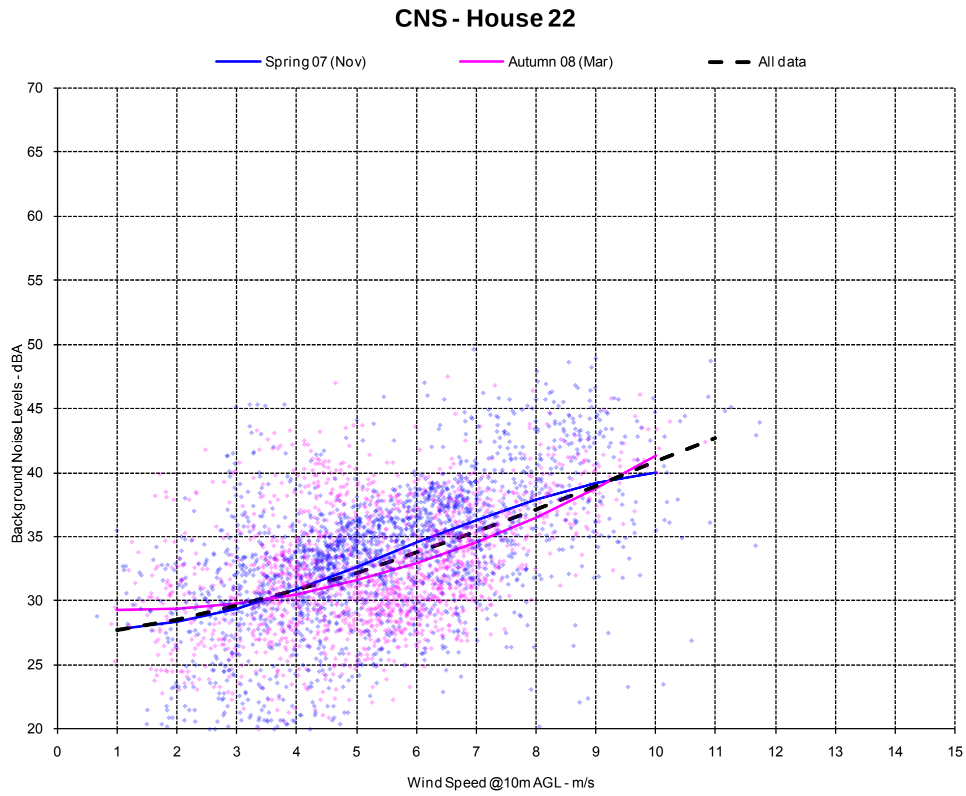
CNS - House 22
Spring 07 (Nov)
Autumn 08 (Mar)
All data
Background Noise Levels - dBA
Wind Speed @10m AGL - m/s

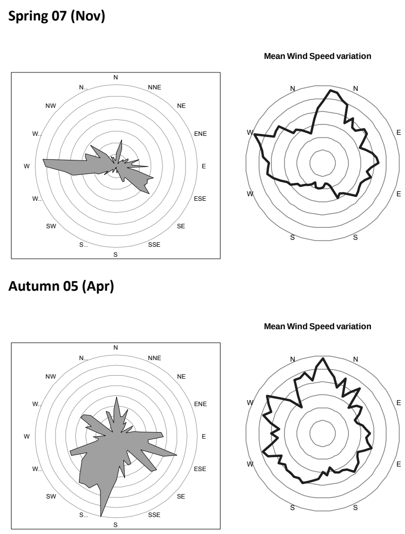
Spring 07 (Nov)
Mean Wind Speed variation
Autumn 05 (Apr)
Mean Wind Speed variation

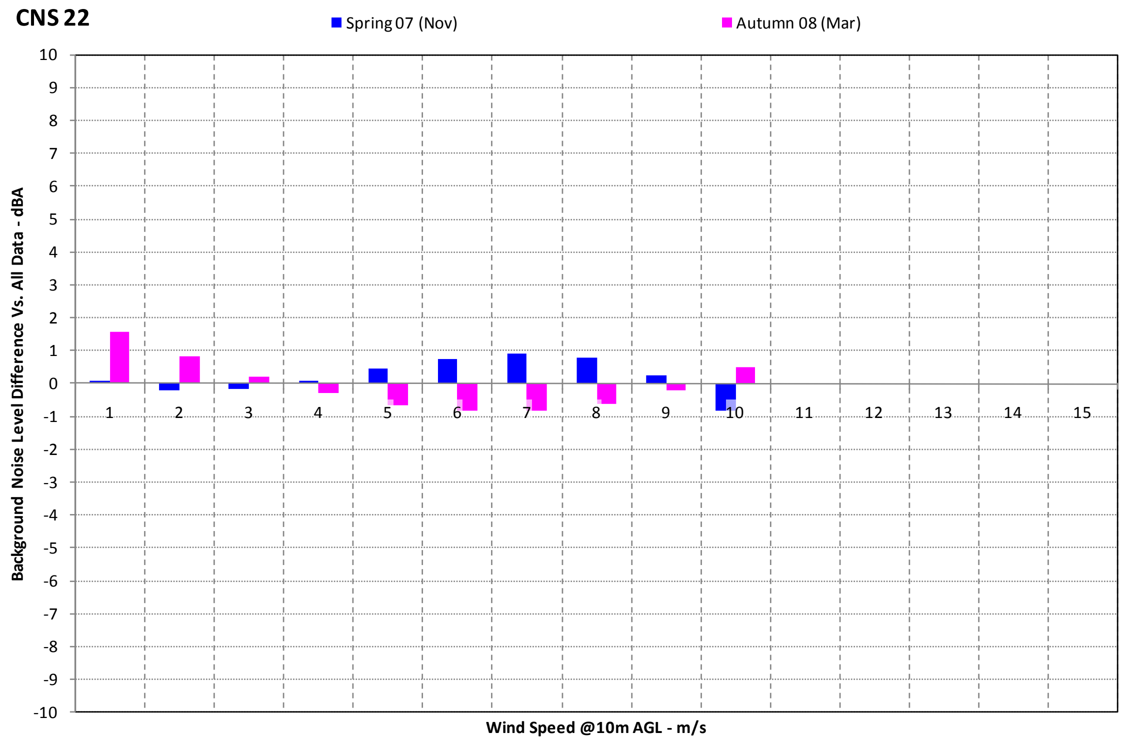
CNS 22
Spring 07 (Nov)
Autumn 08 (Mar)
Background Noise Level Difference Vs. All Data - dBA
Wind Speed @10m AGL - m/s

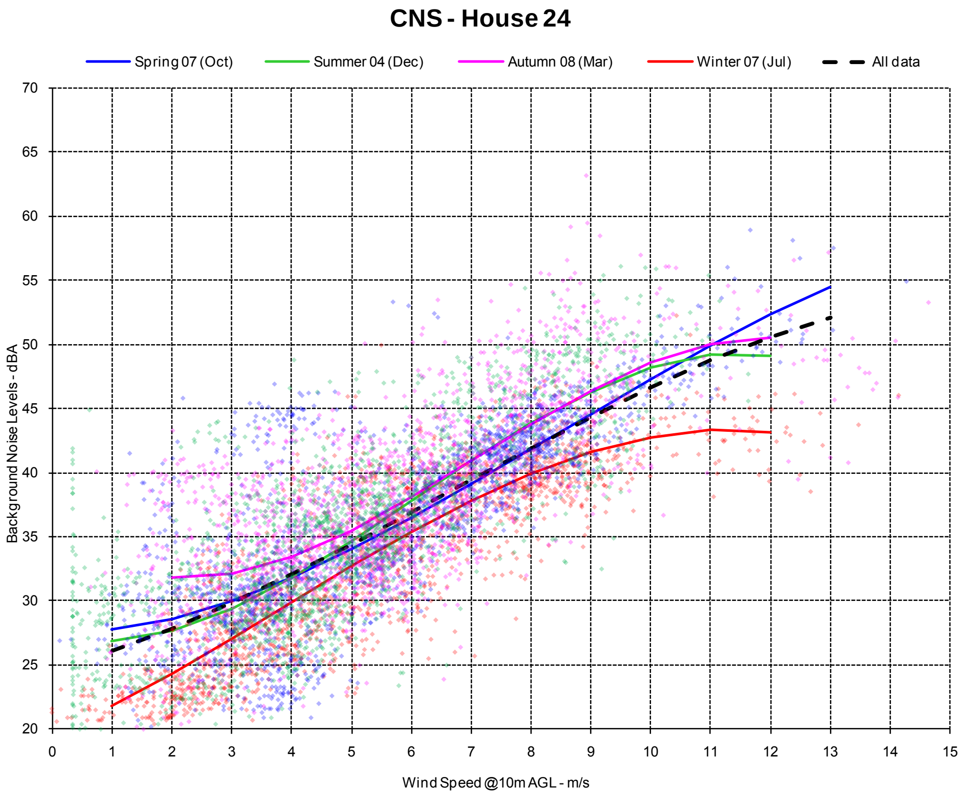
CNS - House 24
Spring 07 (Oct)
Summer 04 (Dec)
Autumn 08 (Mar)
Winter 07 (Jul)
All data
Background Noise Levels - dBA
Wind Speed @10m AGL - m/s

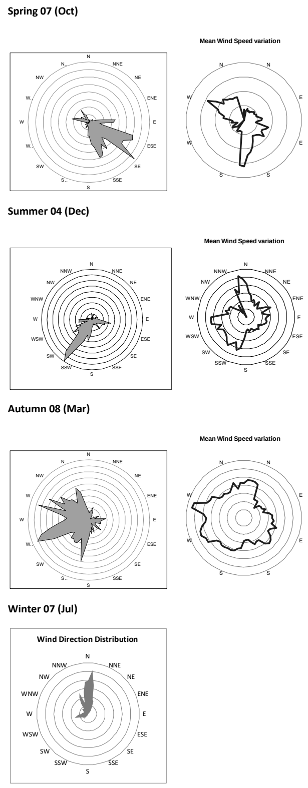
Spring 07 (Oct)
Mean Wind Speed variation
Summer 04 (Dec)
Mean Wind Speed variation
Autumn 08 (Mar)
Mean Wind Speed variation
Winter 07 (Jul)
Wind Direction Distribution

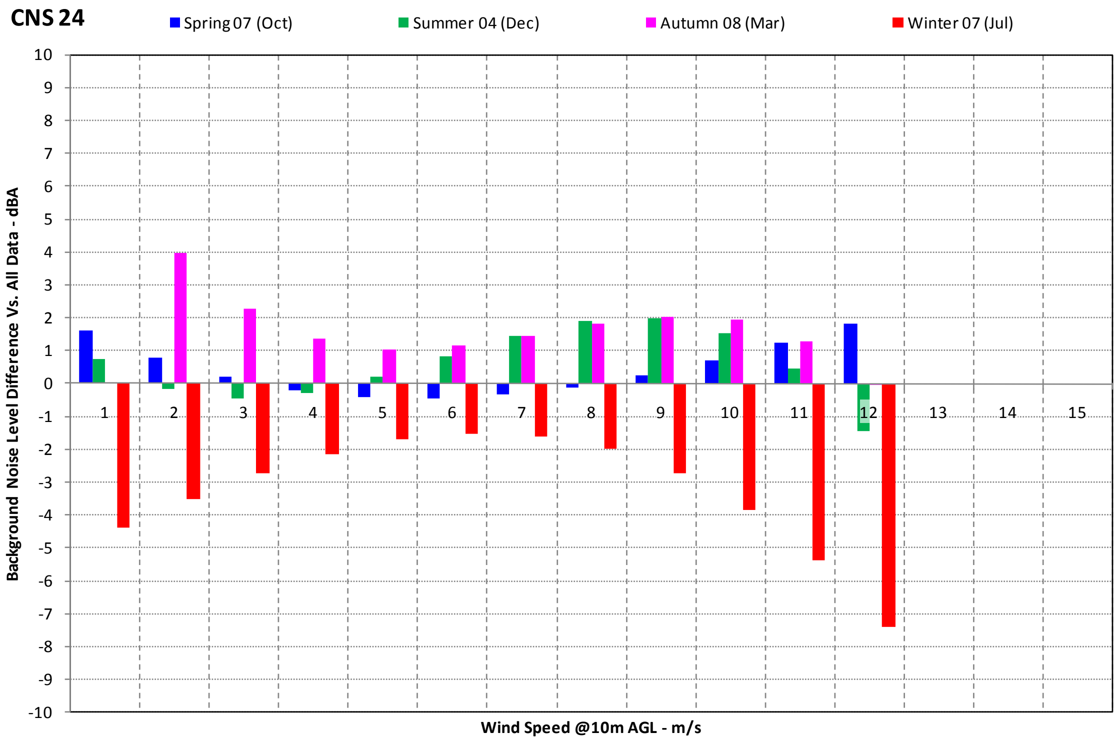
CNS 24
Spring 07 (Oct)
Summer 04 (Dec)
Autumn 08 (Mar)
Winter 07 (Jul)
Background Noise Level Difference Vs. All Data - dBA
Wind Speed @10m AGL - m/s

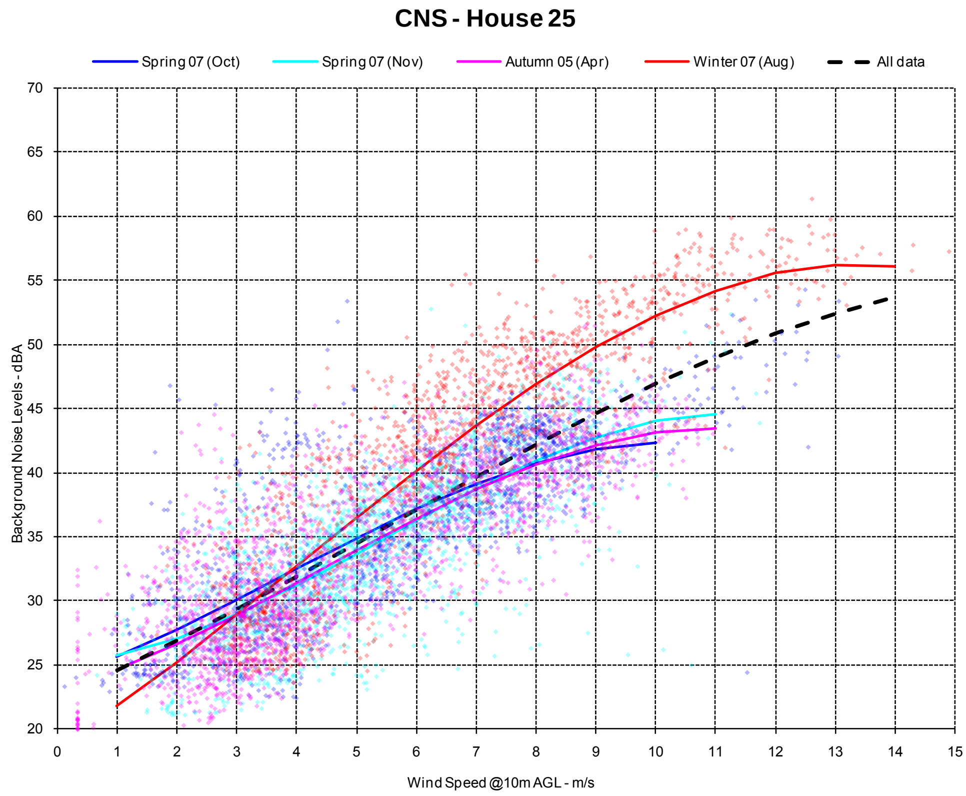
CNS - House 25
Spring 07 (Oct)
Spring 07 (Nov)
Autumn 05 (Apr)
Winter 07 (Aug)
All data
Background Noise Levels - dBA
Wind Speed @10m AGL - m/s

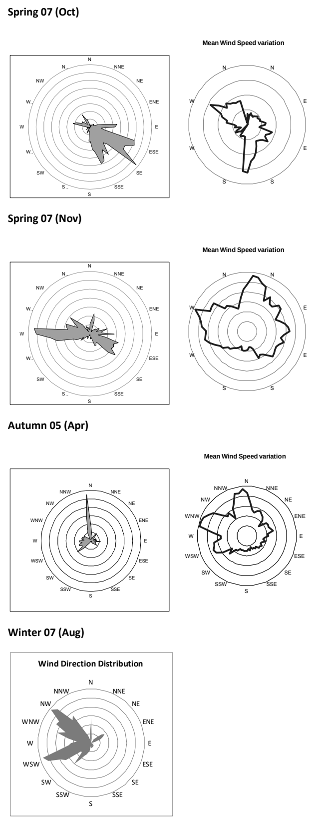
Spring 07 (Oct)
Mean Wind Speed variation
Spring 07 (Nov)
Mean Wind Speed variation
Autumn 05 (Apr)
Mean Wind Speed variation
Winter 07 (Aug)
Wind Direction Distribution

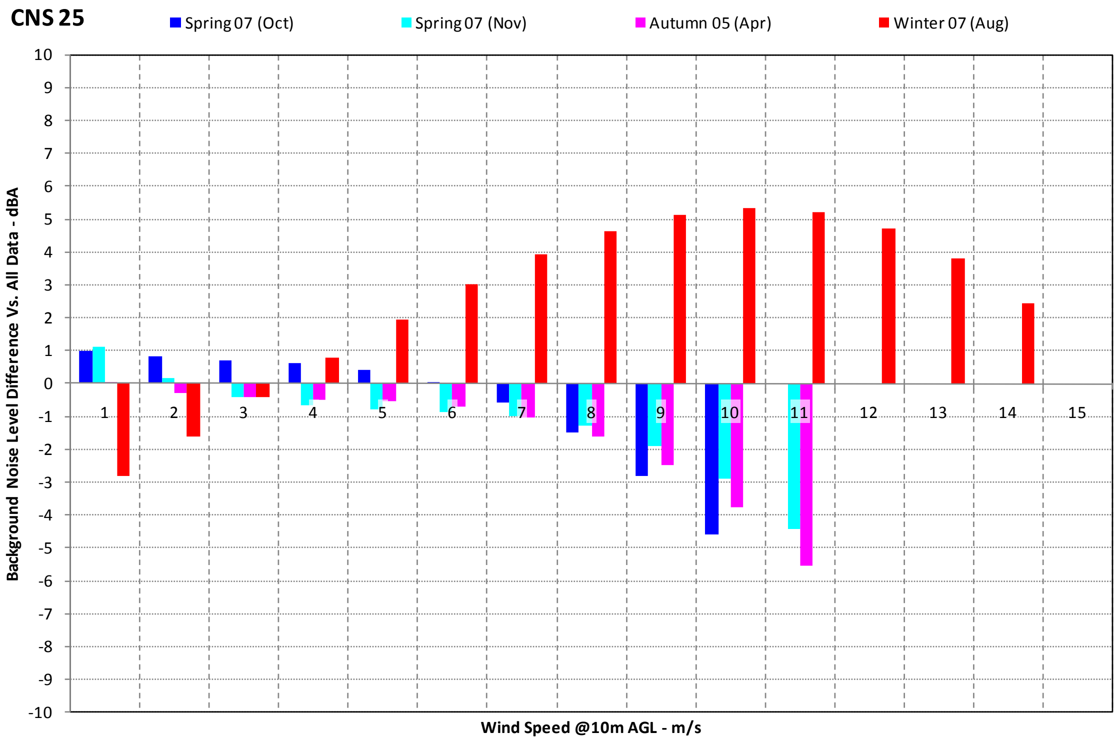
CNS 25
Spring 07 (Oct)
Spring 07 (Nov)
Autumn 05 (Apr)
Winter 07 (Aug)
Background Noise Level Difference Vs. All Data - dBA
Wind Speed @10m AGL - m/s

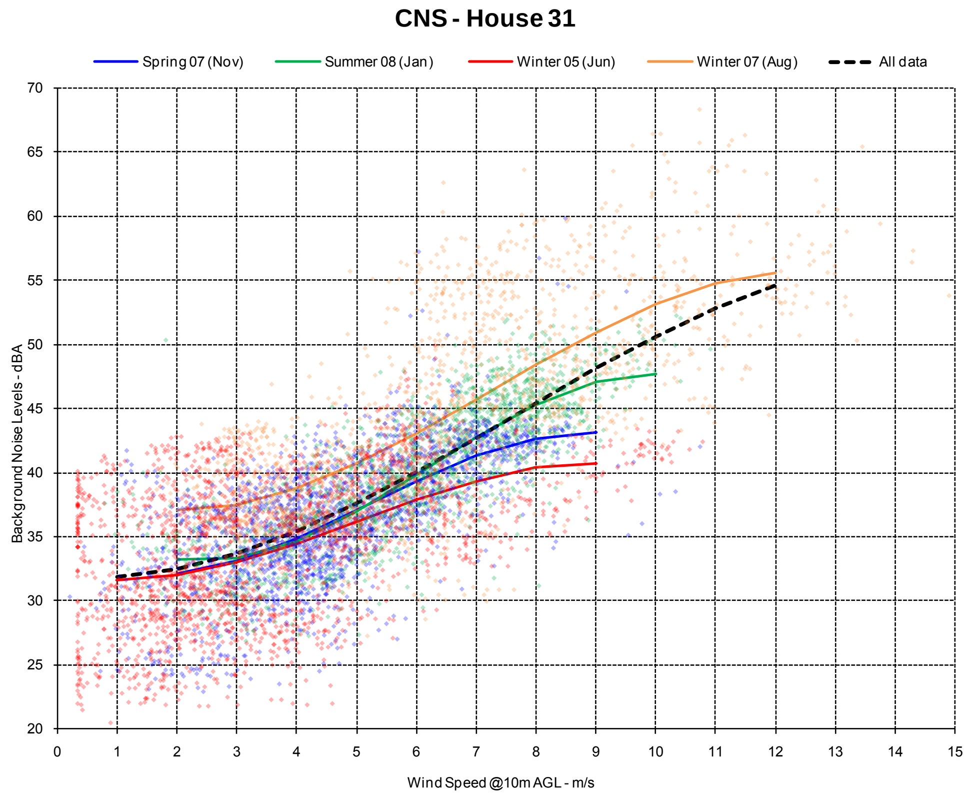

CNS - House 31
Spring 07 (Nov)
Summer 08 (Jan)
Winter 05 (Jun)
Winter 07 (Aug)
All data
Background Noise Levels - dBA
Wind Speed @10m AGL - m/s

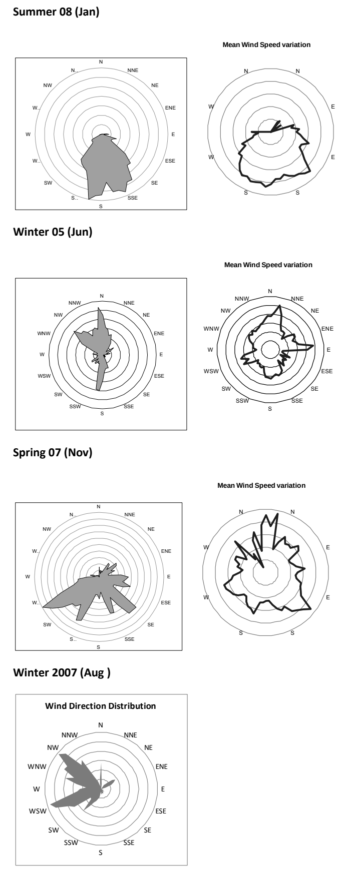

Summer 08 (Jan)
Mean Wind Speed variation
Winter 05 (Jun)
Mean Wind Speed variation
Spring 07 (Nov)
Mean Wind Speed variation
Winter 2007 (Aug)
Wind Direction Distribution

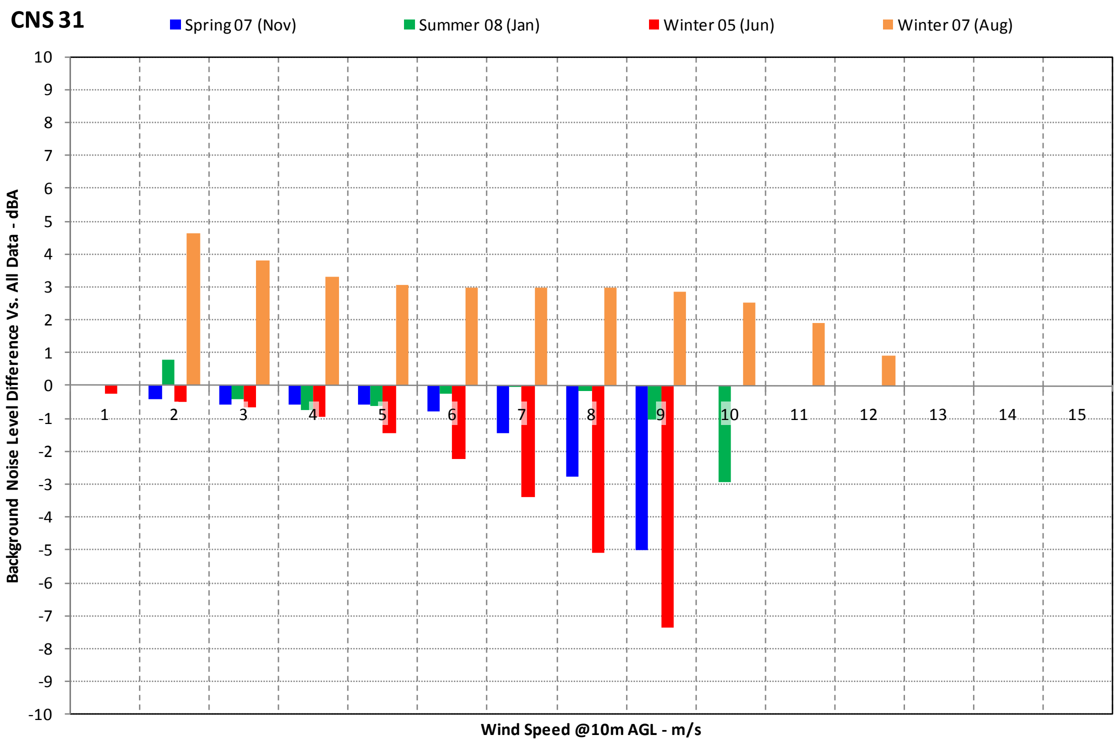

CNS 31
Spring 07 (Nov)
Summer 08 (Jan)
Winter 05 (Jun)
Winter 07 (Aug)
Background Noise Level Difference Vs. All Data - dBA
Wind Speed @10m AGL - m/s

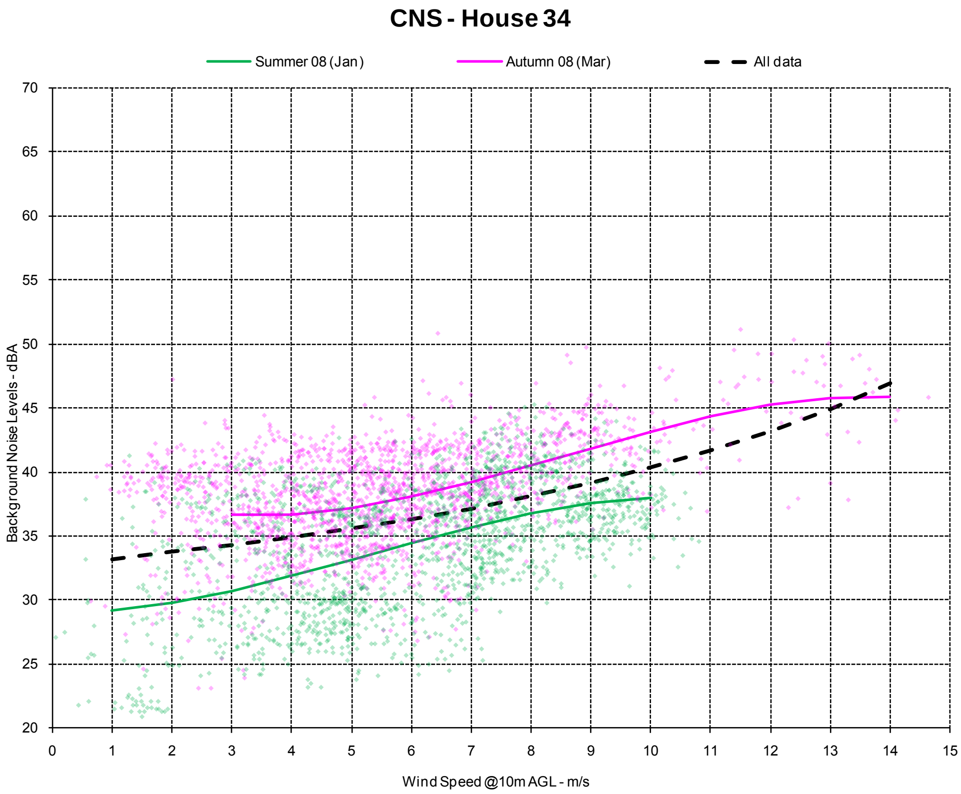

CNS - House 34
Summer 08 (Jan)
Autumn 08 (Mar)
All data
Background Noise Levels - dBA
Wind Speed @10m AGL - m/s

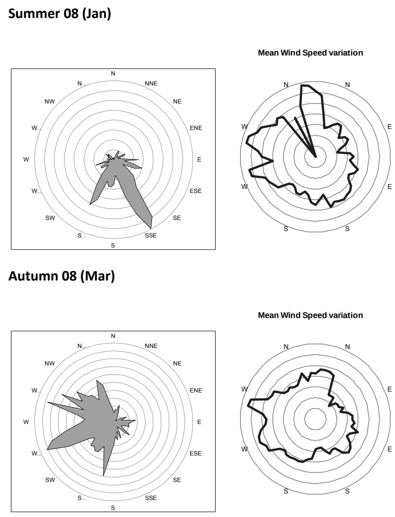

Summer 08 (Jan)
Mean Wind Speed variation
Autumn 08 (Mar)
Mean Wind Speed variation

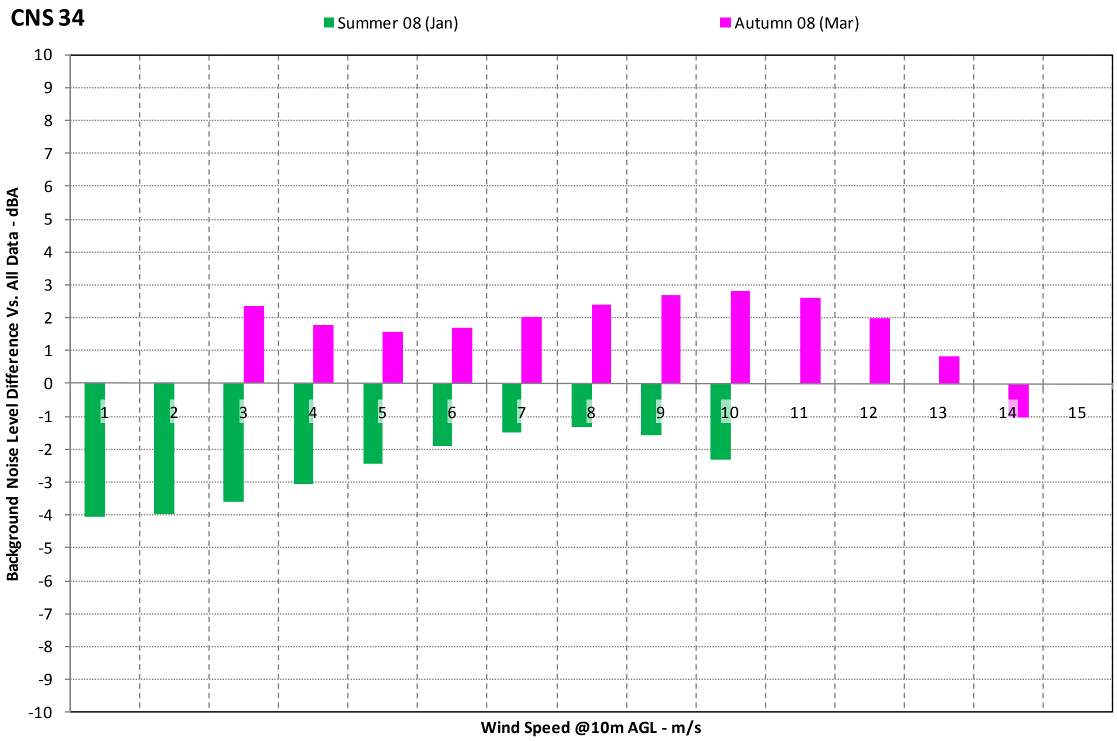

CNS 34
Summer 08 (Jan)
Autumn 08 (Mar)
Background Noise Level Difference Vs. All Data - dBA
Wind Speed @10m AGL - m/s

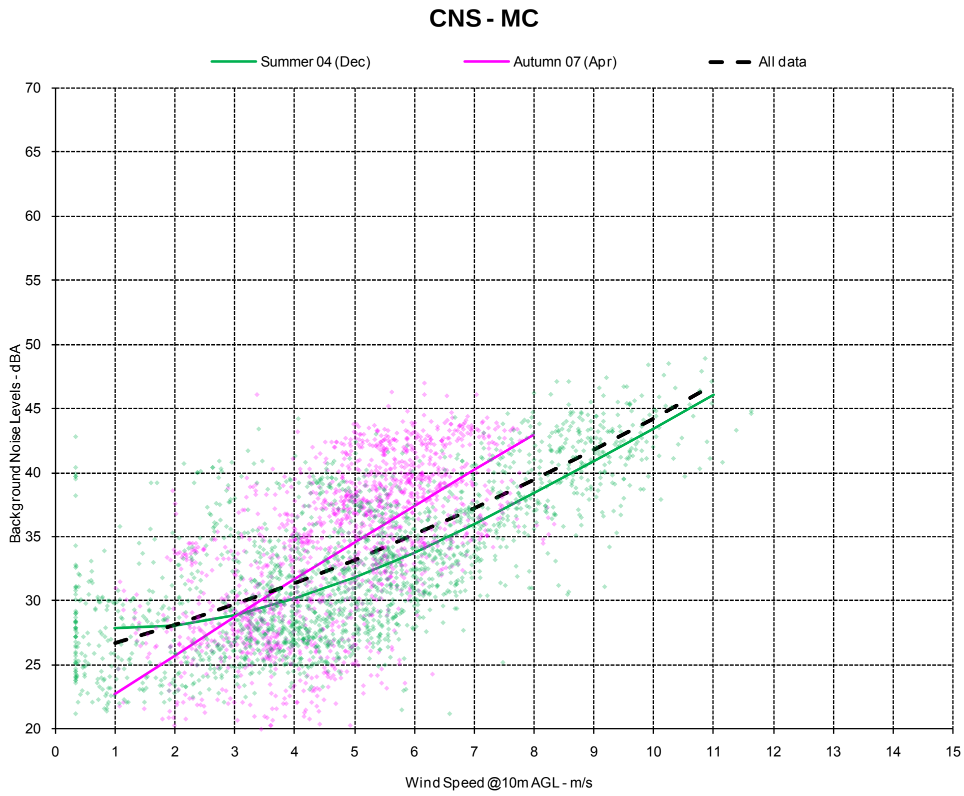

Summer 04 (Dec)

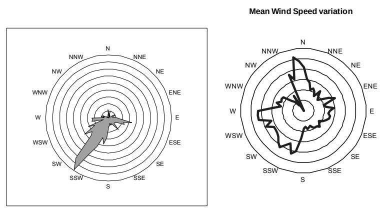

Autumn 2007 (Apr)

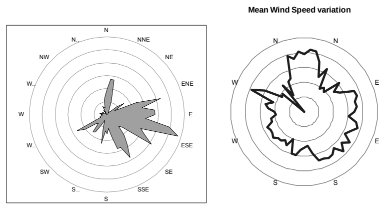

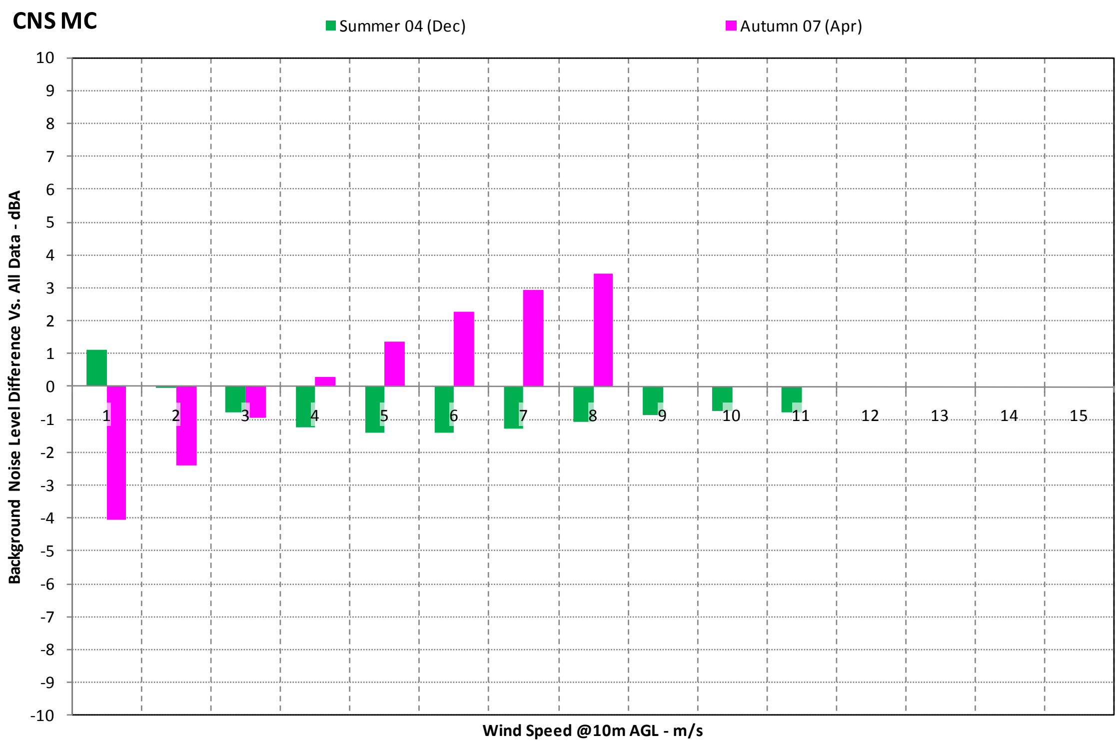

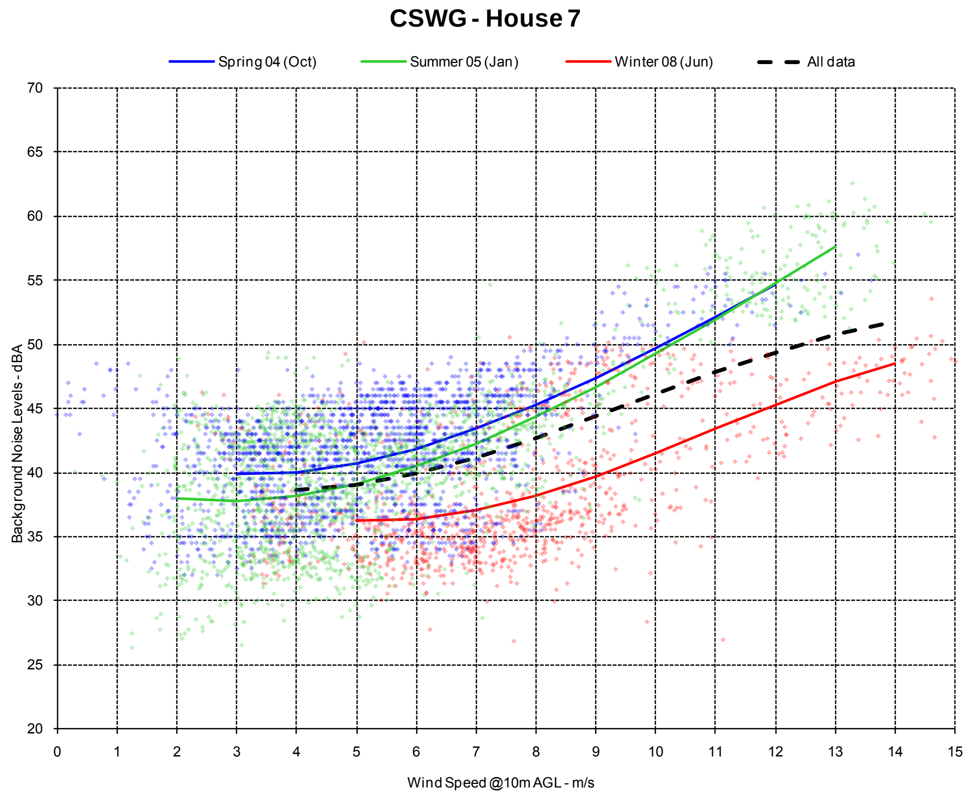
CSWG - House 7
Spring 04 (Oct)
Summer 05 (Jan)
Winter 08 (Jun)
All data
Background Noise Levels - dBA
Wind Speed @10m AGL - m/s

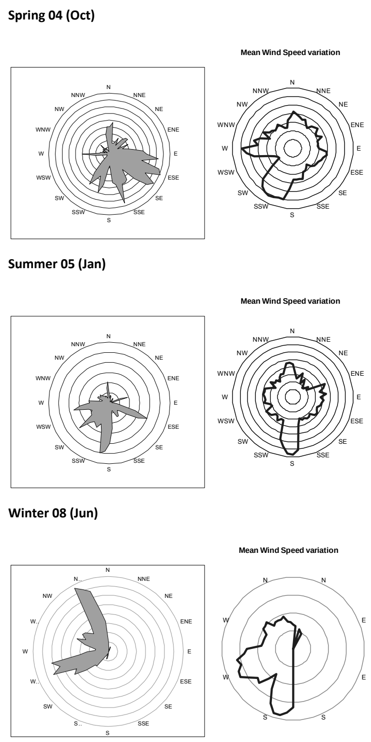
Spring 04 (Oct)
Mean Wind Speed variation
Summer 05 (Jan)
Mean Wind Speed variation
Winter 08 (Jun)
Mean Wind Speed variation

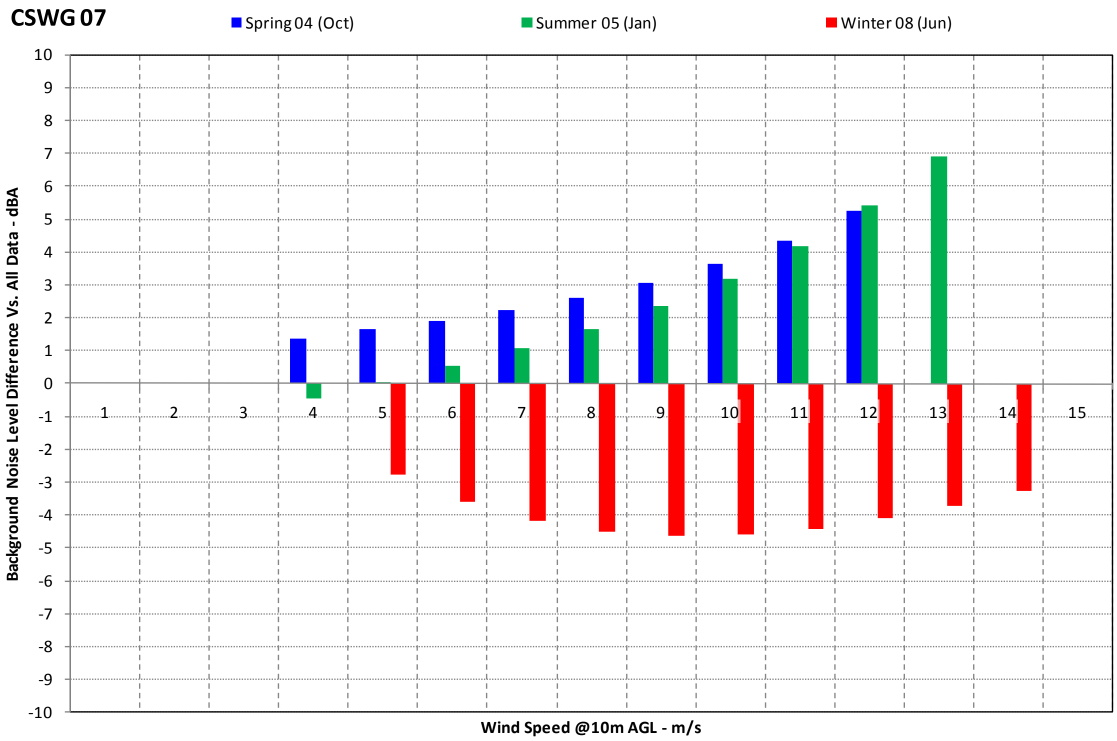
CSWG 07
Spring 04 (Oct)
Summer 05 (Jan)
Winter 08 (Jun)
Background Noise Level Difference Vs. All Data - dBA
Wind Speed @10m AGL - m/s

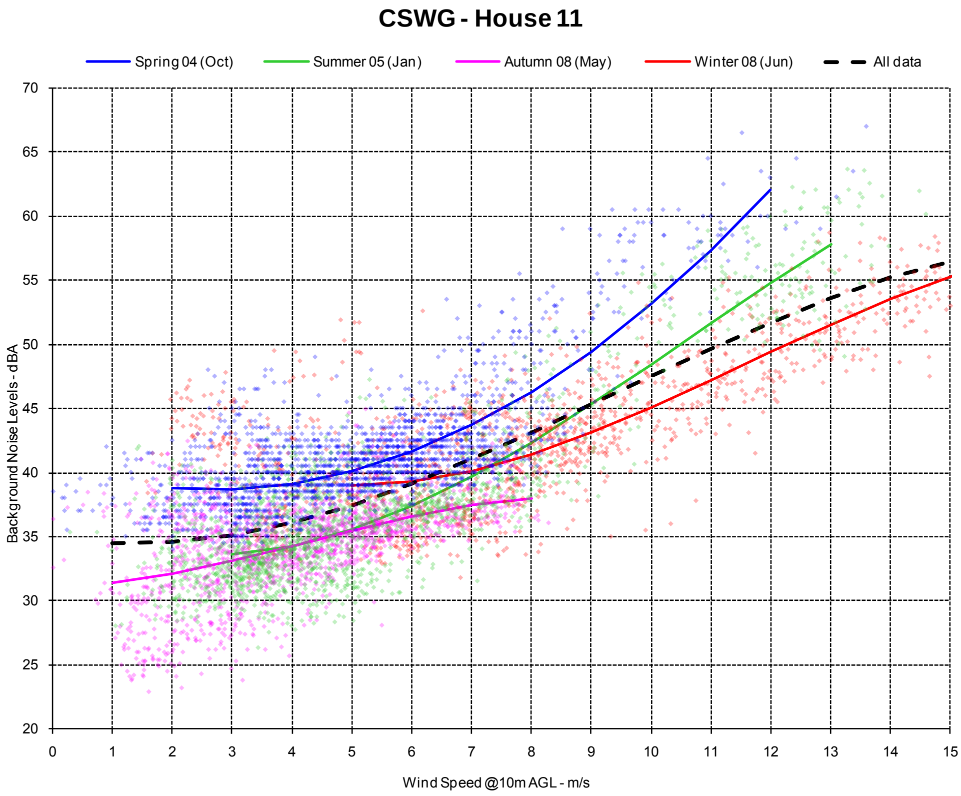
CSWG - House 11
Spring 04 (Oct)
Summer 05 (Jan)
Autumn 08 (May)
Winter 08 (Jun)
All data
Background Noise Levels - dBA
Wind Speed @10m AGL - m/s

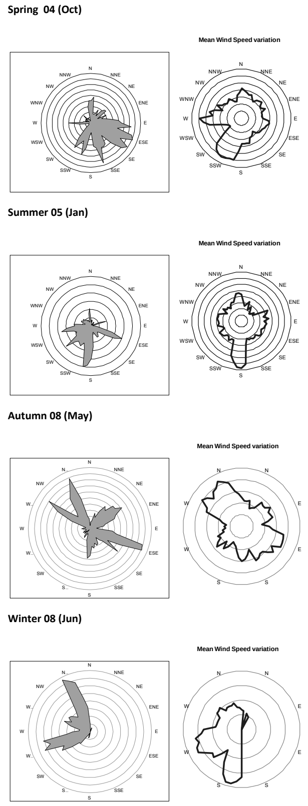
Spring 04 (Oct)
Mean Wind Speed variation
Summer 05 (Jan)
Mean Wind Speed variation
Autumn 08 (May)
Mean Wind Speed variation
Winter 08 (Jun)
Mean Wind Speed variation

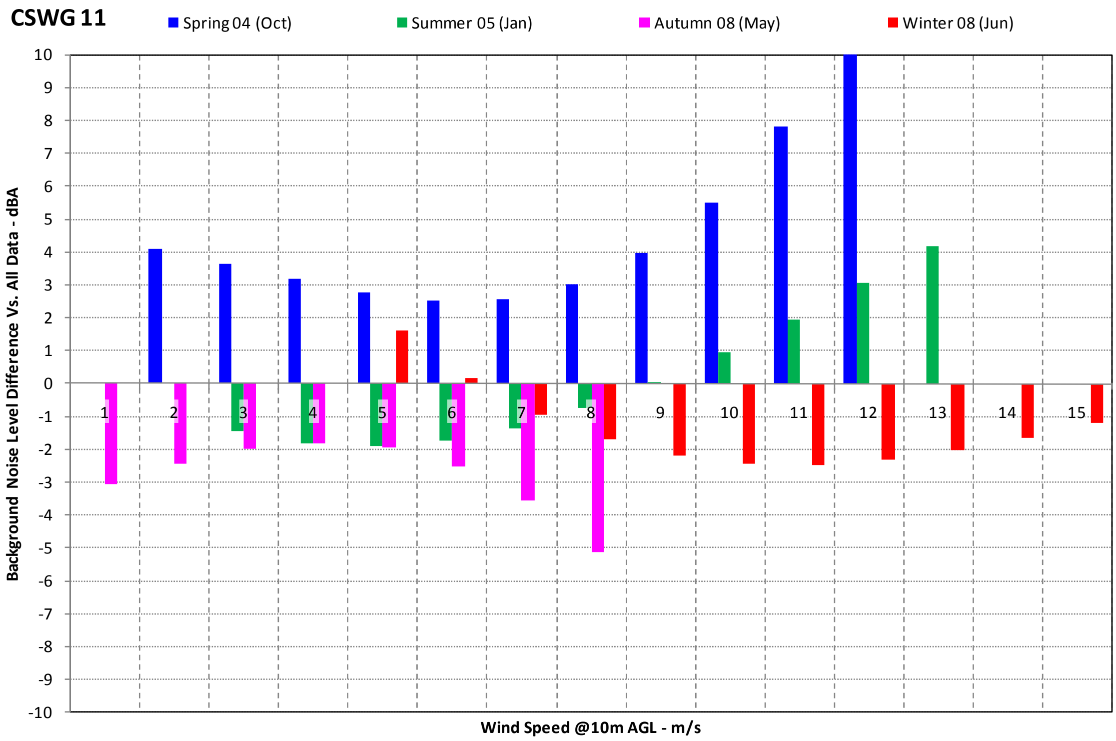
CSWG 11
Spring 04 (Oct)
Summer 05 (Jan)
Autumn 08 (May)
Winter 08 (Jun)
Background Noise Level Difference Vs. All Data - dBA
Wind Speed @10m AGL - m/s

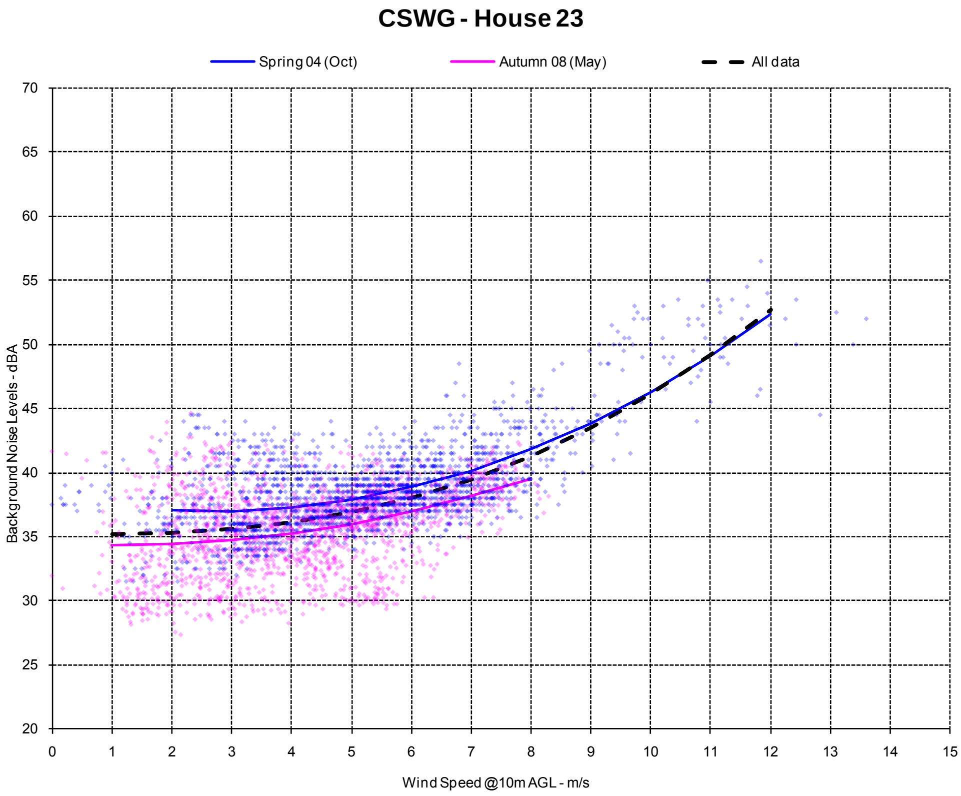
CSWG - House 23
Spring 04 (Oct)
Autumn 08 (May)
All data
Background Noise Levels - dBA
Wind Speed @10m AGL - m/s
70
65
60
55
50
45
40
35
30
25
20
0 1 2 3 4 5 6 7 8 9 10 11 12 13 14 15

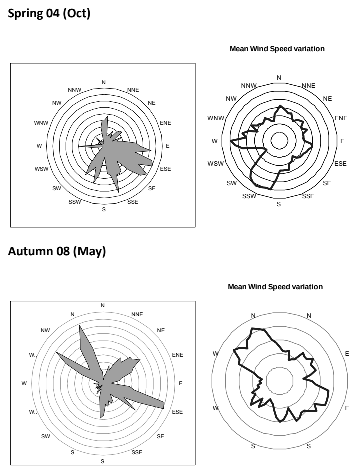
Spring 04 (Oct)
Mean Wind Speed variation
Autumn 08 (May)
Mean Wind Speed variation

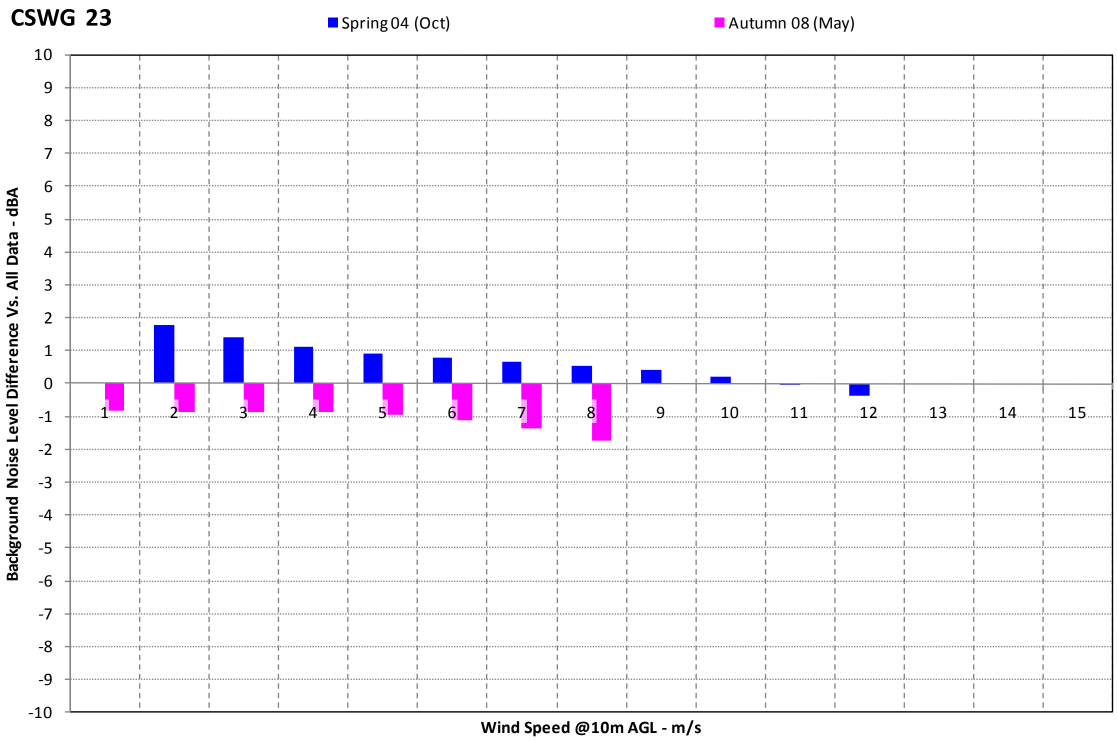
CSWG 23
Spring 04 (Oct)
Autumn 08 (May)
Background Noise Level Difference Vs. All Data - dBA
Wind Speed @10m AGL - m/s
10
9
8
7
6
5
4
3
2
1
0
-1
-2
-3
-4
-5
-6
-7
-8
-9
-10
1 2 3 4 5 6 7 8 9 10 11 12 13 14 15

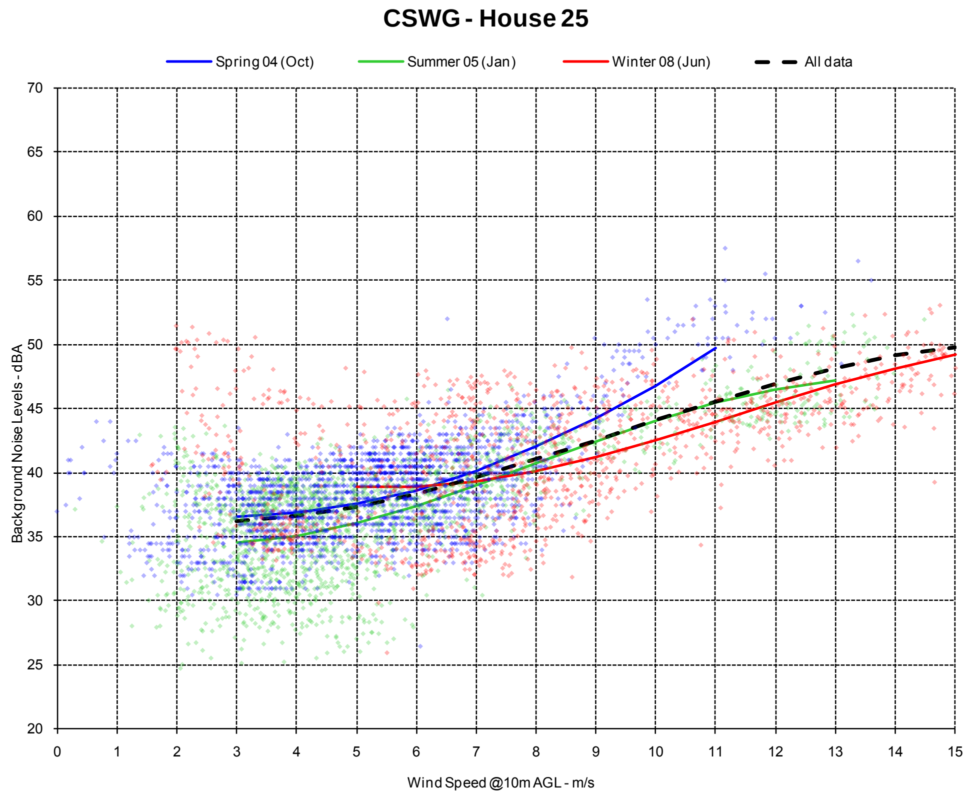

Winter 08 (Jun)

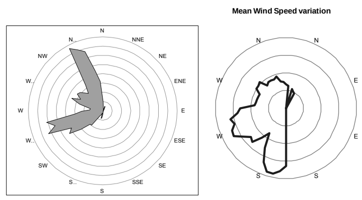

Spring 04 (Oct)

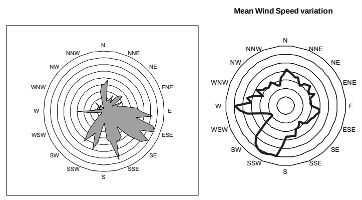

Summer 05 (Jan)

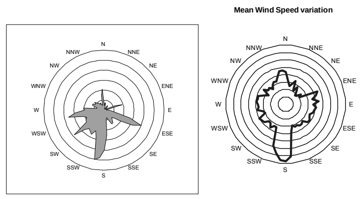

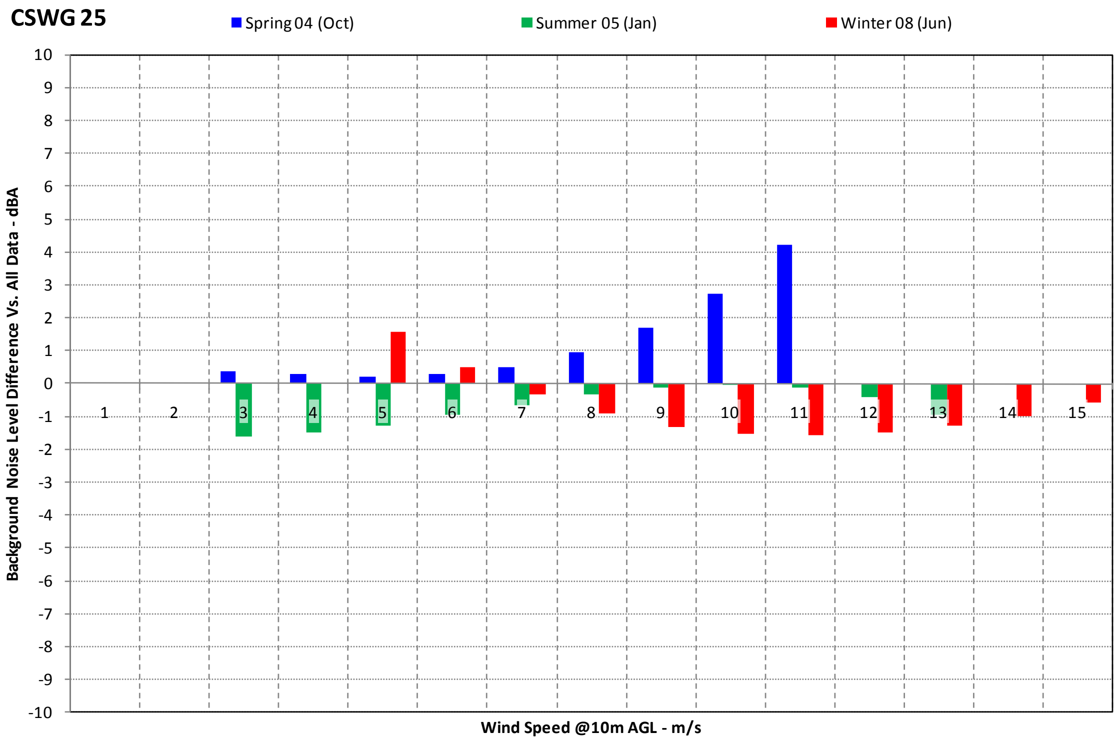

APPENDIX C

SUMMARY OF PARAMETERS

a, b, c and d in tables below correspond to the constant in the background noise regression curve equation.

$$y = a \cdot x^3 + b \cdot x^2 + c \cdot x + d$$

where y is the background noise level and x the wind speed.

If a does not contain any value, then a 2nd order regression was used instead of 3rd order.

R^2 is the coefficient of determination of the regression curve

PWEP II – CBS

		Monitoring period	Logger Location	Avg. wind speed	Max. wind Speed	Correlation Coefficient	a	b	c	d	R^2	Average difference between survey period and all data between 6-10m/s
CBS 01	All data	-			14	0.86	-0.01087	0.2660	0.4885	24.33	0.75	
	Summer 05 (Jan)	06.01.2005 to 19.01.2005	A	6	13	0.71	-0.00556	0.1504	1.0160	24.66	0.51	-0.1
	Winter 06 (Jul)	14.07.2006 to 28.07.2006	A	6	14	0.90	-0.02354	0.5488	-1.3110	26.26	0.83	-0.9
	Spring 06 (Oct)	11.10.2006 to 23.10.2006	A	6	14	0.90	-0.01125	0.2906	0.1675	26.15	0.81	0.7
CBS 02	All data	-			14	0.79	-0.00761	0.1958	1.2770	22.00	0.63	
	Summer 05 (Jan)	06.01.2005 to 20.01.2005	A	6	13	0.72	-0.00190	0.0163	2.6060	19.20	0.52	-0.8
	Winter 06 (Jun)	01.06.2006 to 13.06.2006	B	4	13	0.86	-0.00770	0.2704	0.3773	22.42	0.77	-1.9
	Spring 06 (Sep)	26.09.2006 to 09.10.2006	B	6	14	0.80	0.00842	-0.1272	3.0040	20.90	0.64	0.4
	Autumn 07 (Apr)	02.04.2007 to 15.04.2007	B	5	10	0.67		0.0477	2.0330	22.18	0.46	0.8

PWEP II - CBN

		Monitoring period	Logger Location	Avg. wind speed	Max. wind Speed	Correlation Coefficient	a	b	c	d	R^2	Average difference between survey period and all data between 6-10m/s
CBN 46	All data	-			14	0.67	-0.01300	0.3443	-0.6487	29.59	0.46	
	Spring 05 (Nov)	17.11.2005 to 02.12.2005	A	5	12	0.75	0.00435	-0.0490	2.7150	22.78	0.56	3.9
	Winter 06 (Jul)	07.07.2006 to 21.07.2006	A	6	13	0.68	-0.04773	1.0280	-4.8390	39.12	0.52	1.7
	Summer 07 (Feb)	23.02.2007 to 07.03.2007	A	6	13	0.60	-0.03872	0.6187	-1.3990	26.46	0.38	-5.4
	Spring 07 (Oct)	03.10.2007 to 16.10.2007		7	14	0.77	-0.00174	0.1165	0.8269	26.15	0.60	-0.4
CBN 54	All data	-			18	0.83	-0.01220	0.2627	0.5338	26.50	0.69	
	Summer 05 (Jan)	21.01.2005 to 03.02.2005	A	6	15	0.85	-0.02984	0.5828	-0.8203	24.83	0.73	1.5
	Winter 06 (Jul)	21.07.2006 to 04.08.2006	A	6	15	0.45	-0.01910	0.5446	-3.1100	36.31	0.28	-0.8
	Spring 06 (Sep)	26.09.2006 to 10.10.2006	A	5	14	0.43	-0.01804	0.5072	-2.9690	37.37	0.28	-0.5
	Summer 08 (Jan)	31.01.2008 to 13.02.2008	A	6	10	0.61	-0.03150	0.6326	-2.8620	35.93	0.41	-0.4
CBN 55	All data	-			18	0.83	-0.01220	0.2627	0.5338	26.50	0.69	
	Summer 05 (Jan)	21.01.2005 to 03.02.2005	A	5	15	0.85	-0.02984	0.5828	-0.8203	24.83	0.73	-1.3
	Autumn 06 (Apr)	24.04.2006 to 08.05.2006	A	6	15	0.89	-0.01723	0.3883	-0.3867	28.06	0.80	-0.3
	Winter 06 (Jun)	16.06.2006 to 30.06.2006	A	4	12	0.66	0.00485	-0.1014	2.4050	25.87	0.43	-0.1
	Spring 06 (Sep)	12.09.2006 to 26.09.2006	A	6	18	0.87	-0.00212	0.0364	1.8140	25.81	0.76	0.3
	Spring 06 (Oct)	27.10.2006 to 09.11.2006	A	6	11	0.81	-0.06030	1.1610	-4.1030	32.51	0.67	1.3
CBN 63	All data	-			15	0.83	-0.02585	0.5592	-1.0170	31.22	0.69	
	Summer 05 (Feb)	22.02.2005 to 08.03.2005	A	5	12	0.62	-0.06507	1.3010	-5.1500	36.93	0.47	-0.4
	Autumn 06 (Apr)	04.04.2006 to 18.04.2006	A	6	14	0.87	0.00114	-0.0705	3.1850	22.83	0.75	-1.2
	Winter 06 (Jun)	30.06.2006 to 13.07.2006	A	6	13	0.87	-0.02624	0.4811	-0.0827	29.74	0.77	0.6

	Spring 06 (Oct)	11.10.2006 to 25.10.2006	A	6	15	0.83	-0.03502	0.8363	-3.1820	36.67	0.71	1.3
CBN 70	All data	-			16	0.62	-0.02706	0.7088	-3.7530	50.24	0.44	
	Summer 05 (Dec)	22.12.2005 to 05.01.2006	A	6	16	0.63	-0.04726	1.2100	-7.1430	55.04	0.45	-0.6
	Winter 06 (Jul)	31.07.2006 to 12.08.2006	A	5	13	0.64	-0.00942	0.3109	-1.5400	47.43	0.51	-1.5
	Winter 07 (Aug)	22.08.2007 to 04.09.2007	A	6	16	0.64	-0.02211	0.5495	-2.4580	48.53	0.44	0.9

PWEP III - CNS

		Monitoring period	Logger Location	Avg. wind speed	Max. wind Speed	Correlation Coefficient	a	b	c	d	R^2	Average difference between survey period and all data between 6-10m/s
CNS 01	All data	-			18	0.66	-0.01657	0.2684	1.0170	25.80	0.45	
	Summer 05 (Jan)	06.01.2005 to 20.01.2005	A	6	15	0.63	-0.00661	0.0291	2.4880	22.98	0.41	-1.3
	Winter 07 (Jul)	19.07.2007 to 01.08.2007	A	6	14	0.74	-0.02294	0.2709	2.0520	23.50	0.57	2.6
	Spring 07 (Oct)	17.10.2007 to 29.10.2007	A	5	18	0.56	-0.01109	0.2319	0.2339	28.63	0.32	-2.8
CNS 02	All data	-			11	0.70	-0.01642	0.3901	-0.4480	27.49	0.51	
	Autumn 05 (Apr)	20.04.2005 to 04.05.2005	A	5	11	0.78	-0.01242	0.2489	0.6751	26.24	0.61	0.7
	Spring 07 (Nov)	14.11.2007 to 25.11.2007	A	4	11	0.50	-0.04046	0.7274	-2.1040	29.22	0.26	-2.7
CNS 22	All data	-			12	0.53	-0.00355	0.1235	0.4901	27.12	0.28	
	Spring 07 (Nov)	30.11.2007 to 14.12.2007	A	5	12	0.55	-0.02463	0.4227	-0.5628	27.97	0.31	0.4
	Autumn 08 (Mar)	15.03.2008 to 27.03.2008	A	5	11	0.48		0.1543	-0.3614	29.51	0.25	-0.4
CNS 24	All data	-			19	0.78	-0.01008	0.2025	1.1680	24.78	0.61	
	Summer 04 (Dec)	14.12.2004 to 28.12.2004	A	5	12	0.79	-0.03708	0.6784	-0.9787	27.20	0.65	1.5
	Winter 07 (Jul)	19.07.2007 to 01.08.2007	A	6	14	0.86	-0.01646	0.1829	2.1520	19.44	0.76	-2.3
	Spring 07 (Oct)	29.10.2007 to 12.11.2007	A	6	19	0.81	-0.01303	0.3303	-0.0104	27.43	0.67	0.0
	Autumn 08 (Mar)	20.03.2008 to 04.04.2008	A	6	15	0.71	-0.04104	0.8732	-3.2980	35.26	0.53	1.7
CNS 25	All data	-			15	0.79	-0.00703	0.1151	1.9930	22.52	0.62	
	Autumn 05 (Apr)	20.04.2005 to 04.05.2005	A	5	11	0.81	-0.02023	0.2702	1.3300	23.05	0.67	-1.9
	Winter 07 (Aug)	03.08.2007 to 14.08.2007	A	7	15	0.88	-0.01459	0.1793	3.0280	18.63	0.79	4.4
	Spring 07 (Oct)	29.10.2007 to 11.11.2007	A	6	13	0.67	-0.01989	0.2270	1.5680	23.86	0.47	-1.9
	Spring 07 (Nov)	30.11.2007 to 14.12.2007	A	5	12	0.75	-0.02594	0.4242	0.2465	25.09	0.56	-1.6

CNS 31	All data	-			15	0.45	-0.01928	0.4388	-0.6101	32.11	0.55	
	Winter 05 (Jun)	30.06.2005 to 14.07.2005	A	4	11	0.45	-0.03652	0.5501	-1.0390	32.18	0.24	-4.5
	Winter 07 (Aug)	03.08.2007 to 14.08.2007	B	7	15	0.72	-0.03438	0.7479	-2.7090	39.82	0.52	2.9
	Spring 07 (Nov)	14.11.2007 to 27.11.2007	B	5	11	0.57	-0.05557	0.8686	-2.2540	33.56	0.44	-2.5
	Summer 08 (Jan)	31.01.2008 to 12.02.2008	B	6	11	0.81	-0.07030	1.3060	-5.1490	38.89	0.69	-0.9

PWEP III – CNS (cont.)

		Monitoring period	Logger Location	Avg. wind speed	Max. wind Speed	Correlation Coefficient	a	b	c	d	R^2	Average difference between survey period and all data between 6-10m/s
CNS 34	All data	-			12	0.65		0.0653	1.2290	25.43	0.42	
	Summer 08 (Jan)	11.01.2008 to 23.01.2008	A	6	11	0.52	-0.01602	0.2541	-0.0335	28.97	0.28	-1.7
	Autumn 08 (Mar)	20.03.2008 to 03.04.2008	A	6	15	0.46	-0.01749	0.4505	-2.5070	40.65	0.26	2.3
CNS MC	All data	-			12	0.65		0.0653	1.2290	25.43	0.42	
	Summer 04 (Dec)	14.12.2004 to 28.12.2004	A	5	12	0.70	-0.01091	0.3250	-0.6253	28.15	0.53	-1.1
	Autumn 07 (Apr)	02.04.2007 to 13.04.2007	B	5	8	0.66		-0.0296	3.1550	19.55	0.44	2.9

PWEP IV - CNN

		Monitoring period	Logger Location	Avg. wind speed	Max. wind Speed	Correlation Coefficient	a	b	c	d	R^2	Average difference between survey period and all data between 6-10m/s
CNN 12	All data	-			12	0.77	-0.02824	0.5739	-0.9008	26.49	0.62	
	Spring 04 (Nov)	30.11.2004 to 13.12.2004	A	5	12	0.78	-0.01392	0.3154	0.1312	26.81	0.62	-0.5
	Autumn 08 (May)	30.05.2008 to 12.06.2008	A	4	11	0.73	-0.01277	0.4599	-0.7087	25.63	0.59	1.0
CNN 26	All data	-			12	0.72	-0.02533	0.6098	-1.3180	28.55	0.56	
	Spring 04 (Nov)	30.11.2004 to 13.12.2004	A	5	12	0.77	-0.00731	0.2453	0.6653	27.23	0.61	0.6
	Autumn 08 (May)	28.05.2008 to 11.06.2008	A	3	9	0.48	-0.03844	0.7494	-2.0790	28.99	0.27	-3.1
CNN 28	All data	-			12	0.67	-0.02667	0.5881	-1.3680	28.82	0.48	
	Summer 04 (Dec)	14.12.2004 to 28.12.2004	A	5	12	0.70	-0.01091	0.3250	-0.6253	28.15	0.53	-1.1
	Autumn 07 (Apr)	02.04.2007 to 13.04.2007	B	5	8	0.66		-0.0296	3.1550	19.55	0.44	2.9

PWEP IV - CSWG

		Monitoring period	Logger Location	Avg. wind speed	Max. wind Speed	Correlation Coefficient	a	b	c	d	R^2	Average difference between survey period and all data between 6-10m/s
CSWG 07	All data	-			21	0.51	-0.01624	0.4732	-2.8510	43.53	0.31	
	Spring 04 (Oct)	18.10.2004 to 31.10.2004	A	5	14	0.50	-0.01204	0.4170	-2.3440	43.52	0.33	2.7
	Summer 05 (Jan)	21.01.2005 to 03.02.2005	A	5	15	0.73	-0.00989	0.3725	-1.8300	40.20	0.58	1.8
	Winter 08 (Jun)	24.06.2008 to 03.07.2008	A	8	21	0.61	-0.02106	0.6905	-5.6310	49.83	0.45	-4.3
CSWG 11	All data	-			21	0.79	-0.01177	0.3310	-0.8920	35.10	0.64	
	Spring 04 (Oct)	18.10.2004 to 01.11.2004	A	5	14	0.73		0.2666	-1.4040	40.49	0.67	3.5
	Summer 05 (Jan)	21.01.2005 to 03.02.2005	A	5	15	0.85	-0.01684	0.5376	-2.5330	36.86	0.79	-0.6
	Autumn 08 (May)	30.05.2008 to 10.06.2008	A	4	8	0.50	-0.02341	0.3032	-0.0853	31.26	0.26	-3.7
	Winter 08 (Jun)	24.06.2008 to 04.07.2008	B	9	21	0.81	-0.01776	0.6161	-4.9260	50.49	0.75	-1.4
CSWG 23	All data	-			14	0.57	0.00529	0.0685	-0.1312	35.25	0.39	
	Spring 04 (Oct)	18.10.2004 to 01.11.2004	A	5	14	0.63	0.00135	0.1536	-0.8589	38.18	0.52	0.5
	Autumn 08 (May)	28.05.2008 to 10.06.2008	B	4	8	0.36		0.1100	-0.2497	34.51	0.14	-1.4
CSWG 25	All data	-			21	0.67	-0.01091	0.3075	-1.3580	37.80	0.48	
	Spring 04 (Oct)	18.10.2004 to 01.11.2004		5	14	0.60	-0.00175	0.2264	-1.2380	38.30	0.46	1.2
	Summer 05 (Jan)	21.01.2005 to 03.02.2005	A	5	15	0.70	-0.01873	0.4575	-1.9950	36.94	0.51	-0.4
	Winter 08 (Jun)	06.01.2005 to 20.01.2005	B	9	21	0.61	-0.01431	0.4907	-4.1350	49.11	0.47	-0.7

Third International Meeting On Wind Turbine Noise Aalborg Denmark 17 – 19 June 2009

Case Study: Wind Turbine Noise in a small and quiet community in Finland

Carlo Di Napoli, Pöyry Energy Oy
Tekniikantie 4 A, 02151 Espoo, Finland
carlo.dinapoli@poyry.com

Abstract

I work as a noise consultant in an engineering and consultancy company (Pöyry Energy Oy) in Finland. This particular case study came to my attention in 2007, just before the second WTN conference in Lyon. The Finnish wind turbine projects have been relatively small compared to the situation in other European countries and have comprised many sites with only one to three installed turbines.

This particular site is located at the west coast of Finland in a small community with local residents and many vacationers with summer cottages, which are located close to the sea shore. Site has just one pitch regulated 1MW wind turbine and the closest resident has a summer time vacation cottage at about 750 m distance from the turbine. Over 20 vacationers have summer cottages close to the shore line within a range from 750 m to 1,3 km from the turbine. After the turbine start up, the turbine owner received many complaints of turbine noise from the vacation residents, but not from the nearest permanent residents.

Overnight noise measurements were performed in windy conditions in a downwind location. Measurements and sound propagation modelling revealed that wind turbine noise has to be measured in a specific weather condition in order to estimate the full impact of the sound level at immission points. No specific wind turbine noise measurement or modelling rules exists in Finland (yet), which made it also difficult to perform straight forward comparisons against national noise regulations. This case also revealed the importance of correct sound level estimation for a wind turbine park in pre-engineering phase in order to minimize the developer's own risks for further complaints.

1 Introduction

Wind power production has been quite limited in Finland and the current total capacity of 143 MW (300 GWh) is still very small compared to many EU countries. However there are large potential areas for off-shore production in the Baltic sea and in Finnish Lapland (total estimated capacity potential of about 19 TWh). Current installations are mainly located at the west and south coast of Finland, some wind parks are also located in Lapland where anti-icing blade systems has been tested for several years in rather rough climatic conditions. Current typical installations include only 1-5 turbines except the latest near-shore installations. Along The Finnish coast line there are over 40 000 small islands which dominate the landscape in some particular areas. Not surprisingly the coast line is also popular for it's recreational value with thousands of summer cottages located here and there. This particular case is located at the west coast close to the coast line in a small community with many holiday residents, who typically spent their time only in the summer in this community. The distance to the closest holiday residents is about 750m from the 1 x 1MW pitch regulated wind turbine with the tower height of 66m.

2 Initial Status

I work as a noise consultant in Engineering and Consultancy Company (Pöyry Energy) focused mainly to power industry and Wind Turbine Noise (later "WTN") issues have been one (interesting) part of my total work field. Before this project came to my attention in 2007, the wind turbine owner had already made once the immission noise measurements by using another company based on the noise complaints of local holiday residents. However, the local environmental office rejected the first test report and the measurement results arguing, that the noise measurement was done with methods too simple for proper verification of WTN (although no specific national WTN immission measurement rules exists) and issued new measurements to be performed with measurement plan included. After negotiations with owner and other participants, I received the measurement project and started working with the measurement plan. This work phase also included reviews of the initial material including the rejected noise report and a short environmental study prepared prior to the Wind Turbine installation mainly as an appendix in the construction permit papers. After reviewing the material, it soon became clear that that environmental study and the first measurement were done lightly with many errors or just without proper knowledge of the substance issues related to wind turbines not mentioning the complex WTN.

No specific WTN immission measurement rules exist in Finland (yet). Therefore I had to adapt new measurement instructions to the measurement plan, which included instructions for simultaneous night time (22-07 o'clock) sound power measurement at "IEC" point and downwind sound pressure measurements at immission point with highest possible wind conditions in order to test the sound power level of the installation and at the same time to test influence of the night time atmospheric stability to sound propagation and background sound levels./1/ The plan was accepted by the authority and other parties involved and the project could move on to the measurement phase done in mid August on 2007 after forecasting the proper weather conditions.

3 Measurement Phase

The turbine is located on top of a small hill (23 m above the sea level) and the coast line (with many summer vacation cottages) including a small harbor is located of about 900 m north to northwest from the turbine.

Picture 1. Turbine seen from the sea

The complete measurement project was still scaled as "small" with only one overnight measurement. Sound power equipment together with immission point sound pressure level equipment was put on place in the afternoon. The weather condition was perfect; plenty of wind (peaks of 13 m/s) from prefect direction after a low pressure area and especially it's center was just moved to north east over the project area.

3.1 Sound Power Measurement - Surprises Ahead

The sound power test was considered to test the actual in situ sound power of the constructed turbine, although it was clear that the turbine type was tested thoroughly with IEC type tests prior to this test. This measurement method also gave the opportunity to make sound attenuation comparisons with and basic sound pressure results (e.g. logged L_{Aeq}, L_{AFmax}, L_{AFmin} results) measured simultaneously at immission point.

Right after the first equipment tests and after the start of the first official test, the prevailing wind speed accelerated to a level over 10 m/s at the nacelle height. To my surprise, the turbine tower started to resonate with a frequency of about 40 Hz (was clearly visible in live 1/3 octave spectrum) and a loud and low “rumble” structure borne sound started to emit from the turbine. The resonance strength, which was clearly the tower natural resonance frequency, was highly depended on the wind speed (blade rotational speed) and thus could be heard again whenever the wind speed increased above 9-10 m/s. Data-analysis showed later, that the frequency range was wider and at A-weighted 1/3 spectrum, two 1/3 octaves were about 5-10 dB above the “normal” level of that particular frequency range. This phenomenon did not appeared later in the night as the wind speed decreased below 10 m/s at the nacelle height.

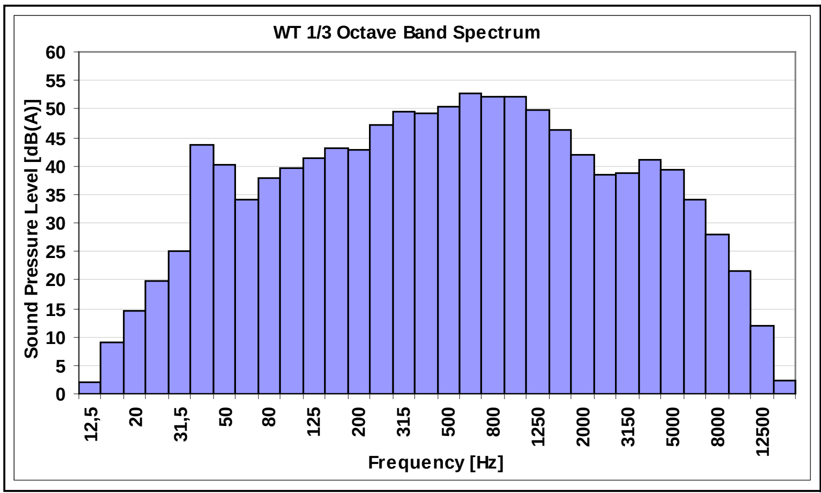

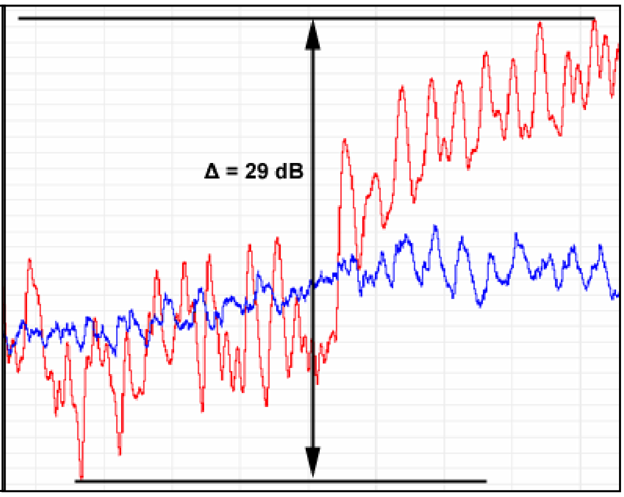

Picture 2 (on left): Basic A-weighted 1/3 octave spectrum. Picture 3 (on right): Sound recording revealed that the total sound level increase was about 30 dB, when wind speed exceeded the “limiting” level. Blue curve is the basic A-weighted amplitude modulated sound at “IEC” point and red curve is the filtered frequency of 40 Hz in dB(C).

Another low frequency noise peak was found later during data-analysis, but not heard easily at site. The source of the second low frequency noise peak of 31,8 Hz was not found in this measurement session.

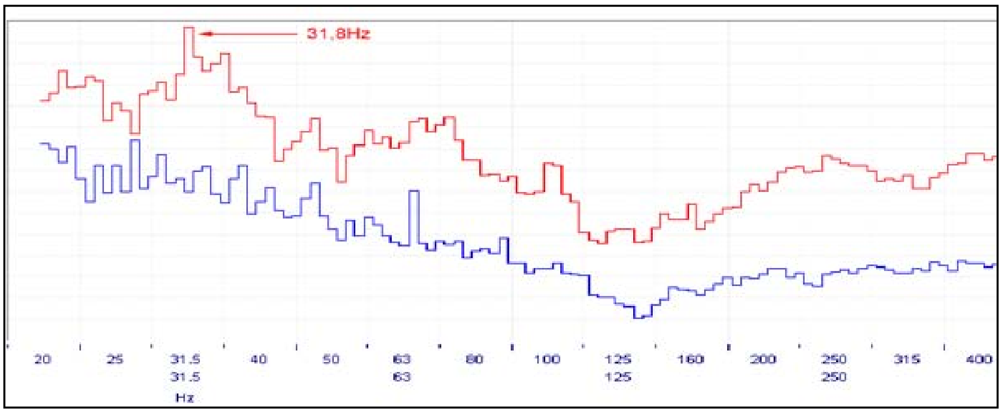

Picture 4. Red Curve: L_{pL} 1/24 octave band sound spectrum values of sound recordings at immission point measurement when wind turbine was on. 31,8 Hz had a sound pressure of 42 dB(L). Blue Curve: Background 1/24 octave band sound spectrum at immission point. The time difference of both these measurement is 10 minutes.

The wind turbine was shut down 3 times during the whole measurement period to test background sound level of sound power and immission measurement points. The sound power measurement point was found to have no wind induced sounds, the background sound included only the humming sounds of nearby trees. The LAeq background sound difference to the sound pressure level of nominal rotational speed (about 25 rpm) was 25 dB, although most of the time during afternoon sound power measurements, the average wind speed at nacelle was 9-10 m/s. Measurement revealed, that the turbine sound power level increases rapidly in the lower wind speeds (about 5,5dB per 1m/s) and then stabilizes to a constant level of LAeq = 106-107 dB(A) in the higher speeds (7-12 m/s). LAFmax values were permanently about 3 dB higher than LAeq values throughout the measurement.

3.2 Immission Point

The main immission point measurement was 530m away from the turbine. Between the turbine and the immission point, there was mainly rock based landscape with a thick layer of undergrowth above it and in the middle a drainage swamp surrounded with thick fence of bushes and trees.

Main goal of the immission measurement was to verify the sound propagation during night time in full downwind conditions and to test the current applicable sound prediction models, especially the influence of the ground absorption. Therefore it was decided to measure the whole session in this particular point, although the point was not very close to any local holiday residents. Other immission point sound levels were decided to solve by sound propagation modeling.

Logged immission point sound levels varied from 51 dB(A) to below 30 dB(A). During turbine shutdowns, the background sound was measured to vary between 29-34 dB(A), so even this point has hardly any wind induced noise nor any other background sounds except the sounds some of humming trees closer to the turbine.

The wind speed decreased slowly (3,5 m/s at nacelle height at 6:30 in the next morning) and direction turned during night time but the best “steady state” wind speed (and thus sound power level) with optimum downwind direction was measured in the evening. A three hour continuous measurement LAeq results was 43 dB(A) although the measurement continued during the whole night. The simultaneous sound power level was about 106 dB(A), so the total attenuation was 63 dB. Sound pressure at that time at the IEC board was about 60 dB(A), so the sound pressure difference was about 17 dB(A). The total night time (22-07) LAeq was 39 dB(A).

Logged LAeq (and LAFmax and min) values were compared to the IEC board sound pressure levels in order to prove the immission point noise source. The congruity of sound was visible especially in LAeq values.

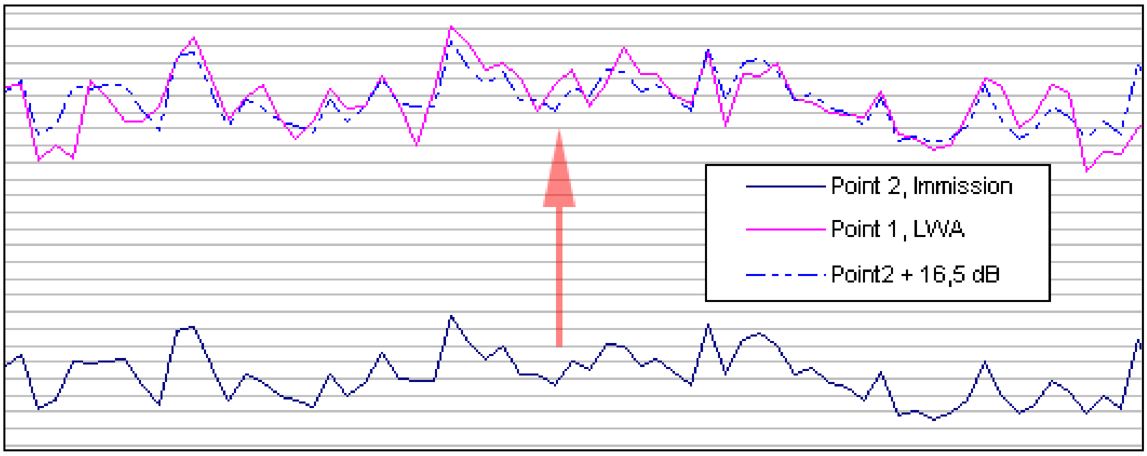

Picture 5. The congruity of sounds

3.2.1 Amplitude Modulation of Sound

Amplitude modulated sound (later “AM”) was recorded with 16bit, 44 kHz sound recorder later in the evening. Data-analysis revealed that the sound level during recording time (24:00-01:00) changed rapidly along with changing wind speed.

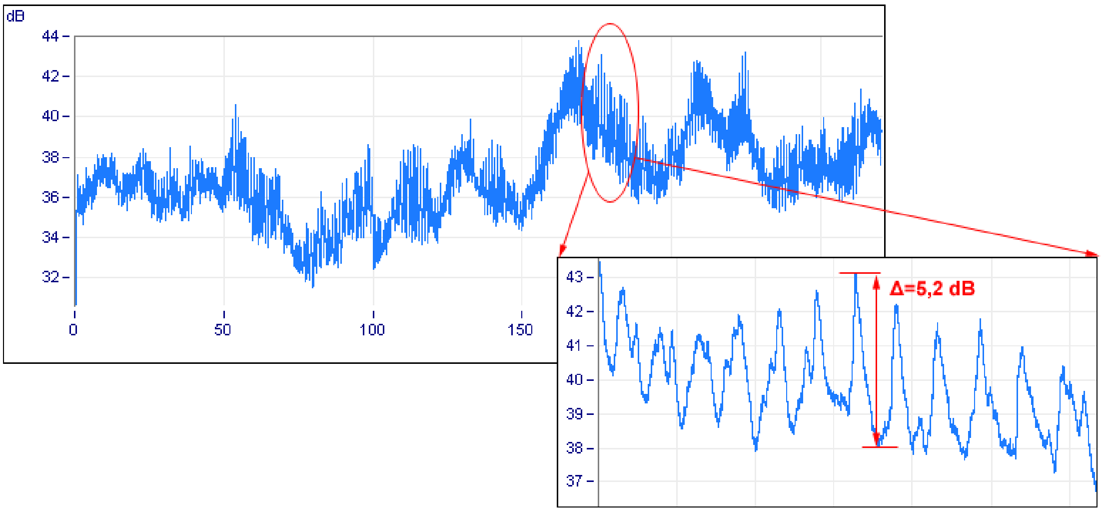

Picture 6. Amplitude modulation of WT sounds

The highest recorded AM strength was 5,2 dB (from bottom to top) and highest peaks were typically measured during decreasing wind speed or during the end of an wind speed acceleration and blade rotation speed. Also many double pulses were analyzed probably emitted from WT when the blade passed the tower at lowest rotational point. The AM pulse was visible in every recording graph in any wind condition, even at the lowest possible condition where sound pressure level of the turbine was about the same level as background sounds. During one recording session of just 3 minutes, the AM sound level changed 12 dB (bottom to top) at that time (it corresponds to wind speed change of 5 m/s).

4 Data Analysis, Modelling and Measurement Report

Measurement report was done few weeks after the measurement night which now included all the major results, the sound propagation models and final comparisons to the current valid guideline values for recreational areas during night time (LAeq = 40 dB(A)). Current practice of result comparison includes a thorough analysis of measurement uncertainty, which was done to both measurement points.

4.1 Sound Propagation Modeling

Nordic Prediction Method is widely used in Finland (DAL32) for calculating the sound propagation for any sound sources. Typically this is done by using modern GIS based computer models with more or less detailed terrain models including buildings. Ground absorption is typically set to zero, so for majority of sound sources, the calculated immission point values are higher than averaged values. This is then corrected (or not) by different environmental correction methods depending on the final target of the modeling project.

In the initial environmental study, the border of the LAeq 40 dB(A) was though to have a distance of 250 – 400m to the turbine with no other information given.

Below is a summary on different model results to this case. The calculated value represents a result with one wind speed point at rated level of 8 m/s at 10m.

Table 1. Sound propagation modeling results to point 2 (530m from the turbine) in different cases

Cases	ISO 9613	DAL 32	ISO 9613 + Concawe**	Simple Propagation Model for WTN /2/
Case 1, GA* = 0	42	42	47	46
Case 2, GA = 0,5	39	39	44	43
Case 3, GA = “real”	38	39	43	43

* GA = “ground absorption”, ** = Concawe weather correction, stability class D, corrected wind speed and direction “as measured”

The calculated results show clearly, that for basic prediction and for short distances, standardized point-to-point (without sound ray “curvatures”) models can give reliable results but only if the ground absorption is set to zero (no attenuation). If more fixed and realistic ground absorption is used, basic WTN noise model (1/3 octave band) and ISO with Concawe weather correction (Pasquill stability class D was used with corrected wind speed and wind direction) gave good results as well compared to the measured results. Other important immission points were calculated based on the ISO+Concawe model, as the GIS based program gave opportunity to create special areas for ground absorption. The total calculation area was well known and thoroughly mapped.

4.2 Comparisons with Guideline Values

Only the calculated immission values close to every noise sensitive holiday residents were compared to the national guideline values (which in many cases are understood as limit values), so this time an indirect method was used. It quickly became clear, that two different LAeq values had to be used, one with nominal wind speed (downwind condition, “as measured”) and one with averaged wind speed with correction for wind direction for the whole summer period (when most of the holidaymakers are present)./3/ For this data, more measured wind data was received from the client representing the wind direction and speed distribution in the whole area at nacelle height. Most of the LAeq values with averaged night time wind speed for the whole summer period, especially after uncertainty calculation, did go below the national night time guideline of 40 dB(A) value for recreational areas. Downwind condition values (as measured) however went above in some cases, so in the end I had to conclude, that whenever the weather condition is favorable for sound propagation and sound production (enough wind speed to produce the sound power, low wind speed at the ground level to minimize the background sounds, downwind conditions), guideline values can be exceeded in vicinity of some summer cottages. Especially this is the case, when the “semi narrow band” structure borne sound is emitted during high winds, although the calculated sound energy of 40 Hz frequency at summer cottages is just 3-4 % of the total value after A-weighting.

5 Conclusions

This short measurement case revealed, that modern wind turbine has a potential for many types on noises, not only just aero acoustic AM sounds generated by rotating blades. The tower and it’s support may create a potential for low frequency structure borne sounds especially in higher winds, where the tower and rotational equipment stress load increases. Finland has typically difficult weather conditions during winter with heavy blizzards and cold and this issue might appear in the future, where turbine blade icing may cause different types of dynamic instabilities.

With even simple sound propagation models it was possible to predict downwind sound levels with reasonable accuracy. Commercial software’s can give more detailed picture of the total sound propagation area for short (up to 1-1.5km) distances.

The ever changing weather conditions also create noise verification difficulties during typical immission tests as the wind turbine sound emission and propagation is so heavily depended on the weather conditions. Therefore specific rules (national or international) for proper wind turbine noise measurement procedures (immission side) and especially interpretations against the guidelines would harmonize the results, as the weather conditions are almost opposite (there must be wind in order to produce the sound power) to the conditions limited by the current national noise measurement rules (max wind limit of 5 m/s etc). /3/

References

/1/ van den Berg, G.P. The sounds of high winds. Elsevier Science Direct, University of Groningen, Netherlands 2006.

/2/ Ljud från vindkraftverk, raport 6241. Naturvårdsverket, Sverige, december 2001.

/3/ Guidelines for Environmental Noise Measurement. The Finnish Ministry of Environment, publication 1/1995.

Third International Meeting
on
Wind Turbine Noise
Aalborg Denmark 17 – 19 June 2009

The Parabolic Microphone for Directional Measurements on Wind Turbines

Lars Enggaard, DELTA
Erhversvej 2a, 8653 Them, Denmark
len@delta.dk

Abstract

The parabolic microphone has earlier been used for measuring noise from wind turbine blade sections. In connection with an investigation of noise from wind turbines in partial wake DELTA has designed a parabolic microphone and improved the performance by using a directional microphone together with a larger reflector. The principles behind the parabolic microphone are presented and perhaps some measurement results.

Index terms – Parabolic Microphone Measurement System (PMMS)

Introduction

The new parabolic microphone measurement system has been designed in relation to the project EFP07-II "Noise Emission from Wind Turbines in Wake” [1] which is about noise measurements on blade sections on full scale rotors. DELTAs part of the project is to measure the noise using the PMMS at approximately 100 m distance downwind on a full scale rotor in different degrees of wake. The PMMS results will be correlated with the results from high frequency surface pressure microphones mounted on one of the blades. These measurements are conducted by Risø-DTU.

The project is publicly funded by Danish Energy Agency under journal nr. 33033-0191 and co funded by DONG Energy, Statkraft Development, StatoilHydro and Vattenfall A/S. The project partners are DELTA (Project manager), Risø-DTU, EMD International and DONG Energy.

DELTA has improved the performance of the parabolic microphone by using a directional microphone and a larger reflector compared to earlier work [2]. The PMMS is presented in next section which describes the system more in details.

The new measurement system can for example be used to reveal local differences in the noise characteristics of different blades and different blade sections.

Description of the Parabolic Microphone Measurement System

The parabolic microphone measurement system is based on the properties of a parabolic reflector. A parabolic reflector amplifies the sound coming at normal incidence thus suppressing the sound coming from the sides. This gives the parabolic microphone its useful directivity which enables focused measurements.

The parabolic reflector is mounted on a trailer which makes it easy and fast to set up the PMMS for measurements. Figure 1 shows the parabolic microphone mounted on the trailer.

Figure 1: Parabolic microphone mounted on trailer. The microphone is placed in the focus point.

The reflector can easily be adjusted in all directions by use of its hydraulic system. The exact position of the reflector is indicated by two displays showing the azimuth and elevation angles. On the trailer board are mounted level tubes that make it possible to align the trailer horizontally by adjusting the four corner stands.

The PMMS is equipped with a telescopic sight which is used to locate the desired measurement spots on the wind turbine blade. The sight is adjusted for the present measurement situation. The procedure for the adjustment is explained later.

The parabolic microphone measurement system is a multi channel system. The software part of the system is programmed in LabVIEW and developed by DELTA.

The inputs of the system are:

- 4 acoustic inputs (parabolic microphone, +6 dB ground board measurement and two optional acoustic inputs)
- 3 trigger inputs. The PMMS is designed to work with trigger inputs to distinguish between the three blades on the rotor. One trigger for each blade. The trigger is used to find the relevant time window for a blade passage.
- 5 input from the wind turbine system (Power, nacelle wind, pitch etc.)

Directional Microphone

An improvement of the PMMS is the use of a cardioid microphone placed in the focus point of the parabolic reflector pointing towards the dish. The reason for choosing the cardioid microphone is because of its suppression of the direct sound on the PMMS. It minimizes interference patterns since the direct sound will be attenuated and mainly the normal incidence reflections on the dish will be measured.

Larger dish

The directivity of a parabolic reflector is dependent on its physical size. Generally a parabolic reflector has a small aperture angle at high frequencies while it becomes larger with decreasing frequency. The designed PMMS uses a dish having a diameter of 2.4 m instead of a dish of 1.8 m used earlier at DELTA [2]. The improvement of using the larger dish is that the parabolic reflector microphone will be more capable of focusing at a given point at the wind turbine blade.

Test the PMMS directivity

The directivity of the PMMS has been tested at DELTA. The PMMS was placed 22 m away from a loudspeaker sending out pink noise. Figure 2 shows the results. The angles are off-axis angles and the curves are all normalized to the on-axis response.

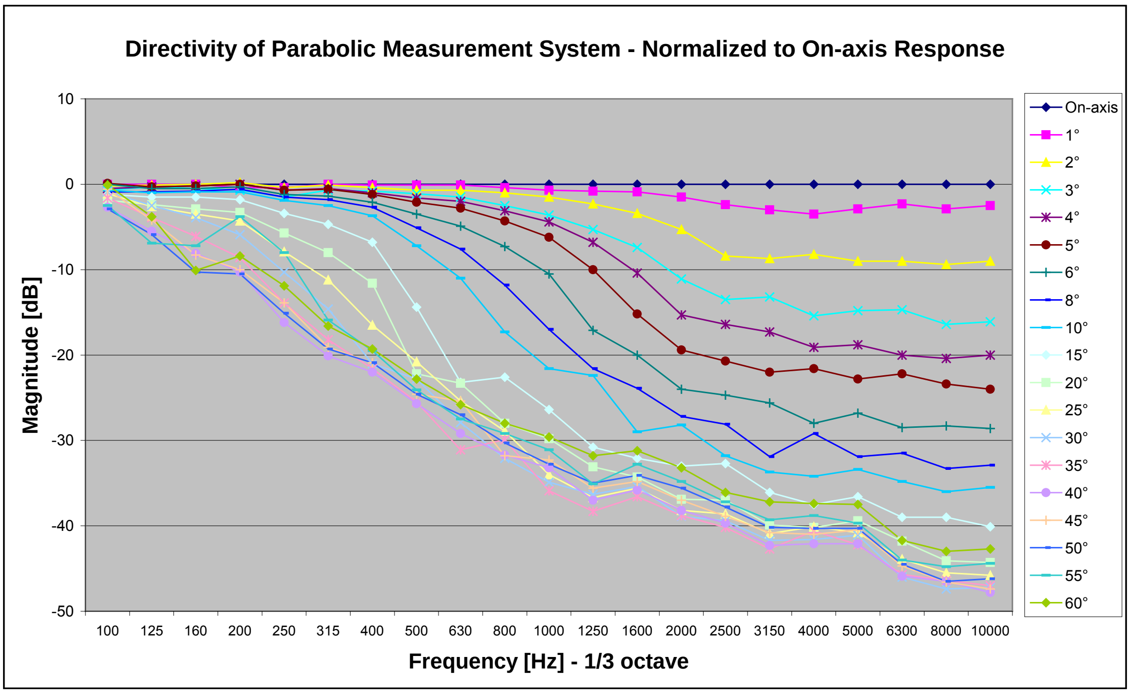

Figure 2: Directivity of the parabolic microphone measurement system.

It is seen from figure 2, that the directivity of the PMMS varies with frequency. The system is therefore not expected to be useful at lower frequencies. Figure 3 shows the aperture angles of the PMMS related to the 1/3-octave filter band damping. The aperture angle equals two times the off-axis angle from figure 2.

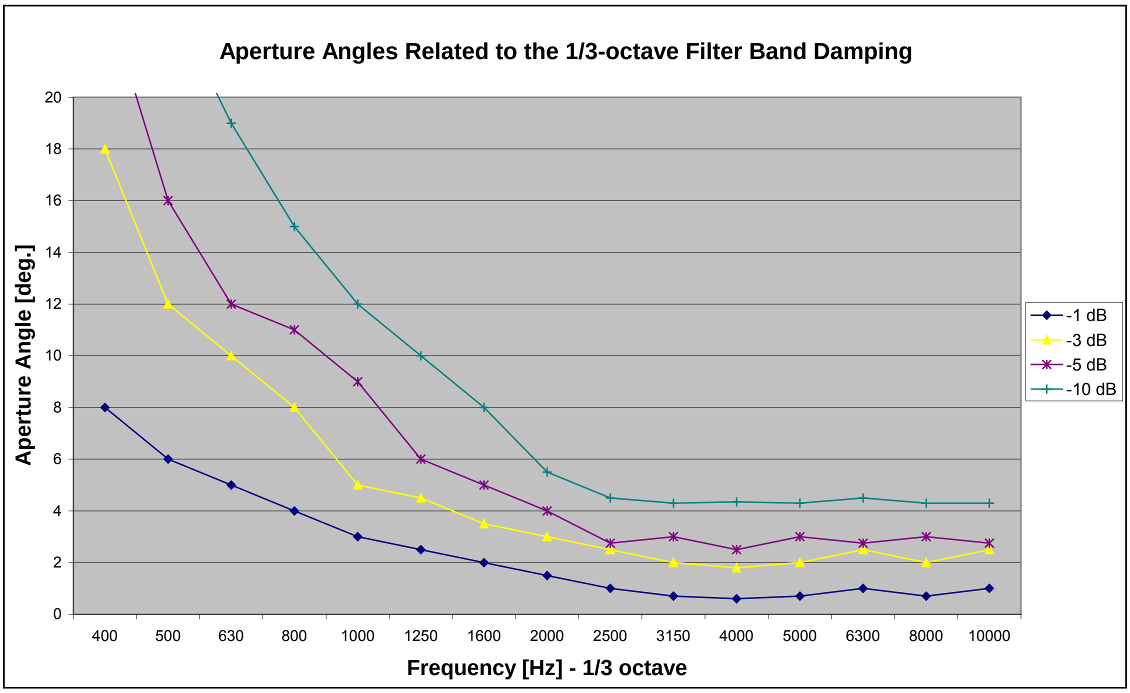

Figure 3: Aperture angles of the parabolic microphone measurement system.

For example, the PMMS has an average aperture angle of ~ 3° related to a 3 dB damping if the frequency range of the blade noise is expected to reach from 1 kHz – 4 kHz. The diameter of the measurement area for the PMMS with an aperture angle of 3° is approximately 5 m at a distance of 100 m. A similar figure for the old parabolic microphone of 1.8 m is presented in figure 4.

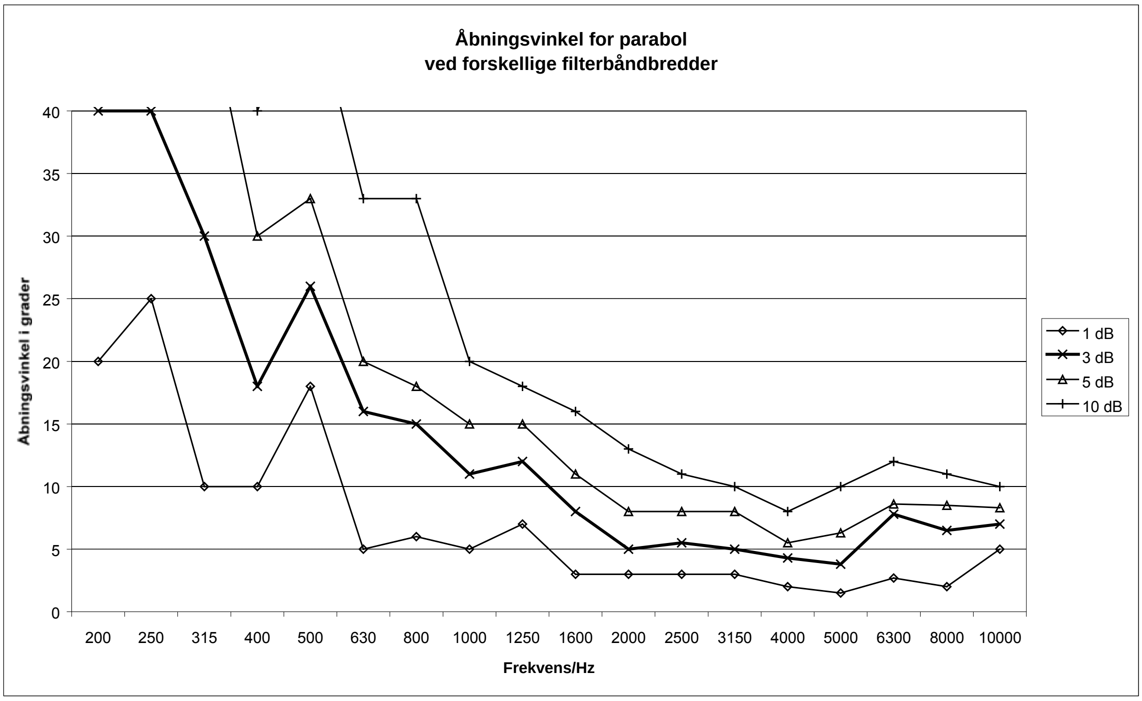

Figure 4: Aperture angles for the old parabolic microphone of 1.8 m related to the 1/3-octave filter band damping [2].

The parabolic microphone of 1.8 m has an aperture angle of approximately 7° for the same situation. The diameter of the measurement area for the 1.8 m parabolic microphone with an aperture angle of 7° is ~ 12 m at a distance of 100 m.

Aiming of the PMMS and Gain Measurement

One of the issues to deal with using the PMMS system is the aiming of the parabolic microphone. The first thing to ensure is that the parabolic microphone points at the desired target from an acoustical point of view. The procedure is to place a loudspeaker at the top of the nacelle sending out pink noise and afterwards adjust the parabolic microphone to point at the loudspeaker. This can be difficult because of the fast meteorological variations which cause the noise level to move up and down especially at high frequencies.

To overcome this problem DELTA has designed a procedure that reduces the disturbance of these level variations when aiming the system. The method is based on a subtraction of a standard ground board measurement from the parabolic microphone measurement in a chosen filter band. The two measurements both contain the level variations due to the meteorological conditions. Therefore only the variations in level due to the gain of the parabolic microphone are left. By listening and maximizing the level difference in the chosen filter band between the parabolic microphone and the ground board measurement it is easier to aim the parabolic microphone correct. The frequency of the used filter band should not be chosen to low because of the low directivity of the parabolic microphone at low frequencies. Neither should the frequency be chosen to high because of the sound disturbance due to the meteorological variations. From figure 3 it is seen that the directivity generally starts to get lower beneath approximately 2 kHz. Therefore a filter band with a centre frequency of 2 kHz is the preferred choice when aiming the system acoustically.

The telescopic sight is adjusted to point at the loudspeaker when the PMMS is pointing at the loudspeaker. Afterwards the telescopic sight is used to navigate to the given measurement spot.

The gain of the PMMS is determined as part of each measurement campaign by use of the loudspeaker on top of the nacelle and with reference to the +6 dB ground board measurement which will be correct for. The gain is afterwards used to correct the PMMS measurement when absolute sound pressure levels are required as free field results.

Alternative to Phased Microphone Array Technique

The PMMS is a low cost alternative to the phased microphone array technique. The array technique uses several microphones when the PMMS uses only one microphone. The microphone arrays are big and are therefore more time consuming to set up.

The phased microphone arrays measure the noise from the entire rotor plane at once. This way, the noise distribution in the rotor plane is measured dynamically. Afterwards, the delays between the microphones can be set to steer around the main lobe of the system.

The PMMS measures one spot at the time on the blade. Therefore the measurement spot has to be moved in steps to cover an entire blade or rotor plane. The measurement results from a blade section are therefore an average of several time windows where the blade passes the focused measurement area of the PMMS.

Conclusions

The parabolic microphone measurement system can be used to measure noise from wind turbine blade sections and reveal information of the differences in the noise characteristics. The system can also be used when comparing the noise from different blade designs.

The PMMS is based on a one-microphone technique and is thereby a low cost alternative to phased microphone array setups. The parabolic microphone has been improved by a larger dish having a diameter of 2.4 m together with a directional microphone. The larger dish and the microphone both improve the directivity of the system.

The PMMS has an average aperture angle of ~ 3° related to a 3 dB damping if the frequency range of the blade noise is expected to reach from 1 kHz – 4 kHz. The diameter of the measurement area for the PMMS with an aperture angle of 3° is approximately 5 m at a distance of 100 m.

The old parabolic microphone of 1.8 m has an aperture angle of approximately 7° for the same situation. The diameter of the measurement area for the 1.8 m parabolic microphone with an aperture angle of 7° is ~ 12 m at a distance of 100 m.

A recording and analysis software program has been developed and designed in parallel with the construction of the parabolic microphone.

References

[1] Project application, EFP07-II "Noise Emission from Wind Turbines in Wake", J.nr. 33033-0191, DELTA, Risø-DTU, EMD International, DONG Energy.

[2] "Measurement of Aerodynamic Noise From Wind Turbines" (in danish), 2001-03-28, project nr. 12016, UVE-project j. nr. 51171/97-0005, Bent Andersen, Bo Søndergård.

Third International Meeting
on
Wind Turbine Noise
Aalborg Denmark 17 – 19 June 2009

A study of the seismic disturbance produced by the wind park near the gravitational wave detector GEO-600

Irene Fiori[1], Lara Giordano[2], Stephan Hild[3], Giovanni Losurdo[4], Emanuele Marchetti[6], Gillian Mayer[3], Federico Paoletti[1,5]

(1) European Gravitational Observatory, S.Stefano a Macerata, Pisa, Italy;
(2) University of Salerno, and INFN sez. Napoli, Italy;
(3) Albert Einstein Institut and University of Hannover, Germany;
(4) INFN, sez. Firenze, Italy;
(5) INFN, sez. Pisa, Italy;
(6) University of Firenze, Dept. Of Earth Science, Italy.

Irene.Fiori@ego-gw.it, Federico.Paoletti@ego-gw.it

Abstract

Noise emissions from wind turbines might disturb the operation and deteriorate the sensitivity of Gravitational Wave (GW) detectors. These detectors aim to an extremely precise measurement (of the order of 10^{-18}m) of the difference in path lengths between interfering light beams from two optical cavities. Seismic ground vibrations and air pressure waves in the low frequency might couple to the detector especially in correspondence to mechanical modes of the seismic isolation system. A wind turbine park exists in the vicinity of the German GW detector GEO-600 (near Hannover) and two parks are planned for construction close to the detector VIRGO in Italy (near Pisa) which has enhanced sensitivity to low frequency GW signals. We have studied some characteristics of the seismic noise emission of the wind park near GEO-600, and developed a simplified model of the attenuation of the seismic wave. We used the model to predict the excess seismic noise that a wind park might produce near VIRGO, and to set a safety distance from the detector for the location of the new wind parks.

Introduction

Several detectors are nowadays operative to reveal the space-time deformations which, according to Einstein theory of general relativity, are produced when large massive objects undergo fast acceleration variation. Detectable gravitational waves are expected to be produced in astrophysical processes, like supernova explosions, coalescence of binary systems, spinning neutron stars. A class of GW detectors works on the principle of the Michelson interferometer [1]. A laser beam is split in two by a semi-reflective mirror. The two beams are made to resonate in two long orthogonal optical cavities (arms) consisting of one pair of “free falling” mirrors. A gravitational wave would cause a differential variation of the length of the two arms (one stretches a tiny bit, while the other compresses). This results in a phase difference of the two beams which is measured with a photodiode looking at the interference of the beams out of the two arms. Detectors of this kind are: GEO-600 in Germany, VIRGO in Italy, LIGO detectors in USA, TAMA in Japan [2]. These are able to measure a length variation of the order of 10^{-18}m over a 3km distance, and over a frequency band of 10Hz to 10kHz. Second generation detectors, now in construction phase, aim to measurements at least ten times more accurate.

Optical cavity mirrors and benches (carrying optics used for readout and control) are decoupled from ground through seismic isolation systems. These are typically effective above about 10 Hz. Intense low frequency seismic noise might overcome the isolation system and deteriorate the detector sensitivity. A major concern is that low frequency periodic disturbances might match and excite the low frequency modes of the isolation systems, seriously compromising its operation.

In 2004 the EGO laboratory (hosting the VIRGO detector) was notified that two wind parks were planned for construction in its vicinity (few km away from VIRGO experimental buildings). A concern arose about the possible effects of such plants on the detector operation. In particular, the EGO laboratory was interested to asses which would be the effect of such plants in terms of increase of the local anthropogenic background noise, and of the frequency content of the noise which might match critical resonant modes of VIRGO.

A work by Schofield (2001, [3]) had shown that wind turbines produce intense low frequency seismic disturbances that might be still effective (above the local anthropogenic seismic background) at considerably large distance (10-20 km) from turbines. This is confirmed also by the comprehensive and detailed work by Style (2005, [4]) whose report is successive to the time of our study.

Indeed, the seismic excess as function of distance from the plant does depend on the absorption characteristics of the soil, i.e. its composition (rocks or limes) and on the anthropogenic background noise level. A wind park (“Schliekum”) does exist in the vicinity of the GEO-600 detector. Its effect on the site seismicity and on the detector had not been studied, although no significant effect had been ever noticed. However, the VIRGO has enhanced (ten times better) sensitivity in the low frequencies (10-100Hz) and a different isolation system design, and the impact of wind turbines noise might be more relevant.

The authors performed a study of the seismic noise emissions of the wind park near GEO-600. The soil composition of the GEO site (cultivated soil, and layers of lime and sand deposits) and its seismicity (industrial area, with high density population and road traffic) are similar to those of the VIRGO site. This fact permits a reasonable extrapolation of the data to the VIRGO case. Measurements were carried out during four days in July 2005. A first report was presented at [5]. The study had two main goals: (i) asses and quantify the presence of a seismic wave field from the wind park at the GEO site, (ii) derive a model of the seismic wave absorption which would permit to reasonably quantify the impact of the planned wind parks near EGO, and eventually to define a distance of respect from EGO for the turbines location.

Here below: Section 1 describes measurement location and equipment; Section 2 describes some characteristics of the wind park seismic emissions; Section 3 describes the study of turbines-induced seismicity at GEO site and measurements of the velocity of the seismic wave field derived from correlation measurements with an array of seismometers working in coincidence; Section 4 describes a measurement and modelling of the attenuation of the seismic wave with distance; Section 5 describes the use of the model to predict the turbine noise impact for VIRGO.

1. Measurement sites and equipment

The GEO-600 site is located 25 km South of the city of Hannover in Germany (Figure 1). The detector is surrounded by agricultural cultivated soils. Soil is composed, up to a depth of 20-50m, by lime and sand sediments. Figure 2 shows the site seismicity compared to Peterson LNM, which indicates it to be a relatively high seismicity site. The EGO laboratory site, hosting the VIRGO detector, is located 10 km from the city of Pisa, Italy. The EGO site characteristics are similar to GEO-600 with respect to all mentioned aspects. The seismicity of EGO site is depicted in Figure 2 as well.

The “Schliekum” wind park consists of 8 turbines placed at a distance of 220m to 370m from each other. Turbines are aligned approximately along the North-South direction, at an average distance of 1.0 and 1.6 km respectively from the GEO-600 North and Central experimental buildings (Figure 3).

Schliekum turbines are of different manufacturer and model and differ to some extent in size and power (Table 1). Common relevant features are: (i) a three-bladed rotor head mounted on a steel tower sitting on a concrete foundation; (ii) an active control on the blades pitch angle assure an optimal and constant power output against wind speed changes in the range from 3 to 25 m/s, outside this range windmills are automatically stopped to avoid damage or reduced efficiency. The blades pitch control changes the rotor speed approximately between 9.5 and 20 rmp; (iii) an active control of the nacelle yaw angle keeps the rotor head aligned to the wind direction; (iv) the power generator (asynchronous type, located in the nacelle) runs at variable speed between 700-1400 rmp [6].

Figure 1. Geographical location of the GEO detector (three house markers at center of figure) and wind parks around it: Schliekum wind park (red crosses) and other seven ones (green flag markers).

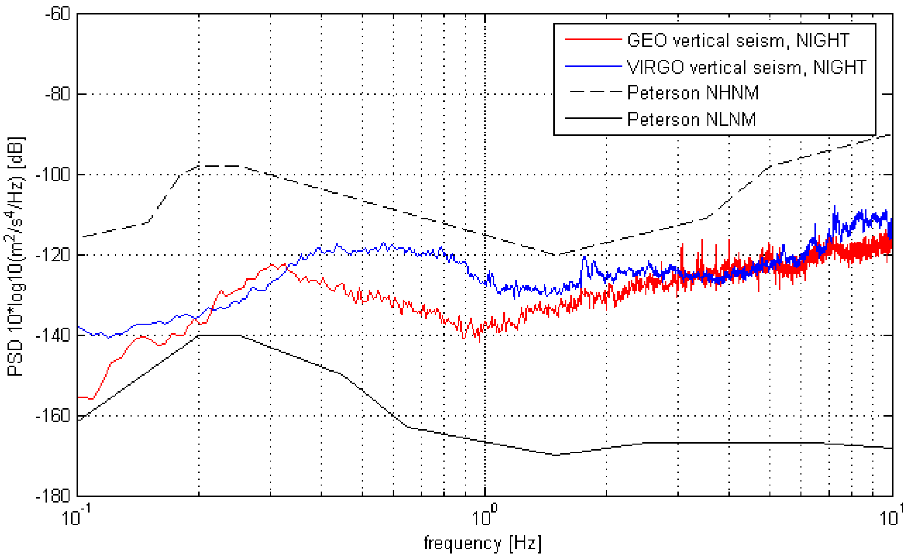

Figure 2. Typical vertical seismic spectra recorded at GEO-600 (red) and VIRGO (blue) experimental buildings during quiet night time periods, compared to Peterson Low and High Noise Models [7].

Manufacturer and Model	N. of turbines	Names	Power [MW]	Tower height [m]	Rotor diameter [m]
Nordex N90	3	Domink, Ole, Malte	2.3	100	90
Nordex S77	2	Daniela, Kerstin	1.5	85	77
EnronWind 1.5s	2	Lutz, Robert	1.5	85	65

EnronWind 1.5	1	Isabelle	1.5	85	65

Table 1. Tech. data of Schliekum wind turbines. Names have been assigned by us to identify turbines.

A first set of measurements aimed at the characterization of the seismic noise produced by the single turbines. Recordings were taken at the basement platform of each windmill using two geophones (Sercel L-4, 1Hz) laid along the vertical and one horizontal directions. Results are discussed in Section 2.

A second set of measurements aimed at the investigation of the seismic wave-field by the turbines. These data were recorded during July 25th through 28th 2005. We used: (i) two portable seismic stations, each consisting of one tri-axial low frequency seismometer (Lennartz 3D/5s, 100mHz), AD converter, hard disk, and GPS receiver; and (ii) three fixed tri-axial low frequency seismometers (STS2, 8mHz) permanently deployed on the floor of each GEO-600 experimental building. Seismometers were GPS synchronized, and the 3-axes were aligned along geographical NS, EW and vertical directions ($\pm 2°$). Seismometers were used for coincidence measurements described in Section 3.

We took our own record of the wind speed. We used one anemometer, positioned at 5m height close to GEO-600 central station. However, it is known that wind speed increases logarithmically with height up to some hundreds meters from soil. Therefore, the wind speed values we measured and we quote thorough this report note are systematically lower than wind speed at the turbine blades (80-100m height). Nevertheless, they provide a useful reference for correlation studies (see section 3); but in case we need to compare to wind turbines working set point a scale factor has to be considered.

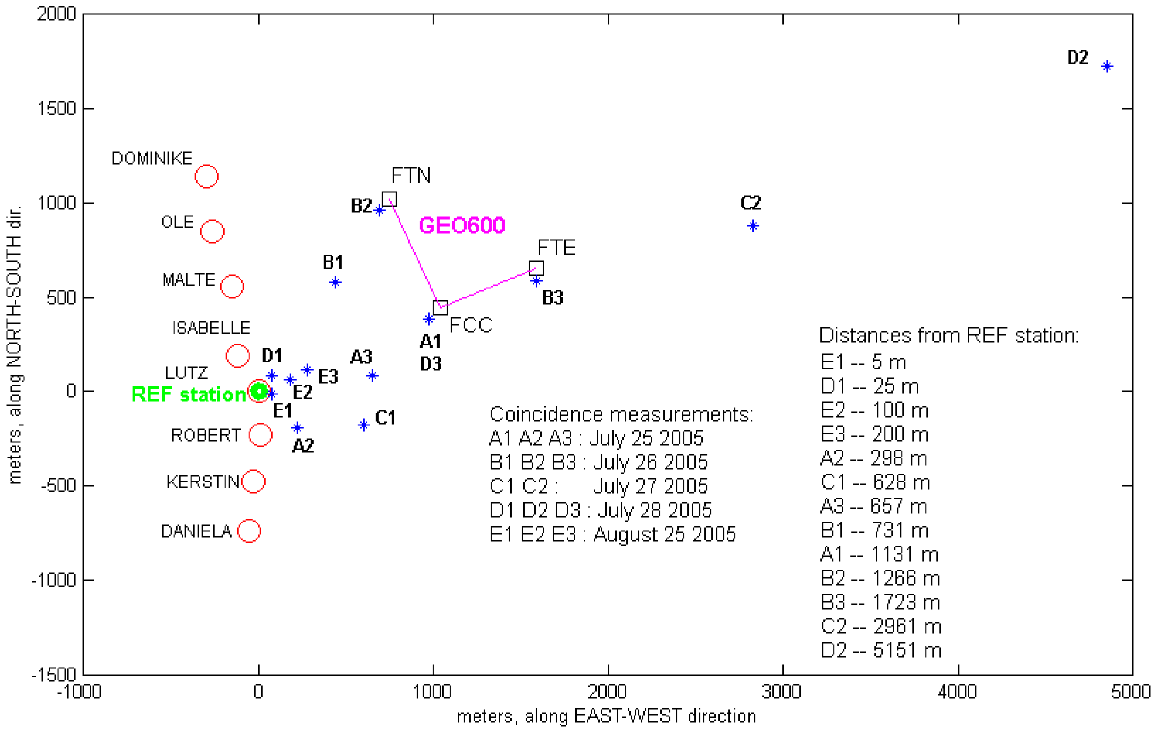

Figure 3. Location of: Schliekum wind turbines (red circles), GEO-600 experimental buildings (black squares), sites of seismic recordings (blue stars), and reference site at turbine “Lutz” (green circle).

2. Characteristics of wind turbine seismic emission

Seismic tracks recorded at turbine platforms contain intense and persistent spectral components which can be associated to structural or functional resonances of the windmills. Figure 4 shows the time evolution of the spectral composition of one seismic record. Figure 5 compares spectral composition of seismic records of different turbines. Figure 6 compares the spectral composition of tracks recorded during different wind speed conditions. Figure 7 shows seismic excitations associated to reorientation of one turbine head.

A family of equally spaced and stationary frequency components (we name “functional” peaks) are associated to the revolution frequency of the rotor (around 0.2 Hz) and to the rotor blade-pass frequency (three times the rotor frequency, 0.6 Hz) and its harmonics (1.2Hz, 1.8Hz, 2.4Hz, etc…). Peaks up to the 10^{th} harmonic are clearly distinguishable. Often peaks are broad. But sometimes, particularly in conditions of low wind speed, they are very sharp and steady (we suspect that this is associated to a peculiar regime of operation of the turbine feedback control but we do not have records of turbines operation status to investigate further). One intense, always sharp peak sweeping between 10Hz and 20Hz seems associated to the generator frequency (Figure 4, top). All these peaks sometimes do coherent sweeps (frequency changes up to 20%), which look associated to variations of rotor and generator speed (we hypothesize that this occurs when blades pitch angle changes to follow variations of wind speed or direction). Functional peaks disappear when the turbine is stopped (Figure 4).

A few other peaks persist when the turbine is stopped and never change their frequency: the most intense one is around 0.3 Hz (0.37 Hz for the two N77), less intense ones are at 2.5Hz, 4Hz and 6 Hz (Figure 4 and Table 2). These frequencies seem associated to turbine structural modes. According to a simulation study by Shaumann and Seidel [8] the 0.3 Hz frequency might be associated to the pendulum mode of the heavy rotor head and tower, and higher frequencies to flexural modes of the tower.

We took seismic records of the motion of all turbines base platform. We found the amplitude and spectral composition of records of same type turbines are indeed quite similar, while the frequency and shape of peaks differs slightly but significantly among different turbine models (Figure 5).

The root mean square (RMS) of seismic amplitude of the functional peaks increases proportionally to wind speed, and the scaling factor seems the same for all frequencies (Figure 6). Approximately a factor ten variation of RMS is associated to the operation of the turbine at different wind speed conditions within the working range. On the other hand, the amplitude of structural peaks looks independent on wind speed.

Intense seismic bursts with a typical exponential decay (decay time of 1 to 2 minutes) are produced when the turbine head is reoriented in correspondence of wind direction variations. A spectral analysis of the burst signals show that the structural modes are largely excited (2 to 5 times more than during typical conditions). Also some other frequencies (1Hz, 3Hz, and a few above) are excited, which might correspond to other structural modes not much excited during the normal turbine operation.

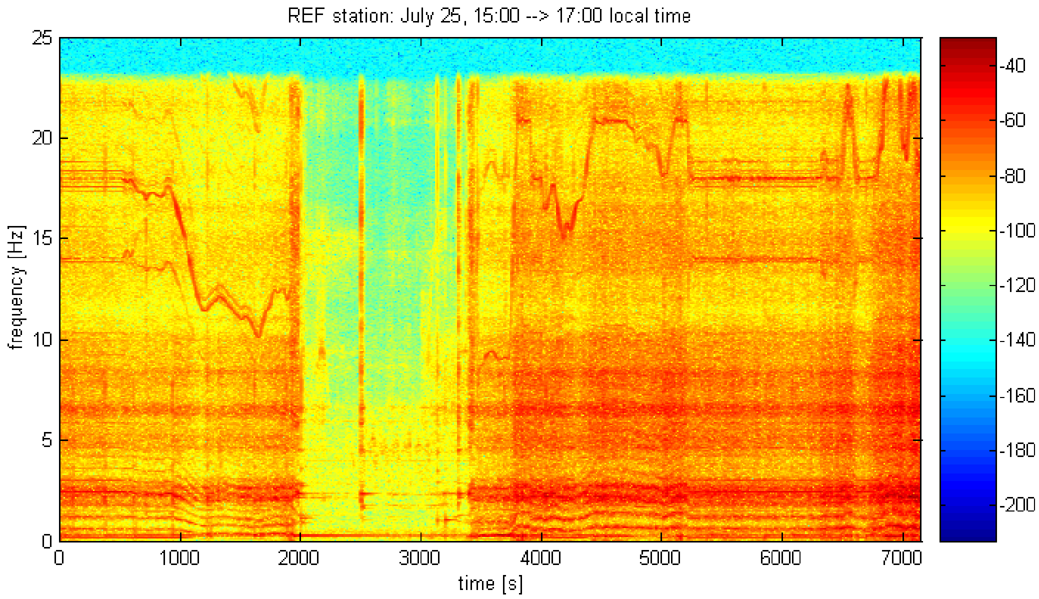

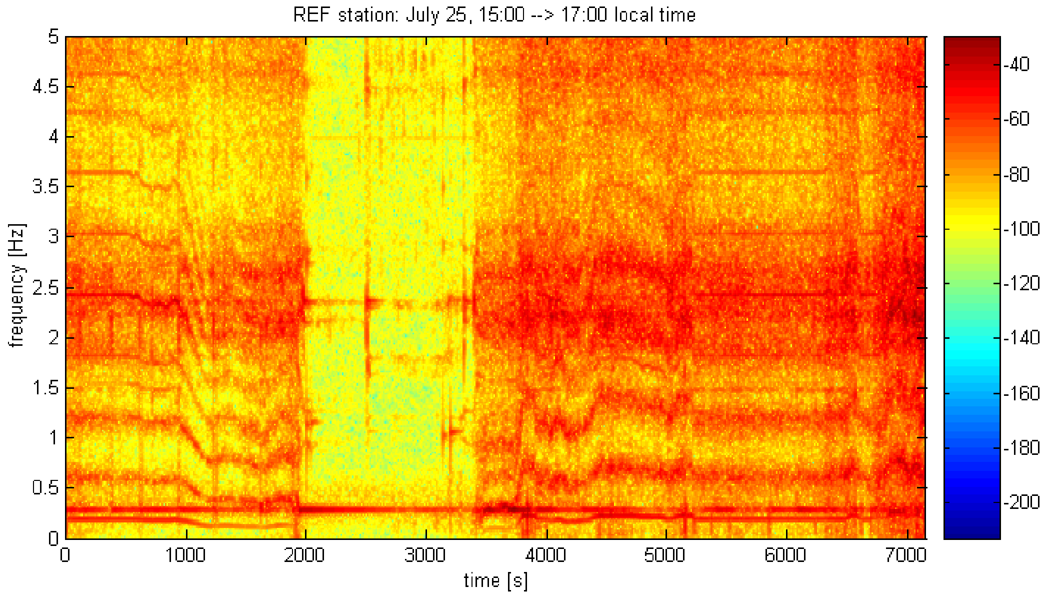

Figure 4. Spectrograms of 2hour seismic record at the Lutz base platform. In the period 2000÷3500s the turbine was stopped. The bottom plot is a zoom of the upper one in the 0÷5 Hz frequency region.

Turbine	Pendulum mode f_0 [Hz]	Flexural mode f_1 [Hz]
Nordex S77	0.37	2.45
Nordex N90	0.29	1.9
Enron Wind 1.5	0.29	2.3
Enron Wind 1.5s	0.29	2.2

Table 2. Measured frequency of the first and second structural modes of the four turbine models.

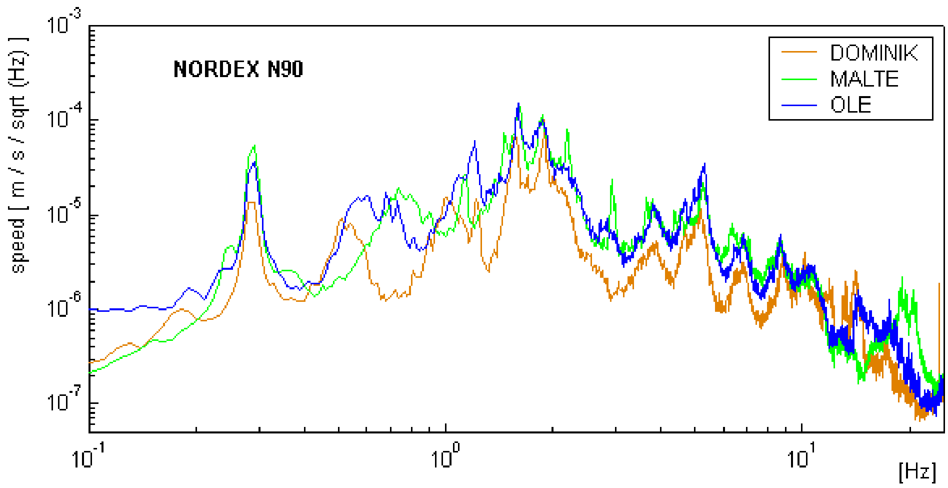

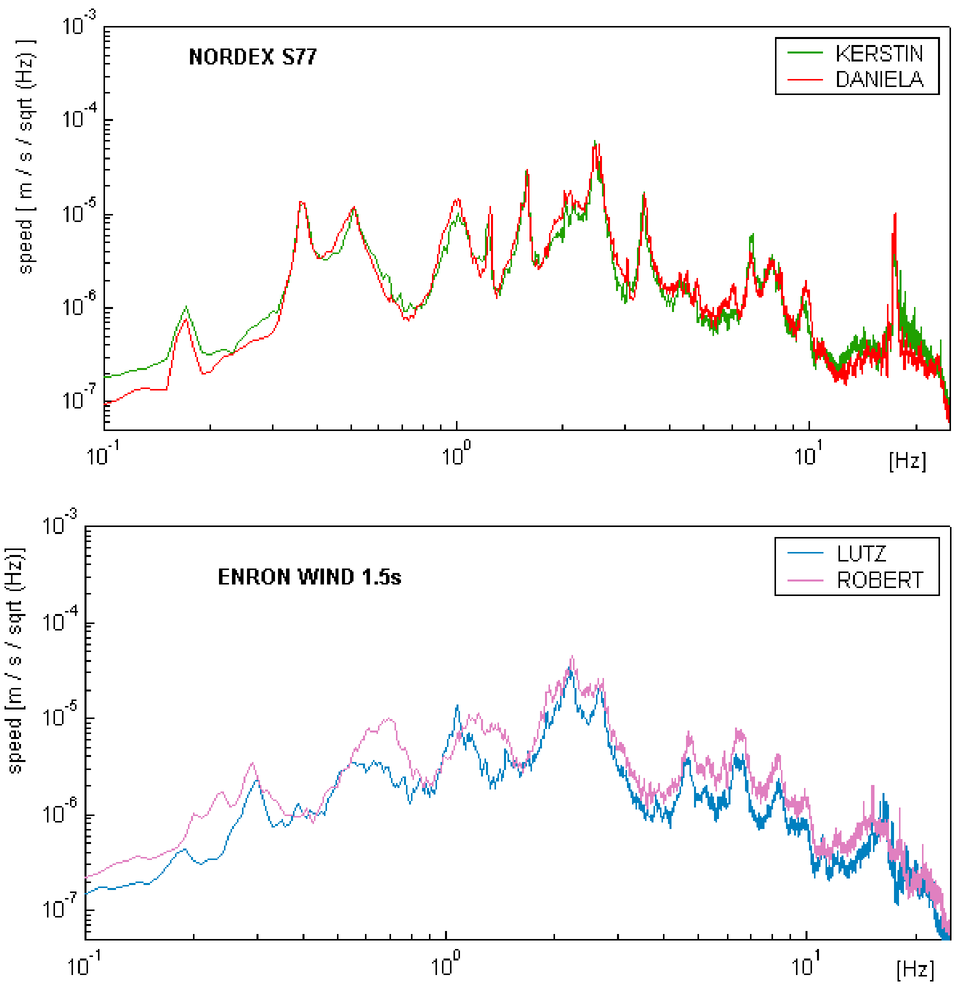

Figure 5. Amplitude of seismic vibration of turbines basement. Three turbine models are compared.

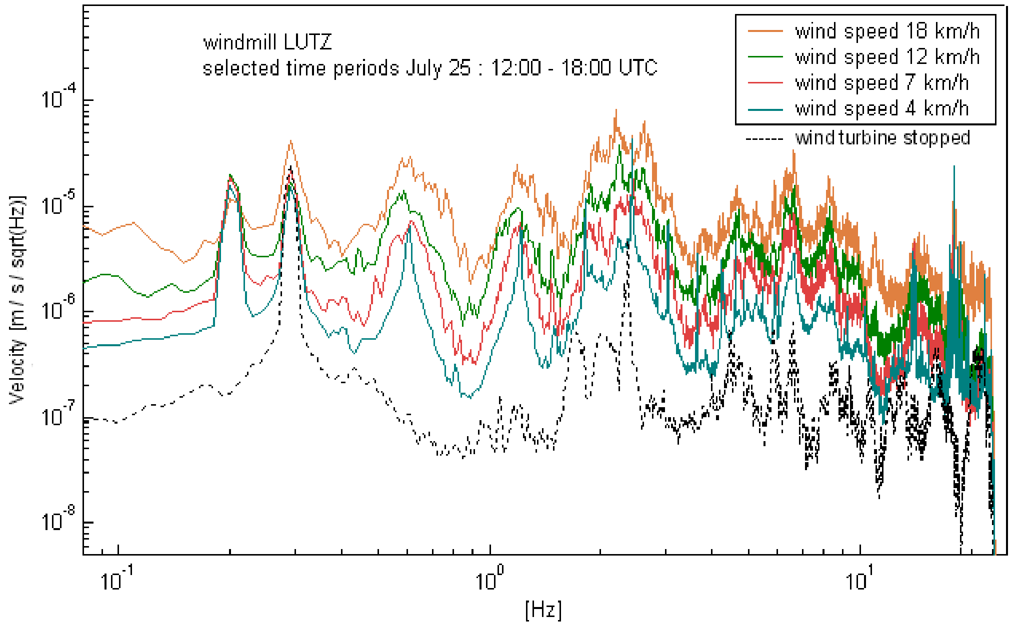

Figure 6. Solid lines are seismic amplitude spectra measured at Lutz base platform in different wind speed conditions; the dotted line is a measurement taken while the turbine was stopped. Quoted wind speeds are measured at soil level.

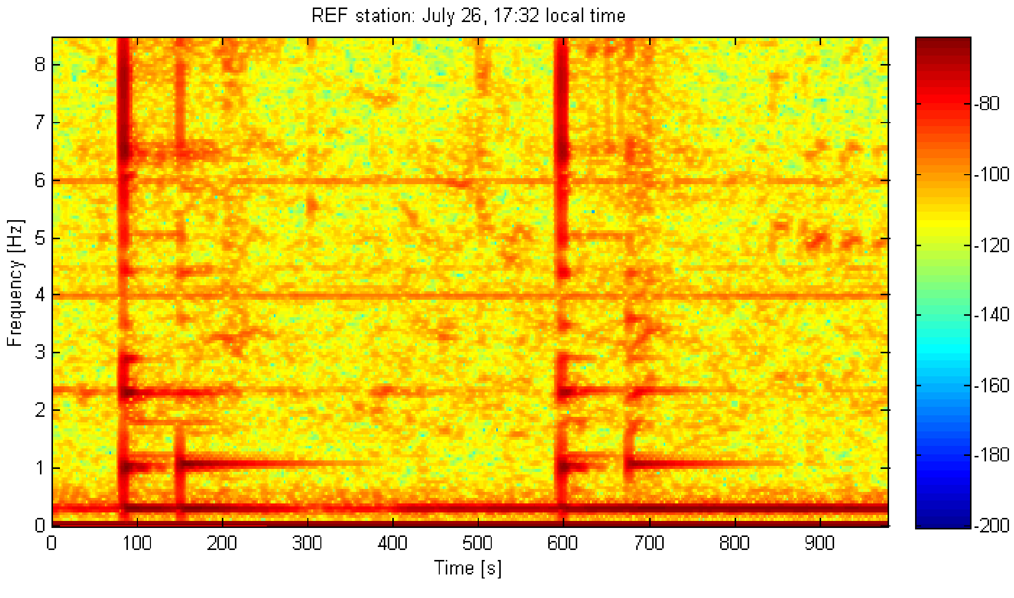

Figure 7. Spectrogram of a 15minutes seismic record at the Lutz basement. Temporary increases of seismic amplitude correspond to re-orientation of the turbine nacelle while the blades were stopped .

3. Characteristics of the seismic wave-field from turbines

It is expected that turbines vibrations transmit to the soil through basements and generate persistent seismic surface wave travelling to some distance from the wind-park. A method to detect and study this seismic wave-field, particularly in conditions of elevated background noise, is that of coincidence measurements with an array of seismometers.

We used two tri-axial seismometers, GPS synchronized and aligned. We left one seismometer permanently positioned at Lutz basement platform; while we moved the other one to 13 different out-field sites at variable distances, up to 5km away. A map of recording sites is shown in Figure 3. Three tri-axial seismometer permanently located on the floor of each GEO experimental building were also part of our seismic array.

At least 8 hours of continuous recording was taken at each site. The two most distant sites are located 3km and 5km away and there the seismometer was left recording over-night to catch more quiet times. Most sites are actually in the “near-field” with respect to the wind-park. This was dictated by the need to investigate on the noise produced at the GEO site, and also by the fact that it was not possible to find suited measurement sites, sufficiently distant from roads and houses, at farther distance from the wind-park.

The computation of coherence between the seismic signal at Lutz platform and the signal at out-field stations permitted us to track and study the seismic wave of this particular turbine.

Figure 8 compares horizontal and vertical seismic spectra recorded at Lutz and at increasing distances from it. Figure 9 shows spectral coherences between the seismic record at Lutz and at distant stations. Shown data records were taken with not too different wind conditions, wind speeds at soil ranging from 7 km/h to 11 km/h. For more distant stations (B2 and B3) night-time data are used, because day-time records are dominated by anthropogenic noise from other sources. Seismic records at the two most distant stations (3km and 5km) are dominated by anthropogenic noise also at night-times.

Below 1 Hz all spectra show a persistent seismic peak at 0.3 Hz (Figure 8), which happen to correspond to the frequency of the turbines first structural mode. Between 2Hz and 10Hz the stacked spectra give evidence of a seismic noise component whose amplitude gradually decreases with distance, and which is still detectable at 2 km from the turbines (Figure 8). This noise component is characterized by intense spectral peaks, which reasonably well associate to turbines frequencies. At these peaks, significant coherence is measured between the out-field stations and the vibrations of Lutz platform, this coherence decreases with distance from Lutz (Figure 9). Instead, quite surprising, no coherence is found in correspondence to the intense 0.3Hz spectral component (Figure 9).

The 2-10Hz seismic noise component from the turbines is sensed by the seismometers inside GEO-600 buildings. This is demonstrated by a study shown in Figure 10: comparing seismic spectra recorded during a few night-time periods when the turbines were stopped and when turbines were running. A clear excess (about a factor 5 above background) is detected between 2 and 10 Hz. Typical turbine peaks are spotted. During day-times the excess is less evident; it is partially covered by human activities related noise.

The 2-10 Hz seismic noise looks richer in horizontal than vertical components. This is shown in Figure 11, displaying the ratio of horizontal to vertical spectra recorded by station A1, deployed in the soil close to the GEO central building. This is true also for the background noise, recorded when turbines are stopped. In conditions of strong wind the horizontal to vertical ratio is enhanced in correspondence of the frequencies of turbines emission.

The presence of coherence between Lutz station and the out-field stations (Figure 9) persisting over long periods, points to the existence of a persistent seismic wave in the soil produced by the turbines. The propagation time (and thus the velocity) of this wave can be measured by looking for the maximum of the correlation function between the seismic signal at Lutz and the signals at one out-field station, for different time shifts between the two signals [9,10]. This computation is represented with a “correlogram” plot.

Figure 12 shows correlogram plots which measure the propagation time of the seismic wave between station “REF” at the Lutz platform and station “A1”, located 1130m North-East from REF. The four correlograms in Figure 12 analyze the seismic wave-field in four different frequency bands (2-3Hz, 4-5Hz, 6-7Hz and 8-9Hz). This is done by band-pass filtering the signals before correlating them. The propagation times measured in Figure 12, together with similar ones measured from correlating REF signal with other stations, seem consistent with the hypothesis of a seismic wave propagating in radial direction from Lutz with a particularly slow velocity. We measured: v=(450±50)m/s for the 2-4Hz component, v=(260±50)m/s for the 4-10Hz component. We thus derive indication of a slowly propagating seismic wave whose speed decreases with frequency. These characteristics, including the fact that the seismic signal is richer in horizontal than vertical components, seem consistent with a shear type of seismic wave (also known as Love waves [11]) travelling in aerated soils as are the agricultural cultivated soils surrounding the Schliekum park and GEO.

We performed a similar correlation analysis for the 0.3Hz seismic component. This is particularly interesting since its frequency coincides with the structural mode of the turbines. The 0.3Hz signals is detected by all out-field stations; it is coherent among all stations, although it is not coherent with the seismic signal at Lutz. The result of the correlation analysis is that: (i) the 0.3Hz signal is quite stable (both in frequency and amplitude) and persistent over the four days; (ii) it is associated to a seismic wave field which travels from the North-East direction (48°±4° N, i.e. opposite to the wind park) with velocity = 800±50m/s. Indeed, the dominant 0.3Hz signal detected by out-field stations is not originating from the Schliekum wind park. We initially hypothesized the 0.3Hz might be the 1st harmonic of oceanic microseism (whose typical fundamental frequency is 0.1÷0.15 Hz [12].

A subsequent study revealed that the typical oceanic microseismic signal at GEO has a dominant 150mHz component, and propagates from North, with a velocity of the order of 6 km/s. One alternative hypothesis is that the observed 0.3Hz peak originates from another wind park. The closest one in the North-East direction from GEO is located about 4.5 km far and counts 10 turbines. This wind park is older than the Schliekum and might have more unbalanced and noisy turbines. However, the origin of the 0.3Hz seismic component, although interesting, remains unknown.

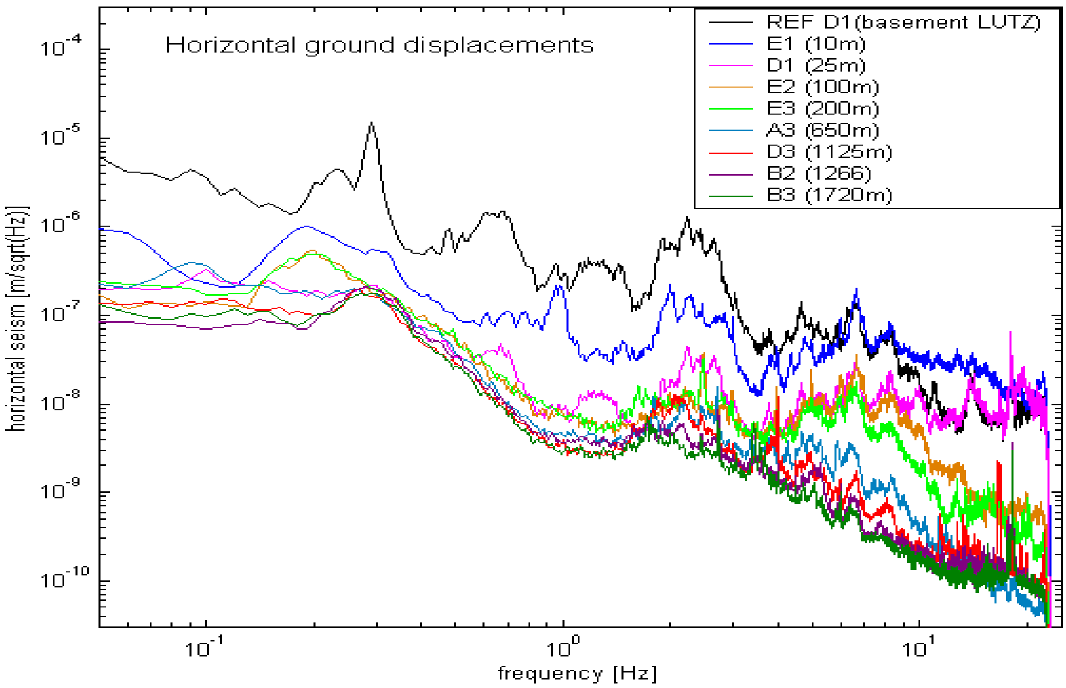

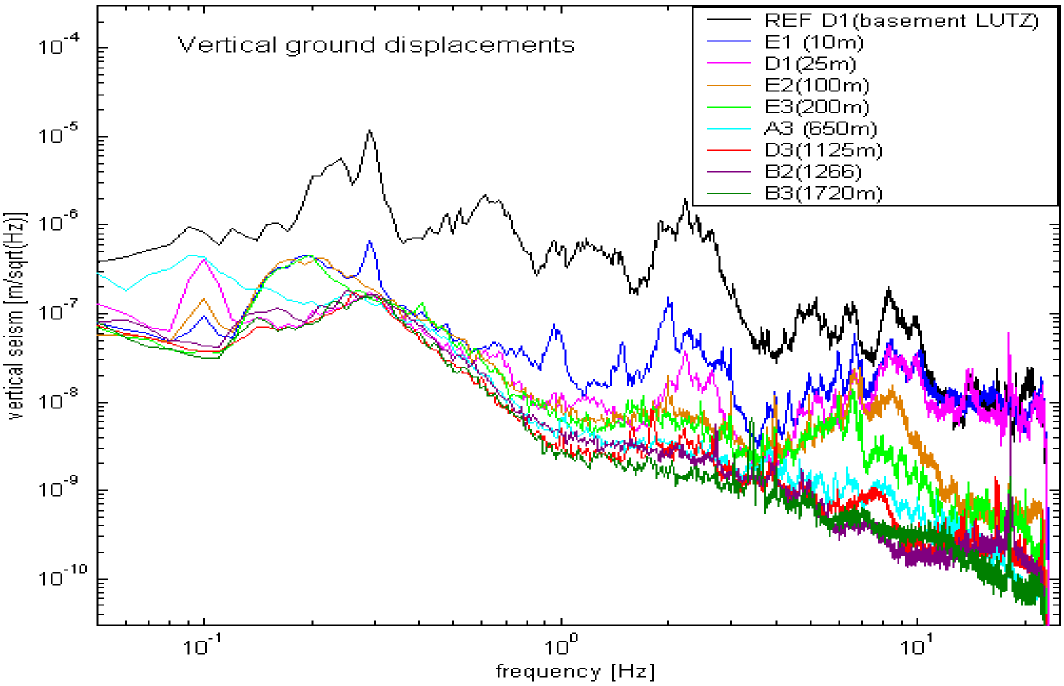

Figure 8. Displacement seismic spectra at Lutz platform (black), and at increasing distance towards GEO-600 and beyond (in colors). Each spectrum is averaged over about one hour. Top plot shows the average soil displacement noise measured along two orthogonal horizontal directions; Bottom plot shows soil vertical displacements.

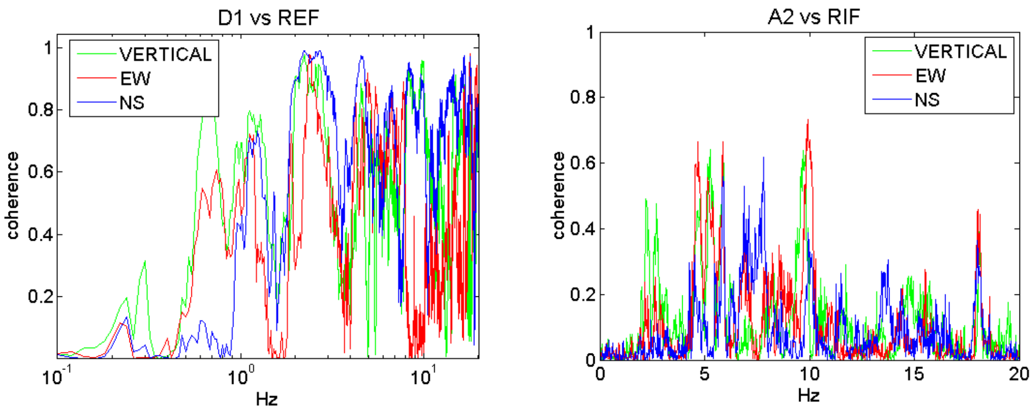

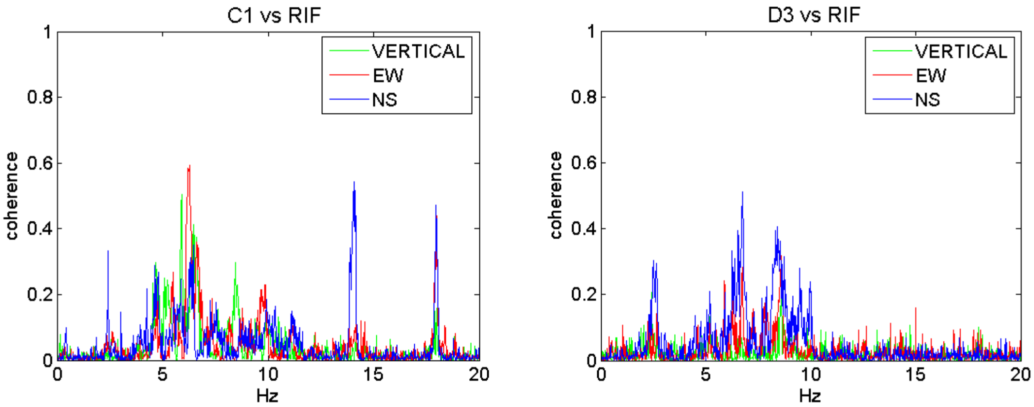

Figure 9. Coherence between the seismic signals at Lutz and at four locations at increasing distance from it: 25m, 300m, 630m and 1130m (clock-wise from top-left). The first plot is displayed with a logarithmic x-axis, to evidence the absence of coherence at the 0.3 Hz peak.

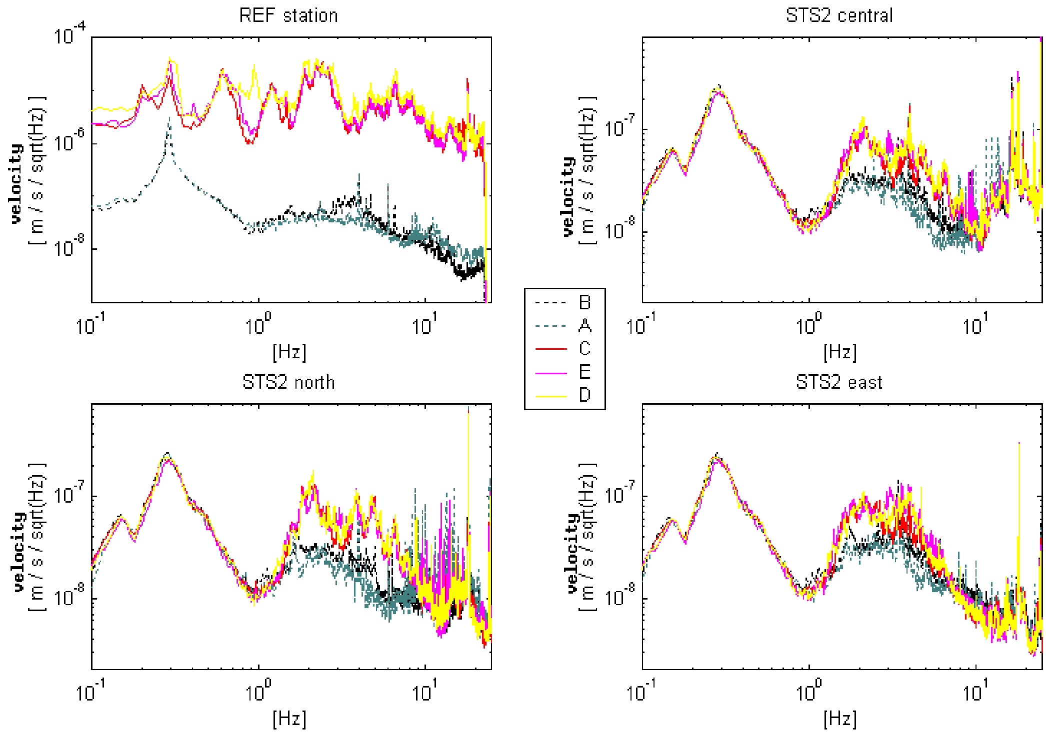

Figure 10. Seismic spectra at windmill Lutz and three GEO buildings corresponding to two night-time periods with all turbines stopped (A,B) and three night-time periods with turbines running (C,D,E).

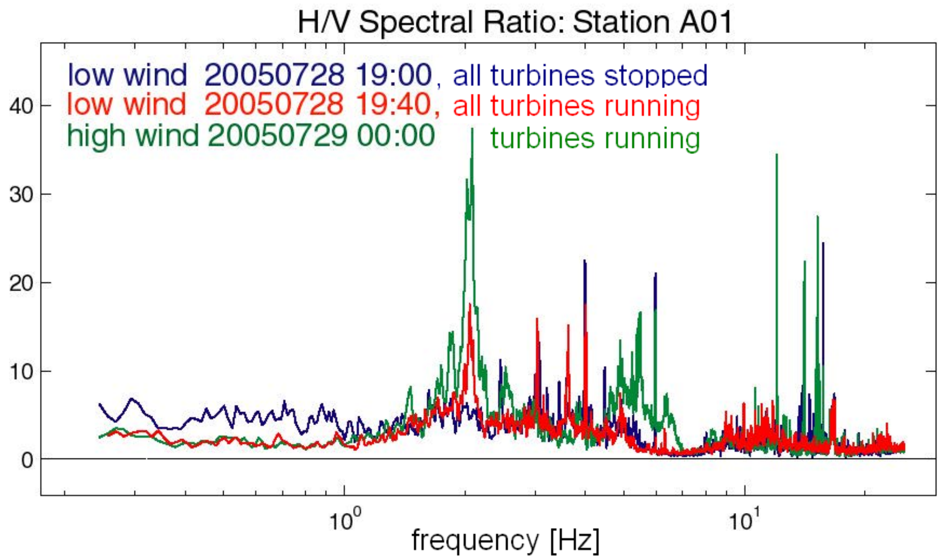

Figure 11. Ratio of horizontal and vertical seismic spectra measured by station A1. Three conditions are compared: all turbines stopped (blue), all turbines running with low wind (red) and all running with strong wind (green).

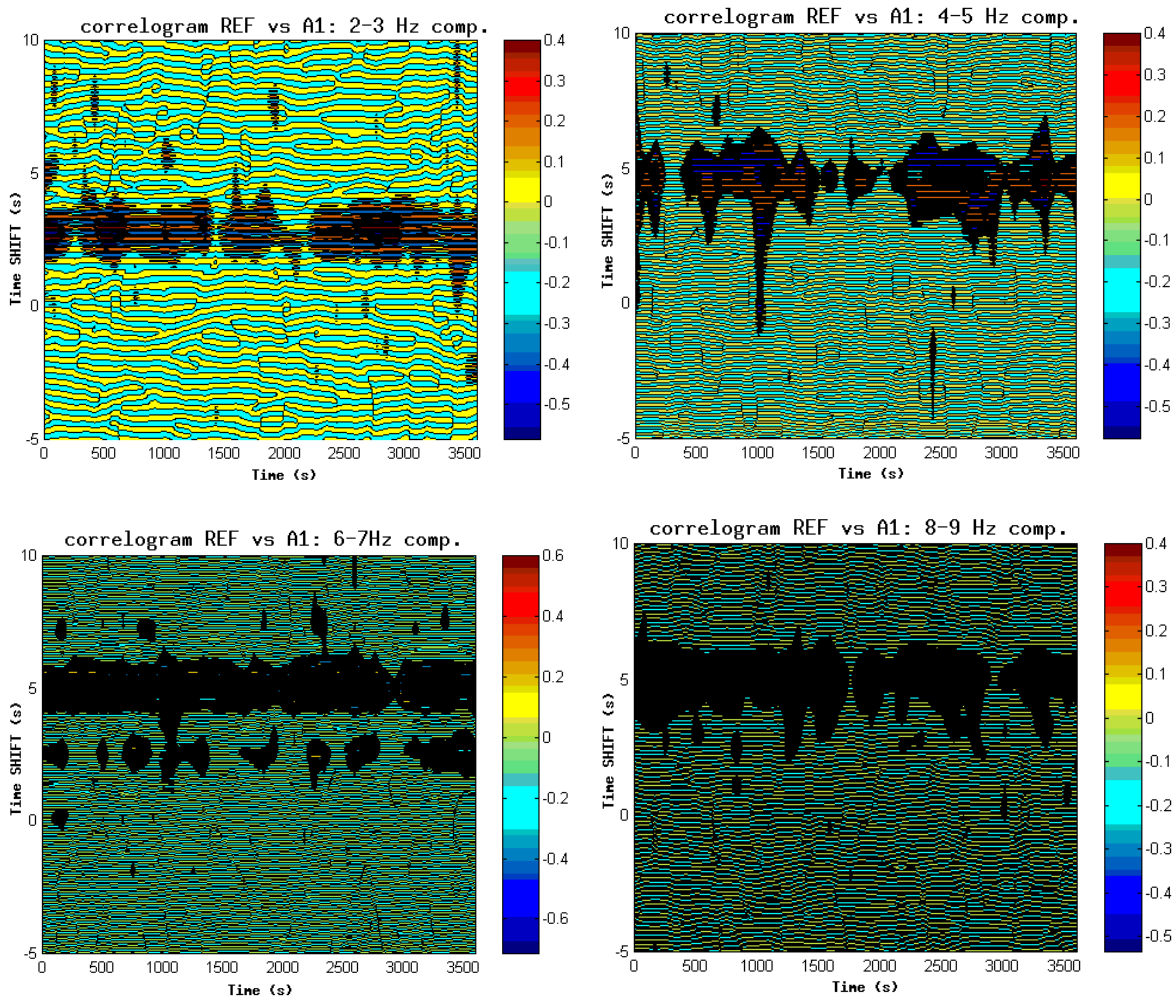

Figure 12. Correlation analysis of seismic tracks recorded by stations REF and A1 (1130m away). Signals were first band-pass filtered. The four correlogram plots are produced correlating the REF and A1signals filtered in four different frequency bands (clock-wise from upper left: 2-3Hz, 4-5Hz, 6-7Hz and 8-9Hz). In each plot the dark region identifies the maximum of the correlation function of the two signals as function of time. For the upper left plot, the maximum correlation occurs when the REF signal is delayed by +2.5s with respect to REF. This measured delay is constant as function of time (over 1 hour). This indicate for a persistent wave-field propagating from REF to A1 with a velocity of 450 m/s. Similar considerations apply to the other plots.

4. A model for seismic wave absorption

We used coincident records to measure the attenuation of the seismic wave-field as a function of distance from the wind park. As discussed in Section 3, the measured wave-field does not contain well identified spectral peaks which could be tracked in all recording sites. On the other hand, both the coherence studies (Figure 9) and the comparison of distant seismic spectra (Figure 8), indicate that the seismic wave field from the turbines is richer in frequency components between 2Hz and 10Hz. Thus, we measured the attenuation of this composite wave-form. The advantage is that we maximize the signal to noise ratio by including all the most intense signal components. The drawback is that we average over a possible frequency dependence of the absorption law.

We proceeded by selecting, for each measuring site, about 4 hours of clean data, having excluded periods with turbine stopped or transients (transient events, like those caused by passage of cars, are identified with visual inspection of the data in the time frequency domain by means of spectrogram plots). We then extracted the wave form component by filtering the data with one Butterworth band-pass filter with 2Hz and 10Hz cut-offs. We did the same for the coincident recordings of the REF station and of the far station. We then computed the amplitude root mean square (RMS) of both filtered signal. We analyzed separately horizontal and vertical components (we averaged the two orthogonal NS and EW components to one effective horizontal component). We then computed the ratio of the RMS at the far station over that of REF station. In the reasonable hypothesis that the amplitude of seismic emission of all Schliekum turbines is affected by wind speed in the same way, this operation factors-out the effect of variations of the wind speed during measurements. Finally, we normalized the RMS ratios to the horizontal seismic RMS value recorded at station E1 (Figure 3), which was buried in the ground close to Lutz foundation[1].

The normalized RMS ratios are plot in Figure 13, separately for the horizontal and vertical components. We find indication that the horizontal and vertical components

---

[1] The seismic signal measured onto the turbine platform appears not to be a good reference for measuring attenuations, since the basement can amplify seismic vibrations. Qualitatively this effect can be observed in Figure 8, comparing the seismic spectrum measured by the REF station on the concrete with spectra measured by station E1 deployed in the soil but very close to the basement edge. It seems that vertical vibrations are amplified by about a factor two more than horizontal ones. In addition, the basement seems to enhance low frequencies up to 5-6 Hz.

of the seismic wave-field from the wind park follow the same attenuation law, although the amplitude of the vertical component is about a factor 1.75 smaller than the horizontal component at any distance from the turbines (this is consistent with measurements discussed in Section 3). At distances greater than 1.5km we note a saturation effect. This indicates that the turbines RMS noise is overcome and masked by anthropogenic noise from other sources.

A simple model for the propagation of a seismic wave from a surface source, as for example the wind turbine, assumes that the seismic energy is radiated uniformly from the source along a circular wave-front. The attenuation of the wave amplitude with distance is then described by the formula [11]:

(1) $$A_R = A_r \frac{\sqrt{r}}{\sqrt{R}} \cdot \exp\left(\frac{-\pi \cdot f \cdot (R-r)}{Q \cdot v}\right)$$

Where: R is the distance from source where the signal amplitude is A_R, r is the distance of a reference nearer (r<<R) location where the signal amplitude is A_r. The exponential term accounts for the energy dissipation in the soil. This is parameterized with a quality factor Q which …, v is the wave velocity and $\omega=2\pi f$ is the wave frequency.

We applied this model to the multiple incoherent sources of the Schliekum wind park. We computed the total seismic (A_j) amplitude at one measuring location *"j"* as the quadratic sum of the seismic amplitude at *"j"* of the seismic waves from each turbine, $A_{i,j}$ (the index *"i"* identifies the turbine: *"i"*=1,…8):

(2) $$A_j = \sqrt{\sum_i A_{i,j}^2}$$

(3) $$A_{i,j} = \frac{K}{\sqrt{R_{i,j}}} \cdot P_i \cdot \exp\left(\frac{-\pi \cdot f \cdot R_{i,j}}{Q \cdot v}\right)$$

(4) $$K = A_0 \sqrt{r_0} \frac{1}{P_0} \exp\left(\frac{\pi \cdot f \cdot r_0}{Q \cdot v}\right)$$

Where: $R_{i,j}$ is the distance of turbine *"i"* from location *"j"*, P_i is the power of turbine *"i"* (see footnote [2]), and K is a constant factor which accounts for the seismic amplitude measured at one reference distance from one reference turbine.

The parameters we use in the model are the following:

- f = 6 Hz, is the central frequency of the chosen RMS frequency range;
- v = 310 m/s, is the weighted average of the measured velocity (Section 2);

[2] Our measurements indicate the turbine seismic amplitude is proportional to wind speed (Section 2 and Figure 6), on the other hand, turbines power is approximately proportional to wind speed in the rated working range. We thus assume seismic amplitude to be proportional to turbines power.

- According to literature [11] a value of Q in the range 20 to 100 is reasonable for a sandy clay type of soil. We tested our model with values of $Q \cdot v$ = 6000, 15000, and 30000.

The hypotheses of uniform radiation and of linear superposition indeed are not strictly valid in the near field of the sources. In fact, the presence of obstacles (buildings, other turbines) or soil non-homogeneities on the wave-field path can cause local build-ups or dilutions of seismic energy. Therefore we do expect the model to have some degree of uncertainty when applied to measurements done in the vicinity of the turbines, at distances smaller that a few times the signal wavelength (in our case $\lambda \approx 50$m).

Figure 14 compares the measured horizontal attenuation to the prediction of the attenuation models. Values of $Q \cdot v$ in the range 15000 to 30000 appear to adequately reproduce the data. This poor estimate suffers mainly of the fact that we could not perform significant measurements beyond 2 km from the windmills, because there the windmills signal was overcome by anthropogenic noise of different origin.

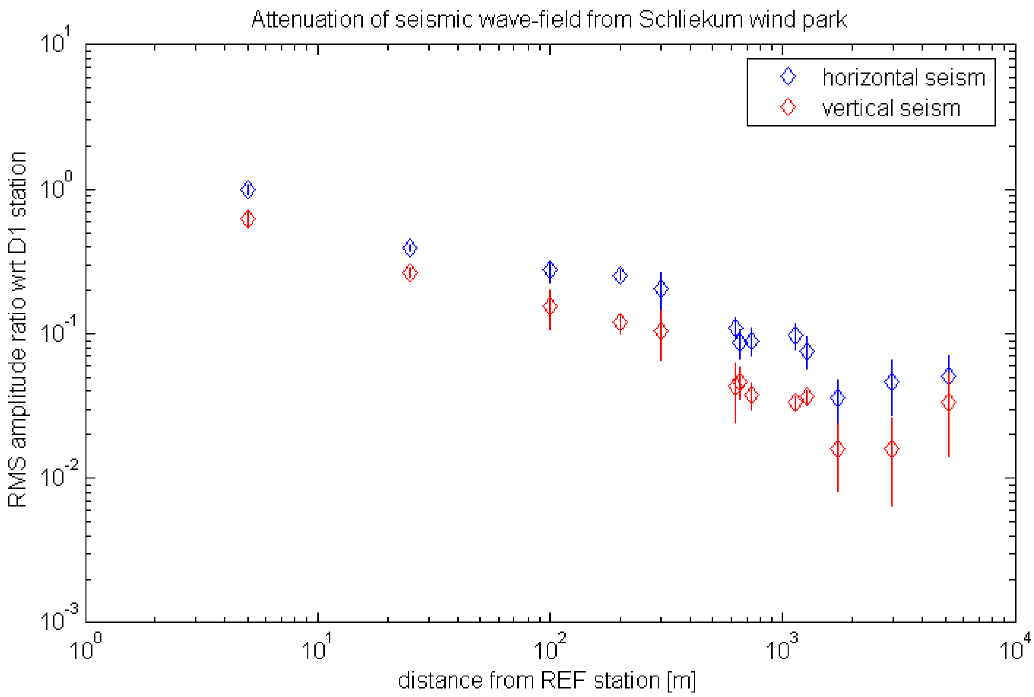

Figure 13. Attenuation of the amplitude of the seismic wave-field from the Schliekum wind turbines: horizontal (blue) and vertical (red) components. The plotted dots are the ratio of the 2-10Hz RMS amplitude measured at out-field stations (A1 to D3), corrected by wind speed, to the horizontal RMS measured at station E1 (5m). On the horizontal axis is reported the distance of out-field stations from REF station on Lutz platform. Each RMS is computed over four hours of data (cleaned from transients

and turbines off periods) at 100s steps. The bars show the statistical uncertainty associated to the variance of RMS values.

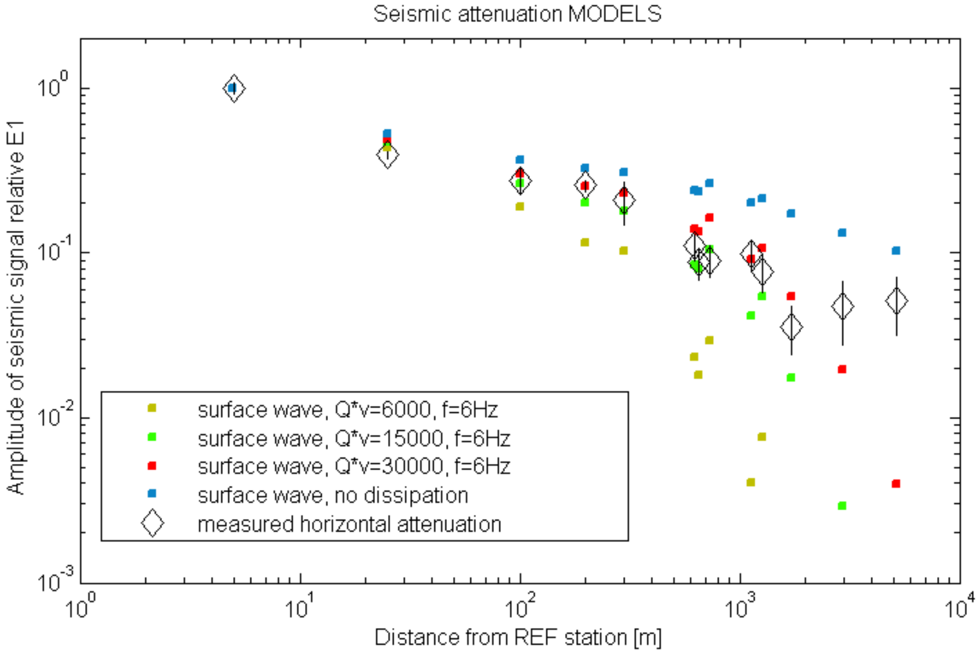

Figure 14. The measured horizontal attenuation as function of distance (blue diamonds) is compared to the predictions of the attenuation model. Squares of different colours correspond to four different values of the $Q{\cdot}v$ parameter, or, assumed a velocity v=300 m/s, four different values of the soil attenuation factor: Q=20, 50, 100. Also the ideal case of a non-dissipative soil is represented.

5. Prediction of seismic noise at VIRGO by "il Faldo" wind park project.

The final goal of our study is to derive an estimate of the seismic disturbance (RMS noise level and spectral composition) produced at the VIRGO site from the wind park "il Faldo" proposed for construction in the vicinity of the site. Figure 15 shows the proposed layout of "il Faldo" composed by 9 turbines, Enercon E82, 2.0MW [13]. The turbines are located approximately S-W of VIRGO at distances between 3 and 4.5 km from the (closest) VIRGO West experimental building.

We used the model described in Section 5, with the following assumptions:

(1) VIRGO and GEO soils have similar transmission properties for mechanical waves, so that the attenuation model we derived for GEO reasonably applies to VIRGO. This assumption is supported by the similar morphology of soils (sandy clay), and by the fact that the velocity of propagation of 2-4Hz surface seismic waves measured at GEO (Section 3) and at VIRGO [14] are similar.

(2) We assume similar characteristics of the seismic emissions by Schliekum and "il Faldo" wind turbines. We indeed expect the coarse features of the signal spectral composition to depend mainly on the blades rotation frequency and the turbines structural parameters, which are similar for Schliekum and "il Faldo" ones. On the other hand, we expect that the relative amplitude of the

frequency components transmitted to the soil would depend mainly on the characteristics of the turbine foundations, which we assume similar.

Thus, we used formula (2), (3) and (4) (Section 4) with the following settings:

- we defined locations "j" where to evaluate the seismic noise of "il Faldo" (black dots in Figure 15);
- we inserted in "r_{ij}" the geometrical layout of "il Faldo" and turbines power P_i;
- being interested in a conservative estimate of the noise produced, we adopted, within the $Q \cdot v$ range determined above, the value $Q \cdot v$=30000, corresponding to a less dissipating type of soil (given a wave speed v≈300m/s, this corresponds to a soil quality factor Q=100),
- we adopted the same average frequency f = 6Hz, and RMS range 2÷10Hz;
- we adopted as reference seismic RMS amplitude (A_0) the seismic noise produced by turbine Lutz (P_0=1.5MW) measured by station E1 in conditions of an average wind speed of 8 km/h (measured at soil level).

Figure 16 shows the predicted RMS seismic amplitude (2÷10Hz) produced by "il Faldo" at increasing distances towards VIRGO, and its expected excursion associated to variations of wind speed in the range 4 to 25 km/h (at soil level). The expected noise is compared to the typical values of 2÷10Hz RMS environmental seismic noise measured at the VIRGO site. In this frequency range, the site seismicity is dominated during working hours by the noise produced by local traffic and follows a daily amplitude variation of about a factor 6 (90% C.L.) [15,14].

The result is that the wind park would produce an observable effect at the VIRGO West station (North and Central stations instead would be substantially unaffected). The increase of seismic noise at the West station would be within the range of RMS variations due to other anthropogenic sources (Figure 16). However, in order to correctly evaluate the impact of the noise on the VIRGO interferometer, we have to consider the spectral composition of the noise. In fact, seismic peaks in correspondence of the mechanical resonances of the mirror suspensions can excite high-Q modes and make the system unstable.

Figure 17 gives an idea of the spectral amplitude of the seismic signal from the "il Faldo" turbines that would be measured at the VIRGO West station. The prediction has been obtained using the amplitude spectrum recorded at E1 and rescaling it to the value of predicted RMS at the West station. An upper limit is computed increasing this spectral noise by a factor three to account for wind speeds up to 25 km/h (soil level). We compare these predictions to the spectral amplitude of the typical seismic noise from (other) environmental sources measured at the VIRGO site. We find that seismic spectral peaks from the "il Faldo" turbines would significantly exceed the present seismic noise, in conditions of moderate-high wind, but only at the Virgo West experimental hall which is the closest (≈3km) to the wind park.

Although the precise frequency position of the seismic peaks between 2 and 10 Hz might be different for the “Il Faldo” windmills, our projection indicate a significant disturbance. The frequency region above 4 Hz appears to be the most exposed. At present the day-time increase of seismic noise in the 2-10 Hz range is due to transient signals associated to road traffic [14,15]. Seismic noise from turbines would be instead of a persistent nature, thus more critical for the VIRGO detector, being capable of exciting mirror suspensions resonances.

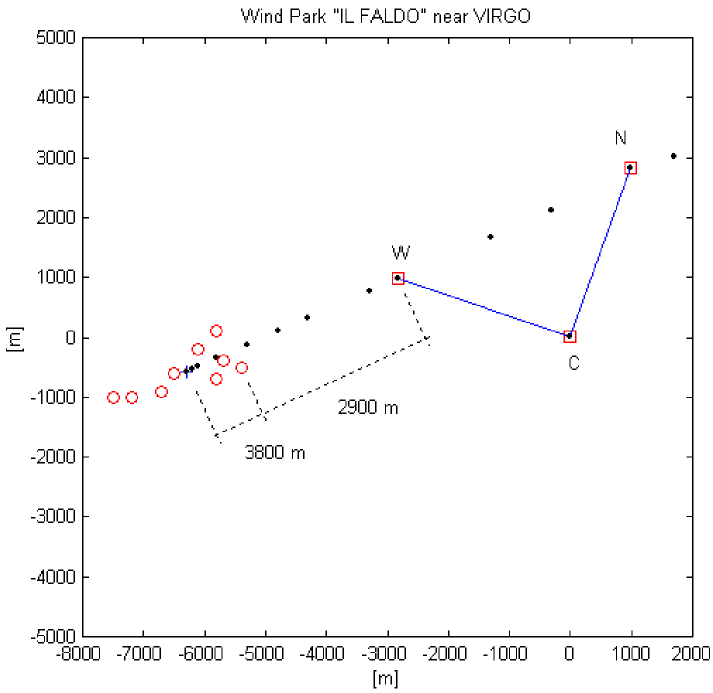

Figure 15. Proposed layout of “il Faldo” wind park. Red circles indicate turbines. Also depicted is the position of VIRGO experimental Buildings (C=central, W=West, N=North). Black dots mark the points where the model prediction was evaluated.

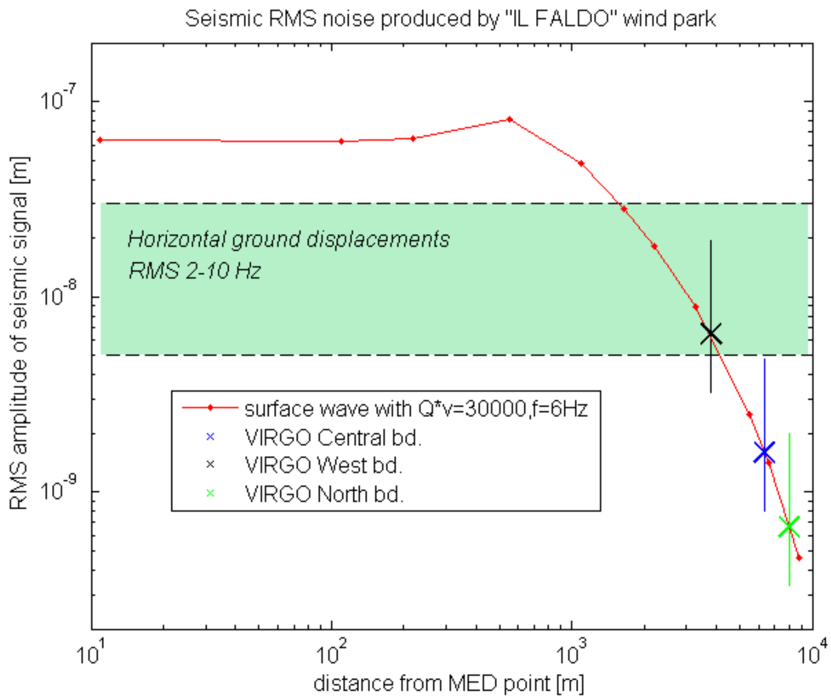

Figure 16. Prediction of seismic RMS displacement (2-10 Hz) produced by “Il Faldo” wind turbines at increasing distances towards VIRGO. Distances are measured for convenience from the geometrical barycentre of the turbines position (MED). The green rectangle delimits the range of RMS seismic noise variation measured at the Virgo site. Crosses mark the RMS noise expectation at VIRGO buildings for a typical average wind speed of 8 km/h. Vertical bars represent the variation in RMS noise we expect associated to variations of wind speed between 4 and 25 km/h. These are wind speed values measured at soil level, we assume they correspond to the minimum and maximum wind speed values of typical operational range of turbines.

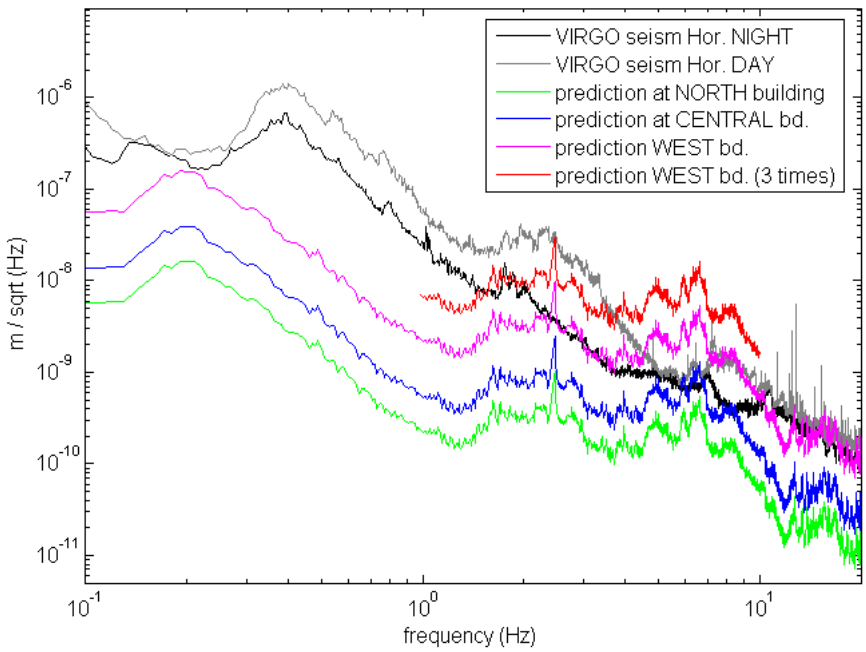

Figure 17. Black and gray curves are typical seismic noise displacement spectra at the VIRGO site, recorded during night-times (black) and day-times (gray). These are compared to the predicted spectral noise produced by the “il Faldo” turbines at the location of the VIRGO experimental buildings (in colors). The parameters used for the attenuation model are the same used in Figure 16. Magenta, blue and green curves are computed for an average wind speed of 8 km/h (measured at soil level), which we assume corresponds to the mid-range wind speed of turbines operation. The red curve shows the expected noise level at VIRGO West building in case of a three times stronger wind, which we assume corresponds to the upper limit of the operational range of turbines.

Conclusions

We studied the seismic wave-field generated by one wind park located in a not particularly quiet seismic area (25 km from the city of Hannover) on a cultivated soil and composed of lime and sand sediments (thus particularly seismically dissipative-type of soil).

We find that the seismic wave-field is particularly rich in the 2 to 10 Hz frequency components, which correspond to functional frequencies of the turbines. The surface seismic wave has the characteristics of a Love wave with a dominant horizontal component. The velocity of propagation is particularly slow, 500÷250 m/s, with evidence of dispersive effects (higher components travel slower). A qualitative indication is that at about 2km distance from the park the wave-field amplitude reduces to a level comparable to the variation of the anthropogenic seismic noise.

A simple model of incoherent superposition of uniformly radiated surface seismic waves from the single turbines seems to reproduce the measured seismic wave-field attenuation with distance, for values of the $Q \cdot v$ parameter in the range 15000÷30000. The uncertainty of the model predictions is however large because we applied it to measurements in the near-field of the wind park.

Based on this model we expect that a similar wind park proposed for construction in the vicinity of the VIRGO detector in Italy, would produce a disturbance significantly above of the typical RMS variation of the site seismicity, up to about 4 km distance.

Based on this result and conservatively accounting for the model uncertainty, we set a minimum “distance of respect” of 6km from each of the VIRGO buildings for the installation of the wind park, counting 9 turbines of 2MW. This distance scales with the square root of the number of turbines and linearly with the turbines power.

References

[1] Saulson P.R (1994) “Interferometric gravitational wave detectors”, World Scientific.

[2] VIRGO: http://www.ego-gw.it/virgodescription/ ; GEO: http://geo600.aei.mpg.de/; LIGO: http://www.ligo.caltech.edu/; TAMA: http://tamago.mtk.nao.ac.jp/.

[3] Schofield R (2001), "Seismic Measurements at the Stateline Wind Project", LIGO T020104-00-Z.

[4] Style P (2005) "A Detailed Study of the Propagation and Modelling of the Effects of Low Frequency Seismic Vibration and Infrasound from Wind Turbines", WTN 1st International Meeting, Berlin, October 2005.

[5] Fiori I, presentation at 2nd ILIAS-GW Annual Meeting, Palma de Mallorca, October 2005.

[6] NORDEX http://www.nordex-online.com/en/products-services/wind-turbines/n90-23-mw/; ex-ENERCON: http://www.gepower.com/home/index.htm.

[7] Peterson J (1993) "Observations and modeling of background seismic noise", U.S. Geological Survey Tech. Rept., 93-322, 1-95.

[8] Schaumann P, Seidel M (2000) "Einschwingverhalten von Windenergieanlagen", Berechnungen und Messungen Hannover.

[9] Marchetti E, Mazzoni M, Ripepe M (2002) "Low frequency seismic wave-field array analysis at Virgo", VIRGO NOT-FIR-1390-220.

[10] Justice J H, et al. (1985) "Array Signal Processing", S. Haykin Editor, Prentice-hall, pp. 432.

[11] Lay T, Wallace T.C (1995) "Modern Global Seismology", Academic Press.

[12] Braun T, Ripepe M et al (1998) "On the origin of the long-period tremor recorded at Stromboli Volcano", Annali di Geofisica, vol.39 pp 311-326.

[13] http://www.enercon.de/.

[14] Fiori I, Holloway L, Paoletti F (2003) "Study of the 1 to 4 Hz seism at VIRGO", VIRGO NOT-FIR-1390-251.

[15] Fiori I (2003) "Properties of seismic noise at the Virgo site", *Class. Quantum Grav.* **21** S433-S440.

Third International Meeting
on
Wind Turbine Noise
Aalborg, Denmark 17 – 19 June 2009

Practical effects of atypical divided rotor blades on aerodynamic noise: a glimpse on future prospects for wind farms and micro turbines

Emmanuel Gadaix
MHG Labs, GRI
43 Moo 5 Soi 19, M. Phetngam Pragkasa 1
Thanon Pragkasa Mai, Ampur Muang
Samutprakarn 10280, Thailand
gadaix@gmail.com

Introduction

Noise, the most often cited problem with wind turbines, is also related to their efficiency and aerodynamic properties. The disturbance to the human ear can be as much a public nuisance as a practical reminder of the energy lost.

Some of the sources of noise in wind turbines can be reduced; for example mechanical noise can be damped by the use of soundproofing and insulation material. For the aerodynamic noise however, numerous efforts were made to reduce the sound created by the interaction of the blades and the disturbed air flow, without any major breakthrough. Attempts at optimizing rotor blades, either through their blade tips or the airfoil shape, have had only a very limited effect so far.

This paper introduces an innovative turbine design based on atypical divided rotor blades. The turbulence levels on this new turbine are significantly lower than traditional designs due to a very different airflow pattern which reduces the noise created by the boundary layer separation. Wind tunnel and field tests have shown that this atypical design does not share conventional turbines' properties, especially on sound.

Applied to all types of turbines (wind, water, gas) as well as propellers (aviation, marine), this design may be a significant contribution in reducing the noise of those applications – often the first and foremost complaint.

A short history of turbines and propellers

7th - 3rd century BC

Archimedes' screw, the ancestor of the propeller, is a machine historically used for transferring water from a low-lying body of water into irrigation ditches. It was one of several inventions and discoveries traditionally attributed to Archimedes in the 3rd century BC, but recent research has shown that an earlier form of this screw was first used by Sennacherib, King of Assyria, for the water systems at the Hanging Gardens of Babylon and Nineveh in the 7th century BC. Others attribute it to King Nebuchadnezzar II.

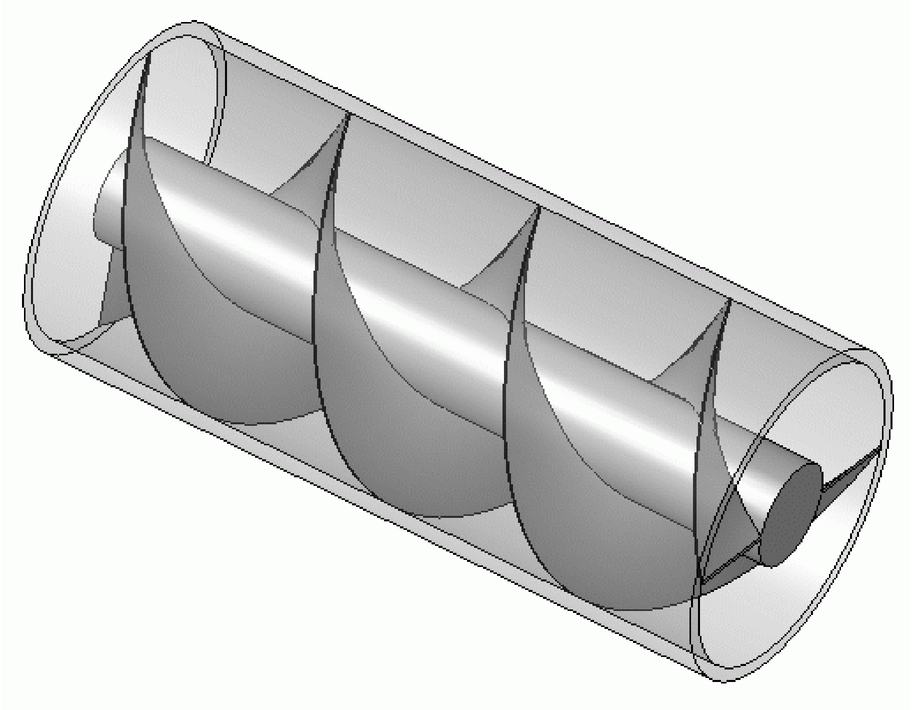

Archimedes' Screw

Modern version of the Archimedes' screw are still in use today, for example sewage treatment plants because they cope well with varying rates of flow and with suspended solids. The principle is also found in pescalators used at fish hatcheries, which are Archimedes screws designed to lift fish safely from ponds and transport them to another location. Leonardo da Vinci adopted the principle to drive his theoretical helicopter, sketches of which involved a large canvas screw overhead.

High viscosity liquids

1500

Leonardo da Vinci drew a sketch of a device, the chimney jack that rotated due to the effect of hot gases flowing up a chimney. It looked like a device that used hot air to rotate a spit. The hot air came from the fire and rose upward to pass through a series of fan like blades that turned the roasting spit.

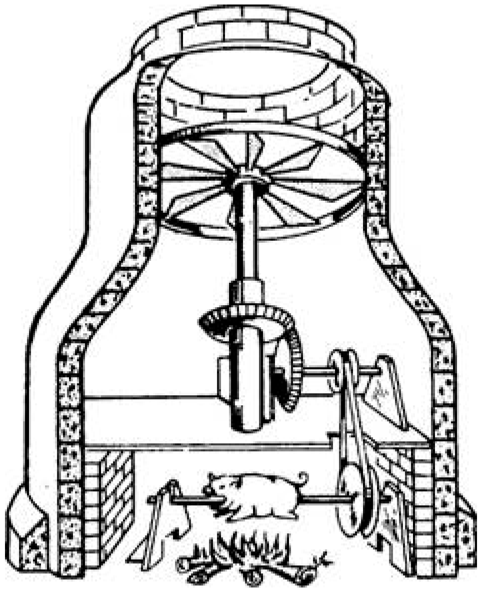

Da Vinci Chimney

1791

John Barber received the first patent for a basic turbine engine. His design was planned to use as a method of propelling the 'horseless carriage.' The turbine was designed with a chain-driven, reciprocating type of compressor. It has a compressor, a combustion chamber, and a turbine.

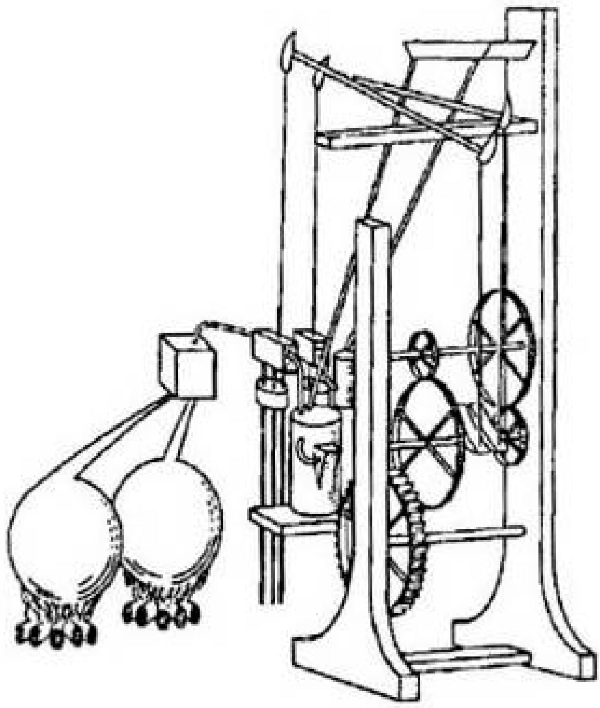

John Chamber Gas Turbine

1752

John Fitch, American steam powered boat pioneer, experimented with a propeller driven boat. His version of a propeller was typical of early propeller attempts, in that it was really a screw, like an Archimedes screw. These early screw designs did not prove to be practical, but inventors kept being drawn back to the idea of a propeller instead of paddle wheels. A successful propeller was not developed for many years, and the propeller did not displace the paddle wheel for many more years.

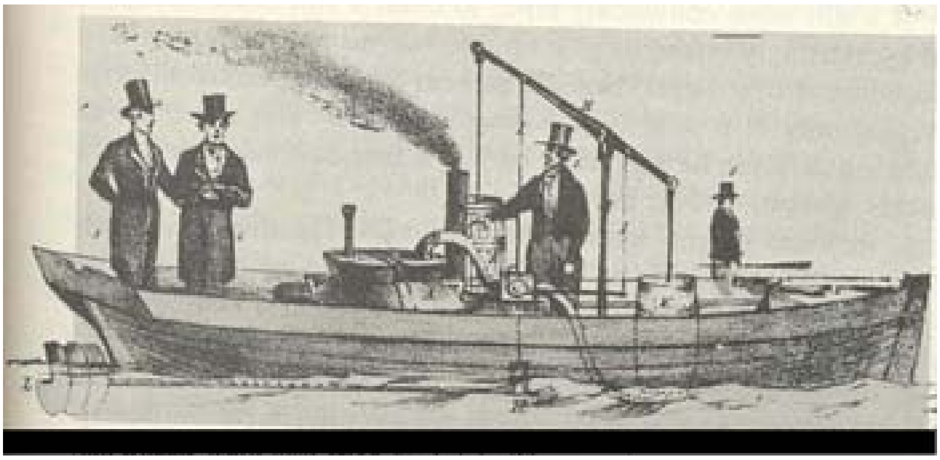

Fitch’s experiments with propellers

1816

James Steedman, a carpenter and cabinetmaker from Scotland's west coast, had an interest in natural history, and his study of fish gave him the idea of rear propulsion; watching a spinning wheel suggested the method. He and gunsmith McCririck made models, one of which was taken by Maxwell Dick, an Irvine fellow inventor, to London in 1830, where - it was alleged - the idea was pirated, and patented without credit to James Steedman.

Steedman’s propeller on his gravestone

1827

Robert Wilson, always interested in boats (seeing paddle-wheels on a fishing boat at age 5; he lost his father in a boat rescue at age 7), had the idea of a propeller from watching a windmill. He worked on the invention while apprenticed to a joiner and cabinetmaker. In 1827, the Earl of Lauderdale unsuccessfully approached the Admiralty, the "Edinburgh Mercury" recorded the "new invention", and in 1828, the first practical screw propeller was trialed on the Union Canal (the model being in the Royal Scottish Museum). The Admiralty again rejected the idea in 1833. Robert Wilson went on to be a highly successful engineer, taking out patents for valves, pistons, propellers and hydraulic and other machinery. In 1880, aged 77, the War Office granted him £500 for the use of his double-action screw propeller as applied to the fish torpedo.

Wilson memorial at Dunbar harbor, 4-tons propeller

<u>1828</u>

Charles Cummerow, a merchant of the city of London, took out a patent for a screw propeller in 1828. His propeller was formed of one complete turn of the blade upon its axis, fixed abaft the rudder and parallel to the line of the keel.

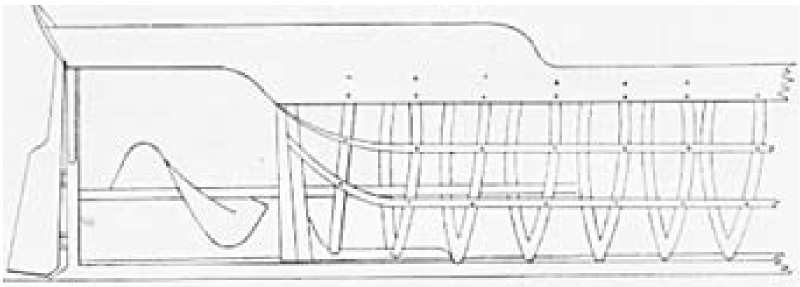

1836

François Petit Smith, a farmer, had a passion since boyhood for constructing models of boats. In 1834, he built a boat with a wooden screw; in 1835, a superior model; in 1836 he took out a patent. Where he got his original idea is not known. In 1839, the "Archimedes", a 237-ton vessel, achieved over 9 knots speed. Isambard Brunel was so impressed that he advised the screw to be adopted as the method for propelling the "Great Britain", which achieved 10 knots on her first voyage. The design was patented in the U.S. in 1838-39. Smith was knighted in 1871.

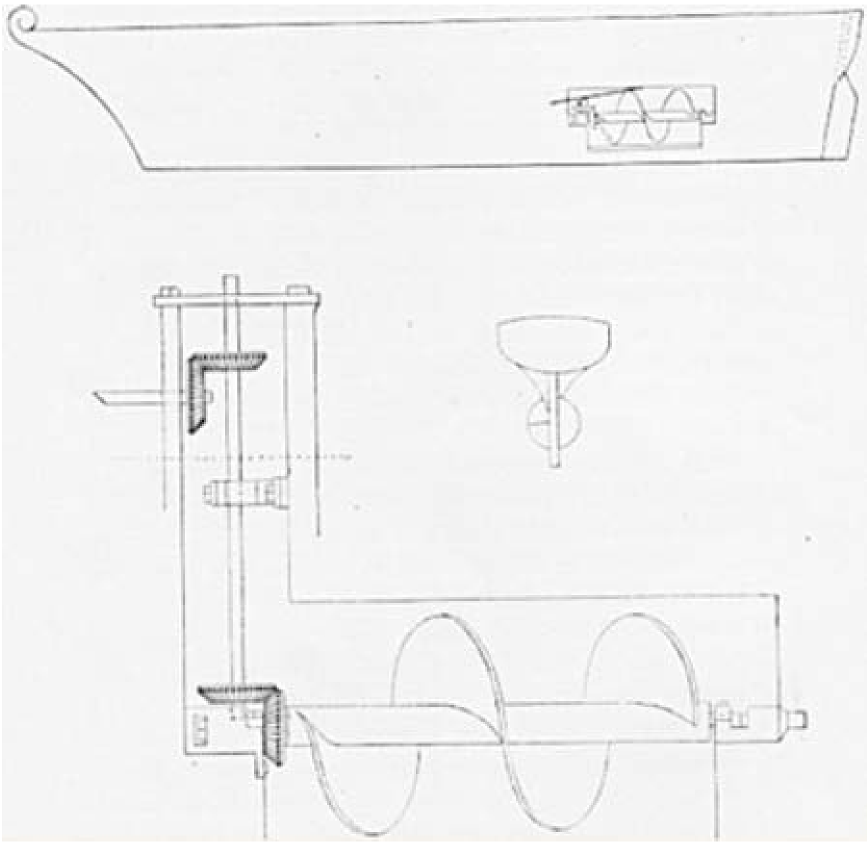

Smith propeller

1838

John Ericsson from Sweden was a born artist, gifted at the drawing board, and his talent in this area lead him eventually to explore engineering. At age 17, Ericsson joined the Swedish army. He became a lieutenant relatively quickly. He continued to do surveying for the army, and also, in his spare time, designed a heat engine that used fumes from fire instead of steam as a propellant. He left the army and moved to England in 1826. Ericsson had been working on a ship propeller when American ship captain Robert Stockton became intrigued by his ideas and asked him to design a propeller steamer for him and bring it to the United States. Ericsson did so, and moved to New York in 1839. His propeller was successfully installed in the SS Princeton, completed in 1843. The vessel subsequently won a race against what had been regarded as the fastest steamer in the world, the SS Great Western, in the fall of that year. In 1839, Ericsson's propellers were introduced into vessels for inland waterways. That year he also began working on building a large frigate for the U.S. Navy , the USS Monitor. This ship incorporated a steam-propelled screw propeller, low in the water. It also had a revolving gun turret, and used iron construction rather than wood. The Monitor was completed in 1862 and is credited with having helped the Northern states stay protected during the Civil War. The screw propeller is still the main form of marine propulsion till now.

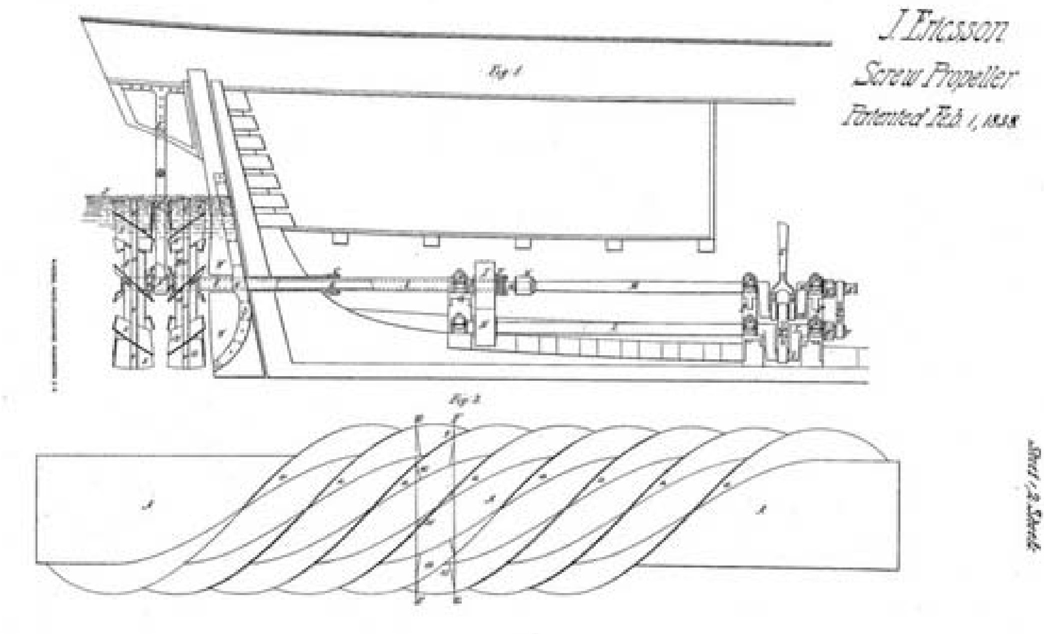

John Ericsson propeller

<u>1887</u>

Charles F. Brush (1849-1929) is one of the founders of the American electrical industry. He invented e.g. a very efficient DC dynamo used in the public electrical grid, the first commercial electrical arc light, and an efficient mehod for manufacturing lead-acid batteries. His company, Brush Electric in Cleveland, Ohio, was sold in 1889 and in 1892 it was merged with Edison General Electric Company under the name General Electric Company (GE). During the winter of 1887-88 Brush built what is today believed to be the first automatically operating wind turbine for electricity generation. It was a giant - the World's largest - with a rotor diameter of 17 m (50 ft.) and 144 rotor blades made of cedar wood. Note the person mowing the lawn to the right of the wind turbine. The turbine ran for 20 years and charged the batteries in the cellar of his mansion. Despite the size of the turbine, the generator was only a 12 kW model. This is due to the fact that slowly rotating wind turbines of the American wind rose type do not have a particularly high average efficiency. It was the Dane Poul la Cour , who later discovered that fast rotating wind turbines with few rotor blades are more efficient for electricity production than slow moving wind turbines.

Brush Windmill

1897

Poul la Cour (1846-1908) who was originally trained as a meteorologist was the pioneer of modern electricity generating wind turbines. La Cour was one of the pioneers of modern aerodynamics, and built his own wind tunnel for experiments. La Cour was concerned with the storage of energy, and used the electricity from his wind turbines for electrolysis in order to produce hydrogen for the gas light in his school. One basic drawback of this scheme was the fact that he had to replace the windows of several school buildings several times, as the hydrogen exploded due to small amounts of oxygen in the hydrogen. La Cour gave several courses for wind electricians each year at Askov Folk High School. La Cour founded the Society of Wind Electricians which in 1905, one year after it was formed, had 356 members. The world's first Journal of Wind Electricity was also published by Poul la Cour.

Lacour test turbines at Askov Folk High School

1942

During World War II the Danish engineering company F.L. Smidth (now a cement machinery maker) built a number of two- and three-bladed wind turbines. Yes, Danish wind turbine manufacturers have actually made two-bladed wind turbines, although the so-called "Danish concept" is a three bladed machine. All of these machines (like their predecessors) generated DC (direct current). 3-Bladed FLS Turbine This three-bladed F.L. Smidth machine from the island of Bogø, built in 1942, looks more like a "Danish" machine. It was part of a wind-diesel system which ran the electricity supply on the island. Today, we would probably argue about how the concrete tower looks, but this machine actually played an important role in the 1950s wind energy study programme in Denmark. In 1951 the DC generator was replaced with a 35 kW asynchronous AC (alternating current) generator, thus becoming the second wind turbine to generate AC.

F.L. Smidth Turbines

1951

Vester Egesborg Turbine The engineer Johannes Juul was one of the first students of Poul La Cour in his courses for "Wind Electricians" in 1904. In the 1950s J. Juul became a pioneer in developing the world's first alternating current (AC) wind turbines at Vester Egesborg, Denmark. In 1951 he started full-scale experiments, first with a two bladed 11 kW windmill, in 1953 with a three bladed, 45 kW asynchronic generator for alternating current, Bogø, and in 1957 his research and innovative ideas resulted in an extremely successful experimental wind mill in Gedser of 200 kW. Demonstrating high reliability and efficiency it was in continuous operation till 1968.

The innovative 200 kW Gedser wind turbine (35K JPEG) was built in 1956-57 by J. Juul for the electricity company SEAS at Gedser coast in the Southern part of Denmark. The three-bladed upwind turbine with electromechanical yawing and an asynchronous generator was a pioneering design for modern wind turbines, although its rotor with guy wires looks a bit old fashioned today.The turbine was stall controlled , and J. Juul invented the emergency aerodynamic tip brakes which were released by the centrifugal force in case of over speed. Basically the same system is used today on modern stall controlled turbines. The turbine, which for many years was the world's largest, was incredibly durable. It ran for 11 years without maintenance.

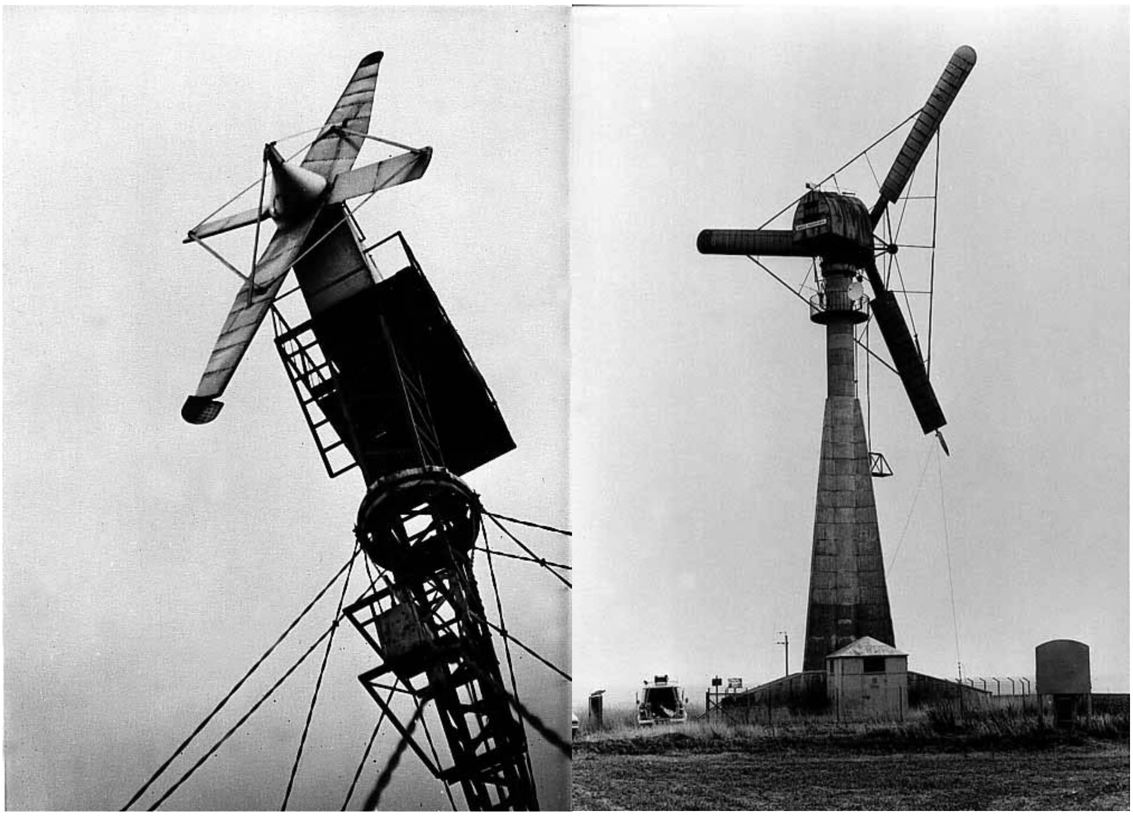

Johannes Juul Turbines

Other honorable mentions

150 B.C., Hero of Alexandria used to drive turbines by the ascending gas from a fire, and directed them through to the turbine by a ventilation shaft.

1629, Giovanni Branca developed a stamping mill, that used jets of steam to rotate a turbine that then rotated to operate machinery.

1678, Ferdinand Verbiest built a model carriage that used a steam jet for power.

1687, Sir Isaac Newton announces the three laws of motion. These form the basis for modern propulsion theory.

1839, Nov. 25. Mr. John Hunt took out a patent for combining a stern propeller and rudder in one; the blades of the propeller were to be of any suitable form.

1839, Nov. 26. Mr. George Rennie patented his conoidal propellor, which differs from all others before proposed in this, that the lines of the screw are obtained from the circumvolution of a thread round a cone instead of a cylinder, whereby the diameter of the screw, rearward of the leading part, is progressively diminished, and in proportion thereto the amount of prejudicial resistance.

1839, Jan. 22. Mr. J. C. Haddan patented the "forming and using of screws with openings, or spaces, in the central portions of the threads," whereby "the velocity of the impinging, or propelling surface, is rendered more equal, and a passage afforded for the water through the centre."

1840, May 28. Mr. George Blaxland patented the use of "one or more inclined planes," (not segments of a screw, but plain blades,) to be fixed at right angles to a revolving, horizontal shaft, placed in the after part of the keel, forwards of the rudder-post, which inclined planes (are to) work in the water below the water line, in an opening formed in the dead-wood of the vessel."

1830, June 13. Captain Carpenter patented the use of two propellers of a trapezoidal form, to be placed in the stern quarters of the vessel.

1843, Jan. 19. Mr. Thomas Sunderland patented a stern propeller, having blades attached, not immediately to the shaft, but to the ends of a cross-bar affixed to it, and of such a curved form that every point of the outer edge is equi-distant from a straight line drawn through the center of the shaft.

1843, Sir George Cayley designs an ingenious convertiplan, equipped with four rotors and twin propellers.

1865, Rankine develops his momentum theory.

1872, Dr. F. Stolze designed the first true gas turbine engine. His engine used a multistage turbine section and a flow compressor. This engine never ran under its own power.

1878, William Froude develops the blade element theory.

1897, Sir Charles Parson patented a steam turbine which was used to power a ship.

1900-1905, The Wright brothers design and test propellers systematically and succeed in 1903, performing their famous first powered flights.

1903, Aegidius Elling of Norway built the first successful gas turbine using both rotary compressors and turbines - the first gas turbine with excess power.

1907, Lancaster publishes his «Aerodynamics», including a theory of optimum propellers.

1910, Coanda tests his piston engine powered jet unit.

1914, Charles Curtis filed the first application for a gas turbine engine.

1918, General Electric company started a gas turbine division. Dr. Stanford A. Moss developed the GE turbosupercharger engine during W.W.I. It used hot exhaust gases from a reciprocating engine to drive a turbine wheel that in turn drove a centrifugal compressor used for supercharging.

1919, Ludwig Prandtl and Albert Betz calculate optimum propellers, having minimum induced loss.

1919, Fixed pitch propellers with metal blades enter service.

1920, Dr. A. A. Griffith developed a theory of turbine design based on gas flow past airfoils rather than through passages.

1924, The constant speed propeller is patented by Dr. H. S. Hele-Shaw and T. E. Beacham.

1930, Sir Frank Whittle in England patented a design for a gas turbine for jet propulsion. The first successful use of this engine was in April, 1937. His early work on the theory of gas propulsion was based on the contributions of most of the earlier pioneers of this field.

1932, Variable pitch propellers are introduced into air force service.

1935, Constant speed propellers become available.

1936, At the same time as Frank Whittle was working in Great Britain, Hans von Ohian and Max Hahn, students in Germany developed and patented their own engine design.

1939, The aircraft company Ernst Heinkel Aircraft flew the first flight of a gas turbine jet, the HE178.

1941, Sir Frank Whittle designed the first successful turbojet airplane, the Gloster Meteor, flown over Great Britain. Whittle improved his jet engine during the war, and in 1942 he shipped an engine prototype to General Electric in the United States. America's first jet plane was built the following year.

1942, Dr. Franz Anslem developed the axial-flow turbojet, Junkers Jumo 004, used in the Messerschmitt Me 262, the world's first operational jet fighter. After W.W.II, the development of jet engines was directed by a number of commercial companies. Jet engines soon became the most popular method of powering airplanes.

1945, The first turboprop engines are tested by Rolls-Royce on a Gloster Meteor.

1980s, NASA and industry perform tests with high speed propellers (propfans and unducted fans) for transport aircraft.

1987, Tasin Al-Majed experiments on a dual-slotted flat blade and patents his early design in Germany in 1988. He is known to have built several prototypes in Sweden, where his invention was largely ignored. His propeller design was awarded the silver medal at the Geneva’s 15th International Exhibition of Inventions.

2007, Mahmood H. Hussain, an Iraqi national living in Baghdad, patents a divided rotor blade with the US patent office. He received the golden prize at the 2nd international invention exhibition in Kuwait in November 2008.

In Summary

The only part of an airplane that hasn't changed is the propeller. The same design observation is true for the wind turbines.

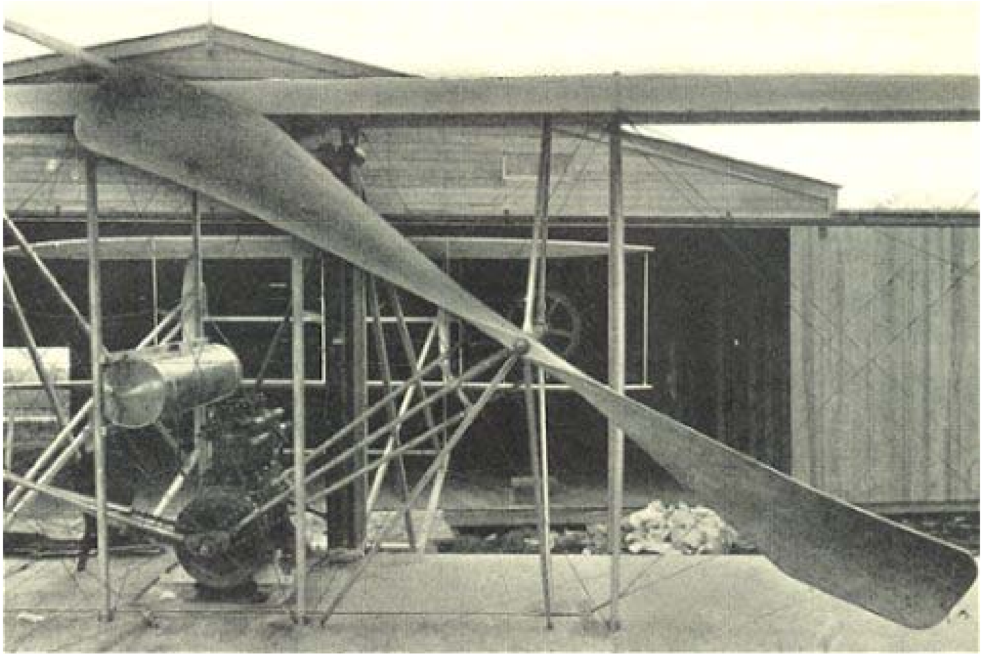

Wright Brothers Propeller

High performance and efficient Model Airplane Propellers

An atypical turbine / propeller design

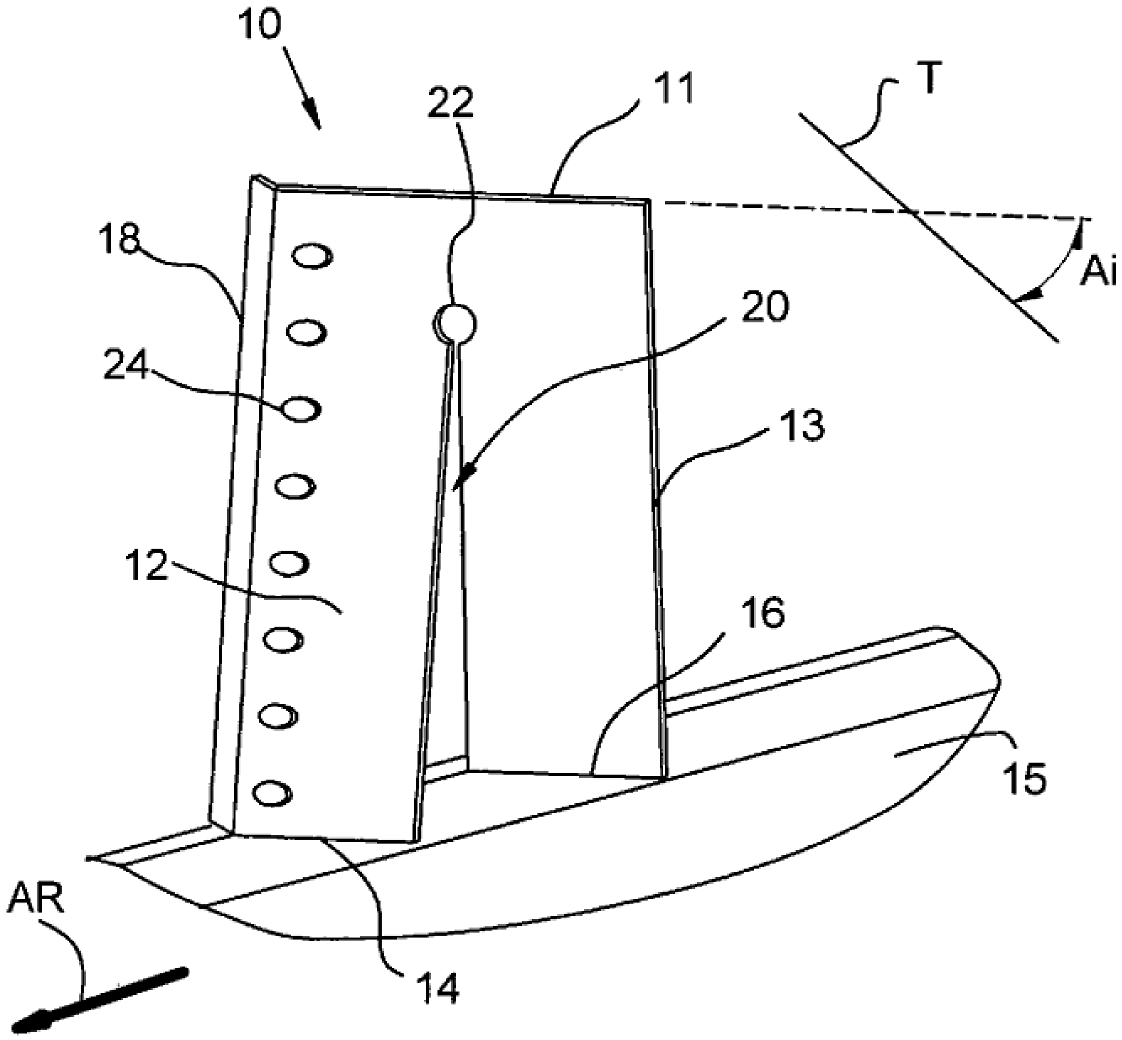

This design has been patented by Mahmood Hussain (patent issued on July 8, 2008). It is applicable to both propeller and turbines.

For propellers, it features a series of holes on its blade to improve the laminar airflow. The angle 45 degrees angle of attack is optimal and impossible to achieve with traditional propellers.

Some of the benefits include:

- Reduced noise dB level for both turbines and propellers
- Higher efficiency
- Reduced boundary layer separation resulting in better flow
- Higher strength allowing operations in hostile environments e.g. desert, storms, ice
- Able to start at lower wind speeds
- Lower production and maintenance costs due to its simple design

- More flexibility in the material that can be used for manufacturing
- Lighter weight (no volumetric increase)

Several prototypes have been built in the following countries:

- Syria
- Iraq
- Kuwait
- Thailand
- Hungary
- Sweden
- Germany
- USA
- France
- Algeria
- Norway

Pictures of the new wind turbine

The regulator concept

The regulator's role is to modify the turbine's angle of attack and thus auto-regulate itself during strong winds, keeping the optimal exposure to ensure both protection of the structure and maximal energy capture. The concept was initially pioneered by Ivan Troëng, a Swedish inventor, in the 1970s.

A propeller being tested in Chonburi, Thailand

Counter-rotating turbine tested in wind tunnel

The sources of noise in wind turbines

The aeronautical noise generated by wind turbines comes mostly from the limitations of the airfoil profile it inevitably uses. While there are thousands of such profiles in existence, practical testing have shown only very little improvements in terms of noise level.

Clearly the shape of the blade of the wind turbine will remain a brick wall when it comes to both efficiency and noise level.

Laminar Boundary Layer Vortex- Shedding Noise

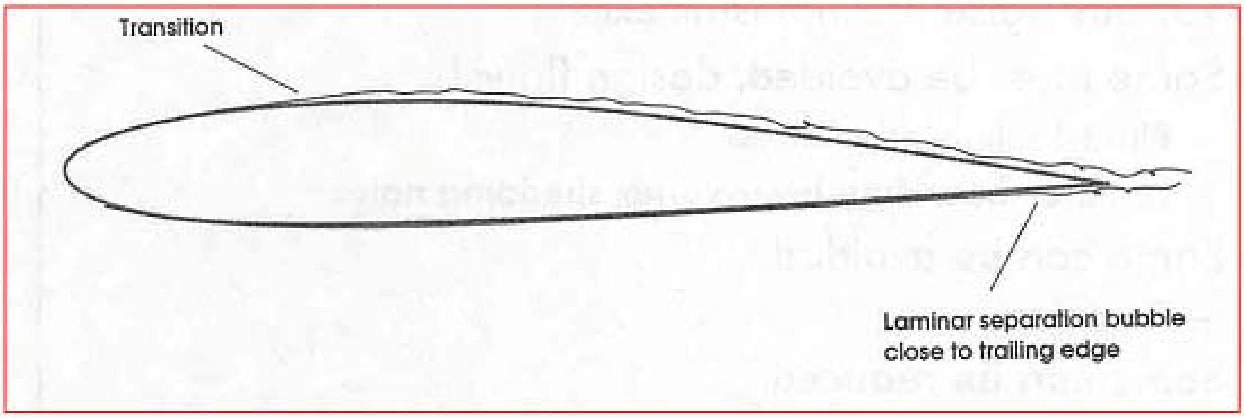

The new turbine/propeller design (with holes and slots) ensure a more continous air flow. We also have a much higher aspect ratio. boundary layer keep in touch

Turbulent Boundary Layer Trailing Edge Noise

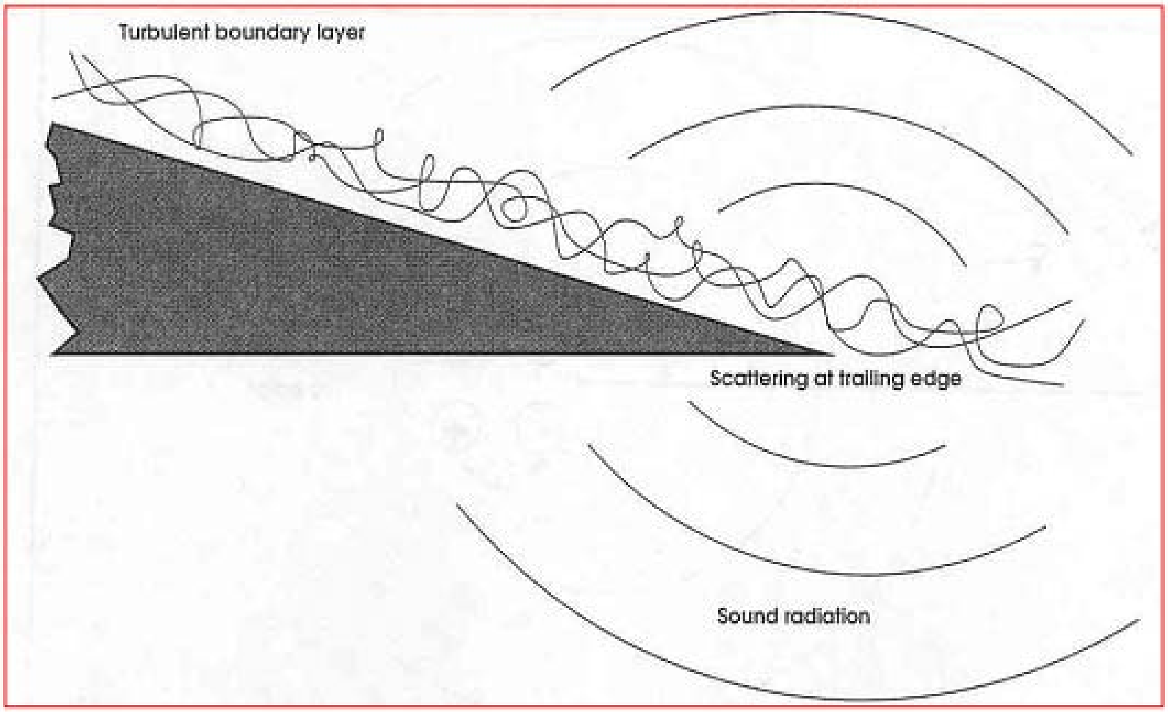

In the new design, the two laminar flows are meeting at edge and prevent the scattering at the edge like shown above.

Leading Edge Inflow Turbulence Noise

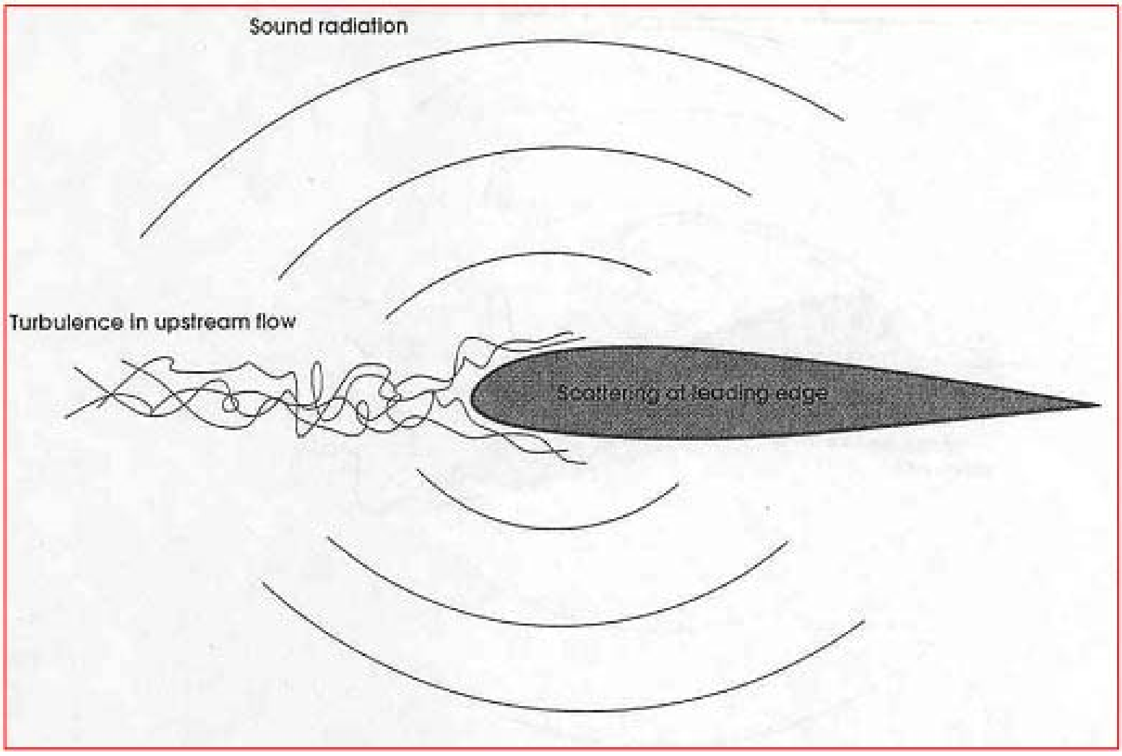

As we are not using an airfoil profile, we do not have a leading edge that creates upstream flow turbulence. We use sharp edges (e.g. like a sword cutting the air), and are hitting the air with a 10 degres angle of attack (Z flow, 10-20-10).

Blunt Trailing Edge Noise

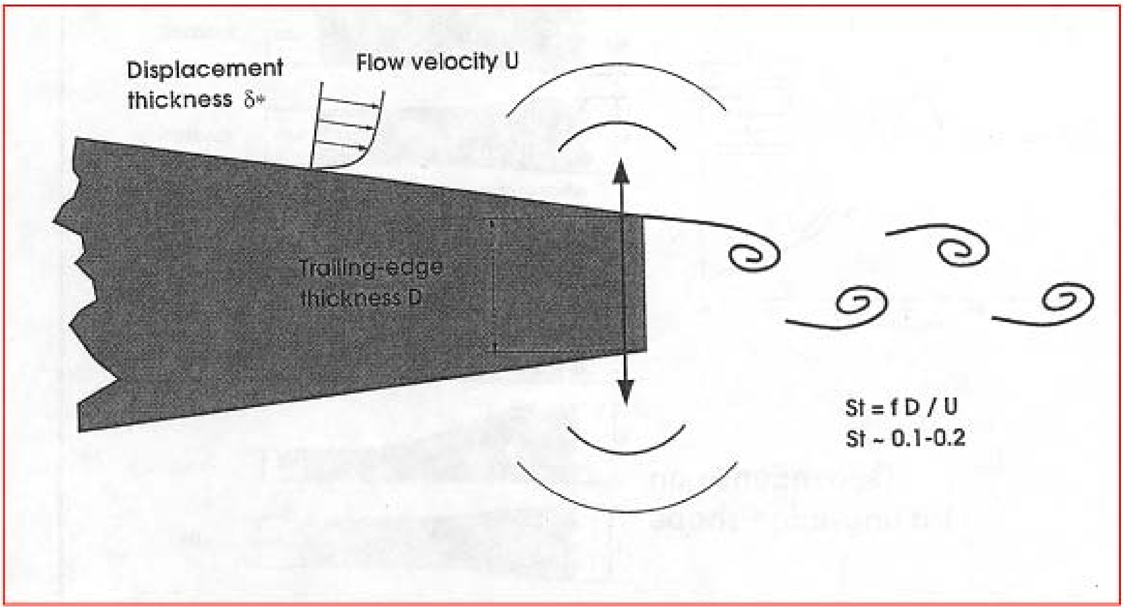

Same observations: flat blade, sharp edge

Separation Noise

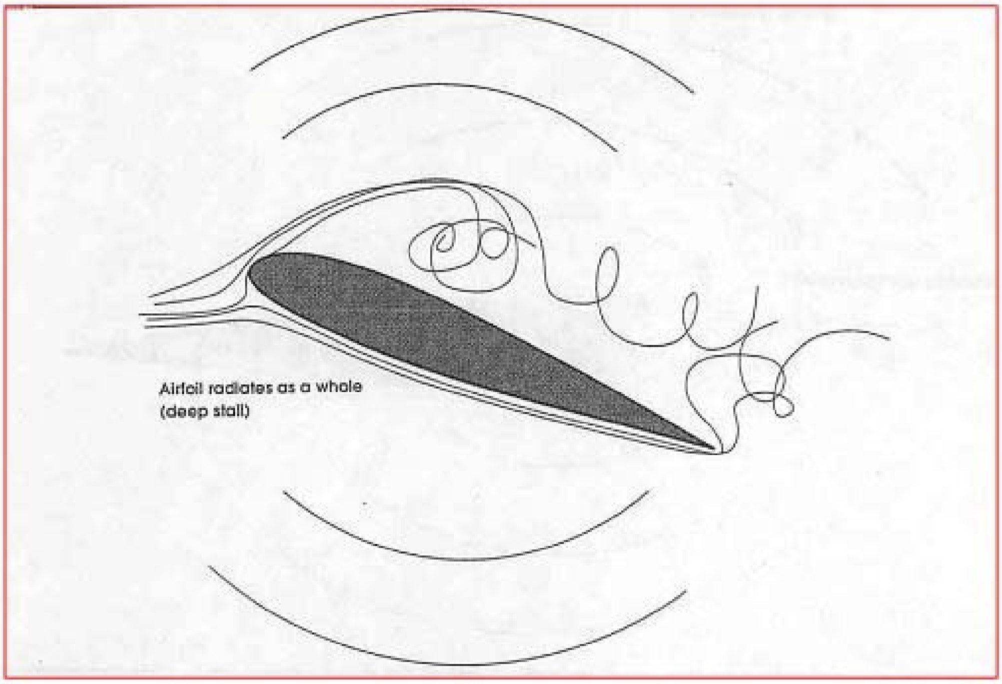

In the new design we have no separation of the boundary layer (divided in 2 parts, each with max aspect ratio, acting alone harmonically, slot+wing)

Blade Tip Noise

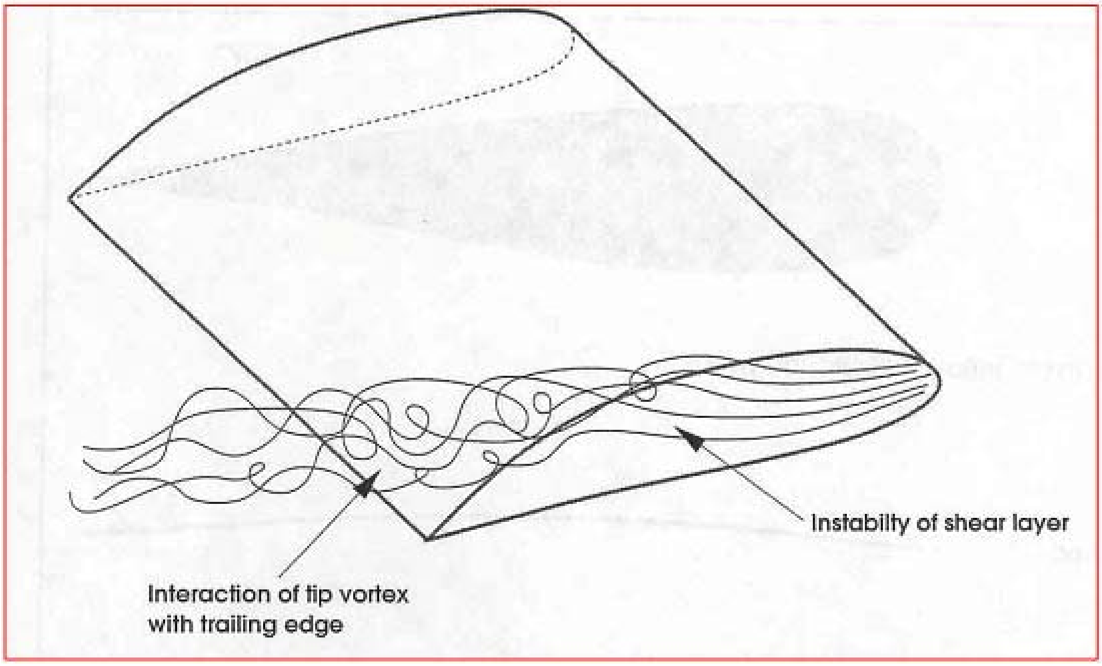

Same observations.

Demonstration

3-blades propeller connected to an electric motor.

Illustrates:

- Thrust generated by flat-blades propeller
- Drop in current intensity
- No tip noise
- Directional airflow

Conclusion

Airfoil profiles, wings, propellers and turbines have not evolved significantly since their discovery. The "twisted profile" shape has outlived its usefulness and it is time to consider alternative, more efficient designs.

Mr. Hussain's patented invention is showing promising results in the fields of aeronautics, marine and alternative energy. Tests results have shown that it is possible to make propellers with a 45 degrees angle of attack without twisting, something that most aeronautical experts would scream to be impossible.

This new design, when applied to wind turbines, gives us a new way of thinking about how to capture wind energy. Its angle of attack, its flat blade design, its high aspect ratio, its lack of boundary layer separation – all those elements open up new possibilities for wind turbine design.

For more information

Contact the author at gadaix@gmail.com

Check US patent no. 7396208 B1

Third International Meeting
on
Wind Turbine Noise
Aalborg Denmark 17 – 19 June 2009

Vibration and noise of a horizontal axis wind turbine

Maria GOLEC, Zdzisław GOLEC

Poznań University of Technology, Institute of Applied Mechanics

Piotrowo 3 Street, 60-965 Poznań, Poland

maria.golec@put.poznan.pl , zdzislaw.golec@put.poznan.pl

Abstract

The paper presents the results of vibroacoustic tests of Danish Bonus and Nordtank wind turbines, each of rated power 150 kW. The vibration and noise tests have been carried out within a single measurement session at a private farm in Radolina, commune Golina, district Konin (eastern part of Wielkopolska). During the tests three wind turbines were installed and operated at the farm: two Nordtank and a single Bonus ones (the farm is under development and further air-generators are to be implemented there). The turbines were manufactured in 1991 and formerly used in Denmark. The vibroacoustic tests included the following:

- the tests of free vibration of the tower and nacelle,
- vibration measurement of the tower of the above mentioned air-generators with the help of a laser vibrometer,
- recording of the rotational sequence of the wind turbine blades with a high-speed camera,
- study of sound propagation in the vicinity of the Bonus turbine.

The physical model of the system including the tower, the nacelle located on its top, and the rotor has been assumed in the form of a restrained homogeneous beam (a pipe of uniform cross-section and wall thickness) with concentrated mass at one end (i.e. the mass of the rotor and nacelle). During the laser vibrometer measurement the displacements and vibration speed have been recorded. Results of the vibration tests are presented in the form of short-duration FFT analyses and the time patterns corresponding thereto. In result of the sequential analysis of the rotation of the Bonus turbine blades recorded with the high-speed camera it was found that the 2D visual information achieved this way does not allow for measuring the displacements of the blades and nacelle, as the nacelle changes its position according to the wind direction. The study of sound propagation in the vicinity of the Bonus turbine consisted in measuring the sound pressure in eight measurement points uniformly distributed every 45º at the circles of the radii 15 m, 30 m, and 45 m from the BONUS turbine. The sound pressure has been measured at the height of 0.6m and 0.3 m above the ground level.

Introduction

Development of wind power plants in Poland is, to large extent, a result of the policy of the European Union member states, focused on promotion of the growth of unconventional renewable energy sources, inclusive of the wind power. During recent years apart from large wind parks many small wind farms or single installation are created, built often by private investors. The smaller wind farms and single turbines are frequently located in the countryside or in the vicinity of individual and dwelling houses. Such location of the noise emitting wind turbines may disadvantageously affect the acoustic climate of the environment. Due to economical reasons in the new small wind farms composed of several stands often the old-type wind turbines are installed, sometimes previously operating in other countries. In Radolina (Wielkopolska) in a private wind farm three Danish wind turbines are operated – two ones of Nordtank and one of Bonus (the farm is under development by further air-generators). The turbines were manufactured in 1991 and formerly used in Denmark.

In order to assess the vibroacoustic processes arising during operation of the turbines the sound pressure around the Bonus turbine and vibrations of both air-generators towers have been measured. Moreover, the sequence of rotation of the Bonus turbine has been recorded. Additionally, a model study of free vibration of the tower with a nacelle has been carried out[1].

Subject of the study – Bonus and Nordtank wind turbines

The vibroacoustic study of wind turbines has been carried out in Radolina village, commune Golina, district Konin (eastern part of Wielkopolska). The farm included three operating wind turbines, each of minimal power 150kW: two Nordtank and one Bonus (Fig. 1).

In the neighbourhood of the wind farm located on an open, flat area there are no terrain obstacles. The wind farm is located about 350m away from the road. Such a location provides comfortable conditions for the vibroacoustic tests as the effect of the traffic on the measurement results may be ignored.

Technical parameters of the considered Bonus and Nordtank turbines insignificantly differ each from other (Table 1). The data are used in model research of free vibration of the tower.

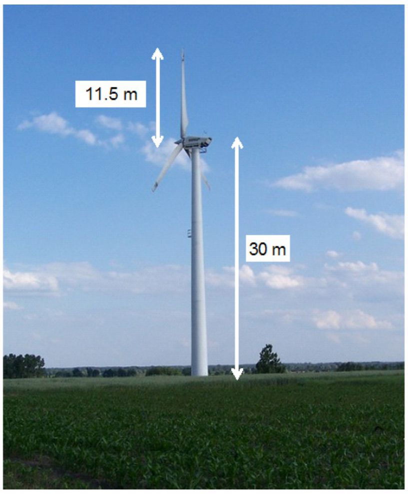

Fig. 1. Subject of the study - the Bonus MK ii 150 wind turbine; Radolina village, Province of Wielkopolska

[1] The study has been carried out within the framework of the Research Project No N501 062 32/4061 “Identification of noise sources and propagation of vibroacoustic processes of air-generator farms”

Table 1. Technical data of the Bonus and Nordtank wind turbines [2,3,4]

	Bonus MK ii 150	Nordtank NTK 150/25
Generator power	150 kW	150 kW
Rotor diameter	23.8 m	24.6 m
Number of the rotor blades	3	3
Area of the rotor profile surface	415 m^2	475 m^2
Rotor rotational speed at rated power	40.4 r.p.m.	38 r.p.m.
Tower shape	Cylindrical	Cylindrical
Tower height	30 m	31 m
Tower mass	15 000 kg	11 000 kg
Nacelle mass	6000 kg	6000 kg
Rotor mass	2500 kg	3900 kg
Blade mass	740 kg	830 kg
Total mass	23500 kg	21000 kg
Total mass per 1sq.m of the rotor	52.81 kg/m^2	44.21 kg/m^2
Thickness of the tower wall	0.015 m	0.015 m

Operation of the wind turbines depends on wind velocity. Both turbines are launched for the wind velocity of 4m/s. Rated power of the turbines is achieved at wind velocity of 13m/s. On the other hand, they must be stopped at wind velocity reaching 25m/s.

Sound propagation test

Noise has been tested within a sole measurement session during operation of all the turbines, i.e. two Nordtank and single Bonus ones. Weather conditions have bee determined by means of the Heavyweather weather station [4]. Wind velocity varied in the range 2-6m/s, temperature in the range 13.0 – 17.5ºC, and pressure from 985.7 hPa to 987 hPa.

Sound propagation test in the neighbourhood of the Bonus turbine consisted in measuring the sound pressure in eight measurement points located evenly at the circles of the radii 15m, 30m, and 45m around the Bonus turbine (Fig. 2). The sound pressure level has been measured at two elevations above the ground:

- At the height of 0.6 m. The test itself and noise acquisition have been carried out with the use of an assembly composed of the SVAN 912AE vibration and noise analyzer, ½' SCO2-C4 microphone provided with a weather cloth, and KA10 Calibrator. Three continuous spectra in the frequency band up to 5kHz and three tertiary spectra in the band up to 16kHz have been recorded. In order to minimize the effect of the ground type existing in particular measurement points around the turbine the microphone stand has been always situated on a sound reflecting laminated panel of the dimensions 1 m×1.2 m.

– At the height of 3 m – the noise has been measured with a DSA-50 meter from SONOPAN. Three tertiary spectra in the band up to 16 kHz have been recorded.

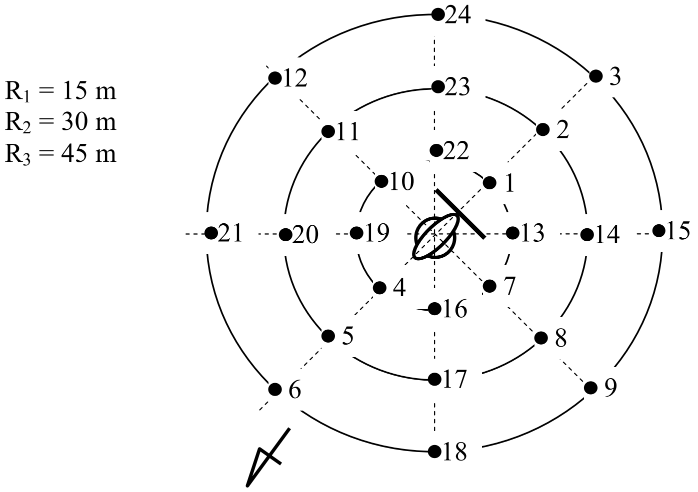

Fig. 2. Location of the points for sound pressure measurement around the Bonus wind turbine

Examples of the sound pressure measurement at the height of 0.6m above the ground at R_1=15m distance from the turbine tower (Figs 3 and 4) show that the Bonus turbine noise is predominated by infrasound and low-frequency ballast. Maximal level of the infrasound and low-frequency noise occurs after the passage of the rotor blades through the tower mast zone from the windward direction: $L_{ip\ max}$< 83 dB.

In higher frequency band within the audible range the noise level is remarkably lower, i.e. amounts approximately to 20 dB. The highest noise level in the whole audible range is also observed after the passage of the rotor blades through the tower mast zone from the windward direction.
At the distance R_2 = 30 m from the turbine tower the sound pressure level exceeds by several dB the one occurring at R_1=15m (the distance $R_2 \cong$ H+0.5 D, where H – tower height, D = 23.8 – rotor diameter).

Hence, significant noise, both in low frequency and audible ranges, is generated after the passage of the rotor blades through the tower mast zone from the windward direction.

At the height of 3 m above the ground level the sound pressure did not exceed 70 dB

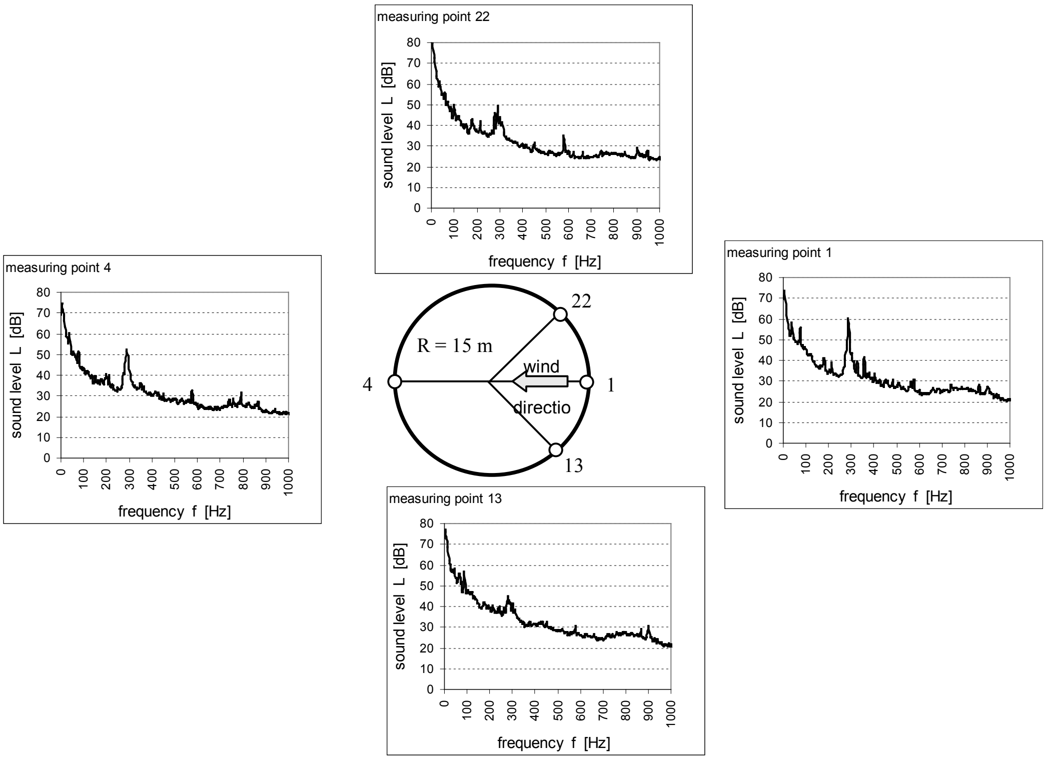

Fig. 3. Averaged noise spectra at the distance R_1=15 m from the Bonus turbine tower

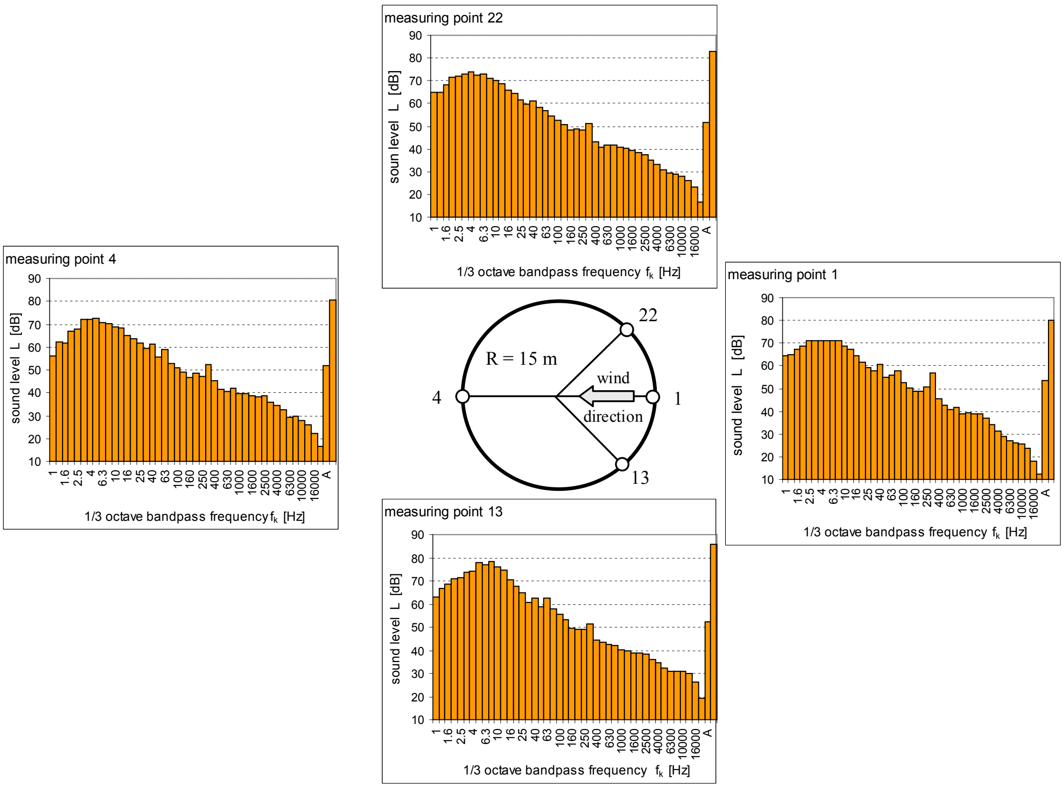

Fig. 4. Averaged 1/3 octave noise spectra at the distance R_1=15 m from the Bonus turbine tower

Study of vibration of the towers of the Bonus and Nordtank turbines

For purposes of vibration measuring of the turbine towers a laser vibrometer composed of the OFV 5000 controller and OFV 505 Polytec head has been used, in connection with SCADAS Mobile dynamic analyzer of LMS provided with Test.Lab software (the Signature Acquisition module). For purposes of analyzing the recorded displacement and vibration velocity time patterns the Time-Variant Frequency Analysis module has been used. The module has been located about 5m away from the air-generator footing.

Anti-reflective paint of the tower made the laser measurement of the vibration difficult or even impossible. Hence, in order to improve the quality of the reflected signal the stripes of antireflective band have been fixed to the measurement points of the tower.

The four measurement points have been located at two levels in 2 vertical planes (Fig. 5).

Results of displacements and vibration velocities measurement are presented in the form of short-time FFT analyses and the time patterns corresponding to them. Examples of tower displacement and vibration velocity measurements are shown in Figs 6 and 7.

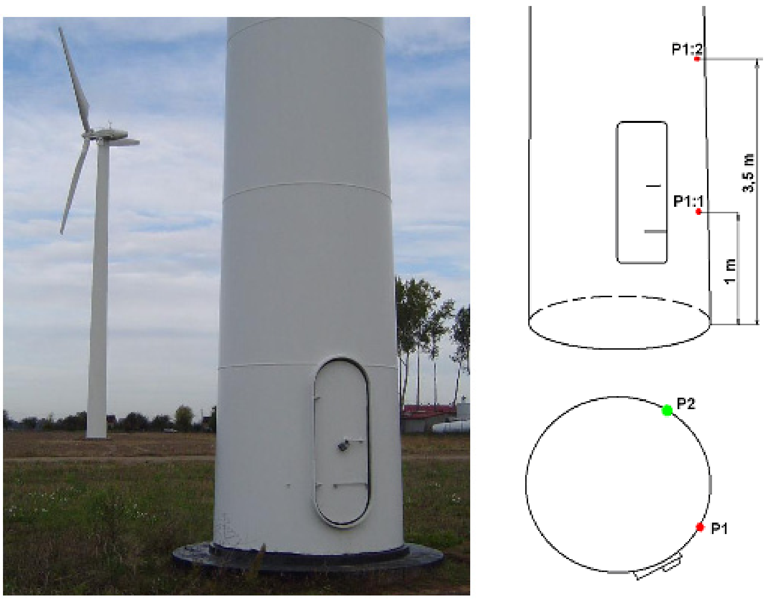

Fig. 5. Measurement points of displacements and vibration velocities of the tower
The point 1:1 – at the height 1m and the point 1:2 – at the height 3.5m
The point 2:1 – at the height 1m and the point 2:2 – at the height 3.5m

point 2:1

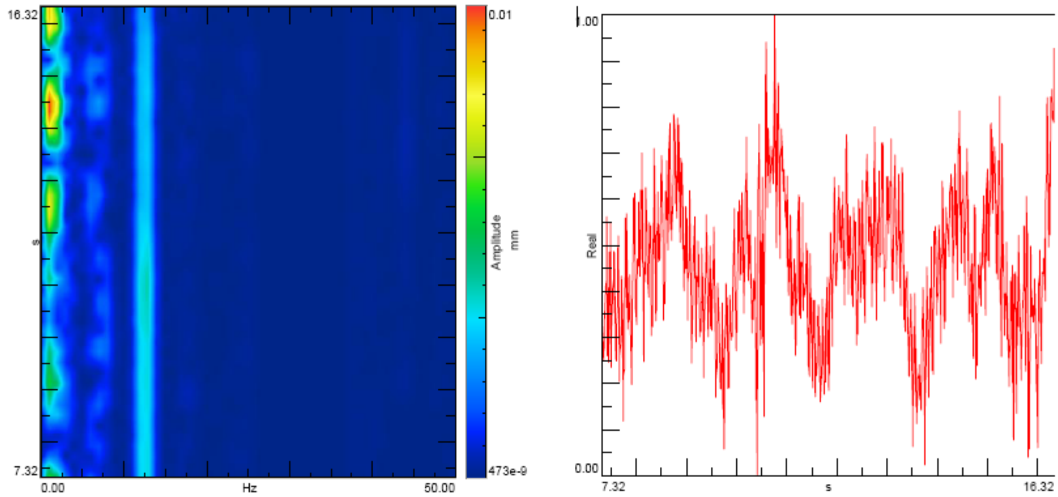

point 2:2

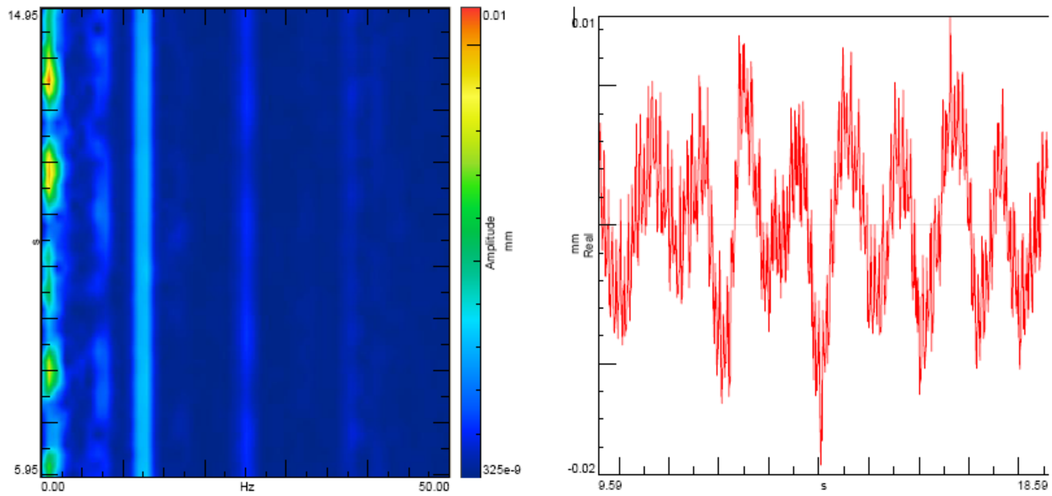

Fig. 6. Bonus turbine – vibration displacements in the frequency range up to 50Hz (points 2:1 and 2:2)

point 2:1

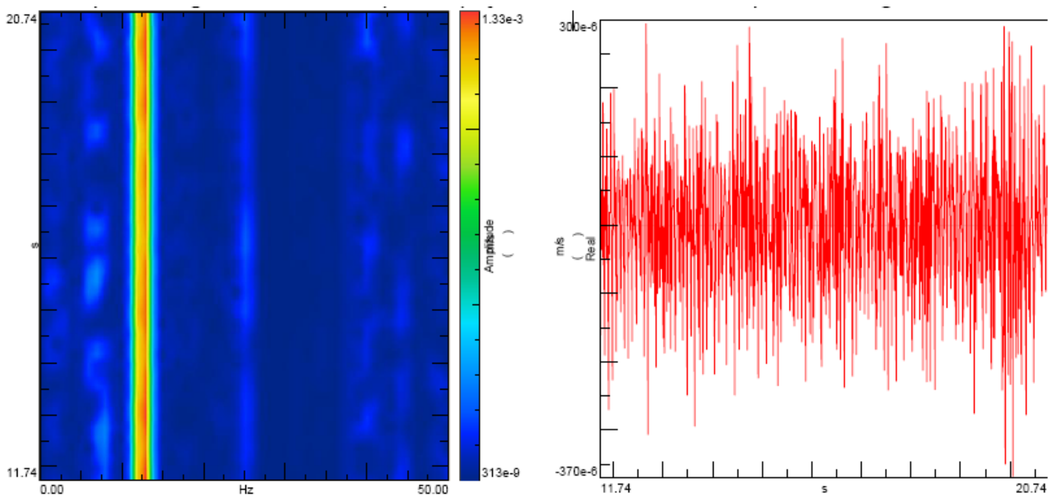

point 2:2

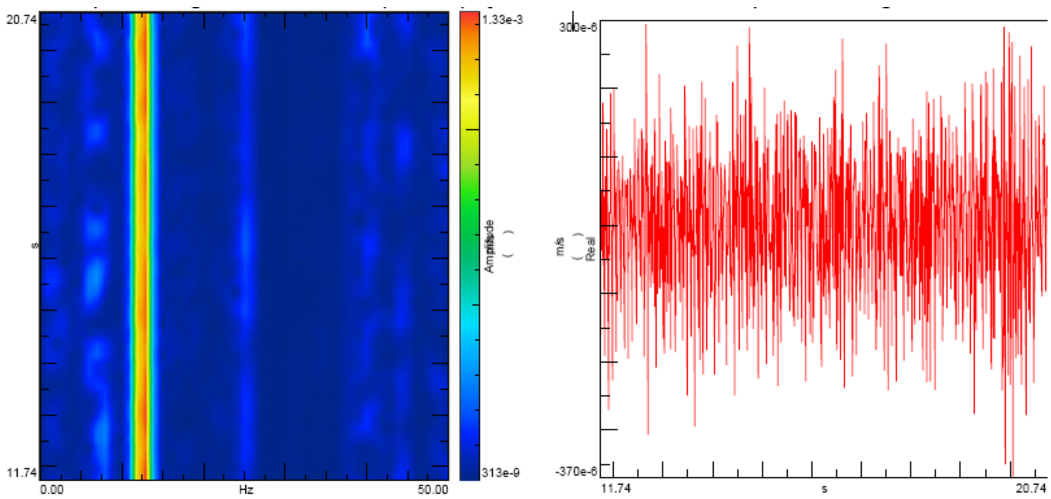

Fig. 7. Bonus turbine – vibration velocities in the frequency range up to 50Hz (points 2:1 and 2:2)

Based on the analysis of the patterns of displacement and vibration velocity measurements of the Bonus and Nordtank towers it was found that:

- for purposes of the tower behaviour observation, i.e. its bending and torsion, the analysis of vibration displacements is more useful;
- the tower vibration generated in result of time-varying external forces (the wind) and induced by the rotor, generator and gear operation includes in the range from 0 to 300Hz;

- in case of both air-generator types the differences in vibration measurement results are small, while the physical phenomena reflected by them are similar, probably due to small difference in the design of these turbines.

The spectrograms of both turbines enable observing vibration amplitude modulations of the towers together with the parts fixed to them.

Recording the rotational sequence of the Bonus turbine blades

In result of recording of the rotational sequence of Bonus turbine blades with the help of the Vision Research rapid camera, model Phantom V.5.1., eleven films have been obtained, generated by conversion of the source material recorded in the cine to avi format, with the use of the XviD MPEG-4 Codec.

The recording of the rotational sequence of the turbine blades was aimed at analyzing the motion and answering the question whether the rotor and nacelle displacements may be measured by analysis of the visual information.

It was found that 2D analysis of the information does not enable measuring the blade and nacelle displacements. This is due to the fact that the nacelle adapts its position according to the wind direction and, therefore, the actual motion in the physical world must not be determined on the grounds of the motion of a given pixel and scale coefficient.

Further stage of the study consisted in determining trajectories of the motion of air-generator blades from various perspectives for each of them. Results of the measurement are presented in graph diagrams (Figs. 8 and 9).

Fig. 8. Trajectory of the motion of Bonus turbine blades

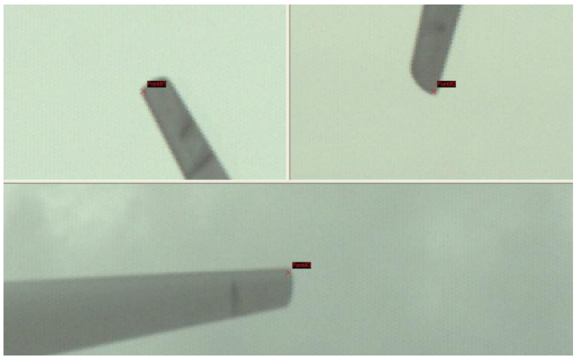

Fig. 9. Reference points of the correlation algorithm

It was found that the correlation algorithm based on watching the characteristic points of the image used in the present procedure is effective for purposes of tracing the air generator blade motion and enables automatic defining of the point coordinates as functions of time.

Study of free vibration of a simple model of horizontal axis wind turbine

The physical model of the tower with the nacelle and rotor located at its top has been assumed as a restrained homogeneous beam (the pipe of constant cross-section and wall thickness) with concentrated mass m (the sum of the rotor and nacelle mass) located at its end (Fig. 10).

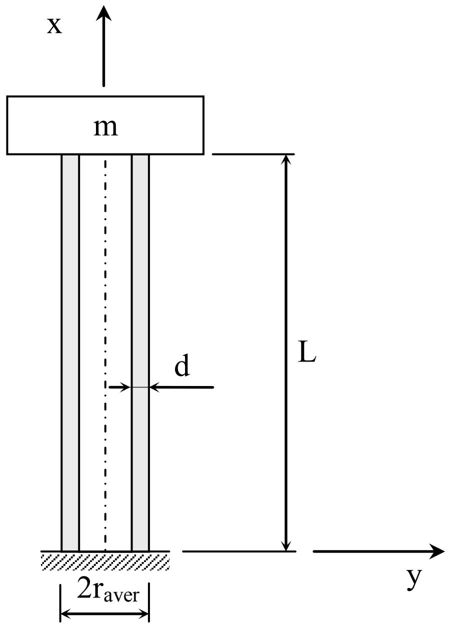

Fig. 10. Physical model of the air-generator: the tower with the nacelle

The equation of motion of the system is formulated as:

$$EI\frac{\partial^4 y(x,t)}{\partial x^4} + \rho A\frac{\partial^2 y(x,t)}{\partial t^2} + m\delta(x-L)\frac{\partial^2 y(x,t)}{\partial t^2} = 0$$

where:

E – Young modulus of the tower material,

ρ – density of the tower material,

$A = \pi d(2r_{aver} - d)$ – cross section area,

$I = \frac{\pi}{4} d\left(4r_{aver}^3 - 6r_{aver}^2 d + 4r_{aver} d^2 - d^3\right)$ – moment of inertia of the cross section with regard to the neutral axis,

$\delta(x-L) = \begin{cases} 0, & x \neq L \\ \infty & x = L \end{cases}$ – Dirac delta function.

The eigenvalues have been computed in the MATLAB(R) environment, with the use of an own program developed within the framework of the present work. Free vibration frequencies of the Bonus air-generator have been calculated with the assumption of the following data: average tower radius r_{av} = 0.69m, the tower wall thickness d = 0.015 m.

First five eigenvalues β_i and natural frequencies f_i of the boundary problem (for μ=0.5667 , the BONUS wind turbine: L= 30 m) are shown in Table 2

Table 2. Approximate eigenvalues and natural frequencies of the BONUS wind turbine

β_i	E [N/m^2]	ρ [kg/m^3]	I [m^4]	A [m^2]	H [m]	f_i [Hz]
1.3897						0.855
4.0941						7.423
7.1778	2.1E+11	7800	0.015	0.064	30	22.816
10.2890						46.881
13.4134						79.677

The modes of free vibration of the model for the calculated eigenvalues are shown in Fig. 11.

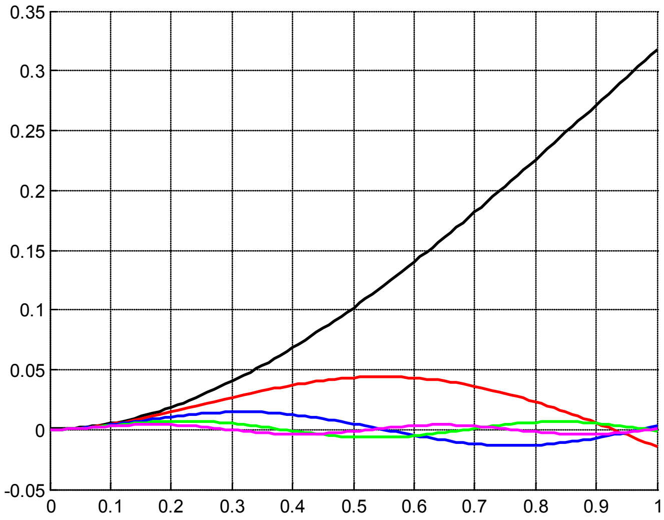

Fig. 11. Modes of free vibration of the Bonus air-generator for μ = 0.5667

In order to compare the model and experimental tests of vibration of the Bonus turbine tower Table 3 specifies the components of the displacement spectrum of tower vibration and free vibration frequencies of the tower model.

Table 3. The frequencies of tower displacement components and frequencies of free vibration of the model of Bonus air-generator tower

Number of the component	Frequency of the component f [Hz]	Frequencies of free vibration	
		Number of the eigenmode r	Frequency f_r [Hz]
1	**0.98**	**I**	**0.86**
2	1.51		
3	2.93		
4	6.49		
5	**7.71**	**II**	**7.42**
6	12.55		
7	**25.15**	**III**	**22.82**
8	37.89		
9	**44.09**	**IV**	**46.88**

Natural frequencies of bending vibration and the frequencies of predominating components of the air-generator tower vibration displacements obtained from experimental tests are close each to other. The differences between the values of natural frequencies and predominating components may be caused by many reasons, as for example:

- too simple mechanical model of the system – the tower should be considered as a pipe of varying diameter, while the model assumes constant diameter;
- vibration of the tower may be of complex character, i.e. of coupled bending-torsion type, while the model considers only bending vibration.

Conclusions

The tests of noise and vibration of the Bonus wind turbine may be considered as a case study for definite weather condition. Nevertheless, the results of the tests give some notion of the distribution of vibroacoustic field of the considered turbine.

Analysis of the 2D visual information did not enable measuring displacements of the blades and nacelle. Technological reasons precluded recording of 3D rotational sequence of the turbine blades, since such an analysis required the use of at least two synchronized cameras. In case of 3D measurement the object might be observed at other than right angle that would allow measuring the displacements of the wind turbine parts.

References

[1] BOCZAR Tomasz: Wind Power Industry. Actual potential utilization (in polish - Energetyka wiatrowa. Aktualne możliwości wykorzystania) Publisher: Pomiary Automatyka Kontrola, 2007, ISBN: 978-83-87982-37-9

[2] SCORE PK 3 – Renewable energy sources – utilization in communal and community economy (in polish: Odnawialne źródła energii – wykorzystanie w gospodarce komunalnej i gminnej): http://www.kape.gov.pl

[3] FIAŁEK Mariusz, ŁUKASIK Roman: Polish Wind Turbine produced by „NOWOMAG" S.A. – engineering state, device quality, development and application perspectives (in polish: Polskie elektrownie wiatrowe produkcji „NOWOMAG" S.A. stan techniki, jakość urządzeń, kierunki rozwoju i zastosowań): http://www.igf.fuw.edu.pl

[4] Technical data of weather station WS 2300: http://www.heavyweather.info

Third International Meeting

On

Wind Turbine Noise

Aalborg Denmark 17-19 June 2009

Using the Noise Perception Index (NPI) for assessing wind turbine noise

George F. Hessler Jr., Bd. Cert. INCE

Hessler Associates, Inc.

3862 Clifton Manor Place, Suite B

Haymarket, Virginia 20169

George@HesslerAssociates.com

Abstract

The author has recently published a detailed noise impact assessment methodology[1] in the Noise Control Engineering Journal applicable to conventional facilities and power plants. The method averages on an energy basis the hourly increase-to-ambient caused by a planned or existing source over a representative minimum length of time to predict the long-term perception and response from adjacent communities. The core foundation used to justify the method is decades of successful experience gained in three States in the U.S. that use the increase-to-ambient or ambient-based approach for permitting facilities. The ambient basis for NPI is the daily minimum hourly LA90 measured typically during calm & still wind conditions. This paper explores the applicability of the NPI method for wind turbine generators (WTG) that only operate during windy conditions. Measurements from a single 1.65 MW WTG over a 14-day sampling period is presented to characterize noise emissions from a typical (WTG) installation. NPI was determined for this installation as well as a planned installation to calculate the NPI index at each. The results of NPI predictions appear promising for assessing WTG noise on a long term equitable basis.

Introduction to the NPI Methodology

The NPI method is based on receiver perception of noise emissions from the subject installation over the long term accounting for the daily operational time of the installation by integrating the increase-to-ambient over a representative time period. For conventional facilities and power plants, a minimum of one week is suggested for ambient measurements. The baseline ambient metric is the minimum daily hourly LA90 measurement arithmetically averaged over the number of sampling days. The community response to the integrated increase-to-ambient or NPI Index is formulated on decades of successful installations in three states in the U.S. that dictate a minimum increase-to-ambient standard.

It is shown in reference 1 that the residual sound level, LA90 is much more suitable than LAeq for defining an ambient baseline to predict *perception* to a new source. The figure below illustrates an increase-to-ambient of 3 dBA for both the measured ambient of LA90 and LAeq caused by a new source set equal to each ambient metric. Even though the increase is 3 dB for each case, the perception of the change is drastically different.

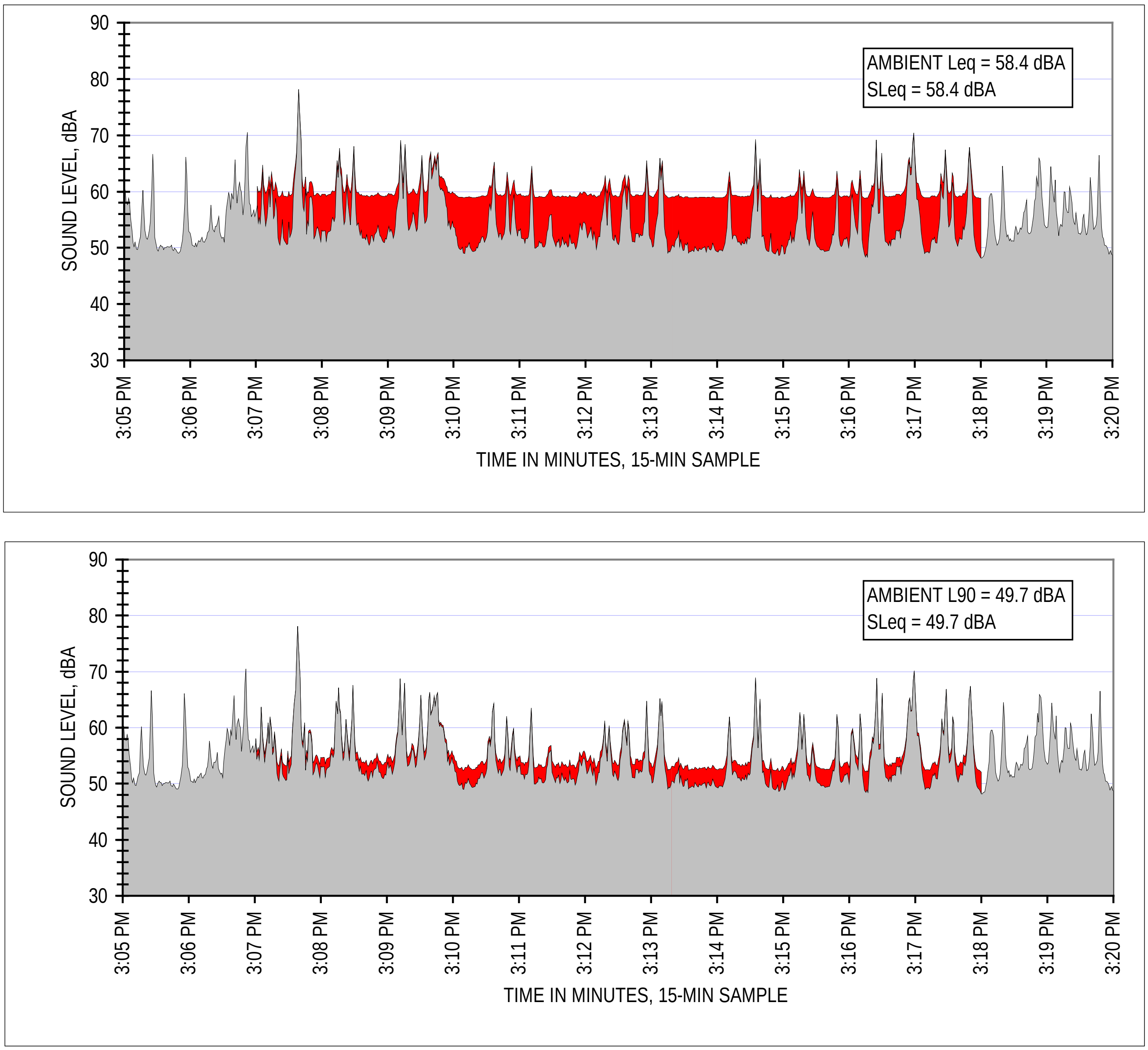

Figure 1: *Increase-to-ambient of 3 dBA for the measured baselines of LA90 and LAeq.*

The perception caused by a new source set equal to LA90 is *barely perceptible* due only to a likely change in character between traffic noise and the source, and only during prolonged lulls in passing traffic. Conversely, if the new source is set equal to LAeq, the source is *readily noticeable* except for very brief seconds when individual vehicles pass-by.

The following graphic illustrates the computation of NPI for an ambient with repeatable daily traffic patterns although it is shown in the article that the technique is also well suited to rural ambient environments where temporal patterns are more random.

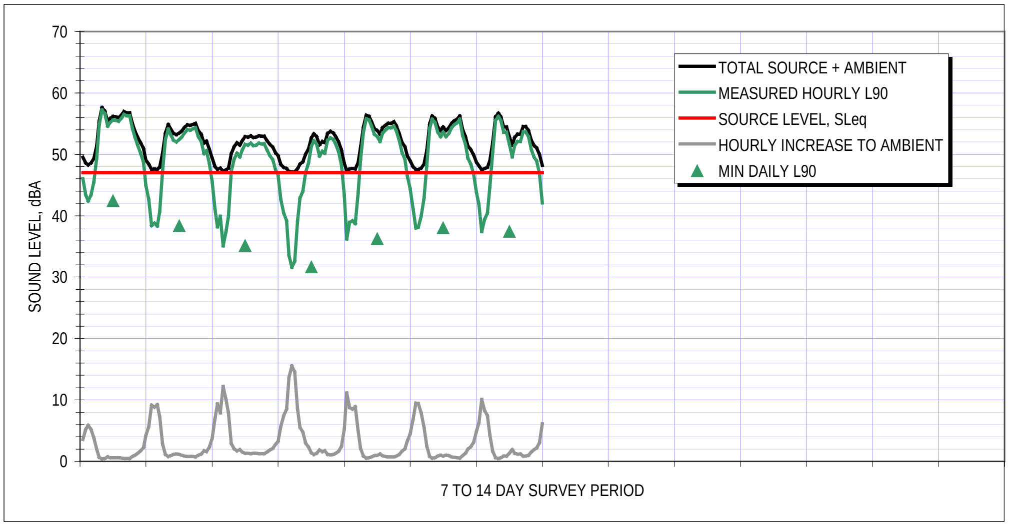

ANALYSIS RESULTS:

10	NOMINAL INCREASE TO BASELINE AMBIENT
37	BASELINE AMBIENT
47	SOURCE LEVEL, SLeq
4.8	NPI INDEX
x	24/7 OPERATION

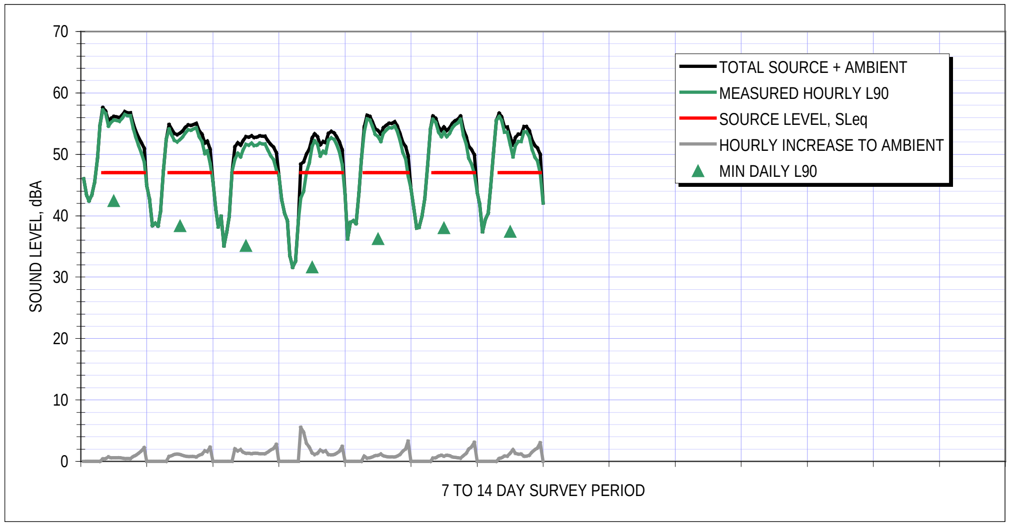

ANALYSIS RESULTS:

10	NOMINAL INCREASE TO BASELINE AMBIENT
37	BASELINE AMBIENT
47	SOURCE LEVEL, SLeq
1.4	NPI INDEX
x	OFF AT NIGHT OPERATION

Figure 2: *Sample calculation of the NPI Index for two power plant operational cycles.*

The hourly LA90 ambient is plotted in green and the new operational source in red. The hourly increase-to-ambient is plotted in gray at the bottom of the figures. It is seen that the NPI Index drops from 4.8 to 1.4 if the facility is not operated during quiet nighttime hours. The NPI computation provides a way of quantifying perception to the time change in operational cycle. The NPI Index is related to expected community response in the following Table.

It remains to apply this methodology to a wind park project that is considerably more complex than a conventional industrial facility of power plant.

Table 1: *NPI Index/Perception/Predicted Community Response.*

NPI INDEX	PERCEPTION	PREDICTED COMMUNITY RESPONSE
<= 3 dBA	GENERALLY IMPERCEPTIBLE	NO RESPONSE
3 TO 5 dBA	BARELY PERCEPTIBLE TO PERCEPTIBLE	NO RESPONSE TO POTENTIALLY ADVERSE RESPONSE
5 TO 10 dBA	PERCEPTIBLE TO NOTICEABLE	POTENTIALLY ADVERSE TO ADVERSE RESPONSE
> 10 dBA	READILY NOTICEABLE	ADVERSE RESPONSE

DEFINITIONS AND CONDITIONS FOR ABOVE TO BE APPLICABLE:

NPI INDEX	The Noise Perception Index (NPI) is the true pressure average increase calculated for each hour over a seven-day(or more) operation of the new source
AMBIENT	The measured hourly LA90 residual level over a minimum seven-day (168 hour) period.
MINIMUM DAILY AMBIENT	The minimum measured hourly LA90 in any hour over each of seven days (or more) ambient survey period
BASELINE AMBIENT	The arithmetic average of the seven minimum daily ambient LA90 measurements
SOURCE LEVEL	The source level, LAeq or LCeq is the equivalent sound level of the source under evaluation
PURE TONE	No pure or prominent tone is permitted at any potentially sensitve receptor location. A pure tone is defined in EPA Report 550/9-76-003
LOW FREQUENCY NOISE (LFN)	Potential adverse impact from LFN must be evaluated if LCeq - LAeq => 20 at any receptor
NOMINAL INCREASE TO AMBIENT	The difference between SLeq and the baseline ambient at any receptor

Typical WTG Noise Emission Patterns and Modeling

A 14-day plot in 10-minute intervals for an operational WTG is given below. The LA90 sound level was measured in three directions at 1000 feet (300m) and in one direction at 2000 feet (600m). The WTG was at the end of a line of turbines and the measured data is essentially from a single 1.65 MW WTG located in a flat soy bean field remote from common air and road sources of environmental noise.

The pattern is complex due to changing and unsteady wind speed and direction, and it is clear the sound level changes from any single 10-minute interval to another. Note there are a couple of periods of detected very high noise generation attributable to fast moving weather fronts. The data also shows that the wind speed can be quite low at ground level while it is high enough to operate the turbine at upper elevations. This adds the complexity of modeling the noise emissions from the WTG as a function of wind speed.

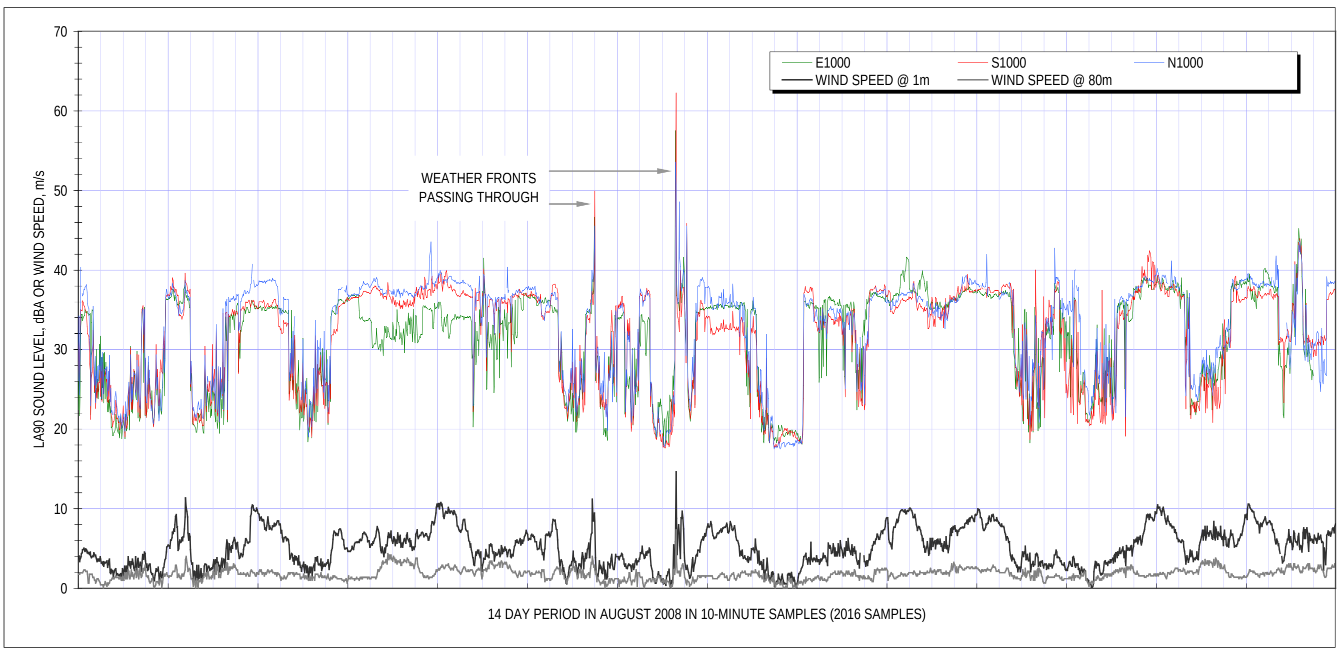

RAW DATA AT 1000' IN THREE DIRECTIONS WITH WIND SPEED AT 1m AND 80m

Figure 3: *Typical WTG noise emissions over a 14-day sampling period.*

Our experience using the ISO 9613 sound propagation model has been good. The major parameter of question is ground effects and if such effects occur in the source range close to the turbine since the source is very high in elevation. A single 1.65 MW turbine is modeled at 1000 feet (300m) below using ground effects from totally reflective to totally absorbent.

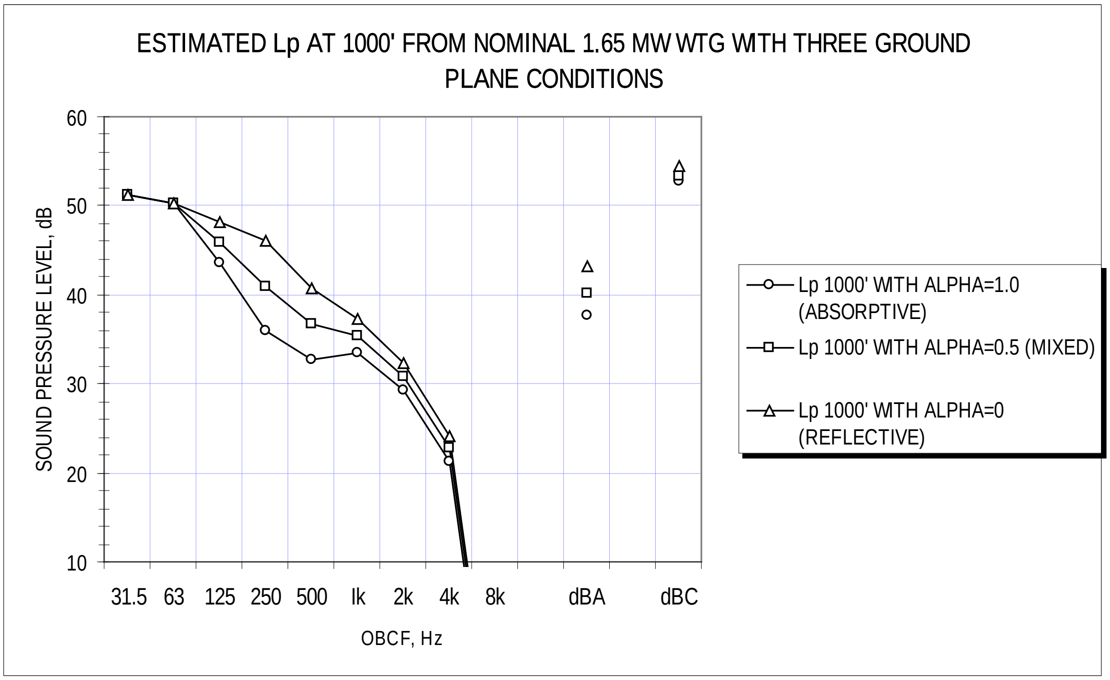

Figure 4: *Estimated Lp at 1000' (300m) for a single 1.65 MW WTG.*

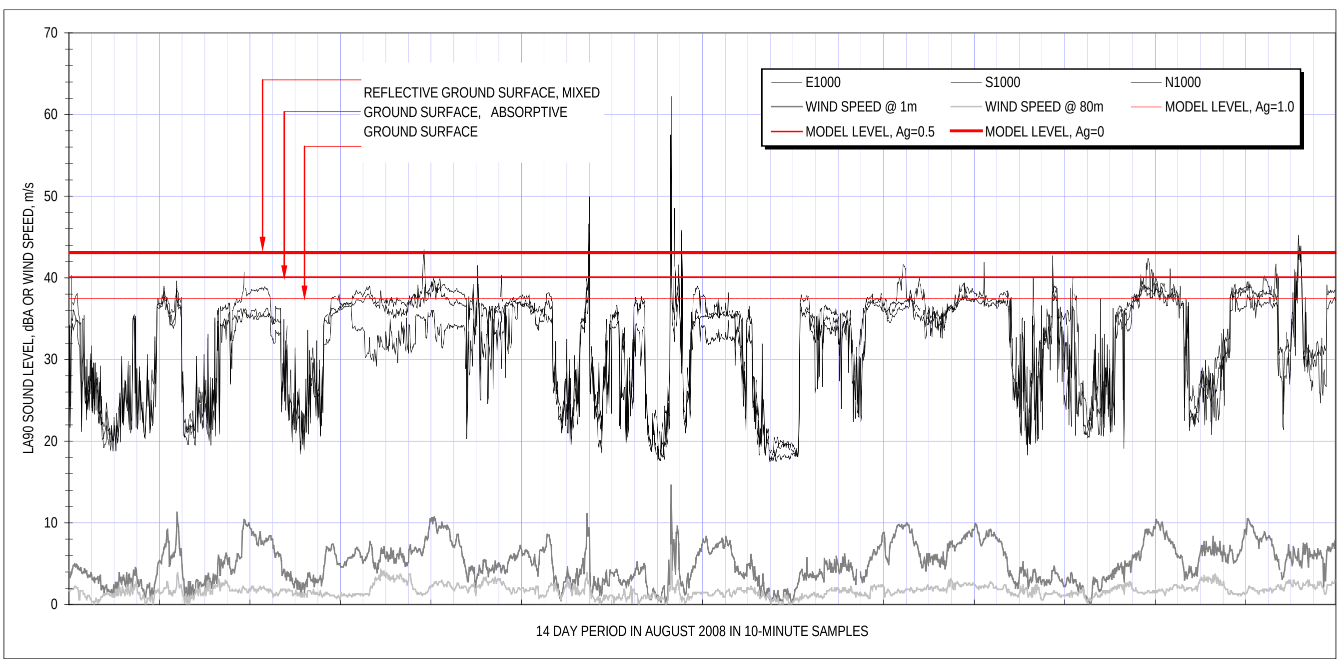

RAW DATA COMPARED TO ISO 9613 PREDICTION ALGORITHMS

Figure 5: *Modeled LA90 versus measured LA90 over a 14-day sampling period.*

Figure 5 above overlays the model estimates onto the measured operational data. One could assume a ground absorption coefficient of 1.0 for a soy bean field with 2 foot (600mm) plants as acoustically soft, but the best fit of the model is Ag = 0.5. Using Ag =1.0 would be unduly conservative. The firm uses 0.5 for all ground appearing to be acoustically "soft".

The real essence of the measured data for this site is illustrated below that plots the WTG noise over an ambient. The plotted ambient was acquired 2 to 3 miles (3 to 5 km) away in a similar field but remote from all audible WTG noise during the same time period.

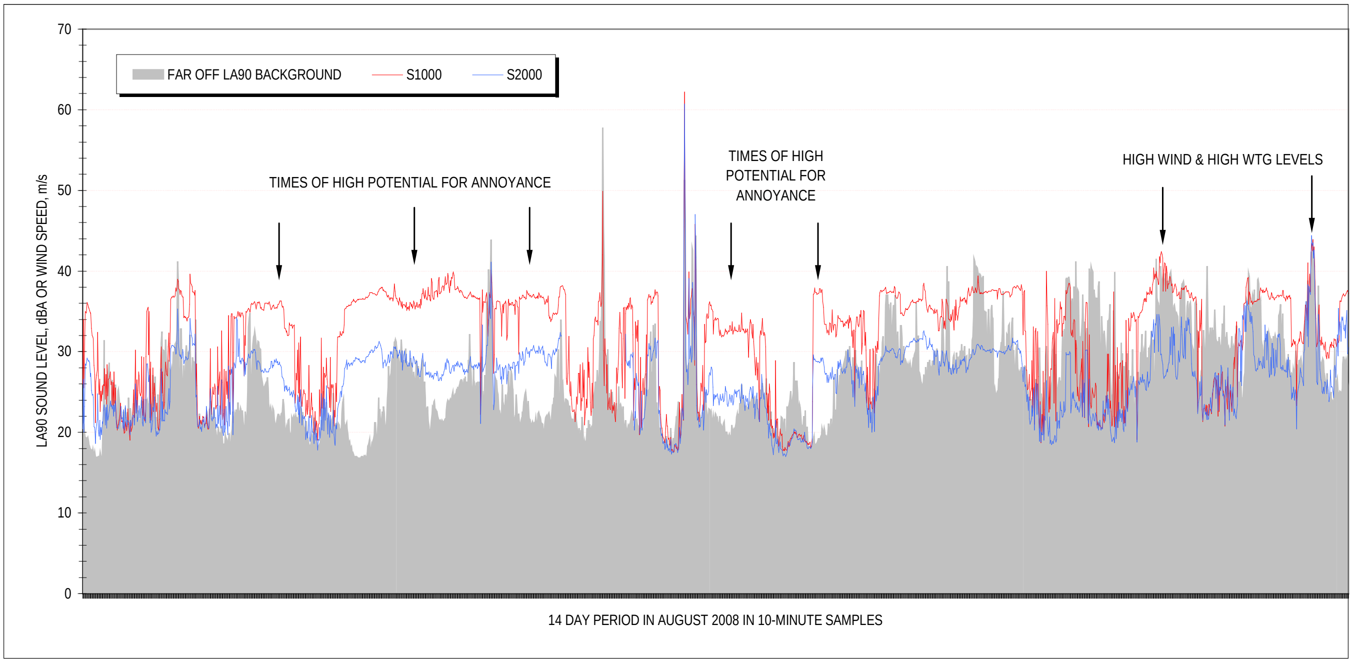

MEASURED LEVELS TO THE SOUTH COMPARED TO REMOTE AMBIENT

Figure 6: *Wind turbine noise emissions at two distances compared to area ambient.*

There are certainly periods of time when the ambient is low with light to no wind at the ground surface but sufficient wind at 80 meter hub-height to drive the turbine. As the wind speed increases, so does ambient noise. So, there is promise that a fair assessment can be made by integrating the increase-to-ambient over time. Another parameter called the percentage of time above (%TA) could also be combined with the NPI computation. The %TA a threshold is gaining acceptance in airport noise analysis because communities can relate to time above a threshold much easier than average DNL (Day Night Sound Level).

Adapting the NPI method to a WTG project

The first step in assessing any site is the measurement of the macro-area ambient sound level. For planned wind turbine projects, it is customary to measure the LA90 residual level in 10-minute intervals over at least a 14 day period. The data is analyzed as a function of simultaneous wind speed to determine LA90 versus wind speed from the cut-in to cut-out wind speed of the wind turbine generator (WTG). The NPI method as now written for conventional power facilities is based on the arithmetic average of the daily minimum LA90 level over a minimum of at least a seven day week to establish a baseline area ambient.

A good argument could be made to define the NPI baseline ambient for wind turbine projects as the average of the daily 10-minute or 1-hour LA90 at a wind speed of 5 or 6 m/s at the referenced elevation of 10m over the 14-day sampling period. At this wind speed, the WTG is making power and the ambient sound level at ground level is still low, but not as low as during calm and still conditions.

For purposes of this paper only, we shall use the currently defined minimum daily hourly LA90 level as a baseline. It is shown below that using the minimum measured 10-minute LA90 data is unduly conservative as opposed to the hourly sampling period by about 2 dBA. One hour data can be obtained from measured 10-minute sampling by simply averaging the six LA90 samples in each hour and the plot illustrates the results. The plot illustrates that on day 11 a single low value for a 10-minute interval occurred, but this value is not representative of the minimum daily level.

CALCULATED NPI BASELINE FROM MEASURED 10-M DATA DAY	FROM DAILY (144) 10-M SAMPLES MEASUREMENTS	FROM DAILY (24) 1-HR SAMPLES (ARTHMETIC AVERAGE)10-M DATA	FROM DAILY (24) 1-HR SAMPLES (POWER AVERAGE)10-M DATA
1	17	17	17
2	18	19	19
3	17	18	18
4	17	17	17
5	20	22	22
6	18	19	19
7	17	18	18
8	19	20	20
9	18	18	18
10	25	26	26
11	20	23	23
12	21	24	25
13	23	25	25
14	23	24	24
NPI BASELINE	19	21	21
MIN DAILY HOURLY LA90	19.35	20.70	20.77

Table 2: *Computation of Hourly LA90 from 10-minute measured data.*

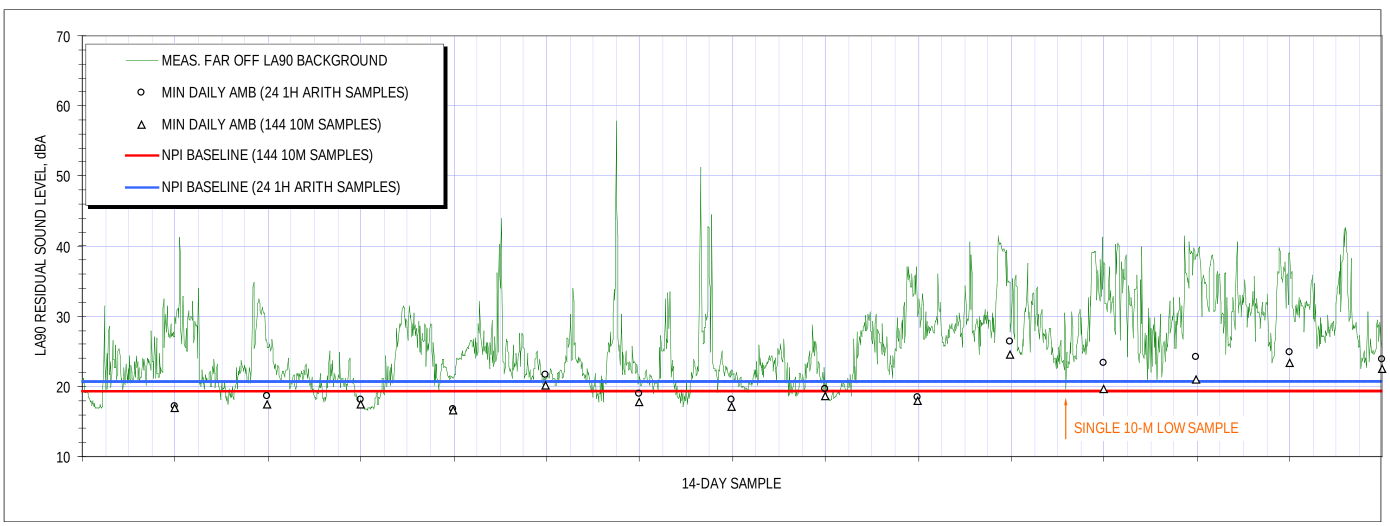

Figure 7: *14-day 10-minute samples and daily 1-hour minimums*

Computation of NPI Index for a Completed Wind Turbine Project

The completed site above is near a 'worst-case scenario' with a very low ambient of 21 dBA. NPI can be computed directly from the data by determining the increase to ambient over the 2016 samples by simply subtracting the measured levels near the turbines from the remote ambient levels. This is plotted below for the data at 1000 and 2000 feet from the WTG.

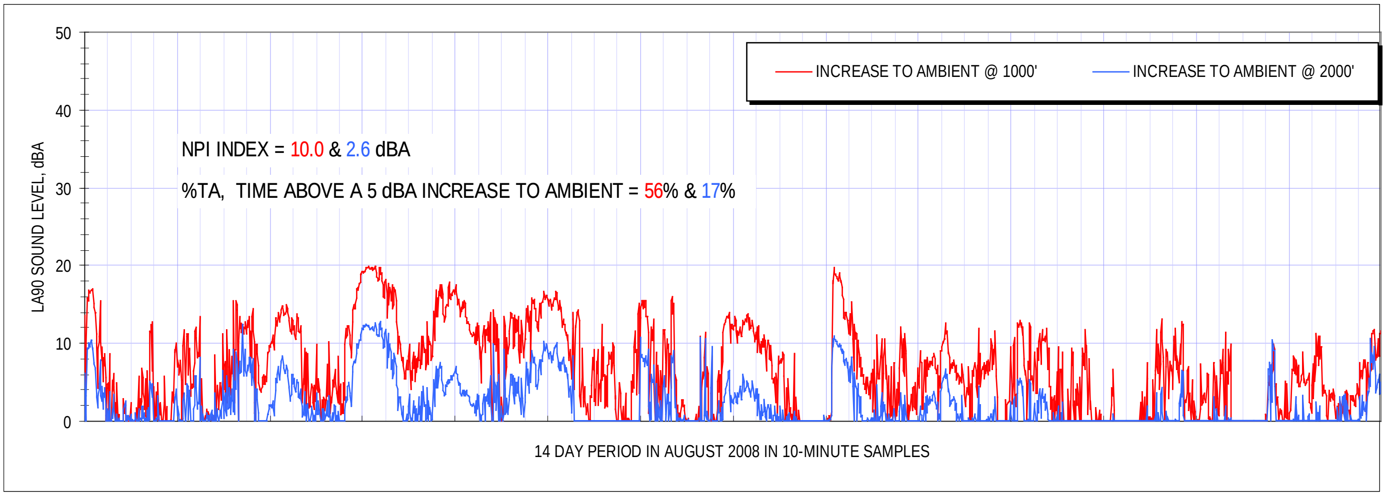

Figure 8: *Increase-to-ambient at 1000 and 2000 feet from a WTG.*

NPI is a value of 10.0 dBA at 1000 feet that predicts a high probability of adverse response but drops to only 2.6 dBA at 2000 feet where no adverse response would be predictable. Note also that the time above a threshold of 5 dBA increase reduces from 56 to 17% of the sampling time between 1000 and 2000 feet.

It should be noted this data is applicable to a single WTG and does not include cumulative effects from adjacent units. There have been no adverse effects for this project as the area contains many large acreage farms and distances from the turbines to residences is correspondingly large.

Computation of NPI Index for a Planned Wind Turbine Project

The plots below show a typical ambient measurement of hourly LA90 over a 14-day sampling period in a rural farmland environment under consideration for a WTG project. The upper plot is at three locations representing the whole project area. The outlier peaks are farm activity near the monitor al location 2. The bottom plot is the averaged macro-area ambient (with farm activity removed) compared to the average wind speed measured at met towers near the noise monitoring locations. The green triangles show the daily hourly minimum LA90 that is averaged to define a baseline ambient of 27 dBA in this example.

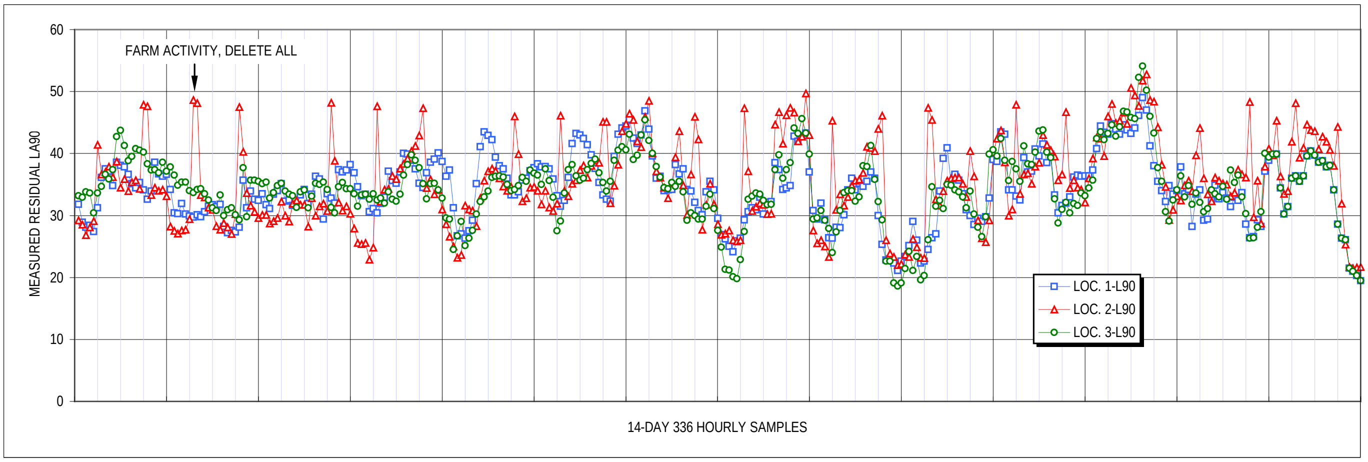

HOURLY RAW DATA -PRECONSTRUCTION SURVEY

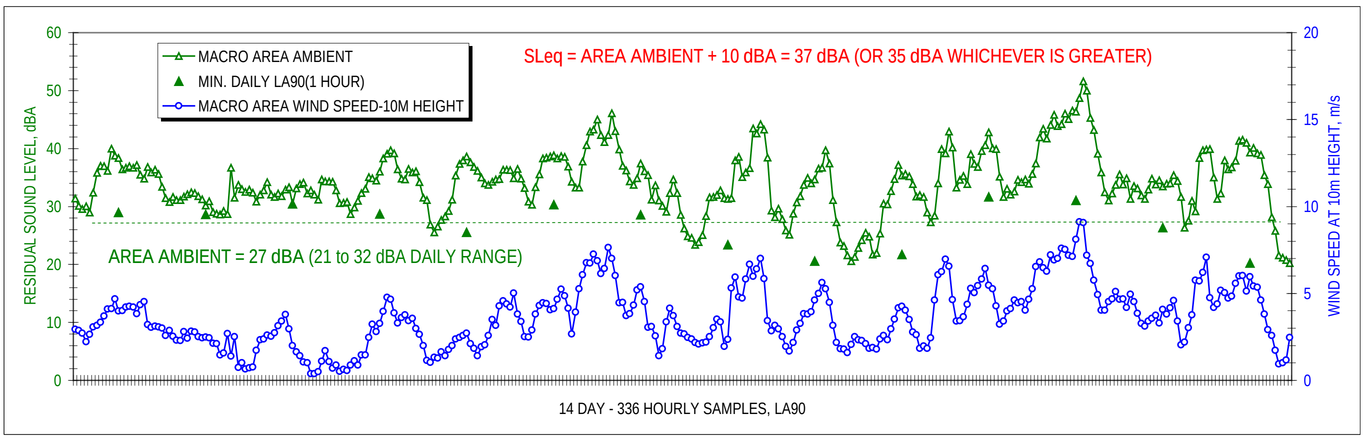

AVERAGED DATA FOR MACRO AREA AMBIENT

Figure 9: *Upper plot is raw data at 3 locations. Lower plot is the averaged macro area ambient with the farm equipment noise removed from data.*

It is easy enough to determine when the WTG units would operate when the wind speed exceeds the WTG cut-in speed of 3 m/s for this turbine model. This data is needed for the NPI computations.

What is not so easy is modeling WTG noise emissions as a function of wind speed for each operating period. Experience is accumulating that the most sensitive operational time is just beyond cut-in speed; 3 to 4 m/s measured at the standard elevation of 10m for most turbines of current design.

Most turbine models emit more noise as wind speed increases above cut-in speed until a steady level of maximum emissions occurs at about 5 to 6 m/s for most WTG models. For ease, we can make the *conservative* assumption that WTG emissions are at this maximum level whenever operating for computation of NPI even though the ambient baseline occurs during calm and still periods.

The NPI computations are best shown graphically below. Firstly, the macro baseline ambient for the 14 days is 27 dBA in this particular area and is the arithmetic average of the 14-day minimum hourly levels. Experience in the three states over many decades demonstrates that adverse community response is avoided if the increase-to-ambient is in the range of 5 to 10 dBA over a minimum baseline ambient. The range evolves since the definition of the baseline ambient differs from state to state. For example, one state allows a 10 dBA increase to the minimum measured single hourly LA90 level over a 24-hour period, while another allows a 5 dBA increase over the average of the minimum four consecutive hours. These converge to somewhere between 5 and 10 BA.

For our example, we can set the WTG level at 37 dBA, 10 dBA above the baseline ambient and compute NPI. The resulting NPI Index is 2.7 dBA which is below the threshold for adverse response with the prediction that community response to WTG noise would not be adverse. This is not too surprising a result for an intruding source of only 37 dBA that is not continuous.

The %TA above an increase-to-ambient of 5 dBA is calculated at 12% indicating the wind turbine noise could be noticeable to an out doors observer for this percentage of time over the 14-day sampling period. The maximum hourly increase-to-ambient does not exceed 10 dBA.

WTG = 37 dBA LIMIT

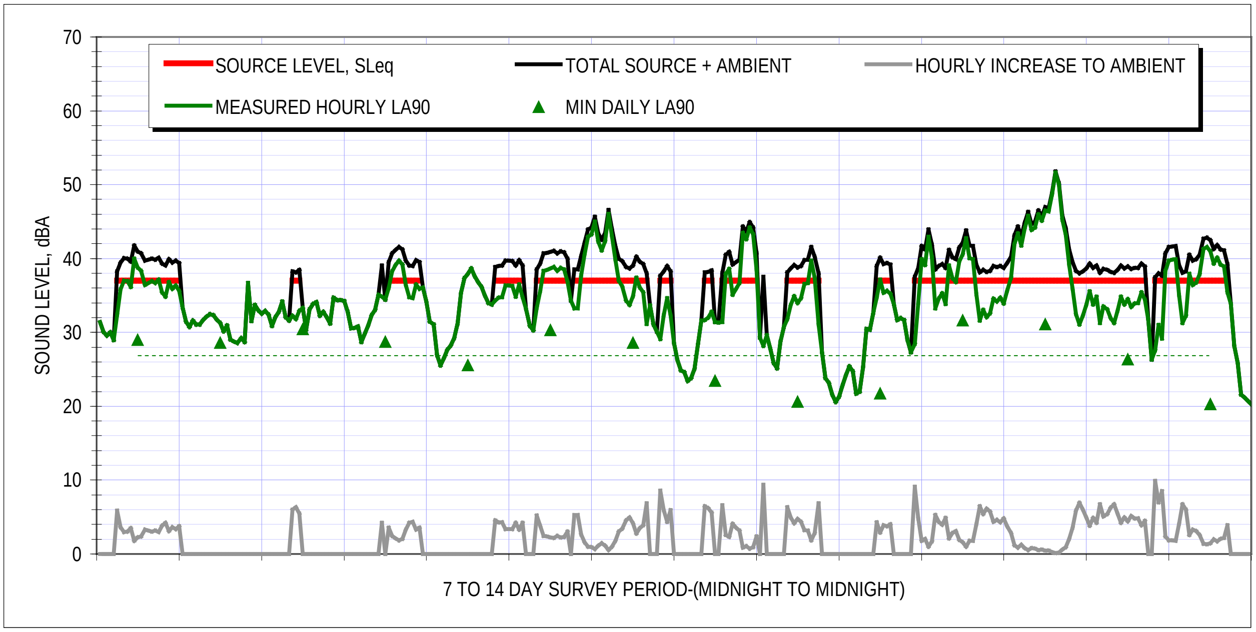

ANALYSIS RESULTS:

10	NOMINAL INCREASE TO BASELINE AMBIENT
27	BASELINE AMBIENT
40	SOURCE LEVEL, SLeq
2.7	NPI INDEX
x	OPERATION ABOVE CUT-IN SPEED
12	%TA, % OF TIME INCREASE-ABOVE-AMBIENT IS > 5 dBA

PREDICTED LONG TERM PERCEPTION AND COMMUNITY RESPONSE

NPI INDEX	PERCEPTION	PREDICTED REACTION
=< 3 dBA	GENERALLY INPERCEPTIBLE	NO ADVERSE RESPONSE
3-5 dBA	BARELY PERCEPTBLE TO PERCEPTIBLE	THRESHOLD OF POTENTIAL ADVERSE RESPONSE
5-10 dBA	PERCEPTIBLE TO NOTICEABLE	INCREASING PROBABILITY OF ADVERSE RESPONSE
=> 10 dBA	READILY NOTICEABLE	HIGH PROBABILITY OF ADVERSE RESPONSE

DEFINITIONS AND CONDITIONS FOR ABOVE TO BE APPLICABLE:

NPI INDEX	The Noise Perception Index (NPI) is the true pressure average increase calculated for each hour over survey..
AMBIENT	The measured hourly LA90 residual level over a minimum seven-day (168 hour) period.
MINIMUM DAILY AMBIENT	The minimum measured hourly LA90 in any hour over each of seven days (or more) ambient survey period
BASELINE AMBIENT	The arithmetic average of the seven minimum daily ambient LA90 measurements
SOURCE LEVEL	The source level, LAeq or LCeq is the equivalent sound level of the source under evaluation
PURE TONE	No pure tone is permitted at any potentially sensitve receptor location as defined in EPA Report 550/9-76-003
LOW FREQUENCY NOISE (LFN)	Potential adverse impact from LFN must be evaluated if LCeq - LAeq => 20 at any receptor
NOMINAL INCREASE TO AMBIENT	The difference between LAeq and the baseline ambient at any receptor

Figure 10: *NPI calculations for an allowable WTG level of 37 dBA.*

Acceptable Noise Levels for Wind Projects

There is a desperate need in the wind turbine industry in the U.S. for an authoritative study and standard that promulgates allowable WTG noise emissions at residences. Currently, design levels arrived at by consensus between developers and local community officials can range anywhere from 30 to 50 dBA. The low end of the range is espoused by ‘experts’ that would not have *an*y audible WTG noise (or any projects for that matter) while the high end is desired by developers to maximize the number of turbines and minimize risk.

The correct balance should lie somewhere between. For example New Zealand, rich in wind power potential, has promulgated[2] a limit of 40 dBA or 5 dBA above the ambient, whichever is higher, conveniently in the middle of the above range.

The figure below shows the NPI results for the same environment as above in Figure 10, except the WTG noise is increased from 37 to 40 dBA.

The results show NPI to be 4.4 dBA. Most acousticians would agree that an increase of 5 to 6 dBA *over the minimum* LA90 ambient represents the threshold for potential adverse response. Note also that the % time above an NPI of 5 dBA has increased from12% at 37 dBA to 32% at 40 dBA for the sampling time. A level of 40 dBA would be noticeable for approximately 32% of the time to an out-of-doors observer. Sleep interference recommendations would not be exceeded with partially open windows. All that said, this result does not exclude the possibility that the closest neighbors may be annoyed to the point of complaints to the project owner.

Such NPI results as given in Figures 10 and11 beg the questions:

Is 40 dBA the balanced limit?

Will there be significant annoyance complaints at 40 dBA?

Should there be an attitude adjustment (visual, participation, etc.) for WTG projects?

Should there be a character adjustment for atonal WTG projects?

Such questions should be evaluated by an impartial third party committee of experts. In the end, it will involve the number of highly annoyed individuals balanced against the benefits of a clean and renewable source of energy. We expressly state the disclaimer that Hessler Associates, Inc. does not endorse or recommend any level limit at this point in time.

Conclusions

The NPI method gives what appear to be reasonable community response predictions for wind turbine projects based on data from a typical completed project and a planned project at a rural site. It is concluded that the NPI Index method, or a derivative, or any other method that evaluates increase-to-ambient over a representative time period is a promising foundation for fairly assessing wind turbine projects.

WTG = 40 dBA LIMIT

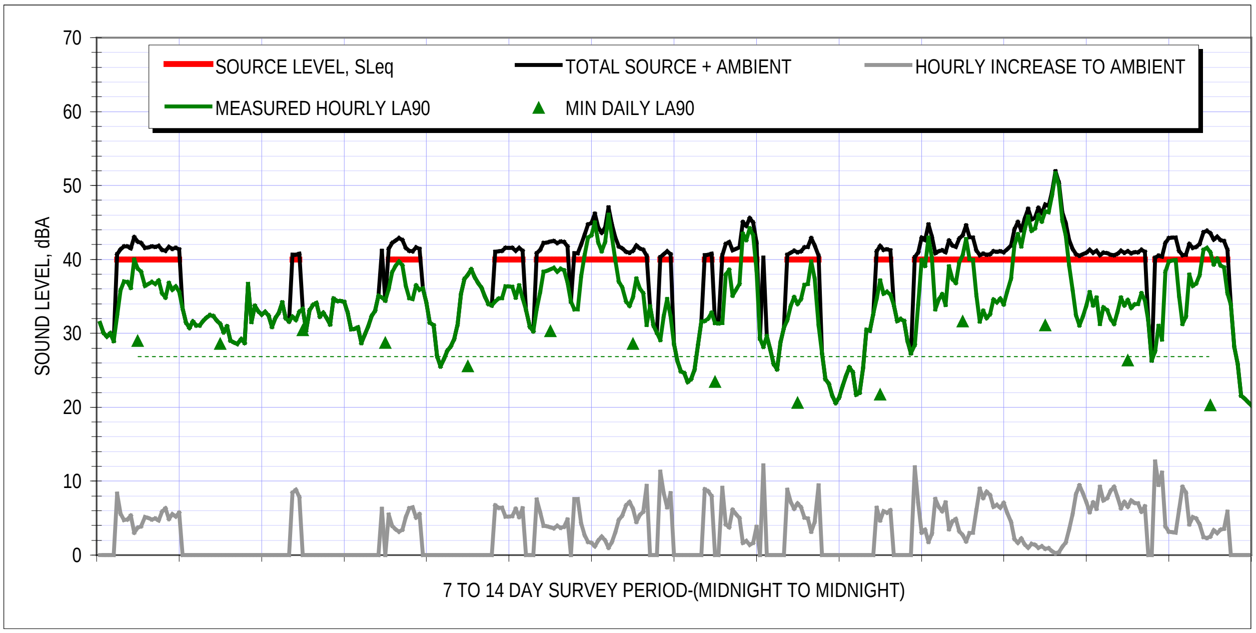

ANALYSIS RESULTS:

10	NOMINAL INCREASE TO BASELINE AMBIENT
27	BASELINE AMBIENT
40	SOURCE LEVEL, SLeq
4.4	NPI INDEX
x	OPERATION ABOVE CUT-IN SPEED
32	%TA, % OF TIME INCREASE-ABOVE-AMBIENT IS > 5 dBA

PREDICTED LONG TERM PERCEPTION AND COMMUNITY RESPONSE

NPI INDEX	PERCEPTION	PREDICTED REACTION
=< 3 dBA	GENERALLY INPERCEPTIBLE	NO ADVERSE RESPONSE
3-5 dBA	BARELY PERCEPTBLE TO PERCEPTIBLE	THRESHOLD OF POTENTIAL ADVERSE RESPONSE
5-10 dBA	PERCEPTIBLE TO NOTICEABLE	INCREASING PROBABILITY OF ADVERSE RESPONSE
=> 10 dBA	READILY NOTICEABLE	HIGH PROBABILITY OF ADVERSE RESPONSE

DEFINITIONS AND CONDITIONS FOR ABOVE TO BE APPLICABLE:

NPI INDEX	The Noise Perception Index (NPI) is the true pressure average increase calculated for each hour over survey..
AMBIENT	The measured hourly LA90 residual level over a minimum seven-day (168 hour) period.
MINIMUM DAILY AMBIENT	The minimum measured hourly LA90 in any hour over each of seven days (or more) ambient survey period
BASELINE AMBIENT	The arithmetic average of the seven minimum daily ambient LA90 measurements
SOURCE LEVEL	The source level, LAeq or LCeq is the equivalent sound level of the source under evaluation
PURE TONE	No pure tone is permitted at any potentially sensitve receptor location as defined in EPA Report 550/9-76-003
LOW FREQUENCY NOISE (LFN)	Potential adverse impact from LFN must be evaluated if LCeq - LAeq => 20 at any receptor
NOMINAL INCREASE TO AMBIENT	The difference between LAeq and the baseline ambient at any receptor

Figure 11: *NPI results for a limit of 40 dBA.*

References

[1] Hessler, G.F., *The Noise Perception Index (NPI) for assessing noise impact from major industrial facilities and power plants in the U.S.*, Noise Control Engineering Journal, Volume 56(5), Sep-Oct 2008.

[2] NZS6808 Acoustics – *“The Assessment & Measurement of Sounds from Wind Turbine Generators.”*

Third International Meeting
on
Wind Turbine Noise
Aalborg Denmark 17 – 19 June 2009

Wind Tunnel Testing of Microphone Windscreen Performance Applied to Field Measurements of Wind Turbines

David M. Hessler, P.E., INCE
Hessler Associates, Inc.
3862 Clifton Manor Place
Haymarket, VA 20169 USA
david@hesslerassociates.com

Abstract

Long-term field measurements of environmental sound levels at rural wind turbine project sites, either prior to construction or after the project is operational, normally show a strong correlation between sound level and wind speed. Unless some other contaminating factor is present, such as man-made noise, flowing water, insects, etc., sound levels will rise with wind speed and diminish during calm periods. The question that arises from this is whether the actual sound level rises and falls due to natural wind-induced sounds or whether wind blowing over the microphone creates a self-generated, false signal. In order to quantitatively address this issue a variety of common windscreens were systematically subjected to known wind velocities in a massively silenced wind tunnel with essentially noise-free airflow. The results of these tests demonstrated that wind does generate a certain amount of false-signal noise in all windscreens and that some work better than others - but in the wind speed range of interest (<10 m/s) it is only the lower frequencies in all of them that are affected by this self-generated distortion. What this means is that A-weighted sound levels measured in moderately windy conditions are largely immune from distortion but that C-weighted levels or levels of low frequency sound in general are significantly skewed upward. Consequently, any casual measurement of sound using a standard windscreen in a windy field will yield ostensibly high levels of low frequency or infrasonic noise - whether a wind turbine is present or not. Such measurements, taken at face value, may be one of the reasons wind turbines are widely, but mistakenly believed to be significant sources of low frequency noise. This paper briefly summarizes the wind tunnel study and applies its findings to actual measurements of an operating wind turbine and the simultaneously measured background sound levels several miles away.

Introduction

Long-term field measurements of environmental sound levels at rural wind turbine project sites, either prior to construction or after the project is operational, normally show a strong correlation between sound level and wind speed. Unless some other contaminating factor is present, such as man-made noise, flowing water, insects, etc., sound levels will rise with wind speed and diminish during calm periods. The question that arises from this is whether the actual sound level rises and falls due to natural wind-induced sounds or whether wind blowing over the microphone creates a self-generated, false signal. In order to quantitatively address this issue a variety of common windscreens were systematically subjected to known wind velocities in a massively silenced wind tunnel with essentially noise-free airflow. The results of these tests demonstrated that wind does generate a certain amount of false-signal noise in all windscreens and that some work better than others - but in the wind speed range of interest (<10 m/s) it is only the lower frequencies in all of them that are affected by this self-generated distortion. What this means is that A-weighted sound levels measured in moderately windy conditions are almost totally immune from distortion but that C-weighted levels or levels of low frequency sound in general are significantly skewed upward. Consequently, any casual measurement of sound using a standard windscreen in a windy field will yield ostensibly high levels of low frequency or infrasonic noise - whether a wind turbine is present or not. Such measurements, taken at face value, may be one of the reasons wind turbines are widely, but mistakenly believed to be significant sources of low frequency noise. This paper briefly summarizes the wind tunnel study and applies its findings to actual measurements of an operating wind turbine and the simultaneously measured background sound levels several miles away.

Environmental Sound Levels and Wind

Long-term field measurements of environmental sound levels at rural wind turbine project sites are often performed in the permitting stage to quantify the background sound level as a function of wind speed for impact assessment purposes. Typically two weeks of 10 minute data are collected at a 6 to 8 positions and then correlated to the concurrent wind speed as measured by 50 m anemometers on one or more met towers within the site area. Consequently, the sound level experienced at ground level is associated with the wind speed well above the surface and similar to what the turbines will ultimately see. A typical survey result is illustrated in Figure 1, where the average site-wide L90(10 min) level is plotted along with the wind speed normalized to the IEC standard [2] elevation of 10 m above grade.

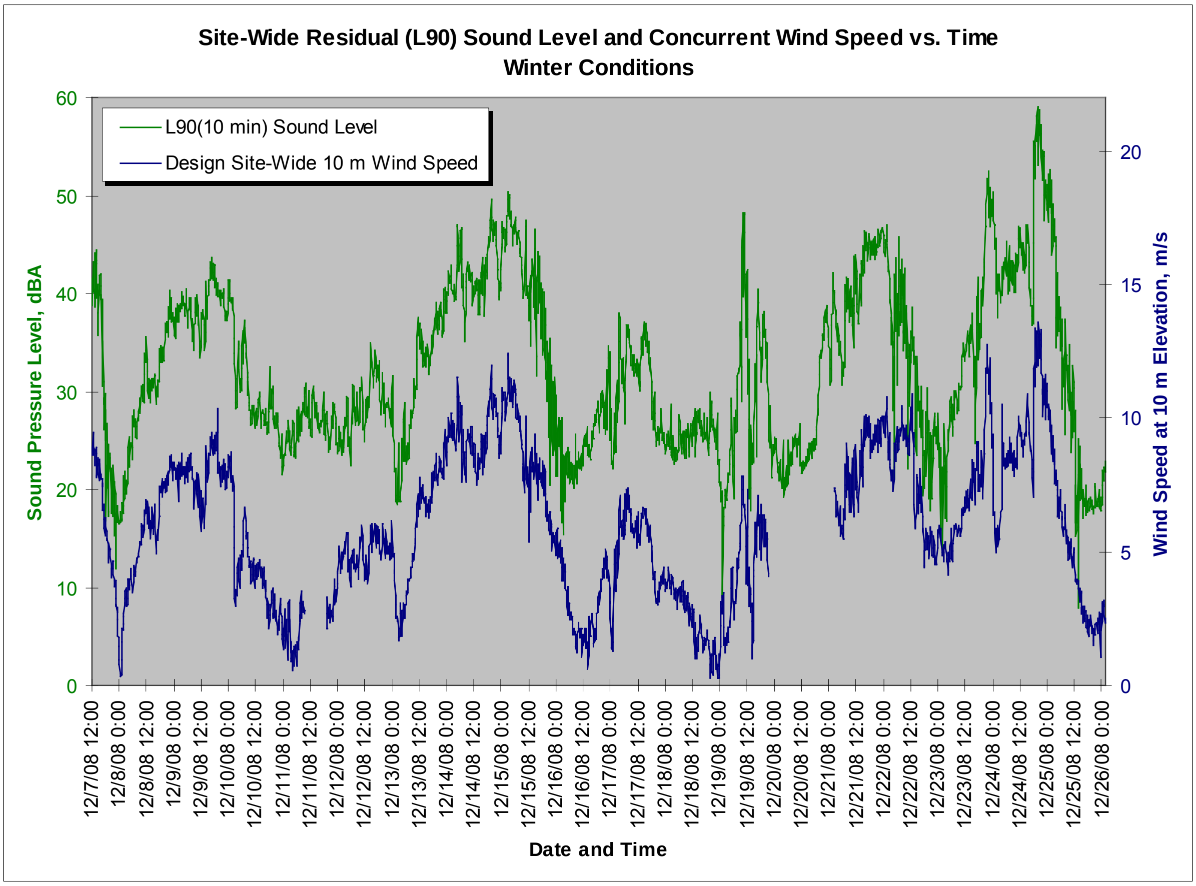

Figure 1 *Measured L90 Background Sound Level Compared to Concurrent Wind Speed - Typical*

The dependency of sound levels on wind speed is subjectively evident in the plot and quantified in the regression analysis in Figure 2 where sound levels are plotted as a function of wind speed rather than time.

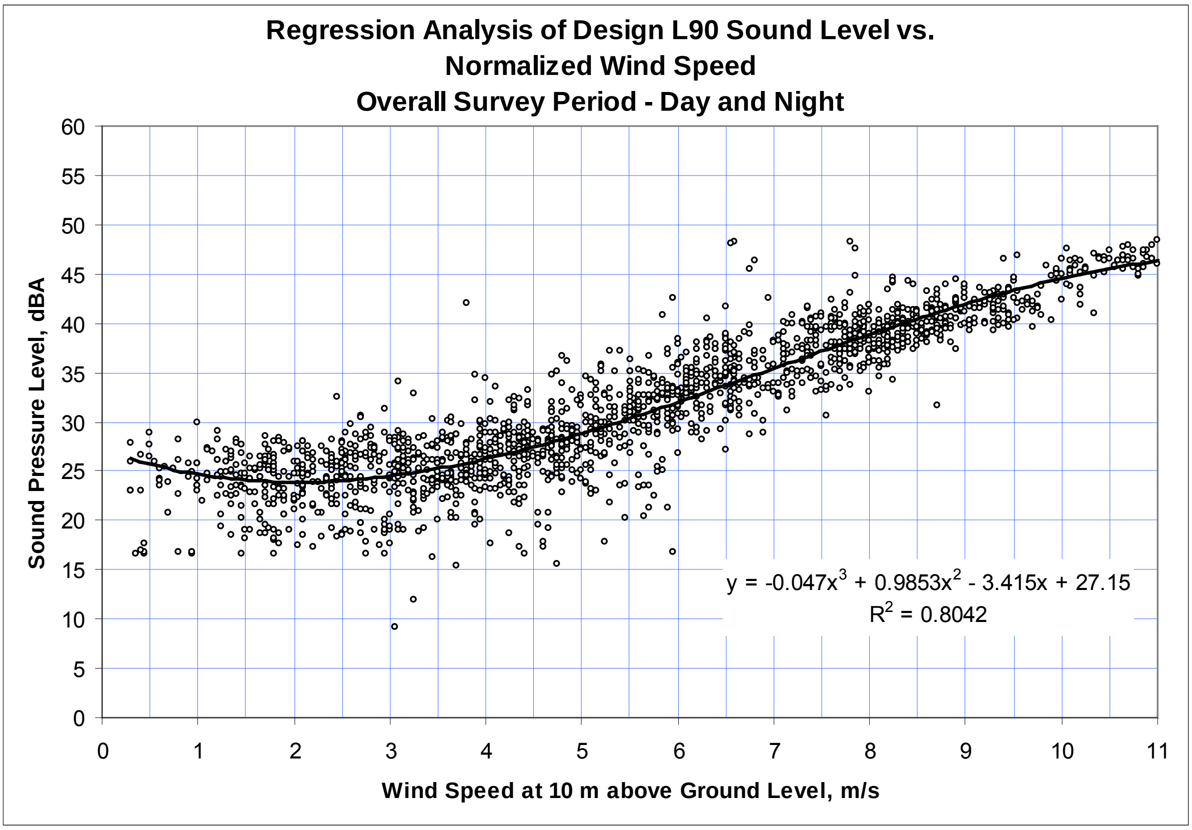

Figure 2 *Regression Analysis of Measured L90 Background Sound Levels and Concurrent Wind Speed – Typical*

The question that arises from this close relationship between sound and wind speed is whether the actual sound level rises and falls due to natural wind-induced sounds, such as trees or grass rustling, or whether wind blowing over the microphone creates a self-generated, false signal - which would conveniently explain the parallel behaviour seen in Figure 1.

Windscreen Testing

In order to quantitatively address this question, a wind tunnel testing program was devised to directly measure the level of microphone self-noise resulting from a known wind velocity for a variety of common windscreens. The complete results of this study have been published in July-August 2008 edition of the *Noise Control Engineering Journal* [1] so only an outline of the methodology and principal results are given below.

The testing was carried out using the acoustical wind tunnel at the Fraunhofer Institut für Bauphysik in Stuttgart (Figure 3), which is massively silenced to virtually eliminate fan noise from the system.

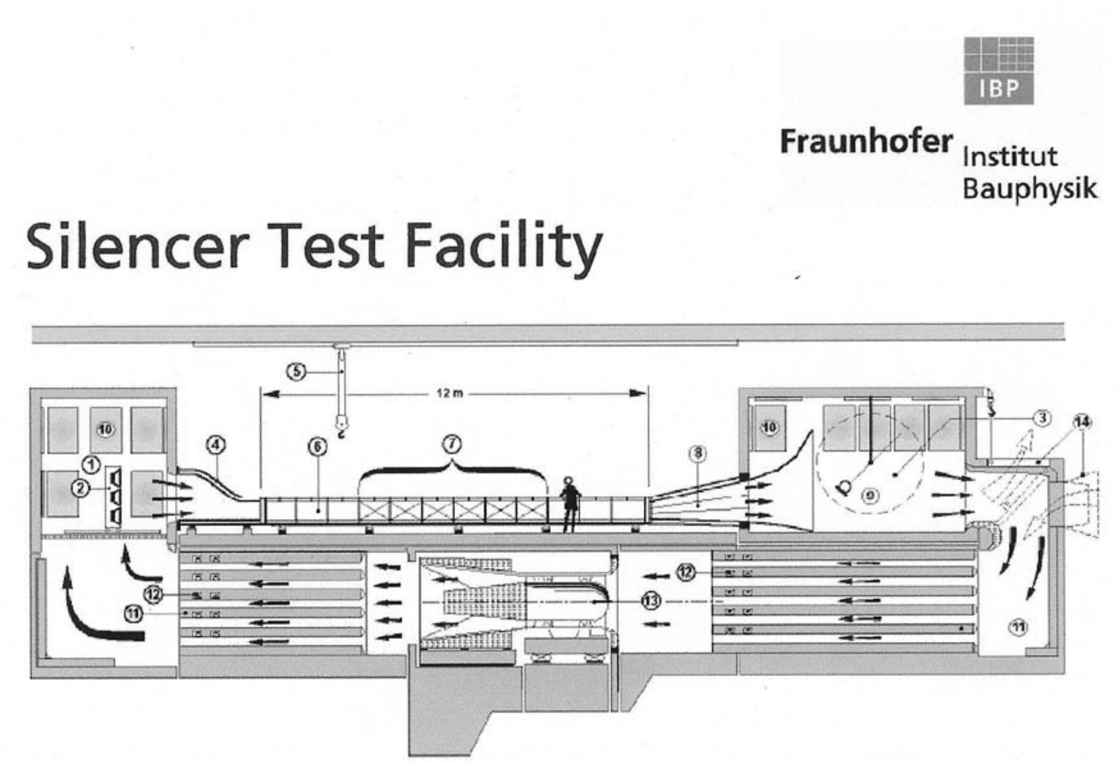

Figure 3 *Cross-sectional View of the Fraunhofer Wind Tunnel*

A series of 9 tests, shown in Figure 4, were run in which 7 windscreens were placed on a typical 1/2" (13 mm) microphone and subjected to controlled wind velocities of 2.5, 5, 10, 20 and 30 m/s normal to the microphone axis. An unprotected microphone and an aerodynamic nose cone were also tested.

TEST 1
NO WINDSCREEN PROTECTION

TEST 2
STANDARD 13mm (1/2") NOSE CONE

TEST 3
NORSONIC MODEL 1212 FOR OUTDOOR MONITORING

TEST 4
GRAS MODEL 41AO FOR OUTDOOR MONITORING

TEST 5
NORSONIC STANDARD 60mm WINDSCREEN

TEST 6
NORSONIC STANDARD 90mm WINDSCREEN

TEST 7
ACO MODEL WS-7-7 (175mm UNTREATED)

TEST 8
ACO MODEL WS-1-80T (75mm TREATED)

TEST 9
ACO MODEL WS-7-80T (175mm TREATED)

Figure 4 *Test Windscreens as Mounted in Wind Tunnel*

The overall test results for the 5 m/s wind velocity case are shown in Figure 5. This plot essentially shows the magnitude of self-generated noise for each windscreen when subjected to a 5 m/s wind.

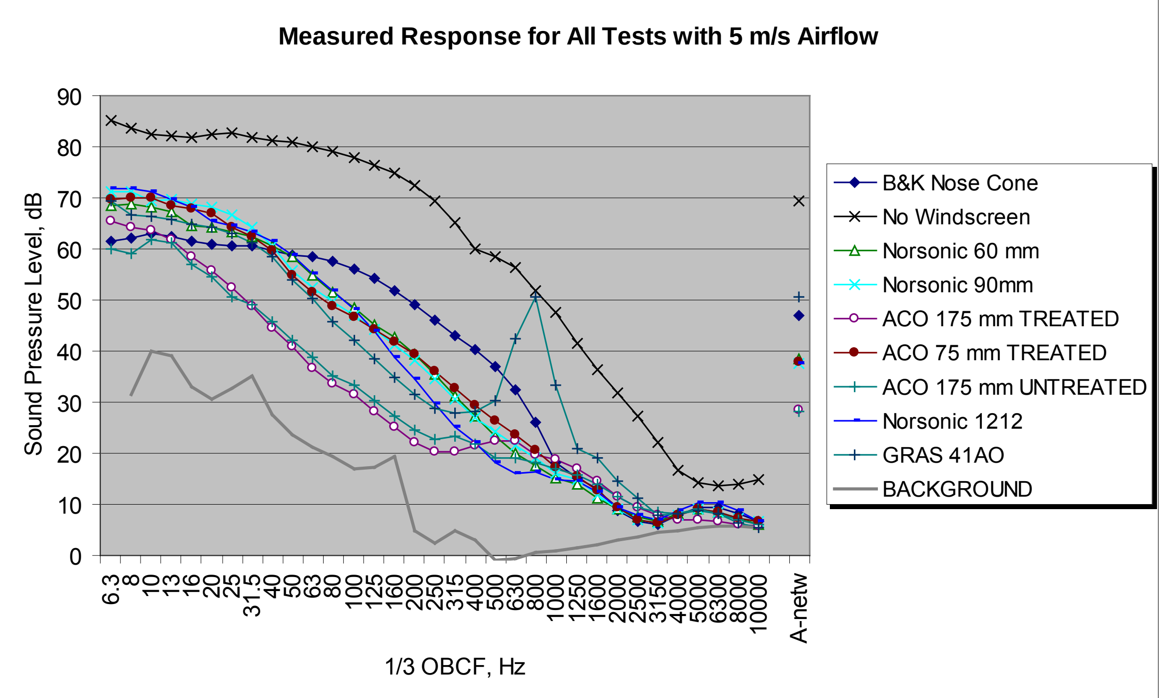

Figure 5 *Test Results – 5 m/s Wind*

Each windscreen or device has a different response but it is the lower frequencies that are most affected in each case. Of key significance are the substantially lower levels of distortion evident in the two larger (175 mm diameter) windscreens. False signal noise is generally 5 to (a very significant) 15 dB lower than the smaller, conventional windscreens in all the lower frequency bands. In terms of overall A-weighted sound levels, the 175 mm windscreens were measured to have a relatively low false signal noise level of about 29 dBA while the windscreens around 75 mm in diameter have a significantly higher distortion level of about 39 dBA for 5 m/s wind conditions. The overall test results for A-weighted self-noise for all wind speeds are shown in Figure 6.

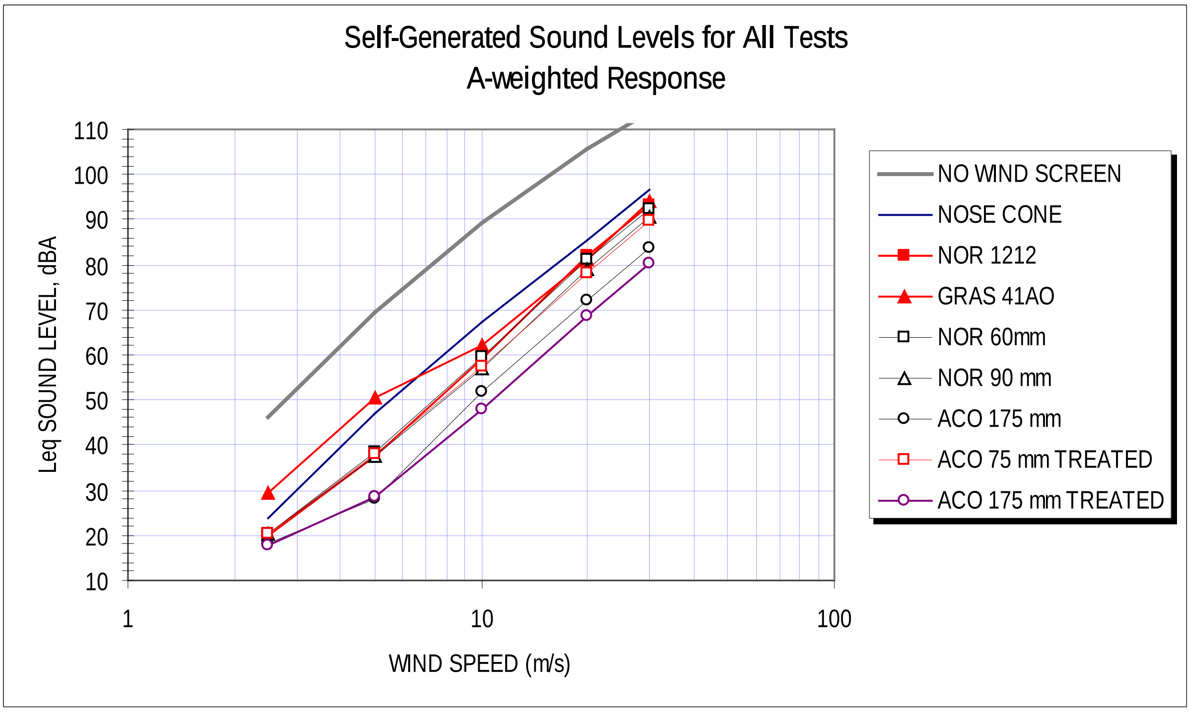

Figure 6 *Test Results – A-weighted Self-Noise as a Function of Wind Speed*

This plot shows that the larger (175 mm) windscreens yield the best results and have minimal levels of flow noise distortion at wind speeds below about 5 m/s, which are normally of the most relevance to wind project design assessments. A correction algorithm can be developed for any of the windscreens tested from the Figure 6 data. For the 175 mm ACO WS7-80T the magnitude of overall A-weighted self-noise can be calculated from Eqn. (1).

$$LpA\ (\text{flow–induced noise}) = 27.4\ Ln(v) - 10.7\ \ dBA \qquad \text{Eqn. (1)}$$

Where v = the flow velocity at the microphone, m/s

Application to Field Measurements

If the wind speed at microphone height is monitored along with sound levels, the measurements can be corrected for self-induced distortion. The use of a large windscreen, however, such as the 175 mm diameter model, typically results in a situation where the A-weighted sound levels need little, if any, adjustment. As an example, the survey data from Figure 1 is re-plotted below along with the measured wind speed at microphone elevation and the corrected sound level where self-noise has been subtracted from each as-measured value depending on the wind speed occurring during that measurement. There are only a few places during the entire two-week survey period when the wind speed at 1 m was great enough to cause the self-noise level to approach the actual sound level and engender the need for a small correction. For most of the survey the magnitude of the adjustment is largely negligible. This figure also illustrates the common result that the wind speed at 1 m generally remains fairly low - in the 3 to 4 m/s range for the most part – and below what might be expected from the IEC 61400-11 shear curve [2], even when the high elevation/10 m wind speed becomes quite significant.

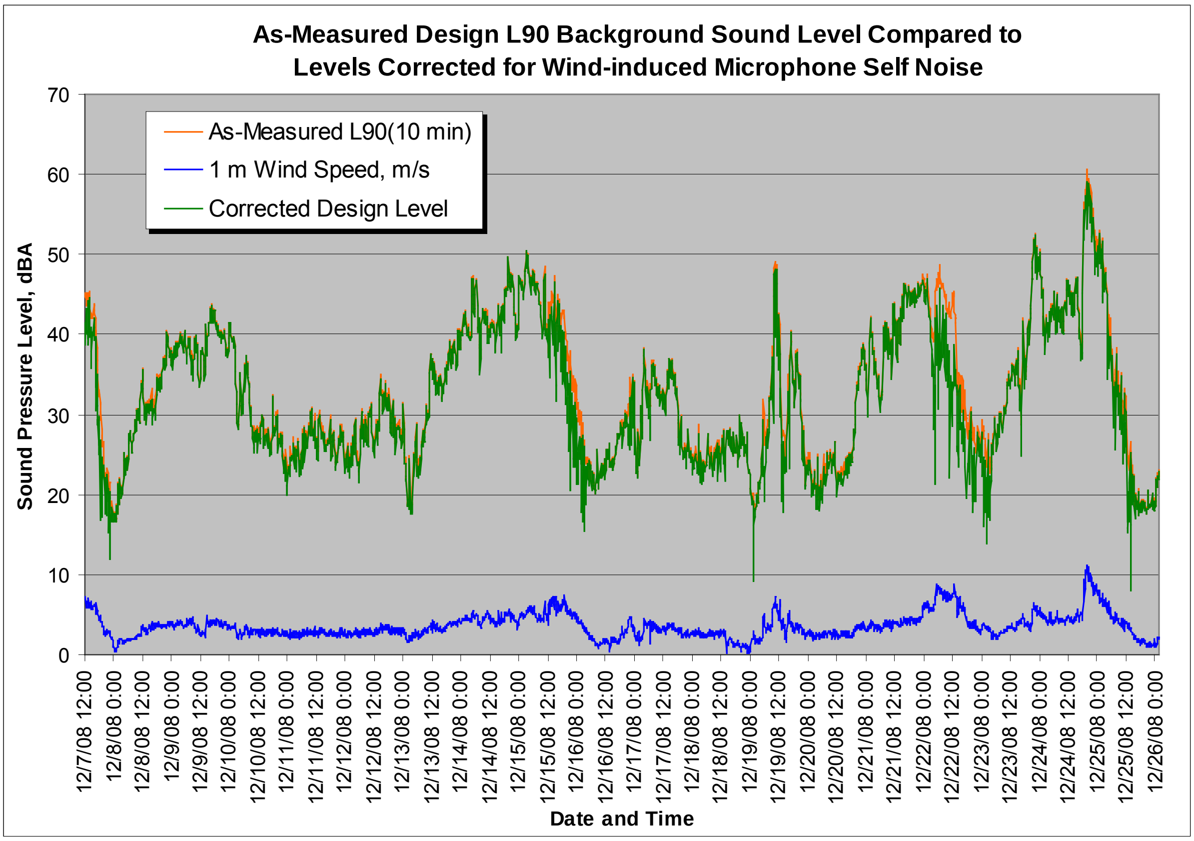

Figure 7 *Survey Results from Figure 1 Corrected for Self-Induced Noise Based on Measured Wind Speed at Microphone Height (1 m)*

Beyond simple A-weighed sound levels, the wind tunnel study results can also be used to evaluate the frequency content of field measurements made in the presence of flow or wind. As with the overall sound levels illustrated in Figure 6, it is also possible to develop an algorithm to calculate the self-noise level as a function of wind speed for each 1/3 octave band for each windscreen tested. Figure 8 shows one of 10 monitoring stations arrayed around a fairly isolated turbine at an open site in a soybean field in the Midwest. This position is 1000 ft. (305 m) away and employs a 175 mm treated windscreen.

Figure 8 *Field Sound Level Monitor 1000 ft. from a Typical Turbine with 175 mm Treated Windscreen*

An identical monitor was also set up in an identical soybean field 3 miles from the project area and completely isolated from any turbine noise. The sound level spectra measured at the same time at this remote position and at the 1000 ft. position on a day when the hub height wind was 13 m/s and the 1 m wind speed was 6 m/s are plotted below.

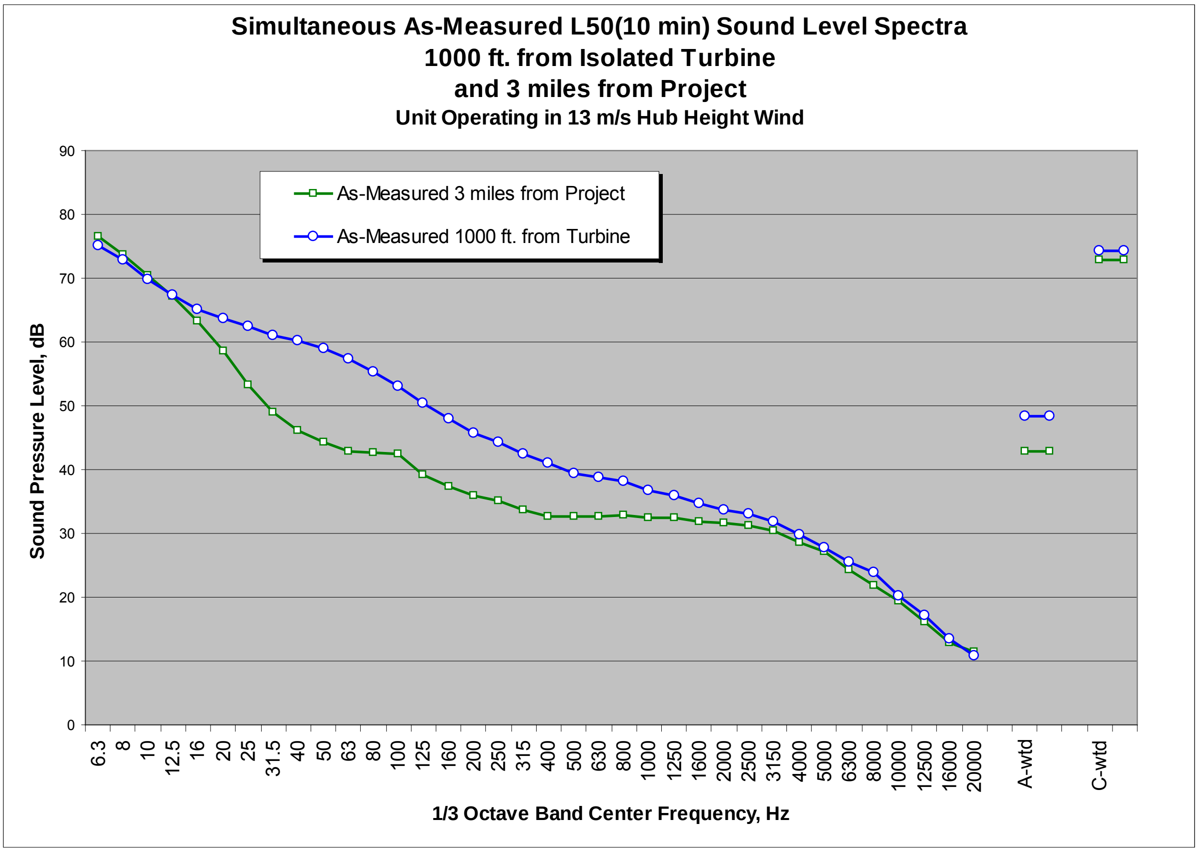

Figure 9 *As-Measured Frequency Spectra 1000 ft. and 3 miles from Isolated Turbine*

This plot shows suspiciously similar levels of very low frequency noise and both measurements have similare C-weighted levels: 74 dBC near the turbine and 73 dBC miles away. Clearly, the lower frequencies in both spectra are displaying false signal noise. In Figure 10 the self-noise level for the WS7-80T windscreen subjected to a 6 m/s normal flow velocity is plotted against the as-measured spectrum at the remote, background position miles from the project. Below about 200 Hz the two levels are intertwined, meaning that the low frequency content of this measurement is completely spurious – to the extent that a reasonably valid correction cannot even be calculated. An actual C-weighted sound level for this measurement can only be very roughly estimated at somewhere around 48 dBC, which, even if not precisely correct, makes much more sense. Because all of this distortion is occurring below 200 Hz, the A-weighted sound level is only minimally affected and its corrected value is only about 1 dBA lower than the as-measured value.

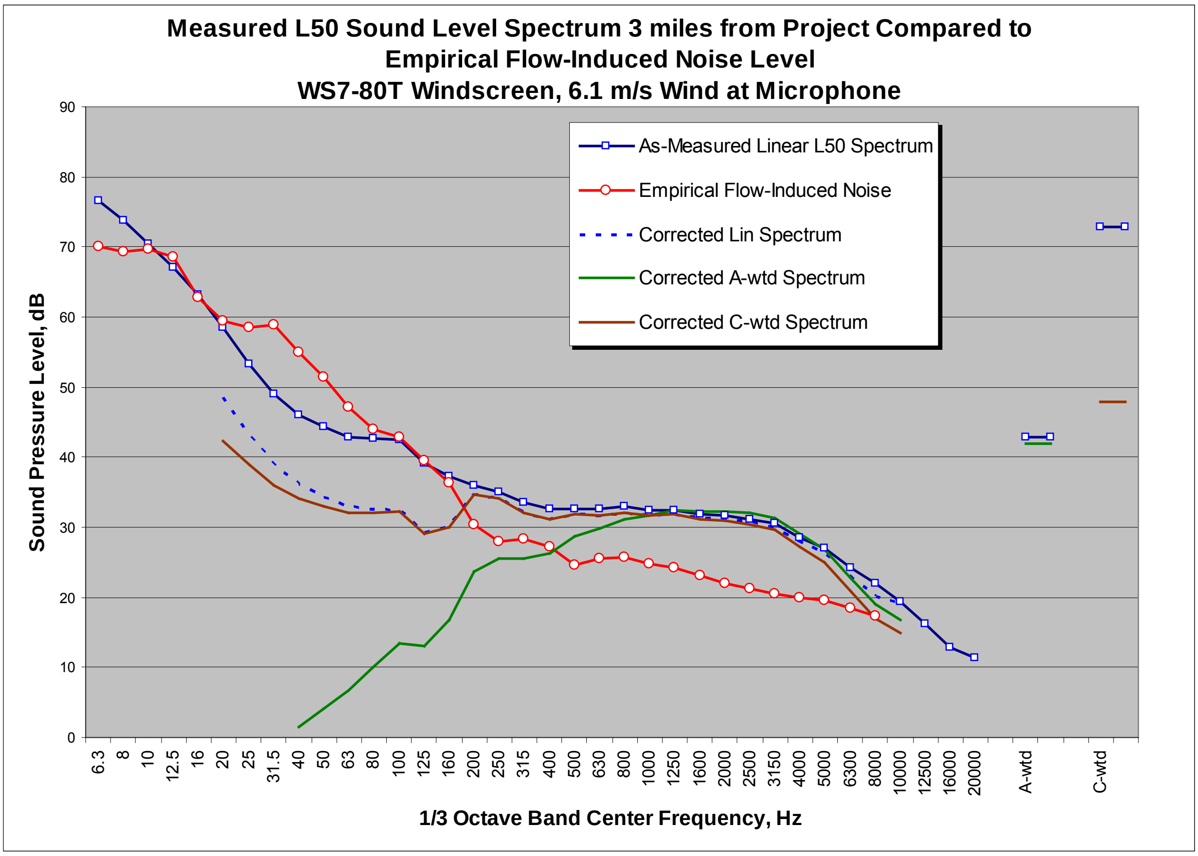

Figure 10 *Measured Frequency Spectrum 3 miles from Isolated Turbine Adjusted for Self-Noise*

At the position close to the turbine (Figure 11) the self-noise sound level meets the as-measured level at a much lower frequency of about 40 Hz because, in this case, measuring fairly close to a turbine operating at essentially full power, there is a moderate amount of actual acoustic energy in mid- and low frequencies. The as-measured levels below 40 Hz can be roughly corrected based on the empirical flow-noise level to yield a more accurate C-weighted sound level. In any event, it is clear that the measured sound levels in the lowest bands are false signals that have nothing to do with the turbine.

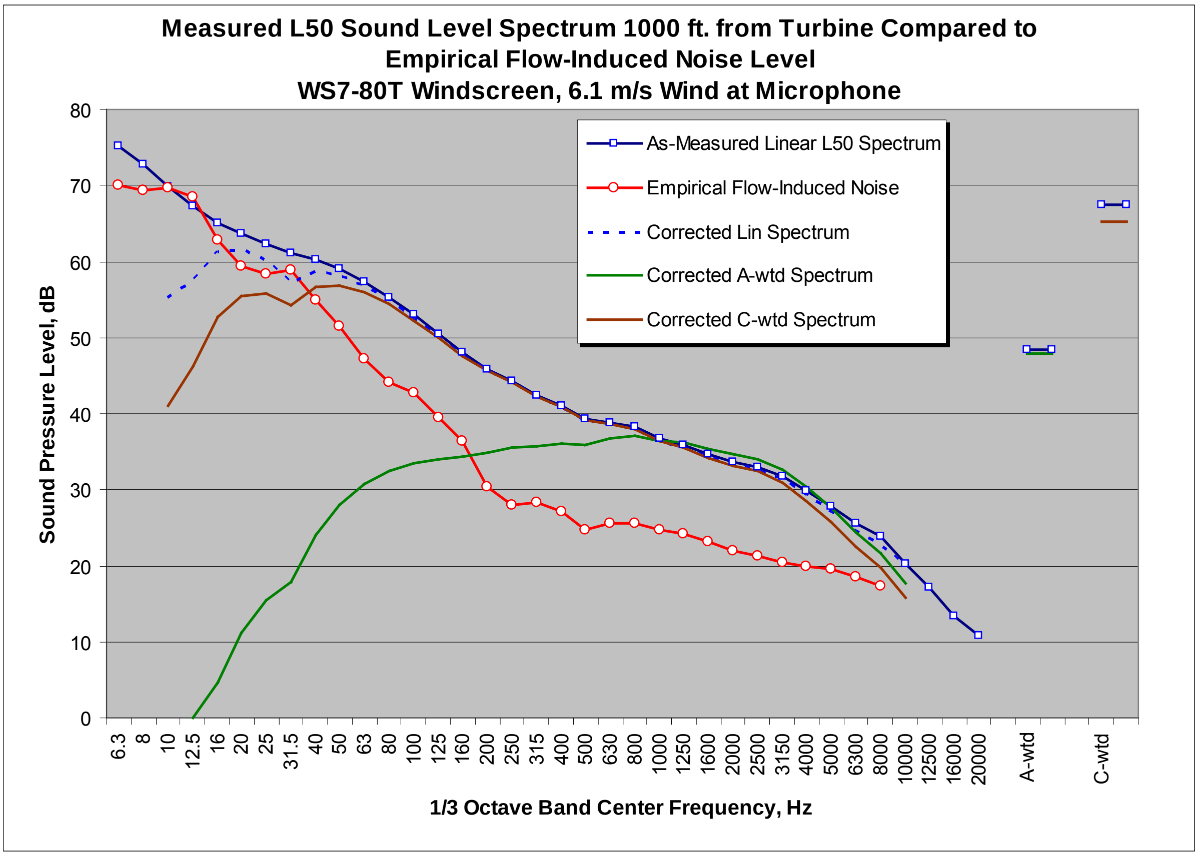

Figure 11 *Measured Frequency Spectrum 1000 ft. (305 m) from Isolated Turbine Adjusted for Self-Noise*

Conclusions

An empirical wind tunnel study of the self-noise distortion due to airflow penetrating windscreens and creating false signal noise revealed that flow noise only has a significant contaminating effect on the low frequency portion of the spectrum. Consequently, measurements made under moderately windy conditions – a virtual necessity for wind turbine analyses - will exhibit erroneously high levels of low frequency noise, which may be one of the principal reasons wind turbines are widely, but mistakenly believed to produce substantial levels of low frequency and infrasonic sound. Because this wind-induced distortion essentially occurs in the lower frequencies, A-weighted sound levels are generally immune from any significant degradation in accuracy as long as an extra-large windscreen on the order of 175 mm in diameter is used and the wind speed at the microphone position is below about 5 m/s. Some distortion in A-weighted levels will begin to occur above this wind speed even with a large windscreen but can be corrected out using the wind tunnel study results. Conventional windscreens in the 75 to 90 mm size range are much less effective and prone to significantly greater error in measuring both A and C-weighted sound levels in the presence of airflow.

References

1. Hessler, G. F., Hessler, D. M., Brandstätt, P., Bay, K, "Experimental study to determine wind-induced noise and windscreen attenuation effects on microphone response for environmental wind turbine and other applications", *Noise Control Engineering Journal*, J.56, July-August 2008.
2. International Electromechanical Commission (IEC) 61400-11:2002(E) *Wind Turbine Generator Systems – Part 11: Acoustic Noise Measurement Techniques*, Second Edition 2002-12.

Third International Meeting
on
Wind Turbine Noise
Aalborg Denmark 17 – 19 June 2009

Recent Developments in Assessment Guidelines for Sound from Wind Power Projects in Ontario, Canada with a Comparison to Acoustic Audit Results

Brian Howe, HGC Engineering
Nick McCabe, HGC Engineering
2000 Argentia Road, Plaza 1, Suite 203
Mississauga, ON L5N 1P7 Canada
bhowe@hgcengineering.com

Abstract

The guidelines of the Ontario Ministry of the Environment (MOE) for the assessment of sound from wind power projects are the most sophisticated in Canada, relying on internationally recognized standards (ISO 9613 & IEC 61400-11) and allowing for a variation in both wind turbine sound power and background sound as a function of wind speed. The MOE completed a technical review of their procedures and published an updated guideline document in October of 2008. The revisions did not change the criteria (essentially 40 dBA at residences in rural areas under moderate wind speeds), but did address the need to consider several factors, such as the wind profile and ground attenuation, with greater specificity. While the revisions help improve the consistency between assessors, there remain some individuals that are critical of the approval process, and in practice there remains a fair degree of variability between the predicted sound levels and those levels occurring under operating conditions. This paper reviews the effect of these improvements, looks at the overall degree of precision versus the variability in sound levels as measured during several acoustic audits of wind power projects recently undertaken by HGC Engineering, and discusses the status of pending legislation that has the potential to modify the assessment process further.

Introduction

The first commercial wind plant opened in the province Ontario in 2002 with 5 wind turbine generators. As of April 1, 2009, eight contractually separate major wind plants were operating in the province of Ontario, with a combined installed capacity of 887 MW [1]. One more, with a capacity of 198 MW is anticipated to go online this year [2]. Numerous other large scale plants are now under development, and the total installed capacity of all current and planned projects is about 1,600 MW by 2012 [2]. To put this into context, the total installed capacity for all types of power plants in Ontario is currently about 27,000 MW.

In Ontario, the environmental noise generated by industrial noise sources is regulated by the provincial Ministry of Environment (MOE). Generally, industrial noise is assessed by the MOE against background sound levels, or certain overriding minimum criteria. As wind turbine generators tend to emit the greatest sound power levels during conditions of higher wind speeds when background sound levels are elevated, the MOE recognized a special case and produced a guideline document in 2004 [3] pertaining to environmental noise from wind power projects.

That guideline defined a prediction method for use in assessing environmental noise from wind turbine generators, identifying ISO 9613 [4] as the model to be used in calculations for sound propagation, and required that source sound power data to be used in the calculations be established using IEC 61400-11 [5]. Specific sound level criteria were also provided. Thus, predictive engineering calculations were established as the basis for environmental noise prediction for wind turbine generators, and for determining setback requirements.

Following adoption of the guideline, areas for improvement were identified in the guideline by a variety of sources. Following a lengthy review and consultation process, the guideline was revised and reissued in 2008 [6]. The new version changed neither the criteria nor the required standards for sound power measurement and environmental noise prediction, but did specify certain analysis assumptions such as the degree of ground absorption, and perhaps most importantly, indicated that site-specific wind shear (wind profile) effects needed to be considered.

At the present time there is a concerted political effort in Ontario to encourage more renewable energy projects. Proposed provincial legislation in the form of a Green Energy Act, 2009 [7] will provide future regulations designed to establish new guaranteed prices for future wind power projects and potentially to exempt wind power projects from various municipal regulations and by-laws, including zoning and development related regulations, in order to streamline the approval process.

As part of the Green Energy Act, the guidelines of the MOE with respect wind power projects are once again open to input from a variety of stakeholder groups. There have been complaints related to noise and the impact on health from Ontario residents living near operating and proposed wind power projects, leading to pressure on the government to implement minimum setback distances between wind turbines and residential dwellings as part of the revised guidelines or as regulations made under the Act. This would be a departure from the current MOE guidelines wherein the setback distance is a function of the acoustic predictions and established criteria.

Noise Guidelines for Environmental Noise, Wind Power Projects

In Canada, environmental regulations for industrial noise sources are under provincial jurisdiction. In Ontario, the applicable regulations for industrial sources pertain to sound level limits at sensitive noise receptors, such as residences, and are based on ambient sound levels at those receptors due to natural sources and road traffic. The guidelines for general industrial sources are based on the minimum ambient sound levels in any given hour which would be expected to occur under windless conditions. As wind turbine generators tend to emit the greatest sound power levels during conditions of higher wind speeds when background sound levels are elevated, the MOE produced a guideline document in 2004 pertaining explicitly to environmental noise from wind turbine projects.

That guideline defined a prediction method for use in assessing environmental noise from wind turbine generators, identifying ISO 9613 as the model to be used in calculations for sound propagation, and required that source sound power data to be used in the calculations be established using IEC 61400-11. Specific sound level criteria, defined in terms of the hourly energy-equivalent average (L_{EQ}) sound level were also provided based on an assumed relationship between wind-induced background sound and 10 metre height wind speeds. These criteria depend on whether the area is defined as acoustically urban or rural, and are summarized in Figure 1.

Figure 1: Summary of Provincial Sound Level Limits

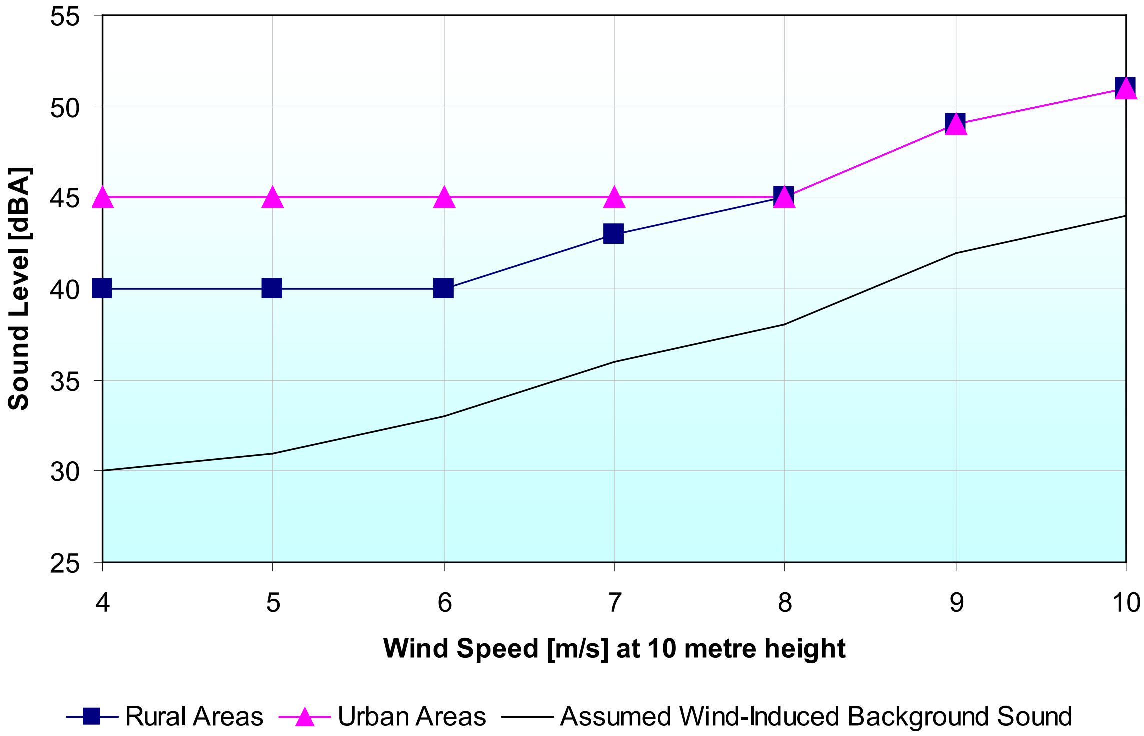

The guideline required predictive engineering calculations using the standards described in the guideline, and thus detailed sound level calculations and definable sound power estimation techniques were established as an important factor in determining minimum setbacks from residencies, and wind plant layout.

However, in practice, the guideline document lead to a great deal of variation in assumptions between different assessors, and therefore to variability in the resulting typical setbacks from residential receptors.

One of the most dramatic variables is related to wind shear (wind profile), and the reference roughness length of IEC 61400-11. As required by IEC 61400-11, most manufacturers list the sound power output of their turbines as a range, correlated with 10 metre height wind speeds under the reference wind profile condition. Because the 2004 MOE guideline did not discuss variation in wind shear, some assessors used the sound power data derived under IEC at face value, and others were taking into consideration site-specific wind shear data.

In practice, then, where the wind shear exponent might vary from 0.05 to 0.45 through a given day, the sound power output from the turbine might vary over the entire published range (which could be 5 to 10 dBA), even while the speed at the reference height remains constant. This can lead to large variation in the calculated setback requirements between one assessor and another.

To address such discrepancies, the MOE published a new document in 2008 replacing the earlier guideline. The 2008 guideline did not alter the numeric criterion values, but did amongst other changes add a requirement that wind profile effects be considered. Specifically, the sound power data should be "adjusted for the average summer night time wind speed profile, representative of the site". Other assumptions to be used in the analysis, such as the effective acoustic absorption of the ground surface or "ground factor", and factors affecting atmospheric absorption were also specified for the first time.

Issues related to the quality of the sound produced by the wind turbines are also addressed by the 2008 guideline by explicitly describing a 5 dB penalty to be added in the event that the manufacture's data indicates that the sound is tonal in nature. While tonal noise is penalized if present, the guideline indicates that tonal characteristics are generally associated with maintenance issues. The amplitude modulation related to the characteristic aerodynamic "swoosh" is not penalized.

The 2008 guideline also addressed in greater detail some practical considerations. These included the cumulative effect of neighbouring wind power projects, the need to consider the transformers as ancillary sound sources, and the need to consider vacant lots that would allow a future residence as a sensitive receptor.

Current Assessment Experience

The 2008 version of the guideline contains a number of considerable improvements over the previous version. However, despite the increased specificity of the current guideline, there remain differences between the practice of different assessors, and more importantly, there remains considerable variation between predictions made using ISO 9613 with IEC 61400-11 and long term sound level measurements made after startup.

HGC Engineering's recent experience in Ontario, measuring noise under different conditions around operational wind plants, indicates that while the typical minimum setbacks have increased over time (setbacks of 450 to 600 metres appear to be typical at present), there is considerable variation between actual sound levels at receptors and the impact predicted during the design of the wind plant. In practice, this fact makes validation of the acoustic performance of a wind plant vis-à-vis the MOE criteria quite difficult.

Figure 2 illustrates the results of a typical sound level monitoring period.

Figure 2: Comparison of Sound Levels Measured at a Residence and Sound Levels Measured Approximately 100m From Nearby Turbine. There is one generator located within 1 km from this residence.

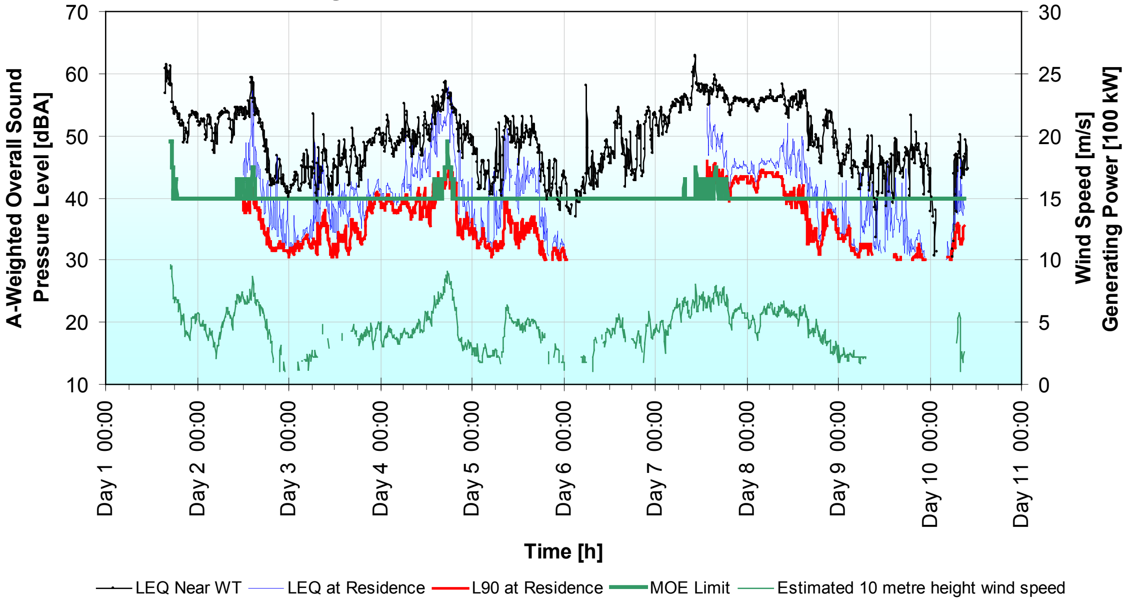

Figure 2 indicates considerable variation in both the energy-equivalent average (L_{EQ}) sound level and the "background" sound level (the L_{90} sound level, or the level exceeded 90% of the time) measured at a residence. Setting aside the strongest peaks in the L_{EQ} sound level, particularly those occurring during daytime hours when man-made sounds would be expected near a residence, there is still a large degree of variation, even for similar 10 metre height wind speeds. This is not unexpected, given the typical diurnal variation in the wind shear exponent, and the fact that the wind direction changes over time.

Figure 3 illustrates the variation another way. The L_{90} sound level measured at the residence is plotted against the wind speed recorded at the nacelle anemometer of the closest wind turbine generators. Considerable variation, on the order of 10 dBA is shown. For comparative purposes, the L_{90} sound level measured close (about 100 metres) from the nearest turbine, at a location where the noise from the turbine is the dominant sound source most of the time is shown in Figure 4. A similar pattern is evident.

Figure 3: L_{90} Sound Level at Residence vs Nacell Wind Speed
All Wind Directions Included

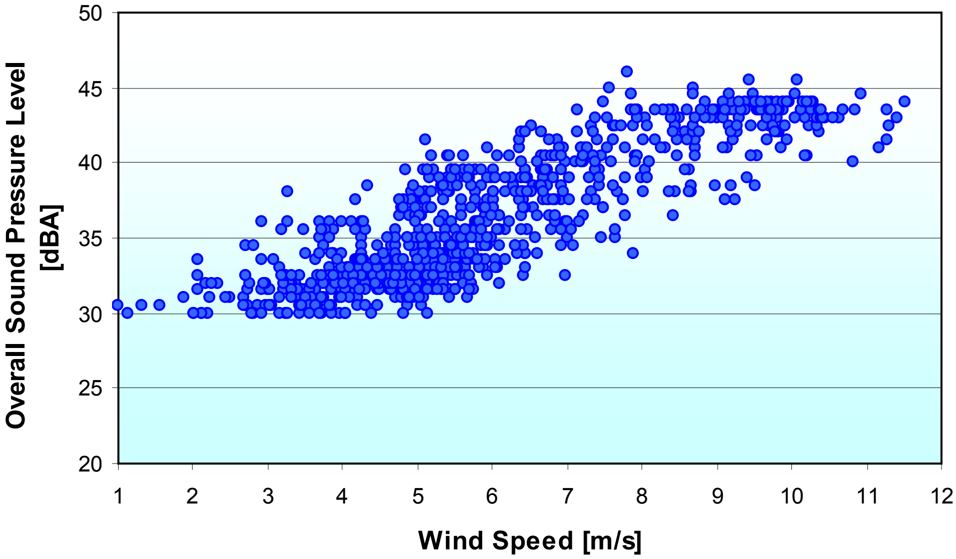

Figure 4: L_{90} Sound Level at WT vs Nacell Wind Speed
All Wind Directions Included

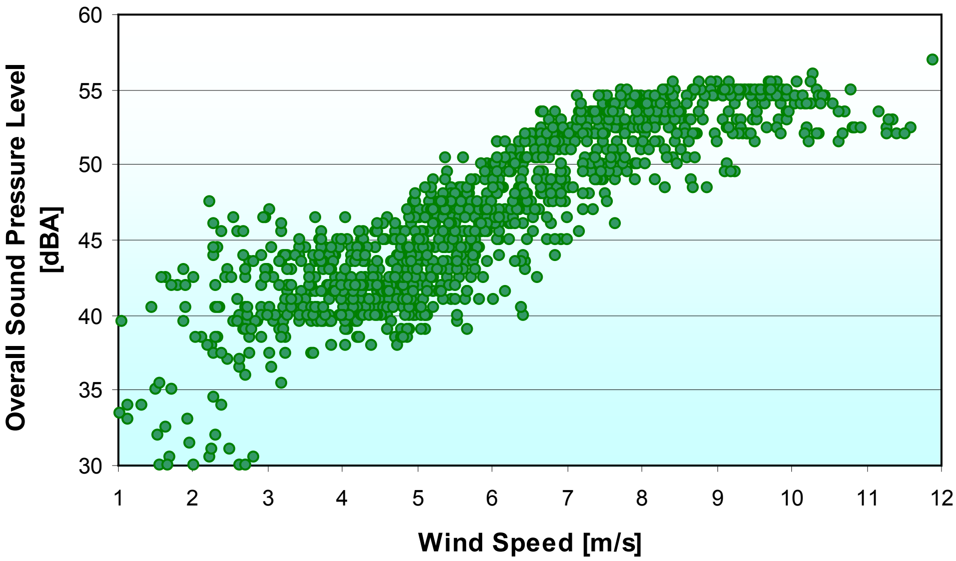

Given the magnitude of the variation, and given that the MOE standard when properly applied will result in a single number prediction for a given 10 metre high wind speed, it should be expected that there will be considerable variation in practice, both above and below the predicted sound level. This has certainly been the experience of HGC Engineering in conducting noise measurements around wind plants. Notice that the L_{90} sound level shown in Figure 1 exceeds the MOE criterion curve by 3 to 4 dBA for period centred around midnight on Day 8, while during periods on Days 2 and 4 with similar 10 metre wind speeds, the L_{90} sound level is effectively at the criterion curve.

The annoyance associated with the audibility of the sound, or with a given sound level impact is a subjective factor. The annoyance issue is complicated by the ability of the ear to become attuned to a particular sound. In one particular case where a homeowner had been complaining about noise from nearby wind turbine generators (there are 5 within a distance of about 1000 metres to this home). The complaints had grown fairly strident. In this case, the wind plant operators had been experimenting with different means to minimize the noise impact, while still allowing turbines in the area to operate. One such test involved a prolonged shutdown of the 5 turbines nearest to the home. The nearest operating turbines were then located at a considerable distance. In this case there were 7 operating turbines between 1000 and 2000 metres from the home. Complaints at this distance would normally be expected to be rare, however, while this operational condition presumably reduced the noise impact for the duration of the test, the homeowner still found the sound of the closest operating wind turbine generators to be objectionable. This highlights the need for prompt attention to any circumstance which may result in temporary increases in the sound levels near a turbine, or changes resulting in a more identifiable or potentially irritating sound such as mechanical wear or damage to blades.

Public Perception and Future Assessment Possibilities

In Ontario, there has been considerable media attention in recent months given to noise-related complaints from people living near to wind turbine generators (notably in range of 400 to 600 metres), and there has been public discussion around the suitability of the MOE guideline limits. At the same time, there is a renewed political impetus to encourage further wind plant development.

Proposed legislation presently in process, the Green Energy Act, 2009, may alter the noise assessment process in Ontario. Historically, wind power projects have required both municipal approval, in terms of zoning and site plan agreements, and provincial approval for sound. This often resulted in conflicting requirements for setback distances and, as both approval processes could be appealed, lengthy approval timelines extending out two or three years have been common. Amongst other things, the legislation proposes alterations to portions of the planning and environmental assessment acts, exempting wind power projects from certain municipal approval processes in order to expedite the development of wind power projects. It remains uncertain what effect the potential loss of these planning tools may have on the noise assessment process.

Interestingly, there has been considerable public discussion surrounding creating regulations under the act that would establish minimum setbacks between wind turbine generators and residences. Such setbacks may well end up being be a fixed limit, not based on an engineering assessment of site-specific factors such as wind profile, the sound power of the turbines, and the number and spacing of the turbines. There is pressure from some in the public, citing health concerns in addition to audibility and annoyance factors, that the setback distance be set at 1.5 km or more, citing recommendations of the French *Académie nationale de médecine* [8] and others.

Mandating a sufficiently large minimum distance would simplify the approval process and reduce the potential annoyance for nearby residents, but would have serious ramifications for the government's goal of increasing green power in the province. From a technical perspective, there are also a number of drawbacks to this approach. A fixed distance, particularly if it is selected to be on the order of 500 m, may not serve the interests of the nearby residents. Depending on the cumulative impact of multiple turbines near or around a given receptor and the sound power of the selected turbines, the noise impact could actually be greater than under the current regime. On the other hand, for projects with only a few smaller wind turbine generators, the distance chosen may be overly conservative, leading to overall inefficiencies in terms of land use and cost. Also, with a fixed setback, the incentive for power developers to select turbines based on sound emission, or to consider a cost premium for low noise models would be removed. Future models may well be larger and generate greater sound levels, but with a fixed distance, there would be little pressure to combat increasing acoustic emissions.

Conclusions

Ontario has been on the forefront of noise assessment for wind power projects in Canada, having produced guidelines for the methodology and criteria in 2004, and updating these in 2008. The guidelines rely on internationally recognized standards, and the updated version has now considered and clarified factors such as the wind profile, penalties for the quality of the sound, and ground attenuation factors. These improvements have increased the consistency between assessments, although there remains in practice variations of at least +/- 5 dB between the predicted impacts and sound levels measured in the field. Despite the relatively robust approval process that is currently in place, complaints related to noise and health effects still occur and there is pressure from a segment of the public to increase the setback distance between wind turbine generators and residential dwellings. This concern is currently of great interest and discussion in Ontario as the province is introducing a Green Energy Act aiming to encourage wind energy projects and to streamline the approval process.

References

[1] Independent Electrical System Operator website:
http://www.ieso.ca/imoweb/marketdata/windpower_projects.asp

[2] Ontario Power Authority website:
http://www.powerauthority.on.ca/Page.asp?PageID=924&SiteNodeID=234

[3] Ontario Ministry of Environment, (2004). Interpretation for applying MOE NPC technical publications to wind turbine generators. MOE PIBS 4709e v1.0.

[4] ISO (1996). Acoustics – Attenuation of sound during propagation outdoors – Part 2: General method of calculation. ISO 9613-2, First edition.

[5] IEC (2002). Wind turbine generator systems – Part 11: Acoustic noise measurement techniques. IEC 61400-11, Second edition.

[6] Ontario Ministry of Environment (2008). Noise guidelines for wind farms. Interpretation for applying MOE NPC publications to wind power generation facilities.

[7] Legislative Assembly of Ontario (2009). An Act to enact the Green Energy Act, 2009 and to build a green economy, to repeal the Energy Conservation Leadership Act, 2006 and the Energy Efficiency Act and to amend other statutes.

[8] *Académie nationale de médecine* (2006). Human Health Repercussions of Windmill Operation

Third International Meeting
on
Wind Turbine Noise
Aalborg Denmark 17 – 19 June 2009

Recent Developments in Assessment Guidelines for Sound from Wind Power Projects in Ontario, Canada with a Comparison to Acoustic Audit Results

Brian Howe, HGC Engineering
Nick McCabe, HGC Engineering
2000 Argentia Road, Plaza 1, Suite 203
Mississauga, ON L5N 1P7 Canada
bhowe@hgcengineering.com

Abstract

The guidelines of the Ontario Ministry of the Environment (MOE) for the assessment of sound from wind power projects are the most sophisticated in Canada, relying on internationally recognized standards (ISO 9613 & IEC 61400-11) and allowing for a variation in both wind turbine sound power and background sound as a function of wind speed. The MOE completed a technical review of their procedures and published an updated guideline document in October of 2008. The revisions did not change the criteria (essentially 40 dBA at residences in rural areas under moderate wind speeds), but did address the need to consider several factors, such as the wind profile and ground attenuation, with greater specificity. While the revisions help improve the consistency between assessors, there remain some individuals that are critical of the approval process, and in practice there remains a fair degree of variability between the predicted sound levels and those levels occurring under operating conditions. This paper reviews the effect of these improvements, looks at the overall degree of precision versus the variability in sound levels as measured during several acoustic audits of wind power projects recently undertaken by HGC Engineering, and discusses the status of pending legislation that has the potential to modify the assessment process further.

Introduction

The first commercial wind plant opened in the province Ontario in 2002 with 5 wind turbine generators. As of April 1, 2009, eight contractually separate major wind plants were operating in the province of Ontario, with a combined installed capacity of 887 MW [1]. One more, with a capacity of 198 MW is anticipated to go online this year [2]. Numerous other large scale plants are now under development, and the total installed capacity of all current and planned projects is about 1,600 MW by 2012 [2]. To put this into context, the total installed capacity for all types of power plants in Ontario is currently about 27,000 MW.

In Ontario, the environmental noise generated by industrial noise sources is regulated by the provincial Ministry of Environment (MOE). Generally, industrial noise is assessed by the MOE against background sound levels, or certain overriding minimum criteria. As wind turbine generators tend to emit the greatest sound power levels during conditions of higher wind speeds when background sound levels are elevated, the MOE recognized a special case and produced a guideline document in 2004 [3] pertaining to environmental noise from wind power projects.

That guideline defined a prediction method for use in assessing environmental noise from wind turbine generators, identifying ISO 9613 [4] as the model to be used in calculations for sound propagation, and required that source sound power data to be used in the calculations be established using IEC 61400-11 [5]. Specific sound level criteria were also provided. Thus, predictive engineering calculations were established as the basis for environmental noise prediction for wind turbine generators, and for determining setback requirements.

Following adoption of the guideline, areas for improvement were identified in the guideline by a variety of sources. Following a lengthy review and consultation process, the guideline was revised and reissued in 2008 [6]. The new version changed neither the criteria nor the required standards for sound power measurement and environmental noise prediction, but did specify certain analysis assumptions such as the degree of ground absorption, and perhaps most importantly, indicated that site-specific wind shear (wind profile) effects needed to be considered.

At the present time there is a concerted political effort in Ontario to encourage more renewable energy projects. Proposed provincial legislation in the form of a Green Energy Act, 2009 [7] will provide future regulations designed to establish new guaranteed prices for future wind power projects and potentially to exempt wind power projects from various municipal regulations and by-laws, including zoning and development related regulations, in order to streamline the approval process.

As part of the Green Energy Act, the guidelines of the MOE with respect wind power projects are once again open to input from a variety of stakeholder groups. There have been complaints related to noise and the impact on health from Ontario residents living near operating and proposed wind power projects, leading to pressure on the government to implement minimum setback distances between wind turbines and residential dwellings as part of the revised guidelines or as regulations made under the Act. This would be a departure from the current MOE guidelines wherein the setback distance is a function of the acoustic predictions and established criteria.

Noise Guidelines for Environmental Noise, Wind Power Projects

In Canada, environmental regulations for industrial noise sources are under provincial jurisdiction. In Ontario, the applicable regulations for industrial sources pertain to sound level limits at sensitive noise receptors, such as residences, and are based on ambient sound levels at those receptors due to natural sources and road traffic. The guidelines for general industrial sources are based on the minimum ambient sound levels in any given hour which would be expected to occur under windless conditions. As wind turbine generators tend to emit the greatest sound power levels during conditions of higher wind speeds when background sound levels are elevated, the MOE produced a guideline document in 2004 pertaining explicitly to environmental noise from wind turbine projects.

That guideline defined a prediction method for use in assessing environmental noise from wind turbine generators, identifying ISO 9613 as the model to be used in calculations for sound propagation, and required that source sound power data to be used in the calculations be established using IEC 61400-11. Specific sound level criteria, defined in terms of the hourly energy-equivalent average (L_{EQ}) sound level were also provided based on an assumed relationship between wind-induced background sound and 10 metre height wind speeds. These criteria depend on whether the area is defined as acoustically urban or rural, and are summarized in Figure 1.

Figure 1: Summary of Provincial Sound Level Limits

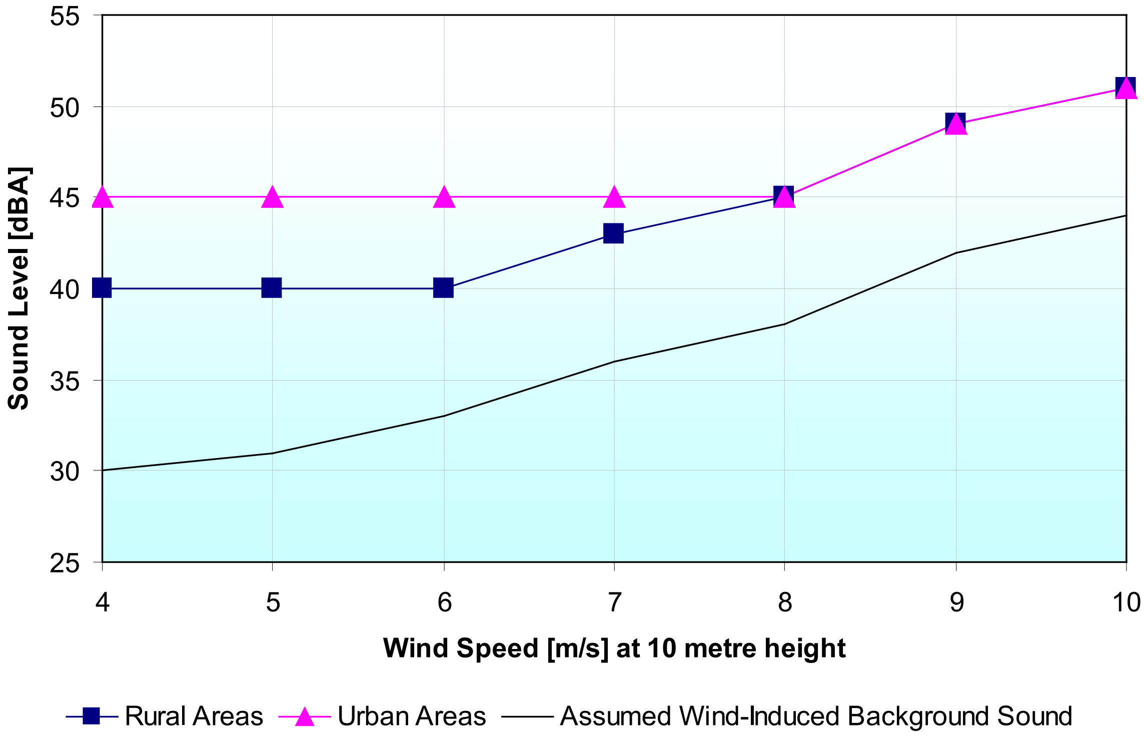

The guideline required predictive engineering calculations using the standards described in the guideline, and thus detailed sound level calculations and definable sound power estimation techniques were established as an important factor in determining minimum setbacks from residencies, and wind plant layout.

However, in practice, the guideline document lead to a great deal of variation in assumptions between different assessors, and therefore to variability in the resulting typical setbacks from residential receptors.

One of the most dramatic variables is related to wind shear (wind profile), and the reference roughness length of IEC 61400-11. As required by IEC 61400-11, most manufacturers list the sound power output of their turbines as a range, correlated with 10 metre height wind speeds under the reference wind profile condition. Because the 2004 MOE guideline did not discuss variation in wind shear, some assessors used the sound power data derived under IEC at face value, and others were taking into consideration site-specific wind shear data.

In practice, then, where the wind shear exponent might vary from 0.05 to 0.45 through a given day, the sound power output from the turbine might vary over the entire published range (which could be 5 to 10 dBA), even while the speed at the reference height remains constant. This can lead to large variation in the calculated setback requirements between one assessor and another.

To address such discrepancies, the MOE published a new document in 2008 replacing the earlier guideline. The 2008 guideline did not alter the numeric criterion values, but did amongst other changes add a requirement that wind profile effects be considered. Specifically, the sound power data should be "adjusted for the average summer night time wind speed profile, representative of the site". Other assumptions to be used in the analysis, such as the effective acoustic absorption of the ground surface or "ground factor", and factors affecting atmospheric absorption were also specified for the first time.

Issues related to the quality of the sound produced by the wind turbines are also addressed by the 2008 guideline by explicitly describing a 5 dB penalty to be added in the event that the manufacture's data indicates that the sound is tonal in nature. While tonal noise is penalized if present, the guideline indicates that tonal characteristics are generally associated with maintenance issues. The amplitude modulation related to the characteristic aerodynamic "swoosh" is not penalized.

The 2008 guideline also addressed in greater detail some practical considerations. These included the cumulative effect of neighbouring wind power projects, the need to consider the transformers as ancillary sound sources, and the need to consider vacant lots that would allow a future residence as a sensitive receptor.

Current Assessment Experience

The 2008 version of the guideline contains a number of considerable improvements over the previous version. However, despite the increased specificity of the current guideline, there remain differences between the practice of different assessors, and more importantly, there remains considerable variation between predictions made using ISO 9613 with IEC 61400-11 and long term sound level measurements made after startup.

HGC Engineering's recent experience in Ontario, measuring noise under different conditions around operational wind plants, indicates that while the typical minimum setbacks have increased over time (setbacks of 450 to 600 metres appear to be typical at present), there is considerable variation between actual sound levels at receptors and the impact predicted during the design of the wind plant. In practice, this fact makes validation of the acoustic performance of a wind plant vis-à-vis the MOE criteria quite difficult.

Figure 2 illustrates the results of a typical sound level monitoring period.

Figure 2: Comparison of Sound Levels Measured at a Residence and Sound Levels Measured Approximately 100m From Nearby Turbine. There is one generator located within 1 km from this residence.

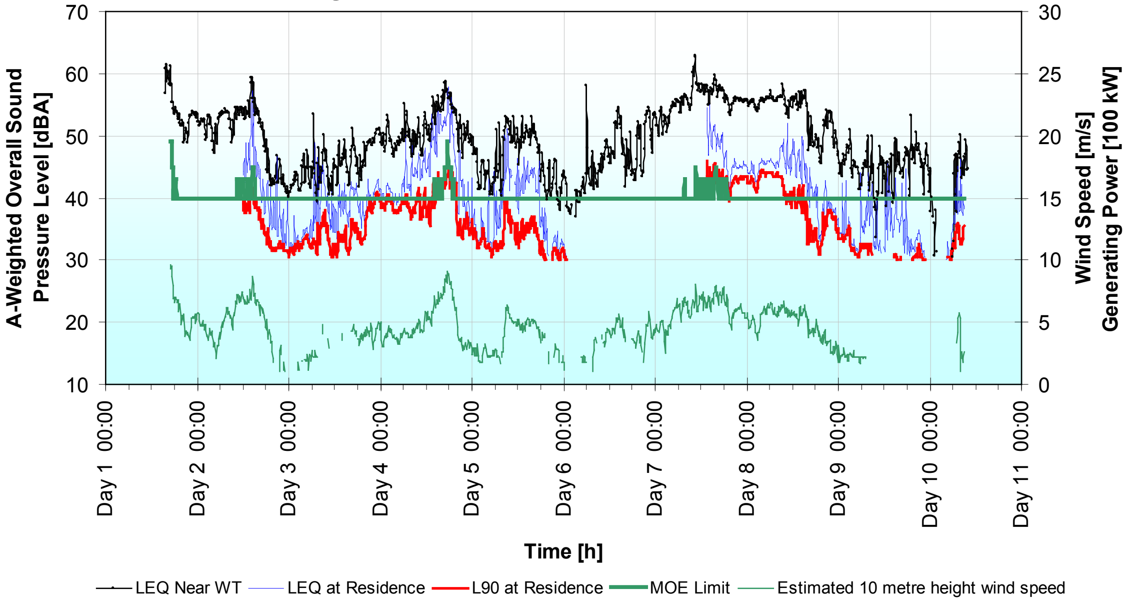

Figure 2 indicates considerable variation in both the energy-equivalent average (L_{EQ}) sound level and the "background" sound level (the L_{90} sound level, or the level exceeded 90% of the time) measured at a residence. Setting aside the strongest peaks in the L_{EQ} sound level, particularly those occurring during daytime hours when man-made sounds would be expected near a residence, there is still a large degree of variation, even for similar 10 metre height wind speeds. This is not unexpected, given the typical diurnal variation in the wind shear exponent, and the fact that the wind direction changes over time.

Figure 3 illustrates the variation another way. The L_{90} sound level measured at the residence is plotted against the wind speed recorded at the nacelle anemometer of the closest wind turbine generators. Considerable variation, on the order of 10 dBA is shown. For comparative purposes, the L_{90} sound level measured close (about 100 metres) from the nearest turbine, at a location where the noise from the turbine is the dominant sound source most of the time is shown in Figure 4. A similar pattern is evident.

Figure 3: L_{90} Sound Level at Residence vs Nacell Wind Speed
All Wind Directions Included

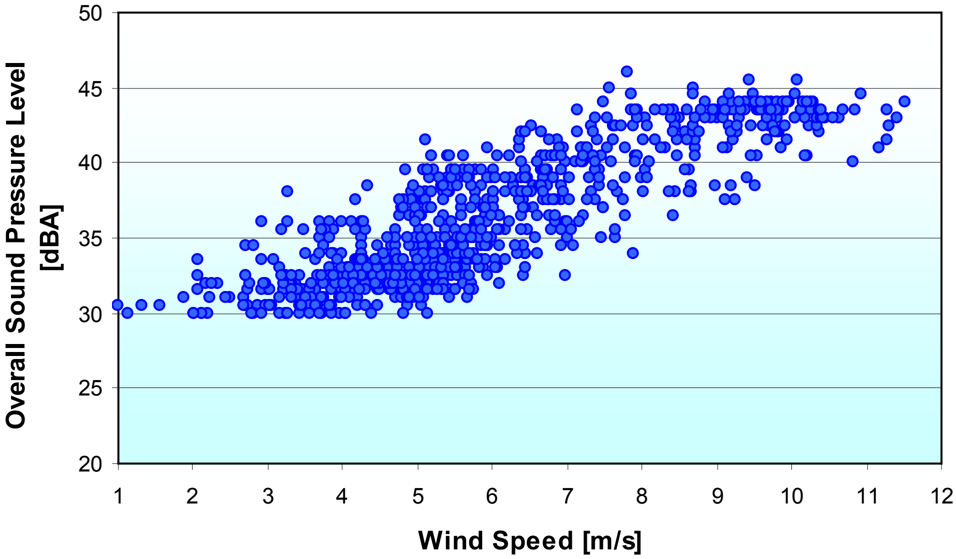

Figure 4: L_{90} Sound Level at WT vs Nacell Wind Speed
All Wind Directions Included

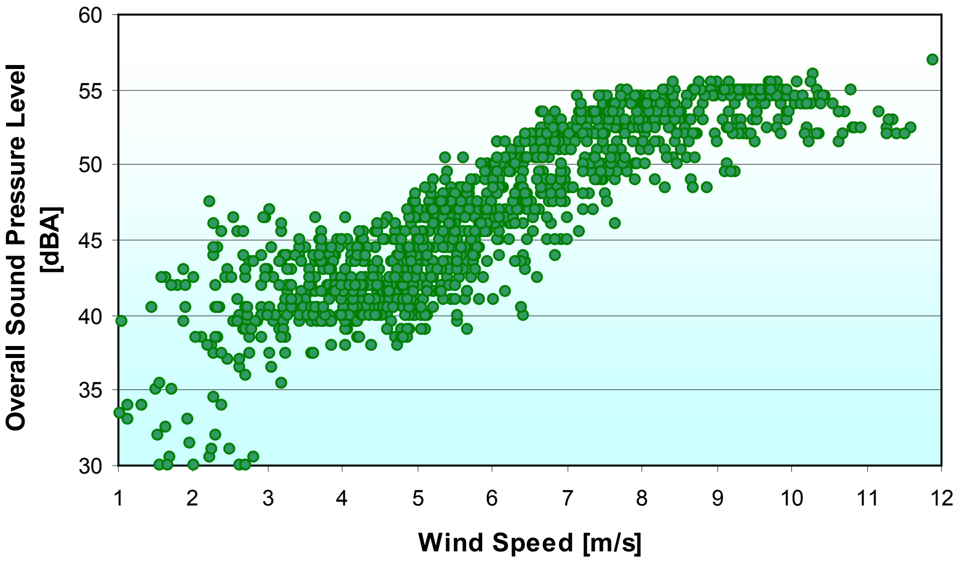

Given the magnitude of the variation, and given that the MOE standard when properly applied will result in a single number prediction for a given 10 metre high wind speed, it should be expected that there will be considerable variation in practice, both above and below the predicted sound level. This has certainly been the experience of HGC Engineering in conducting noise measurements around wind plants. Notice that the L_{90} sound level shown in Figure 1 exceeds the MOE criterion curve by 3 to 4 dBA for period centred around midnight on Day 8, while during periods on Days 2 and 4 with similar 10 metre wind speeds, the L_{90} sound level is effectively at the criterion curve.

The annoyance associated with the audibility of the sound, or with a given sound level impact is a subjective factor. The annoyance issue is complicated by the ability of the ear to become attuned to a particular sound. In one particular case where a homeowner had been complaining about noise from nearby wind turbine generators (there are 5 within a distance of about 1000 metres to this home). The complaints had grown fairly strident. In this case, the wind plant operators had been experimenting with different means to minimize the noise impact, while still allowing turbines in the area to operate. One such test involved a prolonged shutdown of the 5 turbines nearest to the home. The nearest operating turbines were then located at a considerable distance. In this case there were 7 operating turbines between 1000 and 2000 metres from the home. Complaints at this distance would normally be expected to be rare, however, while this operational condition presumably reduced the noise impact for the duration of the test, the homeowner still found the sound of the closest operating wind turbine generators to be objectionable. This highlights the need for prompt attention to any circumstance which may result in temporary increases in the sound levels near a turbine, or changes resulting in a more identifiable or potentially irritating sound such as mechanical wear or damage to blades.

Public Perception and Future Assessment Possibilities

In Ontario, there has been considerable media attention in recent months given to noise-related complaints from people living near to wind turbine generators (notably in range of 400 to 600 metres), and there has been public discussion around the suitability of the MOE guideline limits. At the same time, there is a renewed political impetus to encourage further wind plant development.

Proposed legislation presently in process, the Green Energy Act, 2009, may alter the noise assessment process in Ontario. Historically, wind power projects have required both municipal approval, in terms of zoning and site plan agreements, and provincial approval for sound. This often resulted in conflicting requirements for setback distances and, as both approval processes could be appealed, lengthy approval timelines extending out two or three years have been common. Amongst other things, the legislation proposes alterations to portions of the planning and environmental assessment acts, exempting wind power projects from certain municipal approval processes in order to expedite the development of wind power projects. It remains uncertain what effect the potential loss of these planning tools may have on the noise assessment process.

Interestingly, there has been considerable public discussion surrounding creating regulations under the act that would establish minimum setbacks between wind turbine generators and residences. Such setbacks may well end up being be a fixed limit, not based on an engineering assessment of site-specific factors such as wind profile, the sound power of the turbines, and the number and spacing of the turbines. There is pressure from some in the public, citing health concerns in addition to audibility and annoyance factors, that the setback distance be set at 1.5 km or more, citing recommendations of the French *Académie nationale de médecine* [8] and others.

Mandating a sufficiently large minimum distance would simplify the approval process and reduce the potential annoyance for nearby residents, but would have serious ramifications for the government's goal of increasing green power in the province. From a technical perspective, there are also a number of drawbacks to this approach. A fixed distance, particularly if it is selected to be on the order of 500 m, may not serve the interests of the nearby residents. Depending on the cumulative impact of multiple turbines near or around a given receptor and the sound power of the selected turbines, the noise impact could actually be greater than under the current regime. On the other hand, for projects with only a few smaller wind turbine generators, the distance chosen may be overly conservative, leading to overall inefficiencies in terms of land use and cost. Also, with a fixed setback, the incentive for power developers to select turbines based on sound emission, or to consider a cost premium for low noise models would be removed. Future models may well be larger and generate greater sound levels, but with a fixed distance, there would be little pressure to combat increasing acoustic emissions.

Conclusions

Ontario has been on the forefront of noise assessment for wind power projects in Canada, having produced guidelines for the methodology and criteria in 2004, and updating these in 2008. The guidelines rely on internationally recognized standards, and the updated version has now considered and clarified factors such as the wind profile, penalties for the quality of the sound, and ground attenuation factors. These improvements have increased the consistency between assessments, although there remains in practice variations of at least +/- 5 dB between the predicted impacts and sound levels measured in the field. Despite the relatively robust approval process that is currently in place, complaints related to noise and health effects still occur and there is pressure from a segment of the public to increase the setback distance between wind turbine generators and residential dwellings. This concern is currently of great interest and discussion in Ontario as the province is introducing a Green Energy Act aiming to encourage wind energy projects and to streamline the approval process.

References

[1] Independent Electrical System Operator website: http://www.ieso.ca/imoweb/marketdata/windpower_projects.asp

[2] Ontario Power Authority website: http://www.powerauthority.on.ca/Page.asp?PageID=924&SiteNodeID=234

[3] Ontario Ministry of Environment, (2004). Interpretation for applying MOE NPC technical publications to wind turbine generators. MOE PIBS 4709e v1.0.

[4] ISO (1996). Acoustics – Attenuation of sound during propagation outdoors – Part 2: General method of calculation. ISO 9613-2, First edition.

[5] IEC (2002). Wind turbine generator systems – Part 11: Acoustic noise measurement techniques. IEC 61400-11, Second edition.

[6] Ontario Ministry of Environment (2008). Noise guidelines for wind farms. Interpretation for applying MOE NPC publications to wind power generation facilities.

[7] Legislative Assembly of Ontario (2009). An Act to enact the Green Energy Act, 2009 and to build a green economy, to repeal the Energy Conservation Leadership Act, 2006 and the Energy Efficiency Act and to amend other statutes.

[8] *Académie nationale de médecine* (2006). Human Health Repercussions of Windmill Operation

Third International Meeting on Wind Turbine Noise
Aalborg Denmark 17 – 19 June 2009

The Use of Noise Perception Index (NPI) For Setting Wind Farm Noise Limits

Malcolm Hunt
Principal Acoustic Consultant
Malcolm Hunt Associates
Wellington, New Zealand
mha@noise.co.nz

Lindsay Hannah
Acoustic Consultant
Malcolm Hunt Associates
Wellington, New Zealand
Lindsay@noise.co.nz

Abstract

This paper investigates Noise Perception Index (NPI) as a method for assessing environmental noise from wind farms. NPI is a newly emerging noise assessment tool based on the degree to which pre-existing ambient background sound levels (L_{A90}) are exceeded by the sound under investigation, in this case, wind farm noise.

A practical use of NPI is in the setting of wind farm noise limits. Typically wind farm noise limits of L_{Aeq} 40 dB are recommended as an upper limit for wind farm noise received at residential sites by the New Zealand Wind Turbine Acoustic Standard, NZS6808:1998 *Acoustics – The Assessment & Measurement Of Sound From Wind Turbine Generators* however lower limits may be justified at certain locations, under certain conditions. NPI can assist by identifying sites which exhibit those conditions

This paper describes;

(a) NPI values are derived from a comparison of predicted wind farm L_{Aeq} or L_{A90}sound levels and L_{A90} ambient sound levels for specific wind farm noise receptor sites. The averaged results of this comparison are used to inform whether an alternative, lower noise limit (less than 40 dBA) may be justified based on expected community response;

(b) If the overall NPI indicator value for a receiver site is exceeds NPI 5, NPI can guide on the decibel amount by which the L_{A90} 40 dB limit should be <u>reduced</u> during quiet periods to provide adequate community protection (based on limiting degree to which predicted wind farm sound will exceed ambient sound levels).

Thus NPI assesses receiver sites based on a comparison of predicted wind farm sound levels and measured ambient sound levels to decide if a noise limit <u>below</u> L_{A909} 40 dB can be justified on the basis of expected community response. As indicated above, the NPI also guides on appropriate decibel limits below 40 dBA,

based on a reasonable expectation of community response to the (limited) increase over existing L_{A90} levels.
Importantly, the NPI method allows sub-40 dBA wind farm noise limits to be set on an objective and consistent basis, taking into account the existing environment and the expected scale of potential wind farm noise effects. If the ambient conditions warrant a lowered noise limit, a suitable wind farm decibel noise limit below L_{A90} 40 dB can be derived based NPI's ability to predict community response in the context of site-specific measured L_{A90} sound levels. The overall aim is to assist planning to avoid adverse noise effects for proposed wind farm installations in quiet rural areas.

New Zealand Standard For Wind Turbine Noise NZS6808

The current standard for assessing wind farm noise in New Zealand is NZS6808:1998 *Acoustics – The Assessment & Measurement Of Sounds From Wind Turbine Generators.* This standard was developed specifically for the measurement and assessment of noise from wind turbines (WTG's) and wind farm developments. This 1998 version of this standard was written during the early stages of significant wind farm development in New Zealand.

The 1998 standard has proven to be robust however experience and research over the past decade has brought to light numerous refinements and enhancements which are being considered within a revised draft version of the Standard, DZ6808:2009 *Acoustics- Wind Farm Noise*.

Existing Standard NZS6808:1998 allows for Territorial Local Authorities to set noise limits at values below 40 dBA although no guidance is provided.

DZS6808:2009 recommends a "primary" upper limit for wind farm noise of L_{A90} 40 dBA or 5 dB above the background, whichever is the greater. Recommended wind turbine noise limits are specified using the L_{A90} unit limit rather than L_{Aeq} as previously adopted in NZS6808:1998. The "primary" limit is referred to in the standard as follows: *'In most circumstances the primary noise limit will be adequate to protect health and some degree of amenity. However, at some locations a secondary noise limit may be desirable to afford a greater degree of protection during evening and night-time. A secondary noise limit should only be considered.'* The 2009 standard recommends that wind farm noise limits should not be set lower than L_{A90} 35 dB.

Table A illustrates diagrammatically the recommended noise limits set out in the 2009 standard.

<table>
<tr><th>Background Sound Level</th><th>Primary Noise Limit (L_{A90})</th><th>Secondary Noise Limit (L_{A90})</th></tr>
<tr><td>> 35 dB</td><td>background + 5 dB</td><td rowspan="2">background + 5 dB</td></tr>
<tr><td>30 – 35 dB</td><td rowspan="2">40 dB</td></tr>
<tr><td>< 30 dB</td><td>35 dB</td></tr>
</table>

Table A: DZS6808:2009 Secondary and Primary Noise Limit Summary.

The NPI method is intended to aid the assessment of secondary noise limits referred to within DZ6808:2009.

40 dBA - Primary Noise Limit

The rationale for the upper limit of 40 dBA recommended within the existing Standard (NZS6808:1998) has been reviewed by the DZ6808:2009 committee in the light of available literature and experience with wind farm noise. Much of the earlier research on which NZS6808:1998 was based is described in the ETSU-R-97 document "*The assessment and rating of noise from wind farms*". This document recommends noise from wind farms should be limited to 5 dBA above background noise for both day and night time, with a fixed limit for 43 dBA recommended for night time.

L_{Aeq} 40 dB or the average background sound level (whichever is the higher) is adopted as a limit on wind farm within NZS6808:1998. L_{A90} 40 dB or the average background sound level (whichever is the higher) is recommended in DZ6808:2009. Noise limits of this nature are said within these Standards to provide a reasonable level of protection from the adverse effects of wind farm noise, including during quiet night time periods.

There have been several studies examining the annoyance reaction to sound from wind turbines, mostly relying on predicted sound levels rather than measured levels. Due to wind turbine operation mainly during windy periods means there are commonly difficulties in obtaining field measurements of wind farm sound free from the influence of extraneous ambient sound. One of the most recent surveys was conducted within twelve geographical areas in Sweden which surveyed 1095 people in areas with one or more wind turbines with a nominal power of >500 kW. The results summarised in **Figure 1** support the idea that wind farm sound received at levels less than L_{Aeq} 40 dB do not result in significant proportions of the population expressing high levels of annoyance.

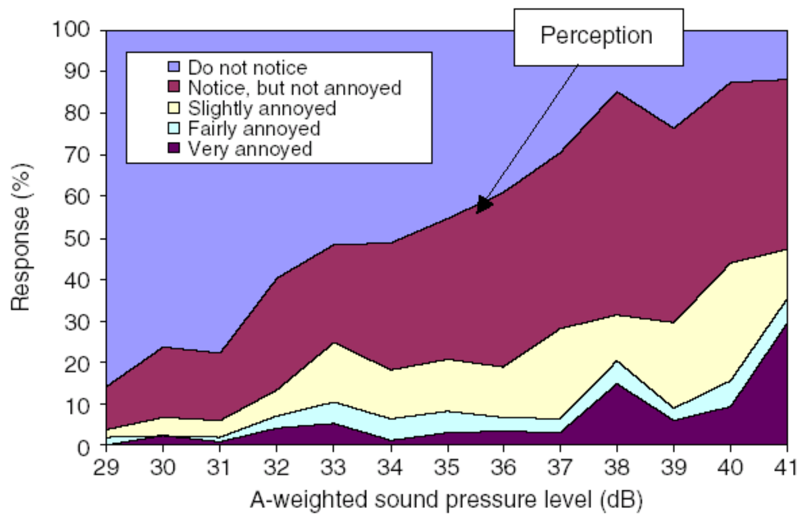

Figure 1 Response to wind turbine noise in relation to A-weighted sound pressure levels outside the dwellings of respondents (n= 1095). E. Pedersen, K. P Waye (2008).

Surveys have purportedly found wind farm noise annoyance higher among people living in more natural environments, i.e. rural versus urban environments, and also among those who lived in areas where the ambient level was classified as “quiet”. These quiet conditions are the conditions under which elevated NPI values occur.

Annoyance expressed at relatively low levels of received wind turbine sound has been used to justify the idea that possibilities for “restoration” are reduced or obviated for the noise receivers when noise from wind farm is detectable (Pedersen and Waye 2008). Whether these are effects of any significance within the spectrum of significant health and amenity effects of environmental noise which need to be regulated against has yet to be established. One fact that is emerging is that surveys of response to wind turbine sounds are greatly affected by visual components (making the environment less natural) and may cause subjects to report added noise impact and reduced possibilities for “restoration”.

Summarising the findings, it is clear that some researchers maintain low and moderate stressors such as low level wind turbine noise could have an impact on health, however there appears no compelling evidence that wind turbine noise at levels below 40 dB could cause health problems other than mild annoyance. Thus, 40 dB as an upper limit on wind farm sound appears reasonable for average daily exposure to wind farm sound. Setting limits below 40 dB indicates a desire to address perception effects associated with the audibility of wind farm sounds.

Wind Farm Noise Limits Below 40 dBA

Whilst the existing Standard NZS6808:1998 states an upper limit of L_{Aeq} 40 dB (or the average background sound level plus 5 dB, whichever is the greater) is adequate to protect people from adverse wind farm noise effects, the Standard allows for lower noise limits to be applied. However no guidance is given.

A number of wind farm projects approved by way of consent orders issued by the Environment Court in New Zealand have included limits of L_{Aeq} 35 dB at dwellings. These lower noise limits have been recommended to the court based on assertions that wind farm sounds will be “unduly audible” under low ambient conditions at residential receiver sites, such as when the background sound level (derived from the scattergraph curve of NZS6808) is calculated to be L_{A90} 25 dBA or less. The aim of the lowered noise limit seems to be to avoid times when the wind farm L_{Aeq} level may exceed the background sound level (L_{A90}) by 10 dB or more.

A L_{Aeq} 35 dB limit is not essential to protect sleep as the established WHO guidelines indicate that negative effects on sleep are avoided when the equivalent indoor sound pressure level does not exceed L_{Aeq} 30 dB for continuous noise. This criteria is achieved indoors even with open windows when wind turbine sound is limited to L_{Aeq} 35 dB or less outdoors. It appears the lowered limit is intended to address the degree to which wind turbine sounds are audible in the environment. This is a low level noise effect far removed from the usual levels of noise effects at which regulatory authorities act to protect public health and protect amenity.

In New Zealand most land use controls for electricity generation facilities are limited to L_{A10} or L_{Aeq} 40 to 45 dB during the quieter night time periods, which are applied in a consistent manner throughout the quietest night time periods. During calm periods (when wind turbines would not be likely to emit any sound) these typical hydro, thermal or geothermal electricity generation facilities located in similar rural areas may emit sounds (within compliance limits) which exceed ambient LA90 levels by 15 to 20 dB. It seems inconsistent that special treatment is accorded to sound from wind farm electricity generation facilities when ambient sound levels are exceeded generally to a lesser degree than other electricity generating facilities located in rural areas.

The current approach of limiting outdoor wind turbine noise at receiver sites for only some selected wind farms in New Zealand to L_{Aeq} 35 dB seems inefficient and leads to inconsistencies. The NPI method set out below indicates when ambient sound levels are sufficiently "low" to warrant the adoption of a lowered noise limit. Where appropriate, the NPI method can guide on whether the sub-40 dBA limit should be 39, 38, 37, 36, or 35 dB. There appears no technical justification for the tradition of setting wind farm noise limits in 5 dB steps below 40 dB. In fact, considerable flexibility is lost in terms of wind farm design when noise limits are not set a 1 dB steps below 40 dB.

Noise Perception Index (NPI)

NPI is an ambient-based noise assessment tool which is well suited to the task of assessing wind turbine noise on low-ambient receiving sites located in vicinity of wind farms. NPI is a based on a concept developed by Hessler and has been promoted based on experience throughout the United States involving noise sources introduced into green field situations.

NPI is defined as a measure of the true pressure *average* of the increases above ambient levels due (in this case) to wind farm noise emissions. A minimum of 2,000 ambient 10 minute sound samples is suggested as adequate to measure the temporal trends of ambient sound levels across representative weather conditions (including calm periods < 5 m/sec local wind speeds).

Using information on measured ambient sound levels and predicted (cumulative) wind farm sound levels, NPI is calculated as follows in spreadsheet notation as follows:

NPI = Sum((10*log(10^(L_{A90} wind farm sound level/10) + 10^(L_{A90} /10)) – L_{A90}))/n ....Eq 1

L_{A90} is the measured 10 minute existing ambient sound level, wind farm sound level is expressed as L_{A90}, and n = number of 10 minute periods included within the ambient measurement.

An example shown in **Figure 2** of NPI values for a sheltered a receiver site where modest wind farm sound levels are predicted to be received at levels between 23 and 32. (NPI=4.7). The sample was taken across 30 days of typical weather. **Figure 2** depicts the relationship between ambient L_{90}, wind farm noise level L_{Aeq}, the wind farm wind speed (m/sec) and calculated NPI(10 min) values for a period of 30 days. This site has a typical average long term NPI value of 4.7.

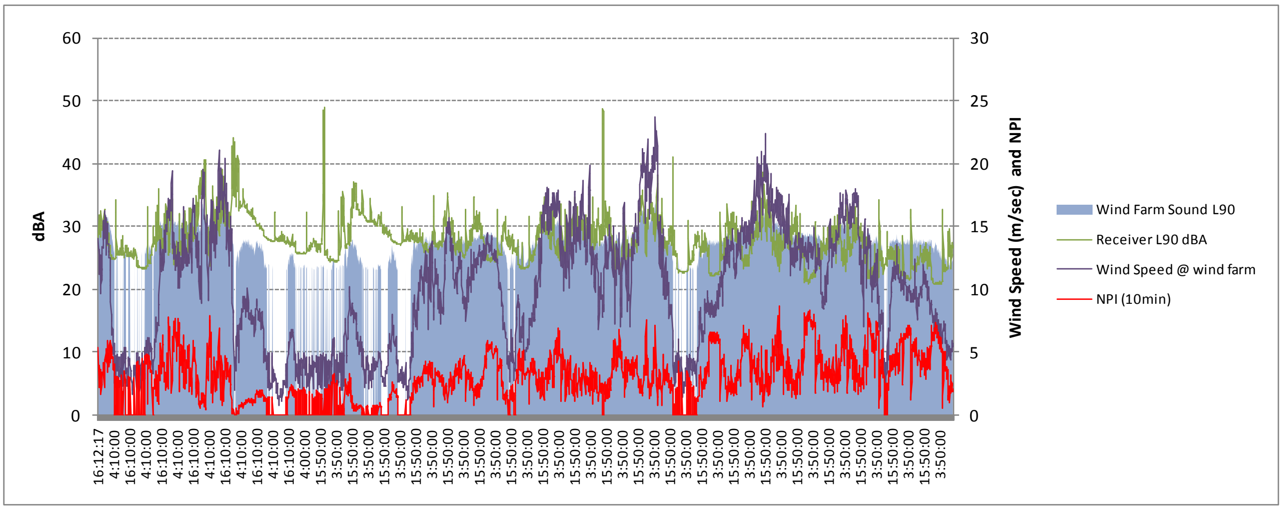

Figure 2: Ambient (dB), wind farm noise level L_{Aeq} (dB), wind farm wind speed (m/sec) and calculated $NPI_{(10\ min)}$ values for a typical low-ambient receiver site.

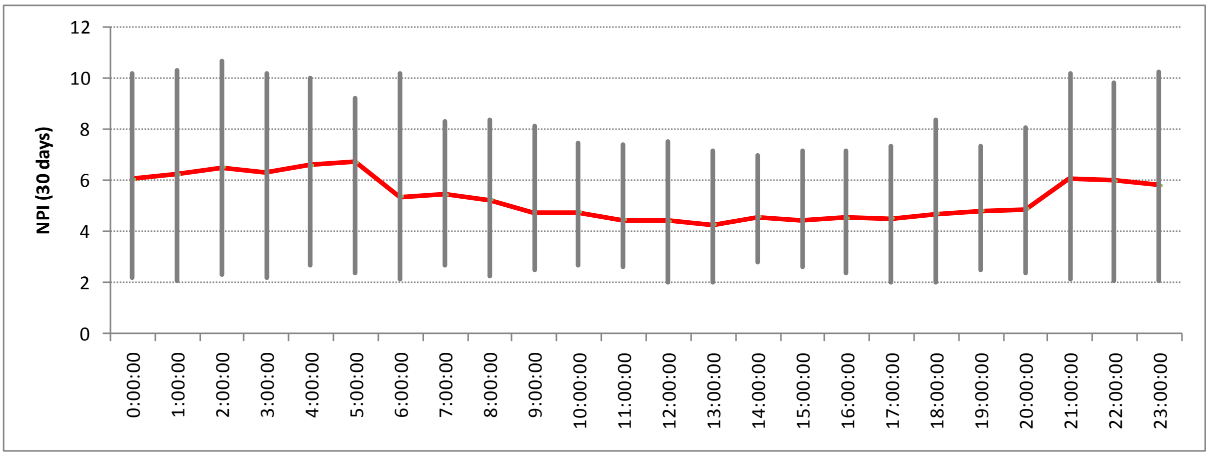

Figure 3: Average hourly NPI (10 min) values across twenty four hours of the day. Higher NPI values occur during times of low ambient L_{A90}.

NPI Values

The NPI rating method returns a single figure NPI value for each measurement site typically 5 or less, but possibly as high as 10 where levels of wind farm sound of 40 dBA or greater are received at very quiet and sheltered receiving sites. Sites with low NPI values are typically remote from wind farm sites (low received levels of wind farm sound) or are on exposed sites with moderate levels of ambient sound from wind related sources (forests, trees, etc).

In terms of interpreting community response, Hessler (2008) proposes NPI values be assessed on a common basis as shown in **Table B.**

NPI	PERCEPTION	PREDICTED COMMUNITY RESPONSE
<= 3 dBA	Generally Imperceptible	No Response
3 To 5 dBA	Barely Perceptible To Perceptible	No Response To Potentially Adverse Response
5 To 10 dBA	Perceptible To Noticeable	Potentially Adverse To Adverse Response
> 10 dBA	Readily Noticeable	Adverse Response

Table B: NPI Values vs. Predicted Community Response (after Hessler 2008).

The main features of NPI when applied to wind farm sound are;

(1) The increase over ambient quantified by NPI reflects the degree to which wind farm sound levels exceed background sound levels. This is the basis from which overall estimates of NPI provide an indicator of potential sound intrusiveness or audibility.

(2) Wind farm sound levels equal to (or less than) 3 dBA above baseline ambient L_{A90} is the threshold. Potential adverse noise effects occur above this level, generally at sites where NPI > 5. At these site a wind farm noise limit L_{A90} <40 dB may be warranted based on the L_{A90} background sound level, and the expected levels of wind farm sound.

Lowered wind farm noise limits at sites with NPI values of >5 and above can be justified on the basis that the wind farm noise above 35 dBA may cause "*Potentially Adverse To Adverse Response*".

Table C shows the NPI values derived from calculations performed for a range of typical receiver sites in the vicinity of proposed wind farms, indicating the relationship between NPI and ambient sound levels.

		Ambient Sound Level (dB) L_{A90}		
Wind Farm Sound Level(dB) L_{A90}		*HIGH*	*MEDIUM*	*LOW*
	LOW	NPI <5	NPI 5 to 6	NPI 6 to 8
	MEDIUM	NPI 5 to 6	NPI 6 to 8	NPI 8 to 9
	HIGH	NPI 6 to 8	NPI 8 to 9	NPI >9

Table C. NPI Index values for a range of receiver sites.

Table C indicates the for the more exposed sites returning a NPI value of 5 or less appear appropriate for the upper noise limit recommended by NZS6808:1998 of L_{Aeq} 40 dB or the background sound level plus 5 dBA whichever is the greater.

In terms by how much should the 40 dBA limit be lowered, the guideline dBA values for these wind farm noise limits where a sub 40 dBA limit may be justified as illustrated in **Table D** provides suggested dBA on the basis on the above NPI analysis.

		Ambient Sound Level (dB) L_{A90}		
		HIGH	*MEDIUM*	*LOW*
Wind Farm Sound Level (dB) L_{A90}	*LOW*	40 dBA	39 dBA	37 dBA
	MEDIUM	39 dBA	37 dBA	36 dBA
	HIGH	37 dBA	36 dBA	35 dBA

Table D: Recommended wind farm noise limits based on NPI values > 5.

The NPI tool is particularly useful for identifying sheltered, low ambient receiving sites expected to receive significant wind farm sound. Sites with an average NPI >5, can be considered sites at which an "effects" threshold is exceeded and where a wind farm noise limit of < 40 dBA may be appropriate at times on the basis of the low ambient sound environment and the scale of the potential wind farm sound levels expected for the site. These circumstances may warrant application of a lowered noise limit as per Table D above, indicating a limit up to 5 dBA lower than 40 dBA for sites where the NPI = >9, see Table C.

In all cases, it is recommended any sub-40 dBA wind farm noise limit criteria only be applied during times of low ambient sound, such as when the background sound level (derived from the scatter graph curve of NZS6808) is calculated to be L_{A90} 25 dBA or less.

Even for the lowest ambient site the above NPI method does not recommend wind turbine noise limits be set at levels below 35 dB at noise sensitive receiver sites. This is because there is no evidence that that sounds at this low level would result in significant adverse environmental health effects.

That is not to dismiss effects of wind farm sound levels received at low levels. What appears to be emerging is the idea that low level wind farm sounds may cause "restoration" be forgone which is classified as a cause of stress and annoyance. This is also coupled with an identified trend towards preserving natural soundscapes in quiet rural areas which do not contain man made sounds.

None of the relevant New Zealand acoustic standards, environmental noise guidelines, or land use planning regimes in place in New Zealand (for example, as implemented through District and Regional Plans) recognise the need to preserve 'soundscapes". There are no stated public policies in New Zealand that support the need to entirely avoid the introduction of detectable man-made sound into quiet rural environments.

The planning regime in New Zealand involves significant public input into the rule-setting process. The relevant noise guidelines on New Zealand do allow for noise from introduced sources so long as the amount of introduced sound is not unreasonable and there are acceptable effects on people and the environment.

In summary, recommendations are made with respect to enhancing the approach of DZS6808:2009 to setting sub 40 dBA wind farm noise limits in New Zealand. The recommendations are in terms of:

1) Using NPI to define which sites, on the basis of the expected levels of wind farm sound and the potential exceedance of ambient sound, would be recommended to have a noise limit of L_{A90} <40 dB.

2) If so, NPI can recommend by how much should the 40 dBA limit be lowered (during specified low-ambient periods) in order to avoid unreasonable wind turbine noise effects during noise sensitive periods.

Conclusions

The "Noise Perception Index" (NPI) offers a workable, objective guide for wind farm noise assessment based on ambient sound levels at receiver sites. The method can be used as a tool to identify low-ambient receiving sites located in vicinity of wind farms that require added protection below the normally applying wind farm noise limit of 40 dBA.

NPI can be used as an aid for setting secondary noise limits under DZ6808 by comparing predicted wind farm sound levels and available data on existing background sound levels. This will identify which sites are recommended to have a sub-40 dBA limit applied; and if so, guiding on how much the 40 dBA limit should be lowered (during specified conditions) in order to avoid unreasonable wind turbine noise effects such as undue audibility.

The method is predicated on the fact that wind farm noise limits of less than 40 dBA can only be justified at receiver sites with demonstrable prevailing low ambient conditions and where future wind farm sound levels are expected to be significant (> 35 to 40 dBA). Such sites exhibit average NPI values of >5.

The recommendations for setting sub-40 dBA wind farm noise limits are designed to avoid "*Potentially Adverse To Adverse Response*" in the community to the expected level of wind farm noise.

The NPI method is promoted to enhance future wind farm development in New Zealand by ensuring sub 40 dBA noise limits are set on an objective and consistent basis taking into account the existing environment and the expected scale of potential wind farm noise effects.

References

ETSU-R-97 (1997) The Assessment and Rating of Noise from Wind Farms" Department of Trade & Industry (UK). See: http://www.dti.gov.uk/energy/sources/renewables/publications/page21743.html

Hessler, G.F. (2008) "*The Noise Perception Index (NPI) for Assessing Noise Impact From Major Industrial Facilities and Power Plants in the U.S.*" Noise Control Engineering Journal, Volume 56(5), Sep-Oct 2008.

Pedersen E, Waye K. (2003) "*Wind Turbine Noise - Dose-Response Relationship" Proceedings ICBEN2003,* The 8th International Congress on Noise as a Public Health Problem. Rotterdam, The Netherlands 29 June – 3 July 2003, pp. 278-279.

Pedersen E, Waye K. ((2008) *Wind turbines—low level noise sources interfering with restoration experience?* Environmental Research Letters 3 (2008) 015002 (5pp)

Pedersen E (2003) "*Noise annoyance from wind turbines - a review*" Naturvårdsverket, Swedish Environmental Protection Agency. Report 5 308.

Standards New Zealand (1998), NZS6808:1998 *Acoustics – The Assessment & Measurement Of Sound From Wind Turbine Generators*

Standards New Zealand (2009), DZ6808:2009 *Acoustics- Wind Farm Noise*. see www.snz.co.nz

Third International Meeting
on
Wind Turbine Noise
Aalborg Denmark 17 – 19 June 2009

National Wind Technology Center Current and Past Testing Activities for Small Wind Turbines

Arlinda Huskey

National Renewable Energy Laboratory
1617 Cole Boulevard, Golden, Colorado USA
Arlinda.Huskey@nrel.gov

Jeroen van Dam

Windward Engineering
1617 Cole Boulevard, Golden, Colorado USA
Jeroen.van.Dam@nrel.gov

Abstract

The National Wind Technology Center (NWTC), part of the National Renewable Energy Laboratory (NREL), has been involved in wind turbine acoustics since the 1980s. The areas of work include measurement technique and standards development, measurement and analysis, prediction code development, and acoustic arrays.

Current noise-emission measurements are conducted to the International Electrotechnical Commission (IEC) standard 61400-11 [1], which is a standard specifically for acoustic measurements of wind turbines. The NWTC has been testing small wind turbines with a modified method based on the IEC 61400-11 methodology. Recently, two small wind turbine–specific standards were issued by the American Wind Energy Association [2] and the British Wind Energy Association [3]. These include methods for measuring and reporting noise levels for small wind turbines. This paper describes the NWTC's past and current testing activities in testing small wind turbines, including the methods and results.

Introduction

The focus of wind turbine noise research and test-method development long has been on large, utility-scale wind turbines. The market for small wind turbines, however, has grown rapidly in the past year [4]. Small wind turbines typically are installed in close proximity to populated areas, and thus noise can be an issue. Small wind turbines generally operate differently than the large wind turbines. The rotational speed of small wind turbines is greater than that of the large wind turbines. Many small turbines operate at variable speed and are free-yaw turbines. Power and rotor speed control methods include stall control, pitch control, furling, and even flutter. These turbines are more active in their response to variations in wind direction and wind speed, resulting in a much more dynamic and less linear noise response. Additionally, consumers buying small turbines should be assumed to be less knowledgeable about acoustics than are industry professionals.

Three draft standards address methods for characterizing noise from small wind turbines. The standards are those of the International Electrotechnical Commission (IEC), the American Wind Energy Association (AWEA), and the British Wind Energy Association (BWEA). The AWEA and BWEA both refer to the IEC standard, as they use the similar instruments and measurement methodologies but differ slightly in the analysis methodology and reporting.

The NWTC has been measuring noise from small wind turbines since the late 1990s. In 2008, the NWTC began an Independent Testing (IT) project to test four small wind turbines—including noise testing. This paper summarizes the noise test results of the small wind turbines tested at the NWTC, and discusses the different standards.

Sound Pressure and Sound Power Methodologies

The current IEC standard determines the sound power levels, one-third octave levels, and tonality. This paper does not discuss one-third octaves or tonality. Sound power levels are reported for wind speeds of 6 m/s, 7 m/s, 8 m/s, 9 m/s, and 10 m/s. One-minute averages are used for data collection. Measurements are taken with the turbine operating and parked (background). A microphone is placed on a board downwind of the turbine. The preferred method of determining the wind speed is to measure turbine power and derive the wind speed using the power curve. Wind speeds are determined at a 10-meter height. The sound pressure levels and wind speed data are used to determine a regression. From the regression the sound pressure levels are determined for 6 m/s, 7 m/s, 8 m/s, 9 m/s, and 10 m/s. Corrections for background are made, then the sound power levels are calculated. The IEC standard is in revision and will include an annex for small wind turbines.

When the NWTC began measuring noise on small wind turbines, the current IEC methodology was used with some modifications. Due to the dynamic nature of small wind turbines, a shorter averaging time of 10 seconds was used. Instead of determining the wind speed through the power curve, the measured wind speed was used. These changes resulted in a more consistent correlation of noise data with wind speed. Due to the sometimes non-linear nature of the sound pressure levels as plotted against wind speed, the bin method was used to determine the sound pressure levels at 1 m/s wind speed bins. Lastly, a broader wind speed range was preferable, because some small wind turbines have power limiting or rotor speed limiting control at higher wind speeds that cause a significant increase in sound pressure levels. The binned sound pressure levels are used to calculate the sound power levels.

The AWEA draft standard largely follows the NREL methodology. Additionally, it defines the AWEA rated sound level. The AWEA rated sound level is the sound pressure level that will not be exceeded 95% of the time, assuming an average wind speed of 5 m/s, a Rayleigh wind speed distribution, 100% availability, and an observer location of 60 meters from the rotor center. The wind speed is defined at a 10-meter height. The wind speed that is exceeded 5% of the time for a Rayleigh distribution (with 5 m/s average wind speed) is 9.8 m/s. Thus, if the sound power level increases with wind speed, then this is the wind speed used to calculate the AWEA rated sound level. This sound pressure level is determined by interpolating between the 9 m/s and 10 m/s bins.

The BWEA draft standard largely follows the IEC standard, but with several modifications. The averaging time changes depending on the rotor diameter, or is four times the rotor diameter with a minimum of 10 seconds. The measured wind speed is used and reported at rotor center. A wider range of wind directions is accepted for a given microphone position, due to the dynamic yaw behavior that small wind turbines can exhibit. One or more linear regressions are used to determine the sound pressure level at 8 m/s and wind speed dependence. The *declared* sound power level is used for reporting. In this case, "declared" means the sound power level with a 95% confidence level as determined from the uncertainty. This follows similar guidelines from IEC 61400-14 Declaration of Sound Power Levels and Tonality [5]. Other reported values include the noise slope immission sound pressure level at 60 meters, immission sound pressure level at 25 meters, and an immission noise map.

Table 1 shows the differences between the methodologies. This paper includes the results for some small wind turbines tested at the NWTC and discusses the different methodologies and reported values.

Table 1. Comparison of Methodologies

	IEC	NREL	AWEA	BWEA
Averaging Time	1 minute	10 seconds	10 seconds	4 * rotor diameter seconds, or 10-second minimum
Wind Speed	At 10 m height	At 10 m height	At 10 m height	At rotor center height
Wind Speed Range	6 m/s to 10 m/s	Minimum 6 m/s to 10 m/s, but as wide as range where wind screen is valid	As wide a range where wind screen is valid	Minimum of cut-in to 11 m/s and up to cut-out for wind turbine with speed-control mechanisms
Acceptable Sound Data	±15 degrees of microphone board	±15 degrees of microphone board	±15 degrees of microphone board	±60 degrees of microphone board
Reporting	Sound power levels, one-third octave levels, tonality	Sound power levels, one-third octave levels, tonality	AWEA rated sound level (sound pressure level at 60 m and 9.8 m/s wind speed), description of obvious changes in sound in wind speeds when speed control happens, observed tones (no analysis required), and IEC-based report	Declared apparent emission sound power level (sound power level at 8 m/s plus standard deviation), noise slope, immission sound pressure level at 60 m, immission sound pressure level at 25 m, immission Noise Map, indication if there is characteristic noise
Labeling	None	None	AWEA rated sound level	Declared apparent emission sound power level, noise slope, noise penalty, immission noise map

Small Wind Turbines

In the last year, NREL has tested four small wind turbines in the Independent Testing program, and acoustic results are available for three of the four. The Gaia 11-kW is a horizontal-axis, downwind, two-bladed, three-phase induction generator, 11-kW wind turbine, and has a rotor swept area of 132.7 m^2. It has an 18.2-m rotor center height. The Abundant Renewable Energy ARE 442 is a horizontal-axis, upwind, three-bladed, three-phase permanent-magnet generator, 10-kW wind turbine, and has a rotor swept area of 41 m^2. It has a 30.9-m rotor center height. The Entegrity EW50 is a horizontal-axis, downwind, three-bladed, three-phase induction generator, 50-kW wind turbine, and has a rotor area of 176.7 m^2. It has a 30.5-m rotor center height. These wind turbines are shown in Figure 1.

Figure 1. Independent Testing turbines (Gaia, ARE 442, EW50)

Prior to the Independent Testing program NREL tested several other small wind turbines [6], and a few of those results are included in this paper. The Whisper H40 is a three-blade upwind turbine with a rated power of 900 watts at a wind speed of 12.5 m/s. As tested, the turbine's 24-volt DC-output grid was connected via a Trace SW4024 inverter. Power and overspeed control are performed by "angle governor" furling. Rotor diameter is 2.1 m and hub height 9.1 m. The Bergey Excel-S, a three-blade upwind turbine with a rated power of 10 kW at a wind speed of 13 m/s. It is connected to a Bergey Gridtek inverter, which provides power to the NWTC electrical grid. The Excel uses a permanent-magnet alternator to produce three-phase variable frequency output at a nominal 240 volts. The three-phase output is rectified to DC power and then converted to single-phase 240-volt 60-Hz AC power in the inverter. The turbine blades are constructed of pultruded fiberglass. In high winds—speeds greater than about 16 m/s—the turbine furls out of the wind to control power and rotor speed. The Southwest Windpower Air X is a three-blade upwind turbine with a power rating of 400 watts at 12.5 m/s. The Air X is a free-yaw turbine that employs stall control, but it occasionally flutters at high wind speeds. The machine tested at the NWTC had a 1.14-m rotor diameter and a 13.3-m hub height.

Methodology Comparison

Data from the Independent Testing project was used to compare the NREL, AWEA, and BWEA methodologies. The results cannot be directly compared because there are slight differences between methodologies. The results, however, show the results of the methodologies in relation to one another.

Table 2 shows the results for sound power levels at 8 m/s, along with the difference in the methodology. The NREL sound power level is calculated for 8 m/s at 10 m height using binning by wind speed. The BWEA sound power level is calculated for 8 m/s at rotor-center height using a linear regression of the wind speed and sound pressure levels. Note that, for this paper, the averaging time for the BWEA method was kept at 10 seconds. The results are similar. The BWEA sound power levels are greater than the NREL levels; this probably results from using a 95% confidence level. There was a distinct difference in the methodologies for determining the sound power levels. The ARE 442 turbine, for example, has more than one linear region (as shown in Figure 2). To determine the sound pressure level at 8 m/s, data between 4 m/s and 10 m/s was used for the linear regression as prescribed by the BWEA standard. For the other turbines all data was used in the linear regression, because there was only one linear region. The Gaia data, for example, is shown in Figure 3. The NREL method binned the data and used interpolation to determine sound pressure levels at integer wind speed values.

Table 2. NREL and BWEA Sound Power Levels

	NREL Sound Power Level	BWEA Declared Apparent Emission Sound Power Level
Definition	IEC sound power level at 8 m/s using wind speed at 10-m height, binning, 50% confidence level	Sound power level at 8 m/s using wind speed at rotor center height, linear regression, 95% confidence level
Gaia	87.23	88.26
ARE 442	86.83	91.76
Entegrity	104.58	105.33

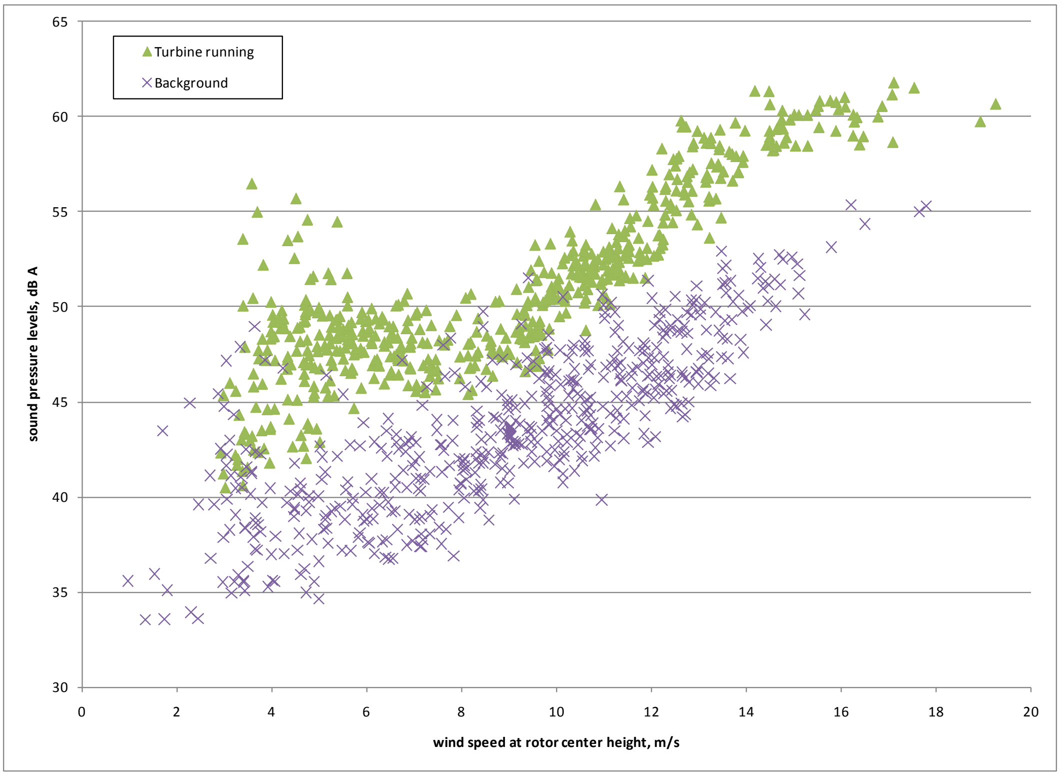

Figure 2. Data for the ARE 442 turbine

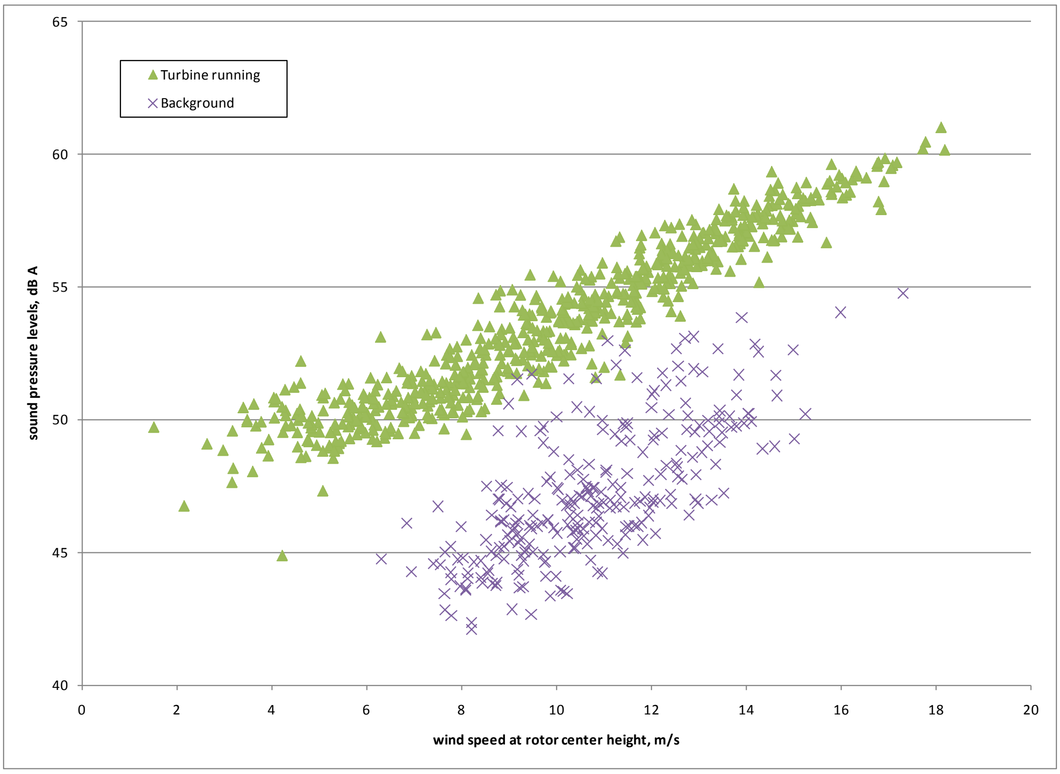

Figure 3. Data for the Gaia turbine

Table 3 shows the results for sound pressure levels at a distance of 60 meters. Again, this is to show the results from the different methodologies even though the results do not directly compare. The sound pressure levels are reported for different wind speeds. In this case the AWEA rated sound levels typically are greater than the

BWEA Immission Sound Pressure Levels. The AWEA number is the sound pressure level that is not expected to be exceeded 95% of the time with 50% confidence. The BWEA number is the sound level at 8 m/s with 95% confidence.

Table 3. AWEA and BWEA Sound Pressure Levels

	AWEA Rated Sound Level	BWEA Immission Sound Pressure Level at 60 Meters
Definition	Sound pressure level at a distance of 60 m and at a wind speed of 9.8 m/s	Sound pressure level at a distance of 60 m and at a wind speed of 8 m/s, and calculated using the Declared Apparent Emission Sound Power Level
Gaia	48.28	47.71
ARE 442	52.14	51.20
Entegrity	65.96	64.77

Although the methods are quite different, the results are similar. AWEA reports at a 9.8 m/s wind speed at 10-m height. BWEA reports at 8 m/s at rotor center (in this case 20–30 m), this is equivalent to about 7 m/s at 10-m height assuming the wind speed profile described in the IEC 61400-11. Thus, the difference in wind speed between the two methods is really about 3 m/s. A typical wind speed dependence of the sound power level is 1 dB per m/s. This means that the BWEA sound power level would be 3 dB less. The BWEA sound power level is the declared sound power level, however, and thus adds 1.645 times the standard uncertainty which typically is approximately 2 dB. Thus, for these turbines, here the numbers are expected to be about the same. They have very different meanings, however, and the difference between the two methods depends on the hub height of the turbine during the measurements.

Small Wind Turbine Sound Power Level Comparison

Small wind turbine noise levels are provided in Acoustic Tests of Small Wind Turbines [6] for several small wind turbines. The IT small wind turbines were added to the table and are shown in Table 4 and Figure 4. All small wind turbines were tested at NREL using the NREL methodology. The results from the Independent Testing project (Gaia, ARE 442, Entegrity) are preliminary. The final reports will be available on the website http://www.nrel.gov/wind/smallwind/independent_testing.html. The turbines tested prior to the IT project (Bergey Excel-S, Whisper H40, Air X) were tested several years ago, and the current models have improved since that time. There are two results for the Bergey Excel-S turbine. The turbine was tested with two different blade sets, the BW03 and SH3052. The SH3052 showed a significant noise improvement with a change in the airfoil, in this case shorter blades. This testing is discussed further in Acoustic Tests of Small Wind Turbines [6].

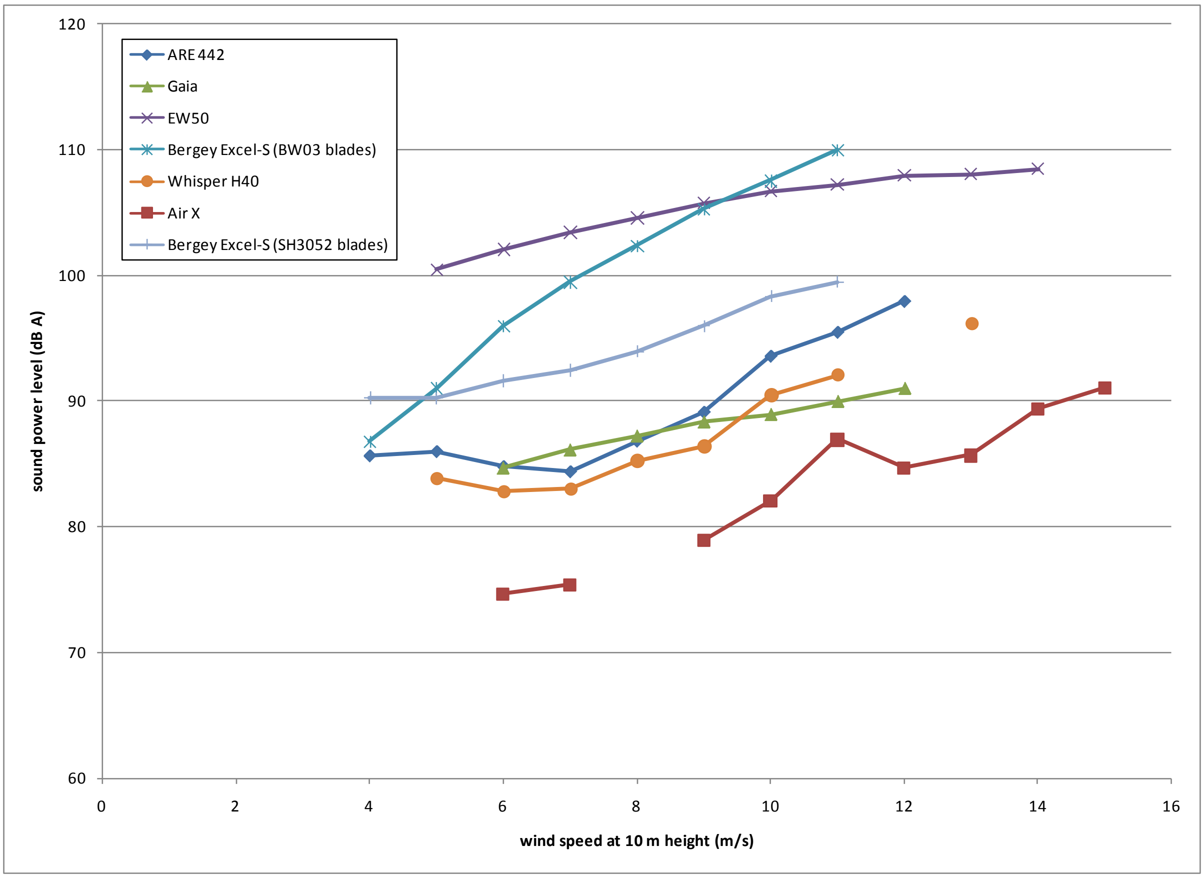

Figure 4. Sound power levels of small wind turbines

Table 4. Sound Power Level of Small Wind Turbines Tested at NREL

Wind Speed	ARE 442	Gaia	EW50	Bergey Excel-S (BW03 Blades)	Bergey Excel-S (SH3052 Blades)	Whisper H40	Air X
4	85.66			86.83	90.25*		
5	86.00		100.46	91.05	90.21*	83.82	
6	84.80	84.68	102.06	96.00	91.60*	82.79	74.69*
7	84.39*	86.12	103.42	99.51	92.43*	83.01*	75.42*
8	86.83*	87.23	104.58	102.37	93.94*	85.25	#
9	89.13	88.36	105.76	105.31	95.97*	86.38*	78.93*
10	93.58	88.95	106.71	107.55	98.33*	90.46*	82.09*
11	95.48	90.00	107.26	109.98	99.48*	92.08*	86.95
12	97.94	91.04	107.96			#	84.68*
13			108.11			96.16*	85.71*
14			108.49				89.39*
15							91.06*

* The difference between the turbine and background was between 3 dB A and 6 dB A.
# The difference between the turbine and background was less than 3 dB A and the sound power level could not be reported.

Conclusions

Not until recently was any work done on the noise testing of small wind turbines. Recently, more activities have taken place and—because there was no well-defined IEC method for small wind turbines available—different methods were developed in parallel. All follow the IEC standard to some extent, but then deviate in the analysis. Although the reported numbers do not seem to vary greatly, they actually differ in the sense that they are reported at different wind speeds and incorporate or do not incorporate the measurement uncertainty. Regardless, getting any measured data to the public will greatly improve the consumer's ability to deal with the noise issues by performing proper siting.

Future Work

The U.K. and U.S. representatives have begun coordinating determination of a unified acoustic noise measurement technique for small wind turbines that can be incorporated as an annex in the next revision of the IEC 61400-11. Further, there is an IEA activity in preparation to devise a unified labeling method.

NREL will continue testing small wind turbines under the second phase of the Independent Testing project. NREL also will provide support in developing regional test centers in the United States. These regional test centers will test to the AWEA and/or IEC standards, thus enabling comparison of test results at different geographical sites.

References

[1] International Electrotechnical Commission (IEC) (2002). 61400-11, "Wind Turbines—Part 11: Acoustic Noise Measurement Techniques."

[2] American Wind Energy Association (AWEA) (2009). "Small Wind Turbine Performance Safety Standard." AWEA 9.1.

[3] British Wind Energy Association (BWEA) (Feb. 2008). "Small Wind Turbine Performance and Safety Standard."

[4] American Wind Energy Association (AWEA). "Small Wind Turbine Global Market Study, Year Ending 2008" (http://www.awea.org/smallwind/pdf/09_AWEA_Small_Wind_Global_Market_Study.pdf).

[5] International Electrotechnical Commission (IEC) (2005). Technical Specification (TS) 61400-14, "Wind Turbines Part 14: Declaration of Sound Power Level and Tonality Values."

[6] Migliore, P.; van Dam, J.; Huskey, A. (2004). "Acoustic Tests of Small Wind Turbines." Collection of the 2004 ASME Wind Energy Symposium Technical Papers at the 42nd AIAA Aerospace Sciences Meeting and Exhibit, 5–8 Jan. 2004, Reno, Nevada. New York: American Institute of Aeronautics and Astronautics, Inc. (AIAA) and American Society of Mechanical Engineers (ASME) pp. 529–542.

Third International Meeting
on
Wind Turbine Noise
Aalborg Denmark 17 – 19 June 2009

Impact of Wind turbine noise in the Netherlands

Jan Jabben, Edwin Verheijen, Eric Schreurs
RIVM, box 1, 3720 BA, Bilthoven, The Netherlands
e-mail jan.jabben@rivm.nl Edwin.verheijen@rivm.nl Eric.schreurs@rivm.nl

Abstract

The Dutch government aims at an increase of wind energy up to 3000 MW in 2011 and up to 6000 MW in 2020 by placing new wind turbines on land or offshore. The Ministry of Housing, Spatial Planning and the Environment commissioned RIVM to explore the possible impact of this policy on the population and available land area for new turbines. The paper gives the preliminary results of the study, in which a national noise map containing all wind turbines in the Netherlands was used for impact assessment. Using the map, consequences of different limit values for Lden in new Dutch noise legislation, both regarding effects on the population and regarding energy policy targets where evaluated and will be discussed.

Introduction

The need for renewable energy has grown strongly the past decennia and is expected to grow even further the next years, as oil and gas reserves are diminishing and carbone emission has become a major problem for effects of climate change.

In particular, this may be the case for wind energy. In the Netherlands, policymakers are now aiming at an increase of up to 3000 MW by 2011, to be realised by windturbines on land or offshore. However, this policy could lead to problems concerning the noise quality on nearby dwellings and may put a heavy claim on the available land space, in order to avoid annoyance and health effects.

In order to evaluate the options depending on the choice of allowable limit values, RIVM has studied the potential effects of an increased wind turbine park on the Dutch population. More specific, the following questions were considered:

- What is the impact of wind turbine noise in the current situation ?
- Does it suffice to set a Lden limit value and if so, how should this be chosen in order to avoid further impact and effects ?
- What are the consequences of available space depending on the limit value ?
- Can low frequency content be an additional problem ?

Current situation

The number of wind turbines in the Netherlands has vastly increased in recent years. In Februari 2009 1.955 turbines were placed on shore, as shown in Figure 1. Also a shift towards larger and more powerful turbines has taken place. The turbines now yield approximately 2 MW.

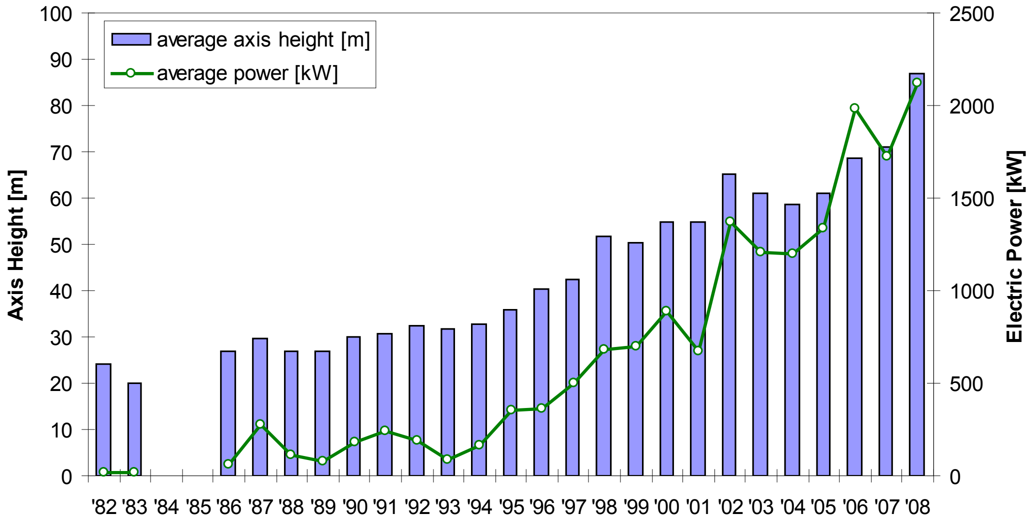

Figure 1 Development towards more and larger turbines in the Netherlands, Source: Wind Service Holland[1]

Data concerning location, axis height, rotor diameter etc were available from Wind Service Holland[1]. This data was used according to the model described in appendix 1 to determine the noise levels on a noise map consisting of a grid of 25 x 25 m. The result is shown in Figure 3. Combining the noise map with locations of dwellings, the exposure of the population was determined, which is shown in Figure 2.

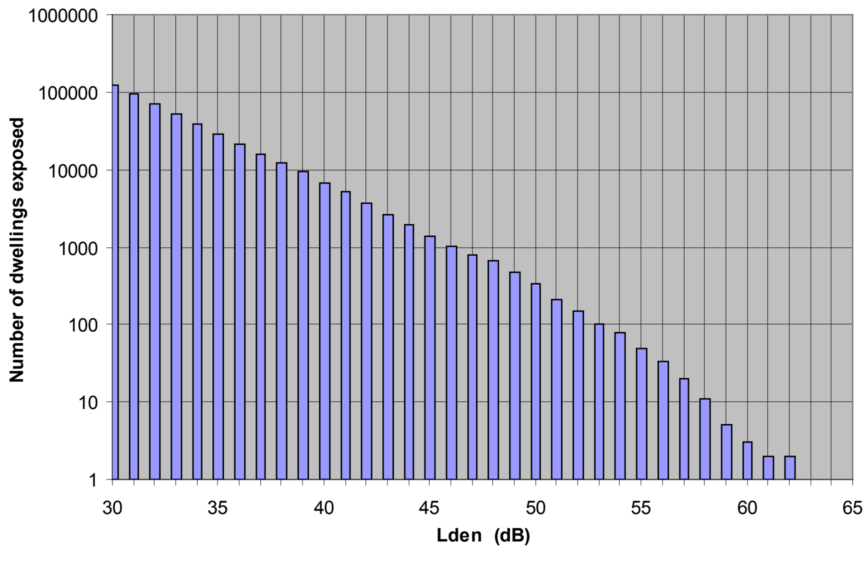

Figure 2: Exposure of dwellings to Wind turbine noise in the Netherlands.

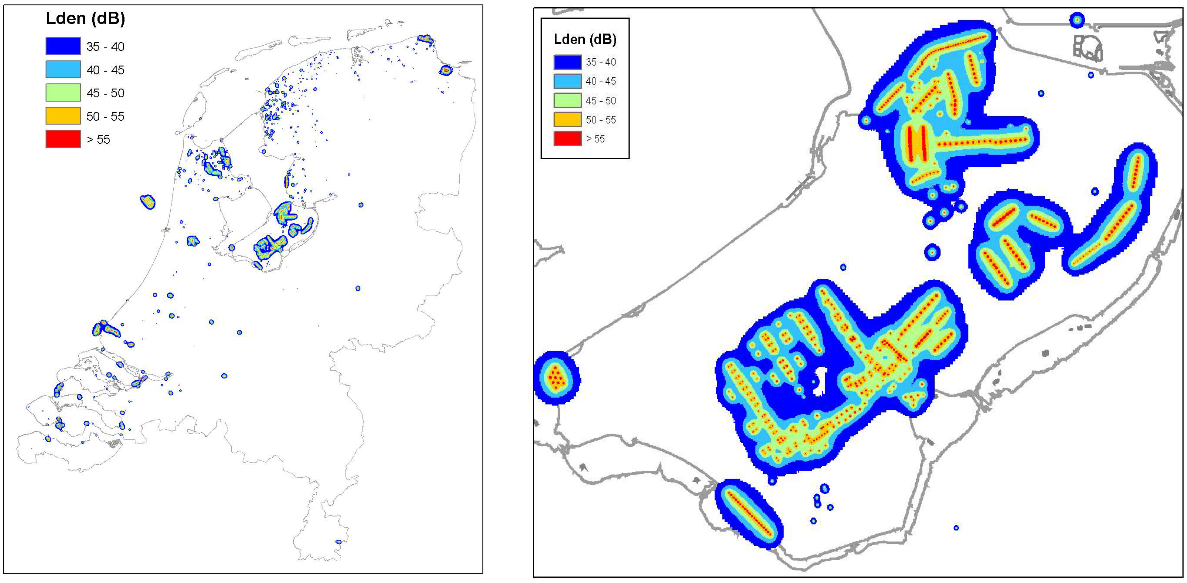

Figure 3: Noise maps for Wind turbines in the Netherlands, the zoomed area is the Flevopolder, just below the 'IJsselmeer' water.

Most turbines are placed in the Northern and coastal areas of the Netherlands. The northern part is the less dense built up area, but also new locations are chosen in more urban regions.

Annoyance

Various studies studies[2][3][4], show that Windturbine noise causes annoyance from noise. Also visual aspects cause annoyance[5]. In order to avoid effects on the population appropriate regulation of admissible impact is therefore necessary. The limit values in Dutch legislation for road traffic noise, railway noise and airport noise are all related to the European noise indicator Lden. For road- and railway traffic the legislation sets a preferred value and a maximum allowable value. If the former is satisfied, no further action is required and noise levels are considered safe with regard to effects on the population. Above the maximum allowable value, permission is denied and in between, stakeholder must evaluate effects and benefits and look at measures for minimizing deterioration of environmental quality, before projects can be executed. For uniformity it is envisaged to also bring new Wind Turbine noise legislation into this framework. For road traffic noise the preferred value is set at 48 dB(A) and the maximum value is set at 55 dB(A). However, choosing the same preferable and maximum Lden values for wind turbine noise would lead to problems, as the type of noise generated by windturbines, at the same Lden level, causes much more annoyance than road traffic noise. To further elucidate this point, Figure 4 depicts the dose response functions for annoyance for a number of different noise sources.

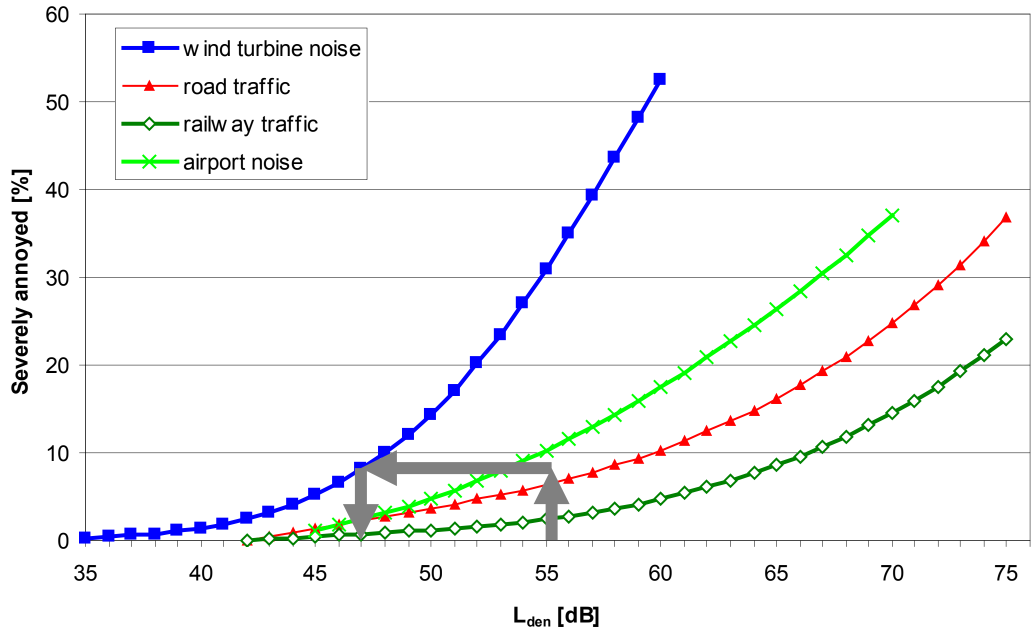

Figure 4 Dose response functions for severe annoyance for windturbine noise[4] compared with railway noise, road traffic noise and airport noise[6].

Annoyance effects caused by noise from windturbines were investigated by Pedersen[2], van den Berg[3] and by TNO[4]. Figure 4 shows the dose response curve according to TNO[4]. Comparison with Miedema's[6] dose response function for road traffic noise shows that the preferred and maximum value for road traffic, Lden 48 and 55 dB(A), correspond to a preferred and maximum value of approximately Lden 40 and 47 dB(A) for wind turbines respectively. At these values both sources may be expected to yield comparable effects. To investigate possible consequences of a choice for the maximum value for wind turbines, the distribution of dwellings in Figure 2 was converted into percentages of severely annoyed inhabitants, by using the WT-dose effect curve[4] as shown in Figure 4. The results are given in Table 1.

noise level (L_{den})	Number of inhabitants affected	Severely annoyed	
		number	percentage of total
More than 29 dB(A)	440.000	ca. 1500	100%
More than 40 dB(A)	15.250	760	52%
More than 45 dB(A)	3.110	400	27%
More than 47 dB(A)	1.810	310	21%
More than 50 dB(A)	740	180	12%

Table 1 Accumulated number of inhabitants affected and number of severely annoyed inhabitants.

It was estimated that 440.000 inhabitants in the Netherlands are exposed to noise from wind turbines of which 1.500 are expected to suffer severe annoyance. It is remarkable that almost half of this number already occurs in within the range Lden 30-40 dB(A). This means that in order to avoid strong increase of annoyance when new turbines are built, the preferred value should not be set too high. As for environmental noise quality, one would like to choose this value as low as possible, e.g at 35 dB(A), but this also means that the available space for new turbines is narrowed considerably. The consequences are further outlined in the next section.

New Turbines

In order to asses the consequences of limit values for available land space, use was made of a 'reciprocal' noise map. Such a map is obtained by attributing a fictitious noise emission to the dwellings instead of the turbines. The resulting noise map indicates the areas where levels are below the limit value. By reciprocity these are also the areas where new turbines can be placed without exceeding the limit on dwellings. An example is given in appendix 2. Not all the 'free' space determined in this manner can be utilized however. In many cases there are restrictions in the sense that space already is reserved for other purposes. Therefore woods, nature areas and airport zones were excluded. The results are summarized in Figure 5. This Figure shows that the available space for placing new wind turbines rapidly decreases, with decreasing limit value.

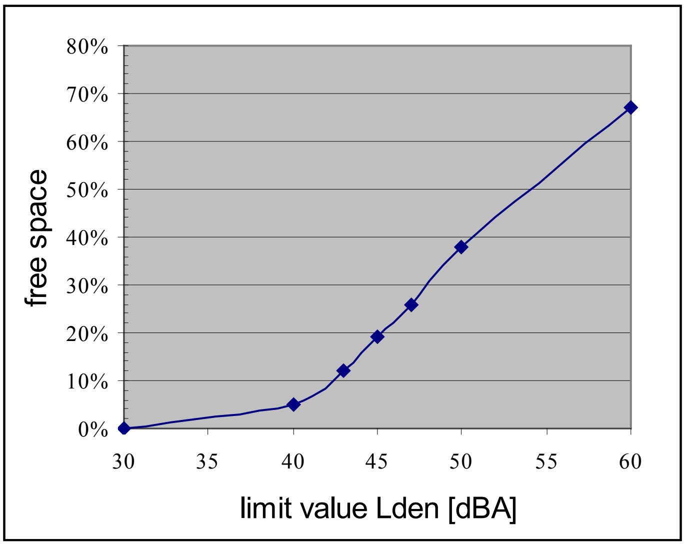

Figure 5 The available space for new wind turbines, depending on the maximum allowable Lden on nearby dwellings in the Netherlands (total area app. 36.000 km^2).

In case a limit value of 40 dB(A) is chosen, approximately 5%, some 1800 km^2, would be available for new turbines. Assuming 2 turbines, each 2MW, could be placed per km^2 this would allow for 3,6 GW, theoretically enough for accommodating a target of 2 GW in 2011 but not enough for accommodating 6 GW in 2020. In the latter case a higher limit value of 45 dB(A) allowing for 19% (4320 km^2 or 8,6 MW) would be needed. At the submission of this paper, further research is still carried out, in order to asses to which extend the “free” space is really available. In any case, from these results it seems clear that the choice or the limit value is critical with regard to the realisation of policy targets for renewable energy.

Is Low frequency noise a problem ?

Wind turbines generate a noise spectrum that contains a large amount of energy in the low frequency region between 20 and 200 Hz. This is shown in Figure xx for the average spectrum of 37 Wind turbines according to Sondergaart[7] and a spectrum of a Vestas V80, according to Rogers[8]

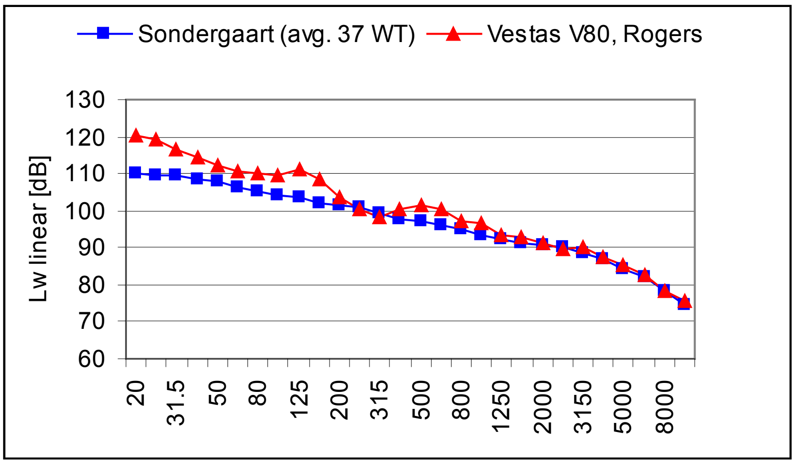

Figure 6 Linear spectra of Windturbine noise; LwA=105 dB(A) avg of 37 WT according to Sondergaart[7] and a Vestas V80, according to Rogers[8], LwA=107 dB(A)

The spectra in Figure 6 were used to asses the possibility that inhabitants of nearby dwellings perceive low frequency noise problems given an *outdoor* Lden value of 40 dB(A). This could be done only by indication as low frequency problems occur *indoor* and the noise attenuation over the propagation path shows a large variability (wind conditions, soil influence, temperature effects, isolation of the dwellings, resonance effects etc.) LF-noise attenuation during propagation was determined using the Harmonoise model[9], modified for point sources, over uncompacted, loose ground (turf, grass, loose soil) with representative flow resistivity σ=80 $kNsm^{-4}$.

Figure 7 gives the linear noise spectrum of a wind turbine (LwA=107 dB(A)) at 800 m distance. The A weighted noise immission level amounts to 34 dB(A), which at continuous operation of the turbine would result in Lden 40 dB(A) (after including penalties for evening and night time and 24-hour averaging). For the isolation of the dwellings, for the low frequency range, a value of 10 dB(A) was subtracted in order to estimate the indoor value.

As for effects from low frequency noise, one can distinguish between annoyance and audibility. In order to evaluate the probability of annoyance, in the Netherlands the Vercammen threshold curve[10] is well known. Exceedence of the Vercammen threshold will likely result in annoyance effects from LFN. In order to evaluate audibility of LFN the Dutch Foundation of Noise Annoyance (NSG) gives the NSG-guideline[11]. Also one can use the ISO266 10% audibility threshold[12]). Exceedence will likely result in audible levels for 10 % of the population. These threshold curves are also given in Figure 7.

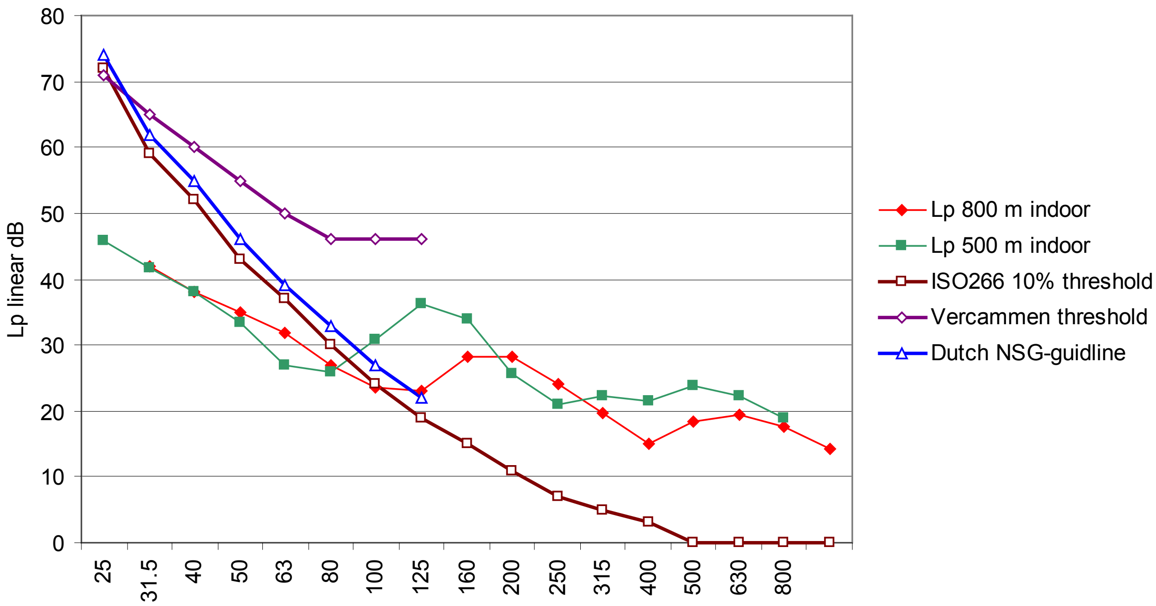

Figure 7 Comparison of linear indoor WT spectra at 500 m (Lden outdoor 45 dB(A)) and at 800 m (Lden outdoor 40 dB(A)) with threshold values for annoyance (Vercammen[10]) and audibility (NSG[11]and ISO266[12]). Source power level windturbine Lw 107 dB(A)

As can be seen from Figure 6, both at 500 and 800 m, according to the Vercammen curve, severe annoyance effects due to low frequency noise are unlikely. Both spectra remain well below the threshold curve. However, as for audibility, according to both the NSG and ISO266 threshold, effects may occur at 500 m (Lden 45 dB(A)), in particular near the 100 Hz frequency. At 800 m (Lden 40 dB(A)), the levels up to 125 Hz seem to remain just below audibility. Although in both cases severe annoyance effects are unlikely, one should be careful in assuming that audibility poses no problems for inhabitants. See for example Kamperman and James[13]. In the evening and night, when ambient noise decreases, audibility could become important, in particular for sleep quality. Also, indoor levels will increase significantly when people have their windows opened. In conclusion, as long as outdoor Lden values remain below Lden 40 dB(A) we expect that low frequency noise impact will remain limited and not cause severe annoyance or health effects. Above this value, the levels become audible and above Lden 45 dB(A) may increasingly cause annoyance, sleep disturbance and health effects.

Conclusions

- It was estimated that 440.000 inhabitants in the Netherlands now are receiving significant noise contribution form wind turbine noise of which 1.500 are expected to suffer severe annoyance.
- It is remarkable that almost half of this number already occurs in within the range Lden 30-40 dB(A). This means that in order to avoid strong increase of annoyance when new turbines are built, the preferred value should not be set too high.
- In the Netherlands (total area app. 36.000 km^2), the available space for placing new wind turbines strongly depends on the limit value that is chosen. In case a limit value of Lden 40 dB(A) is chosen, approximately 5%, some 1800 km^2, would be available for new turbines. At a limit value of 45 dB(A) this increases to 19% (4.320 km^2) and at Lden 50 dB(A), 38 % (13.680 km^2) would be available.
- A limit value of Lden 40 dB(A) seems enough for accommodating a target Wind Turbine power yield of 2 GW in 2011 by turbine on land, but probably not enough for accommodating 6 GW in 2020. In the latter case a higher limit value of Lden 45 dB(A) would be needed if the target for 2020 is to be realized only by turbines on land.
- As far as further increase of annoyance and health effects are concerned, from this study it seems preferable that new turbines do not exceed a limit value of Lden 40 dB(A). This would pose restrictions with regard to the options for new wind parks and finding new locations on land could prove much harder than in the past.
- As long as outdoor Lden values remain below Lden 40 dB(A) we expect that low frequency noise impact will limited and will not cause severe annoyance or health effects. Above this value, the levels become audible and, above Lden 45 dB(A), may increasingly cause annoyance, sleep disturbance and health effects.

References

[1] Wind Service Holland, http://home.planet.nl/~windsh/

[2] E. Pedersen, Human response to wind turbine noise: Perception, annoyance and moderating factors. Thesis, Göteborg University, 2007.

[3] G.P. van den Berg, E. Pedersen, J. Bouma, R. Bakker (2008). WINDFARMperception: Visual and acoustic impact of wind turbine of wind turbine farms on residents. Report FP6-2005-Science-and-Society-20. University of Groningen, Göteborg University

[4] S.A. Janssen, H. Vos en A. Eisses, Hinder door geluid van windturbines, Dosis-effectrelaties op basis van Nederlandse en Zweedse gegevens, TNO-rapport 2008-D-R1051/B, oktober 2008.

[5] E. Pedersen en P. Larsman, The impact of visual factors on noise annoyance among people living in the vicinity of wind turbines, J Environ Psychol doi:10.1016/j.jenvp.2008.02.009, 2008.

[6] Miedema Olsthoorn

[7] B. Søndergaard, D. Hoffmeyer, B. Plovsing, Low frequency noise from large wind turbines, Second international meeting on Wind Turbines Noise, Lyon, 20-21 september 2007.

[8] A.L. Rogers, J. F. Manwell, S. Wright, Wind Turbine Acoustic Noise, University of Massachusetts, januari 2006.

[9] Nota et all, Technical Report HAR32TR-040922-DGMR20, Harmonoise WP 3 Engineering method for road, traffic and railway noise, after validation and fine-tuning

[10] M.L.S. Vercammen, De Vercammen-curve: wat is dat? Achtergronden bij LF-geluid criteria, Congres Geluid Trillingen en Luchtkwaliteit, proceedings GTL2007, Nieuwegein, november 2007.

[11] Nederlandse Stichting Geluidhinder (NSG) 'Richtlijn laagfrequent geluid', Delft April 1999 see www.NSG.nl

[12] ISO. Acoustics–Preferred frequencies for measurements. Geneva, International Organization for Standardization, International Standard ISO 266-1975(E) (1975a).

[13] A.L. Rogers, Wind Turbine Noise, Infrasound and Noise Perception, http://www.windpoweringamerica.gov/pdfs/workshops/mwwg_turbine_noise.pdf

[14] Handleiding Rekenen en Meten Industrielawaai, Ministerie van VROM, Den Haag 2004

Appendix1 : Noise mapping of wind turbine noise

As for setting up a National noise map for windturbine noise, input information containing electrical power, axis diameter and height en coordinates was available from Wind Service Holland[1] The sound power levels of the turbines were estimated according to:

$$L_W = 10\log\left(P_{\text{elek}}\right) + 71\,\text{dB(A)} - \text{C}_{\text{wind}}\,,$$

with $C_{\text{wind,day}}$ = 4 dB(A), $C_{\text{wind,evening}}$ = $C_{\text{wind,nightt}}$ = 2 dB(A), correcting for winds occuring below 8 m/s (at 10 m height)

Sound propagation was modelled using the Dutch Handleiding meten en rekenen voor industrielawaai[14]. It was assumed that turbines operate continuously throughout the year. Only the average variation of wind speed over day, evening and night was taken into account. Al turbines were modeled as point sources with omnidirectivity.

Appendix 2 Estimation of free space using a reciprocity noise map

An example of a reciprocity map is given below in Figure A1.

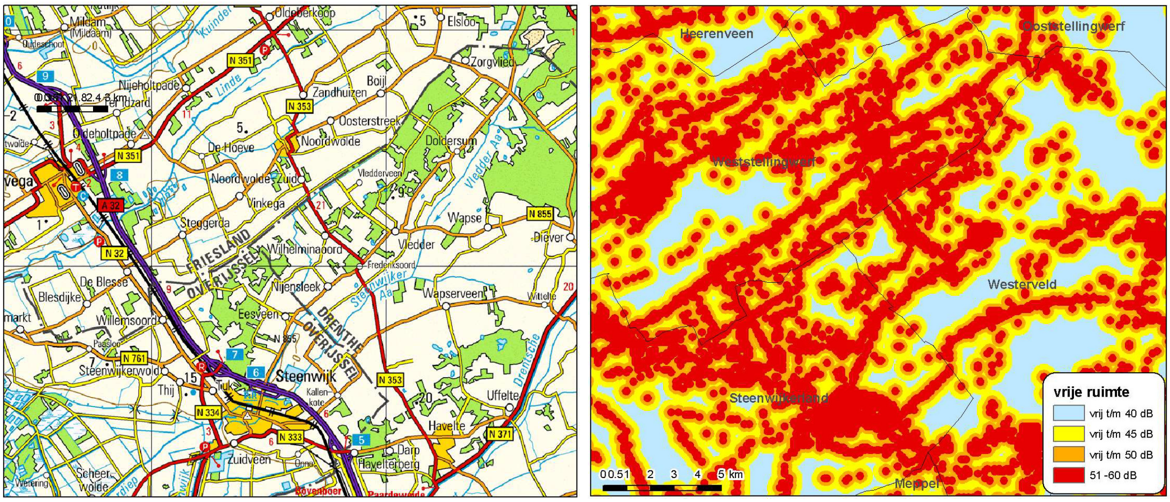

Figure A1 Reciprocity map using built up areas as noise sources.

The dwellings are appointed a fictitious noise emission. The result is given in the map on the right. By reciprocity the grey areas that receive a low (fictitious) noise level by approximation are the areas where new wind turbines can be placed without causing too much noise on the dwellings.

Third International Meeting
on
Wind Turbine Noise
Aalborg Denmark 17 – 19 June 2009

Measurement and assessment of WT noise in the Czech Republic

Ales Jiraska
National Reference Laboratory for measurement and assessment of environmental noise,
Smetanova 1390, 562 01 Usti nad Orlici, Czech Republic
www.nrl.cz
ales.jiraska@zu.cz

Abstract

The Czech Republic has adopted the same scheme of wind turbine (WT) noise limits - $L_{Aeq,8h}$ = 50 dB in the daytime and $L_{Aeq,1h}$ = 40 dB in the nighttime - as for industrial noise. The first wind park in 1995 was a noise disaster, L_{wA} up to 109 dB, $L_{Aeq,8h}$ = 46.5 dB and tonal noise, and it has never got working permission for night operation. It turns out as a stroke of luck, because a noise study was strongly recommended in the permitting procedure since that time and such a disaster has never been repeated.

In the Czech Republic the permitting procedure involves a noise study and according to computing result usually a check measurement and a final calculation assessment. Sound pressure level 35 dB is approximately a dividing line between permission with or without a check measurement. So every WT or farm exceeding this value is checked if the calculation works in the field. Results are usually used as a validation of wind farm area model.

Measurement consists of single WT emission check according to IEC 61400-11, sound propagation between the emission and the nearest imission positions outside and on demand the imission position inside the nearest dwelling. This means about 4 - 6 sound level meters simultaneously measuring WT noise.

Since 2006 a WT boom arrived and brought along infrasound and low frequency (LF) noise questions. Our laboratory has never found out LF noise to be a problem as in Great Britain. The only exception was gearbox - generator shaft mounting failure. In spite of complex measurements and criterion curve third octave assessments we didn't find any exceeding of LF thresholds. It's probably due to lower L_{Aeq} limit and therefore longer distances to the nearest dwelling than in Western Europe (apart from USA).

Our problems are related to A-weighted levels. When the terrain is flat, computation results correspond to field ones. When the terrain is complex, sometimes imission measurement values are greater than in half a distance. This paper discuss this anomaly, measurement conditions and hypothesis of the causes this phenomenon.

Paper is also discussing reflecting surfaces assessment calculation.

It appears that topographical and meteorological conditions can cause a difference between theory and practice. It can be useful to apply reflecting surface in noise studies and (at least in these conditions) check the results by a measurement.

Introduction

National Reference Laboratory for measurement and assessment of environmental noise is established as an advisor of the Czech Ministry of Health for noise issues. It is also National centre for strategic mapping in the Czech Republic.

Our laboratory has long-term experience in environmental measurement, arbitral measurement of problematical cases, developing noise policy and methodical instruction for professionals and help for government and local bodies, ombudsman and public.

Our laboratory processed Czech strategic maps for main railway and roads and made reporting to EC.

We made some research at low-frequency noise including psychoacoustics hearing tests of real records in acoustic chamber. We use Danish and German methods for LF noise assessment and implemented DEFRA criterion curve to the Czech legislation.

We has measured WT noise since 1995 (CDV standard), assisted Czech translation EN 61400-11 standard and measured many cases small and big WT in the Czech Republic.

We pursue health risc assessment for WT project - estimate number of people affected by noise.

Generally we use measurement and calculation technique to assess WT noise in the Czech Republic from project till working permission.

Measurement:

SLMs: BK2250, 2260 and 2270, primary windscreen, third-octave analysis

Emission method: EN 61400-11, lying circle board

Imission method: EN 61400-11, standing circle board, window sticking, rarely tripod

Wind speed and direction derived from WT anemometer, assumption: logarithmic wind speed profile

Calculation:

Software: LimA

Method: ISO 9613-2, max. 2 m contour line, constant building height (4.5 - 6 m), omnidirectional point source L_{wA}, third-octave spectra, climate 10 ˚C, 70 %, without meteorological coefficient, relative calculation height 3 m, planned calculated ground absorption 0, real ground absorption calculated by reverse engineering, default long-term ground absorption estimation 0.2

Assessment range:

wind speed 6 - 10 ms^{-1}, assumption: if wind speed is over 10 ms^{-1} background noise exceeds WT noise (it need not be fulfilled)

wind speed 8 ms^{-1}: assessment value + uncertainty shouldn't exceed the noise limit

wind speed 10 ms^{-1}: assessment value without uncertainty shouldn't exceed the noise limit

Locality Drahany

1 WT Vestas V90 - 2.0 MW, 1 reference MP behind WT at 150 m distance, 2 MP behind WT at 300 m and 575 m, 1 imission MP - the nearest dwelling downwind at 700 m inside, flat terrain

WT noise measurement

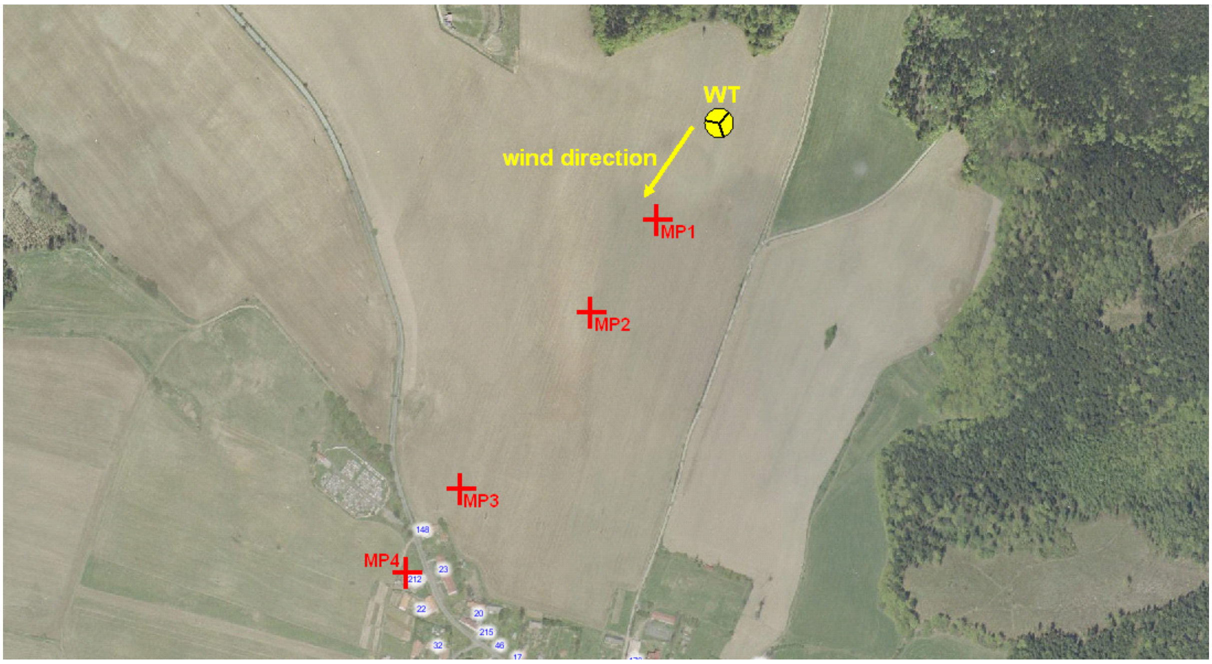

WT noise calculation

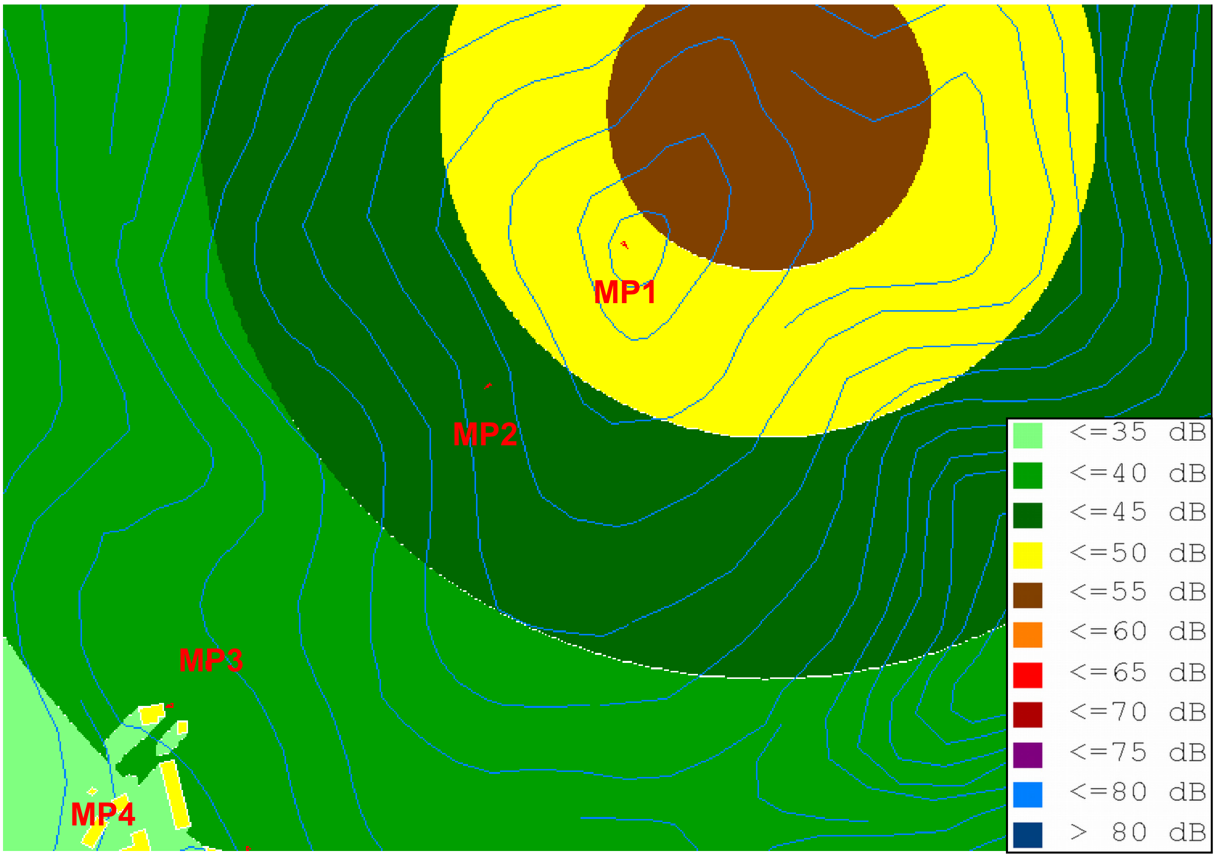

Locality is standard, quiet village place

November 2007, 12:00 - 16:00, overcast, 1.8 °C, 88 %

Measurement results:

Measurement position 1

wind speed v_s **[ms^{-1}]**	$L_{Aeq,T}$ **background [dB]**	$L_{Aeq,T}$ **WT + b [dB]**	$L_{Aeq,T}$ **WT corr. [dB]**	**sound power level** L_{wA} **[dB]**
6	33.2	50.0	49.9 ± 0.9	106.1 ± 0.9
7	33.8	48.2	48.1 ± 0.9	104.3 ± 0.9
8	34.4	46.9	46.6 ± 1.0	102.8 ± 1.0
9	35.0	45.8	45.4 ± 1.0	101.7 ± 1.0
10	35.6	45.1	44.6 ± 1.1	100.8 ± 1.1
11	36.2	44.8	44.1 ± 1.1	100.4 ± 1.1

Measurement position 3

wind speed v_s **[ms^{-1}]**	$L_{Aeq,T}$ **background [dB]**	$L_{Aeq,T}$ **WT + b [dB]**	$L_{Aeq,T}$ **WT corr. [dB]**
6	41.4	41.6	39.4 ± 2.5 *
7	41.2	41.6	39.4 ± 2.5 *
8	41.0	41.6	39.4 ± 2.5 *
9	40.9	41.6	39.4 ± 2.5 *
10	40.7	41.5	39.3 ± 2.5 *
11	40.5	41.5	39.3 ± 2.5 *

Noise calculation results $L_{Aeq,T}$ [dB] in calculation points:

Measurement position	**distance [m]**	$L_{Aeq,T}$ **backgr. [dB]**	$L_{Aeq,T}$ **measured [dB]**	$L_{Aeq,T}$ **calculated [dB]**	**difference meas-calc [dB]**
1	150	34.4	46.6 ± 0.9	46.6	0.0
2	300	34.6	40.2 ± 1.5	41.0	-0.8
3	575	41.0	39.4 ± 2.5 *	34.5	**4.9**

reverse engineering calculated ground absorption 0.38, wind speed 8 ms^{-1}

* too high background noise cause the difference

Third-octave spectra:

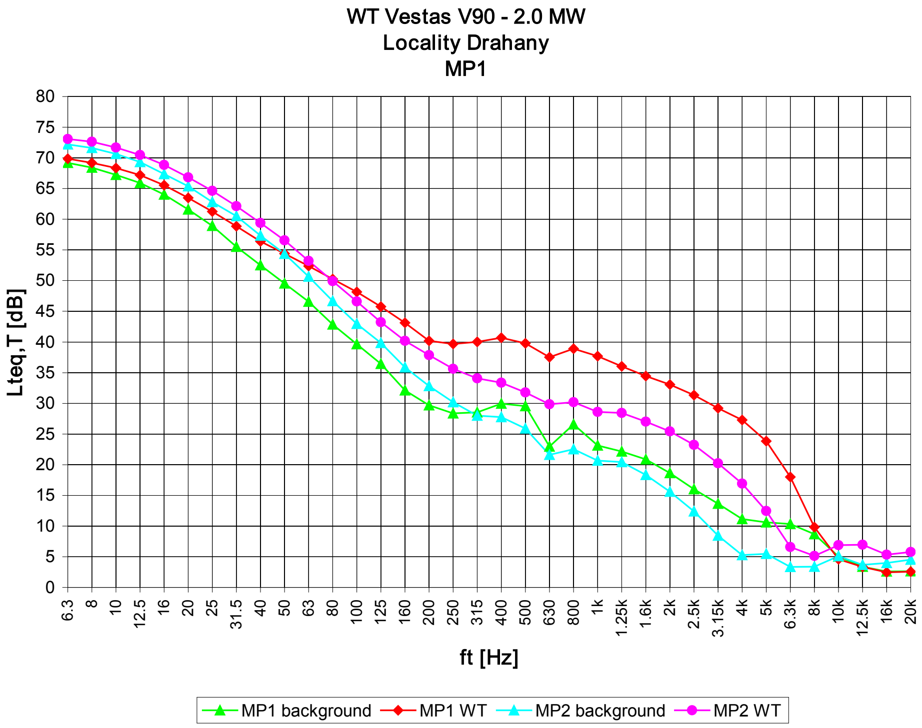

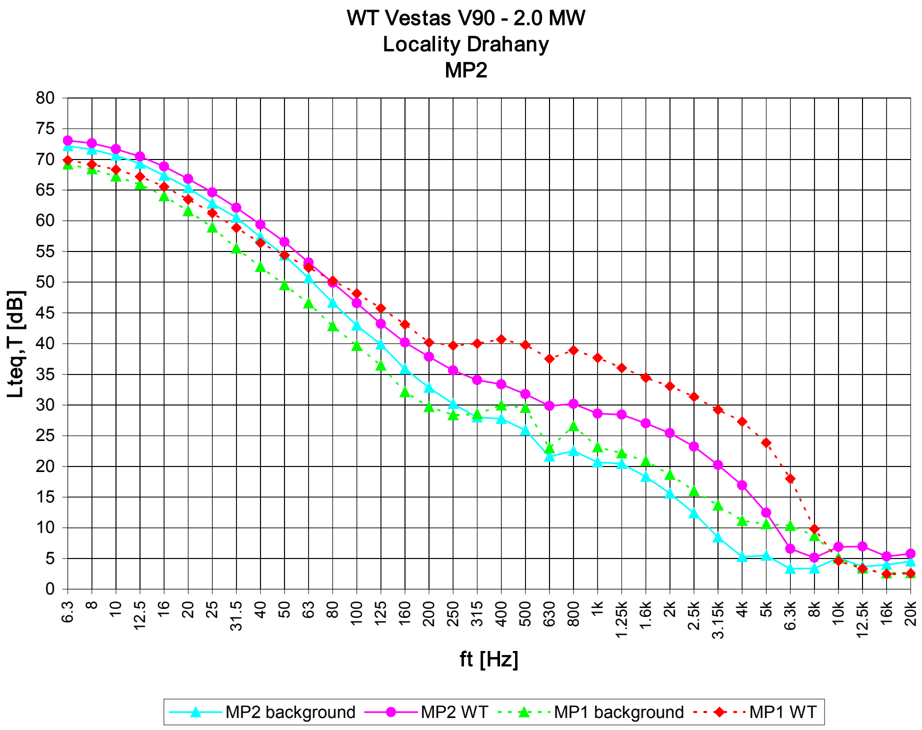

WT Vestas V90 - 2.0 MW
Locality Drahany
MP3

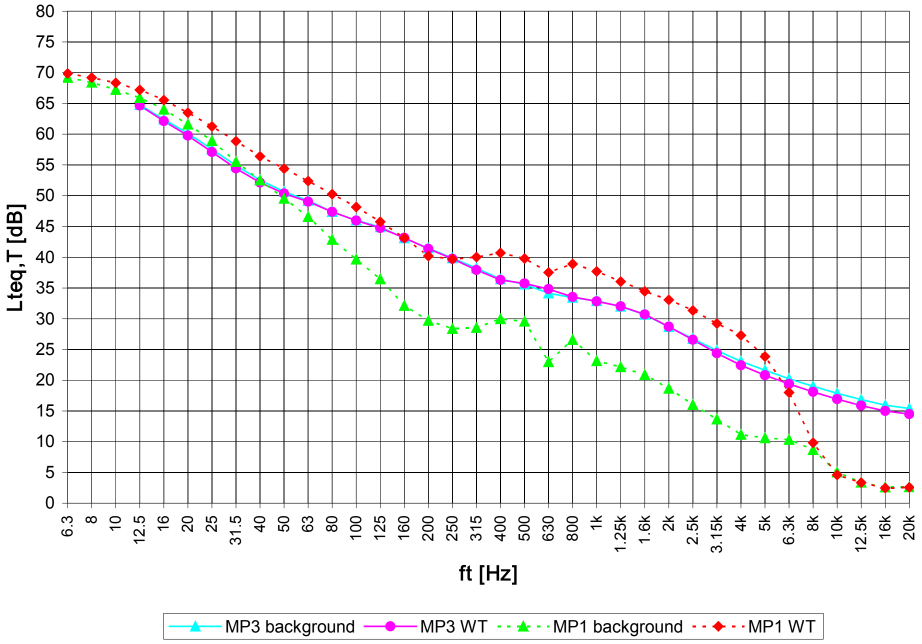

WT Vestas V90 - 2.0 MW
Locality Drahany
MP4

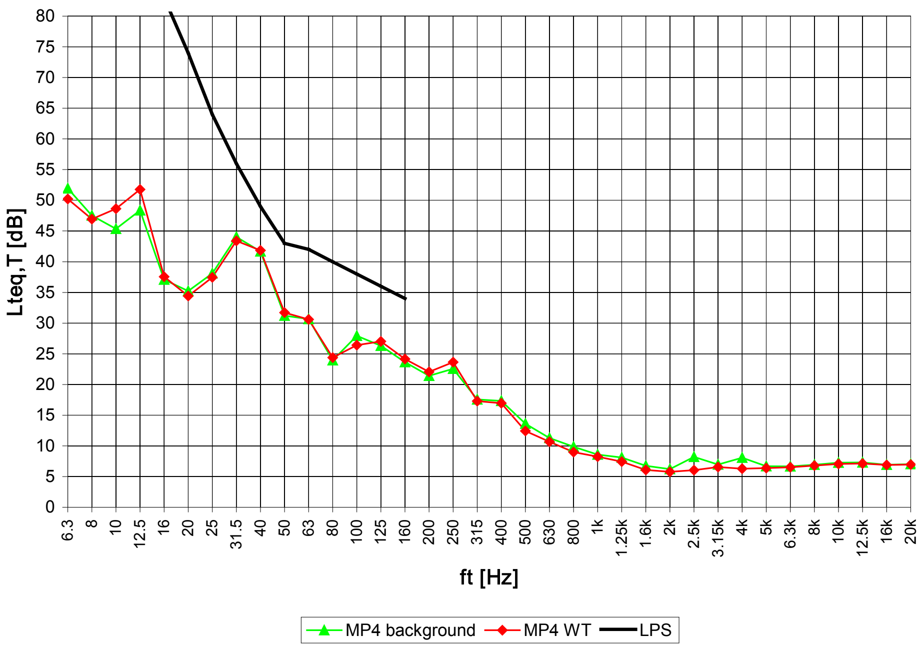

Locality assessment:

Noise is below the nighttime limit 40 dB, LF noise is minimal, WT got working permission.

Residents slightly complained of WT in downwind position, after 1 year complaints disappeared.

Locality Petrovice

2 WT Enercon E70 - 2.0 MW, 2 reference MP behind each WT at 120 m distance, 1 MP behind both WT at 300 m, 3 imission MP - the nearest dwelling downwind at 950 m, microphone outside and inside, dwelling aside at 866 m, hilly terrain

WT noise measurement

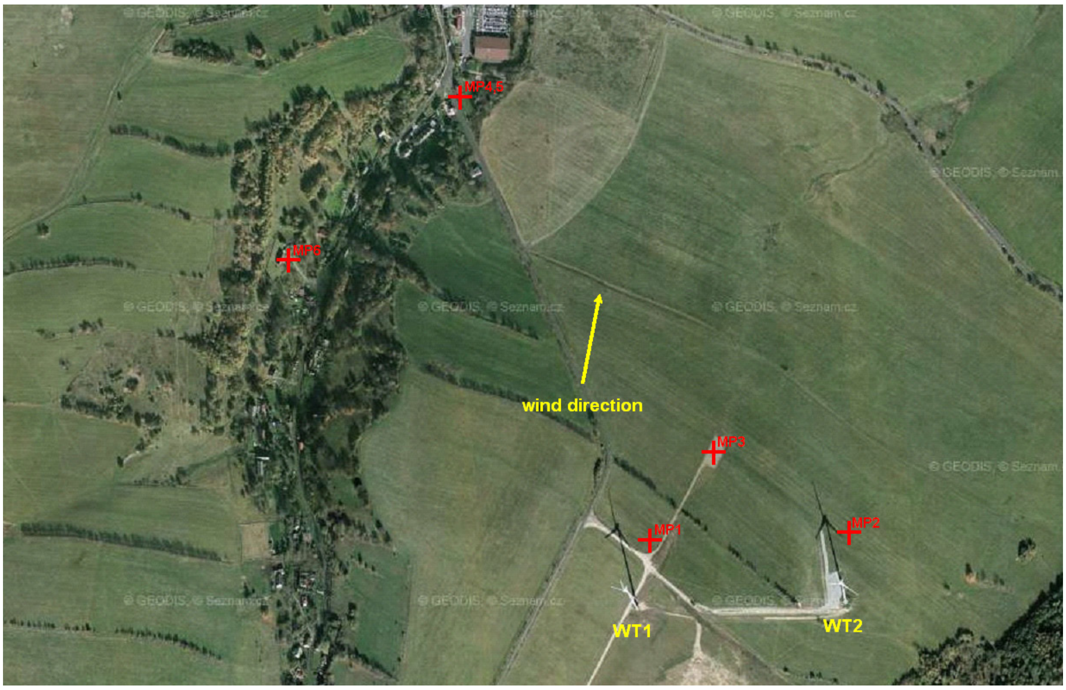

WT noise calculation

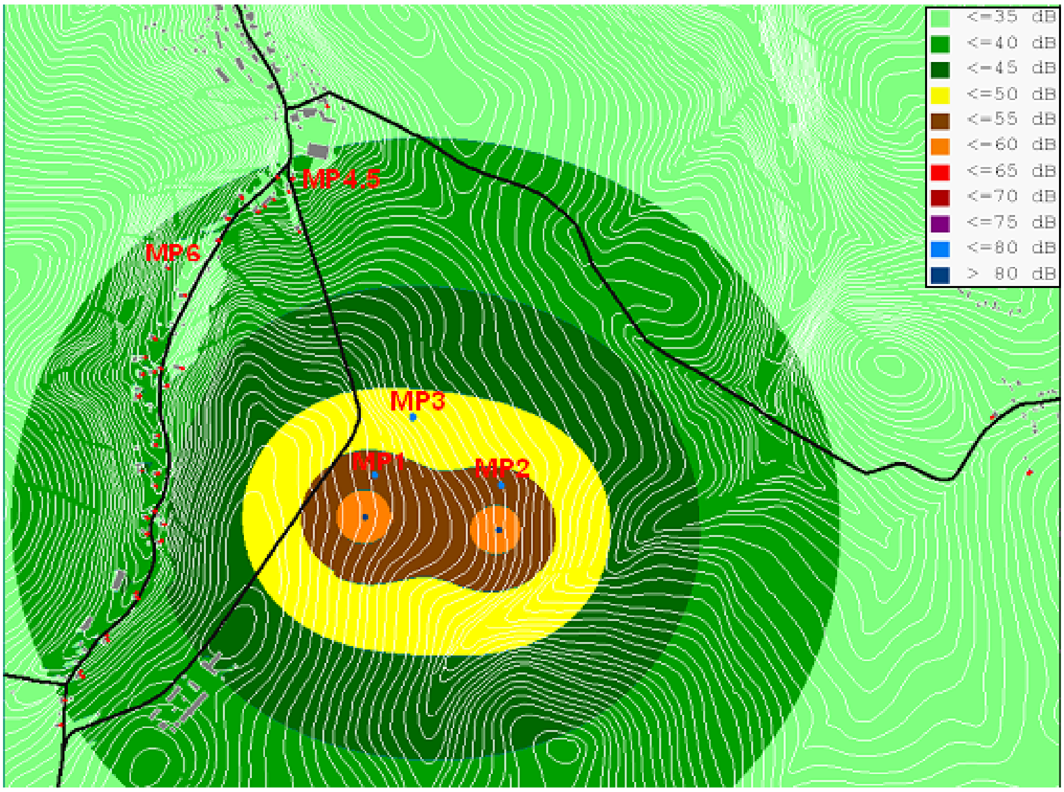

Locality is non-standard on the Czech-German border, high traffic on the road to Germany, new highway 1.6 km from WT1

November 2008, 11:00 - 15:30, cloudy, -0.8 °C, 81 %

Measurement results:

Measurement position 1

wind speed v_s [ms^{-1}]	**$L_{Aeq,T}$ background [dB]**	**$L_{Aeq,T}$ 2 WT + b [dB]**	**$L_{Aeq,T}$ 2 WT corr. [dB]**	**sound power level L_{wA} [dB]**
6	-	46.3	45.9 ± 0.9	100.1 ± 0.9
7	-	49.1	48.8 ± 0.9	103.1 ± 0.9
8	35.9	51.1	51.0 ± 0.9	105.3 ± 0.9
9	-	52.1	52.0 ± 0.9	106.3 ± 0.9
10	-	52.0	51.9 ± 0.9	106.2 ± 0.9

Measurement position 4

wind speed v_s [ms^{-1}]	**$L_{Aeq,T}$ background [dB]**	**$L_{Aeq,T}$ 2 WT + b [dB]**	**$L_{Aeq,T}$ 2 WT corr. [dB]**
1	-	38.2	36.0 ± 0.9 *
7	-	39.7	37.5 ± 0.9 *
8	39.4	40.6	38.4 ± 0.9 *
9	-	41.0	38.8 ± 0.9 *

Noise calculation results $L_{Aeq,T}$ [dB] in calculation points:

Measurement position	**distance [m]**	**$L_{Aeq,T}$ backgr. [dB]**	**$L_{Aeq,T}$ measured [dB]**	**$L_{Aeq,T}$ calculated [dB]**	**difference meas-calc [dB]**
1	120	35.9	51.0 ± 0.9	50.9	0.1
2	120	35.1	50.3 ± 0.9	50.3	0.0
3	300	39.5	44.5 ± 0.9	44.9	-0.4
4	950	39.4	38.4 ± 0.9 *	35.6	**2.8**

reverse engineering calculated ground absorption 0.42, wind speed 8 ms^{-1}

* too high background noise cause the difference

Third-octave spectra:

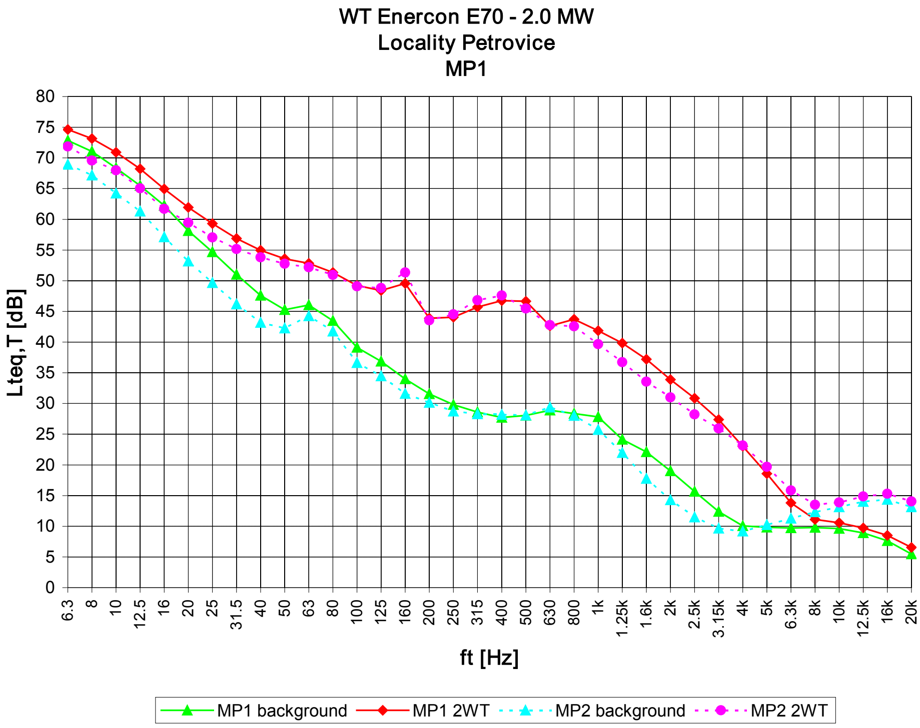

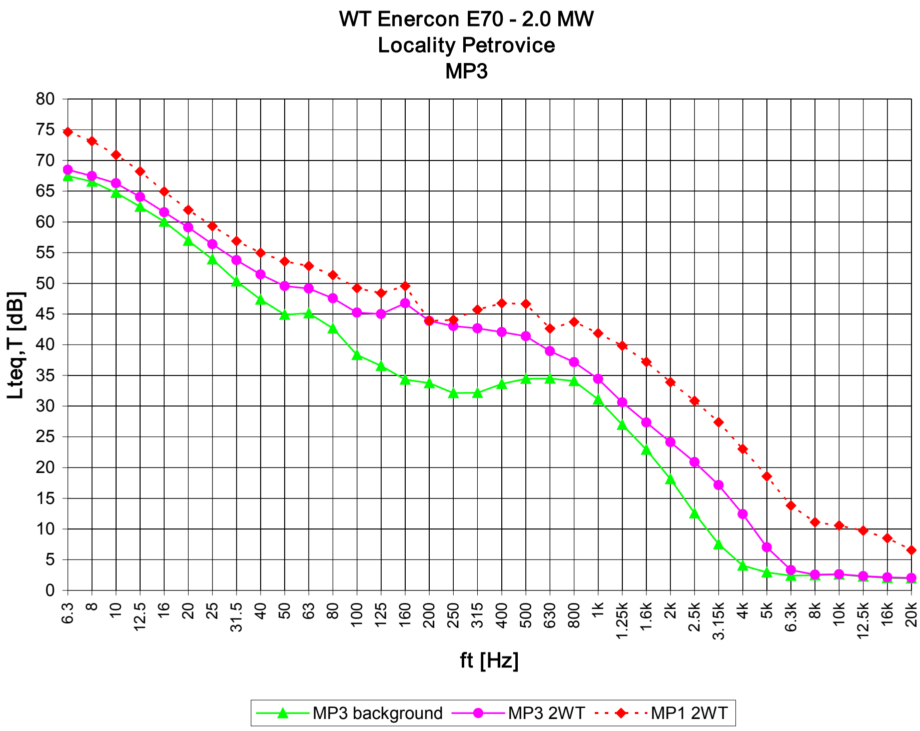

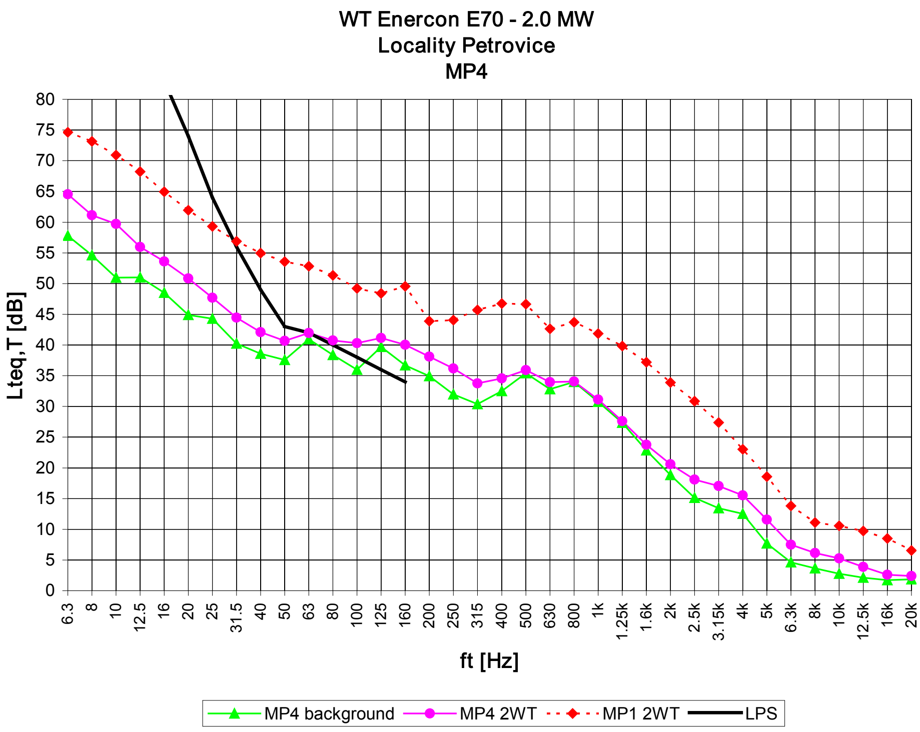

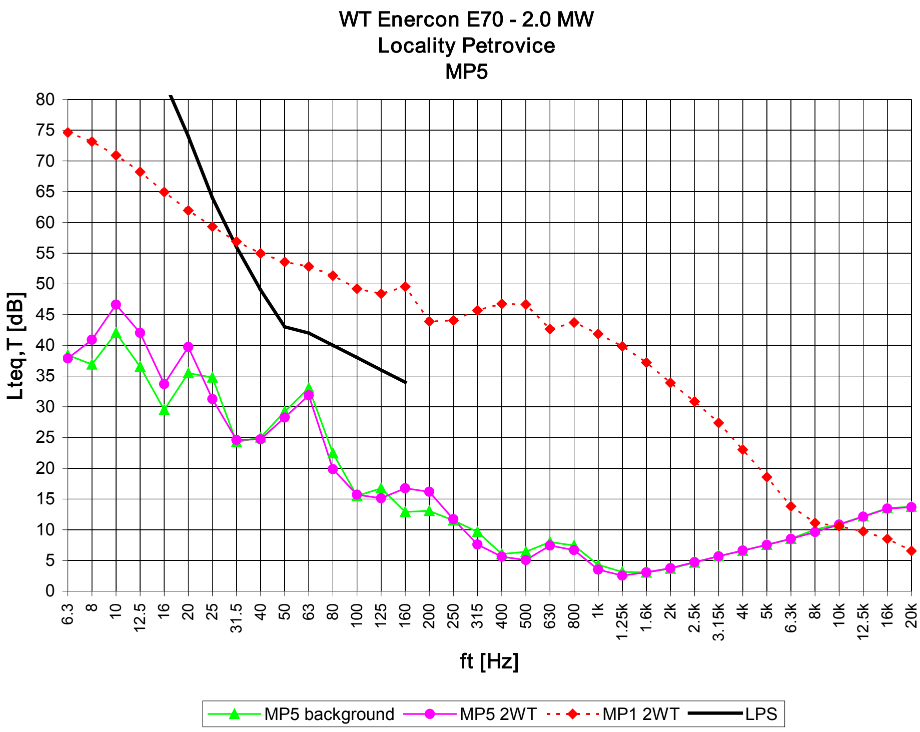

Locality assessment:

Noise is on the edge the nighttime limit 40 dB, LF noise is minimal, 2nd WT didn't significantly worse the situation, 2 WT got working permission, planned 3rd WT failed get building permission due to filling up the locality.

Residents complained of WT in downwind position, today bigger source is highway

Locality Kliny

2 WT Enercon E70 - 2.0 MW, 1 reference MP behind WT at 120 m distance, 1 MP behind WT at 175 m, 1 imission MP - the nearest dwelling downwind at 280 m outside, hilly terrain

WT noise measurement

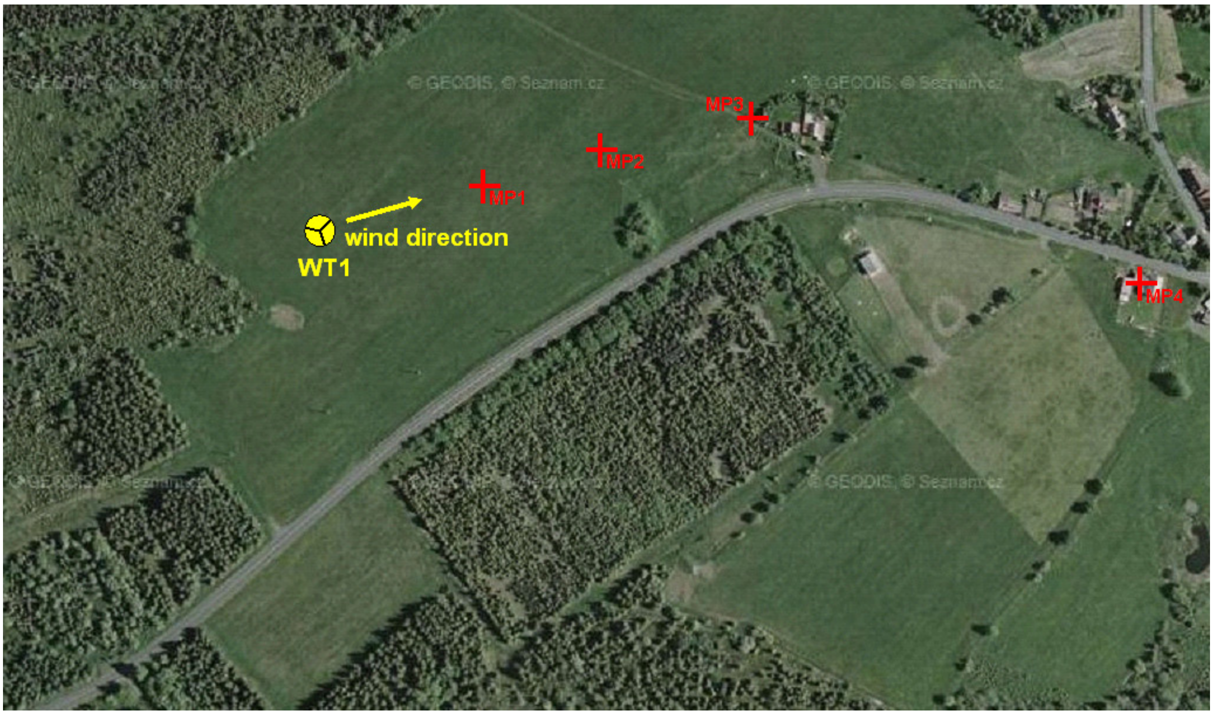

WT noise calculation

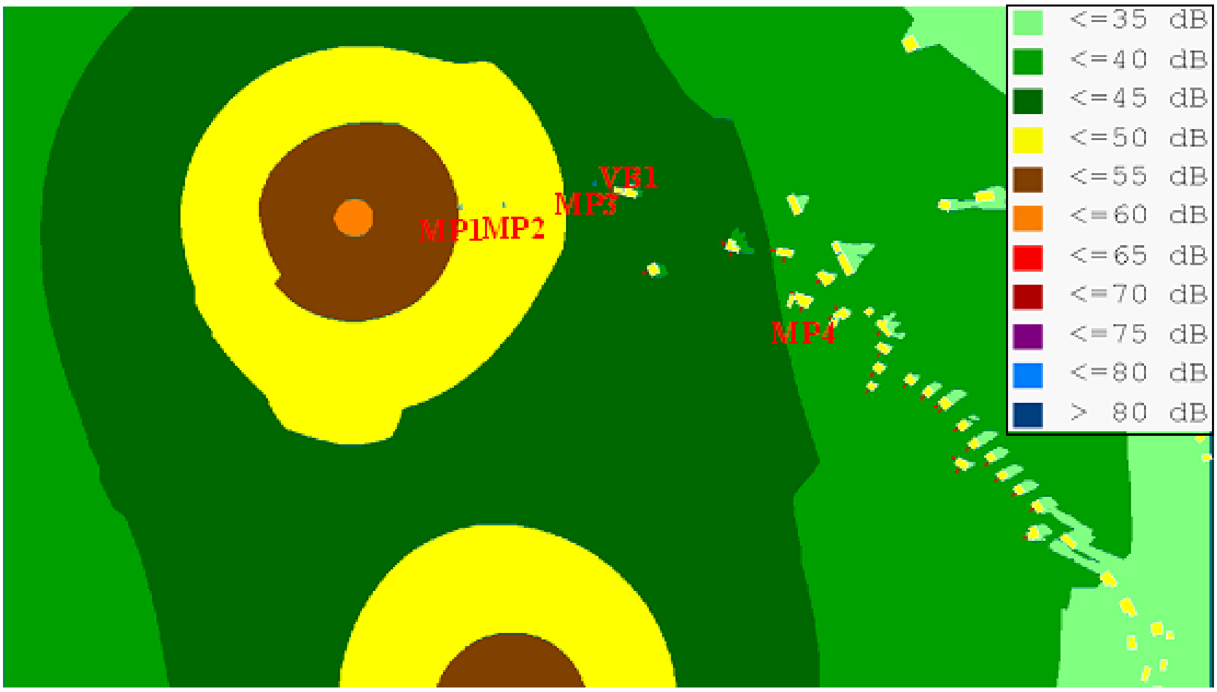

Locality is quiet village place, the nearest dwellings are chalets and cottages; November 2007, 20:00 - 24:00, overcast, after drizzle, 4.3 °C, 95 %

Measurement results:

Measurement position 1

wind speed v_s [ms^{-1}]	$L_{Aeq,T}$ background [dB]	$L_{Aeq,T}$ WT + b [dB]	$L_{Aeq,T}$ WT corr. [dB]	sound power level L_{wA} [dB]
6	20.9	46.4	46.4 ± 1.5	100.8 ± 1.5
7	21.0	48.5	48.5 ± 1.5	102.9 ± 1.5
8	21.1	48.8	48.8 ± 1.5	103.2 ± 1.5

Measurement position 3

wind speed v_s [ms^{-1}]	$L_{Aeq,T}$ background [dB]	$L_{Aeq,T}$ WT + b [dB]	$L_{Aeq,T}$ WT corr. [dB]
6	25.1	43.9	43.9 ± 1.7
7	25.0	46.5	46.5 ± 1.7
8	24.9	47.3	47.3 ± 1.7

Number of data pairs - 67 for WT noise, 39 for background noise

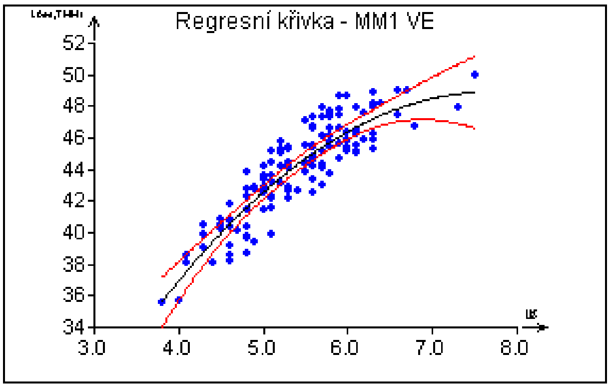

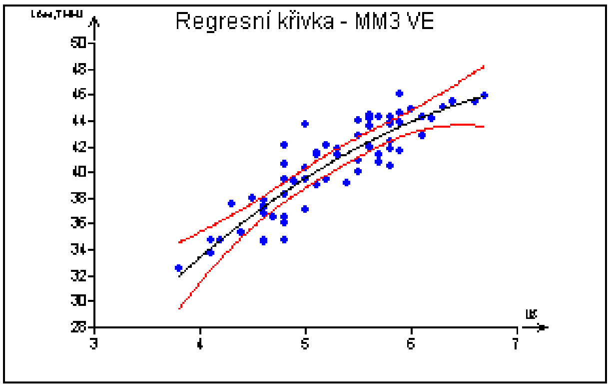

regression curves for MP1 and 3

Noise calculation results $L_{Aeq,T}$ [dB] in calculation points:

Measurement position	distance [m]	$L_{Aeq,T}$ backgr. [dB]	$L_{Aeq,T}$ measured [dB]	$L_{Aeq,T}$ calculated [dB]	difference meas-calc [dB]
1	120	21.1	48.8 ± 1.5	48.9	0.0
2	175	20.3	46.5 ± 1.6	46.4	0.1
3	280	24.9	47.3 ± 1.7	42.9	**4.4**

reverse engineering calculated ground absorption 0.35, forest 1, wind speed 8 ms^{-1}

Third-octave spectra:

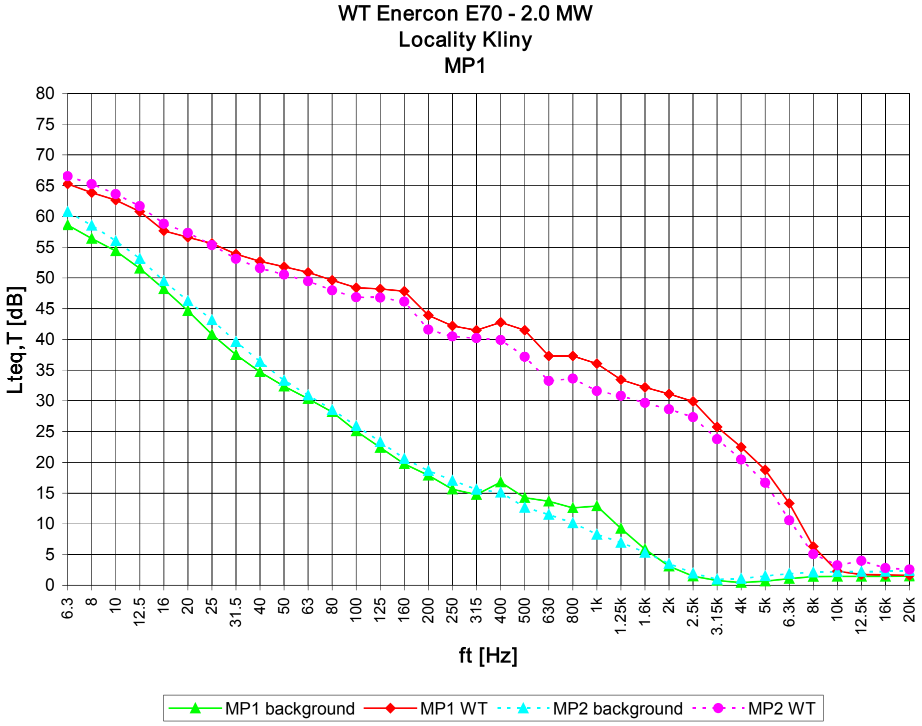

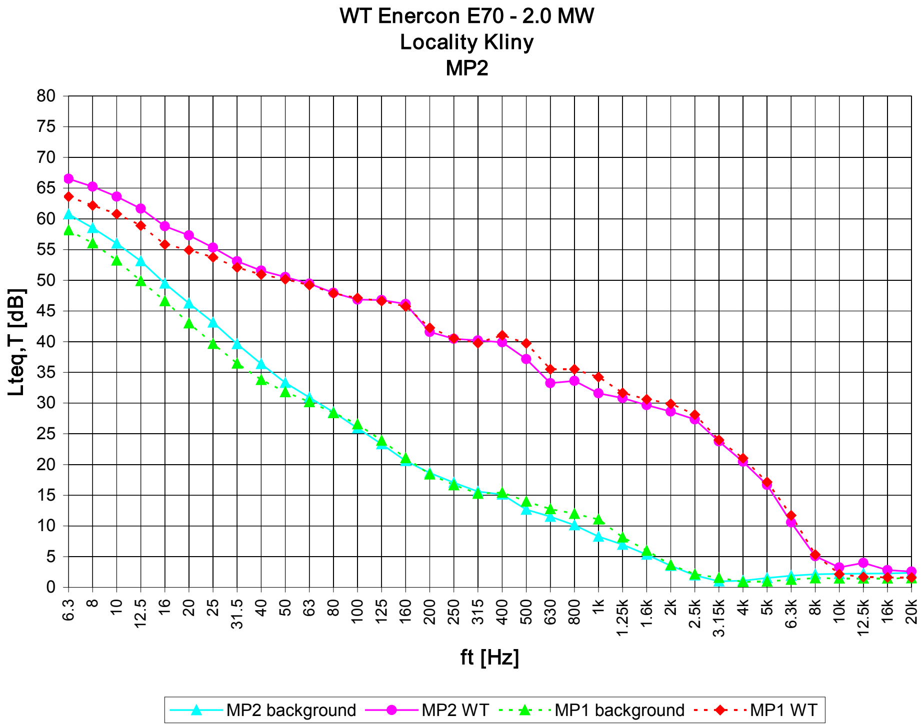

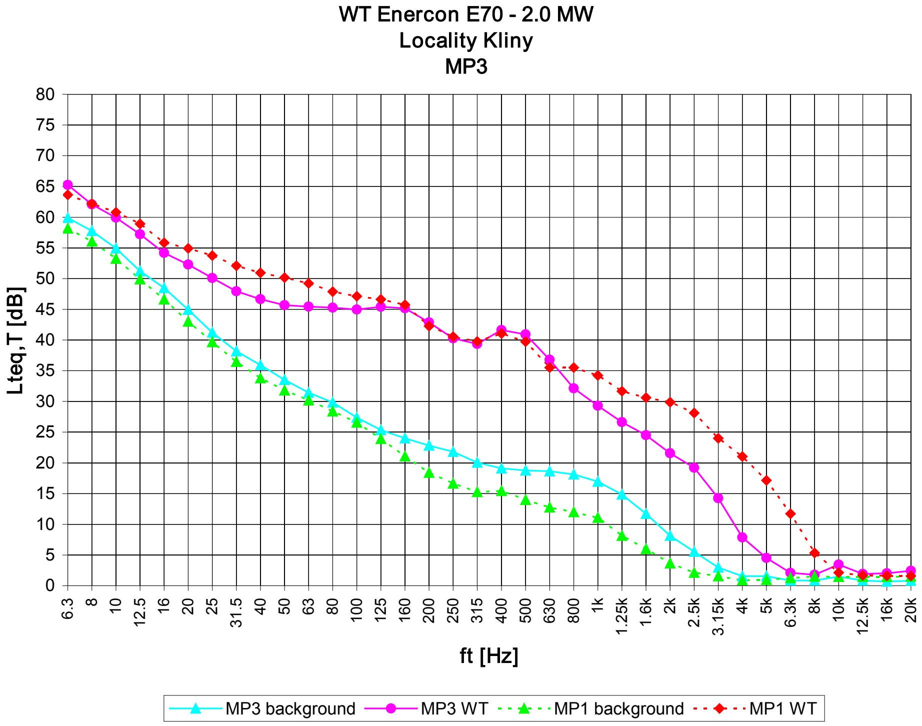

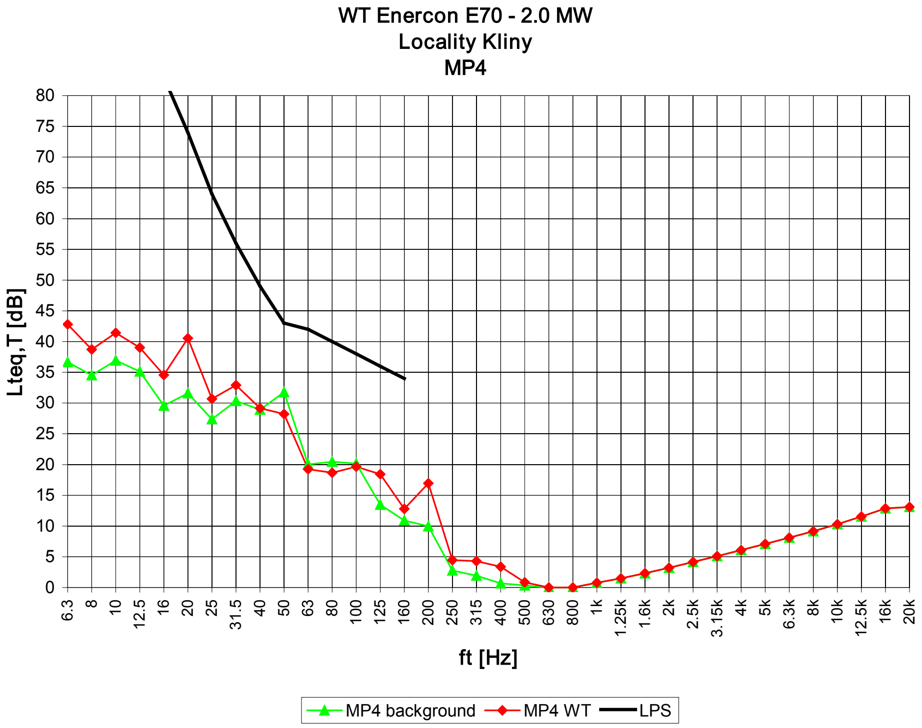

Locality assessment:

Noise is on the edge the nighttime limit 40 dB if WT would operate at reduced power (and we ignore the anomaly), LF noise is minimal, WT got working permission.

Residents haven’t complained of WT, probably because of short-term dwelling.

Locality U Tri Panu

3 WT Enercon E70 - 2.0 MW, 1 reference MP behind WT at 100 m distance (bushes), 1 MP behind WT3 at 120 m, 1 MP behind WT1 at 120 m 80˚ from downwind direction, 1 imission MP - the nearest straight visibility dwelling downwind at 380 m outside, plateau

WT noise measurement

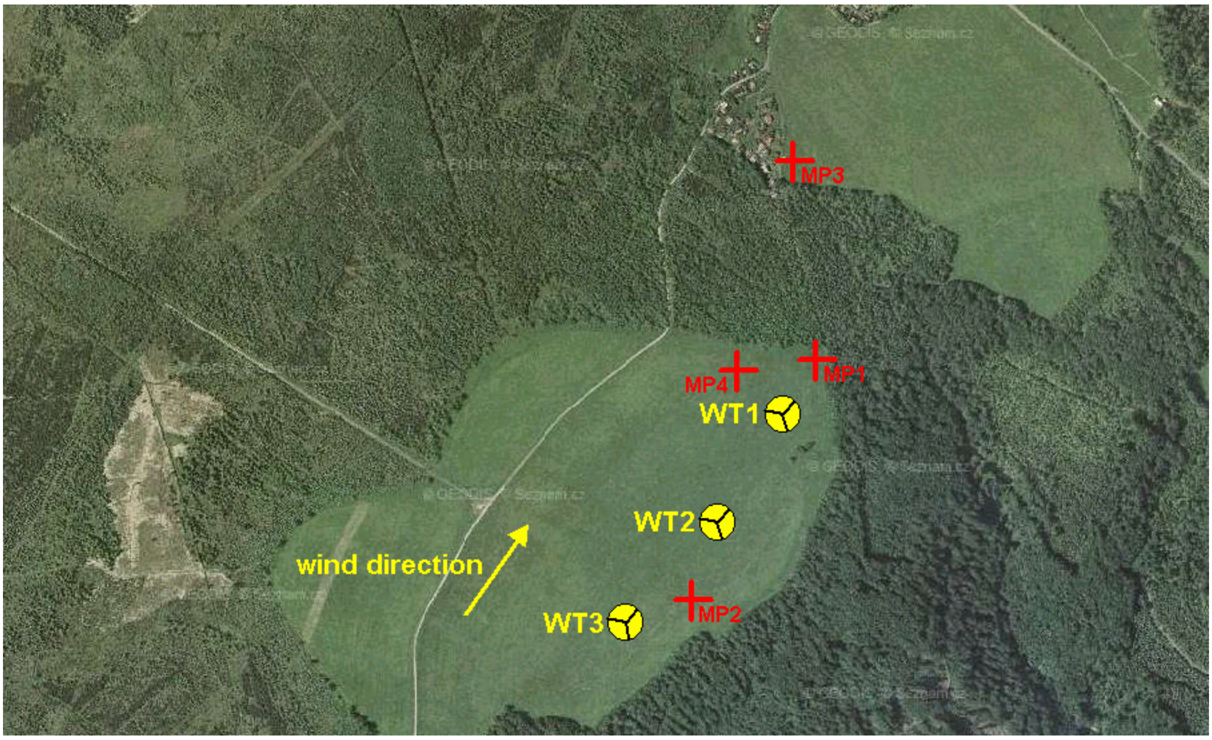

WT noise calculation model

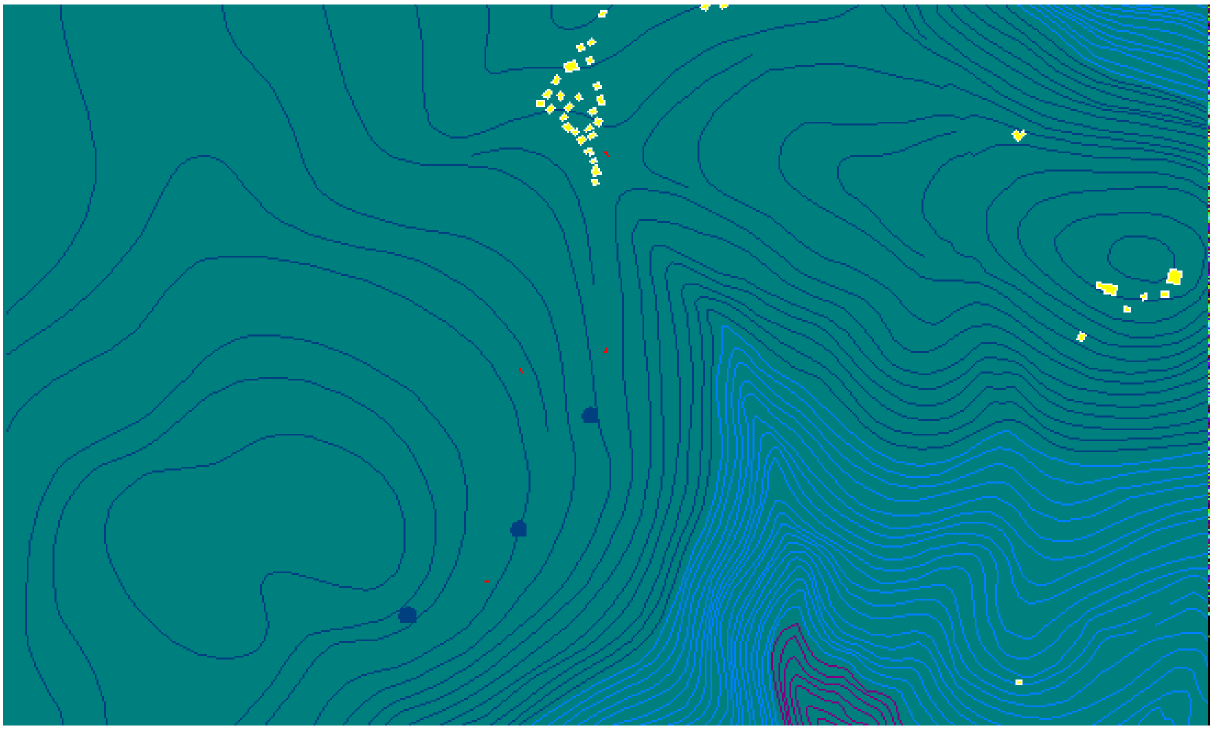

Locality is quiet village place, the nearest dwellings are chalets and cottages; January 2007, 16:00 - 21:00, overcast, drizzle, shower, 2 - 4 °C, 70 - 100 %

Measurement results:

Measurement position 2

wind speed v_s [ms^{-1}]	**$L_{Aeq,T}$ background [dB]**	**$L_{Aeq,T}$ WT + b [dB]**	**$L_{Aeq,T}$ WT corr. [dB]**	**sound power level L_{wA} [dB]**
6	38.4	49.4	49.1 ± 1.6	102.4
7	38.8	50.3	50.0 ± 1.6	103.3
8	39.1	51.1	50.8 ± 1.6	104.1
9	39.4	51.8	51.5 ± 1.6	104.9
10	39.7	52.4	52.2 ± 1.6	105.6

Measurement position 3

wind speed v_s [ms^{-1}]	**$L_{Aeq,T}$ background [dB]**	**$L_{Aeq,T}$ WT + b [dB]**	**$L_{Aeq,T}$ WT corr. [dB]**
6	40.3	39.1	36.9 ± 1.3 *
7	40.5	40.2	38.0 ± 1.3 *
8	40.7	41.0	38.8 ± 1.3 *
9	40.9	41.5	39.3 ± 1.3 *
10	41.1	41.7	39.5 ± 1.3 *

Noise calculation results $L_{Aeq,T}$ [dB] in calculation points:

Measurement position	**distance [m]**	**$L_{Aeq,T}$ backgr. [dB]**	**$L_{Aeq,T}$ measured [dB]**	**$L_{Aeq,T}$ calculated [dB]**	**difference meas-calc [dB]**
1	100	50.4	48.4 ± 2.7 *	47.8	-0.6
2	120	39.1	50.8 ± 1.6	50.8	0.0
3	380	40.7	38.8 ± 1.3 *	38.8	0.0

reverse engineering calculated ground absorption 0.76 (bushes), wind speed 8 ms^{-1}

* too high background noise cause the difference

results raised about 1 - 1.5 dB due to the weather change (higher humidity)

Third-octave spectra:

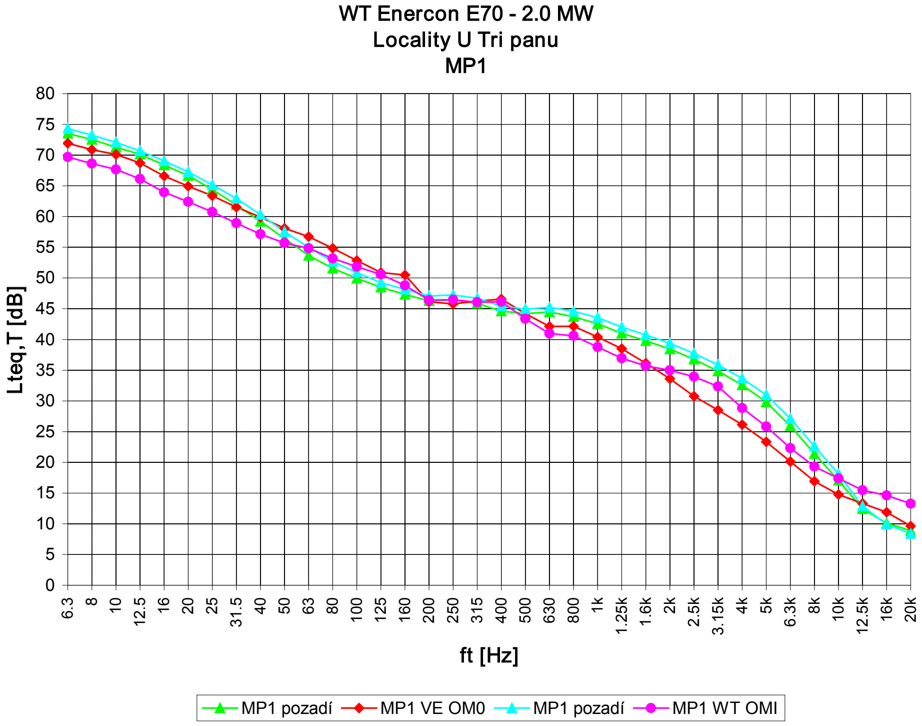

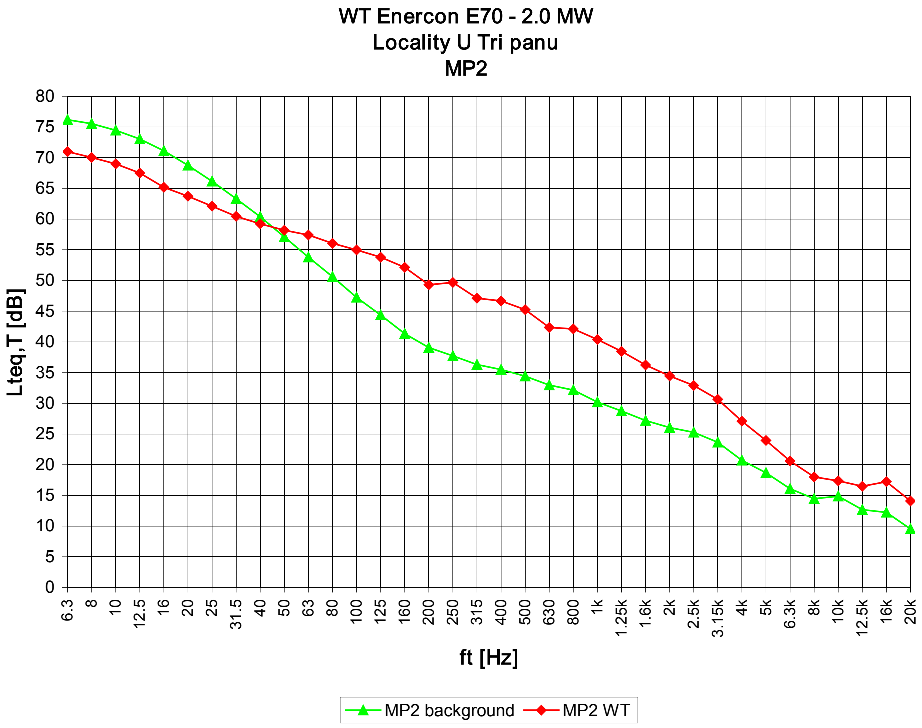

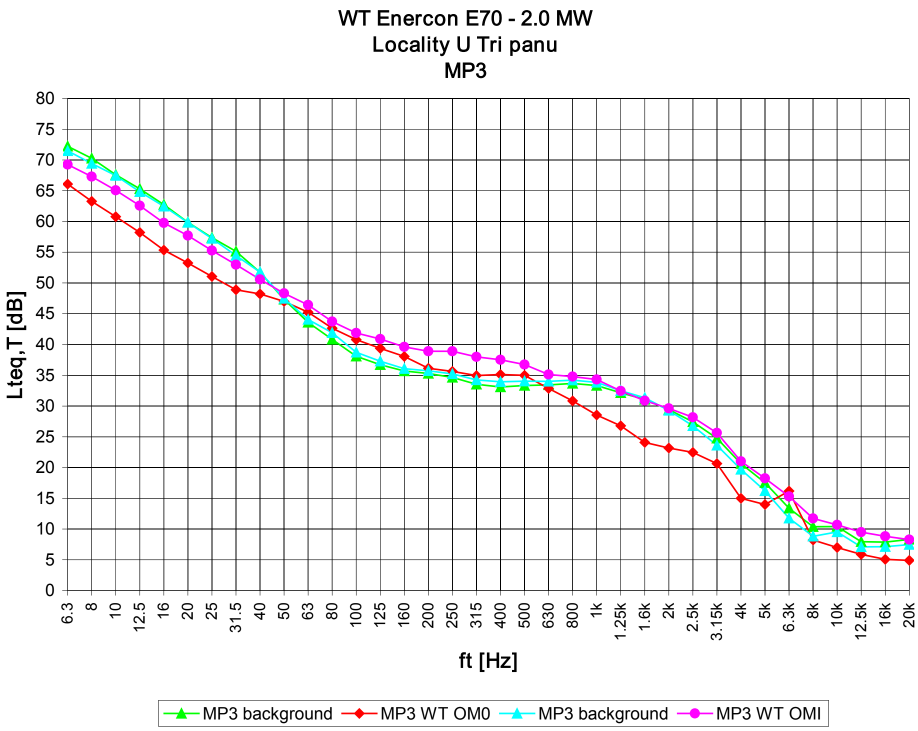

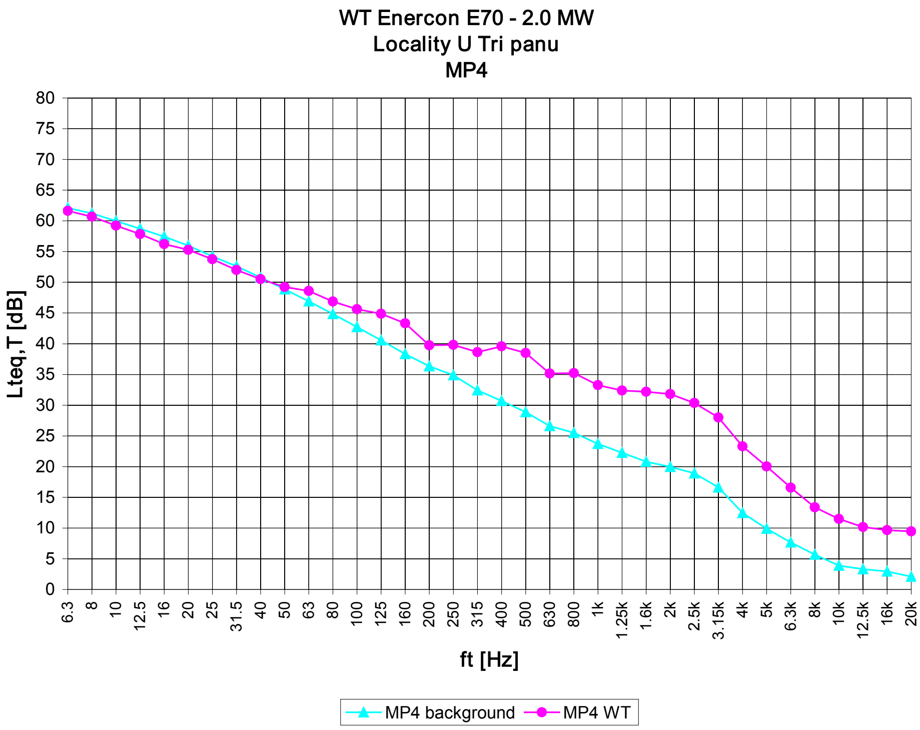

Locality assessment:

Noise is on the edge the nighttime limit 40 dB, WT got working permission.

Residents haven't complained of WT, probably because of short-term dwelling.

Conclusions

1. LF noise isn't common WT problem as looks like from amateur web articles. Tonal LF noise is construction defect diagnostics. See references.
2. Reverse engineering calculated ground absorption of grass or field surface is about 0.4, bushes and conifers about 0.8.

   Recommendation for gravel in LimA (Harmonoise) is 0.6, for soft forest floor 0.95, 0.4 correspond to compact dense ground, 0.8 uncompacted loose ground.

   Real ground absorption is lower then recommended in software. Residents complained of WT in the winter, when ground absorption is even lower, virtually 0.
3. ISO 9613-2 doesn't guarantee real noise values when the terrain is complex. It appears that topographical and meteorological conditions can cause a difference between theory and practice, because the similar sound power level of the same WT type, the similar time of measurement (wind speed profile?).

   This difference occurs in hilly terrain when there is the small slope from WT to imission position.

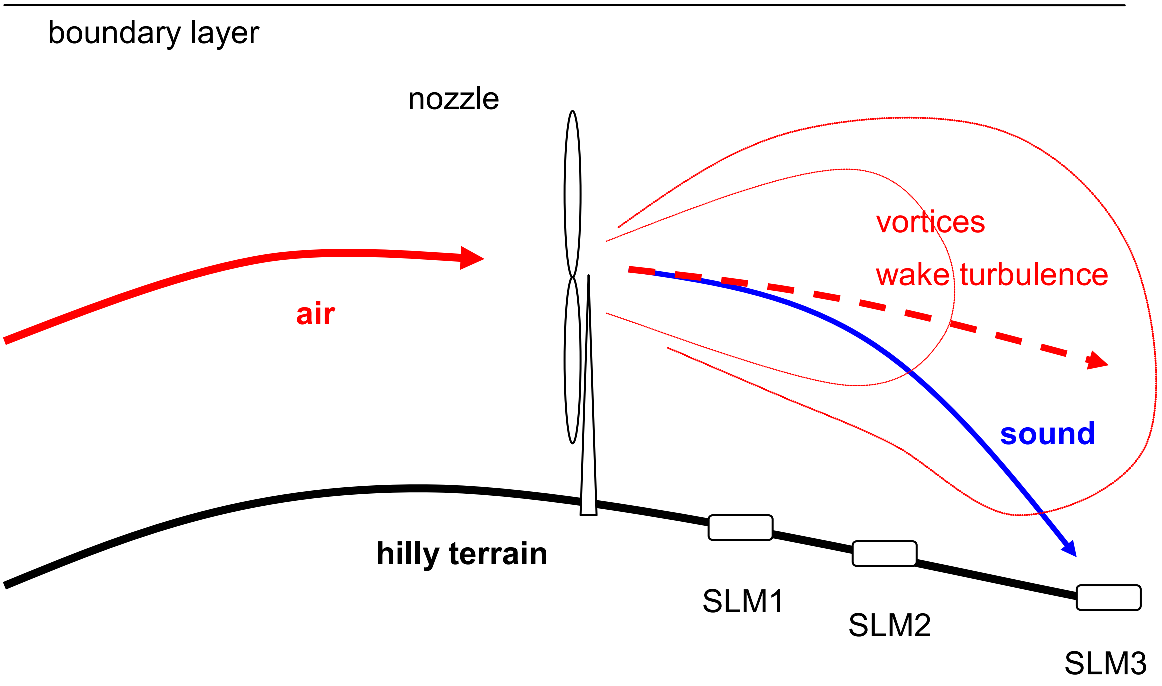

4. It can be useful to apply reflecting surface (ground absorption 0) in WT noise studies generally.
5. It can be useful (at least in complex terrain conditions) to check the results by a measurement.
6. This article should initiate covering more meteorological issues to the WT noise calculation. Inspiration could be ISO/FDIS 13474 standard for calculating a distribution of sound exposure levels of impulsive sound events for purposes of environmental noise assessment.

References

Low Frequency Noise from Large Wind Turbines, DELTA 2008

http://www.deltainspire.dk/C1256ED60045E95F/sysOakFil/Lavfrekvens_publ_4/$File/EFP06-LF%20Noise-Noise%20monitoring%20at%20H%C3%B8vs%C3%B8re%20AV%20139%2008.pdf

Eja Pedersen: Human response to wind turbine noise - perception, annoyance and moderating factors, 2007 (articles from 2003)

http://gupea.ub.gu.se/dspace/bitstream/2077/4431/1/Pedersen_avhandling.pdf

Frits van den Berg, Eja Pedersen, Jelte Bouma, Joel Bakker: Project WINDFARMperception Visual and acoustic impact of wind turbine farms on residents, 2008

http://www.rug.nl/wewi/deWetenschapswinkels/natuurkunde/publicaties/WFp-final-1.pdf

Frits van den Berg: The sounds of high winds: the effect of atmospheric stability on wind turbine sound and microphone noise, 2006 (articles from 2003)

http://dissertations.ub.rug.nl/FILES/faculties/science/2006/g.p.van.den.berg/17_thesis.pdf

Bo Sondergaard: Propagation of Noise from Wind Turbines on-shore and off-shore, 2005

http://www.nationalwind.org/events/siting/presentations/sondergaard-noise_propogation.pdf

Jörgen Jakobsen: Infrasound Emission from Wind Turbines, 2005

http://www.hayswind.com/info/low%20frequency%20noise%20-%20jakobsen.pdf

Weston Wind Turbine Working Group, 2009

http://www.westonturbines.org.uk/wp-content/uploads/2009/01/weston-wind-turbine-working-group-objection-document-14-01-09.pdf

Third International Meeting
on
Wind Turbine Noise
Aalborg Denmark 17 – 19 June 2009

Wind Turbine Acoustic Modeling with the ISO 9613-2 Standard: Methodologies to Address Constraints

Erik J. Kalapinski (Tetra Tech EC, Inc., 133 Federal Street - 6th Floor, Boston, MA 02110, erik.kalapinski@tteci.com)
Tricia Pellerin (Tetra Tech EC, Inc., 133 Federal Street - 7th Floor, Boston, MA 02110, tricia.pellerin@tteci.com)

ABSTRACT

The accuracy of wind turbine noise propagation modeling is dependent on the following factors (1) frequency dependent source data for the full range of operational wind speeds as reported by equipment manufacturers per the IEC 64100-11:2000(E)[1] test measurement standard, (2) site specific topographical, meteorological, and terrain conditions of the project site and the surrounding areas and (3) noise propagation calculation algorithms employed. For wind energy facilities sited in the United States, International Standard ISO 9613-2[2] is most commonly used for evaluation and in support of permitting applications. The engineering methods described in the ISO 9613-2 standard account for geometrical divergence, atmospheric absorption, ground attenuation, screening effects, and favorable meteorological conditions for sound propagation and have proven effective for a wide range of transportation and stationary sources in an outdoor environment.

The purpose of this paper is to identify constraints inherent to the ISO 9613-2 standard with regard to the specialized application of wind turbine acoustics. Methodologies are identified that can be readily employed to accurately describe atmospheric, ground, and lateral attenuation effects for a large diameter elevated noise source. If these effects are

---

[1] International Electromechanical Commission (IEC) 61400-11:2002(E) Wind Turbine Generator Systems – Part 11: Acoustic Noise Measurement Techniques, Second Edition 2002.

[2] International Standard, ISO 9613-2, Acoustics – Attenuation of Sound During Propagation Outdoors, Part 2 General Method of Calculation.

ignored, significant uncertainties may result in the sound levels calculated both in proximity and at distant receptor locations.

Introduction

Comprehensive noise impact assessments are becoming compulsory requiring increasingly rigorous acoustic analyses as wind energy projects shift from largely rural to more populated areas across the United States. With this shift, projects are subject to more demanding state and local regulatory environmental permitting processes. These analyses require the evaluation of received sound levels over the full range of future wind turbine operational conditions at noise sensitive areas such as residences, schools, churches, and parklands. Evaluation of wind energy projects in this setting has brought forth legitimate concerns over the direct application of the ISO 9613-2 standard to the specialized case of wind turbine acoustics. Furthermore, community noise control legislation is becoming more judicious, requiring closer scrutiny of issues related to wind turbine environmental noise, including health-based, activity interference, and perceptibility standards over increasingly extended linear calculation distances. The following paper identifies constraints and suggested methodologies that can that be readily employed to address source levels, atmospherics, and lateral attenuation effects from wind turbines to receptors of concern.

Several international, national, and proprietary acoustic modeling protocols and engineering standards have been developed to calculate noise propagation in an outdoor environment. For wind energy facilities sited in the United States, the International Standard ISO 9613-2, 'Acoustics – Attenuation of Sound During Propagation Outdoors, Part 2 General Method of Calculation' is most the most common and is routinely used in support of permitting applications as required for regulatory approval. In some states and localities, the explicit use of the ISO 9613-2 standard is mandated. This standard is programmed into acoustic engineering computer simulation models such as Datakustic GmBH's Cadna A and Braunstein + Berndt GmbH's Soundplan as well as EMD International A/S WindPro's noise module developed primarily for use by the wind energy project layout designer with limited background in the science of acoustics.

The ISO 9613-2 calculation methodologies for predicting sound pressure levels at a distance from a variety of sources are based on well-established sound propagation algorithms for determining sound attenuation outdoors. The engineering methods consist of frequency dependent algorithms, accounting for the following physical effects: geometric divergence, reflection from surfaces, atmospheric absorption, screening by topography and obstacles, terrain complexity, lateral attenuation due to ground effects, source directivity factors, attenuation through foliage, and meteorological conditions including atmospheric absorption and refraction.

There are several constraints inherent within the ISO 9613-2 standard which has direct implications on the specialized case of wind turbine acoustics. These constraints are related, in part, to wind turbine sound emission data as reported per the IEC 61400-11 test standard, to wind turbine height and area source dimensions, and to meteorological factors effecting the accuracy long-range sound propagation over extended distances:

Non-Standard Atmospherics and Long-Range Propagation: Acoustic modeling uses methodologies that assume near-standard atmospheric conditions. ISO 9613-2 algorithms rely on atmospheric conditions that favor the propagation of sound; however, it does not necessarily represent variations in atmospheric conditions which can effect sound propagation. ISO 9613-2 propagation algorithms account for a range of 'average' downwind wind speeds from 1 m/s to 5 m/s, measured at a height of 3 meters to 11 meters above the ground. Wind speeds outside of this range are not explicitly accounted for in the propagation algorithms. This limiting factor needs to be addressed when assessing wind turbines operating during elevated wind speeds including those corresponding to full rotational operation. At receivers located beyond a distance of 1000 meters from one or more wind turbines, ISO 9613-2 standard spherical divergence calculation methodologies may not hold under certain regularly-occurring atmospheric conditions, both seasonal and diurnal.

Wind Turbine Source Levels and Meteorological Effects: Wind turbine sound emission data as reported by equipment manufacturers is measured and reported using well defined test procedures. The reliability of acoustic modeling under ISO 9613-2 is reliant on the adherence of this source data to the test procedures found in the International Electrotechnical Commission (IEC) 61400-11:2002(E) ‘Wind Turbine Generator Systems – Part 11: Acoustic Noise Measurement Techniques’. Modification of this data to account for site specific meteorological and topographical conditions is required when used in acoustic modeling per the ISO 9613-2 standard to provide a greater level of accuracy.

Wind Turbine Source Dimensions and Lateral Attenuation: Conventional heights of modern utility-scale wind turbines are outside the stated ISO 9613-2 tolerances of 1 to 30 meters above grade for sound source heights. The sound source height is used to define both lateral attenuation and downwind propagation effects. A wind turbine could be effectively characterized as an area source defined by the rotor swept area of the blade. In the United States, however, a wind turbine is often represented as an equivalent point source, which can result in significant under-prediction of sound pressure levels for areas in close proximity to the source.

Non-Standard Atmospherics and Long Distance Propagation

An acoustic wave propagating from a sound source will spread the transmitted acoustic energy over a progressively larger surface in an unbounded uniform atmosphere. As energy is conserved, the sound intensity will decrease in inverse proportion to the distance from the sound source. Spherical spreading is systematically used as a first approximation to evaluate sound transmission loss. It assumes that sound spreads spherically from the source and that the power loss due to the spreading increases with the square of the distance from the source. The classical equation expressing this relationship for an idealized point source is given in equation (1).

$$TL = 10\log r^2 = 20\log r \qquad (1)$$

Where:

TL = transmission loss (dB)

r = distance from the source (m)

In the real atmosphere, sound propagation deviates from spherical spreading due to a number of meteorological factors including absorption of sound in air, non-uniformity of the propagation medium, and interaction of the sound wave with the ground plane. The ISO 9613-2 standard assumes spherical propagation as would occur under moderate downwind propagation conditions. This applies for average meteorological conditions as defined under the standard and is also stated to hold for propagation under a well-developed moderate ground-based temperature inversion. The conditions for downwind propagation given by ISO 9613-2 stipulate a wind direction within an angle of ± 45 to the direction of the path between source and receiver. It also assumes the wind is blowing from the source to the receiver at wind speeds ranging from 1 m/s to 5 m/s measured at 3 to 11 meters above ground level. Outside ISO 9613-2 tolerances, there are regularly occurring anomalous atmospheric conditions which may produce significant deviations in geometric propagation, and impact calculated sound pressure levels at points of reception. When conducting acoustic analyses for wind energy facilities it may be prudent to consider sound propagation under these anomalous atmospheric conditions so as to give a more realistic expectation of future sound levels.

Anomalous meteorological effects include atmospheric temperature inversions, wind inversions, and low level jet streams. Near the ground, vertical gradients in both wind and temperature cause upward or downward refraction of acoustic wavefronts. In the case of a temperature inversion, where a layer of cooler air at ground level sits beneath a warmer layer above, sound rays are refracted downwards toward the earth enhancing propagation in all directions. Large variations in atmospheric temperature gradients, such as what is experienced during atmospheric inversion conditions, tend to occur during calms or at relatively low wind speeds, when wind turbines would not typically be operating.

Low level jet streams are caused by the surface of the earth cooling, causing a reduction in the frictional drag on the wind imposed by the rising convective air, allowing the wind speed to increase. Similar to atmospheric inversion conditions, sound traveling downwind tends to refract back towards the ground, enhancing sound propagation over greater distances. Unlike temperature gradients, wind is a vector quantity defined by both speed and direction, and therefore has a directional effect on sound propagation. For low level jets where the wind gradient increases rapidly over a relatively short distance and at heights above ground level, this effect may become further magnified as sound wave vectors interact with pronounced wind gradients. For low level jets, as the impingement angle decreases, the degree of sound refraction back towards the ground plane will also increase. The propagation medium is limited by both the ground surface and atmospheric layer, which act as a waveguide, effectively confining the sound energy and causing the waves to undergo successive reflections at the boundary interfaces.

Under these conditions, spherical propagation will occur at a distance determined by the strength and height of the wind gradient, often estimated at 1 to 2 times the height of the jet stream. Beyond this distance, the acoustic energy divergence pattern shifts from spherical, to modified-cylindrical at intermediate ranges, and eventually becomes fully-cylindrical, attenuating at a rate given by equation (2). Geometric attenuation under cylindrical divergence is much lower than that under spherical divergence and will result in substantial increases in received sound pressure levels at distant points of reception.

$$TL = 10 \log r \tag{2}$$

Where:

TL = transmission loss (dB)

r = distance from the source (m)

Anomalous meteorological effects have been found to be negligible for sound propagation over short distances but may become increasingly significant at distances greater than 800 meters for elevated sound sources such as wind turbines. These findings have been confirmed through recent work by Boué. Though the effect of these anomalous meteorological conditions can be readily accounted for within the ISO 9613-2 standard, they are infrequently considered in the United States as part of acoustic analyses. ISO 9613-2 accounts for anomalous meteorological conditions during downwind propagation through a meteorological correction factor (C_{met}), shown in equation (3). The C_{met} correction factor is an A-weighted factor and does not include frequency dependent terms. But as shown by Piercy and Embleton, at lower frequencies, which are a principal concern in wind turbine acoustics, the effects of refraction due to wind and temperature gradients are less pronounced. ISO 9613-2 does not provide a correction factor for meteorological effects related to upwind propagation.

$$C_{met} = C_0 \left[1 - \frac{10(h_s + h_r)}{d_p} \right] \quad if \quad d_p > 10(h_s + h_r) \tag{3}$$

Where:

C_{met} = meteorological correction (dB)

h_s = height of the source (m)

h_r = height of the receiver (m)

d_p = distance from the source to receiver (m).

C_0 = factor dependent on local meteorological statistics for wind speed, wind direction, and temperature gradients (dB)

Per ISO 9613-2, a value for C_0 may be estimated from an elementary analysis of local meteorological statistics. The values of C_0 will vary from 0 dB to 5 dB, with values in excess of 2 dB exceedingly rare per ISO 9613-2, when considering long term average meteorological conditions. Conversely, on any given day, a value of C_0 approaching a value of 5 dB should not be unexpected. Neglecting the potential daily variability of C_0 risks the systemic under-predictions of sound levels at distant points of reception from the source. While the conditions that produce the non-standard sound propagation might be infrequent, they are important in capturing the full range of potential received sound levels resulting from wind turbine operation.

Wind speeds and directions are dynamic and constantly shifting. Turbulence due to shifts in wind speed and direction often result in the formation of turbulent eddies. The ISO 9613-2 acoustic modeling algorithms essentially assume laminar atmospheric conditions. In reality, atmospheric inhomogeneity and turbulent eddies commonly occur along the propagation path between the source and receiver, which can scatter sound and enhance attenuation. The scattering effects of an atmospheric inhomogeneity are strongly dependent on frequency and acoustic wavelength. If the atmospheric inhomogeneity is small in relation to the wavelength, the scattering effect will be minor. Due to the complexities of such calculations, the ISO 9613-2 standard does not include adjustments for atmospheric scattering, which leads to added conservatism in modeling results.

Wind Turbine Sound Emission Levels and Meteorological Effects

Accurately defining wind turbine source data for input into the ISO 9613-2 model is critical to ensure the accuracy of acoustic modeling calculations. In order to assist Project developers and acoustical engineers, wind turbine manufacturers report wind turbine sound power data at integer wind speed referenced to a height of 10 meters above grade, ranging from cut-in to full-rated power. The widely accepted IEC standard, currently under review and revision, was developed in part to ensure consistent and comparable sound emission data of utility-scale wind turbines between wind turbine manufacturers. The IEC 61400-11 standard defines procedures to be used in the measurement, analysis and reporting of acoustic emissions of a wind turbine. A thorough understanding of the test procedure and how resultant sound source data is reported is imperative for correct usage in acoustic modeling. Application of the method given in the standard provides the apparent A-weighted sound power levels and frequency spectra at integer wind speeds from 6 m/s to 10 m/s. It has become standard protocol in acoustic analyses in the United States to use maximum sound levels as reported by wind turbine manufacturers for use in assessing regulatory compliance. While this method may be acceptable when assessing regulatory compliance with an absolute noise limit independent of existing acoustic conditions, modeling at multiple wind speeds and operational conditions is required for assessing compliance with regulatory criteria relative to existing acoustic conditions.

Source directivity and tonality may also be determined and reported, though tonality criteria presented in IEC 61400-11 may not concur with applicable regulatory criteria. For area sources, worst case directivity will occur when the majority of the area of emission is visible. For wind turbines, this occurs when the maximum rotor swept area is visible and when a receiver is immediately downwind of the wind turbine tower. Using worst case directivity conditions will provide a level of conservatism when modeling received sound levels at receiver locations.

At higher elevations, the wind is minimally influenced by the surface of the earth. In the lower layers of the atmosphere, wind speeds are affected by friction against the surface of the earth depending on the roughness of the terrain, the presence of obstacles, and the topography of the surface. The aerodynamic roughness length reflects the surface friction imposed on the boundary layer winds and is an important parameter pertaining to the use and manipulation of wind turbine sound power data.

Table 1. IEC 61400-100 Roughness Length Coefficients

Ground Type	z_0 (m)
Water, sand, or snow	0.0001
Open, flat land, mowed grass, bare soil	0.01
Farmland with some vegetation	0.05
Suburbs, towns, forests, many trees and bushes	0.3

The aerodynamic roughness length (z_0) coefficient is the height above a surface at which the logarithmic profile of wind speed versus altitude extrapolates to zero wind speed. It gives a measure of vertical turbulence that occurs when a horizontal wind flows over a rough surface. An increasing roughness length indicates increasing turbulence that arises when the wind passes over a surface. The IEC 61400-11 standard refers to the roughness length as a method of standardizing measured wind speeds to account for actual site conditions. Wind turbine sound source data reported using this standard is referenced to a typical roughness length of 0.03 meters or 0.05 meters. To calculate wind speeds at wind turbine hub height the IEC 61400-11 defines a logarithmic wind profile using equation (4).

$$V_s = V_z \left[\frac{\ln\left(\frac{z_{ref}}{z_{0ref}}\right) \ln\left(\frac{H}{z_0}\right)}{\ln\left(\frac{H}{z_{0ref}}\right) \ln\left(\frac{z}{z_0}\right)} \right] \qquad (4)$$

Where:

V_s	=	standardized wind speed (m/s)
V_z	=	wind speed at height z (m/s)
z_{0ref}	=	reference roughness length (typically 0.05 or 0.03 m)
z_0	=	roughness length (m)
H	=	rotor centre height (m)
z_{ref}	=	reference height (10 m)

z = anemometer height (m)

Under neutral atmospheric conditions and constant surface roughness, the distribution of wind velocity (with height) has been found to be log-linear; however, there has been some debate as to whether assuming a logarithmic wind profile is appropriate for all applications in determining wind turbine source levels. When the atmospheric conditions deviate from ‘neutral’, strong thermal effects begin to influence the shape of the wind profile. Equation (5) is an alternative equation, which accounts for the wind shear exponent used in connection with the power-law wind profile. The surface shear velocity is inversely proportional to the change in velocity with height and is a function of the surface shear stress and the fluid density of the medium.

$$V_s = V_z \left(\frac{H}{z_{ref}} \right)^{\alpha} \tag{5}$$

Where:

V_s = standardized wind speed (m/s)

V_z = wind speed at height z (m/s)

α = wind shear

H = rotor centre height (m)

z_{ref} = reference height (10 m)

Equation (5) is applicable to conditions involving non-complex terrain up to a height of approximately 200 meters above ground and is frequently used in engineering applications. While both valid, using equations (4) and (5) will result in differing resultant wind speeds. The wind shear power-law equation yields comparatively higher wind speeds, resulting in a more conservative dataset.

A study completed by the U.S. Department of Energy-Electric Power Research Institute (DOE-EPRI) Wind Turbine Verification Program included five wind energy facilities in the Midwestern United States (Smith et al, 2002). Long-term sets of validated data were analyzed to determine the timing, magnitude and frequency of ‘wind shear’ and ‘high wind shear’ events at the wind energy facilities. The study showed that for several of these facilities, a strong diurnal shear pattern occurred. During the day, low and sometimes negative wind shear values were measured. During evening and night hours, very high positive wind shear was frequently observed. Klug and Van de Berg also report similar diurnal wind shears during evening and nighttime periods.

This diurnal pattern, while favorable with respect to wind energy generation and production, could also explain occurrences of unexpectedly high received sound levels and complaints during these periods. Higher wind shear levels in the evening and nighttime hours often result in lower operational wind speed at hub height. This wind speed profile can produce a greater than expected differential between operational sound levels and baseline sound level, which may increase audibility at receiver locations. Wind turbines are also physically affected by wind shear. Vertical wind-speed profiles result in a different wind speed at the blades nearest the ground compared to those at the top of the swept area. This in turn influences wind turbine operation by creating a bending moment in the shaft of a two bladed wind turbine when the blades are vertical, and can affect sound generation. If routinely present, diurnal wind shear characteristics should be included in acoustic analysis methodologies when assessing critical design wind speeds relative to existing baseline conditions.

While both equations (4) and (5) can be used to determine wind speed relative to source height, the preferred and most reliable method is to analyze long term historic meteorological wind statistics. By analyzing meteorological wind statistics at various heights above ground level, a site-specific wind speed profile can be developed and the corresponding roughness length and wind shear coefficient can be evaluated in relation to wind turbine source levels. Where historic meteorological data is not available, consultation with a certified meteorologist is another viable option. Naturally, long-term average meteorological statistics are determined based on weather conditions over time, which would include daily variability and atypical events such as the passing of strong weather fronts, microbursts, and other short term events. Therefore, site wind speed characteristics may be resolved using long-term averages and regularly occurring diurnal variations determined from a simple logarithmic or power law profile over the full range of wind speeds. In addition to the wind shear power law and the IEC 61400-100 standard, linear or polynomial curve fitting and/or other regression analysis of site-specific meteorological conditions can be employed to evaluate site wind speed characteristics. While ISO 9613-2 considers long term averages in the calculation of the meteorological correction factor, C_{met}, it has not been adapted to wind turbine acoustics, where generated sound levels are so closely related the prevailing wind speed.

Recent experience has shown for wind energy projects sited in New York state characterized by moderately varying terrain with frequent tree stands, roughness length can vary from 0.12 meters to 0.30 meters. In more complex terrains including wind projects in New Hampshire, Vermont, Colorado, and Washington state, site specific roughness lengths on the order of 0.20 meters to 0.40 meters and greater are not uncommon. When compared to the reference roughness length of 0.03 meters to 0.05 meters per the IEC 61400-100 test standard and presented in wind turbine manufacturer sound power data, it is apparent that the roughness length coefficient corresponding to actual site conditions will differ substantially from those quoted by equipment manufacturers and used for deriving sound source levels. Adjusting the roughness length coefficient to reflect actual site conditions is a procedure often overlooked by acousticians in the United States, which often results in misrepresentation of real wind speed conditions and an underestimation of received sound levels relative to existing baseline levels. At a minimum, localized roughness length should be incorporated into acoustic modeling source terms, even if localized wind shear is determined not to be significant.

Wind Turbine Source Dimensions and Lateral Attenuation

The swept area of wind turbine rotors can be modeled as a disk of point sources, as a ring of point sources at the blade tips or, as is most commonly done in the United States, as an idealized single point source positioned at hub height. The elevated point source at hub height is the most straightforward approach to simulate a wind turbine and is appropriate when the distance from the source to the receiver is large compared to the dimensions of the source. Equation (6) shows the basic outdoor sound propagation equation given by ISO 9613-2.

$$L(DW) = L_W + D_c - A - 10\log\left(\frac{1}{2}\pi R^2\right) \qquad (6)$$

Where:

L(DW)	= equivalent downwind sound pressure level (dB)
L_W	= octave band sound power level relative to a reference sound power of 1 picowatt (dB)
D_c	= directivity correction (dB)
A	= octave band excess attenuation (dB)
R	= linear (slant) distance of L_p from source in meters to calculate geometrical divergence with distance

The directivity correction factor is dependant on the directivity of the source, which for wind turbines is a function of the geometry. Directivity accounts for the variation in sound intensity with orientation relative to the sound source. The directionality of the source may also be affected by the geometry of its immediate surroundings, largely due to the presence of reflecting surfaces. For an omnidirectional point source radiating into free space D_c = 0 dB. The ISO 9613.2 standard calculates downwind propagation using the aforementioned meteorological correction factor. Statements claiming the conservative nature of omnidirectional downwind propagation, though technically accurate, may often be overstated in permitting documents. For receiver locations immediately between discrete wind turbine locations or wind turbine arrays, acoustic modeling may over-predict received sound levels due to omnidirectional downwind effects, depending on the separation distance between source and receiver. If a receiver is located at a distance where it would not be susceptible to these over-predictions, it would still be subject to a level of conservatism due to the inclusion of wind turbine maximum sound directivity.

The octave band attenuation factor given in equation (6) includes attenuation related to atmospheric absorption, topographical features, terrain coverage and ground type, foliage, and/or other natural or man made obstacles such as buildings that can refract sound. The attenuation factor accounting for geometric divergence incorporates distance from source to receiver and the spherical radiation exhibited by the wind turbine point source. Aside from atmospheric stability, wind and turbulence, as discussed previously, propagation can be affected by atmospheric absorption which is a function of humidity, temperature, and air density.

Accurately characterizing source height and dimensions is important when using the ISO 9613.2 calculation algorithms. Not only are these factors essential when calculating sound attenuation caused by geometric divergence, but they are also needed when addressing matters of near-field and far-field effects as well as lateral attenuation. Sound pressure levels in the near-field do not conform to the inverse-square law and therefore sound pressure levels in the far-field cannot be accurately quantified based on near-field measurements. To determine the required source-receiver separation distance in the far-field, it is advantageous to rely on the lower range of frequencies. For instance, under average daytime temperatures, the wavelength of sound in air at 20 Hz is approximately 17 meters, whereas the wavelength of sound in air at 1000 Hz is approximately 0.3 meters.

With respect to wind turbines, potential difficulties associated with calculations made using ISO 9613-2 in the geometric near-field are of concern. The geometric near-field is defined as the region where the distance from a source of sound is less than the largest dimension of the sound source. In the geometric near-field, the effect of source geometry is very significant. Sound sources such as wind turbines are often a composite of many different components. There are two principal types of sound relating to wind turbine operation: mechanical and aerodynamic sound. Mechanical sound is generated at the gearbox, generator, and cooling fan and is radiated from the surfaces of the nacelle and machinery enclosure and by openings in the nacelle casing. Aside from fault upset conditions that may result in aberrant mechanical noise, the dominant sound source generated by utility scale wind turbines is aerodynamic.

Aerodynamic sound is related to air flow and its interaction with the tower and rotor blades when in motion. Air entering the rotor swept area is not completely smooth, consisting of turbulent eddies which generate noise. Air flow occurring across the blade produces turbulence at the surface boundary layer, resulting in trailing edge boundary sound. Trailing edge sound is considered the principal aerodynamic component in wind turbine noise. In addition, tip sound is created by vortex shedding as the blade tips pass through the air. Vortices that are shed from the tips of the wind turbine blades are blown back behind the rotating blades by the wind. When these eddies cut across the shaft of the tower, a characteristic amplitude modulated (time-varying) swooshing sound occurs at the blade-passage frequency. Acoustic modulation is most perceptible in close proximity to the base of the wind turbine tower.

In the region of the geometric near-field, interacting sound waves from various parts of the turbine lead to interference effects and sound pressure levels that do not necessarily decrease at a rate of 6 dB per doubling of distance. Therefore, accurate sound pressure level calculations using ISO 9613-2 may not be possible in this region. In the far-field, the effect of source geometry is negligible as particle velocity and pressure of the contributing waves from the various parts of the source are in phase. As a result, sound pressure level calculations made in the far-field will follow standard propagation rates. It is assumed that the IEC 614-100 test protocol measures source levels at a distance equal to the sum of the height of the rotor above the ground and one-half of the rotor diameter to overcome the potential inconsistencies associated with sound pressure levels measured in the geometric near-field.

Per the ISO 9613.2 standard, an area source may be described by a group or single equivalent point source when the distance from source to receiver exceeds twice the largest dimension of the sources. If a receiver is located within this specified distance, calculated sound pressure levels will be under-predicted when the ISO 9613-2 idealized point source methodology is used. Further adjustments in ground attenuation calculations may be warranted. Potential under-predictions are caused by a portion of the sound source being located closer to the receiver than the representative idealized point source. In the case of wind turbine acoustics, the blade tips would travel closer to a nearby receiver than the idealized point source when positioned at wind turbine hub height.

During the wind turbine siting process, wind turbines are generally sited using setback distances from nearby residential receptors that are much greater than two rotor diameters. As this is the case, the ISO 9613-2 idealized point source assumption would likely only be of concern when assessing compliance at residential property lines, which may be much closer to individual wind turbine locations. Nevertheless, awareness of this possible constraint should be considered if acoustic analysis is required within the geometric near-field region of the wind turbine. Furthermore, when calculations are required in this region and beyond, since the source is largely located above the receiver location, inclusion of a ground attenuation factor is recommended to counteract the occurrence of sound pressure level under-predictions. A ground attenuation factor should be gradually incorporated at the base of the wind turbine until the angle of incidence of the sound generated in relation to the ground dictates otherwise, conservatively estimated to occur at roughly 3 to 4 rotor diameters from the wind turbine. This is of particular importance with reference to the ISO 9613-2 general method of calculation where ground attenuation is mainly the result of sound reflected by the ground, interfering with the sound propagating directly from source. Lateral attenuation is also determined primarily by the ground surfaces near the source and near the receiver. For receivers located immediately below the source and for some distance beyond, lateral attenuation calculation methodology does not hold. The actual angle of incidence will be constant across the entire acoustic study area for fairly flat terrain but will fluctuate in complex terrain depending on the variation in ground height. At mid-range linear distances, including at setback distances typically employed in the United States ranging from 300 to 700 meters, the ISO 9613-2 standard gives a fairly close estimation when compared with field measurement data assuming representative ground attenuation factors are incorporated.

Conclusions

Acoustic modeling software that conforms to ISO 9613-2 has been shown to be an accurate and effective acoustic modeling tool for wind energy projects sited in the European Union, Canada and the United States, when appropriate modeling techniques are employed and site-specific ground, terrain, and topographical features considered.

This paper provides insight into the limitations associated with using the ISO 9613-2 standard as a basis for acoustic modeling calculations. The potential impacts of non-standard meteorological conditions on sound propagation to distant points of reception were investigated. Modification of the ISO 9613-2 calculation algorithms by including a meteorological correction factor was recommended to address wind turbine operations at wind speeds not accounted for by the standard and during anomalous meteorological conditions. Incorporating a meteorological correction factor is necessary to convey expectations to regulators and communities, particularly if the prevalence of these conditions is supported by long-term meteorological data. However, this technique has not been largely adapted to wind turbine acoustics, where generated sound levels are closely related the prevailing wind speed and long range propagation is often of concern. Modifying wind turbine sound source data to reflect a site-specific roughness length coefficient is suggested to accurately characterize the local wind speed profile. In addition, incorporation of a coefficient to account for regularly occurring diurnal wind shear may be included when assessing critical design wind speeds relative to existing baseline sound conditions.

The importance of considering wind turbine source dimensions and their impact on lateral attenuation and downwind sound propagation was discussed. At linear distances less than approximately 200 meters from wind turbine sound sources, depending on turbine rotor diameter and hub height, modeling with ISO 9613-2 software may under-predict received sound pressure levels due to near- field effects, and increasingly so if lateral attenuation effects are included in this region. If analysis is required within the geometric near-field, the inclusion of a ground attenuation factor within this region may assist in offsetting inaccurate modeled sound level results. Field verification and equipment acceptance testing of operational wind energy facilities have demonstrated that with all these factors considered, an accurate representation of future project operational sound levels is possible using the ISO 9613-2 calculation methodologies for wind energy facilities.

References

1. International Electromechanical Commission (IEC) 61400-11:2002(E) Wind Turbine Generator Systems – Part 11: Acoustic Noise Measurement Techniques, Second Edition 2002-12.
2. International Standard, ISO 9613-2, Acoustics – Attenuation of Sound During Propagation Outdoors, Part 2 General Method of Calculation.
3. Smith, K. et al. National Renewable Energy Laboratory. Evaluation of Wind Shear Patterns at Midwest Wind Energy Facilities, May 2002.

4. Blumberg, D.G. and R. Greeley. Field Studies of Aerodynamic Roughness Length, *Journal of Arid Environments*, Vol. 25, (39-48) Academic Press Limited, 1993.
5. Jacobson, M. Fundamentals of Atmospheric Modeling: Edition 2, Cambridge University Press, 1999.
6. Ingard, Uno. "A Review of the Influence of Meteorological Conditions on Sound Propagation," Journal of the Acoustical Society of America, Vol. 25, No. 3, May 1953.
7. Source: Cadna/A Users Manual, Datakustik Co., Grefenberg, Germany, 2007
8. International Standard, ISO 9613-2, Acoustics – Attenuation of Sound During Propagation Outdoors, Part 2 General Method of Calculation. 2005
9. Heier, Siegfried Grid Integration of Wind Energy Conversion Systems. Chichester: John Wiley & Sons. pp. 45. ISBN 0470868996.
10. K. Smith, G. Randall, and D. Malcolm, Global Energy Concepts, LLC, N. Kelley and B. Smith, National Renewable Energy Laboratory. Evaluation of Wind Shear Patterns at Midwest Wind Energy Facilities (Preprint). National Renewable Energy Laboratory. May 2002 • NREL/CP-500-32492.
11. Mathieu Boué, Long-Range Sound Propagation Over the Sea with Application to Wind Turbine Noise. Final report for the Swedish Energy Agency project 21597-3 (TRANS). TRITA-AVE 2007:22 ISSN 1651-7660.
12. Klug H. (2005). A Review of Wind Turbine Noise. Wind Turbine Noise, Berlin.
13. Piercy, J.E. and T.F.W. Embleton, "Review of noise propagation in the atmosphere," Journal of the Acoustical Society of America, Vol. 61, June 1977, p.141.
14. Van de Berg, G. Wind Gradient Statistics up to 200 m Altitude Over Flat Ground. Wind Turbine Noise, Berlin.
15. Van de Berg, G. "The Beat is Getting Stronger: The Effect of Atmospheric Stability on Low Frequency Modulated Sound of Wind Turbines." Journal of Low Frequency Noise, Vibration and Active Control 24(1): 1-24. 2005
16. Van de Berg, G. "Effects of the Wind Profile at Night on Wind Turbine Sound." Journal of Sound and Vibration 277:955-970. 2004.
17. Wagner, s., Bareiss, R. and Guidati, G. Wind Turbine Noise. Springer.
18. Kenneth Kaliski, Edward Duncan, "Propagation Modeling Parameters for Wind Turbines". Presented at NOISE-CON 2007Reno, Nevada October 22-24, 2007.
19. Bies, D. and C. Hansen. "Engineering Noise Control: Theory and Practice", Taylor & Francis, 2003.

Third International Meeting
on
Wind Turbine Noise
Aalborg Denmark 17-19 June 2009

Comprehensive Evaluation and Assessment of Trailing Edge Noise Prediction Based on Dedicated Measurements

M. Kamruzzaman, A. Herrig, Th. Lutz, W. Würz and E. Krämer, S. Wagner
Institute of Aerodynamics & Gas Dynamics (IAG),
Universität Stuttgart, Pfaffenwaldring 21, D-70550, Germany
{kamruzzaman, herrig, lutz, wuerz, kraemer, wagner}@iag.uni-stuttgart.de

Abstract

Turbulent boundary-layer trailing-edge interaction noise (TBL-TE) has been shown to be the main noise source of modern wind turbine designs [1]. Trailing-edge noise prediction models are usually based on the evaluation of boundary-layer and turbulence properties to derive the spectrum of the wall pressure fluctuations in the vicinity of the trailing edge. The far-field noise emission is then calculated by means of an appropriate diffraction model [2]. Such a TBL-TE noise prediction model has been developed [3, 4, 5, 6] at the Institute of Aerodynamics & Gas Dynamics (IAG), University of Stuttgart and successfully applied, e.g. in the frame work of the EU project SIROCCO (SIlent ROtors by aCoustiC Optimization), to design new, less-noisy airfoils for the outer blade region of two different wind turbines in the MW class [7]. As a part of IAG activities in the EU project UpWind a RANS based noise prediction scheme, Rnoise [4] has been implemented. The main features of the Rnoise approach are the direct derivation of the required turbulence noise source properties and the consideration of anisotropy effects by means of different turbulence models.
In the present paper, an extensive assessment and validation of each step of the TBL-TE far-field noise prediction scheme [5, 6, 8] has been conducted. For this purpose detailed measurements of the turbulent boundary-layer properties like two-point turbulent velocity correlations, the spectrum of the associated wall pressure fluctuations (WPFs) and finally the emitted trailing-edge noise spectrum have been performed in the Laminar Wind Tunnel (LWT) of the institute. The measurements were performed for the NACA 0012 airfoil [9]. The availability of these measurement data enabled the comprehensive step by step validation and assessment of the prediction of the turbulence noise source parameters, the description for the wall pressure fluctuation spectrum, and the calculation of the far-field noise spectra.
Most of the investigated cases show that the numerical WPF and far-field radiated noise models capture the measured peak amplitude level as well as peak position remarkably well, if the turbulence noise source parameters are estimated properly including turbulence anisotropy effects.

1 INTRODUCTION

To identify the main noise sources of wind turbines operating in certain terrain and to reduce the noise emission is one important issue in design and application of wind turbines. Flow induced noise represents the dominant noise source of modern turbines. Field tests by Oerlemans et al. have shown that, in particular, turbulent boundary-layer trailing-edge interaction noise (TBL-TE) dominates the overall noise emission for the examined on-shore turbines [1]. Considerable effort, therefore, has been spent to develop and improve accurate and consistent TBL-TE noise prediction models. To predict the noise emission, in general, simplified analytical models [3, 6, 10, 11], semi-empirical models [12, 13] and finally numerical CAA methods [14, 15, 16, 17] or Stochastic Noise Generation & Radiation (SNGR) [18] approaches can be distinguished. All these approaches require information about the turbulence noise source data, i.e. the turbulence properties of the boundary layer. These noise source data can be obtained either by means of a dedicated semi-empirical post-processing of data from an integral or Finite-Difference boundary layer calculation (BL) methods, from RANS analysis, detailed LES simulations, or from measurements.

In order to develop an efficient noise prediction tool that can be used to enable aero-acoustic airfoil and blade design, TBL-TE noise prediction models have been extensively studied and analyzed in the Institute of Aerodynamics & Gas Dynamics (IAG), University of Stuttgart (see Figure (1) in Ref. [8, 10]). The models were applied for example in the frame work of the EU project SIROCCO [6, 7, 19] and currently in UpWind to design new, less-noisy airfoils for wind turbine applications. The noise prediction scheme is essentially based on the well-known TNO-TPD approach proposed by Parchen [4], which makes use of Blake's approach to derive the spectrum of the wall pressure fluctuations and Chandiramani's diffraction model [2]. In order to calculate the required noise source parameters three different aerodynamic prediction methods are used at the IAG, namely the coupled panel integral boundary-layer code XFOIL [20], the Finite-difference boundary-layer code EDDYBL [21] and finally the RANS code FLOWer [22]. As these methods differ with regard to modelling accuracy and output data the procedure to derive the turbulence noise source data is different. For convenience the three resulting noise prediction methods are denoted Xnoise (XFOIL based), XEnoise (EDDYBL based) and Rnoise (RANS based).

In the present paper the main foundations of the three prediction models are summarized and each calculation step is validated and assessed. For this purpose dedicated boundary-layer turbulence and aero-acoustic measurements on a NACA 0012 airfoil section were conducted at the Laminar Wind Tunnel (LWT) of the IAG. Shortcomings of the different prediction models will be discussed and conclusions will be drawn.

2 THE NOISE PREDICTION MODEL

The TBL-TE noise prediction model considered in the present study follows the spectral solution of the Poisson equation for the surface pressure fluctuations underneath a turbulent boundary layer following Kraichnan [23], Panton and Linebarger [24], Blake [3], and the evaluation of the noise emission from the trailing edge due to this fluctuating pressure by solving the diffraction problem [2]. Following the spectral solution of the Possion's equation [3, 23, 24], the wave number-frequency spectrum of the wall pressure fluctuations for the source spectrum $\Phi_{22}(y_2, y_2', \mathbf{k}, \omega)$ is given by

$$\mathbf{P}(k_1, k_3, \omega) = 4\rho^2 \left(\frac{k_1^2}{k_1^2 + k_3^2}\right) \int_0^\infty \Lambda_2(y_2) \left[\frac{dU_1(y_2)}{dy_2}\right]^2 \cdot \tilde{\phi}_{22}(y_2, k_1, k_3) \cdot \phi_m(\omega - k_1 U_c) \cdot \langle u_2^2(y_2)\rangle \cdot e^{-2|\mathbf{k}|y_2} dy_2, \quad (1)$$

where $\tilde{\phi}_{22}(y_2, k_1, k_3)$ is the normalized wave number spectra of the vertical velocity fluctuation u_2, i.e.

$$\tilde{\phi}_{22}(y_2, k_1, k_3) = \frac{\Phi_{22}(y_2, k_1, k_3)}{\langle u_2^2(y_2)\rangle}, \quad (2)$$

Λ_2 represent the vertical integral length scale for the eddy field, and $\phi_m(\omega - k_1 U_c)$ is the moving axis spectrum. The final form of the far-field pressure density spectrum $S(\omega)$ can be expressed as [6],

$$S(\omega) = \frac{L}{4\pi R^2} \int_{-\infty}^{\infty} \frac{\omega}{c_0 k_1} \mathbf{P}(k_1, 0, \omega) dk_1, \text{ single-sided } G(\omega) = 2 \cdot S(\omega),\ k_1 \in [0, \infty] \quad (3)$$

where R is the distance to the observer from the trailing edge and L is the wetted length of the trailing edge.
The determination of the total sound pressure level according to the present scheme involves three nested numerical integrations: The integration in wave number direction k_1, the integration in wall normal direction across the boundary layer and finally the integration vs. angular frequency ω. An evaluation of the integrals shows that especially the integration in k_1 direction requires special care since the integrand behaves quite different for different wall normal distances and considered frequencies. Furthermore, sharp peaks can show up. Therefore, a special adaptive numerical integration scheme was developed [25], inside which the integration limit $k_{1,max}$ is selected by an iteration procedure, while $k_{1,min} = 0$. That means, single-sided spectra are assumed, though the double-sided spectra $S(\omega)$ have not been multiplied with a factor of two. This inconsistency was corrected now.

3 TURBULENCE NOISE SOURCE MODELLING

It is obvious that the accuracy of the noise prediction depends on the accurate modelling of the turbulent noise source terms, i.e. $\phi_{22}(y_2, k_1, k_3), \Lambda_2(y_2), \langle u_2^2(y_2)\rangle$ etc. In the present study three different aerodynamic analysis methods have been used in order to approximate the turbulence data. The resulting prediction schemes are denoted Xnoise, XEnoise and Rnoise (see Sec. 1)) and will be discussed elaborately in the following sections.

3.1 Basics of the Noise Prediction Schemes

Xnoise

Within Xnoise the well established airfoil design and analysis tool XFOIL [20] is applied to calculate basic boundary-layer properties in the vicinity of the trailing-edge. As XFOIL only provides integral boundary-layer parameters several approaches to derive the properties required to set up the $k-\omega$ spectrum are applied. First of all, the unknown mean velocity profile is approximated in two different ways, namely the Coles law of the wall & the Swafford profile family showing the same boundary-layer thickness and skin friction as calculated by the XFOIL boundary-layer procedure. From this approximated mean profile the required turbulence properties are determined by means of a mixing-length approach and some semi-empirical relations as proposed by Parchen [4]. The Xnoise prediction scheme is basically comparable to the NAFNOISE code [26].

XEnoise

Previous investigations within the SIROCCO project have shown that the Xnoise method yields quite reasonable results at least for ”usual” types of airfoil pressure distributions. For stronger deviations, however, the model shows some inconsistencies, i.e. the impact of airfoil shape modifications and variations of the freestream conditions could not be predicted properly. This is attributed to the simplified estimation of the turbulence properties and the application of the local mixing-length approach. As a consequence the Finite-Difference boundary-layer code EDDYBL developed by Wilcox [21] was linked to the prediction model. With an FD method the boundary layer is discretised in streamwise and wall-normal direction and thus, the mean profile along with the distribution of the time-averaged turbulence data is a direct result of the calculation. Within the present study the Wilcox stress-ω turbulence model was applied, that accounts for anisotropy effects of the velocity fluctuations and potentially captures history effects more accurately compared to isotropic turbulence models [21]. To obtain the initial and the boundary conditions required for the EDDYBL analysis, a standard XFOIL analysis is performed in a first step. The resulting “viscous” outer flow velocity distribution is then used as boundary condition for a subsequent EDDYBL analysis of the turbulent flow domain. The initial conditions are taken from the XFOIL boundary-layer analysis. For more details about the implementation of XEnoise see Ref. [6]

Rnoise

Within Rnoise [5, 10] the CFD code FLOWer [22] is used for the aerodynamic prediction. FLOWer solves the compressible, two- or three- dimensional Reynolds- (Favre-) averaged Navier-Stokes equations in integral form. A cell-centered based finite-volume formulation on block-structured grids was utilized for computations presented here. The convective fluxes of the main equations were discretized in space applying a second-order central scheme with a blend of second- and fourth-order artificial damping terms, whereas diffusive fluxes were discretized purely central. The turbulence equations were discretized by a flux difference first-order upwind scheme. Time integration to steady state for the main equations was accomplished by an explicit five-stage Runge-Kutta scheme with local time stepping, where convergence was accelerated by a multigrid method on three grid levels with implicit residual smoothing. The main feature of RANS based implementation is the direct derivation of the required turbulence noise source properties by means of different turbulence models, i.e. one/two equation (k-ω, SST) and Explicit Algebraic Stress Model (EARSM). The FLOWer analyzes were performed on C-type meshes consisting of $672 \times 128 = 86.016$ cells in streamwise- and airfoil-normal direction (238 cells along the airfoil surface). The y^+- values on the surface of the airfoil and in relevant regions of the viscous wall are below 1 in all computations, providing a sufficient boundary-layer resolution.

3.2 Mean Velocity Profile

To derive the mean velocity profile from the standard XFOIL calculated integral boundary-layer properties, either a Coles Law of the Wall combined with the Law of the Wake representation or an approach proposed by Swafford was used in Xnoise. The parameters of these analytical profile families are iterated until the corresponding integral boundary-layer parameters match the values resulting from the XFOIL analysis. The mean velocity U_1 and its gradient in the boundary layer is reconstructed by the well known Coles [21] and Swafford profiles [20] in Xnoise method. Four different coupling procedures are available to derive the value of the Coles' wake-strength parameter Π and Swafford constants a and b inside the Xnoise code.

The mean profile along with the distribution of the time-averaged turbulence data is a direct result of the EDDYBL code. Hence, the velocity gradient can be easily found from this discrete $U_1(y_2)$ data. Also the RANS flow solver FLOWer [22] provides all the time-averaged flow variables over the complete flow field including turbulence parameters.

3.3 Turbulence Energy Spectra & Velocity Correlation

One of the most renowned definitions of the turbulence length scale in turbulence theory is Prandtl's (1925) mixing length theory. Prandtl postulated that [21].

$$- \langle u_1 u_2 \rangle = l_{mix}^2 \cdot \mid \frac{dU_1}{dy} \mid \frac{dU_1}{dy} \tag{4}$$

Townsend [21] stated that in most turbulent shear flows, measurements indicate

$$- \langle u_1 u_2 \rangle \approx c \cdot \sqrt{\langle u_1^2 \rangle} \cdot \sqrt{\langle u_2^2 \rangle}, \text{ where constant } c = 0.3 - 0.6 \tag{5}$$

Consequently, the mixing length implies that $\sqrt{\langle u_1^2 \rangle}$ and $\sqrt{\langle u_2^2 \rangle}$ are of the same order of magnitude. This is generally true although $\sqrt{\langle u_1^2 \rangle}$ is usually 25% to 75% larger than $\sqrt{\langle u_2^2 \rangle}$ for typical shear flows [21]. This difference in the Reynolds stress components is known as anisotropy feature of the flow. It is possible to derive an expression to consider anisotropy effects of the turbulent flow from two-point correlation measurement data. If all the normal

Reynolds stress components are known, then turbulence kinetic energy can be found from the equation

$$k_T = \frac{1}{2}\left(\langle u_1^2\rangle + \langle u_2^2\rangle + \langle u_3^2\rangle\right) \tag{6}$$

For isotropic turbulence all Reynolds stress components are identical, i.e. $\langle u_1^2\rangle = \langle u_2^2\rangle = \langle u_3^2\rangle$. Now assume that the flow is anisotropic and the Reynolds stress anisotropy is given by $\langle u_1^2\rangle : \langle u_2^2\rangle : \langle u_3^2\rangle = a : b : c$. Therefore, for an airfoil boundary layer assume that

$$\frac{\langle u_1^2\rangle}{\langle u_2^2\rangle} = \frac{a}{b} = f_{12} \tag{7}$$

Substitution of Eqn. (7) into Eqn. (5) along with Eqn. (4) leads to

$$\langle u_2^2\rangle = \alpha\,\frac{-\langle u_1 u_2\rangle}{c} = \frac{\alpha}{c}\cdot l_{mix}^2 \cdot \mid \frac{dU_1}{dy} \mid \frac{dU_1}{dy},\ \text{where } \alpha = \frac{1}{f_{12}^{1/2}} \tag{8}$$

Parchen [4] proposed that the vertical fluctuating velocity can be approximated by

$$\langle u_2^2\rangle = \alpha \cdot k_T,\ \text{where } k_T = \sqrt{\frac{\left(l_{mix}^2 \cdot \mid \frac{dU_1}{dy} \mid \frac{\partial U_1}{\partial y}\right)^2}{C_\mu}} \tag{9}$$

where α is an empirical constant which is set 0.45 for the suction side and 0.35 for the pressure side and $c = \sqrt{C_\mu} = 0.3$. In Xnoise the vertical fluctuating velocity has been approximated by means of Eqn. (9).

Within XEnoise, the EDDYBL code features a Reynolds stress turbulence model, namely the Wilcox stress-ω model that accounts for anisotropy effects and provides the complete Reynolds stress tensors. Consequently, $\langle u_2^2\rangle$ is a direct result of the EDDYBL code. The same holds for the Rnoise prediction if a Reynolds stress turbulence model is chosen for the RANS analysis. If a two-equation turbulence model is chosen, e.g. the Wilcox k-ω or the Menters SST model, then the Reynolds stresses are determined in the post-processing by the constitutive relation based on an extended Boussinesq eddy viscosity hypothesis [21]

$$\tau_{ij} = 2\nu_T\left(S_{ij} - \frac{1}{3}\frac{\partial U_k}{\partial x_k}\right) - \frac{2}{3}k\delta_{ij} \tag{10}$$

Calculation of the $\langle u_2^2\rangle$ value in Rnoise method by above equation is denoted by $\langle u_2^2\rangle\,|_{aniso}$. Also, if flow is assumed to be isotropic and homogeneous then from the RANS computed k_T the vertical Reynolds stress can be evaluated by $\langle u_2^2\rangle\,|_{iso} \equiv \langle u_2^2\rangle = 2/3k_T$.

3.4 Vertical Integral Length Scale Λ_2

The length scale Λ_2 is related to the vertical extent of the turbulent eddies. More precisely, it is defined as the integral of the normalized spatial two-point correlation coefficient $R_{22}^{(12)}$

of the vertical velocity fluctuations [27],

$$\Lambda_{22}^{(2)} \equiv \Lambda_2 = \int_0^\infty R_{22}^{(12)}(r_2)dr_2 = \int_0^\infty \frac{\langle u_2(y_1, y_2, y_3, t) \cdot u_2(y_1, y_2 + r_2, y_3, t)\rangle}{\sqrt{\langle u_2^2(y_1, y_2, y_3, t)\rangle \cdot \langle u_2^2(y_1, y_2 + r_2, y_3, t)\rangle}} dr_2 \tag{11}$$

This is vertical integral length scale of the vertical velocity component at separation in vertical direction. The length scale Λ_2, however, is not provided by any established turbulence model or boundary-layer procedure. To derive Λ_2 from known quantities, usually, a calculated turbulence length scale l or the mixing length l_{mix} is multiplied by an empirical scaling factor. Previous investigations suggest that the required scaling factor depends on the boundary-layer development and motivated the derivation of empirical scaling laws [6].

Prandtl (1929) postulated that for flows near solid boundaries the mixing length is proportional to the distance from the surface. Also it is generally agreed that the mixing length does not increase linearly through the complete BL. With these constraints in mind, the expression of Schlichting was used to model the mixing length within the Xnoise scheme

$$l_{mix} = \delta \cdot 0.085 \left[\tanh\left\{\frac{\kappa}{0.085}\left(\frac{y}{\delta}\right)\right\}\right], \tag{12}$$

together with the Klebanoff damping function near the boundary-layer edge

$$l_{mix} = l_{mix} / \sqrt{1 + 5.5\left(\frac{y}{\delta}\right)^6}. \tag{13}$$

Finally, the vertical integral correlation length scale necessary for the noise prediction scheme is approximated by

$$\Lambda_2 = \frac{l_{mix}}{\kappa} \tag{14}$$

where $\kappa = 0.41$. This equation is applied in the Xnoise method to determine the vertical integral length scale.

XEnoise and Rnoise provide the wall normal distribution of the turbulence kinetic energy and dissipation by solving their own transport equation. Consequently, a more elaborate approach can be used to derive an expression for Λ_2 either based on the predicted wave number of the energy containing eddies k_e or turbulence length scale l, but the order of magnitude of l and Λ should be same [28]. For the present analysis the integral length scale has been modeled by the following ways.

Λ_2 as function of the isotropic turbulence length scale l

If a RANS computation is performed with a two-equation $k - \varepsilon$ turbulence model, then Λ_2 can be derived [28] by the relation defined as [6, 5]

$$\Lambda_2|_{iso} \equiv \Lambda_2 = 0.748 \cdot \frac{l}{1.37} \approx 0.547 \cdot l \text{ where } l = \frac{k_T^{3/2}}{\varepsilon} \tag{15}$$

The same relation is also valid for a $k - \omega$ type two-equation turbulence model with length scale $l = \frac{\sqrt{k_T}}{C_\mu \omega}$. It is very important to note that this derivation implies that turbulence is isotropic and Λ_2 is nothing but the longitudinal integral length scale Λ_f derived by assuming $\langle u_1^2\rangle \equiv 2/3 k_T$.

Λ_2 based on the wave number of the energy containing eddy k_e

The wave number k_e can be determined from the predicted turbulence kinetic energy k_T and the dissipation rate ε by comparing the asymptotic behavior of the Kármán spectrum to the Kolmogorov spectrum for the inertial subrange. In terms of the RANS predicted k_T and ε the final expression can be written as [6]

$$\Lambda_2|_{iso2} \equiv \Lambda_2 = 0.39 \cdot \frac{k_T^{3/2}}{\varepsilon}. \tag{16}$$

Anisotropic Λ_2 based on an anisotropic factor f_{22}^{aniso}

Beside the above discussed isotropic length scales, a model according to Ref. [5] for the calculation of anisotropic vertical integral length scale has also been implemented in Rnoise method. The final form of the modeled anisotropic length scale equation is

$$\Lambda_2|_{aniso} \equiv \Lambda_2 = \Lambda_2|_{iso} \cdot (f_{22}^{aniso})^{3/2}, \text{ with } f_{22}^{aniso} = \frac{\langle u_2^2 \rangle}{2/3 k_T} \tag{17}$$

where $f_{22}^{aniso}(y_2)$ is an anisotropic factor and can be evaluated from the RANS calculated k_T and $\langle u_2^2 \rangle$ using Eqn. (10). First two methods from the above discussed models have been used in XEnoise to compute the integral length scale.

3.5 Vertical Turbulent Velocity Spectra

In order to evaluate the normalized vertical velocity spectra $\tilde{\phi}_{22}(k_1, k_3, y_2)$, the von Kármán isotropic 3D energy spectrum model $E(k)$ is incorporated with the isotropic 3D velocity spectrum tensor Φ_{ij}. The energy density spectrum for the vertical velocity fluctuations in the $k_1 - k_3$ plane parallel to the surface finally reads as follows [5],

$$\Phi_{22}\,(k_1,\ k_3, y_2) = \frac{4}{9\,\pi} \cdot \frac{1}{k_e^2} \cdot \frac{(k_1/k_e)^2 + (k_3/k_e)^2}{\left[1 + (k_1/k_e)^2 + (k_3/k_e)^2\right]^{7/3}} \cdot \left\langle u_2^2 \right\rangle. \tag{18}$$

Within all prediction schemes Xnoise, XEnoise and Rnoise $\phi_{22}(k_1, k_3, y_2)$ is evaluated by Eqn. (18). Also for the moving axis spectrum the model proposed by TNO-TPD [4] has been used in all prediction schemes.

3.6 Wall Pressure Fluctuations Point Frequency Spectrum

In order to compare the measured WPF spectrum with the wave-number frequency spectrum model $P(k_1, k_3, \omega)$ one needs to find the point frequency spectrum. This can be easily deduced by integrating the WPF spectrum model Eqn. (1) in k_1, k_3 direction. From any symmetric double-sided wave number spectrum, the single sided point frequency wall pressure fluctuation spectrum can be found as [29]

$$\Phi_{pp}(\omega) = 2 \cdot \int_0^\infty \int_0^\infty \mathbf{P}(k_1, k_3, \omega) dk_1 dk_3 \tag{19}$$

Also another useful relation between the spectrum in angular frequency to cyclic frequency is [30]

$$G_{pp}(f) = 2\pi \cdot \Phi_{pp}(\omega) \tag{20}$$

Within all the prediction schemes such as Xnoise, XEnoise and Rnoise the WPF spectrum is computed by Eqn. (20).

4 EXPERIMENTAL SETUP

4.1 Wind tunnel and airfoil section

The measurements were performed in the Laminar Wind Tunnel (LWT) [31] of the Institute of Aerodynamics and Gas Dynamics (IAG), University of Stuttgart. The LWT is an open return tunnel with a test section of $0.73\,\mathrm{m} \times 2.73$ m and 3.15 m length and a turbulence level of $Tu_x \approx 0.02$% ($f = 20 - 5000$ Hz) at $U_\infty = 30$ m/s.
The NACA 0012 ('NA0012_04b') airfoil section with a chord length of 0.4 m was made at the IAG workshop in CNC machined negative moulds to ensure maximum contour accuracy. Trailing-edge thickness was made sharp ($h = 0.22 \pm 0.01$ mm) compared to the original design coordinates, to avoid blunt TE noise. The center part of the model was covered with graphite paint coating to get an electrically conducting surface as end contact for hot-wire measurements (not described herein).
In total 62 pressure taps were installed in two oblique rows on suction and pressure side to measure c_p-distributions, employing a PSI module with full scale range of 170 mbar. These c_p-measurements were used to fine-adjust AOAs in order to achieve symmetric pressure distributions, when traversing systems were installed in the test section. Before the detailed BL measurements, polar measurements were performed to determine aerodynamic properties.

4.2 Wall Pressure Fluctuations

Measurement of the wall pressure point spectrum close to the TE – the region of interest for acoustic radiation – was desired for comparison to the theoretical models in an intermediate step. A total of five Kulite LQ-062-15-A ultra-miniature pressure sensors with 15 psi full-scale range were flush mounted 4.6 mm upstream of the TE at x/c=0.989 in a non-equidistant spanwise array on the airfoil (see right of Fig. 1). Their extremely small thickness of about 0.8 mm allows mounting very close to the trailing edge of wind tunnel models. No venting port for static pressure exchange is required, as absolute pressure is sensed. This way the sensors could be fixed in cutouts in the model by a sticky compound and embedded in plasticine. The test matrix included clean and tripped cases at angles-of-attack of -10 to 10 deg and Reynolds numbers of 0.8 to 1.9 million. Because the airfoil is symmetric, pressure and suction side point spectra can be investigated without remounting the sensors.
The sensors were equipped with a B screen protection – a circular array of 8 holes of 0.2 mm diameter on a 1.2 mm diameter circle. Their small size shifts the limit of spatial

resolution to relatively high wave-numbers. Also the dead volume of the sensors is very small, avoiding Helmholtz resonator effects in the frequency range of interest. Disadvantage is a relatively low sensitivity of the sensors of typ. 6.7 mV/psi at 10 V excitation, which requires strong amplification of the signals for purposes of flow measurements at low stagnation pressures.

Keeping electronic noise at a minimum was a target selecting the components of the measurement chain. Bridge amplifiers made by Cosytec based on the INA103 instrument amplifier were used to operate the Kulite sensors from separate ± 12 V lead gel batteries. The AC part of the signals was amplified by 60 dB. A high-pass filter with specified 110 Hz corner-frequency separates AC and DC part and provides pre-emphasis.

AD-conversion of the amplified pressure signals is accomplished by a 24 bit audio-system RME Hammerfall Multiface DSP at a sampling rate of 44.1 kHz per channel. The $\Delta\Sigma$-AD converters with 64 times oversampling provide excellent anti-aliasing filtering at half the data rate. Pressure signals were recorded for 2 min.

The time signals were Fourier transformed using Hanning windows of 4096 points with 50% overlap. The filter responses were corrected subsequently. For correction of spatial resolution, which reduces sensor response at high wave-numbers (in the prevailing case at frequencies above a few kHz), the Corcos correction function [32] with an effective diameter of $d = 1$ mm was employed. Finally the wall pressure spectra of the five sensors were averaged.

4.3 Two-point Turbulent Velocity Correlations

Measurements of turbulent BL characteristics and two-point velocity correlations were performed 1.5 mm downstream of the airfoil TE in the near wake TBL with the wind tunnel operated in constant Re-number mode ($Re = 1.5 \times 10^6$, corresponding to $U_\infty \approx 56$ m/s). Intention was to determine and validate the vertical integral length scales – a crucial parameter in the noise prediction.

A new BL traverse had been developed at LWT especially for the correlation measurements. It was equipped with three Faulhaber high precision gear-motors to provide independent movement of two probes in transversal and movement of one of them in lateral direction. In order to minimize probe vibrations, which can significantly spoil correlation measurements, the whole probe traversing system is tightly connected to the airfoil section via two short pylons on the lower side, see Fig.1. The moving probe support frames were free of play and allowed positioning with an accuracy of $\pm 35\,\mu$m in transversal and $\pm 10\,\mu$m in lateral direction.

X-wire probes were used, which were manufactured completely at IAG to match the requirements of the correlation measurements in the relatively thin BLs. A minimum separation distance of 1.1 mm of the probe centers without contact of the ceramic tubes used for mounting the prongs. Spatial resolution of the probes should be superior over standard Dantec probes, so a wire length of 1 mm was chosen, i.e. a transversal prong separation of 0.7 mm. In lateral direction the prongs are also separated by a distance of 0.7 mm. To improve signal-to-noise ratio at higher frequencies, thinner wires of only $2.5\,\mu$m diameter were used. The four DISA 55M10 CTAs were adjusted to an overheat ratio of $a = 1.8$.

Before the measurements the probes were subjected to complete angular and velocity

calibration in a small calibration wind tunnel. Additionally a static pressure probe is placed at the boundary layer edge to correct small velocity magnitude deviations caused by drifts of ambient temperature, changing the overheat ratio, and contamination of the wires.
Before acquisition with a Keithley DASH16 DAQ card at an aggregate sampling rate of 80645.16 Hz, the signals were split into AC and DC part via 1 Hz low-pass filters. AC part was amplified with programmable gain amplifiers, adjusted indiviually to maximize dynamic range of the AD converters. The filter response and the phase error due to multiplexing were removed via transformation into frequency domain. After back-transformation into time domain the DC part was added and the signals were transformed to velocities using the outlined calibration procedure and subjected to the correlation analyses.

4.4 Acoustic CPV Measurements

The hot-wire based Coherent Particle Velocity (CPV) method [33, 34] was employed for measurements of trailing edge noise on exactly the same airfoil section in the same wind tunnel. Two 45 deg slanted hot-wires (Dantec P12 probes, ø2.5 μm$\times$1.4 mm wires) are placed on both sides of the airfoil in the cross sectional plane upstream of the TE, at a distance being much larger than the boundary layer thickness. The low-noise probe supports made from carbon fibre are mounted approximately 0.6 m downstream of the wind tunnel model in such a way that its wake can pass between them, avoiding extra turbulent inflow noise from the supports and probe vibrations.
The strongly non-isotropic directional sensitivity of the wires is exploited to improve the emergence from the background noise, which is the main advantage of using hot-wire sensors as acoustic sensors. The wires are positioned such that the reception of the airfoil noise is maximized, but background noise approaching from downstream is damped by 3 dB.
Like for the correlation measurements, the hot-wires are operated at an overheat ratio of $a = 1.8$ by very low-noise Dantec 55M10 CTA-bridges, which are adjusted to deliver a flat frequency response up to about 80-120 kHz. Calibration of the hot-wires is done in-situ by variation of the tunnel speed.
The signals of the hot-wire bridges are AC-amplified by AMI-321A ultra low-noise amplifiers (1 nV/$\sqrt{\mathrm{Hz}}$ eqv. input noise) with a gain of 1,000. Final AD-conversion is done by a 24 bit audio-system (RME Hammerfall DSP) at a sampling rate of 44.1 kHz per channel. Additionally one-pole RC low-pass filters at 15 kHz remove excessive high-frequency noise.
Typically, time traces of 10 min are recorded and then processed by Fast Fourier Transforms of blocks of 4096 points to calculate the complex cross spectrum G_{12}. The phase difference $\varphi(f) = \arctan(\mathrm{Im}(G_{12}(f))/\mathrm{Re}(G_{12}(f)))$ is a crucial information for selecting the frequency range, where the airfoil noise is sufficiently higher than the background noise and can therefore be measured. Sound pressure (and particle velocity) radiated from the TE is of dipole type, leading to 180 deg phase shift with a symmetric setup, while the tunnel background noise approaching from downstream shows up with approx. 0 deg phase.
For obtaining quantitative far-field values of sound pressure, a simulation of the response of the whole CPV system to the TE line source is performed to correct non-isotropic sensor response, distance scaling of sound field and source directivity. The results are finally

given as third-octave band sound pressure levels L_p produced by a trailing edge of $L = 1$ m at a distance of $r = 1$ m and an observer placed at a reference angle of 90 deg to the airfoil chord.
A post-processing procedure was developed for correction of the TE noise amplitude loss due to superposed coherent background noise components at the lower end of the measurement range. In case of the 0.4 m NACA 0012 mainly the first two third-octave bands are noticably altered.

5 COMPARISON OF THEORY & EXPERIMENTS

A large database of measured BL quantities for a multitude of test cases at different flow conditions was finally established for several airfoils. In the present paper we want to concentrate on the symmetric case of the NACA 0012 at 0 degrees angle-of-attack, because it is connected with the smallest uncertainties of the flow-field calculation.

5.1 Turbulent boundary-layer profile parameters

The wall normal distributions of the Xnoise, XEnoise and Rnoise predicted turbulence noise source parameters such as $\langle u_2^2 \rangle$, Λ_2 and U_1 at $\frac{x}{c} = 0.999$ and associated trailing-edge noise spectra for NACA 0012, $Re = 1.5e6, Ma = 0.166, AOA = 0°$ are compared with wind tunnel measurement data and depicted in Figures 2, 3 and 4 respectively. A comparison plot of the Xnoise predicted and measured data can be seen in Fig. (2). The figure legends Xnoise_mp131 and Xnoise_mp241 denote the BL methods based on Swafford and Coles law of wall respectively. The measured data for the same flow condition are denoted by legend Exp. LWT (HW). From the left most plot it can be clearly seen that the agreement of wall normal U_1 distribution is reasonably good, with a small shift. The same plot shows suction and pressure side $\langle u_2^2 \rangle$ distribution (solid line: suction side, dashed: pressure side). A huge disagreement between measured and predicted data is clearly visible at the near wall region as well as the maximum of $\langle u_2^2 \rangle$ position. It should be noted that within Xnoise, Eqn. (9) has been employed in order to model $\langle u_2^2 \rangle$. It has been observed that for the suction side, Xnoise predicted $\langle u_2^2 \rangle$ values are almost always over-predicted, and for some cases it even shows unphysical results, i.e. for a symmetric NACA 0012 airfoil at $c_l = 0$ the suction and pressure side BL development should be same, but it is not the case as depicted in the Figure 2. Moreover, approximation of different α values at suction and pressure side of the airfoil as proposed by TNO [4] is very crude. If one looks into the mathematical relationships of $-\langle u_1 u_2 \rangle$ and $\langle u_2^2 \rangle$, and also Prandtl's mixing length hypothesis (Eqn. 8), it can be seen that selection of a proper value for α is not trivial. However, from the two-point correlation measurement data it is possible to derive an expression for the parameter f_{12} (see Eqn. (8)) to consider the anisotropy effect.

The XEnoise and Rnoise predicted $\langle u_2^2 \rangle$ and U_1 data for the same test case are depicted in the left most plots of Figures 3 and 4. The agreement between the predicted streamwise mean velocity distribution U_1 with the measured data is pretty much better. Especially, for the Rnoise method it's more promising. It is observable from the Rnoise predicted $\langle u_2^2 \rangle$ data, that the isotropic (legends with Rnoise: SST$\langle u_2^2 \rangle |_{iso}$) approximation matches

reasonably well with a small overprediction, whereas the anisotropic model [5] (legend with Rnoise: SST$\langle u_2^2 \rangle\,|_{aniso}$) tends to capture the measured data more accurately.
Middle plots of Figures 2, 3 and 4 demonstrates the result of the Λ_2 distribution by Xnoise, XEnoise and Rnoise methods together with the measurement data. Clearly, for this particular case, a reasonably good agreement of the predicted Λ_2 distributions is visible for Xnoise and Rnoise method. But for this case XEnoise Λ_2 data is overestimated. It is very important to note that for the current TBL-TE noise prediction model both sides of the turbulence noise sources contribute to the total noise spectra. Therefore, proper estimations of both sides (suction as well as pressure side) turbulence BL parameters are equally important. More validations in previous investigations [5, 6] concluded that at highly loaded BL (high lift cases) the suction side maximum Λ_2 values are almost always over-predicted, whereas pressure side data are underpredicted. The behavior for the very lightly loaded BL (low lift condition) is vice versa [6].
In order to check the accuracy and efficiency of the prediction model Eqn. 3, all the measured turbulence parameters have been directly used as an input to evaluate the total TE noise level. The prediction model captures the total noise level as well as the peak position excellently and can be seen in Fig. 4 and 5 with legend Exp_in.

5.2 Wall Pressure Fluctuations

The point WPF power density spectra predicted with the Rnoise model (following Eqn. (20)) are compared to the averaged spectra measured with the Kulites at AOAs of [0,2,4,6] degrees in Fig. 5. The frequency range where facility noise and 50 Hz harmonics influenced the measured levels significantly is indicated by open symbols. Increasing AOA, the suction side spectra increase in level and maxima shift to lower frequencies, while on the pressure side amplitudes drop and maxima shift to higher frequencies as expected. It can be seen, that the shape and staggering of the predicted spectra is very similar. Maxima are shifted to slightly lower frequencies and amplitudes are a bit lower. Using the measured BL quantities as an input to the prediction model, agreement of the spectrum for zero AOA is even better, which confirms validity of the prediction approach for the wavenumber-frequency spectrum. Recently WPF measurements were performed by RISØ [35] in the LM wind tunnel on a NACA 0015 of 0.9 m chord. Unfortunately direct comparisons of measurements cannot be performed, as the most downstream microphone position was at $x/c = 0.567$, far upstream of the TE, and the airfoil contour is different.

5.3 Far-field Trailing-Edge Noise Spectra

The impact of each input noise source parameter into the total predicted far-field noise levels at 1 m distance can be seen in the right most plots of Figures. 2, 3 and 4. The Xnoise variants underpredict the measured spectra significantly. In particular the Swafford profile formulation produces spectra with an unphysical dip around 3 kHz. The Coles profile version avoids that, but amplitudes in the high frequency range are too low. XEnoise provides significantly improved predictions, which reflect the shape of the measured spectrum perfectly. It can be realized easily, that this is aresults of the more realistic distributions of vertical velocity fluctuations. It should be noted, that length scales evaluated from the experiments according to the new formulation (R_{22} normalized by $\langle u_2^2 \rangle (\mathbf{y}, t)$ data only in Eqn. 11) are not optimally suited for comparison, because they are distorted. This issue is discussed in [27]. Looking at the Rnoise predictions it is obvious, that the general shape is also close to the measurements and levels match very well. Best agreement is achieved, when the measured BL parameters are fed into the prediction model, which makes the far-field spectrum practically collapse with the measured one. Some uncertainties in all the measured magnitudes may compensate, however this shows nicely the validity of the present noise prediction model.

6 CONCLUSIONS

A detailed evaluation and assesment of a TBL-TE noise prediction model (Eqn. (3)) has been conducted based on three different sets of measurement data namely, turbulence parameters, wall-pressure fluctuations and far-field TE noise spectra. The investigated test cases show that the numerical WPF and far-field radiated noise models capture the measured peak amplitude level as well as peak position remarkably well, if the turbulence noise source parameters are estimated properly including turbulence anisotropy effects. Among other methods (i.e. Xnoise, XEnoise) the RANS based prediction scheme Rnoise shows most promising results.

7 ACKNOWLEDGEMENTS

A part of the present work is conducted in the frame of the EU project UpWind and the authors would like to acknowledge the European Commission. Furthermore, Andrey Ivanov is thanked for valuable discussions about length scale evaluations.

References

[1] S. Oerlemans and B. Méndez López. Localisation and quantification of noise sources on a wind turbine. *Wind Turbine Noise: Perspectives for Flow Control, Berlin, October 17-18*, 2005.

[2] K.I. Chandiramani. Diffraction of evanescent wave with application to aerodynamically scattered sound and radiation from unbaffled plates. *J. Acoust. Soc. Amer.*, 55:19–29, 1974.

[3] W.K. Blake. *Mechanics of Flow-Induced Sound and Vibration Vol. I and II*. Academic Press, INC., 1986.

[4] R. Parchen. Progress report draw, a prediction scheme for trailing-edge noise based on detailed boundary-layer characteristics. Report, TNO Institute of Applied Physics, The Netherlands, 1998. TNO-report HAG-RPT-980023.

[5] M. Kamruzzaman, Th. Lutz, A. Herrig, and E. Krämer. RANS based prediction of airfoil trailing edge far-field noise: Impact of isotropic & anisotropic turbulence. In

AIAA-2008-2867-685, 14th AIAA/CEAS Aeroacoustics Conference Proc., Vancouver, Canada, 5-7 May 2008.

[6] T. Lutz, A. Herrig, W. Würz, M. Kamruzzaman, and E. Krämer. Design and wind-tunnel verification of low-noise airfoils for wind turbines. *AIAA Journal*, 45(4):779–792, 2007.

[7] J. G Schepers, A. Curvers, S. Oerlemans, K. Braun, Th. Lutz, A. Herrig, and W. Würz. SIROCCO: SIlent ROtors by aCoustiC Optimization. In *Conf. Proc. , Wind Turbine Noise-2007, Lyon, France*, September 2007.

[8] M. Kamruzzaman, K. Nübler, Th. Lutz, and E. Krämer. IAGNOISE: An airfoil noise prediction tool with graphical frontend. Poster, EPFDC, Keele, UK, July 2008.

[9] A. Herrig, W. Würz, Th. Lutz, and E. Krämer. Trailing-edge noise measurements using a hot-wire based coherent particle velocity method. *24th Applied Aerodynamics Conference, San Francisco, California, 5 – 8 June 2006*, (2006-3876), 2006.

[10] M. Kamruzzaman, Th. Lutz, and E. Krämer. An approach to RANS based prediction of airfoil trailing edge far-field noise. In *Conf. Proc. , Wind Turbine Noise-2007, Lyon, France*, September 2007.

[11] S. Glegg, B. Morin, O. Atassi, and R. Reba. Using RANS calculations of turbulent kinetic energy to provide predictions of trailing edge noise. *14th AIAA/CEAS Aeroacoustics Conference, Vancouver, Canada, 5-7 May, 2008*.

[12] T. F. Brooks and T. H. Hodgson. Prediction and comparison of trailing edge noise using measured surface pressures. (80-0977), June 1980. Presented at the AIAA 6th Aeroacoustics Conference, Hartford, CT.

[13] Thomas F. Brooks, D. Stuart Pope, and Michael A. Marcolini. Airfoil self-noise and prediction. Reference Publication 1218, NASA, 1989.

[14] B. A. Singer, K. S. Brentner, D. P. Lockard, and G. M. Lilley. Simulation of acoustic scattering from a trailing edge. 1999-0231, 1999.

[15] R. Ewert and W. Schröder. On the simulation of trailing edge noise with a hybrid LES/APE method. *Jornal of Sound and Vibration*, 270:509–524, 2004.

[16] M. Meinke R. Ewert and W. Schröder. Computation of trailing edge noise via LES and acoustics perturbation equations. Paper 2002-2467, AIAA, 2002.

[17] Alison L. Marsden, Meng Wang, J. E Dennis Jr, and Parviz Moin. Trailing-edge noise reduction using derivative-free optimization and large-eddy simulation.

[18] Mattias Billson, Lars-Erik Eriksson, Peter Jordan, and Lars Davidson. Anisotropic formulation of the velocity correlation tensor. Internal Report 04/02, Department of Mechanical Engineering, Chalmers University of Technology, Sweden, 2004.

[19] J.G. Schereps, A.P.W.M. Curvers, S. Oerlemans, K. Braun, T. Lutz, A. Herrig, W. Würz, and B. Méndez López. SIROCCO: Silent rotors by acoustic optimisation. *Wind Turbine Noise: Perspectives for Flow Control, Berlin, October 17-18*, 2005.

[20] Mark Drela. Xfoil: An analysis and design system for low reynolds number airfoils. In T. J. Mueller, editor, *Low Reynolds Number Aerodynamics (Conference Proceedings)*, pages 1–12, University of Notre Dame, Paris, June 1989.

[21] David C. Wilcox. *Turbulence Modeling for CFD*. DCW Industries, Inc., 2nd edition, 1998. ISBN 0-9636051-5-1.

[22] N. Kroll, C. C. Rossow, D. Schwmborn, K. Becker, and G. Heller. MEGAFLOW – a numerical flow simulation tool for transport aircraft design. In *Proceedings of the 23rd International Congress of Aeronautical Sciences*. ICAS, 2002. Toronto.

[23] R. A. Kraichnan. Pressure fluctuations in turbulent flow over a flat plate. *Journal of Acoustics Soc. America*, 28:378–390, 1956.

[24] R. T. Panton and J. H. Linebarger. Wall pressure spectra calculations for equilibrium boundary layers. *Journal of Fluid Mechanics*, 65:261–287, 1974.

[25] Thorsten Lutz, Werner Würz, and Siegfried Wagner. First periodic progress report SIROCCO, design and analysis of low noise airfoils. Report, Institute of Aerodynamics and Gas Dynamics, University of Stuttgart, June 2003.

[26] P. Moriarty. Nafnoise: A program for calculating 2-d airfoil noise. Design code, National Wind Technology Center, USA, December 2003.

[27] M. Kamruzzaman, Th. Lutz, A. Ivanov, A. Herrig, W. Würz, and E. Krämer. Evaluation of measured anisotropic turbulent two-point correlation data for the accurate prediction of the turbulence noise sources. In *15th AIAA/CEAS Aeroacoustics Conference Proc., Miami, USA*, 10-13 May 2009.

[28] J. O. Hinze. *Turbulence*. McGraw-Hill, 1975.

[29] Julius S. Bendat and Allan G. Piersol. *Random Data, Analysis and Measurement Procedures*. John Wiley & Sons Inc., 3 edition, 2000.

[30] Peter D. Lysak. Modeling the wall pressure spectrum in turbulent pipe flows. 128:217–222, 2006.

[31] F. X. Wortmann and D. Althaus. Der Laminarwindkanal des Instituts für Aero- und Gasdynamik an der Technischen Hochschule Stuttgart. *Zeitschrift für Flugwissenschaften*, 12(4):129–134, April 1964.

[32] Richard M. Lueptow. Transducer resolution and the turbulent wall pressure spectrum. 97(1):370–378, 1995.

[33] Andreas Herrig, Werner Würz, Thorsten Lutz, and Ewald Krämer. Trailing-edge noise measurements using a hot-wire based coherent particle velocity method. 24th Applied Aerodynamics Conference, San Francisco, California, 5-8 June 2006. AIAA 2006-3876.

[34] Andreas Herrig, Werner Würz, Ewald Krämer, and Siegfried Wagner. New CPV-Results of NACA 0012 Trailing-Edge Noise. Novosibirsk, 30.06.-06.07. 2008. Int. Conference on Methods of Aerophysical Research ICMAR.

[35] Franck Bertagnolio. NACA0015 measurements in lm wind tunnel and turbulence generated noise. Risoe report: R-1657(en), RISOE, Wind Energy Department, November 2008.

Nomenclature

Latin & Greek Symbols

c	$[m]$	Chord length
c_d, c_l, c_f	[-]	Airfoil drag, lift and skin friction coefficient
c_0	$[m/s]$	Speed of sound
$\frac{dU}{dy}$	$[1/s]$	Streamwise mean velocity gradient in y_2 direction
$f_{11}^{aniso}, f_{22}^{aniso}$	[-]	Anisotropic factor $f_{11}^{aniso} = \frac{\langle u_1^2 \rangle}{2/3k_T}, f_{22}^{aniso} = \frac{\langle u_2^2 \rangle}{2/3k_T}$
f_{12}, f_{23}, f_{31}	[-]	Anisotropic factor $f_{12} = \frac{\langle u_1^2 \rangle}{\langle u_2^2 \rangle}, f_{23} = \frac{\langle u_2^2 \rangle}{\langle u_3^2 \rangle}, f_{31} = \frac{\langle u_3^2 \rangle}{\langle u_1^2 \rangle}$
$S(f)$, $G(f)$	$[Pa^2/Hz]$	Double-sided (wholeline) & single-sided PSD
k_T	$[m^2/s^2]$	Turbulence kinetic energy
k_e	$[1/m]$	Wavenumber of the energy containing eddy
$k_1, k_2, k_3, \mathbf{k}$	$[1/m]$	Waveno in y_1, y_2, y_3 coordinate direction & wave vector
L, l	$[m]$	Turbulence length scale
$L_p, L_{p,ss}, L_{p,ps}$	$[dB]$	Total, suction & pressure side sound pressure level
$P(\mathbf{k}, \omega)$	$[Pa^2 m^2/Hz]$	Wavenumber frequency spectrum for wall pressure fluctuations
$\tilde{R}_{ij}, R_{ij}^{(1)}$	[-]	R_{ij} normalized by $\sqrt{\langle u_i^2(\mathbf{y}) \rangle \langle u_j^2(\mathbf{y}) \rangle}$, $\mathbf{y}$ position data
$\hat{R}_{ij}, R_{ij}^{(12)}$	[-]	R_{ij} normalized by $\sqrt{\langle u_i^2(\mathbf{y}) \rangle \langle u_j^2(\mathbf{y}+r) \rangle}$, $\mathbf{y}$ & $\mathbf{y}+r$ both position data
U_1, U_2, U_3	$[m/s]$	Streamwise, vertical & spanwise mean velocity
U_c	$[m/s]$	Mean convective velocity of wall pressure fluctuations $\approx 0.7 \cdot U_1$
U_∞, U_e	$[m/s]$	Freestream and boundary-layer edge velocity
$\langle u_1^2 \rangle, \langle u_2^2 \rangle, \langle u_3^2 \rangle$	$[m^2/s^2]$	Streamwise, vertical & spanwise Reynolds stresses
α	[-]	empirical factor for vertical fluctuations from TNO-TPD
$\delta_1, \delta_2, \delta_3,$	[mm]	Boundary-layer displacement, momentum and energy thickness

$\tilde{\phi}_{22}(y_2, k_1, k_3)$	$[m^2]$	Normalized vertical turbulence energy spectra
Φ_m	$[s]$	Moving axis spectra
$\Lambda_{ii}^{(n)}$, $\Lambda_i^{(n)}$	$[mm]$	Integral length scale of i component of velocity separation in n direction
Λ_f, Λ_g	$[mm]$	Isotropic longitudinal and traverse integral length scale
$\Lambda_{22}^{(2)}$, $\Lambda_{22}\|^1, \Lambda_2$	$[mm]$	Integral length scale of $\langle u_2^2 \rangle$ velocity separation in 2 (vertical) direction
$\Lambda_{22,fit}^{(2)}$, $\Lambda_{22,fit}\|^1$	$[mm]$	$\Lambda_{22}^{(2)}$ evaluated by $\tilde{R}_{22}$ curve fitting approach

Subscripts/Superscript/Abbreviations and Acronyms

aniso	Anisotropic turbulence
CPV	Coherent Particle Velocity
exp, EXP	Experimental data
Exp_in	Direct use of experimental noise source data inside the prediction model
EARSM	Explicit Algebric Reynolds Stress turbulence model
iso	Isotropic turbulence
$k-\omega$	Wilcox $k-\omega$ two-equation turbulence model
mp131	Swafford profile for noise source evaluation
mp241	Coles profile for noise source evaluation
RANS	Reynolds Average Navier-Stokes equation
ss, ps	suction side & pressure side
SST	Menter's Shear Stress Transport two-equation turbulence model
SPL	Sound Pressure Level
te, TE	trailing edge
LWT	Laminar Wind Tunnel of the IAG
LM	LM Wind Tunnel at Denmark
RANS	Reynolds-averaged Navier-Stokes
TBL-TE	Turbulent Boundary-Layer Trailing-Edge (interaction noise)
BL	Boundary-Layer
HW	Hot-wire probe measured data
XHW	X type hot-wire probe measured data
Xnoise	XFOIL based TBL-TE noise prediction method
XEnoise	XFOIL and EDDYBL based TBL-TE noise prediction method
Rnoise	RANS based TBL-TE noise prediction method
WPFs	Wall pressure fluctuations

Figures

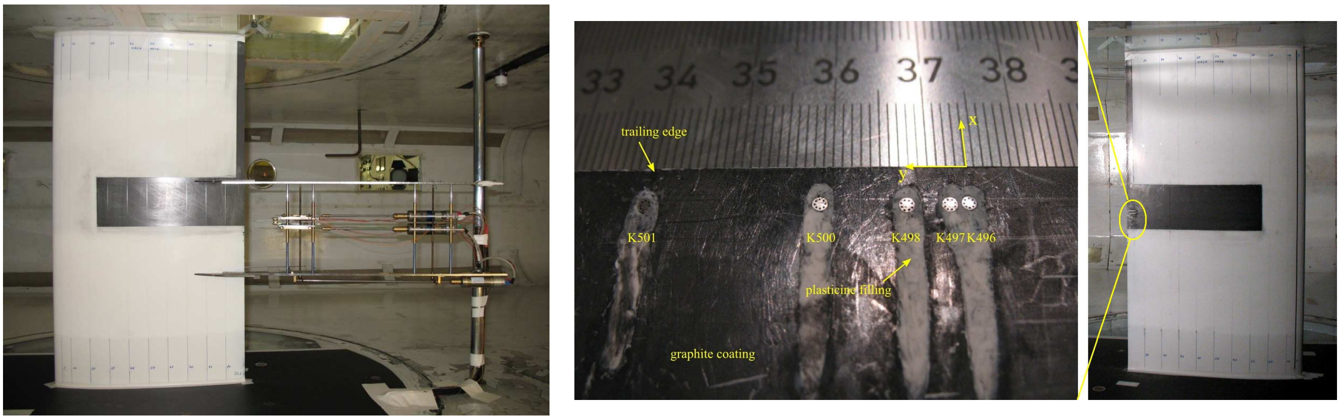

Figure 1: Two-point correlation measurement traversing system (left) mounted together with the NACA 0012 test section & Pressure sensors (right).

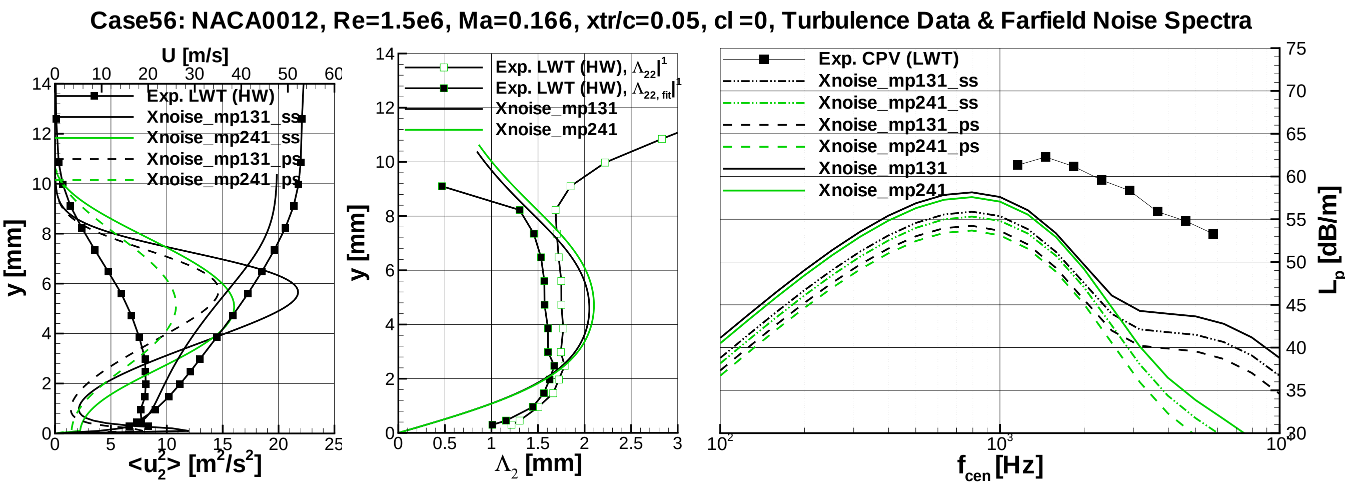

Figure 2: Xnoise predicted suction & pressure side turbulence data and TE noise spectra.

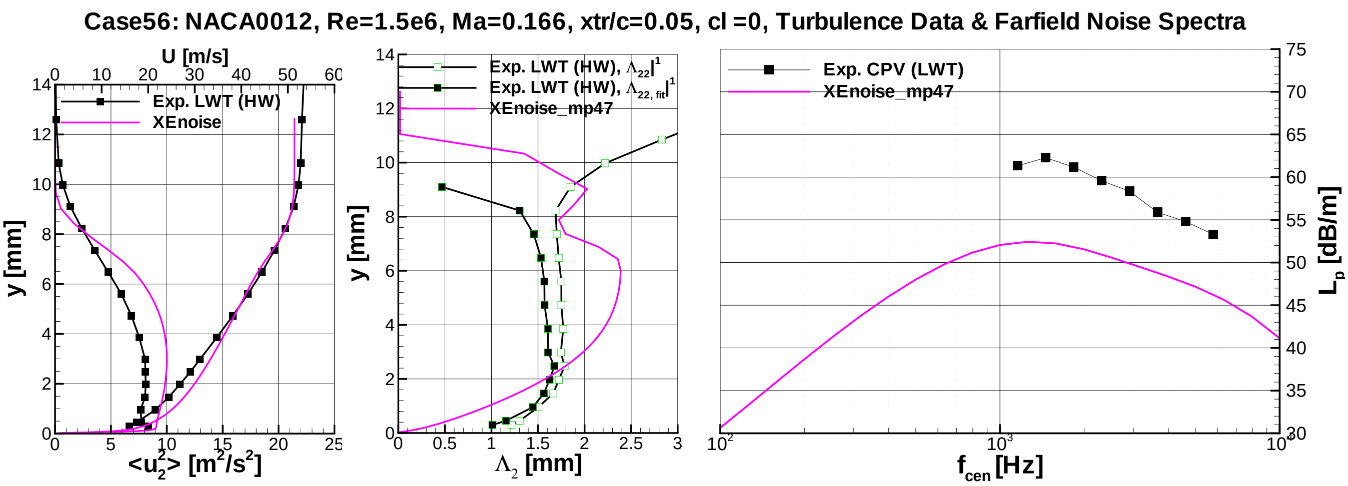

Figure 3: Turbulence parameters and Far-field noise spectra: XEnoise.

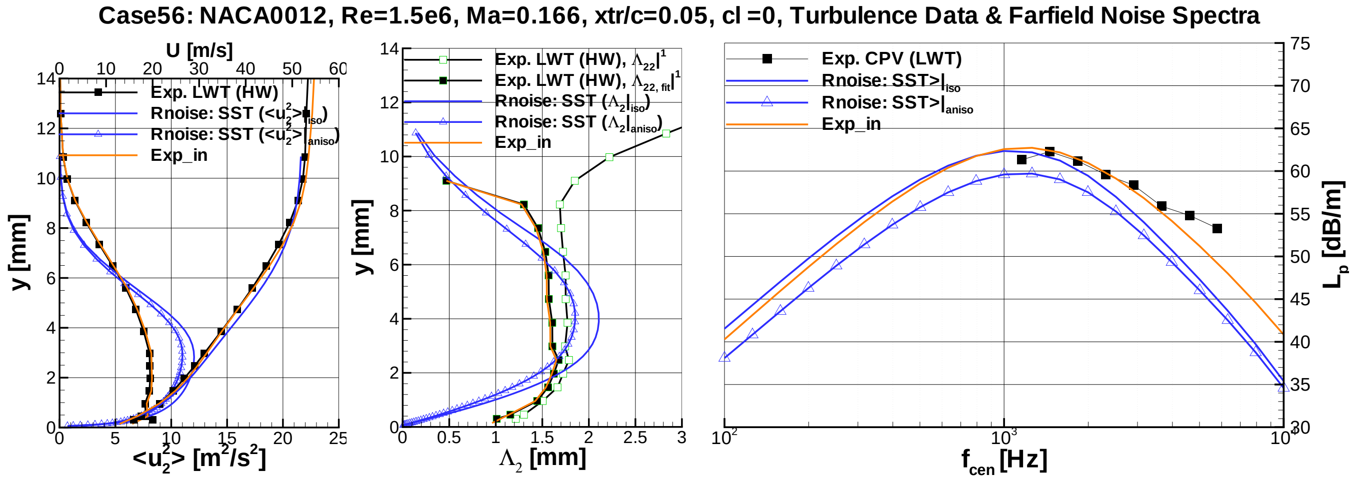

Figure 4: Turbulence parameters and Far-field noise spectra: Rnoise & Exp_in.

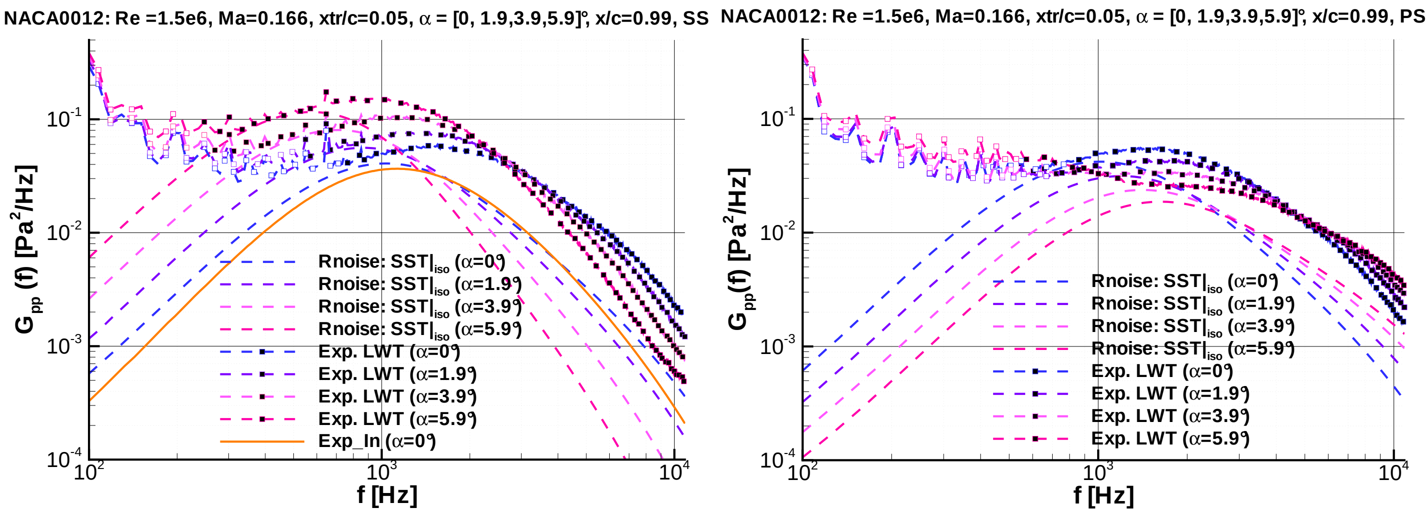

Figure 5: Rnoise predicted & measured WPF spectrum G_{pp} at $\frac{x}{c} = 0.99$: NACA 0012.

Third International Meeting
on
Wind Turbine Noise
Aalborg Denmark 17 – 19 June 2009

An estimation method of the amplitude modulation in wind turbine noise for community response assessment

Seunghoon Lee, Kyutae Kim, Seungmin Lee, Hogeon Kim and Soogab Lee
AeroAcoustics and Noise Control Laboratory
Department of Mechanical and Aerospace Engineering
Seoul National University, Seoul, Korea
kami00@snu.ac.kr, saeroby9@snu.ac.kr, vitamin1@snu.ac.kr, hgmania1@snu.ac.kr, solee@snu.ac.kr

Abstract

Wind turbine noise is known to be easily perceived even when the sound level is low. This may be concerned with amplitude modulation characteristics of wind turbine noise. Several studies have attempted to examine a relationship between amplitude modulation and human perception (or annoyance). However, there are only few studies on quantifying amplitude modulation of sound from wind turbine. In this paper, a practical method to measure amplitude modulation from recorded sound is proposed. This method is based on the assumptions as follows: (1) recorded sound signal has sinusoidal amplitude modulation, (2) blade passing frequency of a wind turbine is known, and (3) fluctuation of background noise is negligible. A double fast Fourier transform was employed to find the modulation depth at each frequency band. Laboratory tests were performed to identify a relationship between noise annoyance and modulation depth of wind turbine noise, which is calculated by the proposed method. The result clearly shows that there is a correlation between noise annoyance and amplitude modulation.

Introduction

One of the most important characteristic of wind turbine noise is amplitude modulation. Near a wind turbine, amplitude modulation in the noise is perceived due to an effect of observer location [1]. This effect decreases as an observer becomes more distant from the wind turbine. However, there are several studies that in certain conditions the amplitude modulation is still perceived even far from the turbines [2]. Amplitude modulation of wind turbine noise makes it difficult to mask by background noise, so that residents near wind turbines can relatively easily detect wind turbine noise [3]. As wind turbines operate continuously for long periods of time, wind turbine noise could have a significant impact on the residents even at low sound levels.

Amplitude modulation characteristic in wind turbine noise also has a possibility to increase annoyance. Previous field study showed that verbal descriptions which imply periodic sound fluctuation such as swishing, whistling and pulsating were highly correlated to noise annoyance [3]. Thus, a study for community response assessment with respect to amplitude modulation should be required.

In order to assess community response, it is necessary to quantify amplitude modulation in wind turbine noise, which is exposed to residents. However, previous measurement methods for amplitude modulation are not appropriate for community response assessment. A common method to measure amplitude modulation is direct measurement of modulation depth. In this method, modulation depth is determined by the difference between L_{max} and L_{min} from a spectrogram [4] or A-weighted sound pressure level with time weighting F [5]. Since this procedure should be treated manually, this method cannot be applied for a long time measurement, which is required for community response assessment. Another method employs percentile sound levels instead of L_{max} and L_{min} [6]. This method defines modulation depth as the difference between L_5 and L_{95}. In ref. 6, one-third octave band spectral modulation depth was obtained by the method. However, it can be applied only when the overall sound level does not gradually increase or decrease. Legarth [7] proposed that fluctuation strength can be a metric for amplitude modulation in wind turbine noise. However, since a model of fluctuation strength is based on temporal variation of a masking pattern [8], scale of fluctuation strength is too large to measure amplitude modulation in wind turbine noise. Fluctuation strength is almost zero until a modulation depth of about 3 dB [8], which is a common modulation depth for wind turbine noise.

The purpose of this study is to make a simple and robust method to measure modulation depth of wind turbine noise for community response assessment. A laboratory test was also performed to examine a relationship between noise annoyance and amplitude modulation in wind turbine noise. Stimuli for the test were created by modifying recorded wind turbine noise. Modulation depth of the stimuli is measured by the proposed method.

Estimation Method

It is difficult to measure modulation depth of wind turbine noise precisely. Also, modulation depth of wind turbine noise is not a single value but a function of frequency. Thus, although amplitude modulation in wind turbine noise is not purely sinusoidal, to find modulation depth simply, we assumed that the wind turbine noise is sinusoidally amplitude modulated. Figure 1 shows the procedure for estimating amplitude modulation in wind turbine noise.

Procedure

First, by applying the fast Fourier transform to each time step of a wind turbine noise signal, a spectrogram is obtained, as shown in Fig. 1.A. The time step should be small enough to identify amplitude modulation of the signal. Next, for each frequency band, the fast Fourier transform is applied again but this time along the time axis.

Fig. 1.B shows a result of the FFT analysis for a frequency band of 1 kHz. If the signal is amplitude modulated at a blade passing frequency, two dominant peaks will be visible, as shown in Fig. 1.B. One peak at 0Hz represents a steady root-mean-square value of the signal. On the other hand, the other peak at the blade passing frequency represents sinusoidal amplitude modulation of the signal.

Figure 1.A **Figure 1.B**

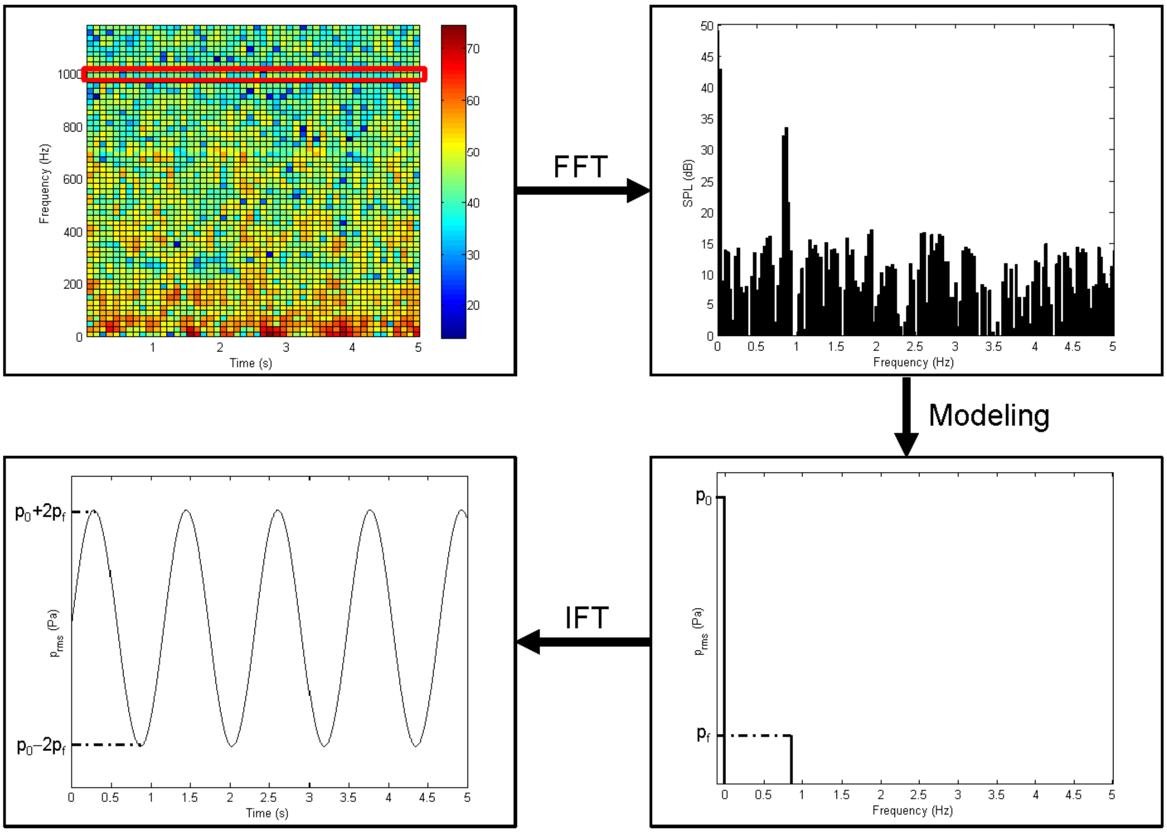

Figure 1.D **Figure 1.C**

Figure 1 The procedure for estimating amplitude modulation in wind turbine noise

Let us assume that all other values except the two peaks are neglected. This assumption is only valid when the peaks are sufficiently higher than other values, which means that the modulation depth should be more than some minimum value. In our experience, this assumption is possible as long as the modulation depth at each frequency band is more than about 1dB. If the two peaks are sufficiently narrow, the result of the FFT analysis in Fig 1.B is also modeled as two tones, as shown in Fig 1.C. Finally, the inverse Fourier transform is applied to the result in Fig. 1.C. The modulation depth is defined as the difference between maximum and minimum value. So the modulation depth at a frequency band is

$$\Delta L = 20\log\frac{p_0 + 2\times p_f}{p_{ref}} - 20\log\frac{p_0 - 2\times p_f}{p_{ref}}$$

Or,

$$\Delta L = 20\log\frac{p_0 + 2\times p_f}{p_0 - 2\times p_f}$$

Modulation depth, ΔL and modulation factor, m are related by [8]

$$\Delta L = 20\log\frac{1+m}{1-m}$$

Thus, the modulation factor at a frequency band is defined as

$$m = 2\times\frac{p_f}{p_0}$$

This procedure is applied to all frequency bands, then the spectral modulation depth or modulation factor is obtained.

Discussion

By applying the double fast Fourier transform to wind turbine noise, the modulation factor at each frequency band can be obtained from a simple formula. It may not be a precise measurement method, but the formula gives a good approximation to the amplitude modulation in the wind turbine noise. If the blade passing frequency of the wind turbine is known or the modulation depth is large enough to detect automatically the modulation frequency, this estimation procedure can be implemented in computer code. Since the method is only valid when the modulation depth is more than about 1dB, it cannot be applied to identify whether the signal is amplitude modulated or not. However, considering that just-noticeable modulation depth for 4Hz sinusoidally amplitude modulated white noise is about 0.7dB [8], the method can provide a good result as long as amplitude modulated noise is detectable.

Listening test

Sound recording

Two sound samples for a listening test were recorded from a 1.5 MW wind turbine, which is manufactured by NEG-Micon. Sound recording was accomplished by Brüel & Kjær 2250 sound level meters. One sample (Sample I) was recorded at a distance of hub height (62 m) at a wind speed of 4~6m/s with opposite wind direction from the turbine. This sample had the amplitude modulation which is described as whooshing sound. The other sample (Sample II) was recorded at a distance of hub height (62 m) from the turbine at a wind speed of 10~12m/s from the right side of the turbine. This sample also had the amplitude modulation, but which is described as swishing sound. The modulation frequency of both samples is 0.865 Hz which is a blade passing frequency of the wind turbine. Figure 2 shows the one-third octave band spectrum of the two samples.

By using the estimation method for amplitude modulation, spectral modulation depth of two samples is obtained, as shown in Fig. 3. Frequency resolution of the modulation spectrum was set to 200 Hz. Maximum modulation depth of Sample I is approximately 5 dB at 1 kHz, while that of Sample II is approximately 12 dB at 8 kHz.

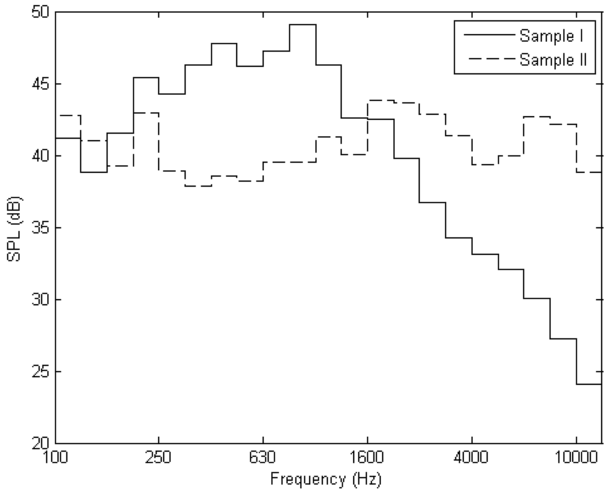

Figure 2 One-third octave band spectrum of Sample I and Sample II

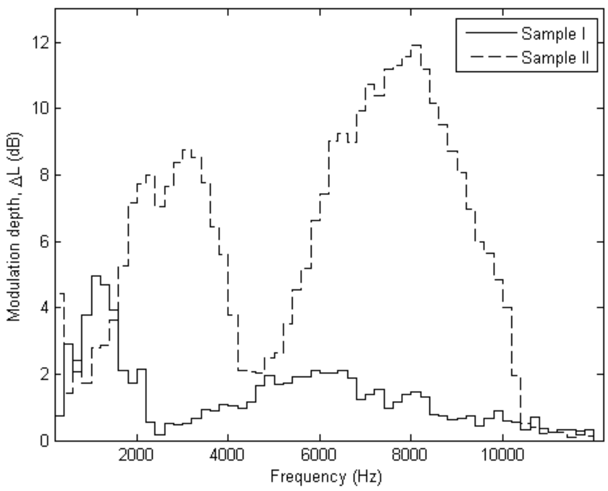

Figure 3 Spectral modulation depth of Sample I and Sample II

Stimuli

In order to conduct a listening test to find a relation between amplitude modulation and noise annoyance, stimuli which have variety of modulation depths are required. In this study, stimuli were designed by modifying the recorded samples.

Figure 4 shows that the signal processing procedure to modify amplitude modulation of sound samples. First, a fast Fourier transform is performed in order to get a frequency spectrum of the sample. This frequency spectrum is used to make a filter whose magnitude is same as the sample. Then, this filter is applied to a white noise, so that the filtered white noise is modeled as an unmodulated sample. This model is reasonable because the aerodynamic noise, which is a dominant noise source of modern wind turbine, is broadband in nature [3] and broadband sound has somewhat random character [9]. The filtered white noise also has the same frequency spectrum as recorded wind turbine noise. Finally, by merging the original sample with the filtered white noise, a new signal whose modulation depth is reduced from the original signal is obtained. Modulation depth of the new signal can be adjusted by the sound level of the white noise.

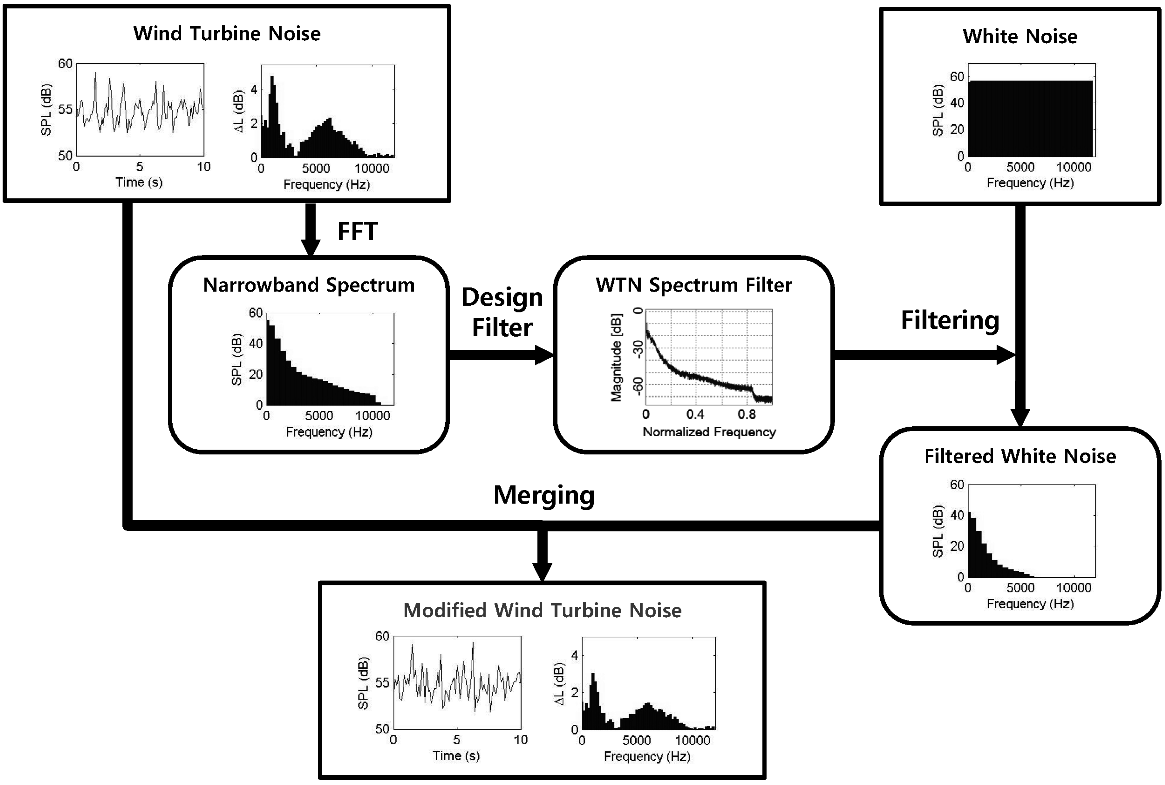

Figure 4 The signal processing procedure for wind turbine noise

A total of 50 stimuli (2 base samples x 5 equivalent sound levels x 5 degrees of modulation) were produced by the procedure in Fig. 4. The equivalent sound level was varied in steps of 5 dB from 35 to 55 dB(A). Figure 5 shows the spectral modulation factors of stimuli at an L_{Aeq} of 35 dB(A). The maximum modulation factor of the stimuli originated from Sample I was varied from 0.28 to 0.10, while that of the stimuli originated from Sample II was varied from 0.60 to 0.12. Figure 6 presents the narrowband spectrum of stimuli at an L_{Aeq} of 35 dB(A). Although the stimuli are modified from the base samples, the frequency spectrum of the stimuli is almost similar to those of the base samples.

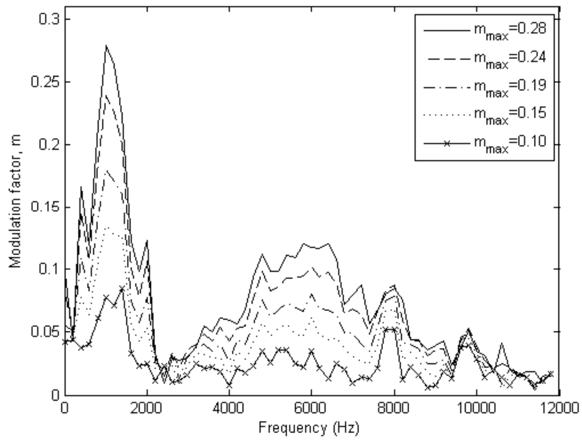

Figure 5.A Sample I

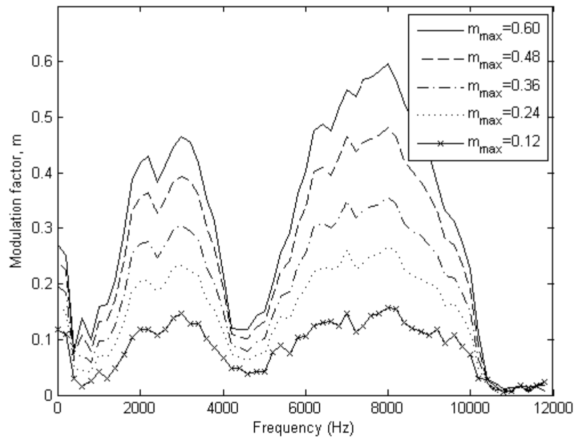

Figure 5.B Sample II

Figure 5 Spectral modulation factors of the stimuli at 35dB L_{Aeq}

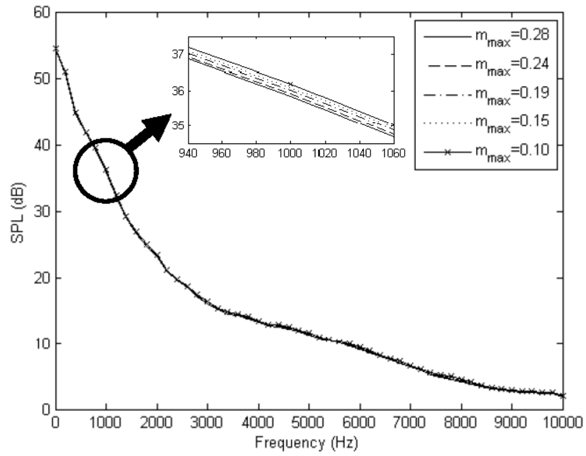

Figure 6.A Sample I

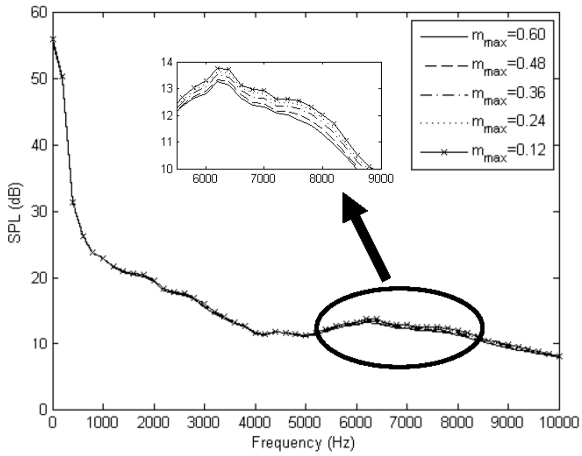

Figure 6.B Sample II

Figure 6 Narrowband analysis of the stimuli at 35dB L_{Aeq}

Listening tests

A total of thirty subjects, fifteen males and fifteen females, between 20 and 30 years of age, participated in the listening tests. The listening tests were conducted in an anechoic chamber (3m x 3m x 2m) where the background noise level was between 20 and 25 dB(A). The subjects were exposed to the stimuli through the supra-aural earphone (Sennheiser HD25-1) calibrated by Brüel & Kjær PULSE Type 3560C and Head and Torso Simulator (HATS) Type 4128.

Prior to the listening tests, a screening test was performed with pure tones which consist of 6 bands at the center frequency of octave band from 250 Hz to 8000 Hz. None of the subjects had a hearing loss greater than 20 dB of reference equivalent threshold sound pressure level (RETSPL) [10].

The subjects were told that they were going to be presented with two kinds of wind turbine sounds. They were instructed to record the degree of annoyance after each stimulus. Response was recorded on an 11-point numerical scale [11].

	Test I	Test II
Base sample	Sample I	Sample II
Number of stimuli	25	25
L_{Aeq}	35~55 dB(A)	35~55 dB(A)
Maximum modulation factor (m_{max})	0.10~0.28 @ 1kHz	0.12~0.60 @ 8kHz

Table 1 The listening tests

The listening tests were carried out in two steps. First, the 25 stimuli originated from Sample I were delivered randomly to the subject. After 3-min rest, the 25 stimuli originated from Sample II were presented in the same manner. Each stimulus lasted for 30 s and the interval between the stimuli was 10 s. The listening tests took approximately 40 min for each subject.

Result

Statistical analysis was accomplished by a two-way analysis of variance (ANOVA) with factors of A-weighted equivalent sound level and modulation factor, followed by pairwise comparisons using Tukey's HSD. A p-value of < 0.05 was regarded as statistically significant.

Mean annoyance ratings for each modulation factor are presented in Fig. 7 and 8. The annoyance rating increased significantly with L_{Aeq} for both tests [Test I : $F(4,725) = 114.7$, $p < 0.00001$; Test II : $F(4,725) = 126.2$, $p < 0.00001$]. The effect of modulation factor on the annoyance level was also significant [Test I : $F(4,725) = 2.93$, $p = 0.02$; Test II : $F(4,725) = 4.03$, $p = 0.003$]. For test I, the annoyance for the stimuli of m_{max}=0.28 was only significantly higher than the annoyance for the stimuli of m_{max}=0.10 [$p = 0.02$]. In case of test II, on the other hand, the stimuli of m_{max}=0.60 and m_{max}=0.48 were significantly more annoying than the stimuli of m_{max}=0.12 [$p = 0.002$; $p = 0.029$].

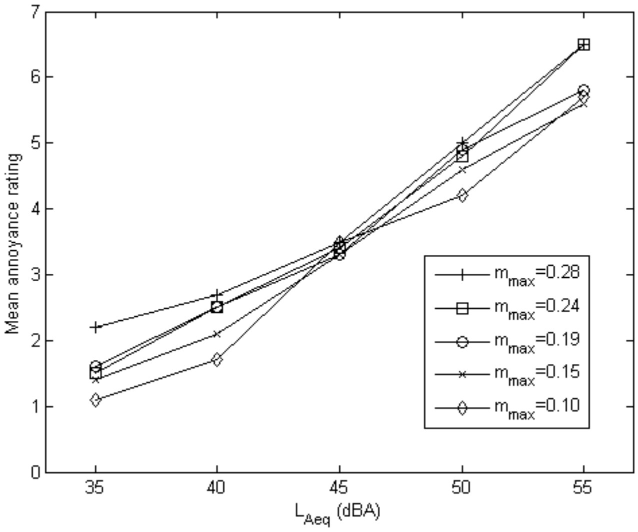

Figure 7 Mean annoyance rating for Test I

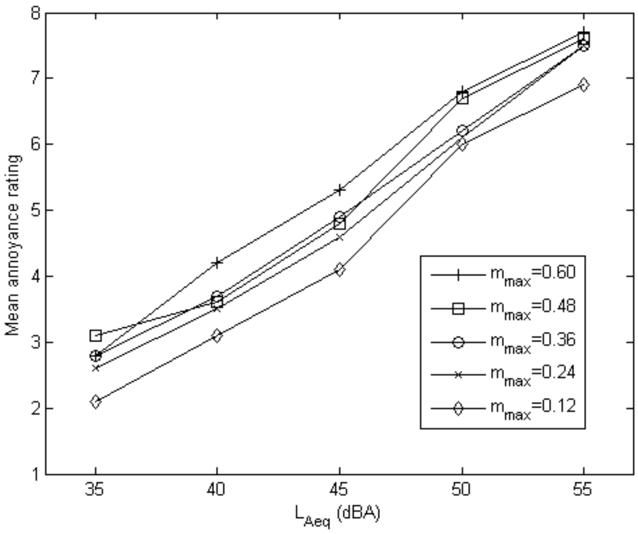

Figure 8 Mean annoyance rating for Test II

Discussion

The results of the study indicated that noise annoyance is clearly related to amplitude modulation in wind turbine noise. This can be one of the reasons why wind turbine noise is more annoying than other community noise at the same A-weighted equivalent sound level [3].

A previous study found that there is a weak relationship between annoyance and equivalent sound level [12]. The reason for this may be that other sound characters can influence on noise annoyance [13]. In this study, however, all other sound characters except modulation factor were unchanged. Consequently, there was a high correlation between noise annoyance and A-weighted equivalent sound level.

Conclusions

An estimation method for quantifying amplitude modulation in wind turbine noise was proposed. The method can be implemented in computer program and applied to various kinds of wind turbine sound signal as long as the modulation depth is more than about 1dB. Thus, it is believed that the method will be a useful tool to measure amplitude modulated noise, which is exposed to residents near a wind turbine or wind farm.

The result of the listening test showed that there is a correlation between noise annoyance and amplitude modulation in wind turbine noise. Therefore, not only equivalent sound level, but also spectral modulation depth should be considered when assessing community response to wind turbine noise.

Acknowledgements

This study is supported by Advanced Aerospace Research Institute, Seoul National University. This work is the outcome of a Manpower Development Program for Energy & Resources supported by the Ministry of Knowledge and Economy (MKE).

References

[1] S. Oerlemans, P. Sijtsma and B. Méndez López, “Location and quantification of noise sources on a wind turbine”, Journal of Sound and Vibration, 299 (2007) 869-883

[2] G.P. van den Berg, “Effects of the wind profile at night on wind turbine sound”, Journal of Sound and Vibration, 277 (2004) 955-970

[3] E. Pedersen and K. Persseon Waye, “Perception and annoyance due to wind turbine noise–a dose-response relationship”, Journal of the Acoustical Society of America, 116 (6), 2004, 3460-3470

[4] K. Bolin, “Investigating the audibility of wind turbines in the presence of vegetation noise”, Wind Turbine Noise 2007, Lyon, France, September 20-21, 2007

[5] IEC 61400-11, Wind turbine generator systems – Part 11: Acoustic noise measurement techniques, 1998

[6] G.P. van den Berg, “The sounds of high winds: the effect of atmospheric stability on wind turbine sound and microphone noise”, Doctoral Thesis, Groningen, Netherlands, 2006

[7] S. Legarth, “Auralization and assessments of annoyance from wind turbines”, Wind Turbine Noise 2007, Lyon, France, September 20-21, 2007

[8] H. Fastl and E. Zwicker, “Psychoacoustics: Facts and Models”, Springer, 2007

[9] A. Moorhouse, M. Hayes, S. von Hünerbein, B. Piper and M. Adams, “Research into aerodynamic modulation of wind turbine noise”, Report to DEFRA, 2007

[10] ISO 389-1, Acoustics – Reference zero for the calibration of audiometric equipment – Part 1: Reference equivalent threshold sound pressure levels for pure tones and supra-aural earphones, 1998

[11] ISO 15666, Acoustics – Assessment of noise annoyance by means of social and socio-acoustic surveys, 2003

[12] M. Rand and A. Clarke, "The environmental and community impacts of wind energy in the UK", Wind Engineering, 14, 319-330, 1990

[13] K. Persson Waye and E. Őhrstrőm, "Psycho-acoustic characters of relevance for annoyance of wind turbine noise", Journal of Sound and Vibration, 250 (2002) 65-73

Third International Meeting
on
Wind Turbine Noise
Aalborg Denmark 17 – 19 June 2009

Large wind turbines - noise and neighbours

Kirsten Nielsen	Bent Christensen
Engestoftevej 64	Helgolandsgade 16, 5 sal tv
4990 Sakskøbing	1653 Copenhagen
Denmark	Denmark

Abstract

Because wind turbines are growing and getting higher and higher, peoples opposition to living next door to wind turbines is also growing. This we have seen all over the world.

The visual influence of the large wind turbines as well as the turbines influence on nature and landscape is worrying the neighbours. People are also anxious about the value of their properties.

The biggest anxiety is the noise from these large machines. We know that large wind turbines are producing more noise than small ones. The low frequency noise is contributing to people’s anxiety. Specialists are not agreeing on the problems from this kind of noise - and they are not agreeing on how to measure the noise or how to read the measurements. Not in Denmark at least. It is very important that scientists find reliable measuring methods for low frequency noise – it is also important to determine how low frequency noise affects people.

In my neighbourhood Kappel, Lolland Denmark – DONG Energy – a firm owned by the Danish State - wants to establish testing facilities for 7 (150 – 200 meters high) off shore wind turbines (40 MW) in an area with 600 houses and 600 summer houses. The testing area is smaller than 3 square kilometres.

Of course people in Kappel are upset and anxious because of all the negative effects these large wind turbines will cause to area and peoples welfare.

Introduction

In recent years the Wind Power Industry has been focusing on producing large – very large – and very effective wind turbines. It seems that the motto for the industry has been:

"Large is good - but larger is even better!"

Once upon a time windmills were every ones possession – if you wanted to. It was possible for ordinary people to buy small turbines which had a size that people could accept and relate to. The people who made a profit on these smaller windmills were also the ones who in general were subjected to the negative side effects the turbines inevitably possessed.

This has now changed.

The Wind Industry has become big business. Only large national or international companies and wealthy investors can afford the massive investments connected to developing and producing modern wind turbines. And as the investors for the most part live far away from the turbines it is easier for them to ignore the visual damage and the noise created by these large structures. Hence problems are often neglected. It is furthermore noticeable that investing in wind turbines can be a very profitable business as the ownership is quite heavily subsidised.

Future neighbours to mastodons like turbines up to 200 meters in height with rotor blades large enough to encircle more than a whole football field does not embrace the prospect.

The understandable anxiety from potential neighbours is met with proclamations like: "No problem – it is only the NIMBY effect – (i.e.: Not in My Backyard)". Wind power enthusiasts are portraying scared neighbours as egotistical ignorant people who don't care about the climate and the future of our planet - while the wind turbine actors are fighting heroically for a better and cleaner world.

It has become politically incorrect to say anything negative about wind power energy.

Noise measurements are often paid by the investors and the companies and therefore the neighbours don't find these measurements to be reliable.

The problems are known all over the world and therefore several organisations like: …

EPAW. www.EPAW.org (European protest against wind power)

National Wind Watch Organisation. www.wind-watch.org

Stilheden. www.stilheden.eu

Svenskt landskapsskydd. www.landskapsskydd.se

Kappelgruppen. www.visigernej.dk (my group)

… are founded. Just to mention a few. There are hundreds of them. A lot of people are reluctant to live in close proximity to mega structures like gigantic wind turbines. Consequentially they are fighting against the wind turbine industry and politicians who advocate for the blind construction of wind farms on land. The neighbours are aware that they are up against very very powerful adversaries.

But it is important to remember what these neighbours groups are fighting for. They are not against wind power as such. But planned constructions of giant wind turbines make people fighting for their environment - for the landscape – nature - and for their quality of life.

The neighbours only have one possibility – to turn to science to get valid information.

Needless to say t is important that the scientists are impartial and unbiased**.** In this respect a conference like this is of great value. You must appreciate that we as potential neighbours have had several bad experiences fighting against our powerful adversaries. As a result of this we have felt very suspicious about measurements sponsored by the wind power industry and the large companies who want to raise giant wind turbines. And we are aware of the fact that the industry has lobbyists placed round governments, municipalities and other places where it is possible to influence decision makers.

EFP06

2006 AAU and Delta started working together on a large project called EFP06[00)]: "Low Frequency Noise from Large Wind Turbines – Quantification of the Noise and Assessment of the Annoyance". Other participants in the project are Risø DTU and DONG Energy.

Unfortunately disagreement arose. AAU did not find the measurements made by DELTA sufficient and had several complaints to some of the measurements which AAU found incorrect.

AAU's scientists retired from the project because they found it was impossible to make genuine scientific analysis of the low frequency noise and annoyance to the neighbours caused by the turbines. The reason was that AAU found that DELTAS measurements and conclusions were somewhat misleading.

Fig. 1) Low frequency noise indoors by 44 dB outdoors [0)]

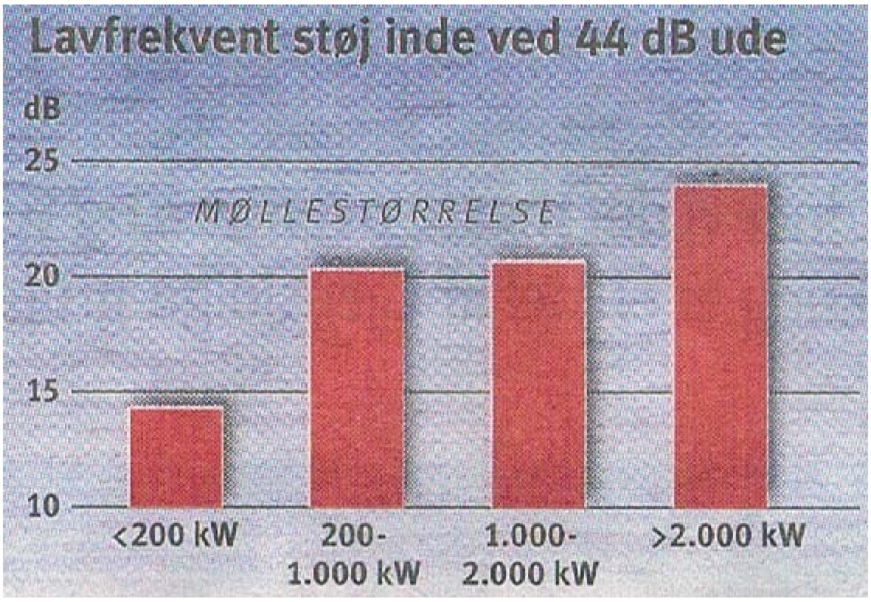

(Berlingske Tidende 08.05.2008) Kæmpemøller larmer mere.

(Giant wind turbines are making more noise than small ones.

Low frequency noise indoors by 44 dB outdoors)

Diagram by Berlingske - on the basis of measurements made by DELTA.

Strangly enough Miljøstyrelsen in Denmark – Danish Ministry of the Environment – decided to support DELTA – even though some of the measurements made by DELTA indicated the limits for low frequency noise were exceeded[0]. (Fig.1)

Again it is politically incorrect to say anything negative about wind power!

Fig. 2) Large Wind turbines are producing more noise than small ones.

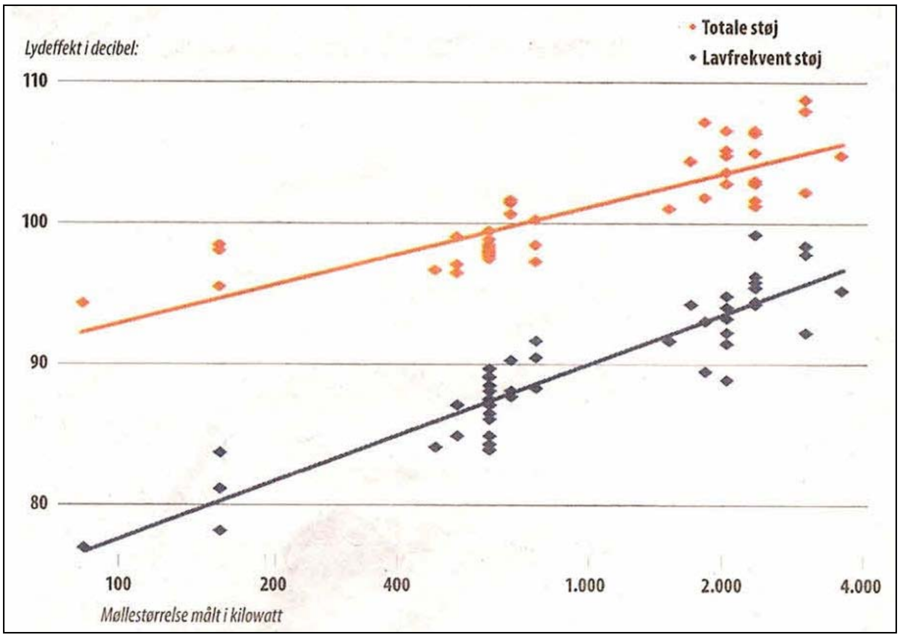

(Berlingske Tidende 03.10.2008)

This curve shows that large WTB’s give more noise than small ones.

The measurements are made by DELTA. The sound is measured near by the turbines.

The curve is expounded by Professor Henrik Møller, AAU.

DELTAS measurements showed excesses for low frequency noise on several occasions. No matter what you call the noise - if the noise from the wind turbines is disturbing the neighbours - it is a very severe thing. People should be granted the indispensable right to relax in their homes.

As laymen we will accentuate following conclusion from DELTAS report[0]:

“The large wind turbines investigated in this project are all prototypes at an early stage of development, subject to changes also with respect to the noise emission. From the measurements in this project on these large wind turbines it was found that there were tones in the noise at low frequencies for several of the investigated turbines. This is not unusual for prototypes and usually the fully developed commercial wind turbines are improved on the emission, especially concerning audible tones in the noise.”

We will ask:

How can DELTA know about that? Why have DELTA made measurements on prototype turbines if the results are more or less useless because they don’t apply to commercial wind turbines?

Large wind turbines must be placed on the sea or in much desolated areas.

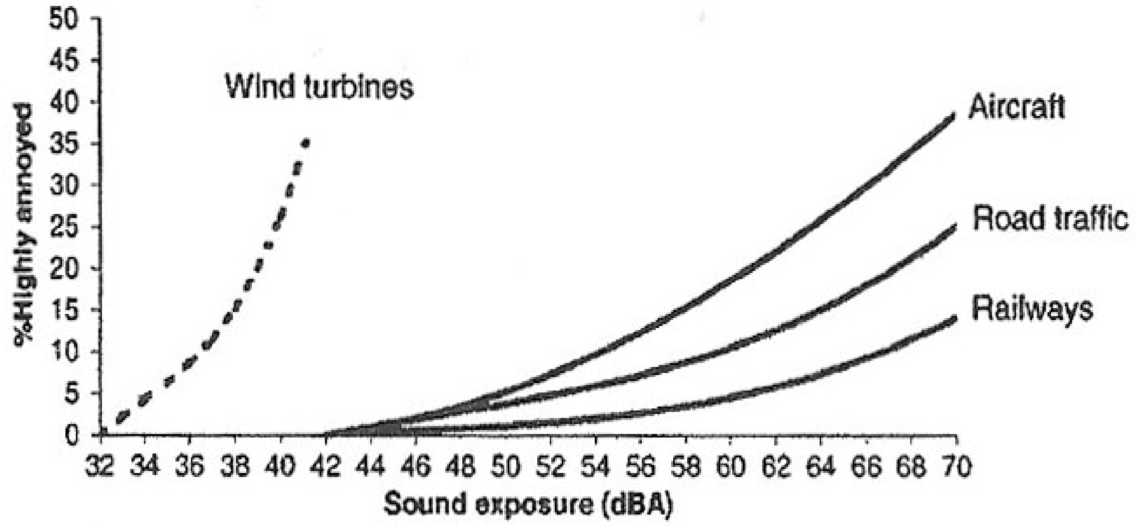

Sound exposure is for wind turbines calculated A-weighted L_{eq} for a hypothetical time period and for transportation DNL.

Fig. 3) From Eja Pedersen and Kerstin Persson Wayes article: Perception and annoyance due to wind turbine noise - a dose-response relationship, Journal of the Acoustical Society of America, vol. 116(6), December 2004, pp. 346-3470.

The curve shows that it is not always easy to live next door to wind turbines. We of course already knew that it is true because we live next to 24 small wind turbines. Depending on the wind and the temperature the noise can be very annoying. One of the results is a decreased sleep quality. Often you must close your windows if you want peace during night time.

Kappel - Lolland – Denmark

Lolland is an island in the south of Denmark. Lolland houses numerous wind turbines. Already now Lollands wind turbines produce more than 100% the electricity people in Lolland need. But most neighbours find that energy produced by wind turbines is OK - as long as the turbines have a decent size and the noise level is reasonable.

For the time being we in Kappel have 24 small wind turbines with a height of 50 meters placed along the coast. The turbines date from 1990. They are owned by DONG ENERGY. DONG Energy is a company partly owned by the Danish state (73 % stock majority).

Fig. 4) Map over Kappel (www.visigernej.dk)

We have learned to live with the 24 small turbines (even though they from time to time produce too much noise in relation to the current levels) – but we say “No thank you!!!” when we are confronted by a project like the one I am going to present to you now.

DONG wants to establish a testing area for off shore wind turbines on land and therefore they want to replace the 24 small wind turbines with 7 turbines ranging from 150 to 200 meters in height accompanied of 2 equally gigantic light towers to warn off flight traffic:

4 turbines with a capacity to produce 5 MW

2 turbines with a capacity to produce 6 MW

1 turbine   with a capacity to produce 8 MW

As you can se these turbines will produce a total of 40 MW – good business for DONG – perhaps good business for the wind power industry - but this grotesque plan is a disaster for the people in Kappel.

The wind turbines will be placed in an area less than 3 square kilometres. Because of noise limits of noise the project demands that DONG Energy buys several properties in the area. If people don't want to sell their houses the Lolland municipality has allowed expropriation.

With the new plan DONG Energy comes close to the existing limits for noise – and even exceeds these limits as you can see from the map. Furthermore the turbines will stand until they are worn out – not only in the test period.

The neighbourhood consists of about 600 houses and 600 summer houses in a distance of 4,5 km.

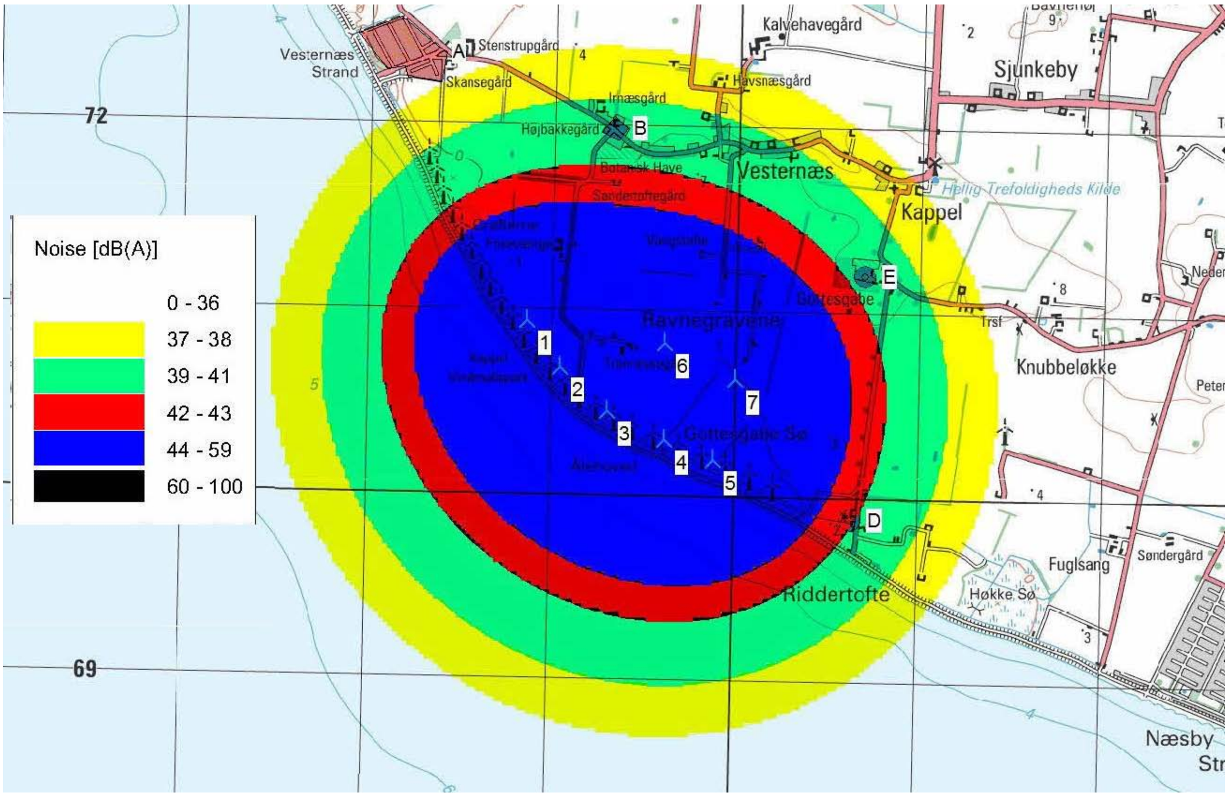

Fig. 5) Map over the testing area for off shore WTB's in Kappel. The map is showing noise from the 7 wind turbines (DONG Energy February 2009).

Rules and regulations for wind turbines in DK

[1)] Distance to neighbours:

Wind turbines must have a distance at 4 times the total height of the turbine to the nearest neighbour.

[2)] Noise:

Upper noise limit at wind speed 6:	37 dB in recreational areas and 42 dB in the open land
Upper noise limit at wind speed 8:	39 dB in recreational areas and 44 dB in the open land

It is furthermore recommended that the shadows cast by the wings of the wind turbine only disturb the neighbouring houses maximum 10 hours a year. **This regulation is not respected**. Not in Kappel at least.

[3)] From the year 2009 it is possible for people in Denmark to be compensated if the value of their property is reduced more than 1 % caused by **new** large wind turbines. The compensation is to be paid by the owner of the wind turbine. The loss will be valuated by an impartial estate agent.

Of course this is better than nothing – but the wind turbine neighbours would certainly prefer to have wind turbines regulations increased.

And how can a few thousand kroner help you if you can not stand to live in your home? and if you are unable to sell your property?

Low frequency noise

A regulation from Miljøstyrelsen (Danish Ministry Of The Environment):

<u>“Orientering nr. 9/1997 om lavfrekvent støj, infralyd og vibrationer i eksternt miljø”</u>

mentions limits for low frequency noise for industries and machines – this limit is normally 20 dB indoors but - strangely –

<u>Danish Ministry Of The Environment has decided that this regulation doesn’t include low frequency noise from wind turbines!</u>

Danish Ministry of the Environment explains this decision by a rather illogical conclusion that: there will be no problems with low frequency noise if limits of “common” noise are observed. If this conclusion is the case you could ask just why wind turbines are excluded.

DELTA’s measurements have actually shown that there are problems with low frequency noise from large turbines (Fig. 1 + 2) – According neighbour’s and AAU’s opinion DELTA tries to underestimate these facts - and therefore the neighbours are even more anxious. They feel that the truth is purposely hidden from them.

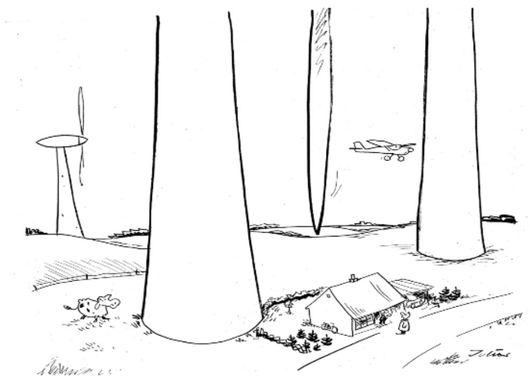

Tænk dog bare på de mange tusinde turister, der kommer for at se havmøllerne på land!

Fig. 6) (”Dagens Julius” Folketidende 02.10.2007

Trods massive protester er kæmpe-vindmøllerne på vej.)

(“In defiance of massive protests gigantic wind turbines are on the way”)

Kan De ikke fortælle mig, hvorfor De ikke vil være med at nedbringe CO2-udslippet med vedvarende grøn energi? (Please tell me why you don’t want to reduce the release of CO^2 by using “green energy”?)

Conclusion

Common people are not able to decide which methods of measurement are correct and give trustworthy results. But common people who will have to live next door to large wind turbines also have to suffer from the noise and the visual effects created by the turbines.

Therefore it is of the utmost importance that also noise problems are taken seriously and scientists can investigate independently of the wind power industry and political authorities.

Wind power gives us electricity without CO^2, but wind power is not without problems.

When deciding where to allow facilities like large scale wind turbines please take into consideration the negative effects on landscape, nature and the local population.

And most of all – consider the neighbours living next door to the turbines. Nowadays the regulations are far from sufficient.

Large wind turbines should only be established on sea or far away from populated areas!

"Not in anyone's backyard!"

NIABY

References:

[00)] EFP06 is financed by Danish Energy Authoritysupported by Vestas Wind Systems A/S, Siemens Wind Power A/S, DONG Energy, Vattenfall A/B Vindkraft and E.ON Vind Sverige A/B. Also Danish Ministry of the Environment and Vindmølle-industrien are participants.

[0)] EFP06, Low Frequency Noise from Large Wind Turbines, Summary and Conclusions on Measurements and Methods, DELTA 2008 (AV 140/08 REV 1)

[1)] Cirkulære om placering for og landzonetilladelse opstilling af vindmøller. (30. juni 1997)

[2)] Bekendtgørelse nr. 1518. Bekendtgørelse om støj fra vindmøller. (14. december 2006)

[3)] VE-loven (18. december 2008)

Kirsten Nielsen

Infralyd & Miljø

Kappelgruppen

Bent Michael Christensen

Infralyd & Miljø

**Third International Meeting
on
Wind Turbine Noise
Aalborg Denmark 17 – 19 June 2009**

Prediction of wind turbine noise directivity and swish

Stefan Oerlemans* and Gerard Schepers¶

***National Aerospace Laboratory NLR, The Netherlands
stefan@nlr.nl**

**¶ Energy research Centre of the Netherlands ECN
schepers@ecn.nl**

Abstract

This paper describes the application of a semi-empirical trailing edge noise prediction method to calculate wind turbine noise. In a previous study, the method was already validated with regard to source spectra, overall sound levels, and the noise source distribution in the rotor plane. In the present paper the prediction method is extended to calculate wind turbine noise directivity and swish. The predictions are validated using measured data at eight microphones on a circle around the turbine. Using a smoothed analytical trailing edge noise directivity function, the turbine noise directivity is predicted within 1-2 dB, and the swish amplitude in different directions within 1 dB. The validated prediction code is then applied to calculate noise footprints of the wind turbine as a function of rotor azimuth. These footprints show that for cross-wind directions the *average* level is lower than in the up- and downwind directions, but the *variation* in level is larger. Even at large distance, swish amplitudes up to 5 dB can be expected for cross-wind directions.

1 Introduction

Wind is a clean and practically inexhaustible source of energy. However, the noise of wind turbines is a major hindrance for the widespread use of wind energy. A recent survey on the perception of wind farms in the Netherlands [1] showed that sound was the most annoying aspect of wind turbines. The swishing character (amplitude modulation) of the noise was mentioned as an important factor explaining the relatively high annoyance, as compared to other sound sources of equal level (air or road traffic). For the design of quiet wind turbines, and for the planning of wind farms, the availability of fast and accurate noise prediction methods is essential. In order to have a wide range of application, prediction codes should capture the physical source mechanisms as much as possible.

For a modern large wind turbine, aerodynamic noise from the blades is generally considered to be the dominant noise source. In previous studies several semi-empirical wind turbine noise prediction methods were developed, which were assessed by comparison with field measurements [2-11]. In most cases the prediction methods included trailing edge noise and inflow turbulence noise. However, since the field results only provided the total sound level of the turbine, and sometimes part of the turbine noise was attributed to other sources, such as tip noise or mechanical noise, only an indirect validation of the prediction codes was possible. Furthermore, in none of these studies the noise directivity or swish amplitude was predicted and compared with experimental results.

Swish is here defined as the amplitude modulation of broadband aerodynamic blade noise at the blade passing frequency (typically around 1 Hz). A number of studies have addressed the swish phenomenon experimentally [12-15]. They reported periods of increased amplitude modulation (also referred to as 'thumping'), which could be observed at large distance. Although various possible causes for this increased amplitude modulation have been suggested, including blade noise directivity, blade-tower interaction, variation of wind speed over the rotor, and interaction between the noise from two or more turbines, the mechanism is still not clear.

Refs. [16-18] reported detailed source localization measurements on two modern large wind turbines, using a large microphone array positioned about one rotor diameter upwind of the turbine. The array results showed that practically all noise perceived on the ground was produced by the outer part of the blades (but not the very tip), during their downward movement. This strongly asymmetric source pattern, which caused the swishing noise during the passage of the blades, was explained by trailing edge noise directivity and convective amplification. Moreover, in Ref. [16] it was shown that the source pattern could *only* be explained by trailing edge noise directivity (and not by inflow-turbulence noise or low-frequency dipole noise).

In Ref. [17], a semi-empirical prediction method for trailing edge noise was applied to calculate wind turbine noise. Using detailed acoustic array data, the method was successfully validated for two modern large wind turbines, not only in terms of source spectra and overall sound levels (as a function of rotor power), but also in terms of the noise source distribution in the rotor plane (as a function of frequency and observer position). These analyses focused on *average* sound levels perceived at the *upwind* array position.

The present paper describes two extensions to the method described in Ref. [17]: first, the *instantaneous* sound level is calculated (i.e. as a function of the rotor azimuth angle), to predict the perceived variation in sound level (swish) during the revolution of the blades, as a result of trailing edge noise directivity and convective amplification. The second extension concerns the calculation of the sound level for different observer positions, to predict the *directivity* of wind turbine noise. The predictions are validated using measured data at eight microphones on a circle around the turbine. The validated prediction code is then applied to calculate noise footprints of the wind turbine as a function of rotor azimuth.

The wind turbine considered in this study is GE 2.3 MW prototype test turbine with a rotor diameter of 94 m and a tower height of 100 m, located on a test site in the

Wieringermeer polder (Netherlands). The turbine is pitch-controlled and rotates in clockwise direction as seen from upwind. A picture of the test set-up is given in Figure 1. More details about the experiments can be found in Ref. [17], which also discusses the array results. For the present paper, which is a condensed version of Ref. [19], only the data from the ground microphones are used.

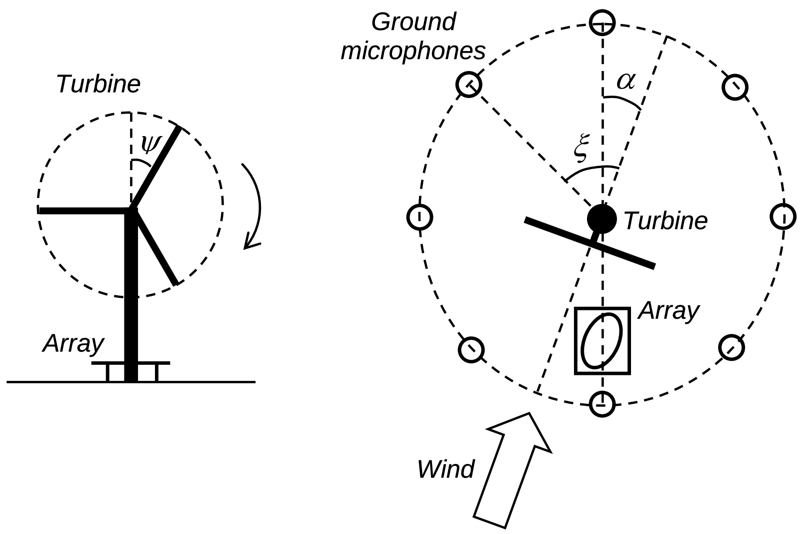

Figure 1: Schematic picture of test set-up: side view (left) and top view (right).

2 Prediction method

Since the field measurements show that broadband trailing edge noise is the dominant noise source for this turbine [17,18], only this noise source is incorporated in the prediction method. The calculation can be divided into three steps: blade aerodynamics, trailing edge noise source strength, and directivity and convective amplification. The resulting noise source distribution on the blades, which depends on rotor azimuth and observer position, can then be used to calculate noise footprints around the turbine. The different steps will be described in the following paragraphs.

2.1 Blade aerodynamics

For the aerodynamic calculations the blade is first divided into a number of radial segments (21 for the present study). Next, for each segment the local Reynolds number and angle of attack are obtained from an aerodynamic wind turbine model, based on the blade element momentum theory [20]. Then, the RFOIL airfoil design and analysis code [21] is used to calculate the trailing edge boundary layer displacement thicknesses on the pressure and the suction side. RFOIL is an extension of XFOIL [22] and takes into account rotational effects. As input to the aerodynamic calculations only the blade geometry and the turbine operating conditions are needed. The blade geometry (including the airfoils) and the aerodynamic profile coefficients were provided by the manufacturer, and the RPM and blade pitch angle were taken according to the turbine control system, as measured during the field tests.

2.2 Trailing edge source strength

Using the boundary layer displacement thickness and local Reynolds number from the previous section as input, the source spectrum for each radial blade segment is calculated using the 2D semi-empirical trailing edge noise prediction code developed by Brooks, Pope, and Marcolini [23]. The model is based on theoretical analyses of a turbulent, low Mach number flow over a half-plane, and basically states that trailing edge noise levels scale with the boundary layer thickness (which is a measure for the turbulence correlation scale) and the fifth power of the flow speed. The peak frequency scales with the ratio between local flow speed and boundary layer thickness. The nondimensional spectral shape is determined empirically on the basis of acoustic and aerodynamic measurements on NACA0012 airfoils, for various wind speeds, angles of attack, and model chords.

2.3 Directivity and convective amplification

In order to obtain the effective source strength for a given blade azimuth angle, as perceived by an observer at a specified position, the effects of trailing edge noise directivity and convective amplification should be applied to the trailing edge source spectrum for each radial blade segment. In Ref. [17], the following analytical directivity function [23] was used:

$$D_s = \frac{2\sin^2(\theta/2)\ \sin^2\phi}{(1-M\cos\zeta)^4}, \tag{1}$$

where θ and φ are defined in Figure 2, ζ is the angle between the blade flow velocity and the source-observer line, and M is the (undisturbed) blade Mach number. The numerator in Eq. (1) describes the trailing edge noise directivity, and is the most important contributor to the asymmetrical rotor noise source pattern [16]. The denominator represents the convective amplification factor for trailing edge noise, and indicates that the source amplitude increases when the source is moving towards the observer.

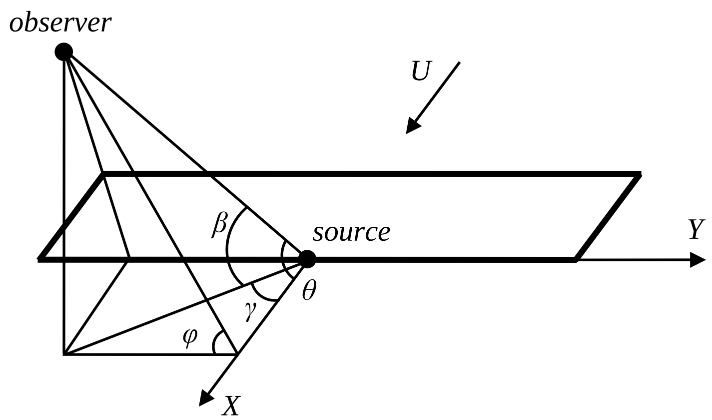

Figure 2: Definition of angles between observer and trailing edge source.

In previous studies Eq. (1) was used for the prediction of noise from helicopters [24] and wind turbines [3,5,9-11], and in Refs. [16,17] it was succesfully applied to explain the rotor noise source distribution as perceived at an upwind observer position. Figure 3 shows the characteristics of this theoretical directivity function (for M =0) in the plane normal to the trailing edge (in terms of the acoustic pressure), and on a sphere around the trailing edge source (in dB). In this figure the flow is in the *x*-direction and the trailing edge runs along the *y*-axis.

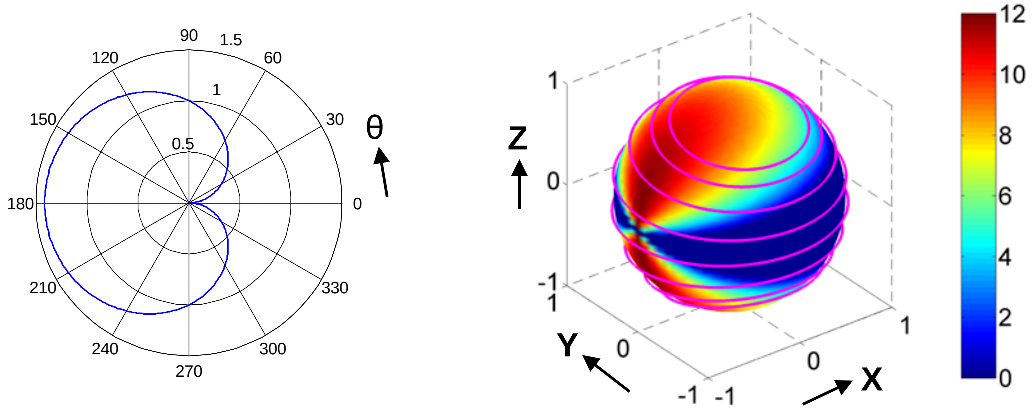

Figure 3: Analytical trailing edge noise directivity function.

In order to assess the influence of the trailing edge noise directivity function on the wind turbine noise directivity and swish amplitude, it is useful to know the position of an observer on the 'directivity sphere'. For this purpose, the 'trajectories' of the eight experimental ground microphones (Figure 1) on the directivity sphere, during one revolution of the blade, are projected as pink circles on the directivity function in Figure 3 (a source radius of 0.9 times the tip radius is used). It can be seen that each ground microphone follows a circle at more or less constant 'latitude' β, where β depends on the microphone angle ξ (the 'longitude' γ depends on the blade azimuth angle ψ). The four lower circles represent the upwind locations, while the four upper circles correspond to the downwind locations. The asymmetry between the upper and lower trajectories is due to the rotor tilt angle, the blade pitch and twist, and the average experimental misalignment angle α of -11°. For a symmetrical turbine (i.e. no pitch, twist, and tilt), the latitude of an observer at large distance would be given by $\beta = |\xi - \pi| - \pi/2$.

Figure 3 illustrates that the directivity measured by the farfield microphones is determined by the *average* level over each trajectory, while the swish amplitude depends on the *variation* of the level along each circle (note that there are three blades on each circle, the contributions of which should be summed). Thus, the ground microphone measurements on a circle around the turbine in fact constitute a measurement of the complete trailing edge noise directivity function, and, vice versa, in order to predict the noise footprint of a wind turbine, the complete directivity function should be known.

Now Figure 3 shows that the directivity function has a discontinuity for $\theta = \pi$, causing unrealistically high swish amplitudes close to the rotor plane. Therefore, the directivity function was smoothed in the region around the discontinuity, by averaging it over a certain range of β and γ. Thus, the resulting smoothed directivity function (Figure 4) is identical to the original function in Eq. (1) for regions away from the plane of the blade. The smoothed function yields good agreement between experiments and predictions (see Section 3), and therefore appears to be a good approximation of the true directivity function for trailing edge noise from an airfoil. In fact, it shows similar characteristics as the theoretical directivity function for a finite-chord flat plate [19].

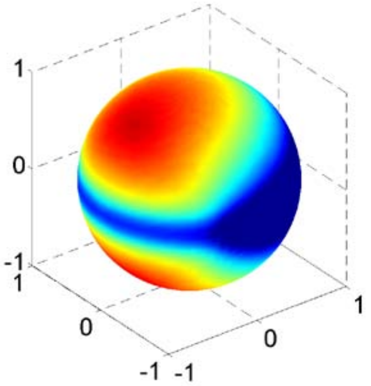

Figure 4: Smoothed analytical directivity function used in present code.

3 Validation against experiment

In Ref. [17] the prediction method was already validated with regard to source spectra, overall sound levels (as a function of rotor power), and the noise source distribution in the rotor plane (as a function of frequency and observer position). Therefore, in this section the predictions are assessed in terms of turbine noise directivity and swish amplitude.

Farfield measurements were performed with eight ground microphones on a 240-m diameter circle around the turbine (Figure 1). An overview of the test conditions is given in Table 1 (the first five columns indicate the number of measurements in the wind speed bins between 6 m/s and 10 m/s).

Table 1: Overview of average test conditions (standard deviation between brackets).

# meas. per U_{10} bin					**U_{nac} (m/s)**	**RPM**	**pitch (°)**	**P (MW)**	**α (°)**
6	**7**	**8**	**9**	**10**					
10	21	15	0	0	10.0 (1.0)	14.6 (0.4)	0.0 (0.0)	1.5 (0.3)	-11 (6)

To determine the directivity of the turbine noise, the average level on each microphone is plotted as a function of microphone angle ξ for each 30 s measurement (Figure 5). The average misalignment angle α for the ground microphone measurements is -11°, and the variation in α is 20°, which explains the eight 'traces' in Figure 5.

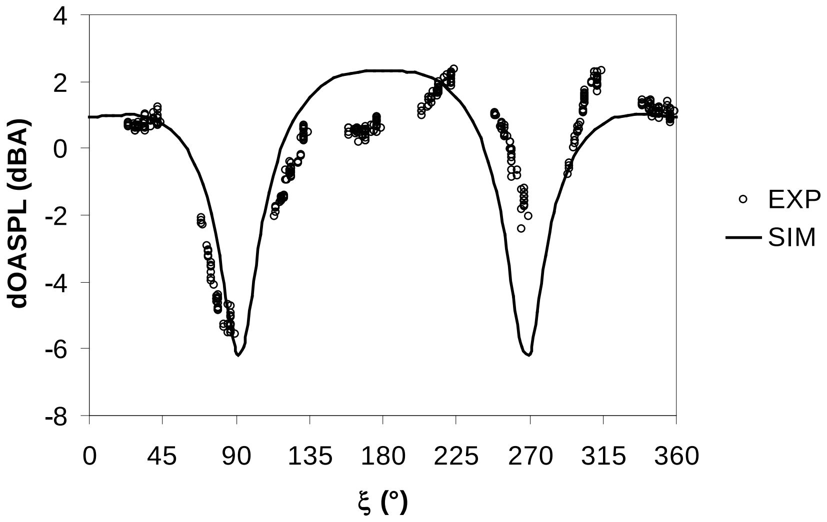

Figure 5: Measured and predicted directivity.

The most distinct feature in the measured directivity pattern are the two 'dips' in the crosswind directions. A similar decrease in noise level close to the rotor plane was also found in [5,8]. Figure 5 also shows the *predicted* directivity on a 240-m diameter circle around the turbine, for a wind speed close to the average experimental wind speed. It can be seen that the predicted curve follows the measured curve within 1-2 dB, with two 6 dB dips in the cross-wind directions. These dips can be understood from the reduced levels of the trailing edge noise directivity function close to the plane of blade (Figure 4).

Next, the *variation* in noise level due to the revolution of the blades (swish) is considered for the different directions. In order to exclude variations due to varying weather or turbine conditions, the overall level on each ground microphone is plotted as a function of the rotor azimuth angle and averaged over all measurements (Figure 6). For each ground microphone three practically identical humps are found, corresponding to the passage of the blades. The *predicted* graphs are shown in the same figure. For the upwind measurement positions (90°<ξ<270°), both the amplitude and the phase of the humps match quite well with the measurements. However, for the downwind microphones the measured amplitude is lower than predicted. Since the signal-to-noise ratio (i.e. the minimum sound level in Figure 6 minus the background noise level with stopped rotor) is generally higher than 9 dB, this does not explain the reduced swish amplitude. However, comparison of the graphs for the individual 30-s measurements (not shown) indicates that slight variations in the phase of the humps reduces the amplitude of the averaged graphs. Due to propagation of the sound through the rotor wake, this effect can be expected to be stronger for the downwind microphones. Thus, in order to obtain a reliable experimental value of the swish, rather than taking the amplitude from the averaged graphs in Figure 6, the amplitude is determined for each individual 30-s measurement, and then averaged over all measurements.

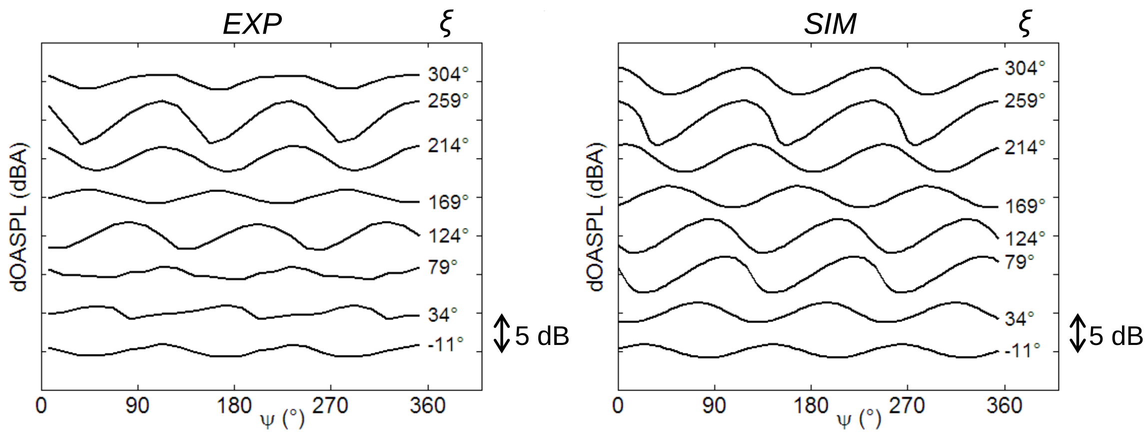

Figure 6: Measured and predicted sound level variation as a function of rotor azimuth ψ, for different farfield positions ξ.

The resulting experimental swish amplitudes are shown together with the predicted values in Figure 7. The error bars indicate the standard deviation in swish amplitude and farfield position. It can be seen that the swish amplitude is predicted within 1 dB for all directions. The relatively low swish amplitude for ξ=79° may be partly explained by shielding of the tower [12,15]. Note that the predicted swish amplitude is closely related to the variation in level along the microphone 'trajectories' (Figure 3) on the trailing edge noise directivity function in Figure 4.

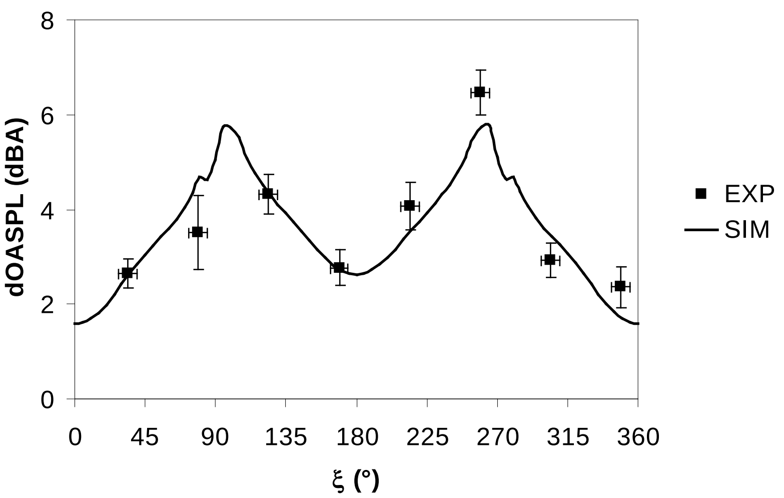

Figure 7: Measured and predicted swish amplitude as a function of farfield position ξ.

4 Noise and swish footprints

The previous section provides a validation of the prediction model against the experimental results, in terms of the turbine noise directivity and swish. The measurements are limited to a 240-m diameter circle around the turbine. However, since the measurements on the circle cover almost the complete trailing edge noise directivity function (Figure 3), the prediction method can also be applied to calculate the noise at larger distances. Figure 8 shows instantaneous turbine noise footprints (top view) for four different rotor azimuth angles, up to a distance of ten times the rotor diameter. The turbine is located at the center of the footprint, and the wind goes from left to right. The rotor azimuth at observer time is indicated in the upper right corner of each footprint. In order to limit the range of the dB scale, the levels are normalized using the horizontal distance r_h to the turbine: $SPL_{norm} = SPL + 20\log r_h$. In this way the levels at a given distance can be directly compared. Note that atmospheric attenuation and sound refraction due to wind shear are not included in the predictions. Refraction may in practice reduce the upwind sound levels.

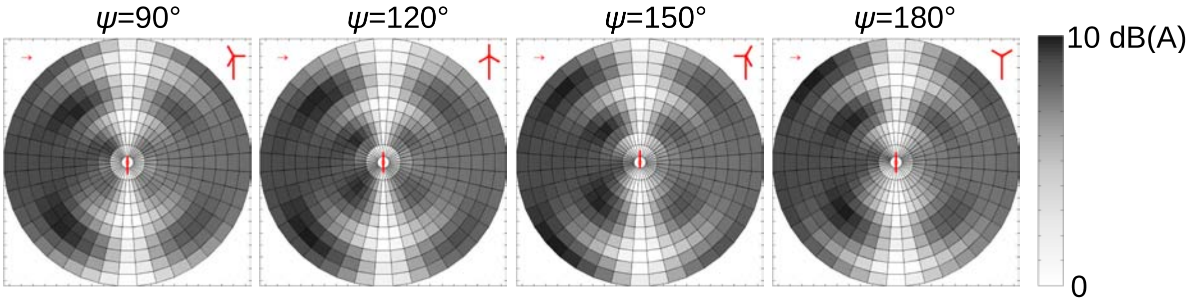

Figure 8: Predicted instantaneous noise footprints for increasing rotor azimuth angle, up to a distance of 10 times the rotor diameter. The wind goes from left to right.

The footprints show two 'waves' of increased sound level, one in each cross-wind direction, which start close to the turbine at ψ =90° and propagate outward with the speed of sound. The wave on the side of the down-going blade is generated when the blade is around ψ =30°, while the wave on the side of the upgoing blade is generated when the blade is around ψ =180°. After ψ =180° the cycle repeats and both waves can be seen to propagate further to the edge of the footprints. The distance between two successive waves is about 5 rotor diameters, which is consistent with the time period of 1.33 s between the passage of two blades (the RPM is 15) and a speed of sound of 340 m/s.

Due to the passage of these sound waves from the blades, the noise levels in the crosswind directions vary significantly, while in the up- and downwind directions the levels are quite constant at large distances. This is illustrated in Figure 9, which shows the average and swish (level variation) footprints for a complete revolution. It can be seen that both footprints do not change significantly beyond a distance of a few rotor diameters. For both cross-wind directions, the *average* level is lower than in the up- and downwind directions, but the *variation* in level is larger. Even at a large distance, trailing edge noise directivity and convective amplification may cause swish amplitudes up to 5 dB in the cross-wind directions. This may be an explanation for the increased amplitude modulation reported in [12-15], although it should be noted that at large distances (beyond several rotor diameters) variations in atmospheric conditions, which are not modeled here, may also cause fluctuations in the perceived noise level. Note that at small distance to the turbine (one rotor diameter) substantial swish is observed in *all* directions, which is consistent with the measurements.

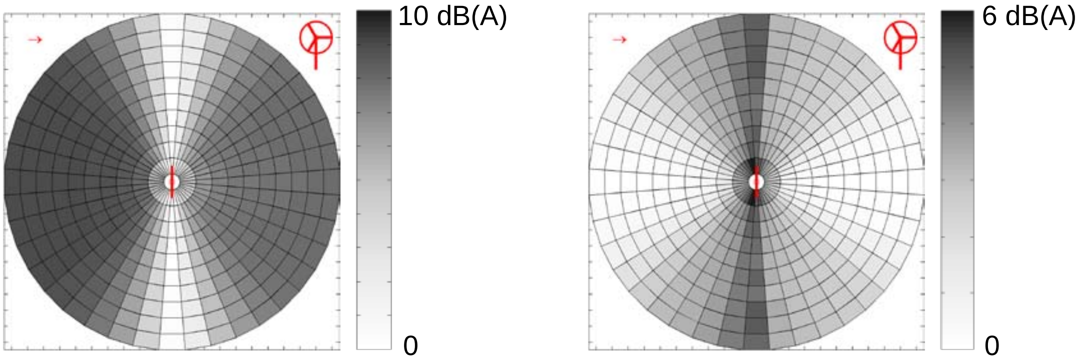

Figure 9: Predicted average footprint (left) and swish footprint (right) for a complete revolution.

5 Conclusions

This paper describes the application of a semi-empirical trailing edge noise prediction method to calculate wind turbine noise. In a previous study, the method was already validated with regard to source spectra, overall sound levels, and the noise source distribution in the rotor plane. In the present paper the prediction method is extended to calculate wind turbine noise directivity and swish. The predictions are validated using measured data at eight microphones on a circle around the turbine. Using a smoothed analytical trailing edge noise directivity function, the turbine noise directivity is predicted within 1-2 dB, and the swish amplitude in different directions within 1 dB. The validated prediction code is then applied to calculate noise footprints of the wind turbine as a function of rotor azimuth. These footprints show that for cross-wind directions the *average* level is lower than in the up- and downwind directions, but the *variation* in level is larger. Even at large distance, swish amplitudes up to 5 dB can be expected for cross-wind directions.

References

[1] F. van den Berg, E. Pedersen, J. Bouma, R. Bakker, WINDFARM perception: Visual and acoustic impact of wind turbine farms on residents - Final report, 2008.

[2] A. de Bruijn, W.J. Stam, W.B. de Wolf, Determination of the acoustic source power levels of wind turbines, *Proceedings of the European Wind Energy Conference*, Hamburg, October 1984.

[3] F.W. Grosveld, Prediction of broadband noise from large horizontal axis wind turbine generators, American Institute of Aeronautics and Astronautics Paper 84-2357, 1984.

[4] S.A.L. Glegg, S.M. Baxter, A.G. Glendinning, The prediction of broadband noise from wind turbines, *Journal of Sound and Vibration* 118 (1987) 217-239.

[5] H.H. Hubbard, K.P. Shepherd, Aeroacoustics of large wind turbines, *Journal of the Acoustical Society of America* 89 (1991) 2495-2508.

[6] M.V. Lowson, Theory and experiment for wind turbine noise, American Institute of Aeronautics and Astronautics Paper 94-0119, 1994.

[7] P. Fuglsang, H.A. Madsen, *Implementation and verification of an aeroacoustic noise prediction model for wind turbines*, Risø-R-867(EN), Risø National Laboratory, 1996.

[8] M.V. Lowson, J.V. Lowson, A.J. Bullmore, Wind turbine noise: analysis of results from a new measurement technique, American Institute of Aeronautics and Astronautics Paper 98-0037, 1998.

[9] P. Moriarty, P. Migliore, *Semi-empirical aeroacoustic noise prediction code for wind turbines*. NREL/TP-500-34478, National Renewable Energy Laboratory, Golden, CO, 2003.

[10] W.J. Zhu, N. Heilskov, W.Z. Shen, J.N. Sørensen, Modeling of aerodynamically generated noise from wind turbines, Journal of Solar Energy Engineering (2005), Vol. 127, 517-528.

[11] G. Leloudas, W.J. Zhu, J.N. Sørensen, W.Z. Shen, S. Hjort, Prediction and reduction of noise from a 2.3 MW wind turbine, *Proceedings of The Science of Making Torque from Wind*, Journal of Physics: Conference Series 75 (2007).

[12] P. Dunbabin, An investigation of blade swish from wind turbines, Proceedings of Internoise 96, 463-469, 1996.

[13] G.P. van den Berg, Effects of the wind profile at night on wind turbine sound, *Journal of Sound and Vibration* 277, 2004.

[14] A. Moorhouse, M. Hayes, S. von Hünerbein, B. Piper, M. Adams, Research into aerodynamic modulation of wind turbine noise: final report, University of Salford, July 2007.

[15] D. Bowdler, Amplitude modulation of wind turbine noise, Acoustics Bulletin of the Institute of Acoustics (UK), Vol. 33, No. 4, July/August 2008.

[16] S. Oerlemans, P. Sijtsma, B. Méndez López, Location and quantification of noise sources on a wind turbine, *Journal of Sound and Vibration* 299, 2007.

[17] S. Oerlemans, J.G. Schepers, Prediction of wind turbine noise and comparison to experiment, *Proceedings of the Second International Meeting on Wind Turbine Noise*, Lyon, France, September 2007.

[18] S. Oerlemans, M. Fisher, T. Maeder, K. Kögler, Reduction of wind turbine noise using optimized airfoils and trailing-edge serrations, American Institute of Aeronautics and Astronautics Paper 2008-2819, 2008.

[19] S. Oerlemans and J.G. Schepers, Prediction of wind turbine noise and validation against experiment, accepted for International Journal of Aeroacoustics.

[20] B.H. Bulder, S.A.M. Barhorst, J.G. Schepers, F. Hagg, Theory and user's manual BLADOPT, ECN-C-01-011, , Energy Research Centre of the Netherlands ECN, 2001.

[21] B. Montgomerie, A. Brand, J. Bosschers, R. van Rooij, Three-dimensional effects in stall, ECN-C-96-079, Energy Research Center of the Netherlands ECN, 1997.

[22] M. Drela, XFOIL: An analysis and design system for low Reynolds number airfoils, Low Reynolds number aerodynamics, T. J. Mueller, Ed., University of Notre Dame, Paris, 1989.

[23] T.F. Brooks, D.S. Pope, M.A. Marcolini, *Airfoil Self-Noise and Prediction*. NASA Reference Publication 1218, 1989.

[24] T.F. Brooks, C.L. Burley, Rotor broadband noise prediction with comparison to model data, American Institute of Aeronautics and Astronautics Paper 2001-2210, 2001.

Third International Meeting
on
Wind Turbine Noise
Aalborg Denmark 17 – 19 June 2009

A New Explanation for Wind Turbine Whoosh – Wind Shear

William K.G. Palmer P. Eng.
TRI-LEA-EM RR 5, Paisley, ON N0G 2N0 Canada
trileaem@bmts.com

Abstract

The cyclic "Whoosh" created by wind turbines are their most recognizable audible feature, often reported as their most annoying aspect. Many references describe that the whoosh is generated due to the interaction between the turbulent air following the trailing edge of the blades, and the downwind tower.

However, this explanation leaves unanswered questions. Why is the whoosh so different from day to night? Neither the tower nor the blades change. A simple empirical test explains part of the mystery. Hold your finger in front of your pursed lips. As you blow on your finger at greater and lesser velocity, you hear that same familiar cyclic whoosh as you do from a wind turbine.

We know that at night the atmospheric profile changes, due to the condition of wind shear, as wind speed at height become uncoupled from lower elevations. We know also from audio / photographic studies that the sound from wind turbine blades is most concentrated at the blade tips.

When the bits we know are melded, a new model develops that explains how the cyclic whoosh of wind turbines can be described by the movement of the blades through high wind speeds at the top to low speeds at the bottom of the blade rotation. The sound increases as the blades go to the top of the circle and decreases as the blades go to the bottom of the cycle.

This knowledge might be used to reduce the annoying cyclic whoosh of wind turbines by a cyclical pitch of the blades as they reach the top of their rotation. This would also decrease stresses on the blades caused by flexure, and might even reduce blade failure probability.

Introduction

People who have followed the debate over wind turbines would readily agree that they would be rich if they had a dollar (or euro) for every article written or every hearing statement by someone saying something like "I went out to the turbine site, stood under the turbine, and could carry on a normal conversation. I don't know what all the fuss is about; there was only a gentle “swish” sound. They aren’t noisy!” However, the wealth accumulated would be quickly erased if the interested data gatherer had to give a dollar (or euro) to every distraught resident from homes surrounding wind turbines, who said, “I just cannot get used to the constant pounding “Whoosh Whoosh Whoosh” that I hear at night from those turbines. Even with my head under the pillow, it is an unwelcome intruder into our home!”

Given the assumption that regardless of their personal opinion one way or another about wind turbines, most people strive to tell the truth, how does the unbiased observer make sense of it all? The speakers cannot all be right, can they? The points of view are exactly divergent. It is too easy to fall into the trap so often set, to accuse the “other side” of not telling the truth, or of just using excuses to explain personal preferences. This paper attempts to provide an explanation to the quandary that is probably one of the greatest mysteries about wind turbines – why they are not noisy to the person who stands under them in the daytime, and yet are unwelcome noisy intruders at night for the resident who lives near them.

It turns out that the explanation may not be so difficult to understand at all, and it may arise from a well-understood climatic condition that is familiar, but which is not well recognized in the acoustical codes prepared for wind turbines.

Common Explanations for Whoosh

A number of references describe the “Whoosh” heard from wind turbines as being due to the interaction between the turbulent air following the trailing edge of the wind turbine blade as it passes the region of slowed wind speed in front of the tower. Other explanations for the Whoosh have been written to describe it as being due to the acoustical Doppler effect, which arises as the wind turbine blades rotate on their downward path approaching an observer on the ground. A paper[i] by Stefan Oerlemans and Gerhard Schepers presented at the Second Wind Turbine Noise Conference in Lyons in 2007 describes the use of an elliptical array of microphones mounted on a board16 metres by 18 metres placed on the ground “roughly one rotor diameter upwind of turbines to measure sound from the blades to measure the distribution of noise sources in the rotor plane and on individual blades” to show that for an observer on the ground, “most of the noise is produced by the outer part of the blades (but not the very tip) during the downward motion.” Their paper shows some pictures of the test set up and typical noise source distributions in the rotor plane.

None of the common explanations proposed to date have suggested a reason for the Whoosh to vary from day to night. As none could explain the anecdotal observations made by residents living near wind turbines, of noise being more pronounced at night, it was necessary to search further.

A New Player Enters the Field – Atmospheric Stability

During the 2007 Ontario Municipal Board hearings related to the appeal by citizens against the Municipality of Kincardine, Ontario zoning bylaws passed to permit erection of wind turbines on 105 lots by the Enbridge Ontario Wind Power development, Meteorological Consultant James W. S. Young Ph.D. P. Eng, presented a paper titled “Analysis of Boundary Layer Winds near Goderich and Their Application to Wind Farms along the Easy Coast of Lake Huron.”[ii] Figure 1 (adapted from Young) shows the first 1000 metres atmosphere above the surface of the earth.

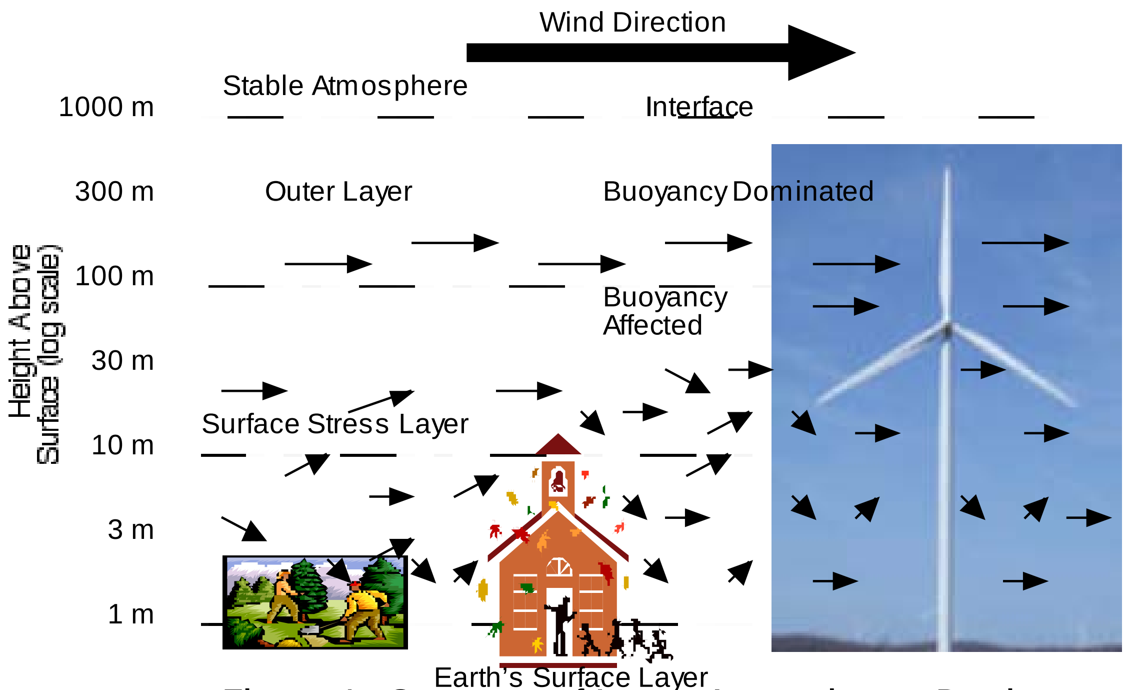

Figure 1 - Structure of Lower Atmosphere - Daytime

Young notes that above about 1000 metres we are in a stable layer of unchanging wind speeds with height, while below that level wind flow is dominated by either buoyancy or surface stress. He states, “The surface stress (or friction) dominates up to about 30 metres. Modern wind turbines typically operate above the surface stress layer in the buoyancy dominated region. In this region the wind flows tend to be less affected by turbulence (instabilities in the atmosphere).”

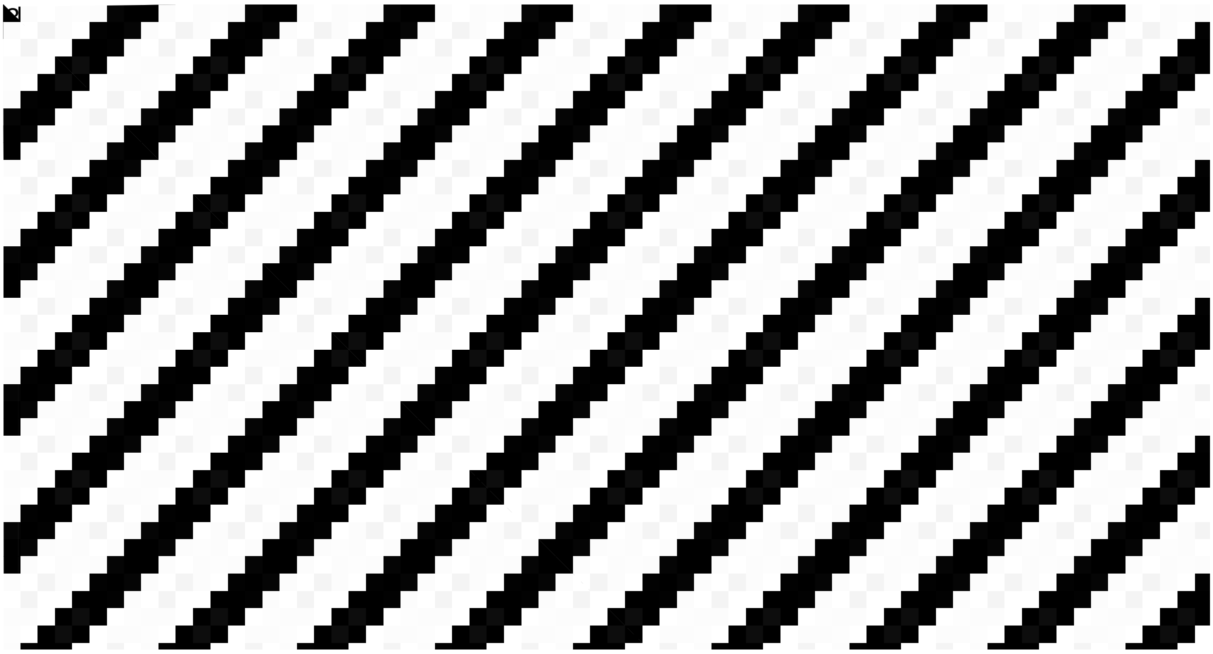

Figure 2 (also adapted from Young's paper) describes the typical patterns that are exhibited by the wind velocity with height as the surface roughness varies over urban (or mountainous) areas, suburbs (or forest) and level country (or water). The figure shows higher wind speeds at lower elevations over flat smooth terrain or water which favours placement of wind turbines in such areas.

The wind velocity with height is normally explained by the power equation:

$$V_h / V_r = (h_h / h_r)^{\alpha}$$

where:

V_h = wind velocity at height h

V_r = wind velocity at reference height (normally 10 metres)

h_h = height in question

h_r = reference height (normally 10 metres)

α = the wind shear coefficient

Young goes on to note that another factor needs to be considered, the stability of the atmosphere. This can be stable, neutral, or unstable. Figure 3 below, also adapted from Young's report, shows the conditions of a neutral atmosphere near the ground, with a stable atmosphere above, or a stable atmosphere near the ground with a neutral condition above.

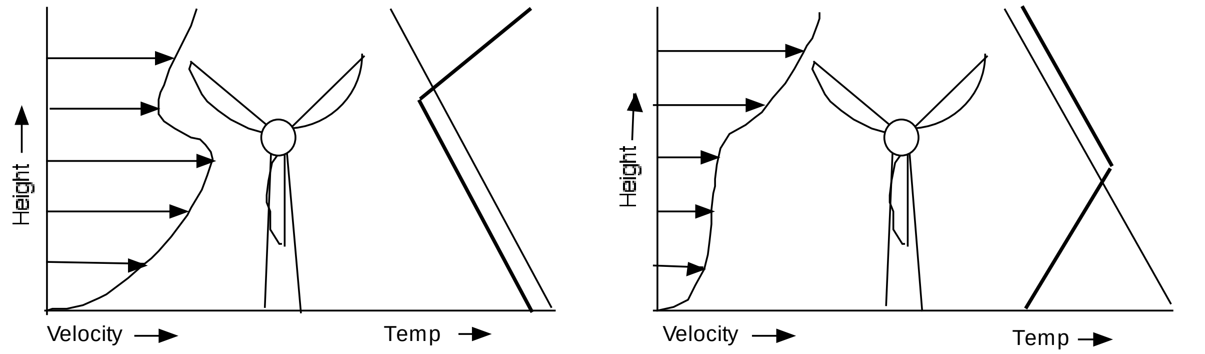

Neutral Atmosphere near the Ground with Stable Above   Stable Atmosphere near the Ground with Neutral Above

Figure 3 - Stability of Atmosphere Can Influence Profile

The sketches in Figure 3 show that neither the wind velocity nor the temperature necessarily follow the power equation of a steadily increasing velocity with height, or the temperature relationship of a decreasing temperature with height. The figure shows a typical wind turbine with a hub height of about 80 metres, at the transition point between the stable and neutral atmosphere condition as might occur.

The temperature reference line shows that in a neutral atmosphere, the temperature can be expected to fall about 1°C per 100 metres, but in the stable atmosphere, the temperature can rise with height. (This is alternately described as a temperature inversion).

The condition of thermal stability above ground elevation can be referenced in other fields of science. The Encyclopaedia of Soil Science shows in an article on Erosion by Wind[iii] that “atmospheric conditions with neutral buoyancy are found with cloudy skies (which reduce radiative heating) and strong winds (which promote atmospheric mixing and prevent temperature stratification.) “ It goes on to describe that “On clear and sunny days (especially in arid or semi-arid areas) strong radiative heating may result in thermal instability (with a steep temperature gradient) which increases buoyancy effects and vertically stretches turbulent eddies … Conversely, atmospheric stability (often occurring at night with radiative cooling of the surface) tends to squeeze turbulent eddies vertically resulting in a strong wind gradient with little vertical mixing.”

Similarly, the doctoral dissertation “The Sounds of High Winds” by G.P van den Berg[iv] discusses the subject of atmospheric stability and notes, “Atmospheric stability has a profound effect on the vertical wind profile and on atmospherical turbulence strength.” Van den Berg discusses both the power law function and the logarithmic wind profile. He notes that the power law has no real physical basis, and that it may not apply under all conditions. Similarly van den Berg notes that the logarithmic wind profile “is an approximation of the wind profile in the turbulent boundary layer of a neutral atmosphere.”

Values of the wind shear coefficient $\propto$ are related to stability classes as defined by the Pasquill classes by van den Berg or the Classification Company Det Norkse Veritas (DNV) as shown in the following table.

Pasquill Class	Name	DNV Class	Shear Coefficient $\propto$
A	Very unstable		0.09
		Unstable	0.16
B	Moderately unstable		0.20
C	Neutral	Neutral	0.22
D	Slightly stable		0.28
		Stable	0.35
E	Moderately stable		0.37
F	(Very) stable		0.41

A slightly different Pasquill Classification was defined in the paper by F. Pasquill "The estimation of the dispersion of windborne material"[v] in 1961.

Table 1: The Pasquill stability classes

Stability class	Definition	Stability class	Definition
A	very unstable	D	neutral
B	unstable	E	slightly stable
C	slightly unstable	F	stable

Table 2: Meteorological conditions that define the Pasquill stability classes

Surface wind speed		Daytime incoming solar radiation			Nighttime cloud cover	
m/s	mi/h	Strong	Moderate	Slight	> 50%	< 50%
< 2	< 5	A	A – B	B	E	F
2 – 3	5 – 7	A – B	B	C	E	F
3 – 5	7 – 11	B	B – C	C	D	E
5 – 6	11 – 13	C	C – D	D	D	D
> 6	> 13	C	D	D	D	D

Note: Class D applies to heavily overcast skies, at any wind speed day or night

The issue of atmospheric stability is an important one for predicting the impacts of releases from chemical facilities, fires, and nuclear facilities. The "Safety Report" of Bruce Nuclear Generating Station A[vi], for example, shows the prevalence of stability class E and F. The 1994 issue of the Safety Report, shows stability classes E and F occurring with the following frequency (based on 4 to 9 years of data for each):

London Ontario	28.4% of the time
Mount Forest Ontario	27.3% of the time
Muskoka Ontario	27.9% of the time
Sudbury Ontario	22.1% of the time
Flint, Michigan	28.5% of the time
Wiarton, Ontario	24.5% of the time

In the 2003 reissue of the "Safety Report"[vii] atmospheric stability was calculated using the Sigma Theta (σ_θ) method, as dictated by the US NRC and US EPA. Using this method the frequency of occurrence of Atmospheric Stability Classes E and F for Wiarton Ontario in the preceding 4 year period was E = 9.3% and F = 9.1%.

Since by definition Pasquill Class E and F can only exist at night (which is less than half of a day in Ontario), the fact that these conditions exist between 18.4 to 28.4% of the time in total in Ontario, suggest that they apply for over half of all nights.

Modelling Atmospheric Stability

It is clear that neither the normal power equation (described above), nor the common logarithmic relationship for wind speed as a function of vertical elevation from International Standard IEC 61400-11 shown below provide any transition to describe the change in atmospheric conditions that occur when atmospheric stability occurs.

$$V_s = V_z \left[\frac{\ln\{Z_{ref}/Z_{oref}\}\ \ln\{H/Z_o\}}{\ln\{H/Z_{oref}\}\ \ln\{z/z_o\}} \right]$$

where:

Z_{oref} is the reference roughness length of 0.05 m

Z_o is the roughness length

H is the rotor centre height

Z_{ref} is the reference height, 10 m

Z is the anemometer height

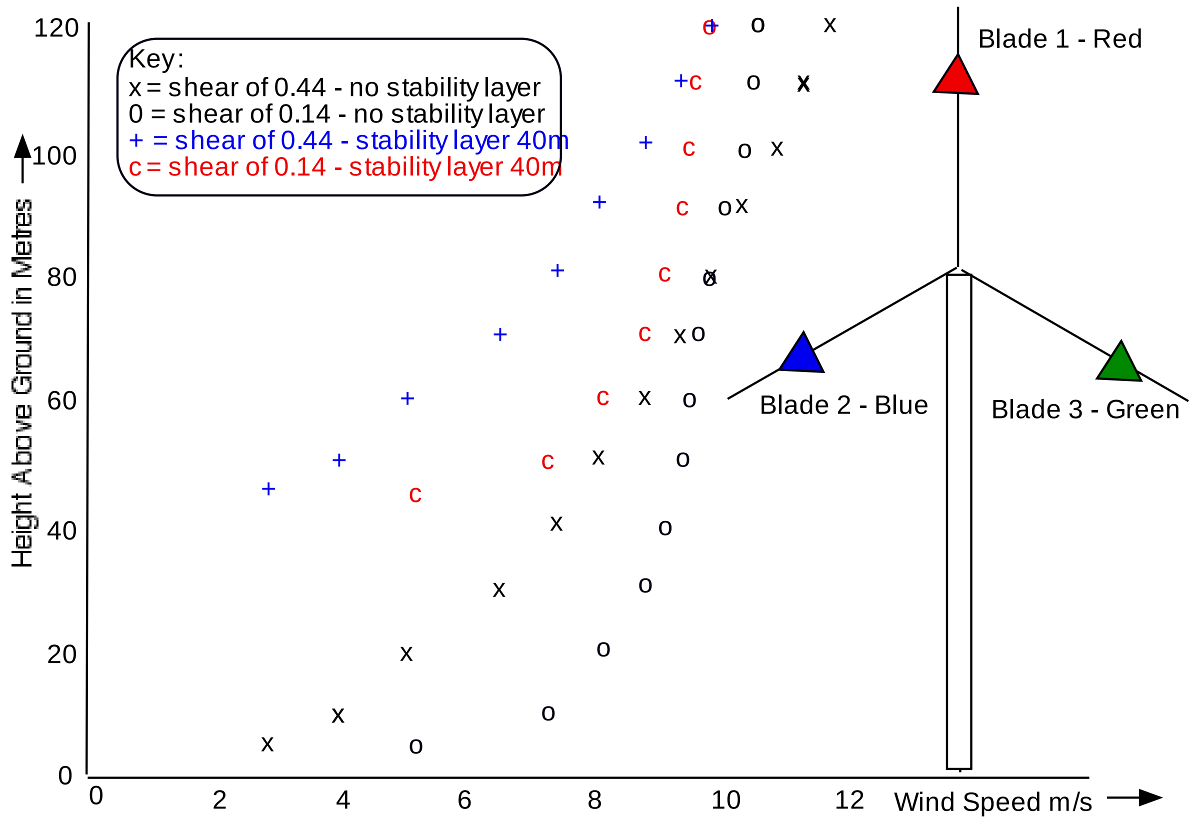

Figure 4 - Effect of Shear and Stability on Incident Wind Speed

Figure 4, on the previous page shows the effect of varying wind shear and on the stability level on the wind speed in metres per second at increasing heights above ground. For the case of no stable layer in the lower atmosphere, the case has been shown where for shears of 0.14 (nominally a neutral atmosphere) and for 0.44 (a stable atmosphere), plotting both cases for the same wind speed of 10 metres per second at the 80 metre hub height of a wind turbine. The curve labelled with the “o”s show that for the case of the wind shear of 0.14 (neutral atmosphere) this corresponds to a wind speed of about 7.5 metres per second at 10 metres above the ground, while for the wind shear of 0.44 (stable atmosphere) the curve labelled with the “x”s shows a wind speed of 10 metres second at 80 metres corresponds to a wind speed of 4 metres per second at 10 metres above the ground. The two shifted curves noted by the “+” and “c” symbols show the case of atmospheric stability that can occur on the majority of nights as shown above for the case of Southern Ontario.

In this case, the wind speed may be low up to the level of the top of the stable layer. This is a familiar phenomenon seen in the smoke that rises vertically from a campfire on the ground or a low chimney at night before sharply changing direction when it reaches the top of the stable layer. The power law is applied as before to calculate the wind speeds above the top of the stable layer once the atmosphere again becomes either neutral or unstable.

Sketched beside the curves of wind speed, as a function of height is a normal wind turbine, with a hub height of 80 metres and a blade diameter of 82 metres. Observation of this figure shows that during the neutral atmosphere with a shear of 0.14 and no stable layer (typical of daytime hours) the wind speed is roughly the same from the top to the bottom of the turbine rotor (varying less than 10% from the top to the bottom of the blade circle.) However, during the condition of a stable atmosphere that can exist on the majority of nights, the variation of incident wind speed across the turbine rotor varies significantly more, ranging from 33% to over 100%. Not only does this variation of wind speed cause high mechanical stresses across the rotor at night as reported by the United States National Renewable Energy Laboratory[viii] it can be shown that it has an impact on the “Whoosh” noise.

Showing the Effect of Stability on Noise

In “The Sounds of High Winds” van den Berg shows the strong influence between angle of attack (the angle between the incoming air flow and the blade chord)[ix] and wind turbine noise in a stable atmosphere. In Figure III.2 of his paper (adapted as Figure 5 below), the local wind velocity divided by the air velocity due to rotation is seen to be the tangent of the flow angle φ.

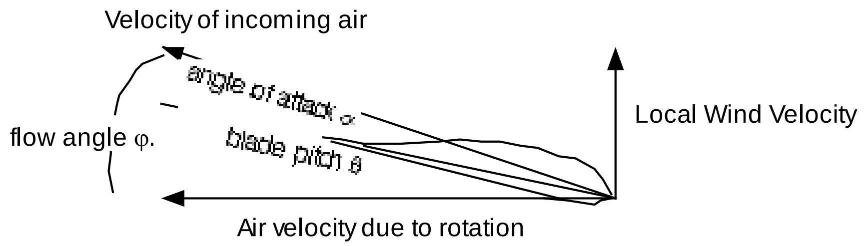

Figure 5 - Air Flow Over Turbine Blade

To display the result of atmospheric stability on the noise produced, an Excel spreadsheet was created to calculate the wind speed incident on the turbine blades as they rotate, in both daytime neutral cases and at night when a stable level is created in the atmosphere typical of the case shown in Figure 4. For simplicity, the turbine blades were designated as the Red, Blue and Green blade, and the elevation was calculated for the point 75% of the distance from the hub on the turbine blade (recognizing the work by Oerlemans / Schepers) for one full rotation of the turbine rotor at each 30-degree increment of the rotation. The rotation direction is clockwise with the Blue blade following the Red blade. See Photos 1 and 2 at the end of the text. The example of a turbine with an 82-metre rotor diameter was used, typical of wind turbines being installed today in Ontario – the Vestas V82, or the Enercon E82.

The wind speed at the location of each of the three turbine blades was then calculated, for the cases of a wind shear of 0.14, 0.26, and 0.44, and for a stable layer at 0 metres, 20 metres and 40 metres, to give 9 cases. The wind speed was calculated using an assumption that the wind speed is constant (and low) up to the top of the stable atmosphere layer, then to increase as given by the power law. The increase is described by the wind shear α after that point. Calculations were made for wind shears from 0.14 to 0.44 (typical of shears shown to exist in the paper[x] presented at 2007 at the Wind Turbine Noise Conference). Actually, the work by Young, presented at the Ontario Municipal Board in 2007 showed that in a number of cases, the wind shear α was greater than 1.0.

Once the local wind speed was calculated incident upon each blade, then the velocity of incoming air was calculated as the resultant vector from combining the local wind velocity and the air velocity due to rotation of the blade. This assumed the rotational speed of 14.4 revolutions per minute at the point 75% from the hub on each 41 metre blade as about 45 metres per second.

Then the “flow angle” of the airflow over the turbine blade was calculated from the tangent relationship described above (the local wind velocity divided by the air velocity due to rotation is seen to be the tangent of the flow angle φ).

In Table B1 of appendix B of his paper “the Sounds of High Winds” van den Berg describes the increase of trailing edge sound with angle of attack α as follows.

A	1°	2°	3°	4°	5°	6°	7°	8°	9°
$\Delta SPL_{TE}(\alpha)$ (dB)	0.4	1.4	2.9	4.6	6.4	8.0	9.4	10.6	11.5

Since van den Berg identifies a linear relationship between the added sound pressure level ΔSPL and the angle of attack, the spreadsheet data was then used to add the angle of attack for each of the three turbine blades for the nine cases of varying wind shear and top of the stable layer. While this would not produce an actual sound power level, the intent was to show the change in the summed flow angles as the blades rotate. Since for modern turbines, the blade pitch does not vary other than for changing power levels, changes in the angle of attack can be derived from changes in the total flow angle as the air passes over the turbine blade.

The results of the curves are discussed in the observations, below. The spreadsheet data is available from the author.

Observations

Chart 1 plots the summed flow angle from all three turbine blades at each rotary position for the nine cases examined. For the assumption of the same 10 metre per second air flow at the 80 metre hub level of the turbine, the greatest summed flow angle exists for the case of the lowest wind shear, as expected since for this case the wind velocity is most constant across the entire turbine rotor. This condition results in the least variation in the summed flow angle as the rotor goes through its circular circuit, and thus a "swish" of little variation. Chart 1 shows that as a stable level in the atmosphere is created, the variation in the summed angle of flow becomes more apparent, and the "Whoosh" would become more apparent. Again, the Chart shows that the greatest summed flow angles are calculated for the smallest wind shear. This is largely a result of the method of calculation, which assumes the same 10 metres per second at the 80 metre level for the case with no stable level.

Chart 2 makes it clear that the most significant changes in the normalized sum of the Angle of Flow exists for the case with the largest wind shear and the top of the stable level at 40 metres. The high shear, coupled with a stable atmosphere produces much more variable effect in the flow angle. Since this is the predominant cause of the turbulent flow condition, and hence the noise, it produces a cyclic nature of the sound. Chart 2 shows that the highest normalized sum for the Angle of Flow occurs when the blades pass the top of their path, and is lowest when the blades pass the bottom of the path. This is contrary to the finding of Oerlmans and Schepers, who determined that "most of the noise is produced by the outer part of the blades during the downward motion" as noted earlier. Figure 6 suggests an explanation of the discrepancy.

ObserverDistance	Rotation when Sound Arrives
82 m	0.4 sec = 0.1 revolution
200 m	0.7 sec = 0.2 rev
400 m	1.2 sec = 0.3 rev
600 m	1.8 sec = 0.4 rev

Figure 6 - Apparent rotation at distance

Field observations taken to confirm the conclusions of this report at a distance of about 400 metres from the turbine pictured did appear to indicate that the "Whoosh" was most pronounced as each blade passed the 4 o'clock position (or 120 to 150 degrees). However, when one considers that at

15°C sound travels at 340 metres per second, one recognizes that at a distance of 400 m the sound takes 1.2 seconds to reach the observer, and in that time, the turbine blade rotates 0.3 revolution. What certainly sounded to this observer to be a sound loudest during the downward motion with the “Whoosh” occurring about the 4 o’clock position, means that the sound was actually generated 0.3 of a revolution earlier, as the blade was just passing the top of its path. This confirms the calculation performed in this report, and supports the observation that the greatest sum of the flow angle, and thus the summed angle of attack occurs when the blades pass the top of the rotation.

One sees that an explanation of the night time “Whoosh Whoosh Whoosh” compared to the daytime gentle “swish swish swish” becomes clear. When the normalized daytime case, for the neutral or turbulent atmosphere is examined, the fluctuation in flow angle, and hence sound levels is barely evident, while the nighttime case with a stable level in the atmosphere case shows a very pronounced cyclic nature.

Conclusions

The anecdotal evidence that wind turbines are more annoying at night, and that the “Whoosh” is more pronounced at night cannot be fully explained by the normal power law, the logarithmic change in velocity with height, by Doppler effects, or by the creation of sound towards the outer limits of the turbine blade on downward motion.

The explanation of the cyclic nature of the “Whoosh Whoosh Whoosh” can be found in the cyclical change of the sound level that occurs, particularly at night, as a stable atmosphere is created. The stable atmosphere creates the greatest change in the summed angle of attack considering the contribution of each blade taken together, as is heard by an observer. This paper has shown that this condition of a stable atmosphere occurs on the majority of nights in Ontario (and likely occurs elsewhere with a similar frequency, as climatic conditions do not observe political boundaries).

The model results displayed in this paper show that when a stable atmosphere exists at night time, the cyclic nature of the sound from wind turbines is more pronounced than it is in the daytime when a stable level in the atmosphere does not exist. Human hearing is capable of resolving a wide variation of sounds, and is particularly sensitive to changes in sound level. Previous work by van den Berg, Pedersen, Bouma, and Bakker, “WINDFARMperception”[xi] published in 2008 showed that “in general respondents perceived wind turbines as being louder in wind blowing from the turbine to their dwelling (and less loud the other way around), in stronger wind ***and at night***.” The report also stated, “In this survey sound was the most annoying aspect of wind turbines. From this and previous studies it appears that sound from wind turbines is relatively annoying: at the same sound level it causes more annoyance than sound from air or road traffic. ***A swishing characteristic is observed by three out of four respondents that can hear the sound*** and could have been one of the factors explaining the annoyance.”

The existence of this condition as shown in this report reinforces the need to apply a penalty to the average sound received from wind turbines at night because the cyclic “Whoosh” produced during stable atmospheres makes them particularly noticeable and annoying, compared to other noise sources.

Photographs

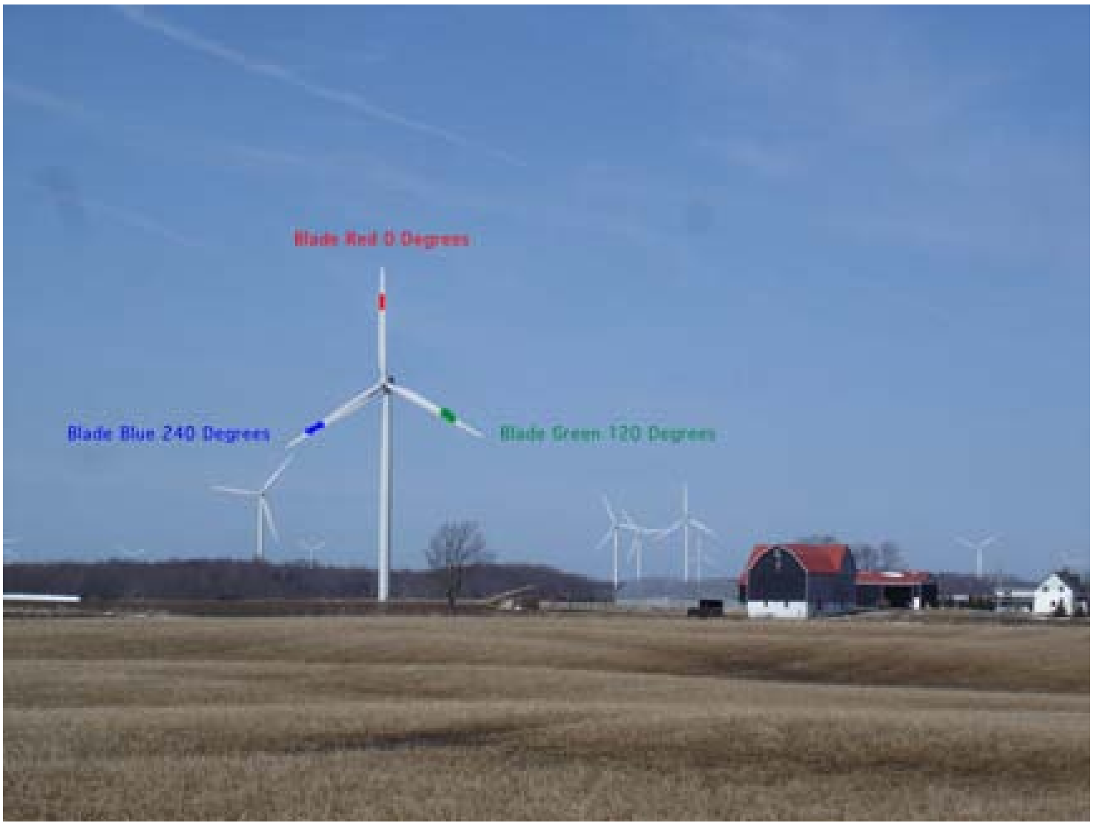

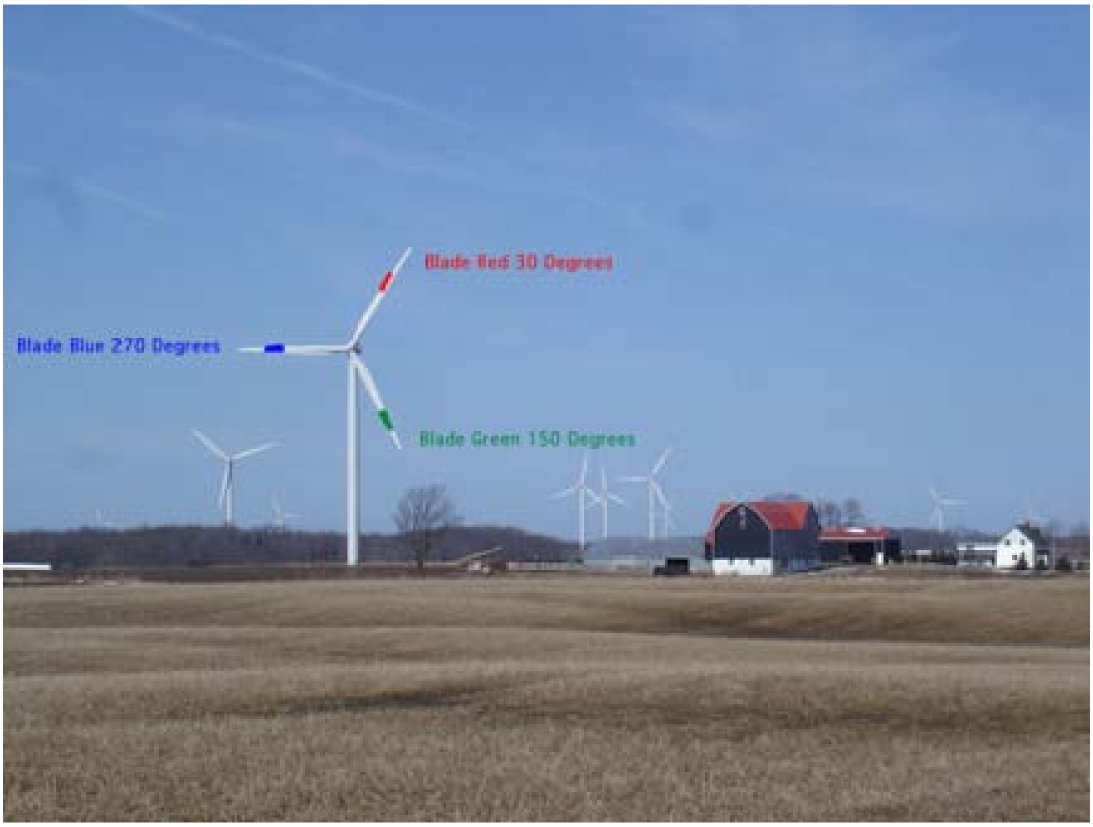

Charts

Chart 1 – Summed Angle of Flow as Turbine Rotates

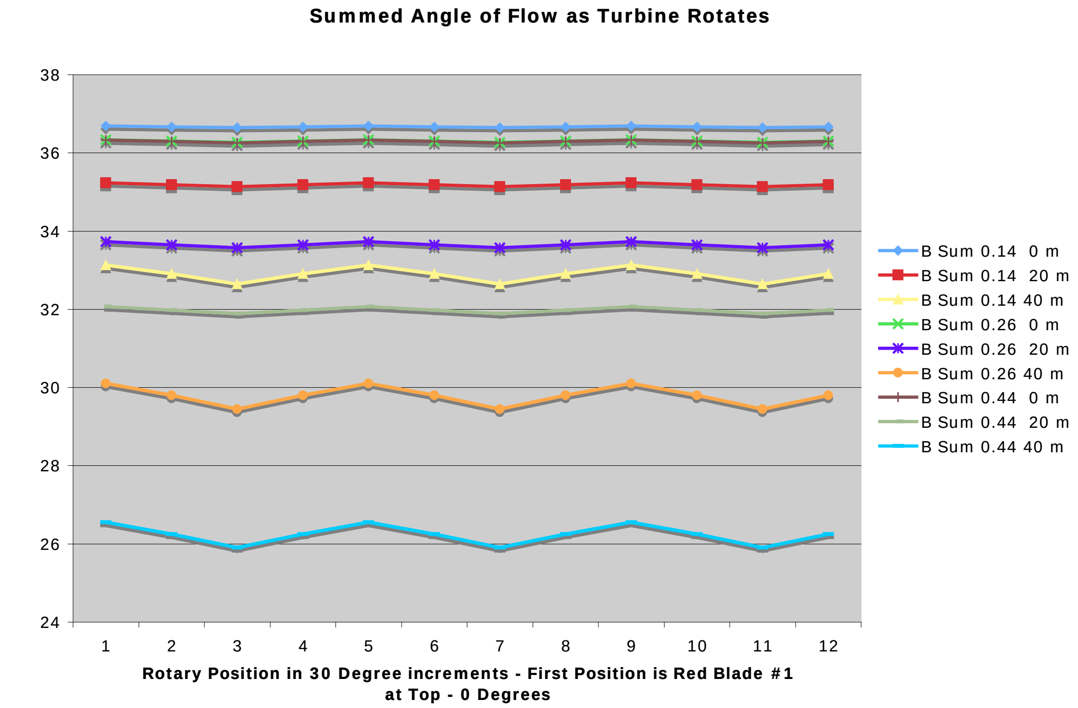

Chart 2 – Normalized Sum of Angle of Flow for All 3 Blades

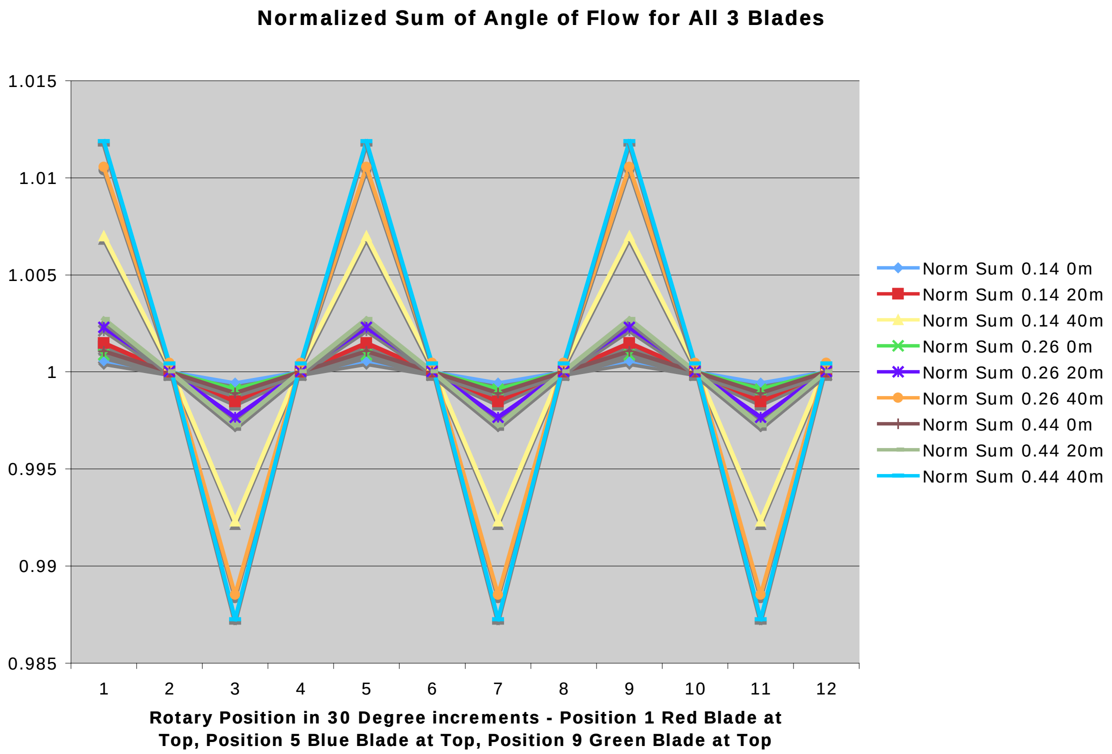

Acknowledgements

I would like to acknowledge the review of a first draft of this paper by the following experts (arranged alphabetically). I do not wish to imply that the reviewers necessarily concur with all content of the paper, but their thoughtful comments helped to clarify the final product for subsequent readers. Thank you sincerely.

- John Harrison, Professor Emeritus, Physics, Queens University, Kingston ON, Canada
- George Kamperman, Acoustical Consultant, Wisconsin Dells, WI, USA
- Nick Kouwen, Professor Emeritus, Civil and Environmental Engineering, University of Waterloo, ON, Canada
- Stefan Oerlemans, National Aerospace Laboratory, NLR, The Netherlands
- Gerard Schepers, ECN Wind Energy, The Netherlands
- G.P. (Frits) van den Berg, University of Groningen, The Netherlands
- Jim Young, Meteorological Consultant, Kincardine ON, Canada

References

[i] Oerlemans, Stefan and Schepers, Gerard, “Prediction of Wind Turbine Noise and Comparison to Experiment” presented at the Second international Meeting on Wind Turbine Noise, Lyon France, September 2007.

[ii] Young, James W.S. Ph.D., P.Eng. “Analysis of Boundary Layer Winds near Goderich and Their Application to Wind Farms along the East Coast of Lake Huron” by as presented at Ontario Municipal Board Hearing PL060986, April 2007.

[iii] Lai, R. “Encyclopaedia of Soil Science” ISBN: 0849350530, Page 618, Erosion by Wind: Micrometeorology.

[iv] van den Berg, G.P. “The Sounds of High Winds, the effect of atmospheric stability on wind turbine sound and microphone noise” submitted as a doctoral dissertation to the University of Groningen, May 12, 2006. Chapter III from pages 27 to 38 discusses the subject of atmospheric stability.

[v] Pasquill, F. (1961). “The estimation of the dispersion of windborne material.” The Meteorological Magazine, vol 90, No. 1063, pp 33-49.

[vi] Bruce Generating Station A Safety Report, Chapter 1, Site Evaluation, Section 2, “Factors Affecting a Release” 1994 Edition, subsection 2.2.1.6 “Atmospheric Stability”

[vii] Bruce Nuclear Generating Station A Safety Report, NK21-SR-01320-00001, Rev 002, July 4, 2003, predicts stability class using the Sigma Theta (σ_θ) method as defined by the US NRC (Nuclear Regulatory Commission) Proposed Revision 1 to Regulatory Guide 1.23: Meteorology Programs in Support of Nuclear Power Plants, 1980, and the US EPA (Environmental Protection Agency) “Guidelines on Air Quality Models” Report No, EPA-450/2-78-027R, Table 9-3, pp 9-21, 1986.

[viii] Kelley N, Smith B, Smith K, Randall G, Malcolm D, “Evaluation of Wind Shear Patterns at Midwest Wind Energy Facilities” National Renewable Energy Laboratory, US Department of Energy, May 2002, Paper NREL/CP-500-32492.

[ix] Van den Berg G.P. . “The Sounds of High Winds, the effect of atmospheric stability on wind turbine sound and microphone noise” submitted as a doctoral dissertation to the University of Groningen, May 12, 2006 (previously also listed as Reference iv) discusses angle of attack and stability on noise in Chapter III, Chapter V, and Appendix B.

[x] Palmer, William K.G. “Uncloaking the Nature of Wind Turbines – Using the Science of Meteorology” presented at the Second International Meeting on Wind Turbine Noise, Lyon, France, September 2007.

[xi] Van den Berg F, Pedersen E, Bouma J, Bakker R, “WINDFARMperception – Visual and acoustic impact of wind turbine farms on residents” University of Groningen, FP6-2005-Science-and-Society-20. Specific Support Action, Project no. 044628, Final Report, June 3, 2008.

Third International Meeting
on
Wind Turbine Noise
Aalborg Denmark 17 – 19 June 2009

Effects of wind turbine noise on humans

Eja Pedersen
Halmstad University
P.O. Box 823, SE-301 18 Halmstad, Sweden
Eja.Pedersen@hh.se

Abstract

Possible adverse health effects due to exposure of wind turbine noise have been discussed since the first modern electrical generating wind turbines were erected in the 1970's. Despite this, only a few large epidemiological studies have been carried out. This paper is based on data from two Swedish studies and one Dutch study in which self-reported health and well-being were related to calculated A-weighted sound pressure levels outside the dwelling of each respondent. The consistencies in results from these studies make it possible to summarize the impact of wind turbine noise on people living in the vicinity of the turbines. The main adverse effect was annoyance due to the sound; the prevalence of noise annoyance increased with increasing sound pressure levels. Disturbance of sleep was furthermore related to wind turbine noise; the proportion of residents reporting sleep disturbance due to noise increased significantly at sound levels close to those recommended as highest acceptable levels at new installations. No other clear associations between sound levels and self reported health symptoms have hitherto been found. However, noise annoyance was correlated with several measurements of stress and lowered well-being. The study design does not allow causal conclusions, but the association indicates a possible hindrance of psycho-physiological restitution. Such a hindrance could in the long term lead to adverse health effects not detected hear.

Introduction

There has been a concern of possible adverse health effects caused by noise from wind turbines ever since the beginning of the modern wind power era in the 1970's. This concern could be due to a common scepticism towards new technique, but could also be traced to bad experiences. The first commercial machines did not just emit aerodynamic noise but also noise from the machinery giving them a reputation as noisy. Furthermore, some were designed as down wind turbines with rather high levels of noise in the low frequency range that was negatively appraised [Hubbard 1982]. The noise was therefore a large issue already thirty years ago. Special for wind turbines are also that they often are placed in rural settings considered as places with low exposure of environmental stressors. Technical induced noise could in such a setting, even when the levels are comparably low, be perceived as a potential health risk.

Several studies concerning the impact of wind farms on residents in wind farm areas are cited in the discussion regarding possible health effects that takes place for example on Internet. Few of these studies have however been published in scientific journals, i.e. they are not critically reviewed and accepted by scientists. As the issue of wind power involves political decisions leading to conflicts where health risks become an argument rather than a fact, it is important to study possible health effects unprejudiced. Conclusions should hence be drawn from well designed experimental or epidemiological studies that have been seriously examined.

The definition of health set up by WHO 1948 is still the guiding principle in public health work. The definition reads as follows:

> Health is a state of complete physical, mental and social well-being and not merely the absence of disease or infirmity [WHO 1948].

Such a definition implicates that when studying the effects of an environmental exposure it is necessary to not just focus on diseases or symptoms of impaired health, but also measure well-being in a wider sense. Response to noise such as annoyance is hence, in the light of the WHO definition, in it self a negative effect that should be avoided in order to retain well-being. However, annoyance could also be viewed upon as a measurable indicator of enhanced risk for chronic unbalance in the physiological stress system; an unbalance that could lead to more severe states such as high blood pressure and, if prolonged, to more severe cardio-vascular diseases. The theory has been confirmed in studies where an association between high exposure of community noise, such as road traffic and aircraft noise, and high blood pressure has been found [e.g. Barregard *et al*. 2009]. The exposure levels were in these traffic studies higher than those relevant for residents living in the vicinity of wind turbines, but it can not be excluded that strong feelings of annoyance, despite sound levels, play a role in endocrine influenced diseases, possibly as inhibitors of physiological restitution [Åkerstedt and Nilsson 2003].

The public concern regarding possible health risks among people living in the vicinity of wind turbines should be treated seriously. The objective of this paper was to explore the relationship between wind turbine noise and potential adverse health effects using data from three epidemiological studies; two published and one soon to be published.

Included studies

All three studies were cross-sectional studies where levels of wind turbine noise were compared to self-reported health status among people living in wind farm areas. Study SWE-00 were carried out in a flat, rural landscape in the south of Sweden year 2000 [Pedersen and Persson Waye 2004]. Study SWE-05 also took place in Sweden but in areas that differed in population density and topography, including suburban sites and hilly terrain [Pedersen and Persson Waye 2007]. Study NL-07 was carried out in the Netherlands 2007, also in a flat landscape, but with different degrees of road traffic intensity [van den Berg *et al*. 2008]. Annoyance and other health effects were measured in postal questionnaires comprising questions of several potential environmental stressors to not lead the respondent towards a focus on wind turbine noise. The questionnaires were delivered during the summer months, i.e. when people supposedly spend time outdoors by their dwelling. A-weighted sound pressure levels (corresponding to downwind condition with wind speed 8 m/s at 10 m height) were calculated for each respondent from the sound power levels of all wind turbines nearby (logarithmically added). Two different algorithms were used for the calculations of the sound propagation; one for the Swedish studies [Swedish Environmental Protection Agency 2001] and another for the Dutch study [ISO 1996]. The algorithms give similar results at the distances relevant in these studies [van den Berg *et al*. 2008] and will therefore in these analyses be treated as correct estimations of the exposure for all respondents outside their dwelling.

The data sets have for this paper been re-analysed in order to assure similar treatment of the data. Only variables available from all three studies are included: response to noise (annoyance), diseases or symptoms of impaired health (chronic disease, diabetes, high blood pressure, cardiovascular disease, tinnitus, impaired hearing), stress symptoms (headache, undue tiredness, feeling tense or stressed, feeling irritable) and disturbed sleep (interruption of the sleep by any noise source), Variables measured in the questionnaires were answered either on binary scales (no/yes) or on ordinal 5-point scales. The latter was for example used for noise annoyance, with the scale “do not notice”, “notice, but not annoyed”, “slightly annoyed”, “rather annoyed”, and “very annoyed”. The variable was for the analyses dichotomized into “not annoyed” (comprising “do not notice”, “notice, but not annoyed” and “slightly annoyed”) versus “annoyed” (comprising rather annoyed” and “very annoyed”). Sleep disturbance due to noise (any source) was measured differently in the three studies. In the Swedish studies, the scale used was binary (no/yes) while in the Dutch study the scale was related to how often sleep disturbance occurred. Sleep disturbance once a month or more often was in this study considered as sleep disturbance.

Several health symptoms are known to increase with age and also have different prevalence among males and females that has to be taken into account. Associations between A-weighted sound pressure levels and self-reported health were therefore tested with binary logistic regression as this method allows adjustments for known confounders. The Dutch study differed from the others in that many of the respondents in the samples with the highest exposures of wind turbine noise reported that they benefited economically from the wind turbines. Almost none of these respondents reported noise annoyance and they also differed from the rest; e.g. they were younger and overall healthier. The results from the Dutch study are therefore reported twice; once with adjusting for economical benefits. The outcome of a logistic regression is the odds ratio (OR) with a 95% confidence interval (95% CI). An OR above 1.00, with a 95% CI with the lower value also above 1.00, indicates a positive correlation between the dependent (health) and the independent variable (sound pressure levels) in the regression model.

A-weighted sound pressure levels were furthermore divided into 5-dB(A) intervals and compared with proportion of respondent annoyed by the noise and disturbed in their sleep by any noise source. Confidence intervals of the proportions were calculated in accordance with Wilson [Altman *et al*. 2000].

Results

A-weighted sound pressure levels were in all three studies related to annoyance with wind turbine noise outdoors (Table 1).

Table 1. Association between A-weighted sound pressure levels (independent, continuous variable) and symptoms of adverse health effects (dependent, binary variable) tested with logistic regression. Statistically significant associations in bold numbers.

	N	OR*	95% CI*
Annoyance (outdoors)			
SWE-00	333	**1.24**	**1.13 – 1.36**
SWE-05	744	**1.14**	**1.03 – 1.27**
NL-07	687	**1.10**	**1.06 – 1.15**
NL-07**	664	**1.18**	**1.12 – 1.24**
Chronic disease			
SWE-00	328	0.97	0.89 – 1.05
SWE-05	742	1.01	0.96 – 1.07
NL-07	697	0.97	0.95 – 1.00
NL-07**	672	0.98	0.95 – 1.01
Diabetes			
SWE-00	333	0.96	0.79 – 1.16
SWE-05	744	**1.13**	**1.00 – 1.27**
NL-07	703	0.97	0.90 – 1.06
NL-07**	678	1.00	0.92 – 1.03
High blood pressure			
SWE-00	333	1.03	0.90 – 1.17
SWE-05	744	1.05	0.97 – 1.13
NL-07	703	0.97	0.94 – 1.03
NL-07**	678	1.01	0.96 – 1.06
Cardiovascular disease			
SWE-00	333	0.87	0.68 – 1.10
SWE-05	744	1.00	0.88 – 1.13
NL-07	703	0.96	0.90 – 1.03
NL-07**	678	0.98	0.91 – 1.05
Tinnitus			
SWE-00	333	**1.25**	**1.03 – 1.50**
SWE-05	744	0.97	0.88 – 1.07
NL-07	703	0.94	0.86 – 1.03
NL-07**	678	0.94	0.85 – 1.04
Impaired hearing			
SWE-00	333	1.09	0.93 – 1.27
SWE-05	744	1.05	0.95 – 1.15
NL-07	703	0.98	0.93 – 1.07

NL-07**	678	1.01	0.94 – 1.10

*Adjusted for age and sex.
**Adjusted also for economical benefits.

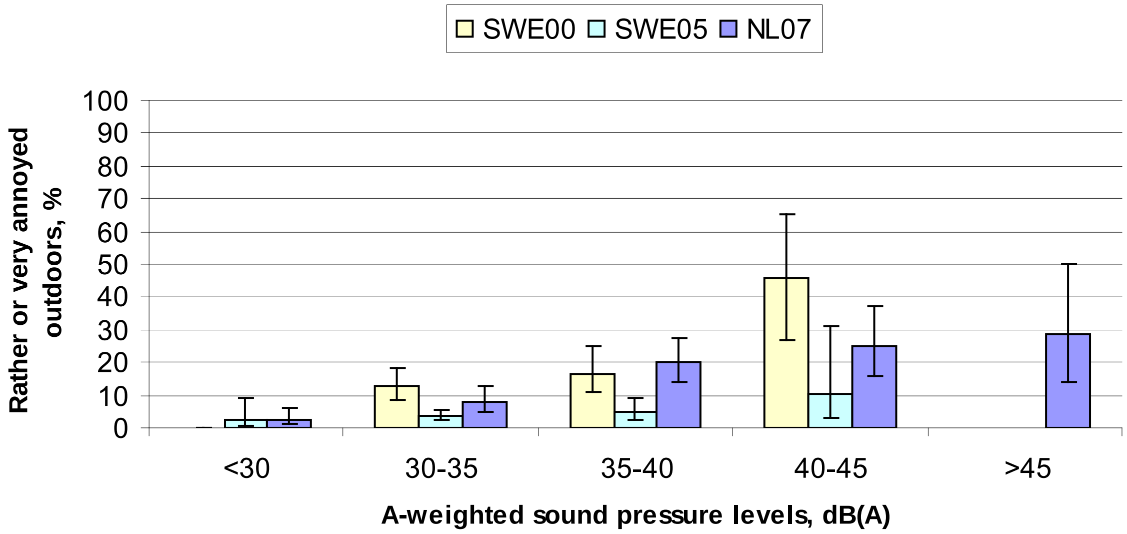

Figure 1. Relationship between A-weighted sound pressure levels (equivalent levels at wind speed 8 m/s, 10 m over the ground) and proportion of respondents rather or very annoyed by wind turbine noise outdoors in three studies: SWE00 (*n* = 341), SWE05 (*n* = 754) and NL07 (only respondents that did not benefit economically from wind turbines; *n* = 586).

The highest increase of annoyance with increase of sound levels was found in the first Swedish study, followed by the Dutch study when adjustments for economical benefits had been made. The prevalence of annoyance was similar in the first Swedish study and the Dutch study up to 40 dB(A) (the recommended highest level in Sweden), but then increased more in the Swedish study than in the Dutch study (Figure 1). Annoyance was low in all sound level intervals in the second Swedish study and differed statically significant from that in the two others studies in the sound level interval 35 – 40 dB(A).

No other variable measuring health or well-being was consistently related to A-weighted sound pressure level throughout the three studies (Table 1). The prevalence of tinnitus was in the first Swedish study positively related to sound pressure levels, but no such relationship was found in the other two studies. An indication of a positive relationship between the prevalence of diabetes and sound pressure levels was found in the second Swedish study. The lower limit of the confident interval was however just above 1.00.

No associations between A-weighted sound pressure levels and variables measuring symptoms of stress were found (Table 2).

Reports of interruption in the sleep by noise of any source were in the first Swedish study related to A-weighted sound pressure levels of wind turbine noise (Table 3). The same was found in the Dutch study when the analyses were adjusted also for economical benefits.

Table 2. Association between A-weighted sound pressure levels (independent, continuous variable) and symptoms of stress (dependent, binary variable) tested with logistic regression.

	N	OR*	95% CI*
Headache			
SWE-00	320	0.95	0.88 – 1.02
SWE-05	720	1.04	0.99 – 1.10
NL-07	661	1.00	0.97 – 1.02
NL-07**	639	1.01	0.98 – 1.04
Undue tiredness			
SWE-00	319	0.95	0.88 – 1.02
SWE-05	725	0.98	0.93 – 1.03
NL-07	662	0.99	0.96 – 1.01
NL-07**	639	1.02	0.99 – 1.05
Tense and stressed			
SWE-00	319	1.02	0.94 – 1.10
SWE-05	721	1.00	0.95 – 1.05
NL-07	663	0.99	0.97 – 1.02
NL-07**	641	1.01	0.98 – 1.04
Irritable			
SWE-00	319	1.03	0.96 – 1.11
SWE-05	724	1.00	0.96 – 1.06
NL-07	666	1.00	0.98 – 1.03
NL-07**	644	1.01	0.98 – 1.04

*Adjusted for age and sex.
**Adjusted also for economical benefits.

Table 3. Association between A-weighted sound pressure levels (independent, continuous variable) and sleep interruption (dependent, binary variable) tested with logistic regression. Statistically significant associations in bold numbers.

	N	OR*	95% CI*
Interrupted in the sleep by noise			
SWE-00	333	**1.12**	**1.03 – 1.22**
SWE-05	738	0.97	0.90 – 1.05
NL-07	703	1.01	0.99 – 1.04
NL-07**	678	**1.03**	**1.00 – 1.07**

*Adjusted for age and sex.
**Adjusted also for economical benefits.

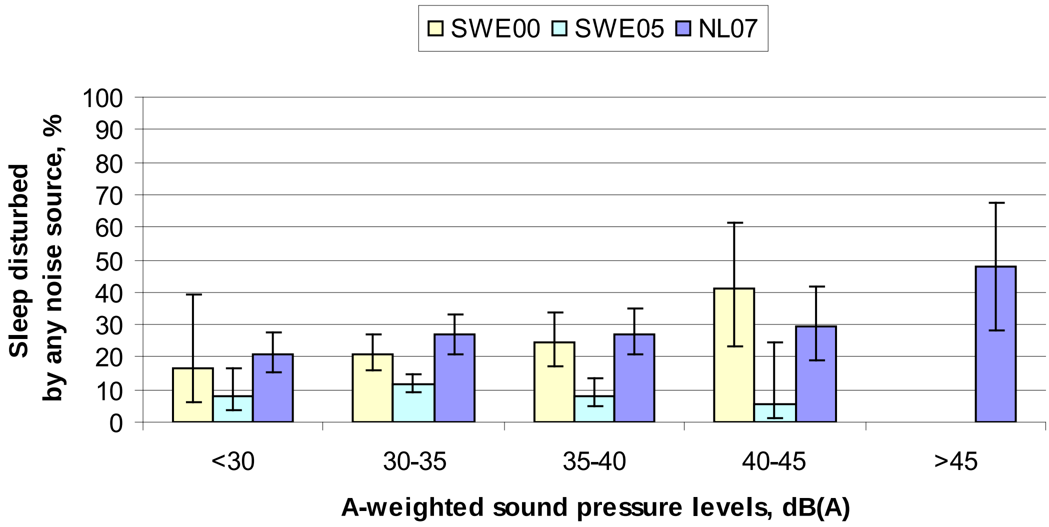

Figure 2. Relationship between A-weighted sound pressure levels (equivalent levels at wind speed 8 m/s, 10 m over the ground) and proportion of respondents disturbed in the sleep by noise in three studies: SWE00 (*n* = 341), SWE05 (*n* = 746) and NL07 (only respondents that did not benefit economically from wind turbines; *n* = 593).

In the first Swedish study the increase of respondents that reported sleep interruption appears to be between the sound level interval 35-40 dB(A) and 40-45 dB(A) (Figure 2). The increase came at higher sound levels in the Dutch study; between the interval 40-45 dB(A) and >45 dB(A).

Several of the variables measuring symptoms of stress were associated with annoyance due to wind turbine noise, also when adjusting for A-weighted sound pressure levels (Table 4). Feeling tense or stressed as well as irritable was associated with noise annoyance in all three studies. Headache was associated with annoyance in the first Swedish study and in the Dutch study. Undue tiredness was associated with annoyance only in one study. The study design do not allow conclusions of cause and effect; annoyance could lead to stress, or stress could enhance the risk for annoyance.

Table 4. Association between annoyance due to wind turbine noise (independent, 5-point scale) and symptoms of stress (dependent, binary variable) tested with logistic regression. Statistically significant associations in bold numbers.

	N	OR*	95% CI*
Headache			
SWE-00	320	**1.24**	**1.01 – 1.51**
SWE-05	720	1.04	0.86 – 1.26
NL-07	650	**1.24**	**1.04 – 1.48**
NL-07**	630	**1.25**	**1.04 – 1.50**
Undue tiredness			
SWE-00	319	**1.22**	**1.00 – 1.49**
SWE-05	725	1.12	0.93 – 1.35
NL-07	652	1.15	0.98 – 1.35
NL-07**	630	1.10	0.93 – 1.31
Tense and stressed			
SWE-00	319	**1.25**	**1.00 – 1.56**
SWE-05	721	**1.22**	**1.00 – 1.50**
NL-07	652	**1.28**	**1.08 – 1.50**
NL-07**	631	**1.27**	**1.07 – 1.50**
Irritable			
SWE-00	319	**1.36**	**1.10 – 1.69**
SWE-05	724	**1.22**	**1.00 – 1.49**
NL-07	666	**1.23**	**1.05 – 1.45**
NL-07**	644	**1.27**	**1.07 – 1.50**

*Adjusted for age, sex and A-weighted sound pressure levels.
**Adjusted also for economical benefits.

Concluding remarks

When a high amount of statistical tests are carried out, some will by random show significant relationships when there in fact are none; if a 95% confidence interval is chosen, theoretically 1 of 20 tests will result in a dubious outcome. Consistent results from three studies enhance the certainty. Annoyance was the only response to wind turbine noise measured in these studies that was directly associated with A-weighted sound pressure levels in all three studies. The increased risk for annoyance with increase in sound levels varied however between the studies. The highest increase in risk, and also the highest prevalence of annoyance at sound levels between 40 and 45 dB(A), was found in the first Swedish study that was carried out in a rural, flat landscape with possibly lower levels of background sound than in the two other studies. It is known from aircraft studies that annoyance response in low background noise regions are much higher than those in high background noise regions, even though aircraft noise levels are the same [Lim *et al*. 2008]. If this is actually due to the noise or to other qualities in the rural landscape is not clear. The prevalence of annoyance was high also in the Dutch wind turbine study; higher than in the second

Swedish study. Common for the first Swedish study and the Dutch study is the flat landscape where wind turbines often are visible in several direction and hence have a substantially impact on the landscape.

A rather high amount of respondents reported that their sleep was interrupted by noise, a nuisance that was found to be related to levels of wind turbine noise in two of the studies (and also to road traffic noise that was additionally measured in the Dutch study). The impact of noise did not increase gradually with noise levels, but rather with a sharp increase around 40 dB(A) in the first Swedish study and around 45 dB(A) in the Dutch study, corresponding well with the recommended highest exposure levels in the two countries. Sleep interruption was not common in the second Swedish study carried out mainly in more densely populated areas with suburban characteristics. It is not clear why sleep interruption was less common in these areas, but a combination of lowered expectations of quietness and higher levels of background noise (without incidents of heavy traffic at night) could be an explanation.

Stress was in these studies not directly associated with A-weighted sound pressure levels, but with noise annoyance. There was a remarkable consistency among the studies for the relationship between feeling tense or stressed and annoyance. This should however not be taken as evidence for a causal relationship from wind turbine noise to stress, mediated by annoyance. The finding could be explained in the light of Lazarus and Folkman's cognitive stress theory [1984] where an individual appraises an environmental stressor, such as noise, as beneficial or not, and act on behalf of this. An individual already in a strenuous situation possibly appraises the noise as an additional threat to psycho-physiological restoration. As in the present case wind turbine noise can not be controlled by the individual, no action can be taken and the response is manifested as annoyance. Being interrupted in the sleep could possibly further increase the feeling of wind turbine noise as a threat.

The results of the studies are not alarming, but call for political action and further research. Annoyance due to wind turbine noise should in the future be avoided by applying proper regulations for shortest distance between wind turbines and dwellings in the surroundings. Further scientific studies should explore the influence of wind turbine noise on sleep in different situations as well as the interaction between sound exposure, noise annoyance and stress.

References

Åkerstedt, T., Nilsson, P.M. (2003) Sleep as restitution: an introduction. Journal of Internal Medicine, 254, 6–12.

Altman, D. G., Machin, D., Bryant, T. N., Gardner, M. J. (2000) Statistics with Confidence, 2nd ed. (BMJ Books, London).

Barregard, L., Bonde, E., Öhrström, E. (2009) Risk of hypertension from exposure to road traffic noise in a population-based sample. Occup. Environ. Med. Published online 2 Feb 2009.

Hubbard H.H. (1982) Noise induced house vibrations and human perception. Noise Control Engineering Journal. 19, 49–55.

ISO (1996) Attenuation of sound during propagation outdoors. Part 2: General method of calculation, ISO 9613-2 (International Organization for Standardization, Geneva).

Lazarus, R.S., Folkman, S. (1984) Stress, appraisal and coping. New York, NY:Springer.

Lim, C., Kim., J., Hong., J., Lee, S. (2008) Effect of background noise levels on community annoyance from aircraft noise. J. Acoust. Soc. Am. 123, 766–771.

Pedersen, E., Persson Waye, K. (2004) Perception and annoyance due to wind turbine noise–a dose-response relationship. J. Acoust. Soc. Am. 116, 3460–3470.

Pedersen, E., Persson Waye, K. (2007) Wind turbine noise, annoyance and self-reported health and well-being in different living environments. Occup. Environ. Med. 64, 480–486.

Swedish Environmental Protection Agency (2001) Ljud från vindkraftverk (Noise from wind turbines), Report 6241. [In Swedish.] Stockholm.

Van den Berg, F., Pedersen, E., Bouma, J., Bakker, R. (2008) WINDFARMperception – Visual and acoustic impact of wind turbine farms on residents. FP&-2005-Science-and-Society-20, Specific Support Action, Project no. 044628. www.rug.nl/wewi/

WHO (1948) Preamble to the Constitution of the World Health Organization as adopted by the International Health Conference, New York, 19-22 June.

Third International Meeting
on
Wind Turbine Noise
Aalborg Denmark 17 – 19 June 2009

Prediction of noise from wind farms with Nord2000. Part 2

Birger Plovsing and Bo Søndergaard
DELTA, Venlighedsvej 4, 2970 Hørsholm, Denmark
bp@delta.dk, bsg@delta.dk

Abstract

The Nord2000 prediction model is an established model for traffic noise and is in the process of being accepted as a Nordtest standard method. Due to the ability of the model to include the influence of meteorological conditions on sound propagation it has been chosen as the prescribed model in Denmark for calculating the yearly average of traffic noise levels.

This paper presents a broad view of the Nord2000 prediction principles for short-term noise levels.

The paper also describes a method for calculating long-term noise levels. In the method the actual weather during the considered time period are distributed on a number of meteorological classes with information on the percentage of occurrence of each class. The noise level for each class is determined by the Nord2000 method on basis of representative meteorological parameters of the class. By this method the calculation of long-term noise level can be limited to calculations for approximately nine meteorological classes.

The model has so far been showing promising results when used to predict noise from wind turbines. Contrary to other available prediction methods, Nord2000 is able to include the propagation effect of varying weather conditions and complex terrain. Predictions by Nord2000 are compared to measured noise levels from a validation project. In the validation project both propagation from an elevated loudspeaker and from a wind turbine are considered and measurements have been carried out for both flat and non-flat terrain.

Introduction

The Nord2000 prediction model is an established model for traffic noise and is in the process of being accepted as a Nordtest standard method. Due to the ability of the model to include the influence of meteorological conditions on sound propagation it has been chosen as the prescribed model in Denmark for calculating the yearly average of traffic noise levels. Contrary to most other available prediction methods, Nord2000 is able to include the propagation effect of varying weather conditions and complex terrain.

Nord2000 has previously been validated for noise sources close to the ground with a satisfactory result [1]. This paper describes the result of measurements carried out for validating Nord2000 for sources placed far from the ground surface. More information about the validation project can be found in another conference paper [2].

Nord2000 prediction principles for short-term noise levels

The Nord2000 calculation principles have been described in a number of reports [3,4,5] and the method has in every detail been described in a proposal for a Nordtest standard method [6].

The limitations in the Nord2000 method are:

- The sound pressure level is predicted in one-third octave bands from 25 Hz to 10 kHz. If necessary, the method can be extended below 25 Hz.
- The Nord2000 method assumes a point source. Therefore, a complex source has to be divided into a number of incoherent point sources and a calculation has to be carried out for each point source. For wind turbines, the experience is that a single point source located at the hub is sufficient in most cases.
- The terrain shape from source to receiver has to be approximated by a number of straight line segments.
- In Nord2000 the effect of weather on propagation (refraction) is determined on basis of the vertical effective sound speed profile and Nord2000 can be used to calculate short-term noise levels for time periods where this profile is almost constant. In the Nord2000 method the profile has to be approximated by a log-lin profile between the source and receiver heights as shown in eq. (1).

$$c(z) = A\ln(\frac{z}{z_0}+1) + Bz + c \qquad (1)$$

In eq. (1) c(z) is the effective sound speed at height z above ground, z_0 is the roughness length of the ground, and A, B, and C are constants. A and B are determined by wind speed profile, the angle between the wind direction and the direction of propagation and the air temperature profile. C is sound speed at the ground determined by the air temperature close to the ground.

In excess of the variables A, B, C, and z_0 in Eq. (1) the Nord2000 meteorological input parameters are:

- C_v^2 and C_T^2 which are structure parameters of turbulent wind speed and temperature fluctuations, respectively
- s_A and s_B which are standard deviation from short-term fluctuations of A and B in excess of what is accounted for by the turbulence parameters
- t and RH which are air temperature and relative humidity used for calculation of air absorption

In general, the log-lin approximation in the range of heights between source and receiver is sufficient for most weather cases. However, in some special weather cases (e.g. low level jets) where the approximation is less good a reduced accuracy of the Nord2000 method is expected. If the weather is changing substantially meaning that the vertical effective sound speed profile is no longer constant with minor fluctuations the method for prediction of long-term described in the following section has to be applied.

Fig. 1 shows three examples of terrain approximated by straight line segments. a) is terrain close to being flat, b) is a valley-shaped terrain, and c) is a terrain where a part of the terrain constitute a sound barrier. When approximating real terrain by straight line segments, it is possible to obtain any degree of perfection by using a sufficiently large number of segments. However, as the calculation time increases with the number of segments the optimum number of segments will be a balance between calculation time and accuracy. In practise no more than 10-15 segments are needed to obtain a sufficient accuracy. In the Nord2000 method source and receiver heights are vertical heights above the segmented terrain.

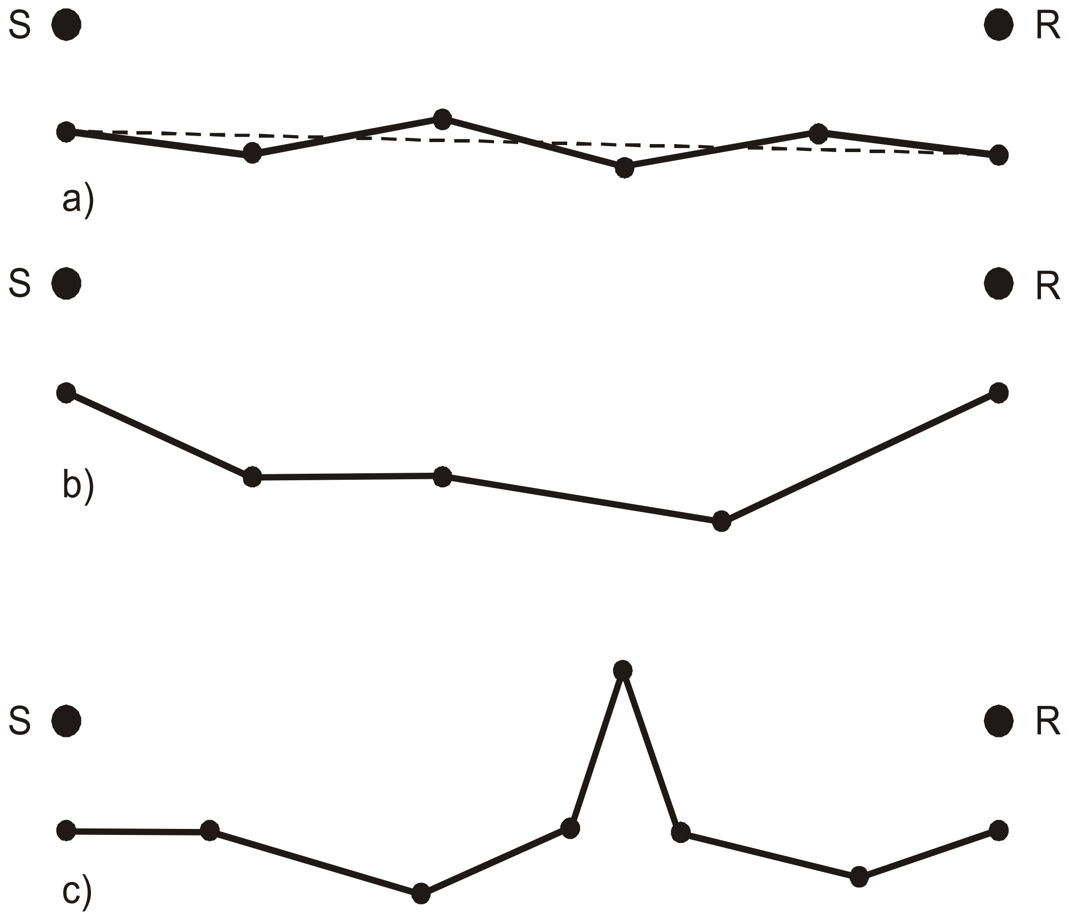

Fig 1. Examples of terrain approximated by straight line segments

In Nord2000 the sound pressure level L_R at the receiver is for each frequency band predicted according to eq. (2). The equation is used for a direct propagation path from source to receiver as well as for a reflection path via a vertical reflector.

$$L_R = L_W + \Delta L_d + \Delta L_a + \Delta L_t + \Delta L_s + \Delta L_r \qquad (2)$$

where

L_W is the sound power level within the considered frequency band,

ΔL_d is the propagation effect of spherical spreading of the sound energy,

ΔL_a is the propagation effect of air absorption,

ΔL_t is the propagation effect of the terrain (ground and screens),

ΔL_s is the propagation effect of scattering zones (like forest or vegetation)

ΔL_r is the propagation effect of obstacle dimensions and surface properties when calculating a contribution from sound reflected by an obstacle. If the ray path is not a reflection path $\Delta L_r = 0$.

Prediction of long-term noise levels by Nord2000

When predicting long-term noise levels the weather conditions are divided into a number of meteorological classes. Each weather class covers a variety of meteorological conditions with almost the same sound propagation. The method used for calculating long-term noise levels is a European method proposed in [7] and later adopted by the Nordic countries [8]. Each class are defined by A and B in the log-lin sound speed profile (5 values of A and B symmetrically distributed around A=0 and B=0). If the occurrence p_i of each meteo-class is known together with the average air temperature t_i and relative humidity RH_i the long-term noise level can be predicted according to eq. (3) where L_i is noise level in the meteo-class i (calculated by Nord2000 using A_i, B_i, C_i corresponding to t_i, $z_0 = 0.025$ m, $s_A = 0$, $s_B = 0$, and typical values of C_v^2 and C_T^2).

$$L_{long-term} = 10\log\left(\sum_{i=1}^{25} p_i \, 10^{L_i/10}\right) \qquad (3)$$

The statistical weights p_i and average temperature t_i and relative humidity RH_i needed for the calculation according to eq. (3) are obtained from normal weather statistics as described in [7] or [8]. For each observation at a synoptical weather station (typically for each hour) the meteorological class given by A and B are determined on basis on wind speed and direction at 10 m and cloud cover in octas and time of the day (day/night). This statistics are obtained for the period of interest (e.g. one year or ten years). Statistics shall be determined each direction of propagation (in 10° intervals according to [7] and [8]).

The experience from creating statistics for calculations of the yearly average noise level L_{den} is that there are no occurrences in almost half of the meteorological classes at selected weather stations in the Nordic countries. Furthermore, in a few classes the percentage is so small that it can be moved to a neighbouring class. In practice the number of classes is therefore no more than 9-10 classes which means that the calculation time can be substantially reduced compared to doing a calculation for each hour in e.g. a one year period.

Validation of Nord2000

In order to validate Nord2000 for high sources such as wind turbines, short-term measurements were carried out as described in [2]. The result of the measurements has been compared to predictions by Nord2000 as described in the following. In the validation project three series of measurement were carried out for single sources:

- Propagation over flat ground using a loudspeaker
- Propagation over non-flat ground using a loudspeaker
- Propagation over non-flat ground from a wind turbine

When comparing measurements and predictions it is a common practice to express the result by the excess propagation effect ΔL defined as the sound pressure level L relative to the free field sound pressure level L_{ff} as shown in eq. (4). The excess propagation effect ΔL includes the effect of the ground surface and air absorption whereas the general reduction of noise level due to spherical spreading of the sound field (6 dB per doubling of distance) is not included. The advantage of this approach is that it is easy to compare results at varying propagation distances.

$$\Delta L = L - L_{ff} \quad (4)$$

In order to calculate ΔL by eq. (4) the free field level L_{ff} has to be estimated. This is done by eq. (5) where L_W is the sound power level and R is the distance from source to receiver.

$$L_{ff} = L_W - 10\log\left(4\pi R^2\right) \qquad (5)$$

To obtain a reliable comparison between measured and predicted noise levels it is essential that L_W has been determined with the highest possible accuracy. For the loudspeaker, L_W has been determined by measurements at short distance. For the wind turbine, L_W has been determined by measurements according to IEC 61400-11:2002 ed. 2.1 (microphone on a plate on the ground approximately 110 m from the wind turbine). Therefore, it must be expected that the accuracy of L_W is less for the wind turbine than for the loudspeaker.

In the analysis comparisons have been made for 1/3 octave bands from 100 Hz to 2.5 kHz determined by the frequency range of the loudspeaker. The analysis also includes comparison of for A-weighted noise levels. In this case the measured spectra have been combined with the source spectrum of Siemens 3.6MW at a wind speed of 8 m/s 10 m above ground

The results for each of the three measurement series are described in the following sections. Details concerning the measurement setup can be found in [2].

Validation of propagation over flat ground using a loudspeaker

Measurements of propagation over flat grass-covered ground were carried out at Høvsøre, Denmark. The source was a loudspeaker placed 30 or 50 m above the ground surface. Measurements were made at three positions (pos. 1, 2, and 3) approximately 500, 1000, and 1500 m from the source with a microphone 2 and 5 m above ground. In the first part of the measurements the measurements positions were located downwind, and in the other part upwind. Measurements in upwind at 1500 m were omitted from the analysis due to too high background noise compared to the loudspeaker noise.

In the measurements sequences of 10 sec. long noise bursts were emitted from the loudspeaker. The first sequence consisted of 5 pink noise bursts limited to the frequency range of the loudspeaker (total duration 50 sec). The second sequence consisted of 5 octave band noise bursts at 63 Hz, then at 125 Hz, 250 Hz, 500 Hz, 1kHz, and 2 kHz (total duration 5 min.). In the analysis both the broad band results and the octave band results were combined into spectra from 100 hz to 2.5 kHz. The reason for using octave band bursts was to increase the loudspeaker output per 1/3 octave band but the analysis showed no significant differences between results obtained by broad band bursts and octave band bursts. Therefore, the analysis does not distinguish between the two kinds of sequences.

Simultaneously the wind speed and direction and the temperature were measured 2, 10, 40, 60, 80, and 100 m above ground and the relative humidity were measured at 2 m. Measured values have been available for the same 10 sec. period used in the noise recordings.

In the analysis measured and predicted excess propagation effects have been compared for each sequence of noise bursts. The predicted values are based on the average meteorological variables within the sequence. The average values have been used to determine the vertical effective sound speed profile used by Nord2000.

For each of group of measurements defined by downwind/upwind, source height, receiver height, and propagation distance the average propagation effect for all sequences has been calculated for each 1/3 octave band. The downwind groups consist in most cases of 15 sequences, and the upwind groups of 11 or 22 for source height 30 and 50 m, respectively.

One example of a downwind result is shown in Fig. 2. Results for the other groups can be found in [9] and are more or less in line with the findings in Fig. 2. The figure shows an excellent prediction of the air absorption at high frequencies.

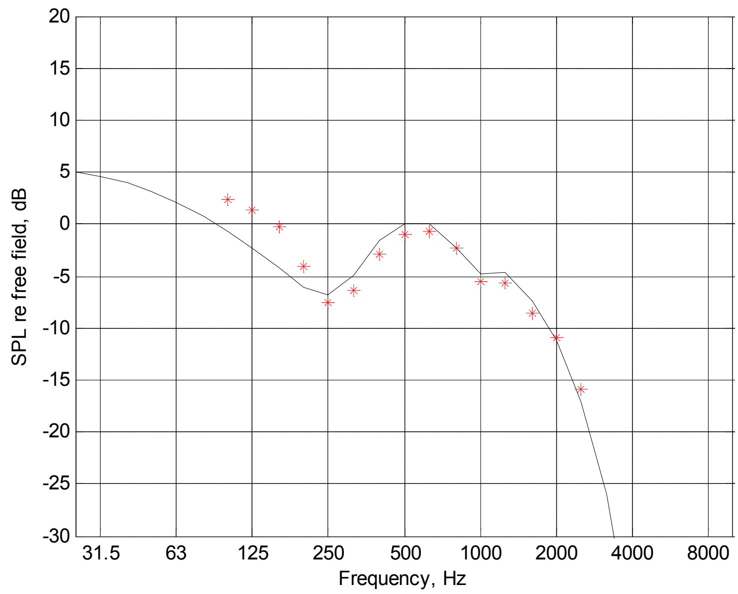

Fig. 2. Average excess propagation effect ΔL in downwind for distance 1500 m, source height 50 m, and receiver height 2 m (black: prediction, red: measurement)

The A-weighted excess propagation effects in downwind and the difference between predicted and measured values are shown in Table 1 and graphically in Fig. 3. The average deviation is -0.1 dB with a standard deviation of 0.7 dB so the agreement is very fine.

Pos.	**h_S (m)**	**h_R (m)**	**Number of seq.**	**Nord2000 (dB)**	**Measured (dB)**	**ΔL_A(c-m) (dB)**
1	30	2	15	-1.4	-2.1	0.7
1	30	5	15	0.0	1.2	-1.2
1	50	2	15	-1.1	-1.4	0.3
1	50	5	15	0.4	0.1	0.3
2	30	2	15	-3.3	-4.0	0.7
2	30	5	15	-1.3	-1.6	0.3
2	50	2	15	-2.7	-3.2	0.5
2	50	5	15	-1.0	-0.9	-0.1
3	30	2	15	-4.3	-3.2	-1.1
3	30	5	15	-2.0	-1.4	-0.6
3	50	2	13	-3.9	-3.0	-0.9
3	50	5	9	-1.6	-1.5	-0.1
Total					Average	-0.1
					Std. dev.	0.7

Table 1. Downwind propagation over flat terrain from a loudspeaker

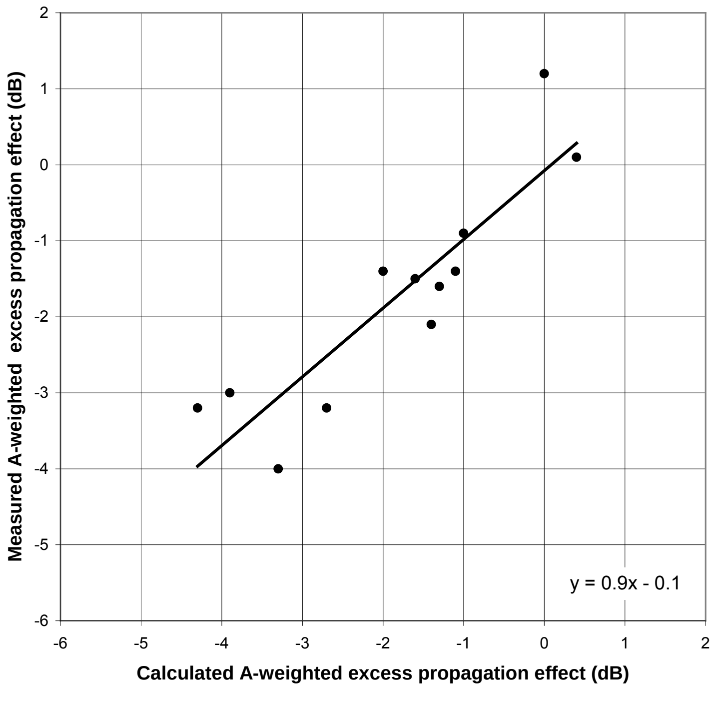

Fig 3. Downwind propagation over flat terrain from a loudspeaker

One example of an upwind result is shown in Fig. 4 where both measurement and prediction show a shadow zone caused by upwind. Results for the other groups can be found in [9] where the general picture is that accurate predictions are difficult when receiver points are close to or just inside the shadow zone.

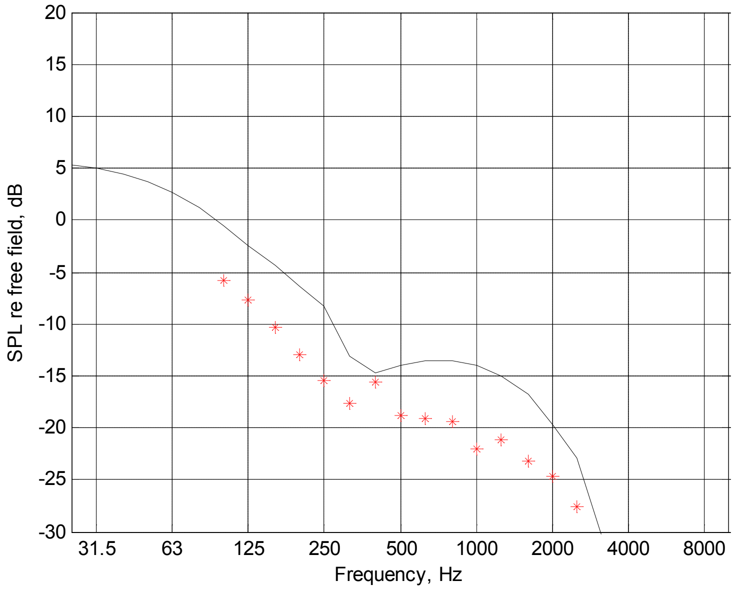

Fig. 4. Average excess propagation effect ΔL in upwind for distance 1000 m, source height 30 m, and receiver height 2 m (black: prediction, red: measurement)

The A-weighted excess propagation effects in upwind and the difference between predicted and measured values are shown in Table 2 and graphically in Fig. 5. The agreement is acceptable although the predicted results on average is 4 dB higher than the measured values taking into account the well-known difficulties of making accurate prediction for an acoustical shadow zone in upwind.

Pos.	**h_S (m)**	**h_R (m)**	**Number**	**Nord2000 (dB)**	**Measured (dB)**	**ΔL_A(c-m) (dB)**
1	30	2	11	-0.8	-8.9	8.1
1	30	5	11	-0.6	-3.1	2.5
1	50	2	22	-1.2	-3.8	2.6
1	50	5	22	0.2	-2.1	2.3
2	30	2	11	-9.4	-14.6	5.2
2	30	5	11	-6.9	-11.5	4.6
2	50	2	22	-5.2	-9.5	4.3
2	50	5	22	-3.3	-8.0	4.7
Total					Average	4.3
					Std. dev.	1.9

Table 2. Upwind propagation over flat terrain from a loudspeaker

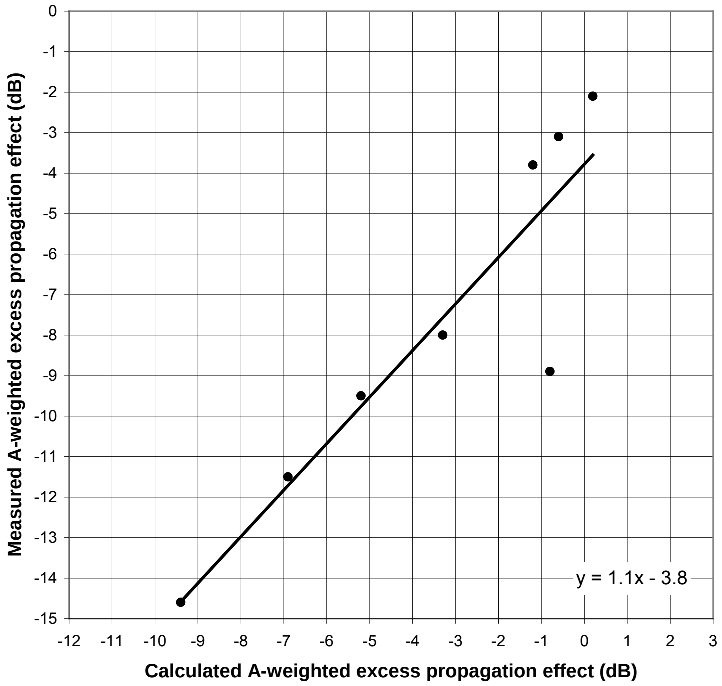

Fig. 5 Upwind propagation over flat terrain from a loudspeaker

Validation of propagation over non-flat ground using a loudspeaker

Measurements of propagation over non-flat ground were carried out at Hitra, Norway. The source was the same loudspeaker used at Høvsøre but this time placed 70 m above the ground surface on a wind turbine nacelle. Measurements in downwind were made at three positions (pos. 1, 2, and 3) approximately 400, 800, and 1000 m from the source with a microphone 2 and 5 m above ground on the first measurement day. On a second day measurements in downwind were made at pos. 1 and 2 alone with the microphone 2 m above ground. Measurements in upwind were made at two positions (1 and 2) approximately 400 and 600 m from the source with a microphone 2 and 5 m above ground on a single day. Terrain cross-sections for downwind and upwind terrains are shown in Fig. 6 and 7, respectively. An impression of the terrain surface type is given in Fig. 8.

The measurement procedure based on 10 sec. noise bursts were the same as applied at Høvsøre.

The wind speed and direction were measured 10, 29 and 70 m, the temperature was measured at 29 m, and the relative humidity at 2 m. Measured values were available for 10 min. periods, only.

In the analysis the vertical effective sound speed profile used by Nord2000 has been estimated on basis of the measured wind in three heights but as the temperature is known only at one height it has been necessary to calculate the temperature profile based on an estimate of atmospheric stability at the time of the measurements.

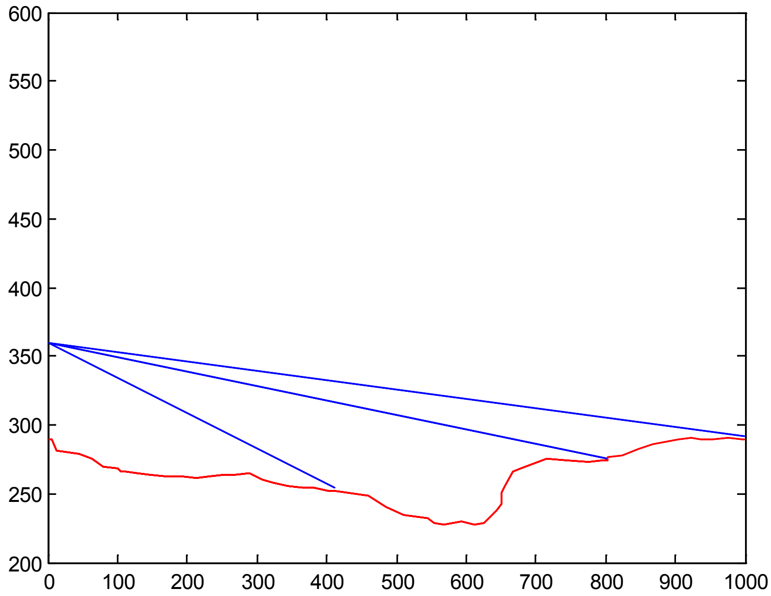

Fig. 6. Terrain cross section (red line) from loudspeaker (at X=0) to downwind measurement pos. 3. The blue lines are line-of-sights between wind turbine and pos. 1, 2, and 3

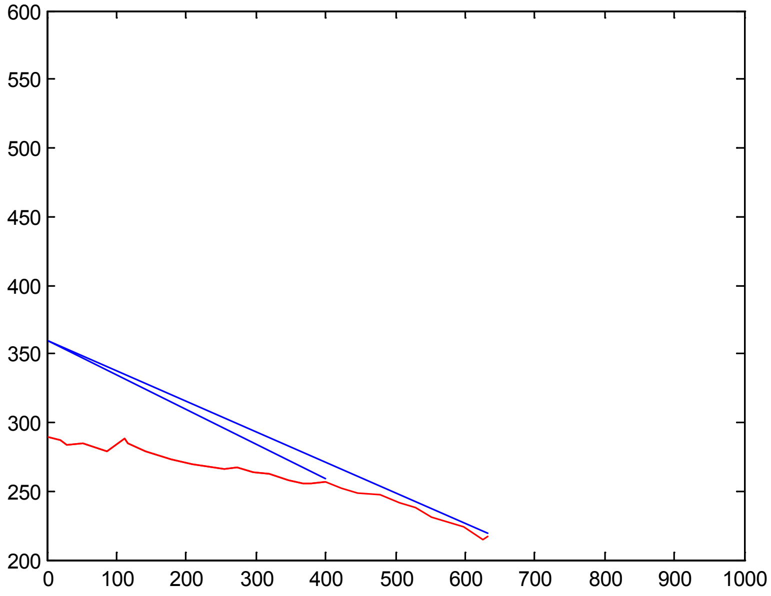

Fig. 7. Terrain cross section (red line) from loudspeaker (at X=0) to upwind measurement pos. 2. The blue lines are line-of-sights between wind turbine and pos. 1 and 2

Fig. 8. View from downwind pos. 2 towards wind turbine with loudspeaker

One example of a downwind result is shown in Fig. 9. Results for the other groups can be found in [9] and are more or less in line with the findings shown in Fig. 9.

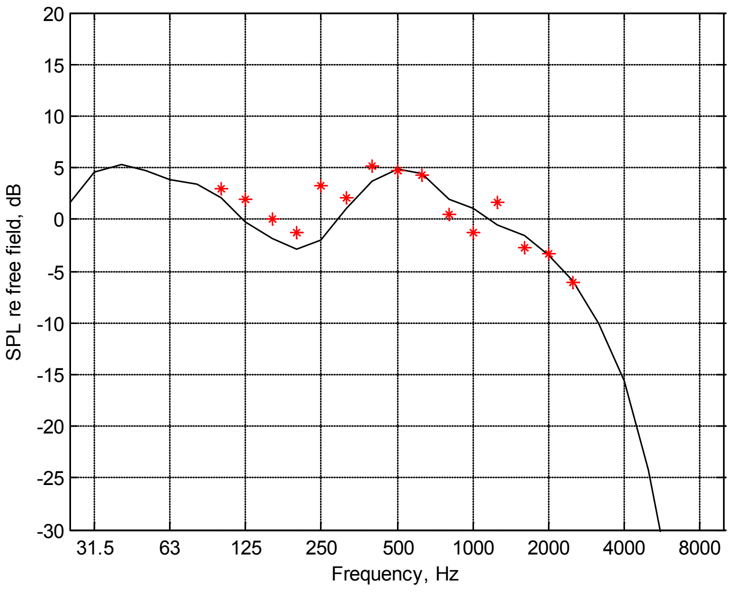

Fig. 9. Average excess propagation effect ΔL in downwind (first day) for propagation distance 800 m and receiver height 2 m (black: prediction, red: measurement)

The A-weighted excess propagation effects in both downwind and upwind and the difference between predicted and measured values are shown in Table 3 and graphically in Fig. 10. The average deviation in all downwind and upwind cases is -0.5 dB with a standard deviation of 1.8 dB which is satisfactory.

Case	Pos.	h_R (m)	Number	Nord2000 (dB)	Measured (dB)	ΔL_A(c-m) (dB)	Group ΔL_A (dB)
Downwind (8-7)	1	2	31	2.0	3.2	-1.2	-1.6
	1	5	31	0.0	2.9	-2.9	
	2	2	31	0.8	1.8	-1.0	
	2	5	32	0.4	3.7	-3.3	
	3	2	32	-8.2	-5.6	-2.6	
	3	5	32	-2.3	-3.5	1.2	
Downwind (11-7)	1	2	4	2.4	1.9	0.5	0.2
	2	2	6	1.4	1.5	-0.1	
Upwind (11-7)	1	2	15	0.6	0.9	-0.3	0.9
	1	5	15	2.6	0.3	2.3	
	2	2	18	-5.1	-7.2	2.1	
	2	5	18	-1.7	-1.3	-0.4	
Total						Average	-0.5
						Std. dev.	1.8

Table 3. Propagation over non-flat terrain from a loudspeaker

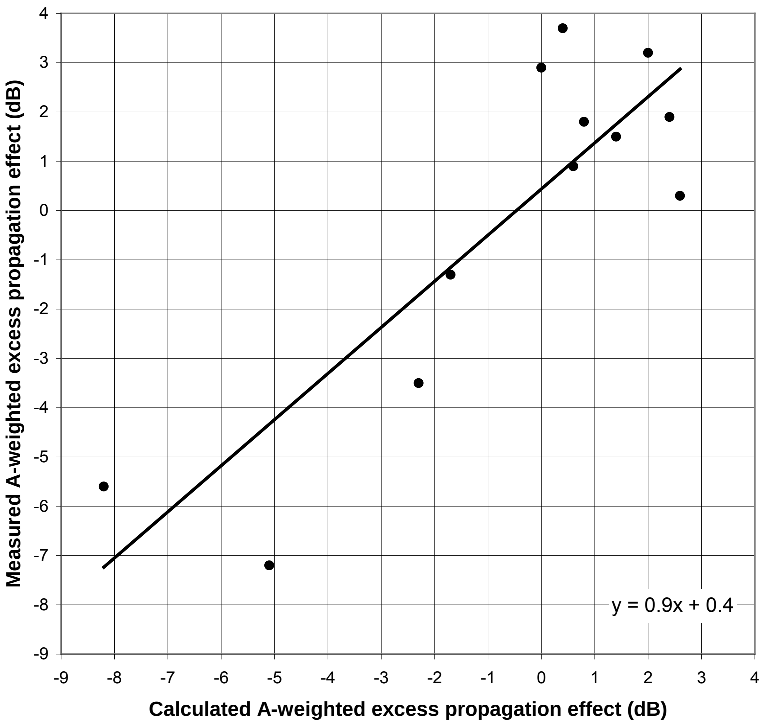

Fig. 10. Propagation over non-flat terrain from a loudspeaker

Validation of propagation over non-flat ground from a wind turbine

Measurements of downwind propagation from a wind turbine over non-flat ground were carried out with the same measurement setup (first measurement day) used in the loudspeaker experiment at Hitra described above. The only differences are that pos. 3 was omitted due to background noise and that the sound power level was estimated based on measurements according to IEC 61400-11:2002 ed. 2.1.

In the analysis the spectrum at the receiver was determined every 10 seconds throughout the entire measurement period and for comparison excess propagation effect spectra were calculated by Nord2000 for each 10 sec. period. A number of measured 10 sec. spectra showed abnormalities mainly due to disturbances and was omitted from the analysis. For the remaining spectra the average predicted and calculated excess propagation effect were determined for each measurement position and receiver height.

One example is shown in Fig. 11. Results for the three other groups can be found in [9]. As indicated by Fig. 11 the agreement between measured and predicted excess propagation effect spectra show as expected larger deviations than seen in the loudspeaker experiments.

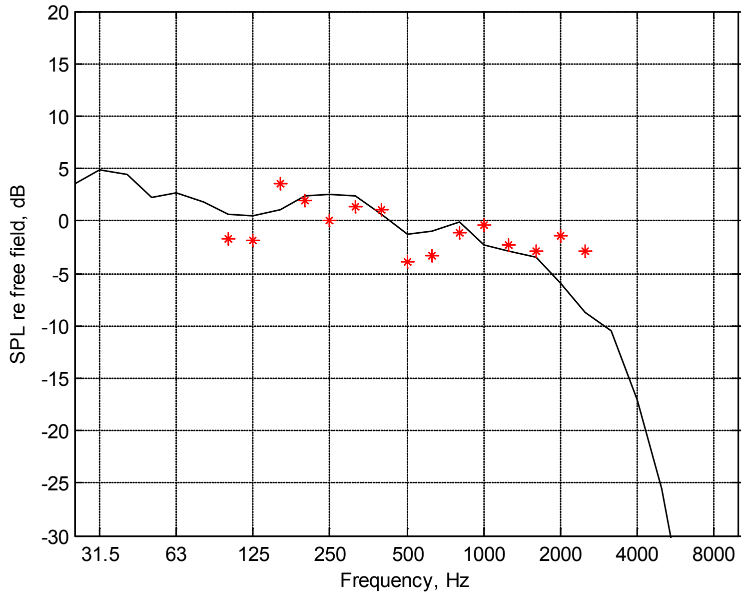

Fig. 11. Average excess propagation effect ΔL in downwind from a single wind turbine for distance 800 m and receiver height 5 m (black: prediction, red: measurement)

The A-weighted excess propagation effects and the difference between predicted and measured values are shown in Table 4. The total average deviation is -1.0 dB with a standard deviation of 2.3 dB which is acceptable.

Pos.	h_R (m)	Duration (sec)	Nord2000 (dB)	Measured (dB)	ΔL_A(c-m) (dB)
1	2	6180	1.8	3.5	-1.7
1	5	4400	0	3.8	-3.8
2	2	2520	0.2	-1.1	1.3
2	5	2890	0.1	-0.3	0.4
Total				Average	-1.0
				Std. dev.	2.3

Table 4. Downwind propagation over non-flat terrain from a wind turbine

Conclusions

The validation measurements for downwind propagation from a loudspeaker over flat grass-covered ground show a fine agreement between measurements and predictions by the Nord2000 method in the considered range of propagation distances (up to 1500 m). The average difference in A-weighted levels is 0.1 dB with a standard deviation of 0.7 dB which is very fine. Also, the agreement between measured and predicted spectra is good.

The validation measurements for upwind propagation from a loudspeaker over flat grass-covered ground show a less good but still acceptable agreement between measurements and predictions by the Nord2000 method considering the well-known problem of making accurate prediction in long-distance upwind cases. On average the predicted A-weighted noise levels are 4 dB higher than the measured levels with standard deviation of 1.9 dB. In principle, the Nord2000 method could be adjusted to give a better fit to the validation measurements but it would be dubious to change the method based on only one experiment. Furthermore, noise levels in an acoustical shadow zone caused by upwind are in general low and very unstable. Therefore, it can be considered an advantage that the prediction in shadow zones are conservative.

The validation measurements for downwind and upwind propagation from a loudspeaker over non-flat terrain show that predictions by Nord2000 is producing A-weighted noise levels which on average are within 0.5 dB of the measured values with a standard deviation of 1.9 dB. This is considered a good agreement taking into account the complexity of the terrain and the meteorological conditions. In downwind pos. 3 at a distance of approximately 1000 m the measured spectra show attenuation at high frequencies which most likely is to the result of an moderate acoustical shadow zone normally seen during upwind propagation. The most likely explanation is that the effect is caused by a wind speed-up effect over the hill-shaped terrain. This is supported by the wind speed measurements showing a lower wind speed at the height 70 m than at 10 and 29 m. Unfortunately the meteorological measurements were made in some distance from the wind turbine, but the predictions by Nord2000 of the shadow zone are in fairly good agreement with the measurement results.

The validation measurements for downwind propagation over non-flat terrain from a wind turbine show less good agreement than obtained for the loudspeaker. However, with an average deviation of 1.0 dB and a standard deviation of 2.3 dB the agreement is still considered acceptable.

Acknowledgement

The project is publicly funded by Energinet.dk under contract no. 2007-1-7389 and co-funded by Dong Energy, Suzlon Energy A/S, Gamesa, StatoilHydro, E.ON Vind Sverige AB, Statkraft Development, and Vattenfall A/S.

The project partners are DELTA (project manager), EMD International and DONG Energy.

References

[1] B. Plovsing: Nord2000. Validation of the Propagation Model, DELTA Noise & Vibration Report AV 1117/06 (2006)

[2] B. Søndergaard and B. Plovsing: Prediction of noise from wind farms with Nord2000. Part 1, 3rd International Conference on Wind Turbine Noise (2009)

[3] J. Kragh, B. Plovsing, S. Å. Storeheier, G. Taraldsen, H. G. Jonasson: Nordic Environmental Noise Prediction Methods, Nord2000 Summary Report. General Nordic Sound Propagation Model and Applications in Source-Related Prediction Methods, DELTA Acoustics & Vibration Report AV 1719/01 (2002)

[4] B. Plovsing and J. Kragh: Nord2000. Comprehensive Outdoor Sound Propagation Model. Part 1: Propagation in an Atmosphere without Significant Refraction, DELTA Acoustics & Vibration Revised Report AV 1849/00 (2006)

[5] B. Plovsing and J. Kragh: Nord2000. Comprehensive Outdoor Sound Propagation Model. Part 2: Propagation in an Atmosphere with Refraction, DELTA Acoustics & Vibration Revised Report AV 1851/00 (2006)

[6] B. Plovsing: Proposal for Nordtest Method: Nord2000 – Prediction of Outdoor Sound Propagation, DELTA Acoustics Report AV 1106/07 (2007)

[7] R. Nota, R. Barelds and D. van Maercke: Harmonoise WP3 Engineering method for road traffic and railway noise after validation and fine-tuning, Technical Report HAR32TR-040922-DGMR20 (2005)

[8] R. Eurasto: NORD2000 for road traffic noise prediction. Weather classes and statistics, Research Report VTT-R-02530-06 (2006)

[9] B. Søndergaard and B. Plovsing: Nord2000 validation measurements (to be published in 2009)

Third International Meeting on Wind Turbine Noise
Aalborg Denmark 17 – 19 June 2009

Wind Turbine Noise Diagnostics

Werner Richarz, Harrison Richarz
Engineering Ltd., Suite 165
Toronto, ON, M9W 1B3, Canada
werner@aercoustics.com
hricharz@gmail.com

Abstract

The dimensions of wind turbines pose special difficulties for the diagnostics of noise emission. Acoustic array data suggests that broadband noise is emitted predominantly during the downward sweep of each rotor blade. It is shown that source motion and source directivity account for the observed pattern. Rotor-tower interaction effects are of lesser importance. Predicted amplitude modulation ranges from 1 dB up to 6dB.

Introduction

The acoustics of wind-turbines are similar to those of conventional propellers. Whereas the latter imparts energy to the air, the former extract energy. For moderate loading and tip speeds the steady forces exerted by the moving blades on the air stream give rise to tones at the blade passage frequency and its harmonics. Broad-band noise is attributable to the turbulent boundary layers on the blades. There is extensive literature on sound generated by propellers.

Wind turbine rotors differ only in scale: their physical dimensions are larger by an order of magnitude, and their rotation rate is approximately two orders of magnitude less. Still, the physics of the noise generation mechanisms remains invariant. This paper attempts to provide a simple source model that is consistent with the physics of sound generation while taking the unique features of wind turbines into account.

Extended Source

The large rotor diameter of a wind-turbine suggests that the sound source is an extended one. Still, it is common practice to use but a single source at the hub height, in acoustic models. Most of the aerodynamic loading of the rotor is on the outer portions of the blade. A suitable first approximation is a single source at 80% of the rotor radius. The validity of this approximation is confirmed by the source visualizations of Schepers et al. [2].

The listener-source distance is:

$$|\mathbf{X}\text{-}\mathbf{Y}| = [D^2+H^2+R^2 + 2R((D^2\sin\theta\square^2+H^2)^{0.5}\cos(\omega t+\phi)]^{0.5};\ \ \tan\phi = (D\sin\theta)/H$$

The source is rotating at a rate ω at radius R (m) about a horizontal axis H (m) above the ground and the listener is at a distance D from the base of the tower, at an angle θ with respect to the rotor axis (Figure 1). This change in distance is shown in figure 2 for a nominal source-observer distance of 400m, a hub height of 80m and a source radius of 32m. The source radius is 80% of the rotor radius (40m).

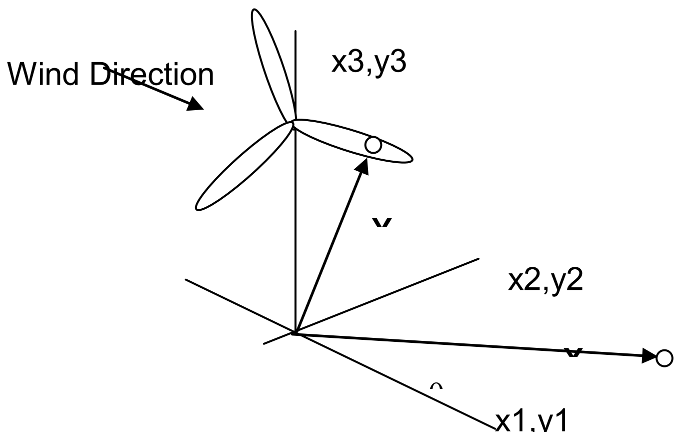

Figure 1 General arrangement.

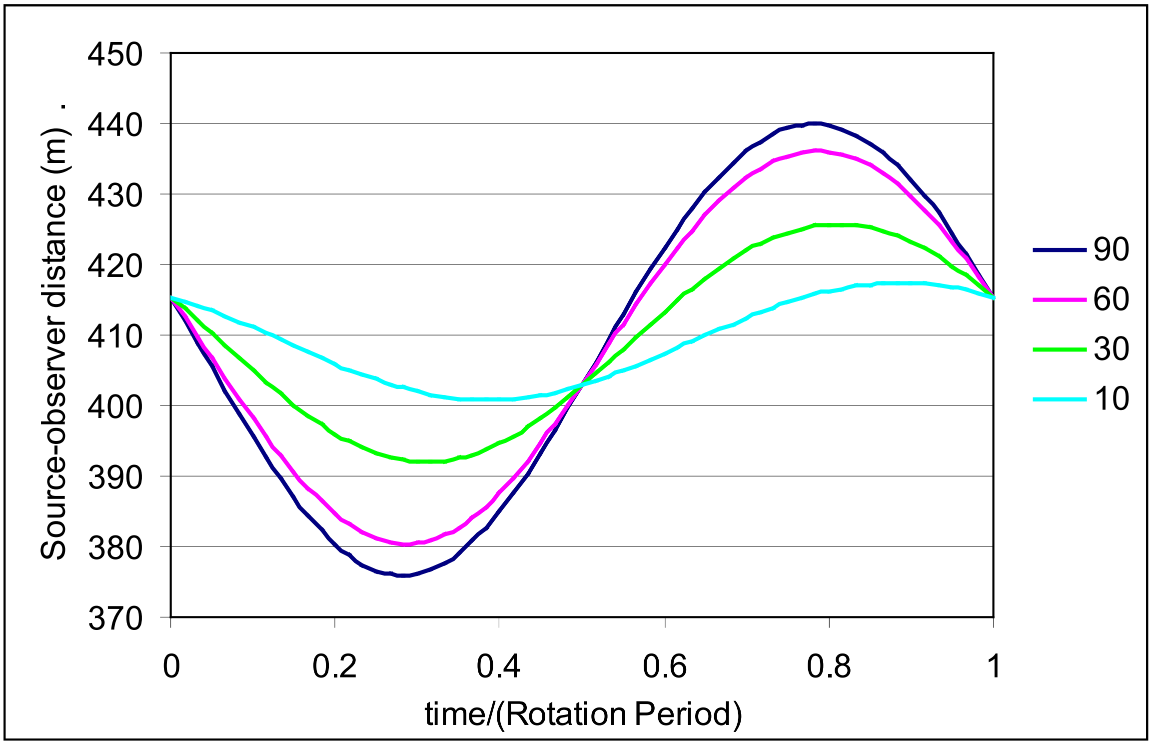

Figure 3 Source-observer distance at selected values of θ. Observer is 400m from the tower, the source moves along a 32 m radius circle at a hub height of 80m.

Source Motion

The sound source moves relative to the listener at a speed:

$$d|\mathbf{X}\text{-}\mathbf{Y}|/dt = -[\omega R((D^2 \sin\theta)^2+H^2)^{0.5}\sin(\omega t+\phi)]/|X\text{-}Y|$$

The speeds, shown in figure 3, are quite considerable, even though from a distance the motion appears to be ‘slow’.

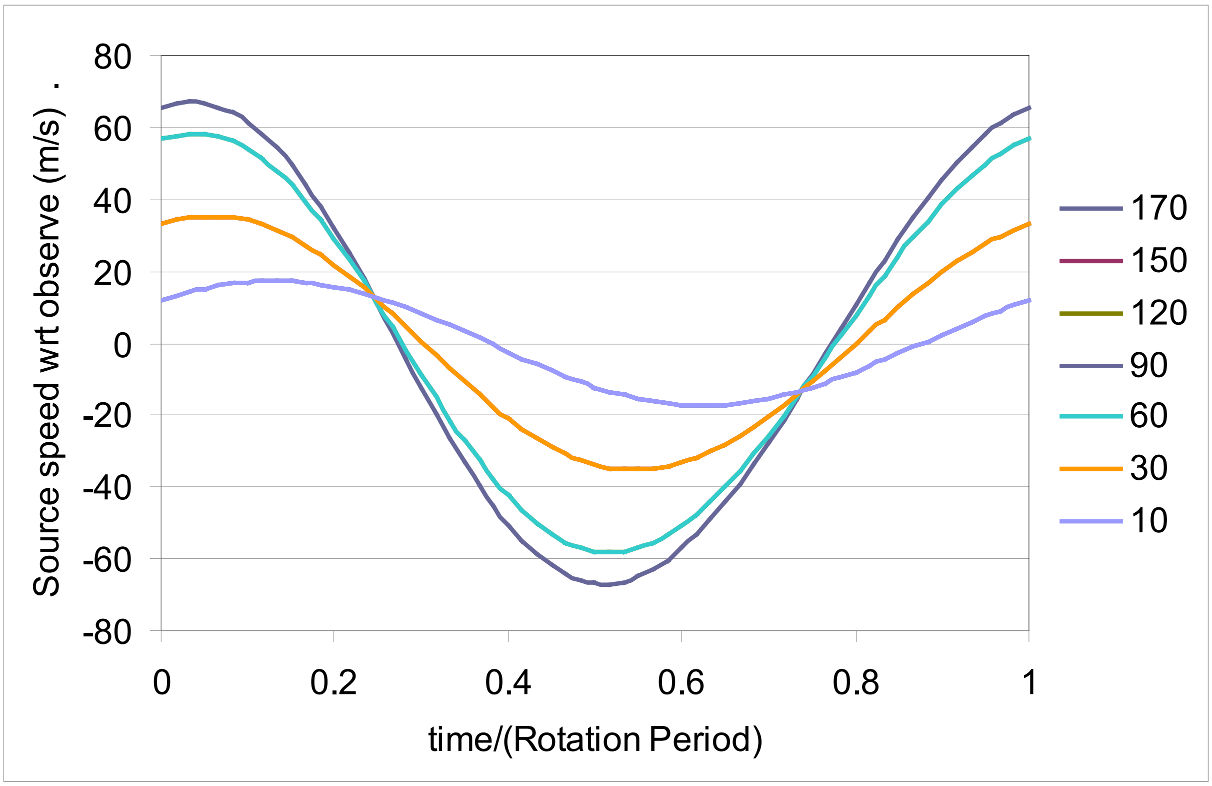

Figure 3 Relative speed between the source and observer at selected values of θ. Observer is 400m from the tower, the source moves along a 32 m radius circle, at a hub height: of 80m.

One would expect that the sound heard by the listener is Doppler shifted. For broad-band noise the Doppler shift is virtually impossible to perceive. The effects of source motion can be illustrated by drawing a set of wave-fronts emitted at successive times by a moving point source. For a stationary source, the wave-fronts are concentric circles. With source motion the pattern is off-set in the direction of motion. The crowding of the wave-fronts in the direction of motion can be used to deduce the frequency shift. If acoustic energy is conserved, the amplitude of the waves must change as well, for the energy is proportional to the mean-square pressure averaged over a complete cycle.

A more precise description follows from the solution of the wave equation of a moving point source:

$$d^2p/dt^2 - \nabla^2 p = f(t)\delta(y_1)\delta(y_2-R\sin(\omega t))\delta(y_3-(H+R\cos(\omega t)))$$

$$4\pi p(x,t) = \int \{f(t')\delta(y_1)\delta(y_2-R\sin(\omega t'))\delta(y_3-(H+R\cos(\omega t')))\delta(t'-t+c^{-1}|\mathbf{X}-\mathbf{Y}(t')|/|\mathbf{X}-\mathbf{Y}(t')|\}d^3y\,dt'$$

The delta functions determine the source position and the time delay between signal reception and emission. From the properties of the delta function it follows that:

$$4\pi p(x,t) = f(t-T)\ [\ |\mathbf{X}-\mathbf{Y}(t-T)|-M_R((D^2\sin\theta)^2+H^2)^{0.5}\sin(\omega(t-T)+\phi)]^{-1}$$

The time delay (T) is set by the source-listener distance at the point of emission. The so-called 1/r term differs from the geometric distance $|\mathbf{X}-\mathbf{Y}(t-T)|$. Even at relatively low tip Mach numbers ($M_R=\omega R/c$) the effect is not negligible. The contribution from the source is greatest, when it is moving towards the observer. The notion that the 'swooshing sound' is due to the downward motion of the blades would be disputed by an observer floating above a wind turbine in a hot air balloon!

The form of the general equation suggests that the sound pressure is a scaled, amplitude modulated replicate of the source function f(t). The amplitude modulation is a periodic function:

$$AM(t)=[\ |\mathbf{X}-\mathbf{Y}(t)|-M_R((D^2\sin\theta)^2+H^2)^{0.5}\sin(\omega(t)+\phi)]^{-1}$$

Further refinements that account for source directivity and rotor tower interaction are addressed below.

Directivity

The broadband noise radiated from the moving rotor blade is a combination of boundary layer noise and trailing edge noise. On the rotor blade a small fraction of the unsteady pressures in the turbulent boundary layer is radiated as sound. When a turbulent eddy flows past the trailing edge, an unsteady lift is induced, which it turn acts as a source of sound. The radiated sound field is not omni-directional (as was assumed in the discussion of source motion). There are several formalisms in the literature. The one given in reference [1] has been used herein:

$$D(\theta_{TE},\theta_c) = |\sin(\theta_{TE})\cos(0.5\theta_c)|$$

The source directivity has not been corrected for source motion. In view of the low Mach numbers, this is at best a second order effect. θ_{TE} is the angle between the trailing edge and the source-observer vector (**X-Y**). ,θ_c denotes the angle between direction of the mean chord and the source-observer vector. Most of the acoustic energy is radiated forward, along the mean chord of the blade. As the blade rotates, these angles change, and the sound pressure increases or diminishes as prescribed by the above equation. The contribution of the source directivity to the change in amplitude is shown in figure 4.

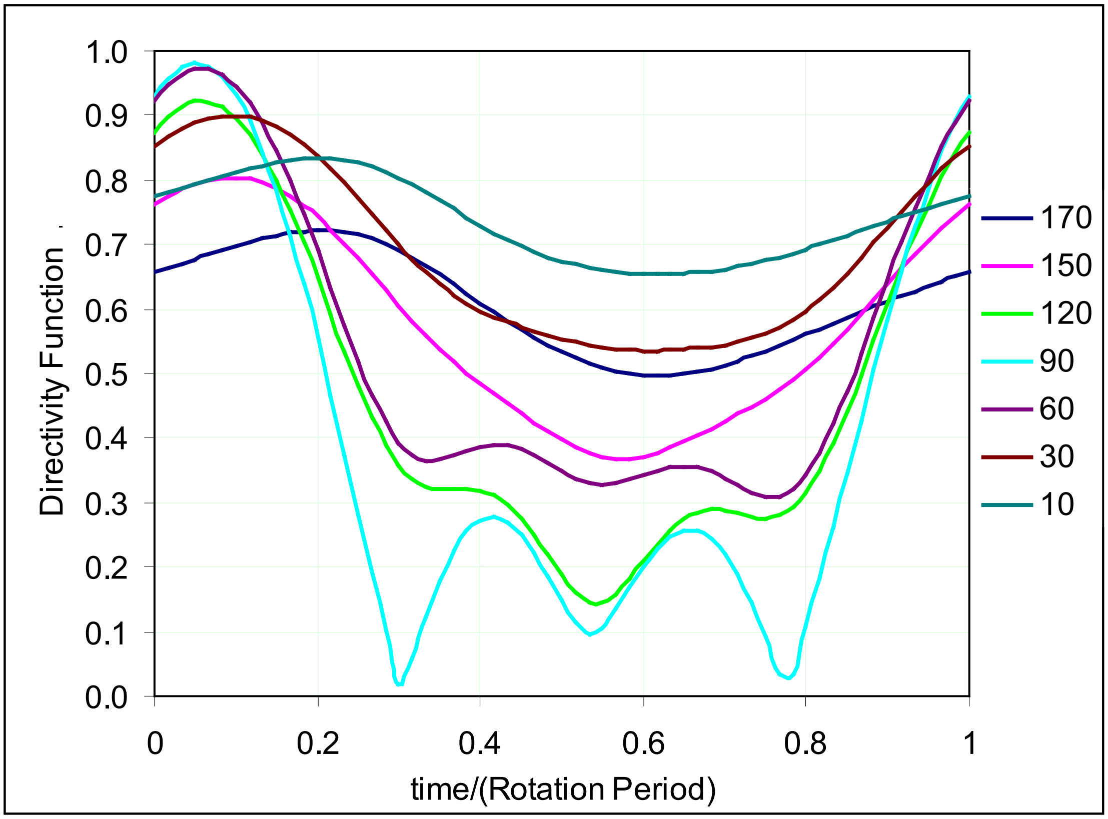

Figure 4 Directivity for selected values of θ. Observer is 400m from the tower, the source moves along a 32 m radius circle, hub height:80m.

Diffraction

For modern wind turbines the aerodynamic interference of the rotor blades and the tower is minimal. The tower does scatter sound. For a nominal cylindrical diameter of the order of 3m this effect is significant for frequencies greater than 100 Hz. This notion has been tested using a CadnaA model as well by scale model measurement. The CadnaA model consists of a collection of point sources distributed over a 32m diameter circle (Figure 5).

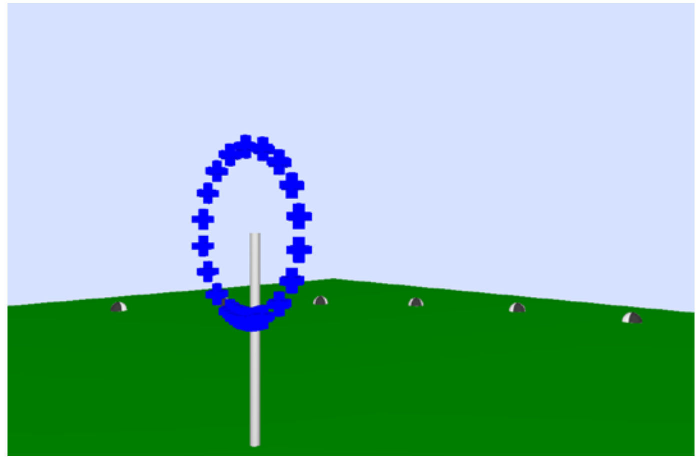

Figure 5 CadnaA model of wind turbine

This simulates the location of the effective sources of broadband noise. Sound pressure levels are predicted for listeners on a 400 m radius centered on the 3m diameter 100m high cylindrical tower. Sound pressure levels from individual sources are shown in figure 6. Upstream observers appear to experience a small increase in sound pressure level, whereas observers downstream of the tower do experience a sudden drop in level as the tower blocks the direct line of transmission for some sources.

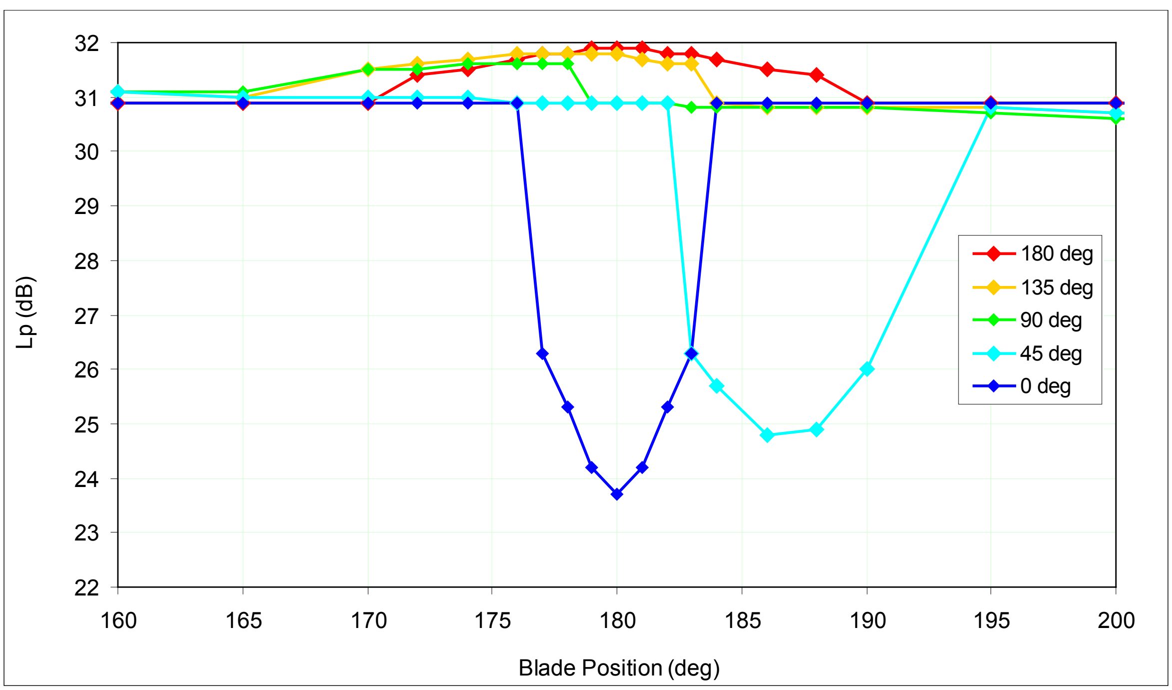

Figure 6 Diffraction due to a 3.5 diameter turbine tower; source frequency 400 Hz.

A scale model was built to validate the predictions. A small loudspeaker attached to a scale model rotor blade served a noise source and a ground-level microphone downstream of the scale model tower measured the sound pressure levels. The results show a 6 dB reduction for *ka* values in the range of 3.5 to 14 (Figure 7). This corresponds to 'full scale frequencies of about 300 to 1200 Hz. One would expect that the shielding effectiveness diminishes for ka values less than unity.

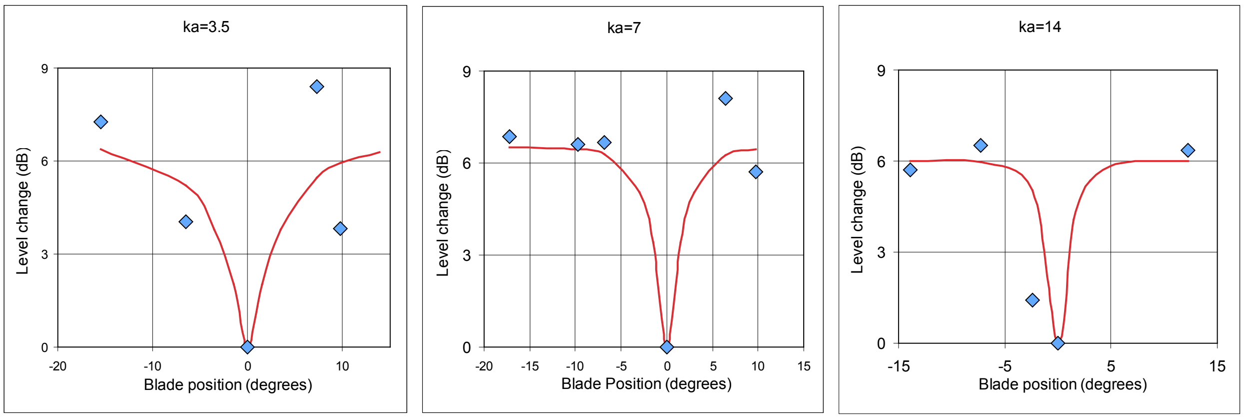

Figure 7 Measured shielding.

Complete Model

All the effects of source motion, source directivity, and tower diffraction have been combined to generate the amplitude variation as the idealized source executes one complete revolution. The resultant patterns are shown in Figure 8. The source motion and directivity effects vary smoothly in time, while the contribution due to diffraction is a rather abrupt notch or pulse, confined to the time when the blade passes the tower.

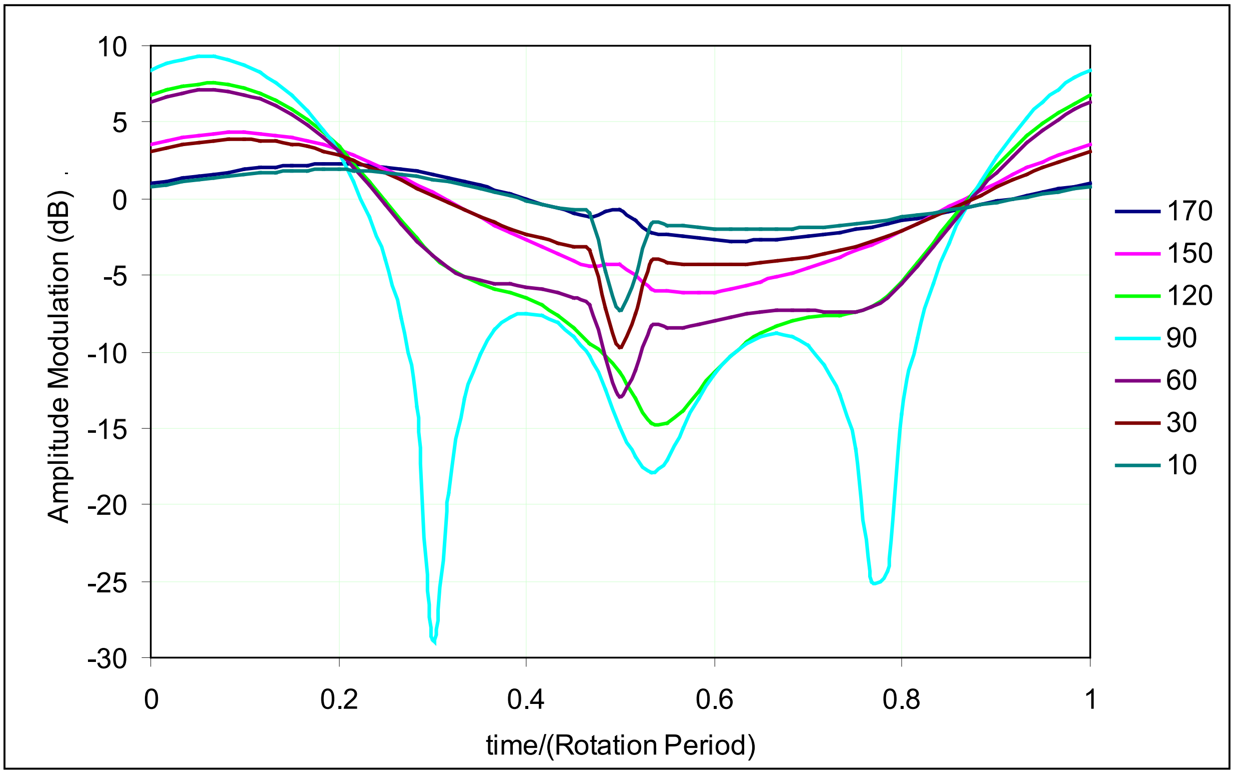

Figure 8 Amplitude modulation of sound radiated from a single rotor blade.

It is reasonable to assume that the broadband noises generated by individual blades are uncorrelated, even if they have similar spectra. Furthermore, the signal strength is taken to be constant, even if the rotor is operating in a slightly sheared flow. Wing-mounted propellers also operate in a sheared flow (generated by the upwash of the lifting wing) and show no signs of amplitude modulation at the blade passage frequency.

The overall amplitude is obtained by adding the amplitude modulation functions. The sound pressures add in the means-square. The amplitude modulation functions must be shifted in time to account for the rotor spacing. The results are shown in Figure 9. The level changes are considerably reduced in amplitude, but should be noticeable to observer downwind of the wind-turbine. Weak periodic pulsing with level changes of the order of 1 dB may also be detectable.

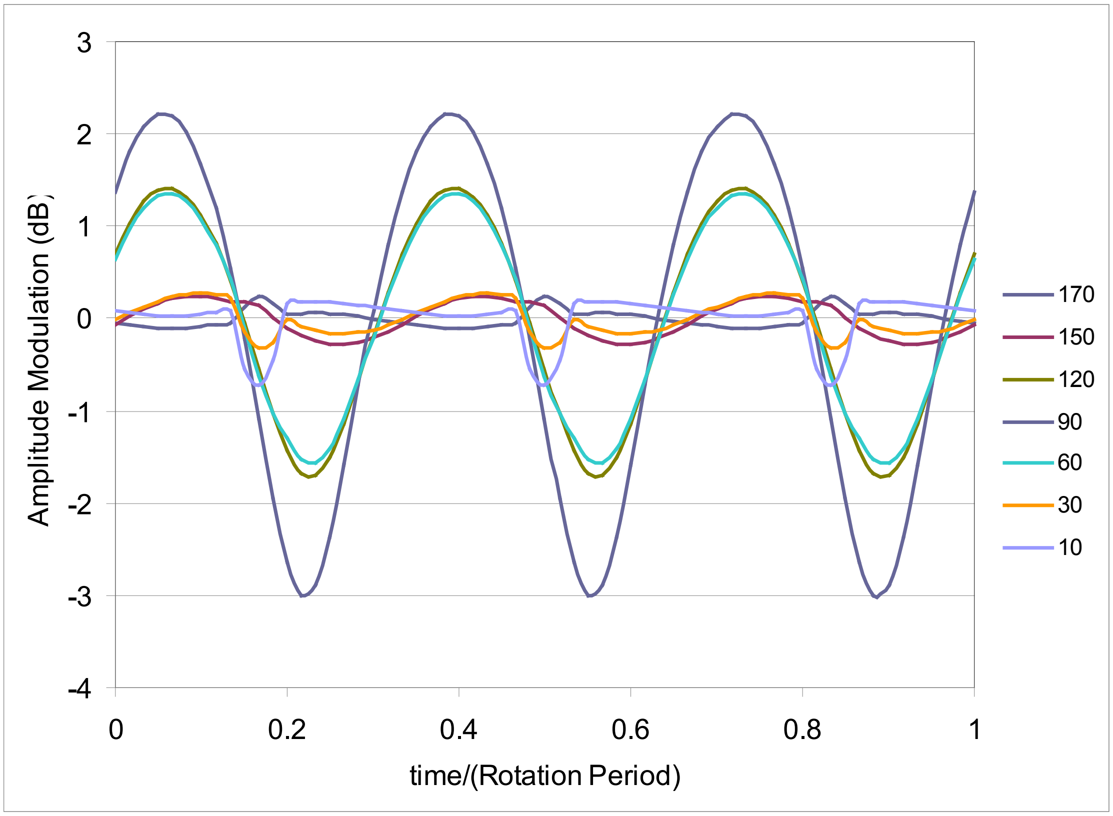

Figure 9 Amplitude modulation of radiated sound for a complete three bladed rotor.

Summary

A self-consistent model for broad-band noise emitted from modern wind turbines has been proposed. Even though the underlying source mechanisms have not been addressed, it is possible to deduce general features of the sound field. Source motion and source directivity appear to be responsible for 'amplitude variations'. The amplitude modulation is likely to make wind-turbine noise more audible, and may, in part, be responsible for subjective annoyance that has been reported in the literature.

References

1] Schepers J. et al. Sirocco: Silent Rotors by Acoustic Optimisation, 2nd Internat. Mtg. on Wind turbine Noise, Lyon, 2007

2] H.H. Hubbard (ed.) Aeroacoustics of Flight Vehicles Vol 1, Acoust.Soc.Amer., 1995, p31, p 397-412

Third International Meeting
on
Wind Turbine Noise
Aalborg Denmark 17 – 19 June 2009

Unsteady Aerodynamics and Inflow Noise

Brian Riget Broe

Address: Frederiksborgvej 399, Build. 776, DK-4000 Roskilde
e-mail: brian.broe@suzlon.com

Abstract

Aerodynamical noise due to atmospheric turbulence has the highest emphasis in semi-empirical models for predicting noise from wind turbines. However it is an open question whether inflow noise has a high emphasis. This illustrates the need to investigate and improve the semi-empirical model for noise due to atmospheric turbulence.
Three different aerodynamical models are investigated in order to estimate the lift fluctuations due to unsteady aerodynamics. Two of these models are investigated to find the unsteady lift distribution or pressure difference as function of chordwise position on the aerofoil. An acoustic model is investigated using a model for the lift distribution as input. The two models for lift distribution are used in the acoustic model. One of the models for lift distribution is for completely anisotropic turbulence and the other for perfectly isotropic turbulence, and so are also the corresponding models for the lift fluctuations derived from the models for lift distribution. The models for lift distribution and lift are compared with pressure data which are obtained by microphones placed flush with the surface of an aerofoil. The pressure data are from two experiments in a wind tunnel, one experiment with a NACA0015 profile and a second with a NACA63415 profile. The turbulence is measured by a triple wired hotwire instrument in the experiment with a NACA0015 profile.
Comparison of the aerodynamical models with data shows that the models capture the general characteristics of the measurements, but the data are hampered by background noise in the wind tunnel. The measurements are in between the completely anisotropic turbulent model and the perfectly isotropic turbulent model. This indicates that the models capture the aerodynamics well. Thus the measurements suggest that the noise due to atmospheric turbulence can be described and modeled by the two models for lift distribution.

Introduction

Noise from wind turbines is a subject which has a considerable public interest in Denmark. It is a subject of much debate before establishing wind turbines at any site. Therefore it is important to gain knowledge of noise from wind turbines.

The noise from wind turbines can be split up into two major sources, a mechanical source and an aero acoustic source (Wagner, Bareiß and Guidati 1996). The mechanical source of noise can be avoided or minimized by engineering means (Henderson 2005). The aero acoustic part can not be avoided but the design of the aerofoil has an important role of how much noise is produced by aero acoustical means.

The aero acoustic source is due to turbulence in the flow around the wind turbine blades. The turbulence is generated by different mechanisms such as atmospheric turbulence and separation and thus the aero acoustic source can be split up into several components (Wagner et al. 1996).

The aero acoustic noise due to atmospheric turbulence is the subject of this paper. It is also called inflow noise. The atmospheric flow is not steady but contains eddies, turbulence (Panofsky and Dutton 1984). The pressure at any point is constant in time when the flow is steady, incompressible, and inviscid. The turbulence create pressure fluctuations. Some part of the pressure fluctuations caused by the turbulence will be emitted as sound (Amiet 1975). The nature of turbulence causes the noise to be emitted in a continuum of frequencies and the inflow noise is of broadband character (Wagner et al. 1996).

The aeroacoustic noise can be treated by computational fluid dynamics (Zhu 2007) which is time consuming and demands powerful computer resources, or it can be treated in a semi-empirical approach which simplifies the physics (Amiet 1975).

The inflow noise has been treated in a semi-empirical approach (Amiet 1975). The semi-empirical approach has the advantage that it is less demanding on computer resources as compared to approaches based on computational fluid dynamics. The semi-empirical approach is suitable for guide- lines for design purposes because an answer is quickly obtained when design parameters are changed.

The semi-empirical inflow model, which is widely used, accounts for the major part of the total aero acoustical noise, Moriarty and Migliore (2003), as seen in Figure 1. According to this model inflow noise is seen to be dominating. However, despite of this the general consensus is that inflow noise is not the most significant aero acoustical noise component. Trailing edge noise is argued to be responsible for major part of the noise emitted aero acoustically (Moriarty and Migliore 2003, Oerlemans, Sijtsmaa and López 2007).

It follows from the discussion above that the semi-empirical model of noise due to atmospheric turbulence must be revised because it has too much emphasis of the total aero acoustical noise compared to trailing edge noise. Other approaches to improve the semi-empirical noise model due to atmospheric turbulence have been carried out by Guidati (2004) and by Moriarty, Guidati and Migliore (2005).

The model of inflow noise shown in Figure 1 is based on the model by Amiet (1975). This model assumes that the noise due to atmospheric turbulence is emitted like a dipole. It is based on isotropic turbulence as described by von Kármán (1948), and the lift distribution (pressure difference) due to turbulence along the chord of the aerofoil described by Adamczyk (1974).

The lift distribution due to turbulence is also described by Sears (1941) and Graham (1970). The models by Adamczyk (1974), Sears (1941), and Graham (1970) are all based on a flat plate. Further a model for the fluctuating lift due to turbulence is described, where the aerofoil is a bend flat plate at an angle of attack (Goldstein and Atassi 1976, Atassi 1984).

This paper is organized in 3 sections: a section that presents the models used, a section that presents data from two experiments conducted on two different profiles, and a section that compares data from experiments with models. Figures are placed in the end of the paper for convenience. The paper is based on the PhD-thesis by Broe (2009).

Both the aerodynamically and the acoustical models are described.

The experiments were carried out in a wind tunnel. Two different profiles were used, a NACA0015 and a NACA63415 profile. The data from these experiments are obtained by various means to get the properties of the flow such as angle of attack, mean wind speed, and surface pressure at the aerofoil.

Models

This section discusses and presents the models used in this paper. The models are aerodynamical and acoustical models. The reader is kindly requested to consult Broe (2009) for a thorough derivation and explanation of the theories below.

The aerodynamical models describe the unsteady aerodynamics when an aerofoil is subject for incoming turbulence. They are based on potential theory and the incompressible and inviscid form of Navier-Stokes equations which are linearized. Expressions for the unsteady lift for each model is given and when possible also expressions for the unsteady lift distribution. The models are defined as 1-D (Sears, 1941), 2-D (Atassi, 1984), and 3-D (Graham, 1970).

The acoustical model predicts the noise due to turbulence in the incoming flow. The model is based on that the force which is responsible for emitting sound pressure is acting as a dipole (Amiet, 1975).

The 1-D model by Sears (1941) is able to predict both the unsteady lift distribution and the unsteady lift due to a gust that acts normal to the plane of a flat plate. The gust incidents perpendicular to the plate, see Figure 2 (in the case of v equal to zero).

The unsteady lift distribution is given as

Eqn. 1: $$l(\theta, \kappa, t) = \rho A_0 \tan\frac{\theta}{2} + 2\rho \sum_{m=1}^{\infty} A_m \sin m\theta$$

where the position on the flat plate (aerofoil) is represented by $x=c/2 \cos\Theta$, c is the length of the aerofoil and Θ is in the interval from 0 to π. The reduced frequency of the gust, κ, is given by $\omega c/(2U)$ where ω is the angular frequency of the gust and U is the velocity of the mean flow. The coefficients A_m is given as

Eqn. 2: $$A_m = 2UWe^{\imath\omega t}\left(\frac{\imath\kappa}{2m}P_{m-1} + P_m - \frac{\imath\kappa}{2m}P_{m+1}\right), m \geq 1$$,

and

Eqn. 3: $$A_0 = 2UWe^{\imath\omega t}\left[C(\kappa)(P_0+P_1)-P_1\right],\ C(\kappa)=\frac{K_1(\imath\kappa)}{K_0(\imath\kappa)+K_1(\imath\kappa}$$

where the coefficients P_m is given by $(-\imath)^m J_m(\kappa)$, $J_m(\kappa)$ is the Bessel function of first kind, $C(\kappa)$ is the Theodorsen function, K_0 and K_1 is modified Bessel functions of second kind, and W is the amplitude of the vertical gust at a given wavenumber. The Theodorsen function is the solution for vertical translation oscillations of a flat plate, Theodorsen and Garrick (1942) and Fung (1969).

The unsteady lift by Sears (1941) is given by

Eqn. 4: $$L'(\kappa)=\frac{1}{2}\rho cUWe^{\imath\omega t}2\pi\left[(J_0(\kappa)-\imath J_1(\kappa))C(\kappa)+\imath J_1(\kappa)\right].$$

A full derivation of the above equations can be found in Broe (2009). The expression in Eqn. 4 is illustrated by the black line in Figure 3 where it is seen that the absolute value of the unsteady lift decreases as the reduced frequency increases. This implies that gusts with wavelength much less than the chord length does not contribute much to the total unsteady lift.

The 2-D model by Goldstein and Atassi (1976) and Atassi (1984) is able to predict the unsteady lift when a flat plate is bend (camber) and has an angle of attack (AOA) to the mean flow as seen in Figure 4. The model is not able to describe the lift distribution. The model has been linearized such that the lift response can be split into a contribution from a flat plate, a contribution due to AOA and a contribution due to camber. The total response becomes

Eqn. 5: $$R_T(\kappa,\mu)=\frac{\kappa}{\sqrt{\kappa^2+\mu^2}}\frac{\overline{S(\kappa)}}{2\pi}+\beta L_\beta(\kappa,\mu)+mL_m(\kappa,\mu)$$

where the line over $S(\kappa)$ means complex conjugated, $S(\kappa)$ is the expression in Eqn. 4 divided by $\rho cUW/2$, β is the AOA in radians, L_β is the lift response due to AOA, m is a bending factor, L_m is the lift response due to the bending, and μ is the vertical component of the wave vector, see Figure 4. The total unsteady lift is given by Atassi (1984) as

Eqn. 6: $$L'(\kappa,\mu)=A(\rho,c,U)(w+u)g(\kappa,\mu)$$

where $A(\rho,cU) = \rho cU/2$, u and w is the amplitudes of the gust in direction of the mean flow and in the vertical, respectively as seen in Figure 4. Further

Eqn. 7: $$g(\kappa,\mu)=2\pi\overline{R_T(\kappa,\mu)}$$

where again overline means complex conjugated.

The unsteady lift is investigated in Figure 6 for different values of the parameters β and m. Figure 6a) and b) show the unsteady lift response due to AOA. It is seen that at low μ the response approaches zero as κ is increased and the larger μ gets the slower it converges to zero. The absolute value of the response approaches to an asymptotic value for values of μ large enough, see blue line in Figure 6b). The camber is approximated to a parabolic line which describes the camber line best, Atassi (1984), and implies that the parameter, m, is describing the amplitude of the parabolic line. Figure 6c) and d) show the response due to camber, L_m. Similar to the response function of the AOA the response function for camber is approaching zero as κ is increased until a certain μ where an asymptotic value of the absolute value of the response is approached, see red and green line in Figure 6d).

The 2-D model is based on the convention that the time part is defined as exp(-ıωt) whereas it is defined as exp(ıωt) in the 1-D model above and in the 3-D model below. In order to compare with these models the complex conjugate of Eqn. 6 is taken. Figure 2.10e) and f) show the complex conjugate of the total response. The complex response and the absolute response is shown, and when the AOA is different from zero the total response is seen to approach an asymptotic value that is not going to zero as κ is increased. The response with camber and AOA=0° is seen to vanish as κ is increased.

The 3-D model is able describe the unsteady lift distribution and lift for a flat plate which impinges by a skewed vertical gust, see Figure 2.

The unsteady lift is given by

Eqn. 8: $L'(\kappa,\nu) = A(\rho,c,U)Wg(\kappa,\nu)$

Eqn. 9: $F(z) \;=\; f_1(z) - 4\nu^2 f_3(z)$

Eqn. 10: $$F(z) = \frac{2}{\pi\sqrt{1-z^2}}\sum_{k=0}^{N}{}''\sigma_k T_k(z)$$

Eqn. 11: $g(\kappa,\nu) = 4e^{\imath\kappa}[\overline{f_2(1)} + \imath\lambda c\overline{f_3(1)}]$

where A(ρ,cU) = ρcU/2, W is the amplitude of the vertical gust, z is the normalized chordwise position defined as x/c, c is the chord length, κ is the chordwise normalized wave number for the vertical gust and v is the spanwise normalized wave number for the vertical gust. The normalization is given as $k_x c/2$ and $k_y c/2$ for the chordwise and spanwise component, respectively. The coefficients σ_k are functions of κ and v, and the functions, $T_k(z)$, are Chebychev polynomials (Fox and Parker, 1968).

The unsteady lift for the 3-D model is seen in Figure 3. It reduces to Eqn. 4 when v = 0, and when the spanwise wave number is different from zero the lift fluctuations approaches zero faster when κ is increasing. Likewise the lift fluctuations is seen to approach zero when κ is fixed and v goes towards infinity. The complex lift indicates a lag in the response of the lift at mid chord in comparison to the inflow at mid chord.

The lift distribution is given by

Eqn. 12:

$$\Delta p(z) \;=\; \frac{1}{2}\rho c U_\infty w_0 \sum_{i=0}^{N}{}'' T_i(z)\left(\frac{2}{\pi\sqrt{1-z^2}}\sigma_i + \sum_{j=0}^{N}{}''\left\{\sum_{k=0}^{N}{}''\frac{1}{\pi}\sigma_k(\nu A_{ij} - \imath\kappa B_{ij})\right.\right.$$

$$\times \left[c_{k+j}(z) + c_{|k-j|}(z)\right] \Big\}\Big)$$

The coefficients A_{ij} , B_{ij}, c_{k+j}, and $c_{|k-j|}$ are found by Chebychev polynomials as

Eqn. 13:
$$\sinh[\nu(z-z')] = \sum_{i=0}^{N}{}''\sum_{j=0}^{N}{}'' A_{ij}T_i(z)T_j(z')$$

Eqn. 14:
$$\cosh[\nu(z-z')] = \sum_{i=0}^{N}{}''\sum_{j=0}^{N}{}'' B_{ij}T_i(z)T_j(z')$$

Eqn. 15:
$$c_h(z) = -\frac{\sin\left(h\cos^{-1} z\right)}{h}, \qquad h \geq 1$$

Eqn. 16:
$$c_h(z) = \frac{\pi}{2} + \sin^{-1} z, \qquad h = 0$$
.

When v is zero in Eqn. 12 the 1-D case is obtained, see Eqn. 1. Comparison of the two models show that they coincide in this case, and this means that Eqn. 1 is validated for the 1-D case. The unsteady lift distribution is decreasing when either the chordwise, the spanwise or both of the wave number are increased (not shown). This is expected because the wave lengths of the gust is so small that the fluctuations are blurred out on the aerofoil in order that the responses become very small or vanish.

Inflow noise is a field of concern. The semi-empirical models that estimate the aerodynamical noise consist of models for different components of noise generated by the flow around an aerofoil. The inflow noise is the dominant component and is the subject below. It is believed based on measurements by Moriarty and Migliore (2003) and Oerlemans et al. (2007) that inflow noise does not have that high importance for the total noise as the inflow noise model suggests. The model for inflow noise is based on Amiet (1975), and this model is presented below. The force that produces the acoustic pressure is a dipole.

The spectrum of the acoustic pressure is by Amiet (1975) estimated to be

Eqn. 17:
$$\begin{aligned} S_{PP}(x,0,z,\omega) &= \left(\frac{\omega z \rho_0 b}{c_0 \sigma^2}\right)^2 U\pi d \\ &\quad \times \int_{-\infty}^{\infty} \delta(k_y)|\mathcal{L}(x,K_x,k_y)|^2 \Phi_{ww}(K_x,k_y)dk_y \\ &\approx \left(\frac{\omega z \rho_0 b}{c_0 \sigma^2}\right)^2 U\pi d|\mathcal{L}(x,K_x,0)|^2 \Phi_{ww}(K_x,0) \end{aligned}$$

where x and z is the horizontal and vertical distance to a receiver, respectively, ω is the angular frequency, ρ_0 is the density of air, b is half the length of the chord, c_0 is the speed of sound in air, d is half the length of the span, $L(x,K_x,k_y)$ is the lift distribution, and $\Phi_{ww}(K_x,k_y)$ is the spectrum of the vertical turbulence as given by von Kármán (1948). The spectrum of the acoustic pressure is used to calculate the SPL in the third octave band as

Eqn. 18:
$$\mathrm{SPL}_{1/3} = 10\log_{10}\left[\frac{2S_{pp}\Delta\omega}{p_{ref}^2}\right], \quad p_{ref} = 2\cdot 10^{-5}\mathrm{Pa}$$

This means that the lift distribution estimated by the 1-D and 3-D model can be used to estimate the SPL emitted due to atmospheric turbulence. The SPL is estimated by Amiet (1975) by using the response function for the lift distribution by Adamczyk (1974) to give

Eqn. 19:
$$\mathrm{SPL}_{1/3} = 10\log_{10}\left[\frac{Ld}{z^2}\frac{\overline{u^2}}{U^2}M^5\frac{\hat{K}_x^3}{(1+\hat{K}_x^2)^{7/3}}\right] + 181.3$$

where L is the typical length scale of the turbulence, overline u^2 is the variance of the wind in the direction of the mean wind, M is the Mach number, and hat K_x is a normalized wave number in mean wind direction.

Data

The aim of the experiments was to obtain knowledge of the acoustics and other dynamic pressure phenomena at the surface of an aerofoil. Microphones were mounted on the surface in order to obtain measurements of high frequency resolution of the pressure fluctuations at different positions at the surface of the aerofoil. Similar previous experiments have been made by Risø, DTU at lower frequency resolution by using pressure tabs to measure the mean pressure.

The wind tunnel used to obtain the measurements analyzed below is owned by the window manufacturer, Velux, and it is located 10 km northeast of Horsens in Denmark. It is mainly used for tests of new product components, and it is rented to external users for multiple purposes. The wind tunnel is an open jet wind tunnel. The maximum wind speed of the tunnel is 40m/s and the turbulence intensity is approximately 1%. The test section of the tunnel is 10.5 m long from the inlet of the jet to the outlet and 7.5 m wide. The height in the test section is 7.5 m. The vertical and horizontal profile of the jet are assumed to be constant. The conditions for measurements in Velux Wind tunnel are treated in detail in Fuglsang, Antoniou, Sørensen and Madsen (1998).

The experiments were conducted in December 2006 and in June 2007. The microphones used in both experiments are of type Sennheiser KE-4-211- 2, and they have a sampling frequency of maximum 50 kHz. The response function given by the manufacturer is constant in the range between 20Hz and 20kHz. Measurements of the pressure fluctuations at the surface of the aerofoil are also obtained with pressure tabs, and they have a sample frequency of maximum 400 Hz but most of the samples are obtained at 100 Hz.

The microphones were placed in a device which was mounted such that it was flush with the surface of the aerofoil. The way the microphone was mounted in the device left a chamber between the membrane of the microphone and the surface of the aerofoil. The chamber caused the signal to be unreliable above a cut-off frequency, which is dependent on the dimensions of the chamber between the microphone and the surface of the aerofoil. The chamber was altered between the two experiments, and thus the cut-off frequency was different for the two experiments. The cut-off frequency is estimated according to the theory of a Helmholtz resonator (Martin, Mus and Mus, 2004), and is estimated to be 3.4 kHz and 13.6 kHz for the experiment in December 2006 and June 2007, respectively. The cut-off frequencies estimated are similar to the cut-off frequencies observed.

The experiments were on a NACA0015 profile with a chord length of 1.0m and a NACA63415 profile with a chord length of 0.6m and both profiles had a span of 2m. The positions of microphones on the latter profile at a section are shown in Figure 5. The first profile is symmetric and has no camber and the other has camber. The NACA0015 profile was equipped with 11 microphones on the suction side only, and the NACA63415 profile was equipped with 67 microphones of which 19 were on the pressure side. The other microphones were placed on the suction side.

The transition and separation points on the aerofoil are recognizable when the standard deviation, σ_p, of the pressure is plotted as function of chordwise position and AOA, see Figure 7. The plot in Figure 7 is to be understood qualitatively because peak values indicate either transition or turbulent transition depending on AOA and chordwise position. The lesson learned from spectra of pressure (not shown) in the experiment with a NACA0015 profile is that σ_p will increase as transition is reached because high frequencies contain nearly as much energy as low frequencies. Then σ_p decreases a little when both looking in the direction of constant AOA and increasing chordwise position and vice versa because low frequencies now contain less energy than at laminar flow. Turbulent transition occurs when the standard deviation of pressure again is increasing in both directions because the energy level at this stage is much higher in all frequencies than at laminar flow. The "mountain ridge" shows the transition position as function of AOA and position. Turbulent transition is not as recognizable but is at the highest AOA and starts at 33.5% chord. Transition is present at AOA 3.4° and 5.0° and turbulent transition is present at 16.0°.

The data from microphones are suitable for analyzing lift fluctuations and lift distribution fluctuations. The data from pressure tabs is not suitable for fluctuations of pressure but give reliable mean pressures. The mean pressure is used to estimate the angle of attack to mean flow of the profile. The measurements by microphones can be used to investigate the positions of transition and turbulent transition of the flow over the chosen aerofoils in the angle of attack and chord wise position space. They capture the fluctuations in a way that they are trusted to give reliable information in the frequency domain when Fourier analyzed (not shown). Data of the flow were obtained by a 5-hole pitot tube and a triple wired hot wire. The data from the 5-hole pitot tube is suitable to describe the mean flow. Hot wire data are used to obtain information of the turbulence in flow. The turbulence intensity is between 1 and 2% and the turbulence is close to being isotropic.

The data from the two wind tunnels experiments are of a quality such they can be used for further analysis. The pressure spectra from microphones show peaks that are ignored because they are characteristic for the wind tunnel.

Analysis

The data has to be used as input in the models in order to obtain pressure spectra and lift spectra. This has to be done to estimate a realistic energy spectrum for the turbulence and to find the amplification factor. The data obtained from a triple wired hotwire is used to estimate the length scale, L, and the mean kinetic energy dissipation, ε. The two parameters are estimated by fitting to the spectra of the three turbulence components, u, v, w. The curves are fitted by the least squares method and L and ε are unique at a given mean wind speed. The hotwire is believed to give reliable results for the turbulence, but the calibration of the instrument was not good enough to be used for the mean wind speed. Hotwire data were obtained only in the experiment with the NACA0015 profile. The estimates for L and ε from the NACA0015 experiment is used for the NACA63415 experiment as well. The flow conditions and turbulence generation are believed to be similar in the two experiments so it is satisfactorily to use estimates of L and ε at similar mean wind speeds for the NACA63415 experiment.

The data from the 5-hole pitot tube is used to estimate the mean wind speed. The mean wind was measured with a cup anemometer. The data from the 5-hole pitot tube are very similar to those of the cup anemometer.

The corrected AOA are found from the pressure data obtained by the pressure tubes. The mean pressure of the data from the pressure tubes are known to be reliable and have been used for estimating corrected AOA's several times with reliable results (Gaunaa, Fuglsang, Bak, and Antoniou, 2004).

The spectra of pressure and lift from the pressure data obtained by microphones have peaks at certain frequencies (wave numbers). The peaks are at different wave numbers because k_x=f/U and the data are not obtained at same mean wind speed at all runs. Furthermore the peaks are ignored when spectra from data and models are compared because the peaks coincide with the peaks in the pressure spectra obtained by a background microphone. Thus the peaks in spectra of pressure and lift are considered not to be of aerodynamical origin but to be due to the wind tunnel. The pressure spectra for models and data are compared in Figure 8. The plots show the data, the 1-D model and the 3-D model for a selection of microphones. The data are chosen for cases at an effective AOA of 0° obtained from the NACA63415 profile. The microphones shown in Figure 8 are all placed 86mm from mid-span to the right of the incoming flow. The order of microphones is from leading edge towards trailing edge by moving from top left to the right and from top to bottom in the plots. The first five microphones are on the suction side. The three last microphones in the plots are on the pressure side. The difference between data and the 1-D model is approximately 1-2 decades at the suction side from the leading edge to about mid-chord. The difference is larger after mid-chord and is increasing to about 2 decades close to the trailing edge. The difference between data and models are larger on the suction side than on the pressure side. The difference at the suction side near leading edge is approximately 1.5 decade and increases to more than 2 decade near trailing edge in Figure 8. It is seen that the pressure fluctuations decrease in magnitude from the leading edge to trailing in the data. The difference between models and data increases from mid-chord to trailing edge. The aerofoils used, NACA0015 and NACA63415, have different properties but they have equal magnitude of difference between data and models (not shown). The difference increases slightly with increasing mean wind speed (increasing Reynolds number). The data are expected to be between the 1-D model and the 3-D model levels. The reason for large difference between the 1-D model and the data might be the properties of the wind tunnel. The wind tunnel is very noisy and might give systematically higher pressure fluctuations than expected. Another mechanism can be the generation of a turbulent boundary layer at the surface of the aerofoil which may create more turbulence at higher frequencies. The difference between data and the 1-D model increases from about mid-chord to trailing edge to more than 2 decades. This may be explained by the generation of a turbulent boundary layer.

The lift was calculated by numerical integration using a trapezoidal method. The lift spectra from the experiment with the NACA63415 profile are shown in Figure 9. It is seen that the data are on top of each other until separation occurs at approximately 11°. The lift spectrum increases after the AOA where separation occurs. The data fall between the 1-D model and the 3-D model in most of the frequency interval. This is expected because 3-D model assumes perfect isotropic flow and the 1-D model assumes completely anisotropic flow, and the data are obtained under near isotropic conditions.

Figure 8 show the lift spectrum for the three models and for the data. It is seen that no effect of AOA is present in the data below the AOA where separation occurs. All data below separation are more or less on top of each other. This is surprising because the 2-D model predicts a difference. The separation is seen in data from both experiments (not shown), but no effect of AOA is seen in data, surprisingly. Errors because of low spatial resolution are expected at high frequencies especially on the NACA0015 profile because few points are used to calculate the lift. This low spatial resolution causes high frequencies not to be captured well. The error because of the low spatial resolution is expected to increase with increasing wave number (frequency) because high frequencies require high resolution to be captured well. The systematic error in pressure seem to be eliminated in the lift because the lift spectra is between the 1-D model and the 3-D model or are just above the 1-D model. The reason for the elimination of the error may be that the background noise is filtered out when integrated. The lift spectrum increases above the angle of separation which is expected to be due to increasing aerodynamical turbulence.

Figure 8 show that the data are in between the 1D-model by Sears (1941) and the 3-D model by Graham (1970).

The SPL is estimated by the model by Amiet (1975). This model is used at different stages dependent on which model for the lift distribution is used. The 1-D model and the 3-D model are implemented into Eqn. 17 and Eqn. 18. The lift distribution used in Amiet (1975) is given by the estimate of the SPL in Eqn. 19.

Figure 10 compare the models of SPL at three different flow conditions. The mean velocity is in Figure 10 from top to bottom 25m/s, 15m/s, and 30 m/s, respectively. The 1-D model and the 3-D model have SPL's that is below the model for the lift fluctuations by Adamczyk (1974) and used by Amiet (1975).

Because the lift spectra for data are in between the 1-D model by Sears (1941) and the 3-D model by Graham (1970) ($kS_{L,1D}(k) > kS_{L,Data}(k) > kS_{L,3D}(k)$) then it is expected that this is also the case for the SPL from data.

There are reasons to believe that the SPL from data would fall in between the SPL's from the 1-D model and 3-D model. The reason for this statement is, that the lift fluctuations from data are in between models and because the lift distribution is integrated over the aerofoil to obtain an estimate the SPL.

Conclusions

Three different models for predicting the fluctuating lift on an aerofoil has been described. These models of lift have been tested against data. The lift distribution is presented for the 1-D model and is developed for the 3-D model. These two models of lift distribution are tested against pressure data. They are also used to predict SPL.

Data are obtained for two different aerofoils. Profiles of a NACA0015 and a NACA63415 are used to obtain pressure data at the surface of an aerofoil. Surface pressure obtained by microphones is tested against models for the lift distribution which in this case is the 1-D model and the 3-D model. The surface pressure data by microphones are integrated numerically to obtain the fluctuating lift. These derived data are tested against models for lift in this case all three models.

The surface pressure is also obtained by pressure holes and these data are able to describe mean pressures at chord wise positions reliably. The pressure hole data are therefore used to get angles of attack of which the mean flow impinges the aerofoil.

The mean wind speeds are obtained from 5-hole pitot tube data and these data are only obtained at the experiment with NACA0015. The data from the 5-hole pitot tube are used in similar conditions for the experiment with a NACA63415 profile. The mean wind speed data are used to get the magnitude of the lift and the lift distribution fluctuations from models in the further analysis.

Data from a 6-armed hot wire are used to get information of the turbulence. The turbulence is close to be isotropic. The turbulence data are used to estimate the length scale of the turbulence and the energy dissipation of the turbulence.

The comparison of data and models seems to be similar for the two aerofoils. The conclusion is that the models predict the different aerofoils equally. The models of lift capture the lift of the data. The data are slightly anisotropic and are therefore as expected between the 1-D model and the 3-D model. The calculated lift from data are similar for different angle of attacks and thus the 2-D model is not able to describe data. Further the difference between pressure spectra of models and data are systematic which highly probably is because of background noise in the wind tunnel. The models of the lift indicates that noise from a wind turbine due to atmospheric turbulence may be the most dominant. The lift spectra and pressure spectra suggest that sound pressure level of data will be between sound pressure level based on the 1-D model and sound pressure level based on the 3-D model.

The sound pressure level of data are not found because the spatial resolution of surface pressure by microphones on the aerofoils did not allow this.

Acknowledgment

This paper is made in close cooperation with Professor Jakob Mann at Risø National Laboratory for Sustainable Energy. The author thus honors the help, discussion, and advice from him.

References

Adamczyk, J. J.: 1974, The passage of an infinite swept airfoil through an oblique gust, Technical Report NASA CR-2395, NASA.Amiet, R. K.: 1975, Acoustic radiation from an airfoil in a turbulent stream, J. Sound and Vibr. 41, 407–420.

Atassi, H. M.: 1984, The sears problem for a lifting airfoil revisited - new results, J. Fluid Mech. 141, 109–122.

Broe, B. R.: 2009, Unsteady Aerodynamics and Inflow Noise, Risø–PhD–47(EN), note: PhD- Thesis to be submitted August 2009 and a copy is available from the author, Risø National Laboratory for Sustainable Energy.

Fox, L. and Parker, I. B.: 1968, Chebychev Polynomials in Numerical Analysis, Oxford University Press.

Fuglsang, P., Antoniou, I., Sørensen, N. N. and Madsen, H. A.: 1998, Validation of a wind tunnel testing fascility for blade surface pressure measurements, Technical Report Risø–R –981 (EN), Risø National Laboratory.

Fung, Y. C.: 1969, An introduction to the Theory of Aeroelasticity, 2 edn, Dover.

Gaunaa, M., Fuglsang, P., Bak, C. and Antoniou, I.: 2004, Open-jet wind tunnel validation using a naca 0012 airfoil, In: Proceedings. Special topic conference: The science of making torque from wind, Delft (NL), 19-21 Apr 2004, Delft University of Technology, Delft, 2004, pp. 37–48.

Goldstein, M. E. and Atassi, H. M.: 1976, A complete second-order theory for the unsteady flow about an airfoil due to a periodic gust, J. Fluid Mech. 74, 741–765.

Graham, J. M. R.: 1970, Lifting surface theory for the problem of an arbitrarily yawed sinusoidal gust incident on a thin aerofoil in incompressible flow, Aero. Quart. XXI, 182–198.

Guidati, G.: 2004, Berechnung und Verminderung von Strömungsgeräuschen an Profilen, PhD thesis, Institut für Aerodynamik und Gasdynamik Universität Stuttgart. In german.

Henderson, G.: 2005, Development of noise reduction technology for a 500 kw prototype wind turbine, Wind Turbine Noise: Perspectives for Control, INCE, Berlin.

Martin, G., Mus, B. and Mus, M.: 2004, Introduction to Sound Recording. Purchased at http://www.tonmeister.ca/main/textbook/index.html.

Moriarty, P. J., Guidati, G. and Migliore, P.: 2005, Prediction of turbulent inflow and trailing-edge noise for wind turbines, American Institute of Aeronautics and Astronautics Paper 2005-2881.

Moriarty, P. and Migliore, P.: 2003, Semi-empirical aeroacoustic noise prediction code for wind turbines, Technical Report NREL/TP-500-34478, NREL.

Oerlemans, S., Sijtsmaa, P. and López, B. M.: 2007, Location and quantification of noise sources on a wind turbine, J. Sound and Vibr. 299, 869–883.

Panofsky, H. A. and Dutton, J. A.: 1984, Atmospheric Turbulence, John Wiley & Sons, New York.

Sears, W. R.: 1941, Some aspects of non-stationary airfoil theory and its practical application, J. Aeron. Sc. 8(3), 104–108.

Theodorsen, T. and Garrick, I. E.: 1942, Nonstationary flow about a wingaileron-tab combination including aerodynamic balance, NACA Rept. 736.

von Kármán, T.: 1948, Progress in the statistical theory of turbulence, Proc. National Akad. Sci. 34, 530–539.

Wagner, S., Bareiß, R. and Guidati, G.: 1996, Wind Turbine Noise, Springer.

Zhu, W. J.: 2007, Aero-Acoustic Computations of Wind Turbines, PhD the- sis, DCAMM Special Report No. S100.

Figures

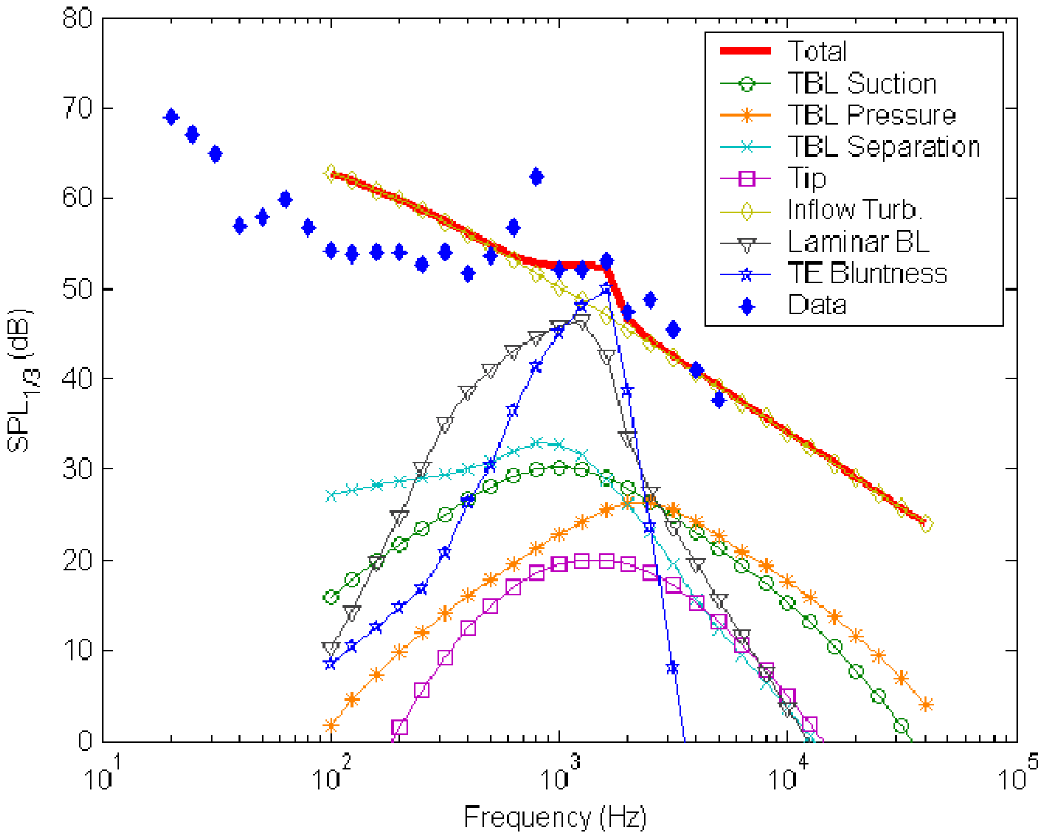

Figure 1: Plot of the $SPL_{1/3}$ at the one third octave frequencies for aero acoustic sources described in Moriarty and Migliore (2003). This figure is identical to Figure 9 in Moriarty and Migliore (2003).

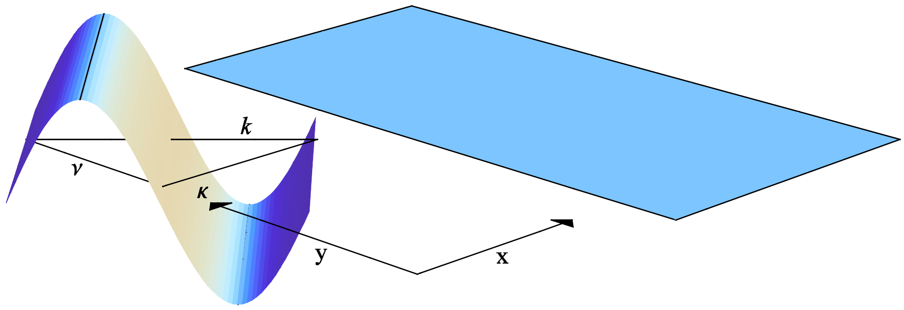

Figure 3: Sketch of a skewed sinusoidal gust entering a flat plate. The width in the x-direction is the chord length, c.

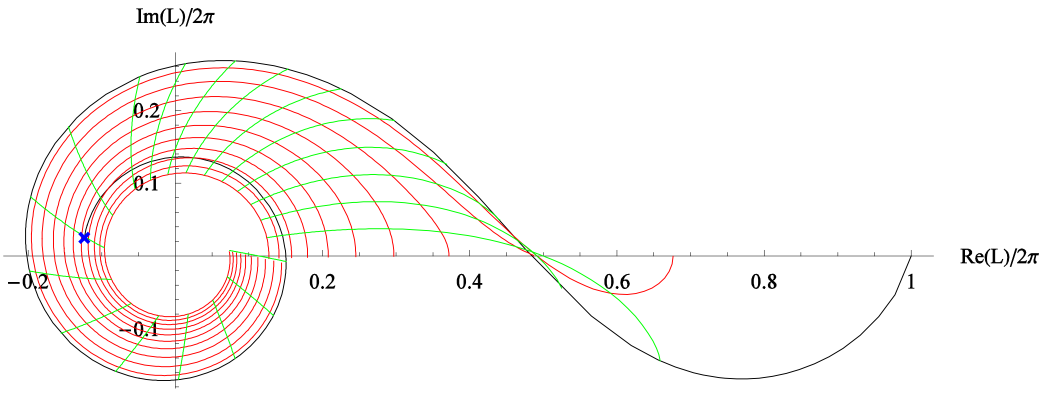

Figure 2: Plot of the lift response due a sinusoidal gust as function of reduced wave number. The black line is due to a 1-D sinusoidal gust on a flat aerofoil by the model of Sears (1941). Note that the absolute value of the lift response |L| is the distance from the origin of the plot to a point on, say, the black line. The argument of L is the corresponding phase of the lift relative to the phase of the gust at the midpoint of the aerofoil to the gust. The green and red lines in the plot show the case of a 2-D sinusoidal gust on a 2-D flat aerofoil by the model of Graham (1970). The red lines are functions of κ for different values of fixed ν, where ν is varied from 0 to 2.5 in steps of .25. The green lines are functions of ν when κ is fixed, and κ takes values from 0 to 2.5 in steps of 0.25 and from 3 to 7 in steps of 0.5.

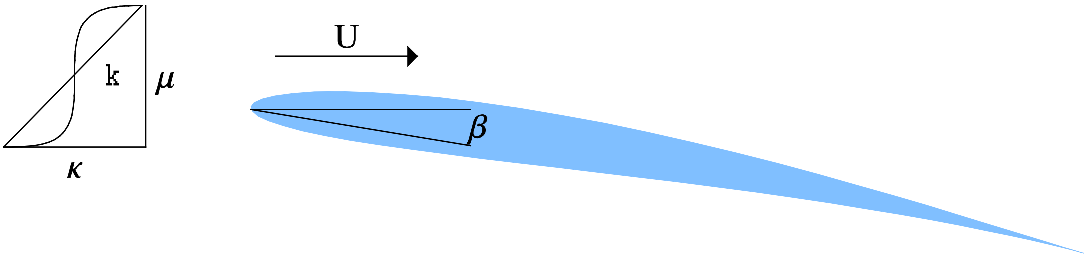

Figure 4: Sketch of a skewed sinusoidal gust entering an aerofoil with thickness and camber at an AOA to the mean flow.

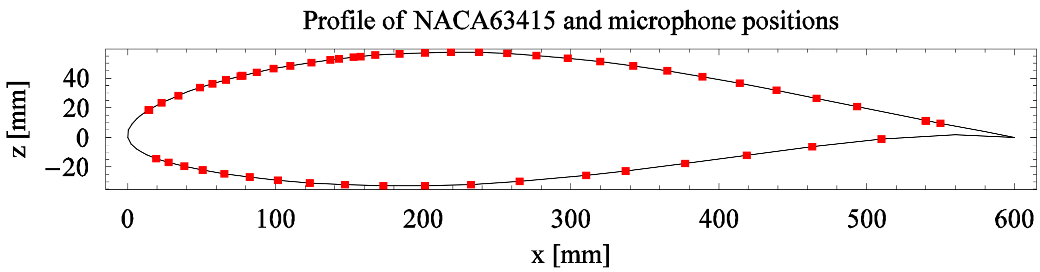

Figure 5: The shape of the NACA63415 profile. The positions of microphones are shown by the red dots.

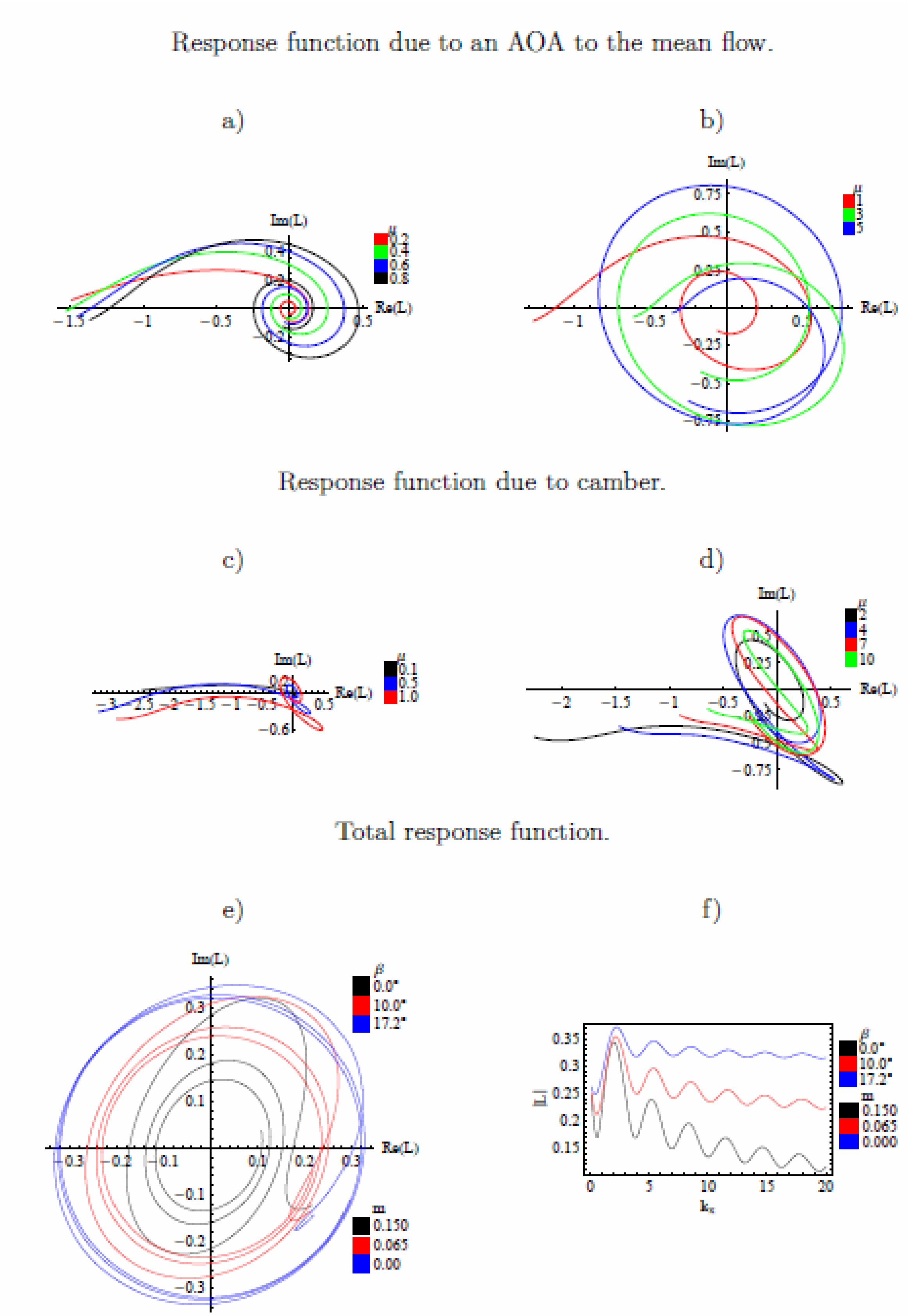

Figure 6: The transfer functions of the 2-D model. The figures a) to e) is similar to the plots in Atassi (1984). The lines are at fixed μ and κ is varied in a) to d). A 2-D gust for which the wave front has an angle of 45° to the mean flow and the wave length of this gust is varied in e) and f).

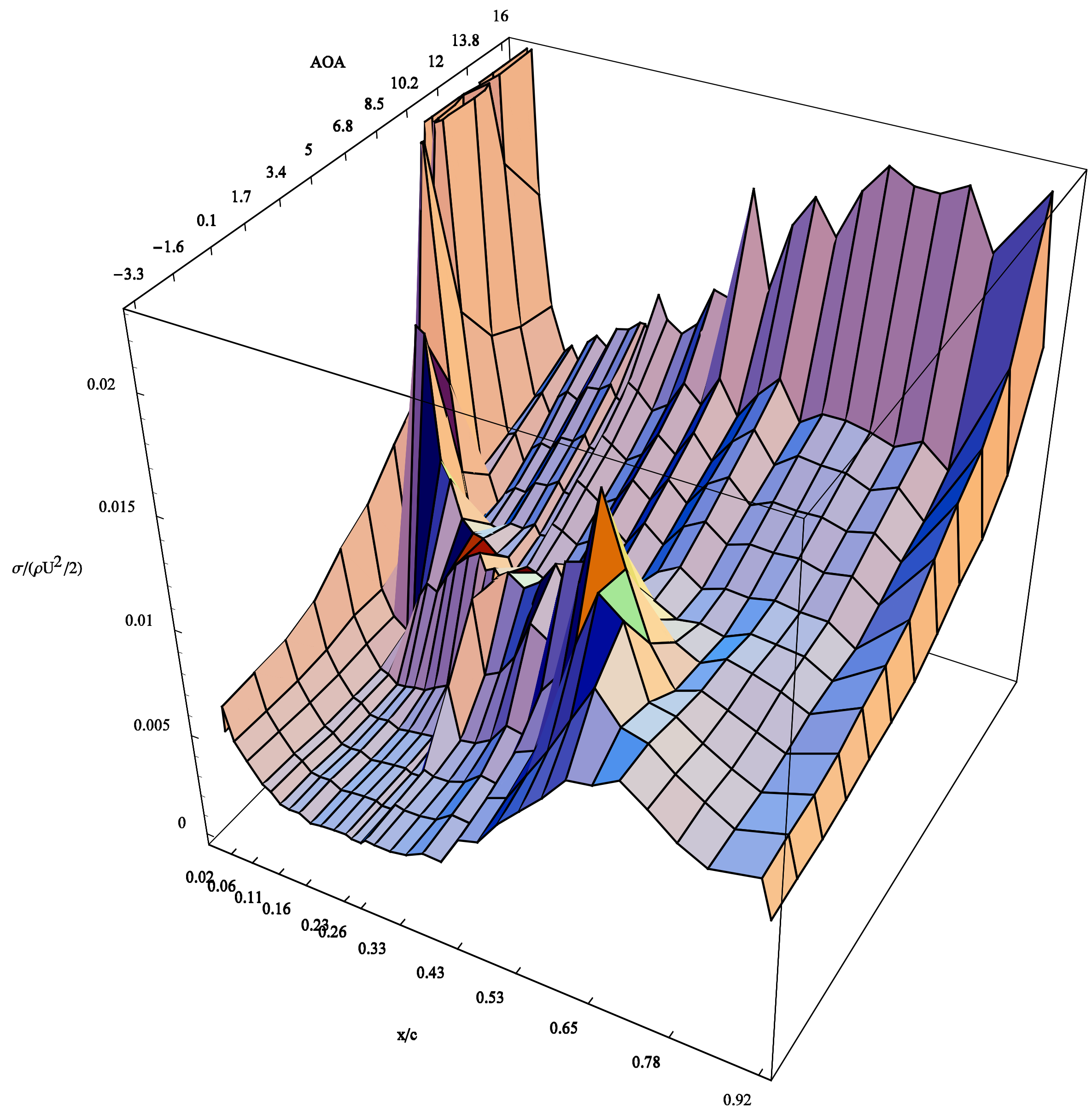

Figure 7: The standard deviation, σ_p, of the pressure normalized with the dynamic pressure. AOA is the angle of attack and x/c is the normalized chordwise position.

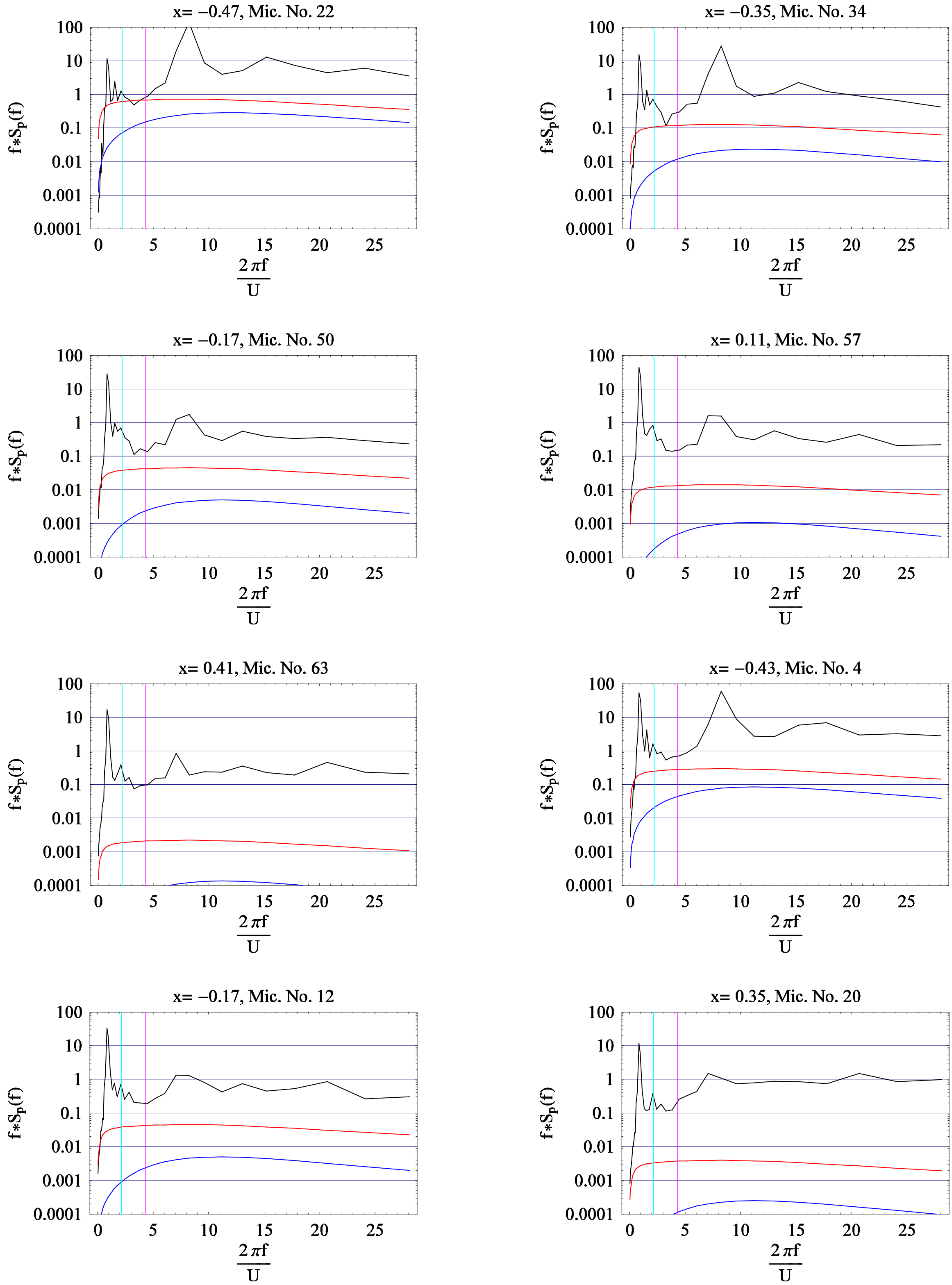

Figure 8: Comparison of pressure spectra from data and models for the NACA63415 profile. The pressure spectra, fSp(f), are plotted against wave number. The data are black, the 1-D model is red and the 3-D model is blue. The data are obtained at a mean wind speed of 30 m/s.

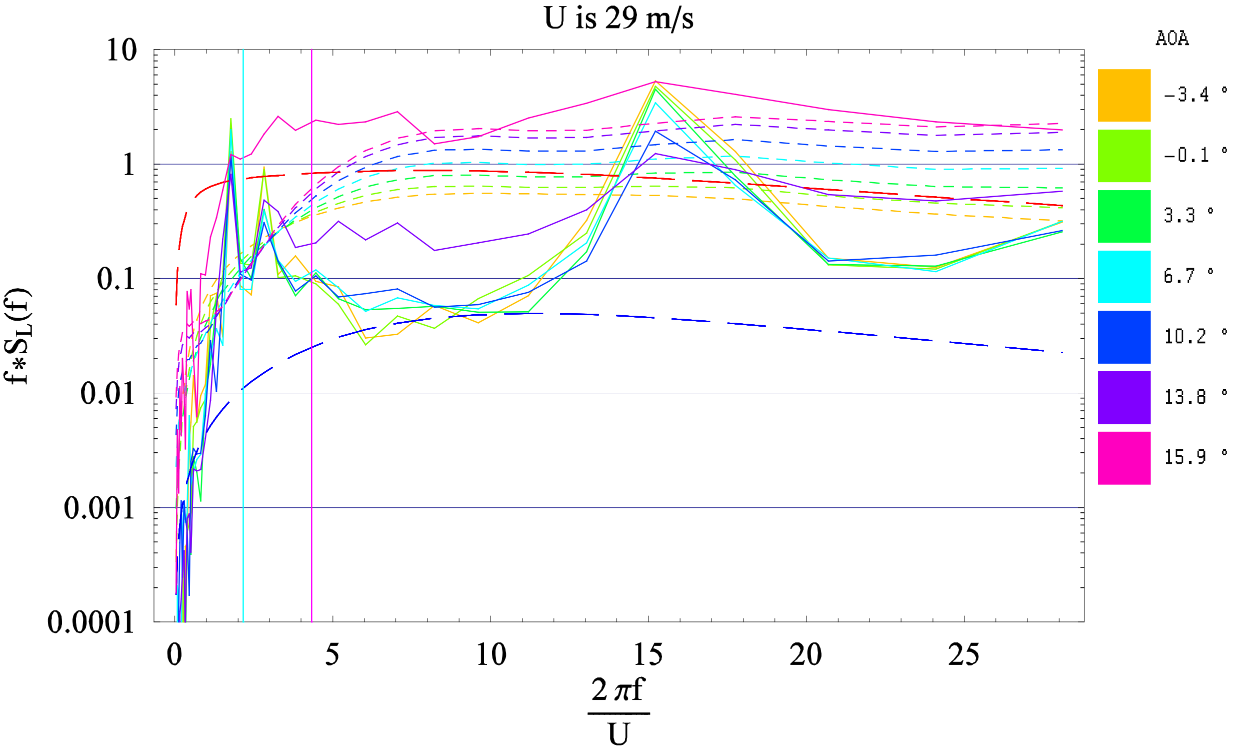

Figure 9: Comparison of lift spectra from data and models for the experiment with a NACA63415 profile. The color legend is for data (full line) and the 2-D model (short dashed line). The long dashed lines represent the 1-D model (red) and 3-D model (blue). The lift spectra, fSL(f), are plotted against wave number.

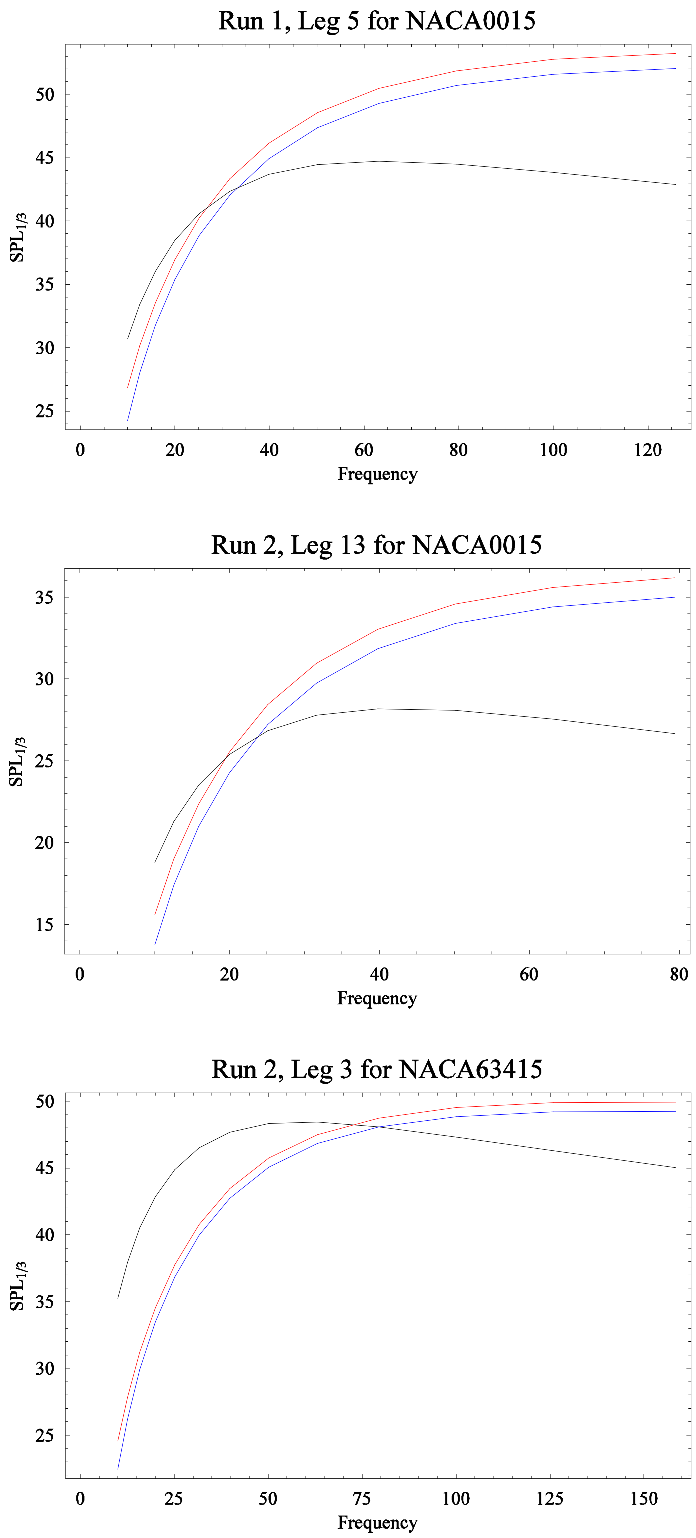

Figure 10: Plot of the $SPL_{1/3}$ at the one third octave frequencies. The 1-D model is represent by red, 3-D model is blue, and the original model (Eqn. 19) is black. The data are chosen as close to zero mean lift conditions as possible.

Third International Meeting
on
Wind Turbine Noise
Aalborg Denmark 17 – 19 June 2009

A critical look at the wind turbine noise regime in Norway.

Sigurd Solberg and Inge Hommedal
Kilde Akustikk, Tvildesvegen 16D, NO-5700 Voss, Norway
sigurd.solberg@kilde.no; inge.hommedal@kilde.no

Abstract

The noise regime formally use the EU-metric L_{den}. In reality, L_{ref}, the noise level for 8 m/s at 10 m height, and an assumption of 80% operation is used. This makes the relation to be $L_{den} = L_{ref} + 5$ dB for a constant downwind assessment.

The recommended noise limit for non-sheltered situation, is $L_{den} = 50$ dB or $L_{ref} = 45$ dB. At locations with wind-shelter (made by the terrain) more than 30% of the year, the recommended noise limit is $L_{den} = 45$ dB. There is no method to assess the terrain and wind into non-sheltered or sheltered situations, and it is recently made at a rough estimate. In addition to the recommended levels, all dwellings within $L_{den} = 40$ dB shall be shown, but the use of this information is not clear.

The calculation is mainly based on a downwind situation, but a calculation for prevailing wind is also required. This means a less strict assessment compared to the main criterion, in practice by up to 2-3 dB. The problem with calculation of propagation at upwind condition is that the existing calculation methods probably are not evaluated for the modern wind turbine hub heights. A test with the EU-Imagine method point-to-point method for a source height of 80 m and a propagation condition similar to upwind indicate a minimum distance in the order of 1000 m before a significant sound reduction is reached. This distance is well above the distance to the recommended limit, $L_{den} = 50$ dB, for typical wind turbines. Until a more holistic regime is made, we advice the Norwegian noise regime to be kept simple, at downwind calculations only, without an uncertain prevailing wind assessment.

Introduction

Still, very little wind power is installed in Norway, only 400 MW (2007). In addition 14.000 MW has been given or has been asked for permission.

The noise regime was originally deducted from industrial noise recommendations, using levels of $L_{A,eq,night}$ = 40 dB, layed out as L_{ref}=40 dB (SFT, 2000) for a receiver in the open land, not wind-sheltered by the terrain.

At the first Norwegian wind park, Fjeldsgård, put into operation in 1998, noise was not a theme in the planning. Following noise complaints when in operation, a new operator took the case to court in 2007 to "clean up", and 9 of the owners of holyday homes were given a post compensation for excessive noise exposure (limit of endurance, neighbourhood law).

General regime of noise abatement

A new national guideline for noise management in planning came into force in 2005, comprising recommended noise limits outside noise sensitive objects (dwellings and holyday homes) for most kinds of environmental noises: from transport, industry, noisy sports, construction activity and wind turbines. The recommended noise levels were mostly formulated in L_{den}-metric and the levels intentionally set where about 20-25% of a normal population was estimated to be annoyed. Thus, the recommended level for road traffic noise was set to L_{den} = 55 dB and the level for wind turbine noise was set to L_{den} = 45 dB, see table 1.

Table 1: Recommended noise limits for new activity or new noise sensitive buildings.
L_{5AF} is defined as the level exceeded by the 5% most noisy events at FAST response.

Noise source	**Noise level outside noise sensitive rooms and on recreation area (dB)**	**Noise level outside bedroom, Night period 23 – 07 (dB)**	**Maximum noise level outside noise sensitive rooms and on recreation area, daytime og evening, 07 – 23 (dB)**
Road traf	L_{den}=55	L_{5AF}=70	-
Rail traf.	L_{den}=58	L_{5AF}=75	-
Air traf.	L_{den}=52	L_{5AS}=80	-
Industry, harbours, terminals	Non-impulsive: L_{den}=55 Impulsive: L_{den}=50	L_{night} =45, L_{5AF}=60	-
Motorsport	L_{den}=45, L_{5AF}=60	There should be no activity	L_{5AF}=60
Shooting	L_{den}=30 , L_{AImax}=60	There should be no activity	L_{AImax}=60
Wind-turbines	L_{den}=45 *	-	-

* Differentiated according to wind sheltering

The recommended limit was differentiated according to the sheltering situation at the receiver. It was estimated that a receiver with low local wind speed because of sheltering would have less wind-induced masking noise from vegetation and potentially provoke a higher degree of noise annoyance(figure 1). If the receiver was sheltered less than 30% of the year, a higher recommended level, L_{den} = 50 dB, was permitted.

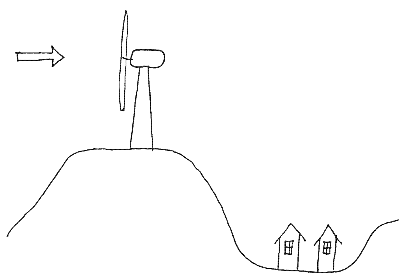

Fig.1: Wind sheltered receiver

The practical regime of wind turbine noise

A practical guide to the guideline and the program for environmental assessment for wind parks make up the practical regime. The guide state an assumption of 80% operation of the turbines and require the noise to be described at wind 8 m/s at 10 m height (L_{ref}). This makes the relation to be L_{den} = L_{ref}+ 5 dB for a constant downwind assessment. The program requires two situations to be modelled: 1) the downwind situation and 2) the situation with prevailing wind. This means a less strict assessment compared to the main criterion, in practice by up to 2-3 dB. The regime permit the general Nordic calculation method for industrial noise to be used. This is a pure downwind method, and the prevailing wind situation may be modelled by ignoring the components in the prevailing upwind sector. The programme requires the contour lines of L_{den} = 40, 45, 50 and 55 dB to be presented.

There is no method to assess the terrain and wind into non-shielded or shielded situations, and it is recently made at a rough estimate. In addition to the recommended levels, all dwellings within L_{den} = 40 dB shall be shown, but the use of this information is not clear.

The typical situation in planned wind parks

The typical on-shore wind parks are planned with 30-100 turbines in mountaineous or coastal areas with small areas only constituting the wind shielded situation (L_{den} = 45 dB). Thus the recommended level L_{den} = 50 dB is the more common in Norwegian wind parks. The typical minimum distance between a noise sensitive object and a wind turbine is 700 -1000 m, Although some holyday homes, because they are found all over the terrain, may be situated within the park at noise levels of L_{den} = 50-65 dB.

The most common remedial action taken is believed to be redemption (pay out, especially the few highly exposed holyday homes within the park) and to rearrange the turbines or remove one or two to satisfy the recommended levels.

3 different, restrictive regimes

The prevailing wind calculation invokes a need for assessment of the calculation method. A simple test of a more comprehensive method (Imagine, P2P-version, 2006) illustrated the problem: significant reduction by upwind refraction of noise from the very high turbines (80-100 m) require a distance of the order of 1 km. The Imagine method is compared to controlled measurements for source height below 20 m and propagation distances below 500 m only. The distance of 1 km is for typical wind turbines well above the distance to the contour of the recommended level, L_{den} = 50 dB. So, at the most common recommended noise level L_{den} = 50 dB the prevailing wind calculations should not differ from a downwind calculation. At lager distances the prevailing wind calculation could be done, but with higher uncertainties compared to downwind calculation, see figure 2.

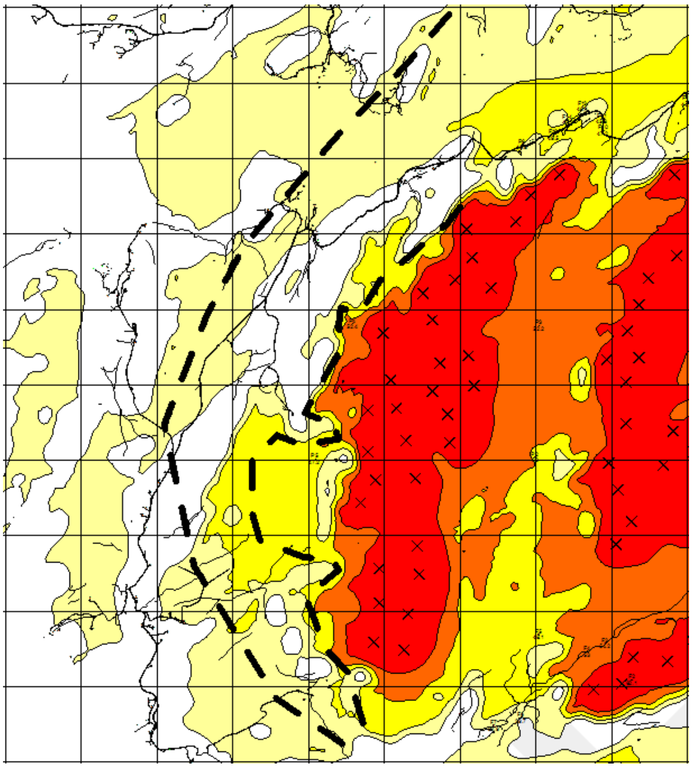

Fig. 2. Excerption of noise map for a large wind park, with contours of L_{den}= 40, 45, 50 and 55 dB. Dashed lines indicate the reduced contours of L_{den}=40 and 45 dB for a prevailing westerly wind. 1 km x 1 km grid.

During the last years investigations of noise annoyance from wind parks in Sweden and The Netherlands have been performed. The assumed relevant results for Norwegian conditions, the response from rural areas in Sweden (low background noise) and the response from non-owners of wind turbines in The Netherlands, both indicate an annoyance score of about 25% for L_{ref}=40 dB (L_{den}=45 dB) and around

30% for L_{ref}=45 dB (L_{den}=50 dB). So, the most common recommended level (L_{den}=50 dB) gives a bit too high annoyance for wind turbine noise compared to recommended levels for the other types of noise. Thus, a practical noise regime following this should rather be more restrictive than less restrictive. 3 possible regimes are outlined here:

- Simple, with safety margins: Omit the prevailing wind assessment and keep the downwind. Do not give more favourable assessment to objects and areas protected by a possible upwind refraction.
- Seek significant differences: assess the uncertainty in the calculations for both wind situations and test for statistical significant differences. Do more favourable assessment in the case of clear differences only.
- Comprehensive, new basis: Assess the annoyance studies more deeply and investigate background noise in a selection of terrain types. Develop a method for terrain shielding assessment, select a better founded recommended noise level and test wind type differences by statistical significance.

We advise the simple method to be used initially, followed by a new basis when experiences come.

References

Eja Pedersen (2007): Human respons to wind turbine noise. Perception, annoyance and moderating factors. Dr. Thesis. Göteborg University.

Frits van den Berg et al (2008): Project WINDFARMperception. Visual and acoustic impact of wind turbine farms on residents. University of Groningen,etc.

SFT (2002): Støy fra vindmøller, (Noise from wind turbines), TA-1738/2000, NVE (Norwegian Water Resources and Energy Directorate) / SFT (Norwegian Pollution Control Authority, Oslo).

Miljøverndepartementet (2005): Retningslinje for behandling av støy i arealplanlegging (noise guideline for area planning). T-1442. (Ministry of Environment). Oslo.

SFT (2005): Veileder til Miljøverdepartementets retningslinje for behandling av støy i arealplanlegging (Practical guide to the noise guideline). TA-2115. (Norwegian Pollution Control Authority, Oslo).

Third International Meeting
on
Wind Turbine Noise
Aalborg Denmark 17 – 19 June 2009

The next version of the IEC 61400-11 measurement method

Søndergaard Bo, DELTA
Erhvervsvej 2a, DK 8653 Them, Denmark
bsg@delta.dk

Abstract

The generally accepted measurement method for noise emission from wind turbines is under revision at the moment. While the basic measurement setup is almost unchanged, significant changes are introduced in the data analysis. The paper will go through the major changes and consequences.

Introduction

The first version of the standard was published in 1998. This means that the work on the standard was initiated about 3 years earlier. The wind turbine size in that period was less than 500 kW and with hub heights up 40 – 50 m. The results of the standard were the apparent sound power level at 8 m/s at 10 m height and the tonality analyzed according to a relatively complex method.

Soon after a revision started with the main aim to improve the standard on the tonality analysis and extending the wind speed range to 6 – 10 m/s at 10 m height. The revision was published in December 2002. To be able to handle the increasing larger wind turbines at wind speeds up to 10 m/s some details in determining the wind speed was changed. As there were some objections to this change an amendment to the standard was prepared and finished in 2005 allowing the use of the nacelle anemometer for wind speeds above 95% of rated power. The amendment was published in 2006 and the version 2.1 of the standard consolidated with the amendment was published in November 2006.

In the mean time the wind turbines continued getting larger and more complex. More advanced control systems and strategies were being developed and it was clear that some of the principles in the standard were not adequate. A full revision of the standard was started up in 2006 with the first meeting in Athens, Greece in May 2006. Since then 7 meetings and a single telephone conference have been held. National comments to the standard are treated at the moment and the standard is expected to be finished during 2010.

At the meeting in Greece in 2006 a list of Work items for the revision was made:

1. Reference height for wind speed.
2. Averaging periods during the measurement should be reviewed
3. A more detailed description of the regression analysis is needed.
4. Customers and authorities demand standardized data in the wind speed range from 3 to 14 m/s. The methods in the standard should be usable at a broader range of wind speeds (In principle all wind speeds)

5. Demands on reduced wind speed ranges for verification purposes should be introduced.
6. Improvements in the procedure for 1/3-octave data are desirable. Using all data.
7. Improvements in the procedure for tonality analysis are desirable.
8. Improvements in the uncertainty analysis should be introduced.
9. Improvements in the demands for the documentation of measurement results should be made.
10. Clarification of the use of power curves in the analysis of measurement results should be included.
11. Small wind turbines.
12. Off-shore wind turbines.
13. Considerations on the use of the nacelle anemometer for background noise measurements.
14. Other aspects of noise are being investigated these years (low frequency noise, infra sound, etc.)
15. Wind farm noise verification.
16. Mandatory secondary windscreen
17. Position of the met mast
18. 95% of rated power clarification
19. Sampling rate for non-acoustic measurements.

The list is quite comprehensive but not all the topics were addressed in the revision.

The major changes between edition 2.1 and edition 3 are:

- Higher order regression analysis is replaced with bin-analysis and the bin size is changed from 1 m/s to 0.5 m/s.
- Analysis is based on 1/3-oktavbands from 20 Hz til 10 kHz
- Averaging time is 10 s previously 60 s
- The reference wind speed is at hub height
- Detailed analysis of uncertainty on the results
- All spectra are used in the tonality analysis
- An annex for small wind turbines

These changes will be commented in this article.

The measurement setup

The setup of the measurements is unchanged and the required amount of data is almost unchanged. This means that the effort in making the measurements is almost unchanged. It is still the weather that determines the measuring time.

Basically the measurements are quite simple. Corresponding values of the noise and the wind speed at hub height are measured for the wind turbine running and stopped and the noise at the centre of bins 0.5 m/s wide is determined after correction for background noise. The noise is measured with the microphone on a ground board at a distance determined as the hub height and half the rotor diameter behind the turbine. Supplementary measurement positions at the same distance but at other directions are optional.

The wind speed is determined by measuring the produced power of the turbine and calculating the wind speed at hub height through a power versus wind speed curve for the wind turbine. For segments of the power curve where the slope is low, typically above 95% and below 5 % of rated power the wind speed measured by the nacelle anemometer is used. During the measurements the nacelle anemometer is calibrated against the wind speed determined through the produced power.

When measuring the background noise the wind speed is measured by a mast mounted anemometer typically at 10 m height. The mast mounted anemometer is also calibrated against the wind speed determined through the produced power. It is not allowed to use the nacelle anemometer during background noise measurements as the in-situ calibration is only applicable for the situation with the turbine running.

Even though this seems simple the discussion on determining the wind speed has been one of the major discussions in the standard from the edition 1 and forward.

Main changes (Regression versus bin-analysis)

In edition 2.1 the noise at a given wind speed was determined through a 3rd or 4th order regression through the measurement data. Even though this is giving good results for most situations it has been necessary to increase the regression order from 2 in edition 2.0 to 4 in edition 2.1. Off course it is possible to increase the regression order further but the method has the unphysical implication that data at low wind speeds influence the results at high wind speeds and vice versa plus there is a tendency to larger deviations at the high and low end of the data set. Using regression analysis also gives the opportunity to extrapolate the results which is very questionable.

It was decided to change to bin-analysis which is simpler and do not have the flaws described above. To be able to get the finer details in the development of the noise with the wind speed the bin-size is set to 0.5 m/s. For the same reason the averaging time is changed from 60 seconds to 10 seconds.

Previously the analysis was based on the total noise level L_{Aeq} and the information on the spectrum of the noise was based on at least three each measured over a period of 1 minute at each integer wind speed. This also applies to the background noise.

In edition 3 the analysis is based entirely on the 1/3-octave band spectra. This means that all measured spectra are included in the analysis. For each bin the spectra are averaged and recalculated to the bin-centre through linear interpolation in each 1/3-octave band.

The interpolation is made between the nearest bin-averages for both the total noise and the background noise before correction for background noise. This approach gives the opportunity to calculate standard deviations on the noise spectra and the wind speed and covariances between the noise in the individual 1/3-octave bands and the wind speed making it possible to calculate the uncertainty on the results in more details. Some of the formulas are shown in Figure 1.

This may look quite cumbersome and unfamiliar to some but is standard statistics and easier to implement than it looks and can be done in a standard spreadsheet.

61400-11 © IEC:2009(E) – 23 – 88/324/CD

$$\begin{pmatrix} V \\ L \end{pmatrix}(t) = (1-t)\cdot\begin{pmatrix} \overline{V}_k \\ \overline{L}_{i,k} \end{pmatrix} + t\cdot\begin{pmatrix} \overline{V}_{k+1} \\ \overline{L}_{i,k+1} \end{pmatrix} \quad (20)$$

$$\overline{V}_k \le V < \overline{V}_{k+1}$$

Using this, the t value at a given wind speed v is calculated as

$$t = \frac{\left(V - \overline{V}_k\right)}{\left(\overline{V}_{k+1} - \overline{V}_k\right)} \quad (21)$$

and the estimated sound pressure level at this wind speed is calculated as

$$L_V(t) = (1-t)\cdot\overline{L}_k + t\cdot\overline{L}_{k+1} \quad (22)$$

The standard deviation on the calculated sound pressure levels at wind speed v are calculated using

$$\sigma_{L_V}(t) = \sqrt{\sigma_L^2(t) - \frac{\sigma_{LV}^2(t)}{\sigma_V^2(t)}} \quad (23)$$

where

$$\sigma_L^2(t) = (1-t)^2\cdot\sigma_{L,k}^2 + t^2\cdot\sigma_{L,k+1}^2$$

$$\sigma_{LV}(t) = (1-t)^2\cdot\frac{\sigma_{LV,k}}{N_k} + t^2\cdot\frac{\sigma_{LV,k+1}}{N_{k+1}}$$

$$\sigma_V^2(t) = (1-t)^2\cdot\sigma_{V,k}^2 + t^2\cdot\sigma_{V,k+1}^2$$

N_k is the number of measurements in wind speed bin k

Figure 1 Calculation of the noise level and the uncertainty of the noise level at a bin centre wind speed through linear interpolation.

The steps in the analysis is shown as a flow sheet in Figure 2 and examples on part of the analysis results are given in Figure 3 and Figure 4.

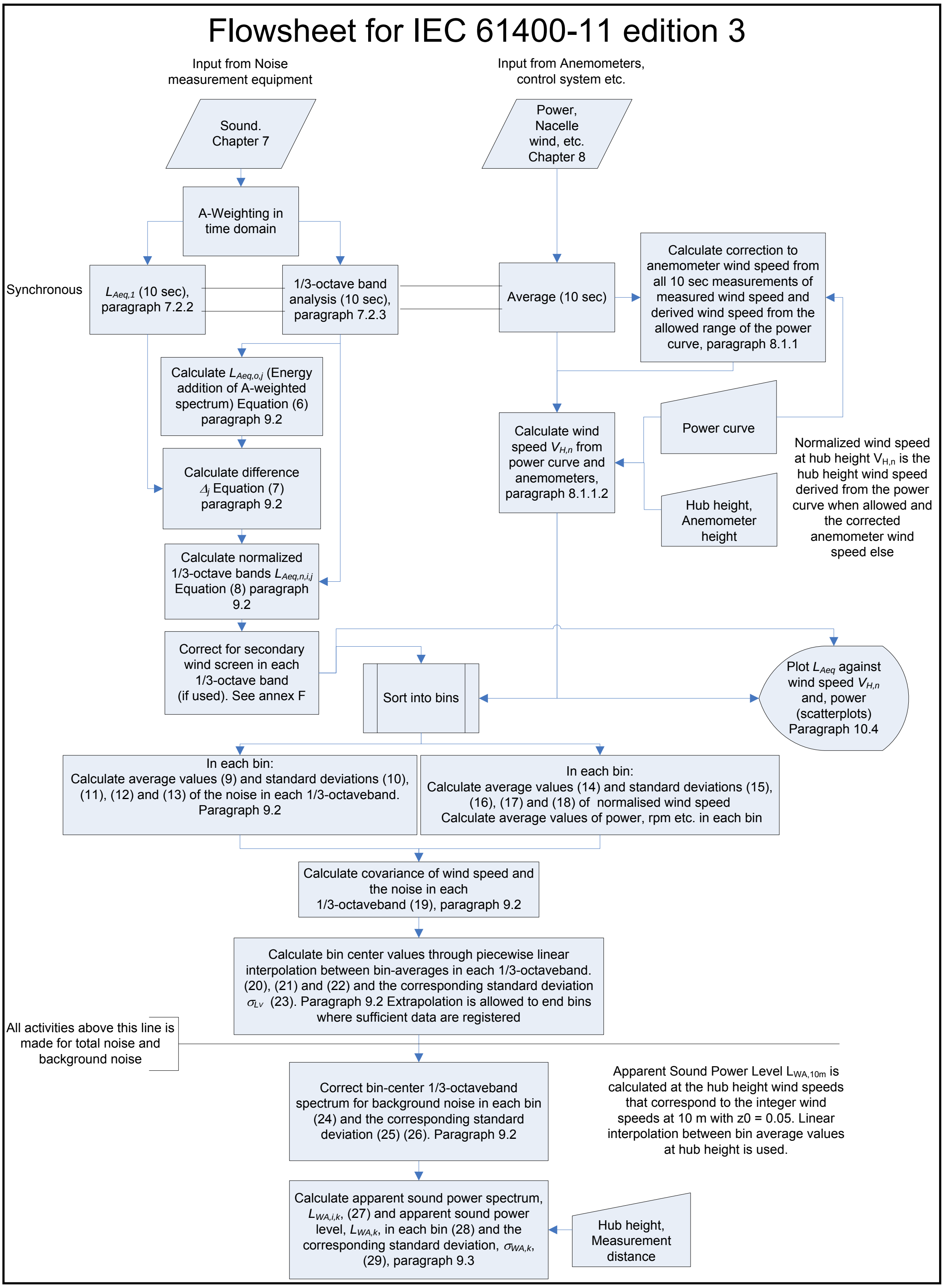

Figure 2 Flow sheet for the analysis in edition 3

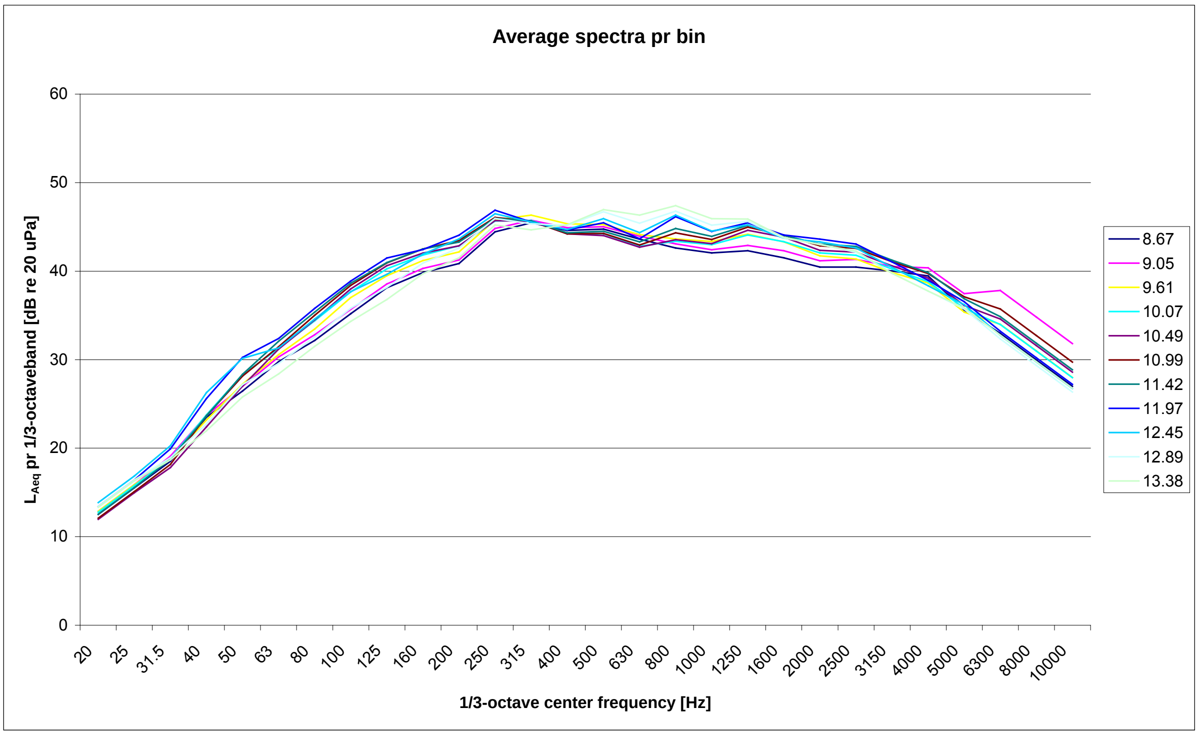

Figure 3 Average spectra for each wind speed bin. The corresponding average wind speed is given in the legend box.

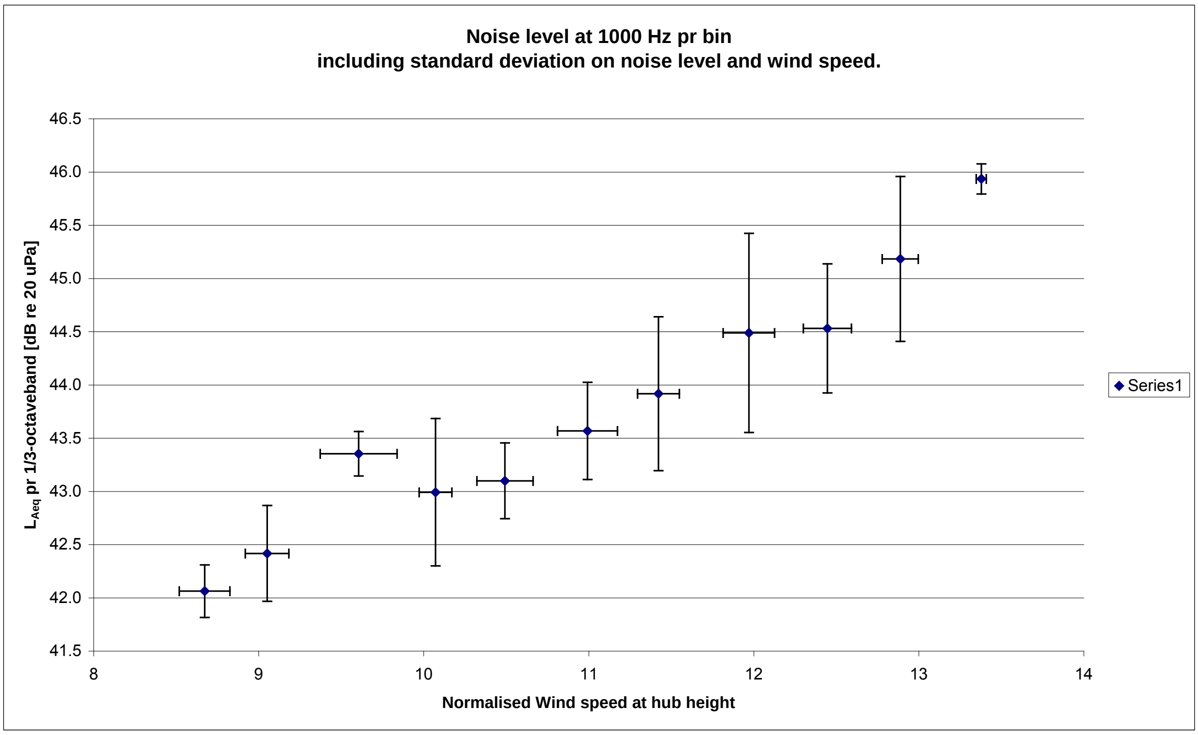

Figure 4 Results from a single 1/3-octave band

Main changes (Reference wind speed)

The apparent sound power level is determined at integer wind speeds from 6 to 10 m/s in edition 2 with a reference to 10 m height. Most of the wind speeds are measured at hub height except when measuring background noise and the recalculation to 10 m height are made for a standardized terrain with a roughness length of 0.05 using a logarithmic wind speed profile given in Equation 1.

$$V_s = V_z \cdot \frac{\ln\left(\frac{z_{ref}}{z_{0ref}}\right)}{\ln\left(\frac{z}{z_0}\right)}$$

Equation 1

Where,

z_{0ref} = reference roughness length of 0.05 m

V_z = Wind speed at height z above ground level

z = The height for which we know the wind velocity (hub height)

z_0 = Roughness length in the current wind direction (z0=z0ref=0.05 m)

z_{ref} = The height for which we want to know the wind velocity (10 m)

The use of a reference height for the wind speed of 10 m has lead to a lot of confusion when using the results for comparison with other wind turbines of for prediction of the noise in the surroundings. As the recalculation to 10 m height is independent of the actual conditions on the site it is always possible to calculate back to hub height but information on hub height does not always follow the noise data. This means that noise measurements made on the same wind turbine construction but mounted at different heights can give different results. The same problem arises when the data are used for noise assessment of a site. If the noise data are measured on wind turbine with another hub height the results of the assessment is less reliable. The problem here is more a lack of understanding among the users of the noise data.

To meet this type of confusion the reference height for wind speed is changed to hub height, facilitating the comparison between wind turbines and the use of the data for noise predictions. The old type of data with a reference to 10 m height is still reported but may be taken out in future revisions.

Main changes (Tonality)

The tonality analysis in edition 2 is based on 12 ten second spectra close to the wind speed in question. A total of 60 spectra for the required wind speed range from 6 – 10 m/s. This means that the analysis of the tonality is only representing a small amount of the data from the measurements and has a random character. The 5 sets of 12 spectra are analyzed according to the method in the standard. The tonality at a given wind speed is then calculated as the average of the tonality for the 12 spectra. If tones are identified only in some of the spectra the tonality is calculated for these spectra. For the other spectra without an identified tone the tonality is given a fictitious low value and the tonality is given as the average tonality for the 12 spectra including the fictitious value. This is for practical reasons rather than for giving good information on the tonality.

In edition 3 it has been decided that synchronously with the 1/3-octave band spectra FFT spectra are measured as well. This is done by most measurement companies already. The FFT spectra are sorted into bins and analysed according to the method described in the standard.

Spectra without identified tones are discarded from the tonality calculation and the tonality for a given frequency at a given wind speed is calculated only from spectra with an identified tone. This means that periods with high tonality are included in the analysis where it was a random choice before

This takes the random character out of the tonality analysis and gives a more reproducible result, even though the measurement period does not include all situations.

Other changes

There is no doubt that the IEC 61400-11 has become more complicated than when the wind turbines were smaller in 1998. For that reason an annex for small wind turbines have been included. The method follows the lines of the main body of the standard but uses the mast mounted anemometer at 10 m height for the wind speed measurements and the analysis is made only for the A-weighted total noise level L_{Aeq}.

The position of the mast mounted anemometer for background noise measurements is changed so the distance between the anemometer and the noise measurements are reduced.

Conclusions

The national comments to the Committee Draft of the standard indicate that the changes are large and that it takes some reading to fully appreciate the changes. However it is worth noting that measurements made according to the previous versions of the standard can be reanalyzed and reported according to edition 3. The measurement requirements are almost unchanged and it is not more difficult to make measurements according to edition 3.

The analysis is heavier but manageable in a standard spreadsheet. It is more general and hopefully it is able to meet the demands when new types of wind turbines are developed. The benefit is that the results are more reliable and the uncertainties on the results are calculated more than estimated.

The has been a large representation in the MT11 group taking care of this revision and many useful discussions have been taken. I hope this means that the new version of the standard will be accepted by the measurement institutes and the users of the results of the measurements.

References

[1] IEC 61400-11:1998 Wind turbine generator systems – Part 11: Acoustic noise measurement techniques

[2] IEC 61400-11:2002 edition 2 Wind turbine generator systems – Part 11: Acoustic noise measurement techniques

[3] IEC 61400-11:2002 ammendment 1:2006 Wind turbine generator systems – Part 11: Acoustic noise measurement techniques

[4] IEC 61400-11:2002 edition 2.1 Wind turbine generator systems – Part 11: Acoustic noise measurement techniques.

Third International Meeting
on
Wind Turbine Noise
Aalborg Denmark 17 – 19 June 2009

Prediction of noise from wind farms with Nord2000. Part 1

Søndergaard Bo, Plovsing Birger, DELTA
Venlighedsvej 4, DK 2970 Hørsholm, Denmark
bsg@delta.dk, bp@delta.dk

Abstract

The validity of noise prediction for wind farms is becoming more important as the wind farms are becoming larger and the wind turbines are becoming more flexible. To be able to exploit the flexibility of wind turbines to the full prediction models that can handle the meteorological influence and the influence of complex terrain on noise propagation are necessary. Nord2000 is such a model and DELTA is testing Nord2000 for use in noise propagation for wind turbines in a development project.

The project is publicly funded by Energinet.dk under contract no. 2007-1-7389 and cofunded by Dong Energy, Suzlon Energy A/S, Gamesa, StatoilHydro, E.ON Vind Sverige AB, Statkraft Development and Vattenfall A/S.

The projectpartners are DELTA (project manager), EMD International and DONG Energy.

A set of field tests have been made with loudspeakers and wind turbines as the source of noise for flat and complex terrain. The measurement campaigns and results will be presented. Detailed results will be presented in part 2.

Introduction

At Wind Turbine Noise 2005 in Berlin an introduction to the benefits of using Nord2000 for noise propagation for wind turbines were given [1]. More about the model can be found in [2], [3] and [4].However for the model to be accepted in general a validation of the method is necessary. The model is already validated for sources and receivers close to the ground and short distances [5]. It was decided to extend this validation to sources with heights relevant for wind turbines through a limited set of tests, mainly based on loudspeaker measurements where the uncertainty is relatively small and to a minor degree on wind turbine noise measurements where the uncertainty is expected to be larger.

The principle used for the validation was to determine the excess propagation effect for the noise propagation relative to the corresponding free field noise level. The advantage of this approach is that it is easy to compare results at varying propagation distances.

The free field noise only includes the spherical spreading of the noise while the excess propagation effect comprises the ground and screening effect and the air absorption. The effect of vegetation is not treated in this investigation as this type of effect is treated similarly in different prediction models.

Measurement setup for loudspeaker tests

As the loud speaker tests were considered most important and reliable a setup was designed for these tests. The source was a was a Cerwin – Vega G212 with 2 12” units in parallel and a Yamaha Professional Series Natural Sound Power Amplifier model P 2200. The noise generator was based on National Instruments Labview software and executed on a Lenovo T60 laptop with the built-in soundcard and programmed to give a cycle of signals as shown in Table 1.

Signal no.	Signal type	Frequency range	Time [s]	Measured Sound Power Level [dB re 1pW]
1	Broadband (pseudorandom)	1/1-octaves from 63 Hz to 2kHz	50	130
2	Pause	-	10	-
3	Broadband (pseudorandom)	63 Hz 1/1-octave	50	123
4	Pause	-	10	-
5	Broadband (pseudorandom)	125 Hz 1/1-octave	50	126
6	Pause	-	10	-
7	Broadband (pseudorandom)	250 Hz 1/1-octave	50	130
8	Pause	-	10	-
9	Broadband (pseudorandom)	500 Hz 1/1-octave	50	130
10	Pause	-	10	-
11	Broadband (pseudorandom)	1kHz 1/1-octave	50	130
12	Pause	-	10	-
13	Broadband (pseudorandom)	2 kHz 1/1-octave	50	130
14	Pause	-	20	-

Table 1 Signal cycle for loudspeaker measurements

The noise level of the source was measured at a distance of approximately 1 m in front of the loudspeaker and registered with the measurement software NoiseLAB developed by DELTA. See Figure 1 and Figure 2.

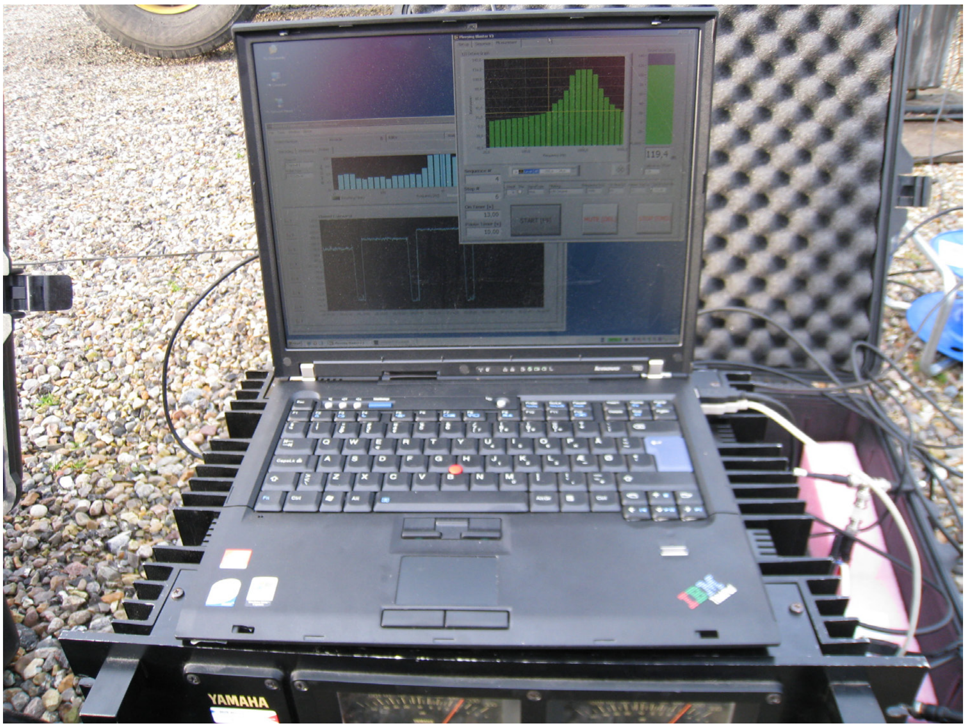

Figure 1 The noise generator and the noiseLAB recorder was running on the same laptop. The noise generator is top left on the computer display and the recorder bottom left. The "stripchart" on the recorder shows the sequence with noise on and noise off. The amplifier is seen under the laptop.

Figure 2 Mounting of the loudspeaker and the microphone in front of the loudspeaker for the Høvsøre measurements. The elevation of the loudspeaker was 50 m and 30 m during measurements.

The tests were made in flat terrain at the DTU-RISØ test site for large wind turbines at Høvsøre and in complex terrain at the Hitra wind farm owned by Statkraft in

Norway. At Høvsøre all meteorological parameters were monitored by RISØ at different heights giving good information on the meteorology during measurements. At Hitra only a standard meteorological mast was available giving the wind speed at 3 heights and the temperature at one height as an average value every 10 minutes. The wind speed was also registered by the nacelle anemometer and averaged to 10 second values.

The noise was measured at 2 m and 5 m height above ground at 3 distances. In flat terrain at 500 m, 1000 m and 1500 m in upwind and downwind. In complex terrain at 400 m, 800 m and 1000 m downwind and at 400 m and 630 m upwind. In flat terrain the loudspeaker was mounted on a lift and the source height was 50 m and 30 m. At Hitra the loudspeaker was mounted on top of the nacelle of a wind turbine at 70 m height see Figure 3.

Figure 3 Loudspeaker position at Hitra. The fact that the nacelle is tubular and extending further than the loudspeaker may have caused reflections that influences the results in the nearest measurement position.

The noise was measured with either G.R.A.S 40AE microphones and 26CA preamplifiers or B&K 4189 microphones, 2639 preamplifiers and a 2658 preamplifier. The noise signals were recorded on hard disc recorders type 744T and 788T from Sound Devices. All microphones were fitted with a secondary wind screen as seen in Figure 4. The insertion loss of the wind screens are measured by DELTA in an anechoic chamber at Aalborg University.

Figure 4 Measurement position at 800 m downwind at Hitra.

Measurement setup for wind turbine test

The measurements with the wind turbine as the source were only made at Hitra in complex terrain. Basically the setup was the same as for the loudspeaker tests. The sound power level of the wind turbine was lower and only the shortest distances could give usable results. The source level was measured according to IEC 61400-11:2002 edition 2.1 [6] at a distance of 111 m. This alone increases the uncertainty of the results compared to the loudspeaker measurements.

Figure 5 Høvsøre testsite. The Loudspeaker position was changed between downwind and upwind measurements. The terrain is clearly flat and typically agricultural. The indicators marked S are source positions and M are receivers. "medvind" means downwind and "modvind" is upwind

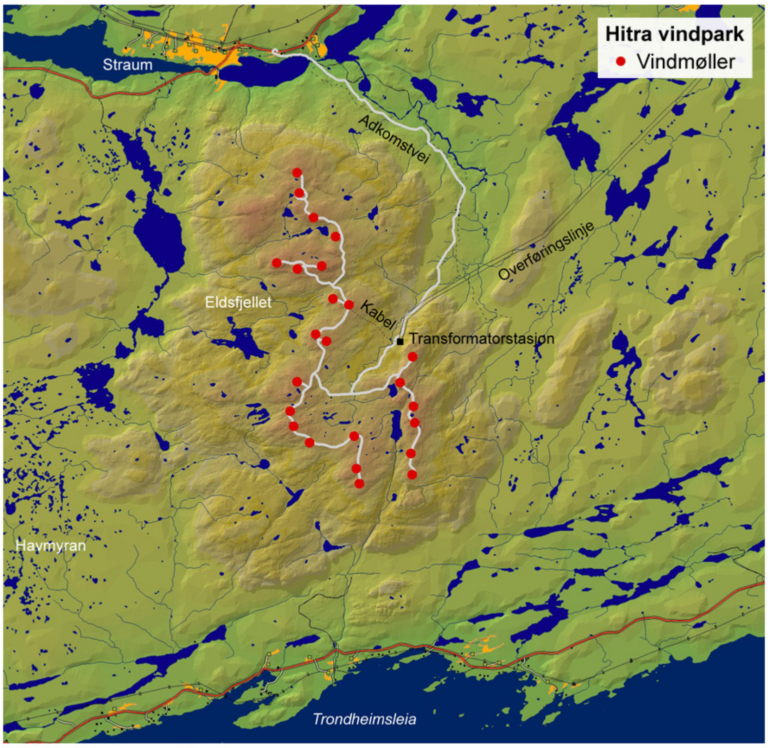

Figure 6 Hitra wind farm. The measurements were made around the wind turbine at the top of the picture. The wind was north easterly

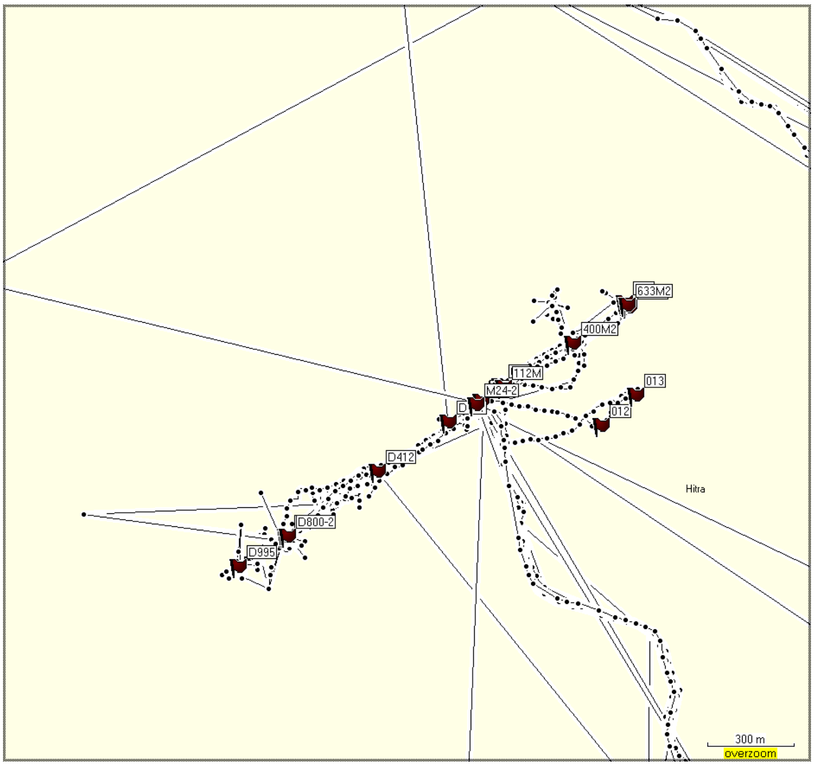

Figure 7 GPS tracking around the test wind turbine at Hitra. The wind turbine position and the measurement positions are indicated on the figure.

Analysis

In the laboratory the recordings were analyzed using NoiseLAB and NoiseLAB Batch to give synchronous values of 1/3-octave band spectra for all measurement positions as 10 second averages. For the loudspeaker measurements this was a relatively easy task due to the noise on/noise off character of the noise. For the wind turbine measurements we had to rely on synchronizing the measurement equipment before each measurements series. Values for the meteorological parameters were analysed an averaged for the same periods based on synchronizing the measurement systems to the meteorological data recording systems. Based on this it was possible to determine the excess propagation effect for the measurements and calculate the corresponding values of the excess propagation effect with Nord2000. More details on the analysis is given in [7]

Results

An overview of the measurements made in the validation is shown in Table 2.

Measurement situation		Downwind Flat				Upwind Flat				Crosswind (Optional)	Downwind Complex				Upwind Complex			
Loudspeaker	Source	30		50		30		50			70				70			
	Wind	Low		Low		Low		Low		-	Low		High		Low		High	
	Receiver	2	5	2	5	2	5	2	5		2	5	2	5	2	5	2	5
	Distance	500 1000 1500	500 1000 1500	500 1000 1500	500 1000 1500	500 1000 1500	500 1000 1500	500 1000 1500	500 1000 1500	-	400 800 1000	400 800 1000	400 800	-	-	-	400 633	400 633
Wind Turbine	Source										70				System failure			
	Wind										Low		High					
	Receiver										2	5	2	5				
	Distance									-	400 800 1000	400 800 1000	400 833	-				
Windfarm	-	Smøla				Smøla					Hitra				Hitra			

Table 2 Overview of the measurement campaigns.

Results given as the Excess Propagation Effect are given in Figure 8 to Figure 11 for Høvsøre

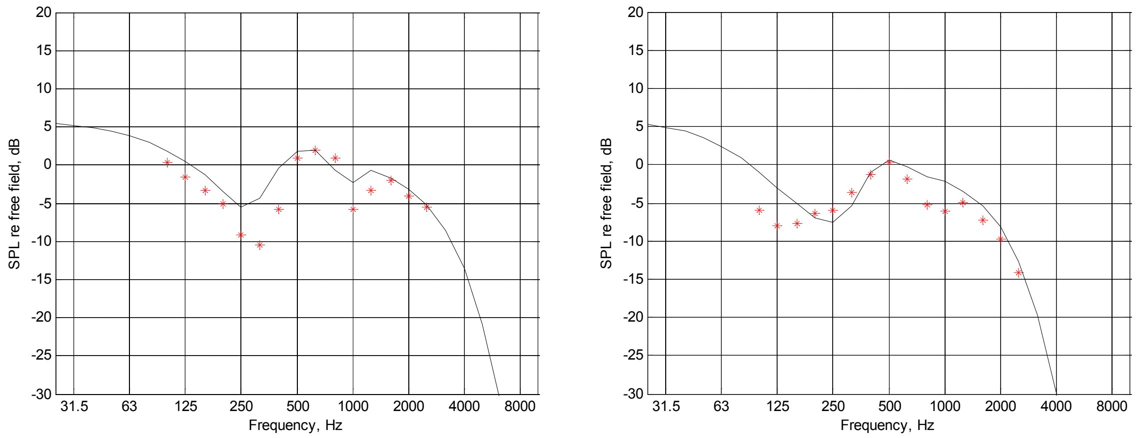

Figure 8 downwind, source 30 m, receiver 2 m, distance 500 m and 1000 m

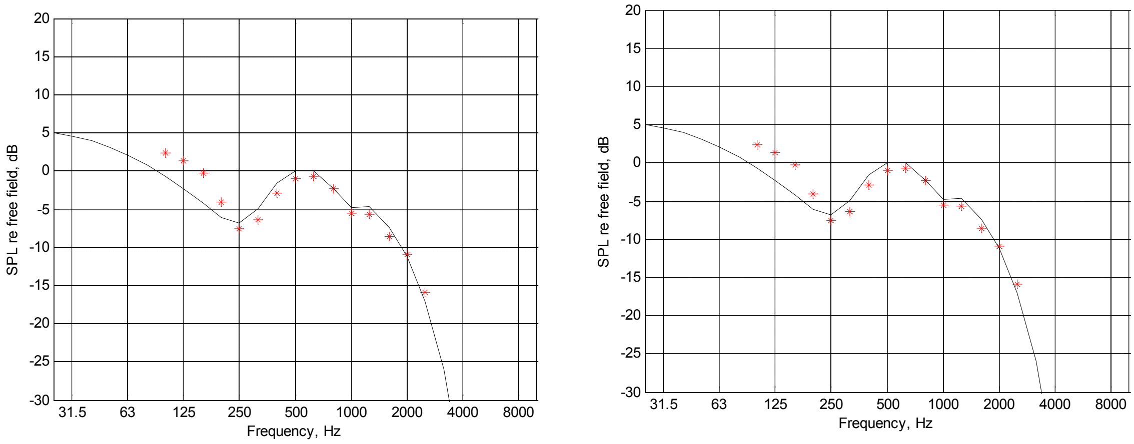

Figure 9 downwind, source 30 m and 50 m, receiver 2m, distance 1500 m

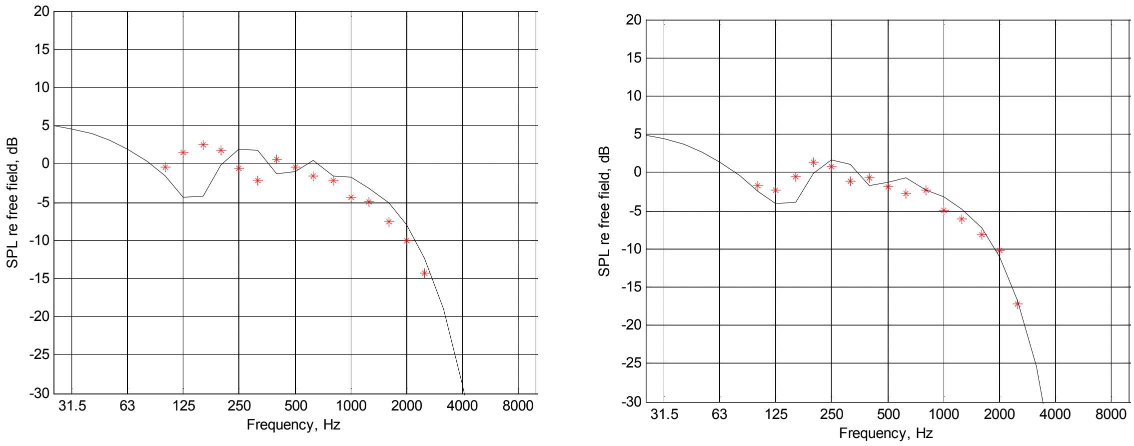

Figure 10 downwind, source 50 m, receiver 5 m, distance 1000 m and 1500 m

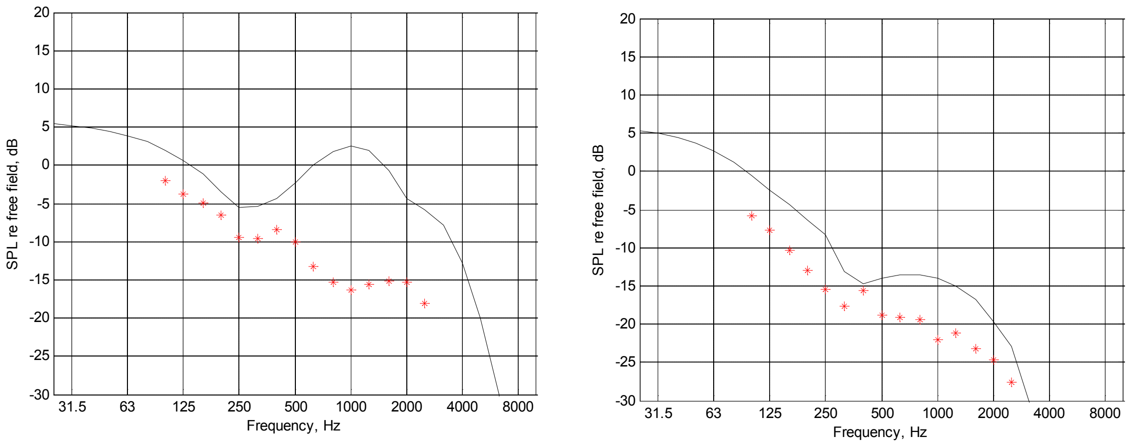

Figure 11 upwind, source 30 m, receiver 2 m, distance 500 m and 1000 m. Notice that at 500 m the shadow zone is present in the measurements but not in the prediction. At 1000 m the shadow zone is present in both measurements and predictions.

Results from Hitra are shown in Figure 12

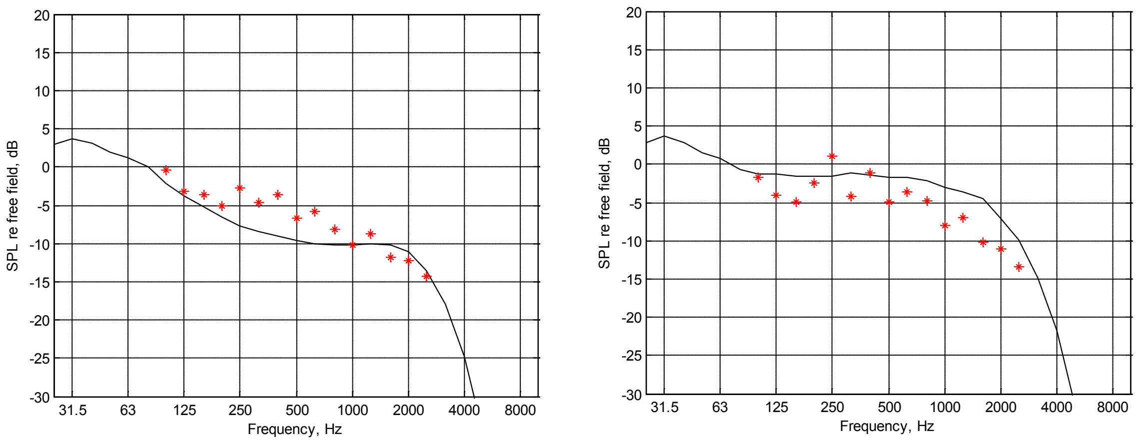

Figure 12 downwind source 70 m, receiver 2 m and 5 m, distance 1000m

Basically the results show very good agreement between measurements and predictions. Difficulties are seen when the shadow zone appears in the upwind measurements e.g Figure 11. The agreement is acceptable taking into account the well-known difficulties of making accurate prediction for an acoustical shadow zone in upwind.

The results from Hitra in complex terrain are similar to the results from Høvsøre and only a special result is shown. In Figure 12 results from a downwind situation is shown. However the result looks more like an upwind situation at the beginning of the shadow zone. The reason for this is that the wind speed was decreasing with the height probably due to speed-up because the wind farm was placed on plateau. The results from Nord2000 are in good agreement with the measurements for this special situation too.

Conclusions

Conclusions on the validation of Nord2000 are given in [7]. However it can be concluded that the planned measurements were actually fulfilling it purposes. It was possible to do reliable measurements with the loudspeaker for distances up to 1500 m in flat terrain and up to 1000 m in complex terrain. The comparison of measurements and predictions with Nord2000 shows good agreement.

It is important to have good information on the loudspeaker performance and directional characteristic as this is essential for the reliability of the measurements.

Even though the microphones were protected with extra wind shields some wind induced background noise did occur due to the tripods, cables etc. For the wind turbines it was not possible to make reliable measurements for the same distances which is good as noise from wind turbines would have been a larger problem than it is today.

References

[1] J. Kragh. B. Plovsing B. Søndergaard. *Prediction of Wind Turbine Noise Propagation over Complex Terrain in All Kinds of Weather with Nord2000* Wind Turbine Noise 2005, Berlin

[2] B. Plovsing and J. Kragh, *Nord2000. Comprehensive Outdoor Sound Propapagtion Model. Part 1: Propagation in an Atmosphere without Significant Refraction,* DELTA Acoustics & Vibration, Report AV 1849/00, 2001

[3] B. Plovsing and J. Kragh, *Nord2000. Comprehensive Outdoor Sound Propapagtion Model. Part 2: Propagation in an Atmosphere with Refraction,* DELTA Acoustics & Vibration, Report AV 1851/00, 2001

[4] J. Kragh and B. Plovsing, *Nordic Environmental Noise Prediction Methods, N2000 Summary Report,* DELTA Acoustics & Vibration, Report AV 1719/01, 2001

[5] B. Plovsing, *Nord2000. Validation of the Propagation Model* DELTA Acoustics and Electronics. Report AV1117/06, 2006

[6] IEC 61400-11:2002 edition 2.1 Wind turbine generator systems – Part 11:Acoustic noise measurement techniques

[7] B. Plovsing B. Søndergaard. *Prediction of noise from wind farms with Nord2000. Part 2.* Wind Turbine Noise 2009, Aalborg

Third International Meeting
on
Wind Turbine Noise
Aalborg Denmark 17 – 19 June 2009

Implementation of the Nord2000 model for wind turbines: New possibilities for calculating noise impact.

Thomas Sørensen[1], Per Nielsen[1], Jens Villadsen[1] and Birger Plovsing[2]
EMD International A/S, Niels Jernesvej 10, 9220 Aalborg Ø[1] and Delta, Venlighedsvej 4, 2970 Hørsholm[2].
ts@emd.dk, pn@emd.dk, jv@emd.dk and bp@delta.dk

Abstract

Implementation of the Nord2000 noise propagation model for wind turbines has created a host of possibilities for examining situations which previously were too complex for calculation. Along with the traditional noise levels new noise descriptors like Lden can be predicted taking into account the influence of meteorology on the noise propagation and the statistical distribution of the meteorological parameters over a period of time. In the first WindPRO implementation, the Nord2000 model can be used for specific terrain and meteorological situations, but more interestingly a method is found to distribute the particular meteorological situations and terrain conditions over the year and day in order to calculate the statistical distribution of the noise impact. This opens up the possibility to calculate average noise levels, uncertainty of the noise level and different probability levels for almost any combination of wind speed and time frame. The model can relate to wind speed at hub height that may vary across the site so realistic calculation can be made in non-uniform complex locations like hills, forests etc.

This presentation is part of the PSO (Public Service Obligation) project: Noise and Energy Optimization of Wind Farms.

Introduction

The PSO (Public Service Obligation) project: Noise and Energy Optimization of Wind Farms has as purpose to prepare the Nord2000 noise model for use with wind turbines. Already the model is used for traffic noise, but the wind turbine case poses some particular problems that need attention before the model can be successfully used for wind turbines.

One aspect is the implementation of the model in a way that can be used to evaluate the noise impact in relation to national noise code regulations. EMD and Delta has made such an implementation for the software package WindPRO. This work has been successful in so far as the model can calculate the noise propagation for very specific situations concerning terrain and weather. However national noise codes usually give a fixed noise limit at receptor with little concern as to whether the noise limit is for worst case, average case or very specific climatic conditions. Therefore a model is needed to aggregate the noise impact over a period of time in a way that can give such answers just as well as national noise codes needs to attend this issue.

Such an aggregation model has been suggested by Eurasto, 2006 for traffic noise and Taraldsen, 2007 has attempted an implementation for wind turbines that would comply with the Norwegian noise codes. This study has like Taraldsen used the meteorological definitions of Eurasto, but taken the model further in a generalisation that should be globally applicable.

The specific case

The specific noise calculation case is the calculation for a setup of wind turbines for a specific terrain and weather situation.

The terrain itself consists of three significant elements:

- Elevation model as described by height contours
- Roughness model to help define the wind profile changes from emitter to receptor
- Terrain hardness, which is a function of soil compactness, unevenness and to some extent vegetation.

While the two first are fairly constant over time, though individual for each emitter-receptor pairing, the terrain hardness may vary over time.

The weather influence is more complicated, but the special strength of Nord2000 is that it can take into account many of the weather parameters. These include:

- Temperature and temperature profile
- Wind speed and wind speed profile
- Humidity

- Turbulence

… and a few other secondary parameters

These elements vary over time in ways that may be linked but often seem to combine in odd ways.

The wind speed parameter contains the added complexity of linking to the noise emission level of the wind turbines. Traditionally the noise emission level of a wind turbine is given for a particular wind speed at 10 m height. This would make the relation to wind speed simple if all turbines were standing in uniform terrain with wide spacing between them. Usually that is not the case. Some turbines may have a higher wind speed than others and therefore a different noise emission level. Also the terrain may be of such a type that a standard profile between 10 m height and hub height may not be valid.

For the specific case, it is therefore possible to set a predefined location as reference point and calculate individual wind speeds for the turbines and thus noise levels. This can be done both for 10 m height and for hub height. In this way noise emission values linked to hub height wind speed can be used, effectively bypassing the problem of non-standard wind profile shear.

Still, all this relates to only the specific case. It is described thereafter how the specific case can be generalized to calculate a statistical distribution of the noise impact depending on meteorological situations and terrain conditions over the year and day.

Theory of meteorological classes

Eurasto, 2006 describes a method of simplifying the task of finding the effective speed of sound which is the core parameter in the calculation of noise damping. This is done by defining meteorological classes into only 25 cases described by the parameters A and B.

$$C = Aln\left(1 + \frac{z}{z_0}\right) + Bz + C(0)$$

Where

z height above ground

z_0 roughness length

A logarithmic coefficient

B	linear coefficient

C(0)	Speed of sound at height z=0

Eurasto gives 5 different wind speed classes and 5 different stability classes (Table 1 and Table 2). These in turn provides parameters for finding the A and B parameters. The complete set of formulae can be found in Eurasto, 2006.

Additionally, the direction difference between the wind direction and the direction from emitter to receptor is considered to define the A and B parameters, meaning that the A and B values may be different between different pairings of emitter and receptor for the same climatic situation.

Table 1. Wind speed classes. (Eurasto, 2006)

Wind speed at 10 m above ground	Wind speed class
0 to 1 m/s	W1
1 to 3 m/s	W2
3 to 6 m/s	W3
6 to 10 m/s	W4
> 10 m/s	W5

Table 2. Stability classes. (Eurasto, 2006)

Time of day	Cloud cover	Stability class
day	0/8 to 2/8	S1
day	3/8 to 5/8	S2
day	6/8 to 8/8	S3
night	5/8 to 8/8	S4
night	0/8 to 4/8	S5

In any case, the A and B parameters are each grouped into 5 different bins giving a total of 25 meteorological cases. This means that for each emitter-receptor pairing all meteorological situations can be calculated in just 25 calculation runs. Combined with the terrain description for the emitter-receptor pairing and average temperature and humidity for each AB class this gives the damping of the propagation model for 25 cases.

Probability of meteorological classes

The question of how often each of these classes occurs was addressed by Taraldsen, 2007 for wind turbines. Their solution inspired our subtly different approach.

While cloud cover is usually not a parameter measured on the local metering mast on site, a regional meteorological measurement series will often (if not usually) contain information of time, wind speed and cloud cover for a time series of reasonable frequency. These are the input data for the meteorological classes and the frequency and pattern of these will typically not differ much from these regional stations to the site. Such a time series can therefore be loaded and the data sorted as frequency of AB combinations for each 1 m/s wind speed bin. An example of this is shown in the table below. If the mast is not a typical 10 m high mast the wind speeds are scaled to 10 m height using a standard profile.

Table 3. Example of observed distribution of climate classes as a function of wind speed (at 10m height).

Climate class	Average temperature	Average humidity	Sum	0	1 m/s	2 m/s	3 m/s	4 m/s	5 m/s	6 m/s	…
A1B1	5	30%	686	0	36	71	115	113	101	81	
A1B2	6	35%	0	0	0	0	0	0	0	0	
A1B3	6	32%	58	0	2	5	5	6	8	10	
A1B4	7	40%	0	0	0	0	0	0	0	0	
A1B5	5	41%	0	0	0	0	0	0	0	0	
A2B1	3	39%	273	0	12	21	37	28	33	29	
A2B2	6	38%	0	0	0	0	0	0	0	0	
A2B3	6	40%	238	0	6	24	16	17	29	26	
…											

It turns out that quite a few AB combinations contain no events at all. Not having to calculate these events greatly reduces the calculation effort.

The distribution of the AB classes in each wind speed bin gives the probability of occurrence of that stability class.

A year worth of incidences.

The average, extreme or other statistical parameters concerning the noise impact at a receptor may perhaps best be described by the distribution of specific incidences over a period of time. If a time series measured on the site for a period of one year is used, the matter is relatively simple for a single emitter-receptor pairing.

For each record in the local time series of data, the wind speed is read. The meteorological class table presented above gives the probability of the meteorological classes for each wind speed bin, so looking up in the relevant wind speed column and picking randomly one of the incidences will correctly distribute the meteorological classes throughout the year. The wind direction has already been taken into account in the definition of meteorological classes and is for the sake of simplification not taken further into account.

The wind speed record also gives the noise emission level for the turbine based on the noise curve for the turbine type, so that we have emission noise – damping = resulting noise level at the receptor.

Going through an entire year the incidences will describe the distribution of the noise suffered at the receptor. This can be sorted into hourly and monthly bins and so statistics can be made on a quite detailed basis.

Table 4. For an emitter - receptor pairing the below table is created. For each time step the resulting noise impact (Res) is stored in the appropriate bin.

				Month		
Hour	Jan	Feb	Mar	Apr	May	...
0	Res 1	Res 1	Res 1	Res 1	Res 1	
	Res 2	Res 2	Res 2	Res 2	Res 2	
	Res 3	Res 3	Res 3	Res 3		
	Res 4			Res 4		
1	Res 1	Res 1	Res 1	Res 1	Res 1	
	Res 2	Res 2	Res 2	Res 2	Res 2	
	Res 3	Res 3	Res 3	Res 3	Res 3	
		Res 4	Res 4	Res 4		
2						
...						

The multi turbine case.

The probabilistic model described above works well for the single turbine case, but falls apart for the multi turbine case. This is because the different turbines may pick different AB combinations for the same time step. A large wind farm will therefore on average have the average climatic condition at all the time and distribution or extreme events will not be recorded.

Linking the emitter-receptor pairs to the same AB combination is not so easy either, because the direction element means that the same meteorologic situation result in different AB combinations for different emitter-receptor pairings.

A compromise solution is therefore to group all turbines together for each receptor. The first turbine decides the wind speed bin to look into and an AB combination will be drawn for that emitter – receptor pairing. This AB class is then used as basis for all the other pairings with that receptor but modified for the difference in direction. This means that for some turbines the AB class may slide to the neighboring classes.

Likewise will the wind speed at the local mast be converted to the wind speed at each receptor, either at 10 m height or hub height in order to find the corresponding emission noise level for each turbine at that record.

So, again each turbine emission noise minus damping gets added together to give total noise impact at that specific receptor for that moment in time. The process is illustrated in below table which is completed for each receptor.

Table 5. The result form to be completed for each receptor before sorting the results (Total noise) in the database in table 4.

Receptor:										
		Turbine 1					Turbine 2			
Date	Time	wind speed	Source noise	angle	Met. Class	Damping	wind speed	Source noise	...	Total noise

New result possibilities

The methodology here presented makes it possible to comply with different national codes to an unprecedented degree, but also offers a number of new possibilities that can be exploited when designing new national codes.

The incidences of noise impact can be subjected to statistical analysis to find the average noise level or the median noise level. These figures will be comparable to many of the existing codes.

For a more conservative noise impact study, the worst case noise impact can be found simply by finding the incident for each receptor with the highest noise level.

The scatter can of course be found, but perhaps more interestingly a critical level of exceedence can be found. For example the noise level that would be exceeded 10% of the time could be calculated thus accepting that, in rare extreme cases,there would be more noise than the critical level, but overall the receptor would not suffer. An example of this is shown in figure 3.

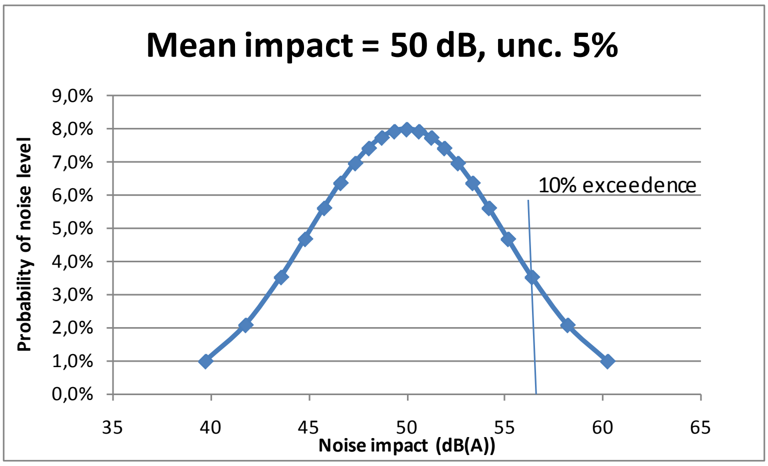

Figure 1. Noise impact distribution over a period of time. Recording all events through a period makes it possible to do statistical analysis and find for example critical exceedence levels (here the 10% exceedence level).

Some codes have different limits for different times of the day, for example Germany and Sweden. This is not a problem as the hourly distributions makes it possible to isolate these periods. This means that these periods can also be weighted in an Lden as required in Norway.

Currently many codes are focussed on specific wind speeds, most commonly 8 m/s or a range of wind speeds from say 4 to 12 m/s. These intervals can also be specified out and statistics be calculated for binned intervals of wind speed.

This methodology has also opened up for overcoming the problem of variable wind speed in the wind farm by defining a reference point for the reference wind speed. Then the relative difference between this point and the turbines can be found.

Finally the method is prepared for using wind speed in hub height as an alternative to wind speed at 10 m height, meaning that discussions on which shear to use for the extrapolation to hub height and modifiers to the source noise level become obsolete.

Conclusion

The Nord2000 model has been successfully implemented in a wind turbine planning software package (WindPRO 2.7). Moreover as the model calculates very specific situations the need arises to devise a methodology that could calculate the noise impact for an average of the encountered situations.

This methodology has been developed based on earlier findings by Eurasto, 2006 and Taraldsen, 2007 to such an extent that the resulting methodology has become very general indeed.

With the calculation possibilities and host of result presentation options a new tool is available for developers and planners, but also for planning authorities in setting up new refined, but probably also simpler codes.

The study is part of the project: Noise and Energy Optimization of Wind Farms, funded by the Danish PSO funds.

Acknowledgements

The project is publicly funded by Energinet.dk under contract no. 2007-1-7389 and co-funded by:

Dong Energy
Suzlon Energy A/S
Gamesa
StatoilHydro
E.ON Vind Sverige AB
Statkraft Development and
Vattenfall A/S

The project partners are
DELTA (project manager)

References

Raimo Eurasto, 2006. “NORD2000 for road traffic noise prediction. WP4. Weather classes and statistics.” VTT-R-02530-06, Technical research centre of Finland.

Gunnar Taraldsen, 2007. “Meteorologi og beregning av støy fra vindmøller i henhold til Eus støydirektiv for industristøy”. Preliminary summary text, SINTEF IKT.

Third International Meeting
on
Wind Turbine Noise
Aalborg Denmark 17 – 19 June 2009

Objective calculation of tonal penalty and its implementation in sound level meters and PC software

**Thorvald Wetlesen, Ole-Herman Bjor, Igor Nikolić
and Svein Arne Nordby
Norsonic AS, P.O.Box 24, N-3421 Lierskogen, NORWAY
Email: info@norsonic.com**

Abstract

Industrial noise like noise from plants and wind mill power stations will be found more annoying if it contains audible tones. Different national and international standards are dealing with the subject of tonal penalty. These standards are quite similar, but differ in some details. This paper describes the difference between the standards and how these tonal evaluations may be implemented in sound level meters and PC software.

Introduction

Most people listening to an unwanted noise of a certain level find the noise more annoying if it contains audible tones. Much industrial noise is either tonal (fans and pumps) or impulsive in nature. Research has confirmed that the frequency weighting A alone is not sufficient to assess sounds characterised by tonality, impulsiveness or strong low-frequency content. To estimate the long-term annoyance to sounds with some of these special characteristics an adjustment (also called penalty), in decibels, is added to the A-weighted sound exposure level or A-weighted equivalent continuous sound pressure level. These adjustments shall only be applied during the time that the specific character is present.

Tonal sound is defined as a sound characterized by a single frequency component or narrow-band components that emerge audibly from the total sound. Adjustments for tonal character should only be applied when the total sound is audibly tonal at the receiver location. Earlier it was common to judge the tonality based on listening to the noise. Today there are standards describing how to obtain an objective measurement of the prominence of tones.

Adjustments for tonal and impulsive sound have been suggested in all versions of ISO 1996 since its inception in 1971. In the newly approved revised version of the International standard ISO 1996-2: “Acoustics – Description, measurement and assessment of environmental noise – Part2: Determination of environmental noise levels”, an objective method for assessing the audibility of tones in noise is described in a normative Annex C of the standard.

A German draft for an objective calculation was published in 1992. The experience since then has led to some modifications and resulted in national standard DIN 45681: Acoustics – Determination of tonal components of noise and determination of a tone adjustment for the assessment of noise emissions.

The need for tonal adjustments is especially emphasized in the measurement and analysis of acoustical emissions by wind turbine generator systems. This problem is addressed by international draft standard IEC 61400-11: “Wind turbine generator systems – Part 11: Acoustic noise measurement techniques”.

This paper describes the difference between those three standards and how the tonal evaluation may be implemented in sound level meters and PC software.

Summary of the methods

All three methods used in the referred standards have three general steps:

1. Narrow-band frequency analysis (FFT analysis)
2. Determination of the average sound pressure level of the tone(s) and of the masking noise within the critical band around the tone(s)
3. Calculation of tonal audibility and the adjustment

The three methods have however slight differences which are described below and summarized in table 2.

In noise assessments, noise levels are usually measured and calculated as A-weighted sound levels or as levels for frequency bands of one- or one-third-octave bandwidth. It is common to add some decibels in penalty to the result if the sound is tonal or impulsive. Although a sound level meter with standardised octave-filter is sufficient for the level measurement, it will in general not be sufficient for judging the tonality.

All three methods are based on the psychoacoustic concept of critical bands, which are bands defined so that tones outside a critical band do not contribute significantly to the audibility of tones inside that critical band. The sound signal is first analysed with a narrow-band frequency analyser, normally of the FFT type. Peaks in the spectrum are regarded as potential pure tones. The level of this tone is compared with the level of the frequencies around the pure tone. The width of the frequency band for the comparison differs in the standards but is always related to width of the critical band. The width of the critical band is a function of the pure tone frequency and is usually 100 Hz for lower frequencies and increases for higher pure tone frequencies. As shown in table 1, the ISO-1996-2 uses a very simple formula. The formula in the DIN and IEC standards is more complicated. The critical bandwidths' dependencies on the tonal frequencies are shown in figure 1.

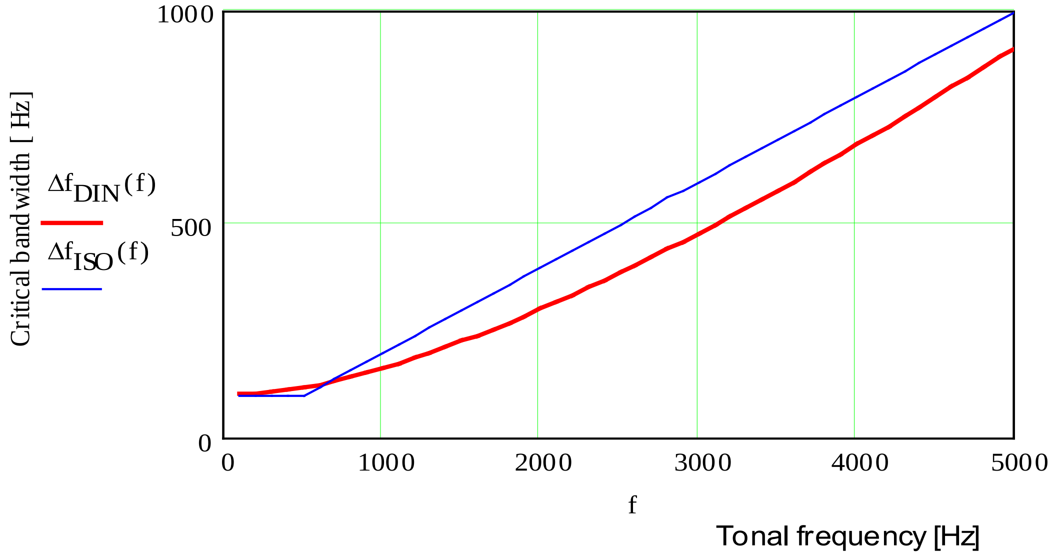

Figure 1: The critical bandwidth in the proposal for ISO 1996-2 and in DIN 45681 (same formula as in IEC61400-1)

If the level of the pure tone is a certain number above the level of the rest of the frequencies within the same critical band, the tone is regarded to be audible. Depending on how much above the detection level the pure tone is found to be, a penalty in the form of a certain number of decibels to be added to the measured A-weighted level is calculated. The penalty is in the range from 0 to 6 dB. All three standards use frequency dependent audibility criterion to compensate for the response of the human ear to tones of different frequency.

The penalty is calculated for each pure tone. Finally, the largest value of all calculated penalty values is used for correcting the overall level.

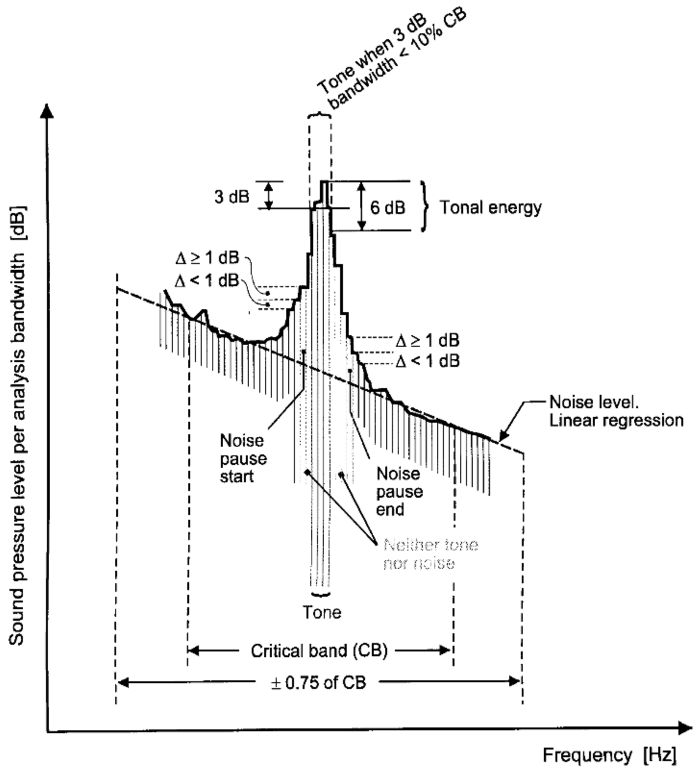

Figure 2: Illustration of the calculation procedure from ISO 1996-2

A pure tone and a noise signal behave differently when they are frequency-analysed. The level of the pure tone will be independent of the frequency resolution in the analysis, while the noise signal level will decrease when the resolution is increased. The noise has therefore to be described by its spectral density. When the tonal component and the noise are compared, the relationship between effective bandwidth of the analyser or FFT-processor and critical bandwidth has to be taken into consideration. For an FFT, which applies a Hanning window function, the effective noise bandwidth is equal to1.5 times the frequency resolution.

Implementation in a sound level meter

Norsonic has implemented the feature of tone detection and adjustment calculation with three models of sound level meters: Nor118, Nor140 and Nor121. All instruments can calculate FFT and averaged auto-spectrum. These data can be exported to a post-processing program that performs tonal analysis. In addition to that Nor121 can perform tonal analysis in real time and show results on the instruments display. The Nor121 and the Nor140 can also store the microphone signal as digital samples of the waveform in a .wav file during the measurement. This gives the possibility to perform both FFT analysis and tonal analysis as post-processing.

Figure 3: The sound level meter Nor-121 for assessment of tonal penalties.

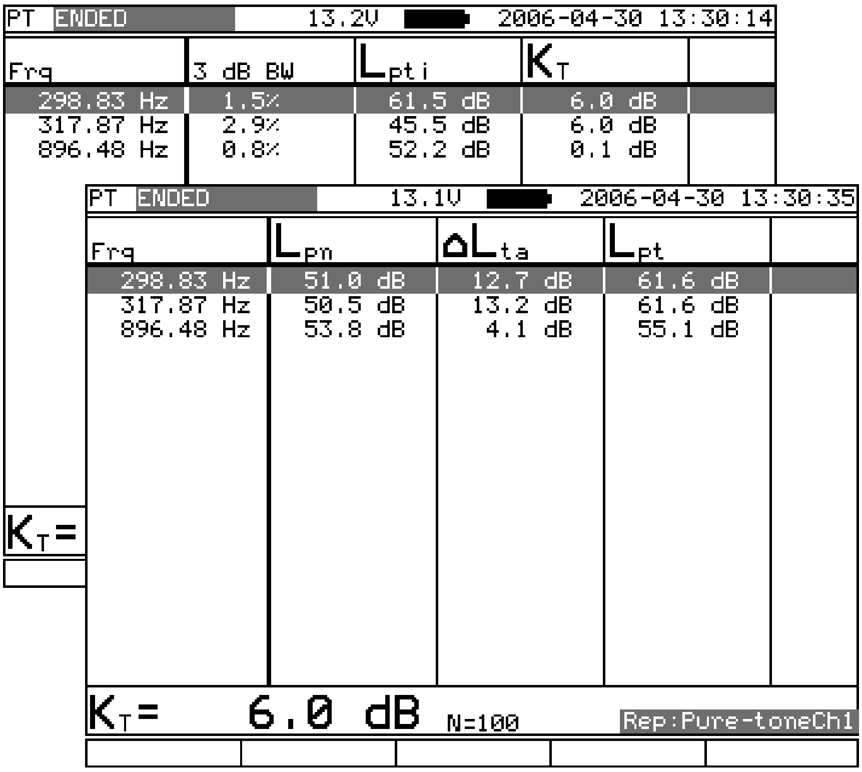

Figure 4: Two displays from Nor-121 show the detected pure tones, together with the associated 3 dB bandwidth of the tone, masking noise level Lpn, the level of the tone Lpt, and the penalty KT. The KT at the bottom shows the number of decibels to be added as penalty to the overall level.

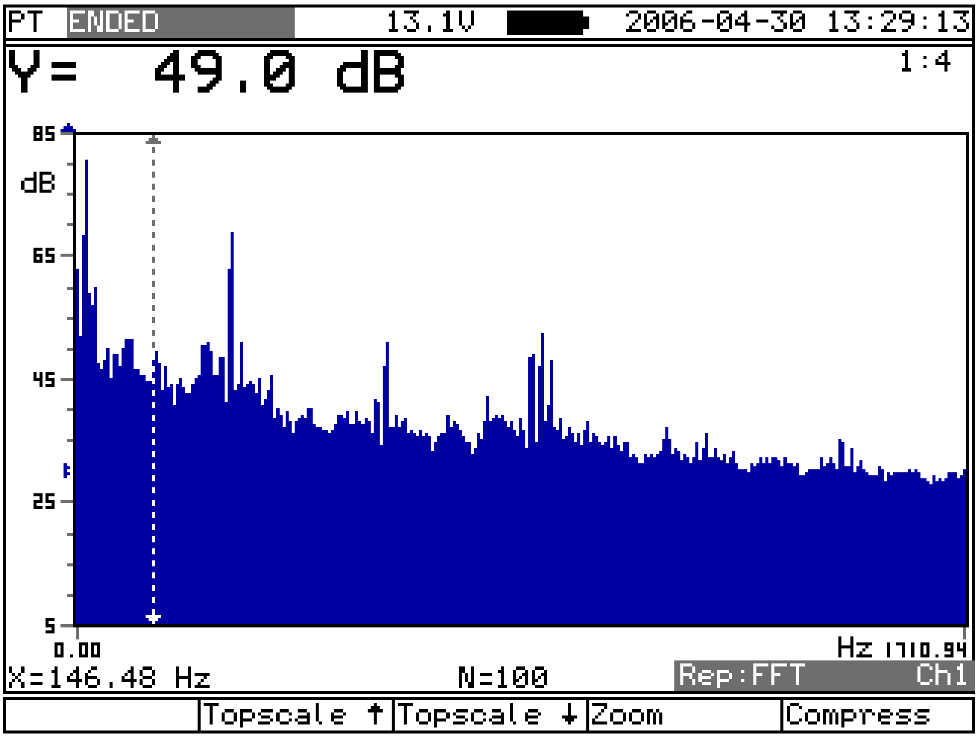

Figure 5: FFT display from Nor-121

The instruments operate normally with a sampling frequency of 48 kHz. However, for the purpose of tonal analysis in the Nor140 the Fast Fourier Transform (FFT) is performed on frequency range up to 24 kHz. The transform has order 14 (16384 samples) and will therefore have a frequency resolution of 1,46 Hz.

Nor121 calculates FFT on the full frequency range and with transform order 14 (16384 samples) its frequency resolution is 2,92 Hz. Figure 5 shows the result of the FFT as presented on the Nor121 display. The display may be zoomed for higher graphical resolution.

The instrument Nor121 uses the procedure specified in the ISO standard for finding audible tones. The result is presented as shown in figure 4. Each detected tone is listed with its frequency, the level of the tone, the A-weighted level of the tone, the bandwidth of critical band, the level of the masking noise, and the penalty value KT. Furthermore, the overall penalty is also indicated.

Implementation in a PC program

The ability to calculate objectively the impact of tonal components in real time in situ, as it is made possible by the Nor121, is doubtlessly an important advantage. It provides the user with immediate information about the noise event as it happens and helps to draw early conclusions. However, equally important is the ability to post process previously recorded noise. This way one can focus on subtle details and perform targeted analyses of selected noise fragments. The ideal tool in that case is a PC software program for presenting and post processing measured noise data. One of the most advanced PC programs for such purposes is NorReview which can do FFT calculations and tonal analysis according to the German DIN 45681 standard. It is also planned to have other standards, such as the ISO 1992-2, implemented.

Post processing of the measurements with NorReview gives the user the advantage to playback and to evaluate the data and then select the most relevant data for tonal analysis. In NorReview the user can easily select the specific part of a recording he wants to analyse.

NorReview uses an audio recording (a wav-file) as source for the calculations. The wav-file must be a mono recording with a sampling rate of 12, 44.1 or 48 kHz with a 16-bit resolution and of minimum one minute duration. The Norsonic instruments Nor121 and Nor140 both provide calibrated wav files. For survey purposes any recording device that produces a wav-file with the specified characteristics may be used.

The report generation is fully automated with NorReview as both the auto spectrum of the noise and the result of the tonal analysis is immediately presented as an extensive report in an Excel workbook. Figure 6 shows an example of an example FFT analysis and table 1 presents the summary of the results from the calculation.

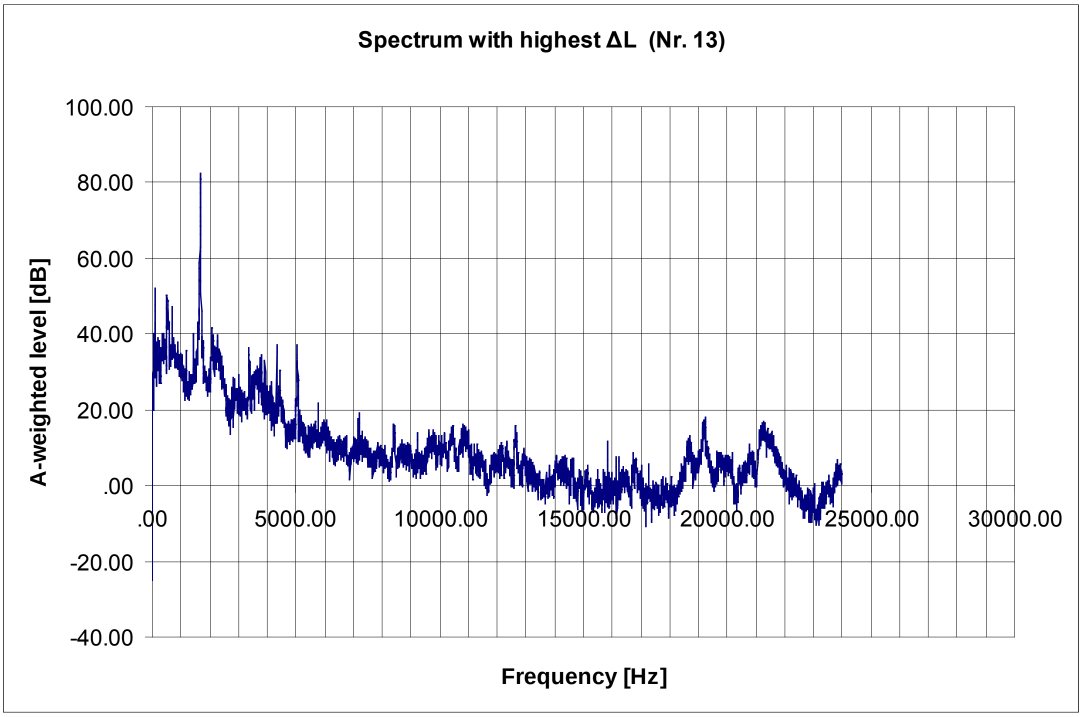

Figure 6: FFT as displayed in Excel after WAV file processing

Table 1: Summary of DIN45681 calculation

Frequency resolution	2.93 Hz
Central Frequency span	87.89 Hz to 18 kHz
Tonal Audibility	34.7 dB
Tone Penalty	6 dB
Uncertainty	0.55 dB

Conclusion

The calculation of the penalty for tonal components in noise assessments can be automatically done in a digital sound analyzer or as post processing of an audio file. For simple investigation tonal analysis can be made directly in a sound analyzer in situ. When further evaluation of the noise and production of more extensive reports is needed, tonal analysis is done as post-processing of a recorded wav-file.

The variety of national and international standards has made tone adjustment a complicated task for equipment manufacturers and confusing for users. Now that the ISO 1996-2 is approved as an international standard the hope is emerging that its procedures for analysis of noise with tonal components will prevail and become internationally accepted and used in practice.

References

[1] ISO/CD 1996-2: Acoustics – Description, measurement and assessment of environmental noise – Part 2: Determination of environmental noise levels (2005)

[2] IEC 61400-11, Ed2: Wind turbine generator systems – Part 11: Acoustic noise measurement techniques (2001) Draft for vote.

[3] DIN 45681 Acoustics – Determination of tonal components of noise and determination of a tone adjustment for the assessment of noise emissions (2005).

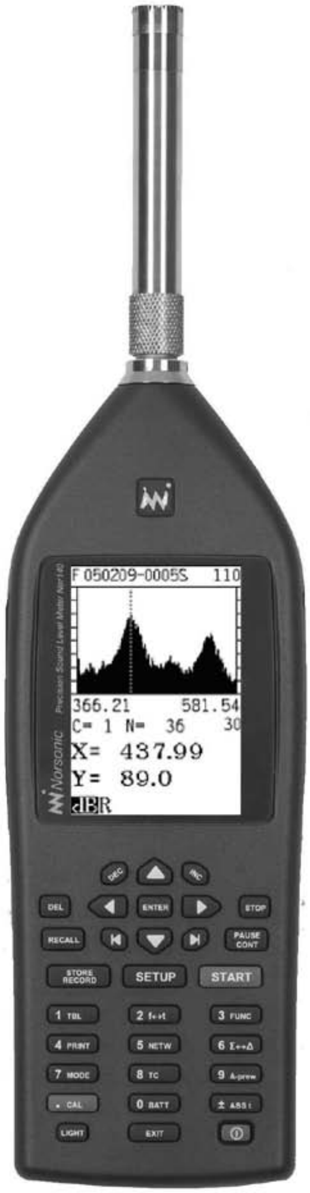

Figure 7: FFT display from Nor140

Table 2 Comparison of Methods

	ISO 1996-2 (2005)	IEC 61400-11	DIN 45681
Frequency resolution	< 3.33 Hz (5 Hz/1.5)	2 - 5 Hz for f < 2000Hz 2 - 12.5 Hz, f ≥ 2000Hz	1.9 Hz ≤ f ≤ 4 Hz
Width of critical band	100 Hz for f ≤ 500 Hz 0,2xf for f > 500 Hz	Formula, starting at 20 Hz	Formula, starting at 100 Hz
Recommended window for FFT	Hanning	Hanning	Hanning
Calculation of the level of the tone	Energy summation of tonal lines	Energy summation of tonal lines	Energy summation of highest lines based on an iterative procedure
Picket fence correction	Yes	Yes	Yes
Masking noise calculation method	Energy summation based on values from linear regression	Energy averaging of values below $L_{70\%}$	Energy summation based on an iterative procedure
Masking noise calculation range	±0.75, ±1 or ±2 critical bands	Critical band	Critical band
Audibility criterion	Dependent of frequency	Dependent of frequency	Dependent of frequency
Level adjustment – penalty	0 – 6 dB, graduated	N/A, only tonal audibility is reported	0 – 6 dB, integer values
Frequency weighting	A	Z	A
Frequency range	100 Hz -17000 Hz	20 Hz - 5000 Hz	90 Hz - 18000 Hz

Third International Meeting
on
Wind Turbine Noise
Aalborg Denmark 17 – 19 June 2009

Wind farm noise measurements and residual noise estimation by modeling

Roberto Ziliani

ISMES – Environment and Territory Division of CESI S.p.A.
Via N.Bixio, 39 - Piacenza - ITALY
roberto.ziliani@cesi.it

Abstract

Long term noise measurements were carried out at a residential premise, located in the surroundings of a wind farm, in the South of Italy. The aim of the survey was to characterise the environmental noise and to obtain an estimate of WTGs noise contribution at the receptor point, in order to check the compliance of the plant with Italian noise regulation. A-weighted and spectral noise levels were collected together with wind speed and direction data and with electrical power output of each wind turbine. The sound power level of a WTG was measured according to IEC 61400-11. The noise contribution of each WTG at the receptor point was calculated by modeling, on the basis of electrical power data. Daytime and nighttime noise immission levels at the receptor point in the relevant wind speed range were evaluated vs. national noise absolute limits. The residual noise vs. wind speed relationship was calculated and the compliance with differential noise immission limit was estimated. The residual noise level of the site was obtained by subtracting the noise contribution of the wind farm from measured ambient noise level.

Introduction

ISMES – Environment and Territory Division of CESI S.p.A. was requested to perform a noise study aimed at characterizing the noise pollution at a residential premise located in the surroundings of a wind farm in the South of Italy and to get an estimate of WTGs noise contribution at the receptor point, in order to check the compliance of the plant with Italian noise regulation.

Italian regulation on noise pollution

The Italian legislation regarding noise pollution is based on the “Framework law on noise pollution” n° 447/95 [1]. Together with the issued implementation decrees, it establishes the fundamental principles and it defines the duties of public bodies (State, Regions, Provinces and City Councils) in charge of regulating, planning and controlling activities. It also establishes parameters and limits for the definition of noise pollution.

The fundamental tool for noise regulation is the noise classification plan (i.e. zoning), that must be set by each City Council. The zoning plan divides the territory into acoustically homogeneous areas which are then assigned to one of the six classes defined by the Prime Minister Decree 14/11/1997 [2], on the basis of the main effective or intended use of the same area. The classes are: class 1 – protected areas, class 2 - mostly residential areas, class 3 - mixed type areas, class 4 - intense human activity areas, class 5 - mostly industrial areas, class 6 - exclusively industrial areas. Emission, immission, quality and warning limits are established with reference to the aforesaid classes for daytime (h. 6.00 ÷ 22.00) and nighttime (h 22.00 ÷6.00) reference times. The noise levels are evaluated as A-weighted equivalent sound pressure levels (L_{Aeq}) during these periods.

Noise emission leve is defined as noise level produced by a specific sound source. Noise immission level is related with ambient noise level, i.e. the equivalent continuous A-weighted sound pressure level produced by all the sound sources acting in a given place at a given time. Ambient noise is composed by the residual noise and by the specific noise contributions of all the annoying sources, with the exclusion of the sound events which can be identified individually as exceptional in relation to the environmental value of the zone. Residual noise is defined as the ambient noise remaining at a given position in a given situation when one or more specified noise sources are turned off. Measurements have to be taken near the receiver's position.

Noise immission limits are distinguished in: (a) absolute immission limits, related to L_{Aeq} of ambient noise and (b) "differential" immission limit, related to the difference between ambient noise and residual noise, measured inside buildings.

Special regulations for roads, railways and airports were defined by implementation decrees of Framework Law. Unfortunately, there isn't any specific regulation for wind farm noise assessment; therefore, wind farms are considered like common industrial sources.

The City Council of the territory where the wind farm is located has not set the relevant acoustic zoning plan yet. Therefore, as established by the Framework Law 447/95, transitory limits stated by the Prime Minister Decree 01/03/91 must be applied. The area surrounding the wind farm corresponds to the generic type of areas defined as *"Tutto il territorio nazionale"*, that means daytime limit of 70 dB(A) and nighttime limit of 60 dB(A) outside of buildings. The facility must also comply with differential noise immission limit: the allowed increase in noise level is + 5 dB(A) during daytime and + 3 dB(A) nighttime, being the maximum difference between the ambient noise (WTGs on) and the residual noise (WTGs off) inside buildings.

Up to now, specific regulations regarding noise surveys in wind farm sites are not enforced in Italy; therefore, all tests were performed in accordance with general national requirements stated by Ministry of Environment Decree 16/03/98 [3].

Site description

The wind farm has a total capacity of about 16 MW; it was completed in 2005 and consists of 24 wind turbines (WTG in the following), located along a ridgeline, at about 800 m a.s.l., with hub height of 45 m a.g.l..

The plant is surrounded by rural area, without settlements next to the wind turbines; only a few isolated rural dwellings are present in the proximity of the turbines. The experimental investigation was conducted with reference to ome of this location, named "Point A" in the following. The nearest WTG is located at about 260 m from the receptor, which is placed at the altitude of about 690 m a.s.l.. The figure at side shows the 3D representation of the wind farm and the surrounding area, with the selected residential premise.

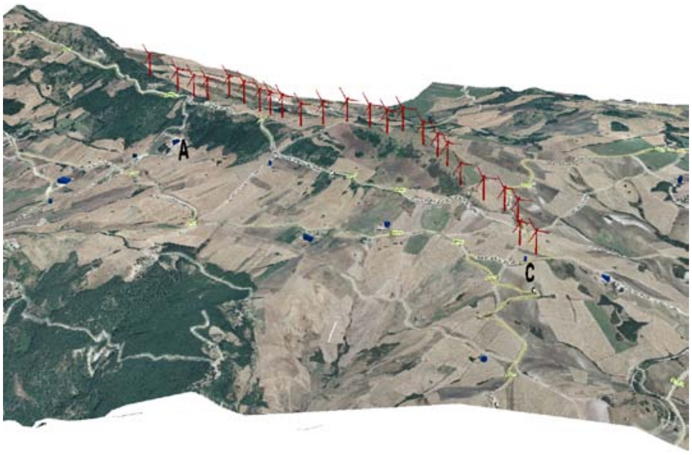

Fig. 1 – 3D view of the area, the wind turbines and the residential premise

The figure below shows the scheme of the wind farm, the location of measurement points and the location of the wind farm anemometer.

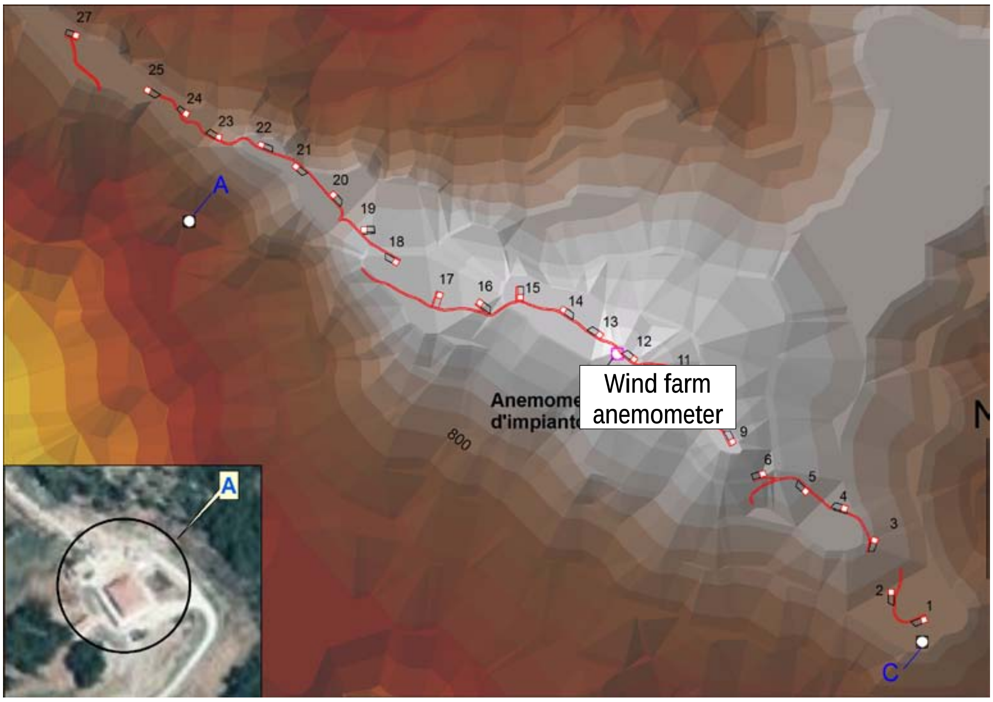

Fig. 2 – Wind farm scheme with the location of WTGs and of measurement points

Description of the study

The study was carried out as follows:

1. experimental campaigns with:
   - automatic long term environmental noise measurements at the receptor location (point A), with synchronous acquisition of sound levels, wind speed and electrical power output of each WTG;
   - measurement in point C (Fig. 2) for the calculation of sound power level of WTG01, according to the standard IEC 61400-11 [4];
2. data processing with:
   - mathematical modeling of the wind farm noise contribution at the receptor location (point A);
   - joint analysis of sound levels, windspeed and electrical power output data, in order to:
     - estimate the residual noise level, as difference between the measured ambient noise level (with WTGs on) and the noise level contribution of WTGs, obtained by the previous mathematical modeling;
     - estimate the absolute and differential noise immission levels with all WTGs operating and verify the results obtained vs. existing environmental noise limits.

Measurement Campaigns

LONG TERM NOISE MEASUREMENTS

The measurement instrumentation (B&K 2260 sound level analyser, B&K 4189 microphone fitted with B&K UA 1404 outdoor microphone kit) was placed in the surroundings of the selected residential premise (point A). The microphone height was set at 4 m a.g.l.. WTG 23, WTG 22 and WTG 24 are the less distant turbines from the receptor, located at 255, 295 and 300 m from the measurement point, respectively. Long term noise measurements were performed automatically for about three months. In the daytime, besides wind farm contribution, the noise level at point A was influenced by sound sources such as dog barking, human activity and single events such as aircraft overflights which sometimes resulted of high intensity.

The continuous equivalent level (L_{Aeq}) and the percentile levels (L_{AN}) were acquired, together with 1/3 octave bands spectra in the range of 12.5 Hz÷20 kHz. Consecutive measurement times of 10' each were selected. Noise levels were collected synchronously with the electrical production parameters of each WTG and with wind speed and direction at the wind farm mast (10 m height), located between WTG 12 and WTG 13 (Fig. 2).

Windspeed conditions and WTGs operation

The figure below shows the wind roses calculated for the whole period of measurement, and for daytime or nighttime reference periods. Data gathered by wind farm anemometer on 10 m mast were used.

<table>
<tr><th colspan="3">Whole measurement period</th></tr>
<tr><th>Total</th><th>Daytime reference period</th><th>Nighttime reference period</th></tr>
<tr>
<td>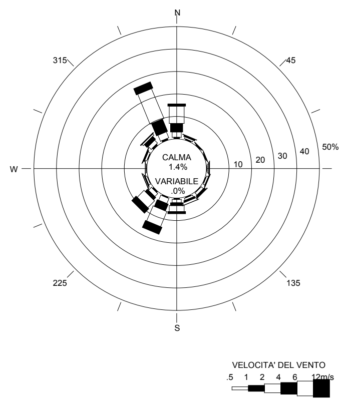
</td>
<td>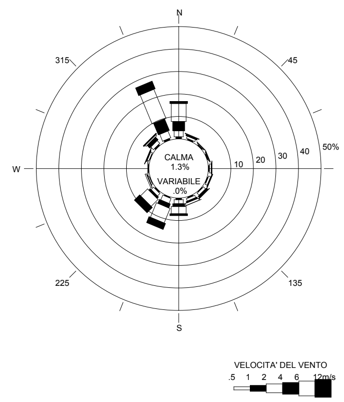
</td>
<td>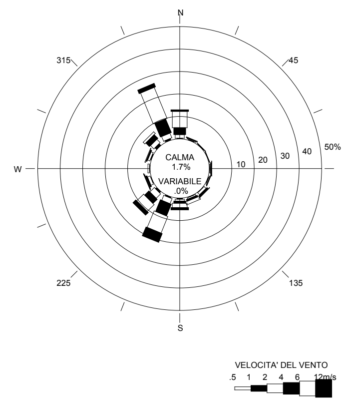
</td>
</tr>
</table>

Fig. 3 – Wind roses for total, daytime and nighttime periods

The prevailing directions were NNW, SSW, N and SW, respectively with about 30%, 20%, 15% and 12% of occurrence. During the survey, the WTGs operated for about 60-65 % of the total measuring time, with an average electrical power of about 310 kW each. The turbine WTG 27 was constantly out of service.

The two graphs below show average V_{hub} and energy production of the WTGs during the measurements. About 4000 samples of 10' each are described. The few interruptions which occurred during the measurements were taken into account. On X axis, WTGs are shown, ranged according to their distance from the receptor.

<table>
<tr><th></th><th>Daytime reference period</th><th>Nighttime reference period</th></tr>
<tr>
<td>Yellow curve:
average V hub [m/s]

Purple bars:
energy production [MWh]</td>
<td>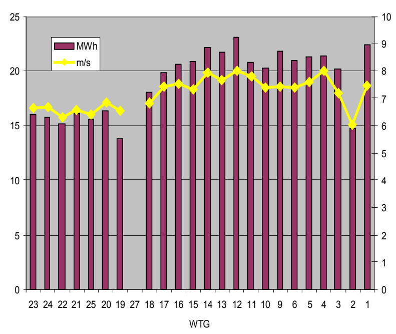
</td>
<td>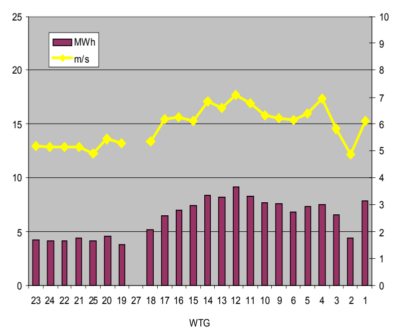
</td>
</tr>
</table>

Average electric power produced by all WTGs vs. average nacelle wind speed are shown in the curves below. The yellow line shows the power curve declared by the manufacturer, using the correct air density of the site, while the magenta curve is a fitting of experimental data (blue points).

<table>
<tr><td></td><td>Daytime period – Average of all WTGs</td><td>Night-time period – Average of all WTGs</td></tr>
<tr><td>X axis:
average wind speed at the nacelle of WTGs

Y axis:
average electric power output of WTGs</td><td>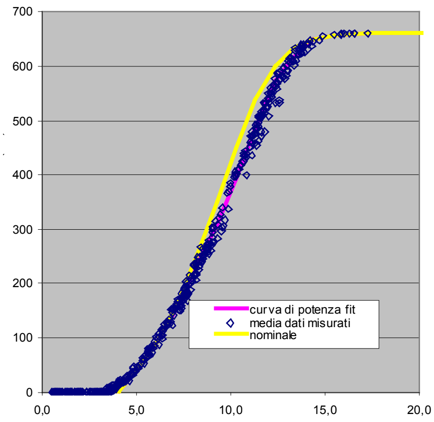
</td><td>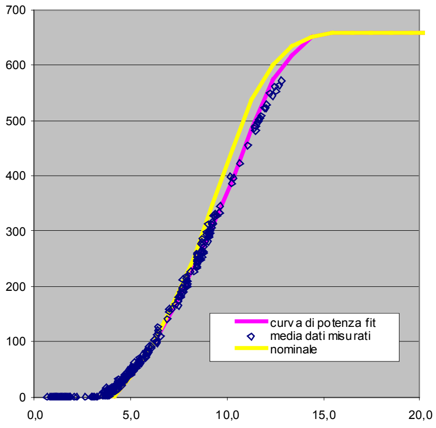
</td></tr>
</table>

<u>Measurements processing and results</u>

Data processing was conducted by B&K 7820 "Evaluator" software and by common worksheets. Inspections of CESI staff, instrumental overloads, intense rainfalls or intervals with the local wind speed > 5 m/s were excluded from data analysis.

In the following charts the time histories of environmental noise, i.e. equivalent level $L_{Aeq,10'}$ and 50th percentile $L_{A50,10'}$, wind speed and wind direction are represented, for a selection (two weeks) of measurement intervals.

The environmental noise of the site consisted of a wind-dependent contribution and of contribution which does not depend on wind conditions, with sometimes high level events. As expected, these events affected the profile of L_{Aeq} (peaked) much more than the more regular profile of L_{A50}.

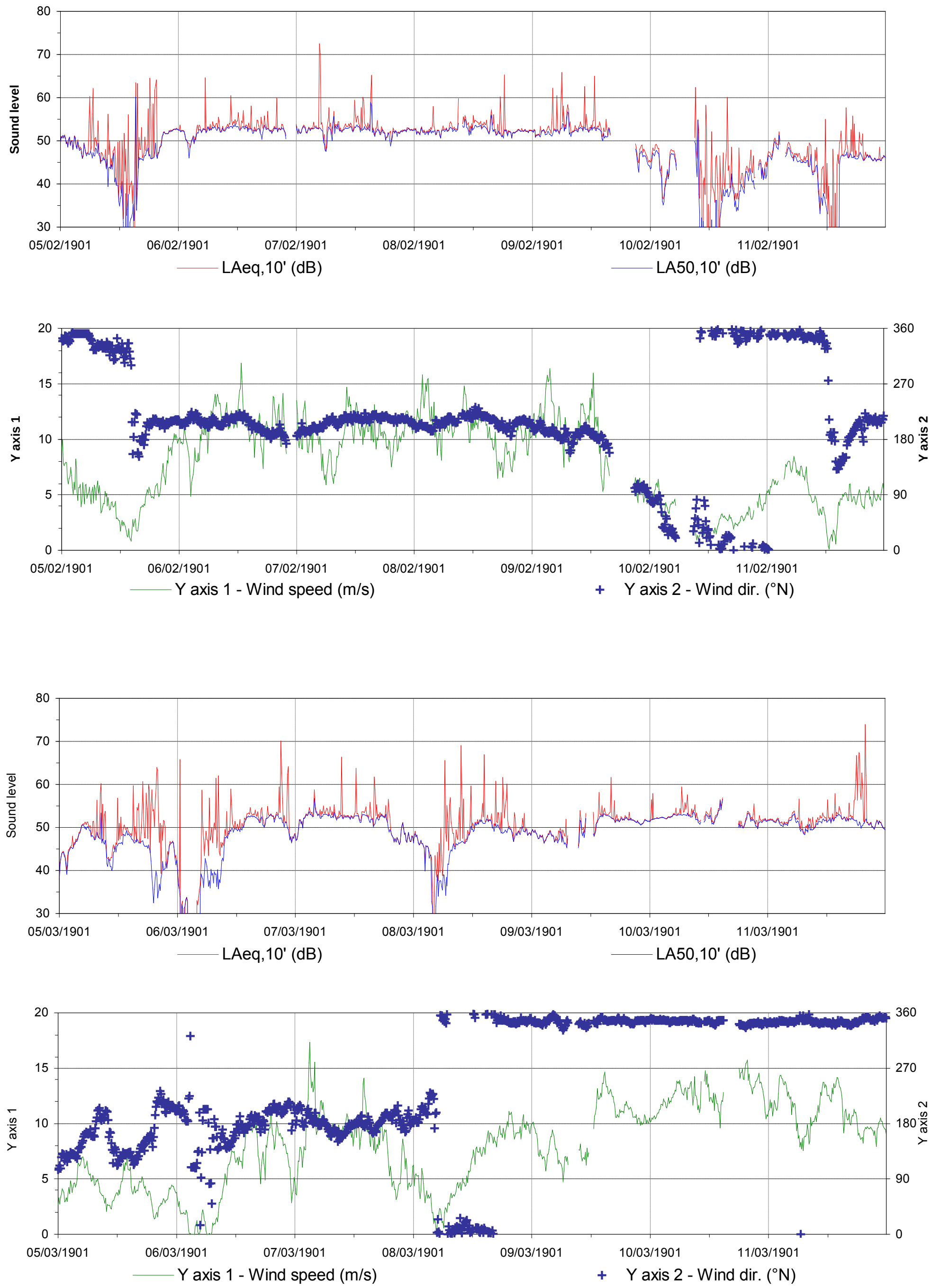

Fig. 4 – Time history of $L_{Aeq,10'}$, $L_{A50,10'}$, wind speed and wind direction – Point A

The following charts show the $L_{Aeq,10'}$ and $L_{A50,10'}$ values vs. the average hub wind speed of WTGs 19÷25. The charts include all the measured data, with the exception of the above mentioned periods (instruments out of order, inspection of CESI staff, periods of intense rainfall, etc.). Data collected during daytime and nighttime reference periods are shown.

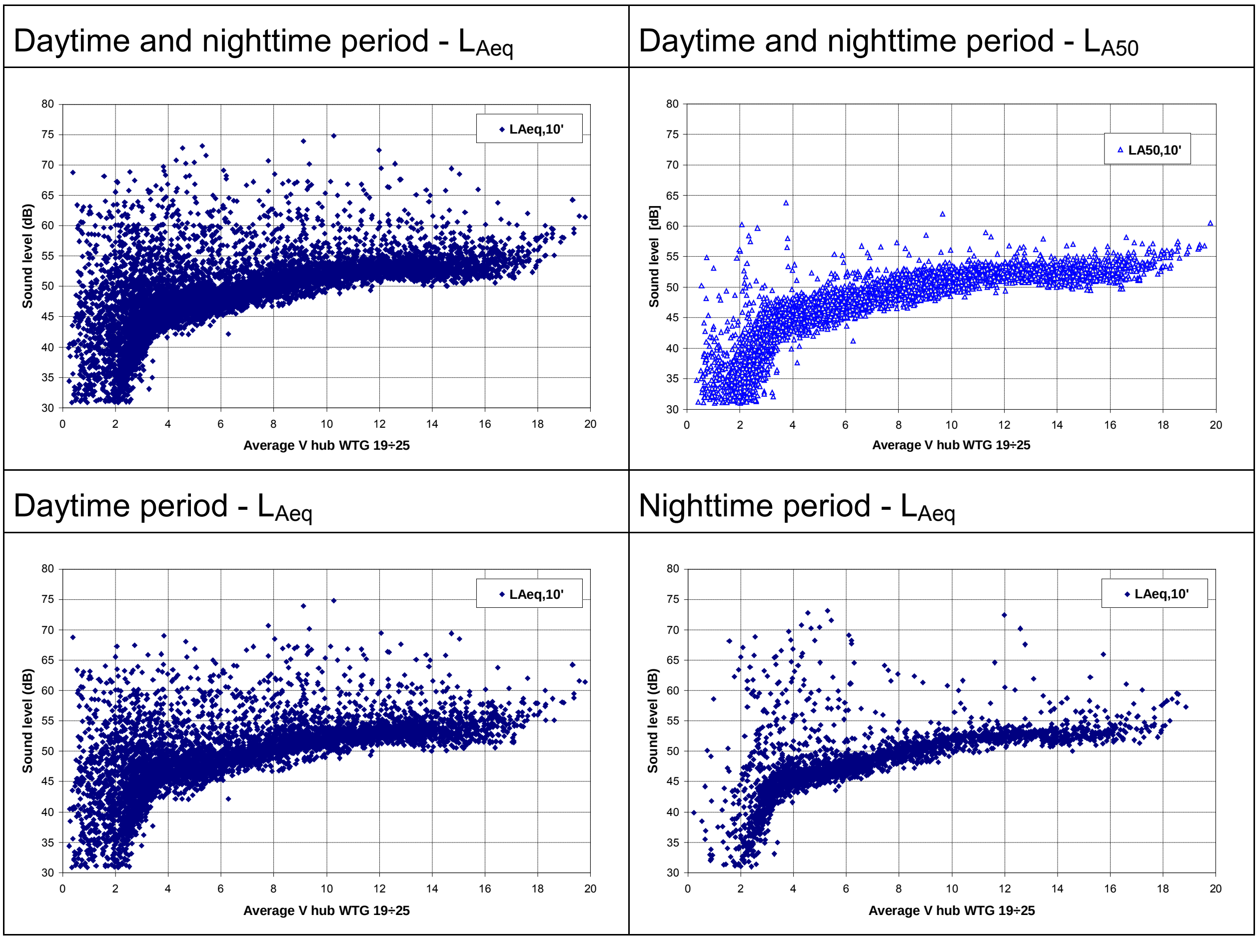

Fig. 5 – Dispersion graphs of the noise at the location A, as a function of average wind speed at hub of WTG 19÷25

The graphs confirm the relationship between environmental noise level at the site and wind speed. During daytime period, we can observe a major dispersion of L_{Aeq} values. It does not depend on wind conditions, but on (sometimes short lasting) noise sources, mainly due to human activities. These events can be excluded through the use of appropriate percentile level, such as L_{A50}; the graph of this parameter shows a lower dispersion than the L_{Aeq} graph. The dispersion of L_{Aeq} values is reduced during the nighttime period, when not wind-dependent noise sources, e.g. human activities, are less incisive.

The environmental noise level, to be compared with the acceptability limits is the L_{Aeq} produced by all the noise sources existing in a given place and during a certain time. It is composed by residual noise level and noise produced by wind turbines. It was considered to select only those samples that are not influenced by short time high level noise events. To make this filtering, the difference L_{Aeq}-L_{A50}, for each sample of 10' was evaluated. Data acquired during the operation of wind turbines, in absence of disturbing events (central hours of the night), show that a value of 5 dB (A) for L_{Aeq}-L_{A50} can be taken as a suitable threshold above which the 10’ period is discarded.

The L_{Aeq} vs. average V_{hub} of WTG 19÷25 in the range 1÷18 m/s~~,~~ for the daytime (6:00 h ÷ 22.00) and nighttime (22:00 h ÷ 6.00) reference periods were obtained. A further analysis considering downwind and upwind conditions was performed. The chart at side shows the results for the first measurement period of nighttime results (n° 661 samples upwind, n° 641 samples downwind).

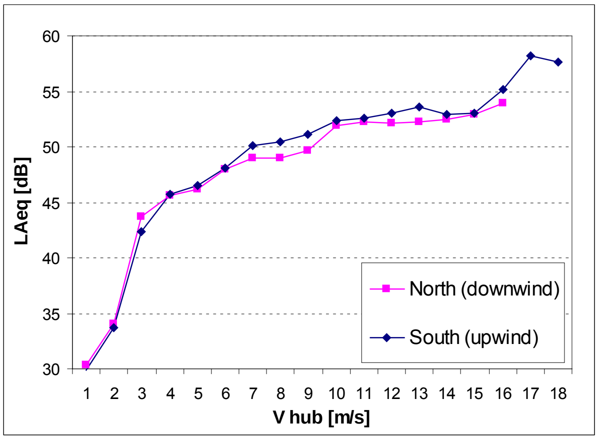

The analysis of nighttime data highlights the following aspects:

- noise levels increase as wind speed increases;
- values for upwind and downwind conditions are similar;
- the minimum value, about 45 dB(A), corresponding to wind speed at hub of 4 m/s, is slightly higher than the cut-in wind speed of this kind of WTG;
- with wind speeds of 11-12 m/s at hub height, the value of L_{Aeq} is between 52 and 53 dB (A).

Behaviour of daytime data was similar, with still slightly higher levels than the corresponding nighttime period. During day and nighttime periods, the noise level was largely consistent with transitory acceptability limits, to be applied in the absence of municipal acoustic zoning, equal to 70 dB(A) daytime and 60 dB(A) nighttime period.

SOUND POWER LEVEL CALCULATION OF WTG01

During the study, a measurement campaign was carried out, in order to calculate sound power level of WTG01 in accordance with IEC standard 61400-11. Measurements were performed automatically, in two phases (total measurement time: about 7 hours) under controlled conditions. All the main global and spectral acoustic parameters were acquired on 1’ consecutive measurement times. The measurement chain was synchronised with electrical power output logging unit of WTG01.

The test procedure states the measurement of noise emitted by a WTG, by means of microphone placed on a reflecting ground board. This measurement set-up leads to a doubling of sound pressure on the microphone.

The figure at side shows the values of $L_{Aeq,1'}$, compared with corresponding values of active electrical power collected by the control system of the WTG01. The obtained distribution is close to a straight line for a wide range of values of electrical power (10 to 300 kW).

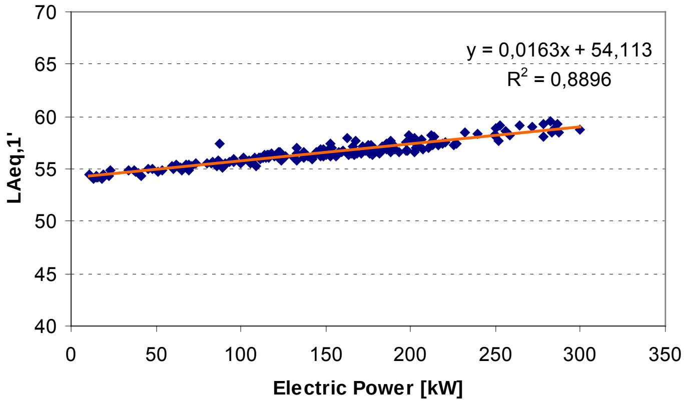

Data have been worked out in the following phases:

1. Calculation of the regression between measured noise level and V_{hub} through a 4th grade polynomial curve. The results of the calculation, reported in the chart below, show a particularly high value of the coefficient of correlation. V_{hub} was calculated from collected electric power data, by means of the power curve of the machine.

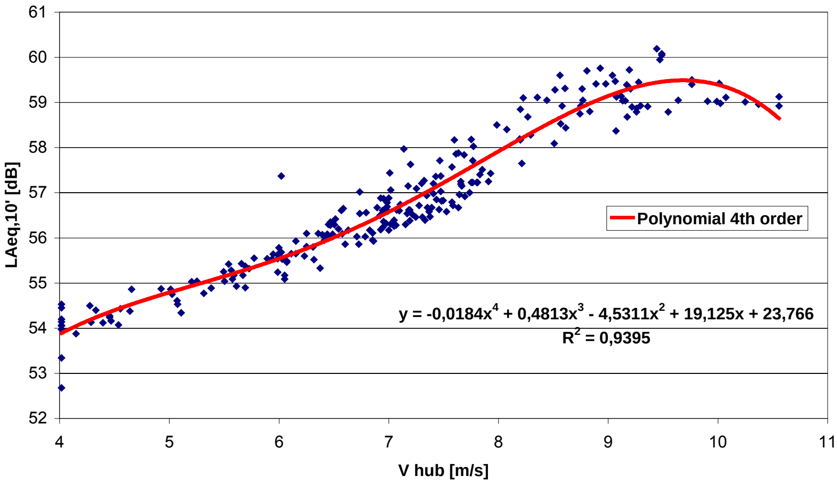

2. calculation of V_{hub}, corresponding to the standard speed V_S from 4 to 7 m/s at 10 m height, with the relation $V_{hub} = V_S \cdot \ln(Z_{hub}/z_0)/\ln(Z_S/z_0)$, assuming Z_s = 10 m, Z_{hub} = 45 m and roughness length z_0 = 0.05 m;
3. calculation the value of sound level at the above mentioned V_{hub}, using the regression curve of the IV order formerly obtained;
4. calculation of apparent sound power level by the relationship

$$L_{WA,k} = L_{Aeq,c,k} - 6 + 10 \log\left[\frac{4\pi R_1^2}{S_0}\right]$$ at the selected V_{hub};

5. calculation of the electric power corresponding to V_{hub} previously obtained;

6. calculation of the regression line between sound power and electrical power generated, to be used in subsequent modeling.

The relationship between sound power level (y) and electrical power output of the WTG (x) is:

$y = 0.0151 \cdot x + 97.095$

as shown in the chart to the side, together with data declared by the manufacturer. The relationship provides a very high correlation coefficient R^2, equal to 0.999.

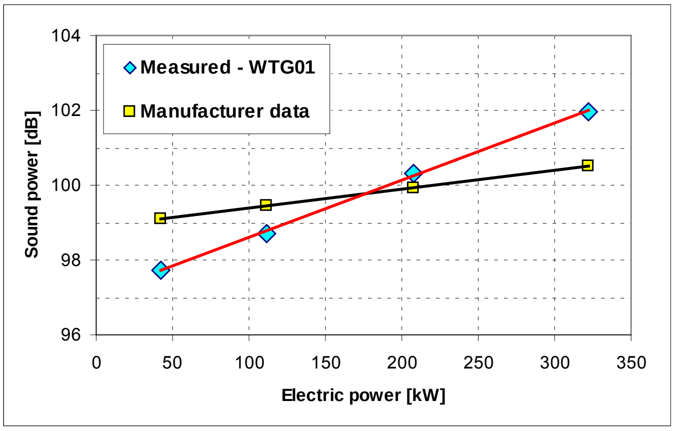

Experimental data for WTG01 differ from the data declared by the manufacturer: the sound power level is slightly different and the slope of regression line is higher, indicating a greater increase in noise with increasing produced electric power.

Data processing

The following steps were carried out for the data processing:

- Step 1: Development of a mathematical model, allowing to estimate the noise contribution of WTGs at receptor location, in function of electric power output acquired during the survey.
- Step 2: Calculation of the residual noise.
- Step 3: Calculation of the immission level with all the WTGs operating.

STEP 1 - MATHEMATICAL MODELING

In the present study the noise propagation model “SoundPlan”[1] was used. The model was operated in accordance with standard ISO 9613-2 [5], which describes a method for calculating the attenuation of sound during propagation outdoors in order to predict the levels of environmental noise at distance from a variety of sources. The method predicts the equivalent continuous A-weighted sound pressure level under meteorological conditions favourable to propagation.

The three-dimensional model of the site covers an area of over 7 km^2 and contains all the informations needed for calculation of noise propagation, such as location of sources and receivers, ground type, shielding effects of natural or artificial barriers, etc. The ground absorption factor (G) was set equal to 0.1 (reflective) around the measurement location and equal to 0.9 (absorbent) in the surrounding area. The isotropic point sources representing wind turbines were placed at the hub of each WTG. The sound propagation between these sound sources and the receiver (point A) is described by the following general relationship:

---

[1] SoundPLAN LLC Braunstein + Berndt GmbH – http://www.soundplan.com/

$$L_p = L_W - \sum_i A_i$$

where:

- L_p, sound pressure level (dB) at the receiver position;
- L_W, sound power level (dB) of the source;
- A_i, attenuation terms: A_{div} (attenuation due to geometrical divergence), A_{gr} (attenuation due to the ground effect), A_{screen} (attenuation due to screening), A_{atm} (attenuation due to atmospheric absorption), A_{misc} (attenuation due to miscellaneous effects like industrial sites, foliage, housing, etc.). Other factors such as wind, temperature gradients and atmospheric turbulence can significantly affect the propagation of sound.

In the present study, SoundPlan code was employed to calculate the noise attenuation terms ($\sum_i A_i$ in the previous relation) between each WTG and the receiver (point A). These parameters have been derived as the difference between L_W of WTG and the sound level contribution of each WTG calculated at the receiver position (L_p). The attenuation terms $\sum_i A_i$, calculated with the standard ISO 9613 for each WTG vs. point A, are shown in the following table where:

- S is the source-receiver distance;
- $\sum_i A_i$ is the sum of the attenuation terms.

WTG	$\sum_i A_i$ dB(A)
WTG 1	**86.7**
WTG 2	**86.1**
WTG 3	**85.7**
WTG 4	**91.4**
WTG 5	**84.1**
WTG 6	**83.1**
WTG 9	**82.2**

WTG	$\sum_i A_i$ dB(A)
WTG 10	**81.5**
WTG 11	**80.5**
WTG 12	**79.4**
WTG 13	**78.5**
WTG 14	**77.2**
WTG 15	**75.8**
WTG 16	**69.6**

WTG	$\sum_i A_i$ dB(A)
WTG 17	**68.0**
WTG 18	**67.9**
WTG 19	**66.1**
WTG 20	**62.3**
WTG 21	**62.6**
WTG 22	**61.4**
WTG 23	**59.8**

WTG	$\sum_i A_i$ dB(A)
WTG 24	**61.3**
WTG 25	**63.5**
WTG 27	**67.9**

As expected, the lower values of attenuation are estimated for WTGs 20÷24, the less distant from the receptor.

The 'A' weighted sound power spectrum of the WTG was derived from data supplied by the manufacturer. The sound power level at the reference value of 8 m/s at 10 m height equals 100.8 dB(A).

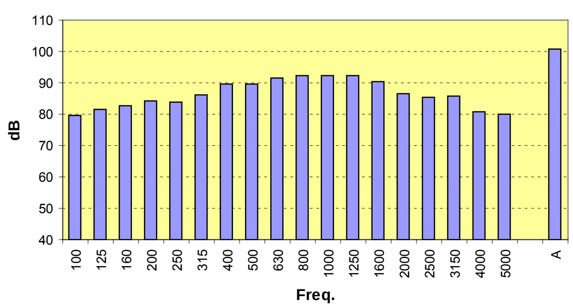

The noise model of the wind farm has been implemented in a spreadsheet program:

- L_W of WTGs is estimated as a function of electrical power through the relationship above described;
- The noise contribution of each WTG ($L_{p,j}$) was calculated by the following relation $L_{p,j} = L_W - \sum_i A_i$
- The noise contribution of all WTGs at the receptor A, denoted L_{WTG}, is thus obtained, by a log-sum of each WTG contribution: $L_{WTG} = 10 \cdot \log_{10}\left(\sum_j 10^{(0,1 L_{p,j})}\right)$.

STEP 2 - RESIDUAL NOISE CALCULATION

The measured L_{Aeq} accounts for the contribution of all sources operating within the measurement time (WTGs contribution + residual). To obtain the residual noise level, i.e. the ambient noise level with WTGs shut down, the noise produced by WTGs, calculated from electrical power output by the method above described, was log-subtracted from individual measured $L_{Aeq,10'}$. The evaluations were carried out with reference to the whole data set, selecting periods with difference L_{Aeq}-L_{A50} < 5 dB (A). Such data filtering is a very cautionary hypothesis, since it excludes from calculus many samples; if they were considered, the level of residual noise could be significantly increased. A regression model, representing the evolution of the residual noise as a function of V_{hub}, was derived. The regression curve is:

$$L_{res} = 10 \cdot \log_{10} \cdot \left(\left(10^{0.1 \cdot L_{base}}\right) + 73 \cdot V_{hub}^{esp}\right)$$

where:

- L_{base} residual noise (in dB) in typical conditions of no wind, i.e. about 35 dB(A);
- V_{hub} wind speed at hub expressed in m/s;
- *esp* exponential coefficient, assumed equal to 3, because of the dependence of the wind energy with the third power of speed.

In the figure at side, the chart shows the dispersion of the values of the residual noise level, depending on the wind speed at the hub, for the nighttime period (over than 1230 samples of 10'). The red curve represents the analytical regression curve described.

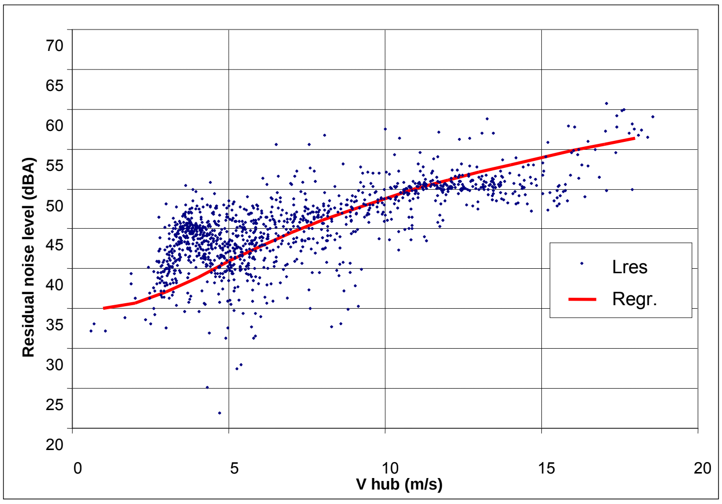

The values calculated by the model at different V_{hub} are reported in the following table.

V_{hub} (m/s)	5	6	7	8	9	10	11
Calculated residual noise level, L_{res}	40.9	42.8	44.5	46.1	47.5	48.8	50.0

In the following evaluations, the estimated nighttime residual noise levels were also assumed for day-time period. This assumption is conservative, because during the daytime period residual noise level could be increased by other noise sources like, for example, human activities.

STEP 3 - NOISE IMMISSION LEVELS

Noise immission level analysis was performed as follows:

1. calculation of the wind farm noise contribution at the receiver position with all WTGs operating by the relationships above obtained;
2. association of each power output value with the corresponding value of V_{hub}, by means of the power curve of WTG (so the noise contribution of all WTGs vs. wind speed at the hub can be evaluated assuming the same wind speed for all WTGs);
3. log sum the noise contribution of WTGs with residual noise determined by the model in the previous step, to get the total L_{Aeq} (i.e. absolute noise immission level);
4. comparison the absolute noise immission level with the residual noise level, given by the model. The arithmetical difference between absolute immission level and residual noise level is an estimate, outside the building, of the differential noise immission level. The following relationship is used:

$$L_{diff} = 10 \cdot \log_{10}\left(10^{0.1 \cdot L_{res}} + 10^{0.1 \cdot L_{WTG}}\right) - L_{res}$$

The following table summarizes, for V_{hub} 5 to 11 m/s:

1. the electric power P, in kW, obtained by the power curve of WTG;
2. the sound power level of WTGs;
3. the noise contribution of all WTGs at the receptor location (L_{WTG});
4. the estimated residual noise level at the receptor location (L_{res});
5. the noise immission level (L_{amb}), calculated as the log-sum of terms 3. and 4.;
6. the differential noise immission level (L_{Diff}).

V_{hub} [m/s]	P [kW]	$L_{WA - WTG}$	L_{WTG}	L_{res}	L_{Amb}	L_{Diff}
5	38	97.7	44.4	40.9	46.0	5.1
6	88	98.4	45.2	42.8	47.2	4.4
7	146	99.3	46.1	44.5	48.4	3.9
8	219	100.4	47.2	46.1	49.7	3.6
9	291	101.5	48.3	47.5	50.9	3.4
10	370	102.7	49.5	48.8	52.2	3.3
11	456	104.0	50.8	50.0	53.4	3.4

The following chart shows conclusive results, valid for both reference periods.

The following parameters are shown, at different V_{hub},:

- Blue curve: noise contribution of all WTG;
- Orange curve: residual noise level;
- Red curve: absolute noise immission level;
- Green curve: differential noise immission level.

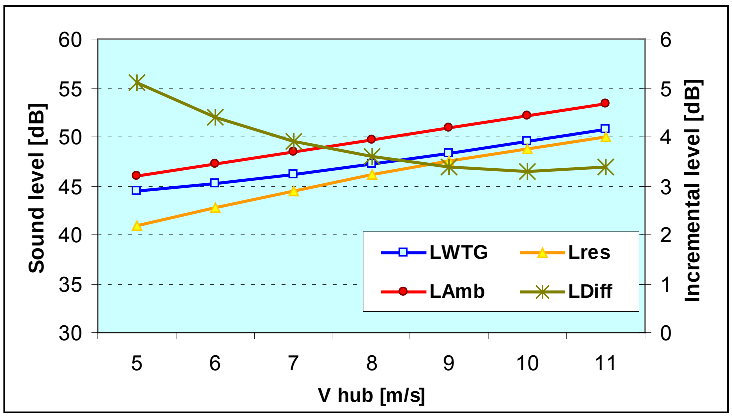

The results of processing highlight the following aspects:

- noise levels increase as V_{hub} increases;
- the minimum noise immission level (about 46 dB(A)), corresponds to V_{hub} of about 5 m/s, i.e. slightly higher than the cut-in speed of the installed WTGs;
- for V_{hub} of 10-11 m/s, the value of the L_{amb} is around 53 dB (A);
- the calculated absolute noise immission level is far lower than 60 dB(A). Therefore, the wind farm is largely compliant with the transitory daytime and nighttime limits valid for areas classified as "Tutto il territorio nazionale", to be applied in the absence of acoustic municipal zoning plan, equal to 70 daytime and 60 dB(A) night time.
- the differential noise immission level, estimated outside the house is between 3 and 4 dB, with wind speeds greater than 7 m/s, and has a growing trend to decrease of the wind speed, up to values of 4-5 dB for speeds from 5 to 7 m/s.

Conclusions

ISMES – Environment and Territory Division of CESI S.p.A. was requested to perform a study aimed at the characterization of noise pollution at a receptor located in the surroundings of a wind farm. The study, based on long term noise measurements, noise, wind and electrical power data processing, predictive modeling, allowed the evaluation of absolute and differential noise immission levels to be compared with the national regulatory framework about noise pollution. The analysis showed full compliance of the plant to the transitory limits of acceptability. Assuming that the differential noise immission level (estimated outside the dwelling) was similar to the situation inside with windows open, the regulatory limits would be exceeded only at night and, significantly, only in the presence of moderate wind speeds. For low wind speed, the plant is off, whereas for high speed winds, residual noise caused by the wind itself tends to mask the noise produced by wind turbines.

References

1. Italian Parliamentary Law no. 447 of 26/10/1995 “Framework Law on Noise Pollution”;
2. Prime Minister Decree 14.11.97 “Noise immission, emission, warning and quality limits determination”;Ministry of Environment Decree 16/03/1998 “Noise pollution description and measurement techniques”;
4. IEC 61400-11 “Wind turbine generator systems - Part 11: Acoustic noise measurement techniques”;
5. ISO 9613-2:1996 “Acoustics -- Attenuation of sound during propagation outdoors -- Part 2: General method of calculation”;
6. ISO 1996-1:2003 “Acoustics -- Description, measurement and assessment of environmental noise -- Part 1: Basic quantities and assessment procedures”